AD 731351

FOREIGN TECHNOLOGY DIVISION

AVIATION ENGINE VIBRATION THEORY AND CALCULATION
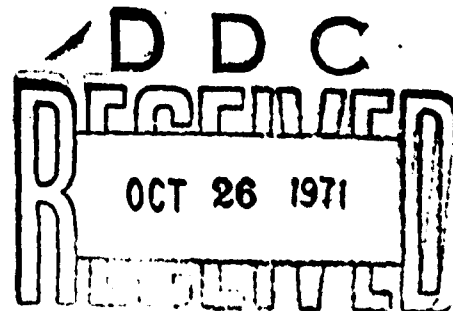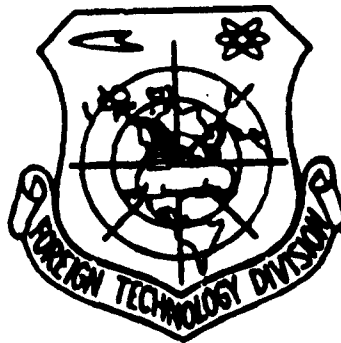
by

D. V. Khronin

DDC

RECEIVED

OCT 26 1971

DOCUMENT CONTROL DATA - R & D

(Security classification of title, body of abstract and indexing annotation must be entered when the overall report is classified)

1. ORIGINATING ACTIVITY *(Corporate author)*	2a. REPORT SECURITY CLASSIFICATION
Foreign Technology Division	UNCLASSIFIED
Air Force Systems Command	2b. GROUP
U. S. Air Force	

3. REPORT TITLE

AVIATION ENGINE VIBRATION THEORY AND CALCULATION

4. DESCRIPTIVE NOTES *(Type of report and inclusive dates)*

Translation

5. AUTHOR(S) *(First name, middle initial, last name)*

Khronin, D. V.

6. REPORT DATE	7a. TOTAL NO. OF PAGES	7b. NO. OF REFS
1970	512	47

8a. CONTRACT OR GRANT NO.	9a. ORIGINATOR'S REPORT NUMBER(S)
F33657-71-D-0057	
b. PROJECT NO. 3066 and 604010	
	FTD-HC-23-780-70
c. T65-04-19A	9b. OTHER REPORT NO(S) *(Any other numbers that may be assigned this report)*
d. DIA Task Nrs T65-01-18A	

10. DISTRIBUTION STATEMENT

Approved for public release; distribution unlimited.

11. SUPPLEMENTARY NOTES	12. SPONSORING MILITARY ACTIVITY
	Foreign Technology Division
	Wright-Patterson AFB, Ohio

13. ABSTRACT

The book deals with basic data on the general theory of
vibrations of linear and nonlinear systems, their application
to calculation of vibrations of parts, units and systems of
aircraft engines. Given are contemporary methods for calcula-
tion of vibrations, which are developing in connection with
the use of high speed computers; the method of initial para-
meters, the method of dynamic rigidities, the methods of dis-
crete models and the integral method. The book represents a
text book for students specializing in the strength of aircraft
engines; it can be useful also to engineers of the aircraft
industry. [AM0132516]

DD FORM 1473 (1 NOV 65)

KEY WORDS	LINK A		LINK B		LINK C	
	ROLE	WT	ROLE	WT	ROLE	WT
Shaft Vibration						
Blade Vibration						
Aircraft Engine						
Complex Stress						

EDITED TRANSLATION

AVIATION ENGINE VIBRATION THEORY AND CALCULATION

By: D. V. Khronin

English pages: 512

Source: Teoriya i Raschet Kolebaniy v
Dvigatelyakh Letatel'nykh Apparatov
(Theory and Calculation of Vibration
in the Engines of Flight Vehicles)
1970, pp. 1-412

Translated under: F33657-71-D-0057

Approved for public release;
distribution unlimited.

UR/0000-70-000-000

This book presents basic information on the general theory of vibrations of linear and nonlinear systems and shows its application to vibration design of components, assemblies, and systems of aviation engines.

In the first part of the book ("Linear Vibrations") we examine multimass systems, rods, and beams operating under various conditions, rapidly rotating turbomachinery shafts and rotors, rotating blades, circular plates and disks. In the second part ("Nonlinear Vibrations") we present the basic methods for determining the stability of periodic vibrations of mechanical systems.

In the book we examine the modern methods of vibration analysis, developed in connection with the application of high-speed computers. These methods include: the initial parameter, dynamic stiffness, discrete model, and integral methods.

The book is intended as a text for students specializing in aviation engine structural design. It may serve as an aid in both curricular and diploma design for students of the corresponding specialities in the aviation colleges, for the initial preparation of graduate students, and may also be useful to engineers in the aviation industry in the analytical and design work. There are ten tables, 173 figures, and 48 references.

Reviewers: I. A. Birger, Dr. Tech. Sci., M. L. Kempner, Dr. Tech. Sci., and the aviation engine structures department of Kuybyshev Aviation Institute.

TABLE OF CONTENTS

<div align="center">PART II</div>

<div align="center"><u>NONLINEAR VIBRATIONS</u></div>

FOREWORD

The present text consists of the lecture course on aviation engine vibration theory and analysis presented by the author for many years at Moscow Aviation Institute, and is intended for students specializing in engine dynamics and structures.

The questions of dynamic strength in aviation engines are of great importance because of the engine design characteristics and operating conditions. Therefore, the book has a broader purpose than the basic objective stated — it may serve as an aid on specialized questions for students in all the specialities related with engine construction, and also for the initial preparation of graduate students.

The book consists of two parts. In the first part we present the fundamentals of the theory and methods for vibration analysis of linear systems; in the second part we examine the vibrations of non-linear systems, their peculiarities, and the basic methods for analysis and calculation of nonlinear systems.

In the presentation of the material, preference is given to the new questions of engineering theory of vibrations which have been developed in recent years and are not adequately covered in the existing literature. Therefore, the material in Chapters IV, V, and VI and in the second part of the book is presented in greater detail. The presentation of the basic questions covered in previous texts is somewhat abbreviated; this applies particularly to Chapters I, II, and III.

Various analysis methods are examined in the book. The application of high-speed electronic computers has had a major influence on the development of analysis methods in recent years. Therefore, we shall examine, in addition to the earlier methods, the more exact and modern methods developed on the basis of computers. These

methods are illustrated by examples which are worked out in detail.

The book is intended for students in the upper courses. Therefore it is assumed that the reader is familiar with the fundamentals of higher mathematics, theoretical mechanics, theory of elasticity and resistance of materials as covered in the usual college programs for the mechanical engineering specialities.

During the preparation of the manuscript, Professor G. S. Skubachevskiy, Dr. Tech. Sci., has been of great assistance and has contributed valuable advice, the author wishes to express his deep gratitude to Professor Skubachevskiy.

The author would also like to thank the reviewers: Professor I. A. Birger, Dr. Tech. Sci., Asst. Professor M. L. Kempner, Cand. Tech. Sci., and also Asst. Prof. V. F. Filekin, Cand. Tech. Sci., and his other colleagues in the department of aviation structures of Kuybyshev Aviation Institute who have made many helpful critical comments on the manuscript.

NOTATIONS

A, A_1, A_2 — amplitudes of free vibrations; amplitude coefficients in general solutions;

B, B_1, B_2 — amplitudes of forced vibrations; amplitude coefficients in general solutions;

C, C_1, C_2, C_3, C_4 — constant coefficients of general solutions of differential equations;

c_p, c_ϕ, c — static stiffness coefficients (subscripts indicate directions of displacements or forces acting);

c_{is} — quasi-elastic coefficients;

e_{im} — dynamic compliance coefficients;

E — modulus of elasticity of the first kind;

G — modulus of elasticity of the second kind;

g — gravity force acceleration;

H — amplitude of disturbing harmonic force;

h — disturbing force amplitude referred to unit mass;

i — imaginary unit;

subscript i — mass number, displacement direction;

J, J_1, J_e, J_p — mass moments of inertia of disks or other system elements (subscript denotes disk number or name of axis about which moment of inertia is taken);

subscript j — vibration mode number;

K — dynamic stiffness coefficient;

k — frequency of natural vibrations of single-mass system;

k — frequency coefficient for rods, shafts, beams with continuously distributed mass;

l — pendulum length;

M — moment;

m, m_1 — point mass (subscript denotes mass number);

n — number, subscript;

2n — viscous friction force coefficient;

P — external force;

p, p_j, p_ν — frequency of natural oscillations (subscript denotes sequential frequency number);

Q, Q_1 — periodic disturbing force;

q, q_s, q_1 — generalized coordinates;

T — kinetic energy; vibration period;

t — time;

$S(k\xi)$; $T(k\xi)$; $U(k\xi)$; $V(k\xi)$ — Krylov functions;

W — plate deflection;

x — point coordinate; section coordinate;

Y — vibration amplitude;

$Y_j(x)$ — rod deflection function;

y — coordinate of point during vibrations; displacement; rod deflection;

z — coordinate;

α_{1s} — influence coefficients;

Δ — determinant of system of homogeneous equations;

Δ_{1s} — minor to element of determinant Δ;

ϵ — angular acceleration of circular frequency or shaft rotational velocity;

ζ — axis notation;

η — axis notation; coordinate of point in ξ, η, ζ moving axes system, rotating about the ζ axis;

θ — angle of rotation of rod section as a result of bending deformation;

ν — in subscript — sequential number of frequency and natural vibration mode of multimass systems, rods, shafts, and plates;

ξ — axis notation; coordinate of point in ξ, η, ζ moving axes system, rotating about the ζ axis;

Π — potential energy;

ρ — density of material or substance;

σ — stress;

τ — vibration period; time;

ϕ — angle of rotation; angle of deflection (pendulum);

ψ — inelastic resistance coefficient

ω — disturbing force frequency; forced vibration frequency;

ω — shaft, rotor, disk rotational velocity;

Ω — angular frequency of disturbance; angular velocity of disturbance vector.

INTRODUCTION

Vibrations are an unavoidable companion of the operation of aviation engines, regardless of their class, type, or size. Vibrations create additional dynamic loads on components, force the structural material to work in fatigue, and are the cause of many engine problems and failures. The presence of vibration reduces engine reliability, Therefore, the reduction of vibration is a very important and urgent problem in modern engine construction.

At the present time the questions of vibration theory and dynamic strength of machines occupy a large number of people in the scientific research institutes, experimental design bureaus of the factories, and in the higher educational institutions. The activity of these specialists is directed toward developing effective means to eliminate vibration and create reliable structures. In view of the complexity of the questions associated with vibration, both theoretical and experimental studies play a major role in the development of these techniques.

We note that the application and development of electronic computers have made it possible to carry out integrated mathematical studies of the problems associated with vibration using computational methods.

At the present time a large number of calculations are made in the engine design process. This makes it possible to select the best solutions with regard to the construction of engine components and avoid many of the difficulties associated with vibrations.

These characteristics of the present status of the question and problem in the field of vibration theory and analysis require that the aviation engine mechanical engineer have thorough and integrated preparation in all the subjects associated with vibrations. Good preparation of the engineers will avoid many of the difficulties in the experimental and production stages and will reduce the un-

necessary expenditure of material resources and human effort in the process of creating new aviation engine designs.

The objective of the courses on "Aviation Engine Vibration Theory and Calculation", and of the present volume intended for use in these courses, is to improve the preparation of the specialists and equip them with the latest engineering methods for the calculation and analysis of vibrations.

The discipline "Vibration Theory" is divided into two major independent divisions — "Linear Vibration Theory" and "Nonlinear Vibration Theory". This division is to a certain degree a methodological approach. It is determined by the characteristics of the problem formulation, the form of the equations which are used to study the systems, and by the analytical methods.

The linear systems are those whose vibrations are defined with adequate completeness and precision by linear equations. The linear equations reflect only approximately the system vibration process and are applicable for small deflections from the stable equilibrium position. However, they do permit the use of very advanced mathematical apparatus which has been developed for linear equations and make it possible to obtain a quite complete picture of small vibrations of systems, and also to develop very advanced computational methods.

The systems for which nonlinear equations are used to describe the vibrations and properties are considered nonlinear systems. The nonlinear equations yield a more correct and complete picture of the system vibrations. In the nonlinear vibration section we examine many complex and important questions which are of great practical value. These include the problems of system stability, effects of real small deviations from system linearity on the vibrations, complex questions of self-excited vibrations, the conditions for the occurrence of parametric resonance, and so on.

The problems associated with nonlinearities of the real systems are taking on increasing importance in modern science and engineering. Therefore the section on nonlinear vibrations is presented in

greater detail in the text. This section includes the necessary minimum of theoretical information on nonlinear vibrations and examines in general form several examples which are particularly important at the present time in engine design.

The studies and development of vibration analysis methods are based on the differential equations which represent the process being studied with a certain precision, within the limits of the assumptions adopted.

There are several ways to formulate the vibration differential equations. In many obvious cases the vibration equations are formulated on the basis of the d'Alembert principle as the equations of equilibrium of all the forces acting on the individual elements of the system. A more general approach is to formulate the vibration equations with the aid of the Lagrange equations. The latter are examined in detail in courses on theoretical mechanics and express the motion in generalized coordinates.

We recall that the LaGrange equations for holonomic systems with ideal constraints with a finite number k of degrees of freedom are written in the following form

$$\frac{d}{dt}\left(\frac{\partial T}{\partial \dot{q}_j}\right) - \frac{\partial T}{\partial q_j} = Q_j \qquad (j = 1, 2, \ldots, k),$$

where q_j — are the generalized coordinates, whose number for a given system must equal the number of degrees of freedom of the system;

    T — is the system kinetic energy, expressed in generalized coordinates;

    Q_j — is the generalized force corresponding to the coordinate q_j.

For conservative systems, in which Q_j is a function only of the generalized coordinates, the Lagrange equation has the form

$$\frac{d}{dt}\left(\frac{\partial T}{\partial \dot{q}_j}\right) - \frac{\partial T}{\partial q_j} + \frac{\partial \Pi}{\partial q_j} = 0 \qquad (j = 1, 2, \ldots, k),$$

where Π — is the potential energy of the system.

Any k independent quantities which define uniquely the system position at a given time can be selected as the generalized coordinates.

In vibration problems the following are usually functions of the potential energy: potential energy of elastic deformation, position energy of the mass in the gravity force field, work of the centrifugal force field. In certain problems we may encounter potential functions of the electromagnetic or electrostatic field forces.

The Lagrange equations lead to second-order differential equations of motion. Usually, with account for all the details, the equations are nonlinear and their integration involves major difficulties. Then the equations are linearized by discarding terms of second and higher orders of smallness in the coordinates and velocities.

The linear equations thus obtained reflect only approximately the system vibration process and are applicable for small deflections from the stable equilibrium position. In this case the discarded terms will not be of significant importance. Moreover, the linear equations give a quite complete picture of the system small vibrations and make it possible to obtain important practical conclusions.

Other widely used and effective methods for the solution of vibration problems are the variational methods — based on the Ostrogradskiy-Hamilton principle. These methods avoid the necessity to formulate and solve the differential equations of motion.

In many cases the solution of problems by the variational methods leads to final results faster and more simply.

The mathematical formulation of the Ostrogradskiy-Hamilton principle is studied in courses on general mechanics.

SYMBOL LIST

Russian	Typed	Meaning
э	e	equatorial
ст	st	static
расч	des	design
кр	cr	critical
в	t	tip
к	r	root
ср	av	average
ш	h	hinge
р	des	design
пр	red	reduced
ж	liq	liquid
с	b	bond
л	b	blade
д	d	disk
кр	tor	torsion
б	s	shroud
в	sh	shaft
уд	sp	specific
ж	r	rigid
до	ah	ahead
за	be	behind
отн	rel	relative
л	l	left
п	r	right
т	f	friction
рез	res	resonant

PART I

LINEAR VIBRATIONS

CHAPTER I

SYSTEMS WITH A SINGLE DEGREE OF FREEDOM

Systems with a single degree of freedom are those whose position at any time t is completely defined by a single generalized coordinate $q(t)$. Some varieties of such systems are shown in Figure 1.1, a, b, c, d, e.
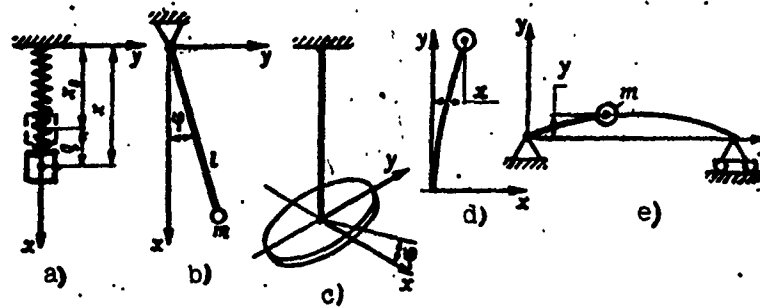
Figure 1.1. Systems with a single degree of freedom

The generalized coordinate q is the defining coordinate. The other system coordinates are related with q — for example, the x, y coordinates, the section rotation angles in bars and beams, and so on. The coordinate coupling equations depend on the concrete form of the system. For example, for the pendulum (Figure 1.1, b) they are expressed by the formula

$$x = l\cos \varphi; \quad y = l\sin \varphi,$$

where the angle ϕ is the generalized coordinate.

A particular system can be considered a system with a single degree of freedom only under several qualifications and assumptions. The most general assumptions are the following: for all systems the elastic elements, such as a spring, pendulum support filament, bar, beam, shaft, are considered to be weightless. The pendulum filament is considered ideally stiff in tension. Concentrated masses are taken to be point masses with zero moments of inertia. In the scheme shown in Figure 1.1,c, the center of gravity of the disk lies precisely on the axis of rotation, and it remains fixed during torsional vibrations. The systems shown in Figures 1.1,d and 1.1,e, can be considered systems with a single degree of freedom only in the case of small deflections, when the projections of the displacements on the y axis can be neglected and these displacements are not significant for the vibrations being examined.

1.1. Free Vibrations of System Without Friction

The small vibrations of the system about the static equilibrium position are described by the differential equation

$$m\ddot{q} + cq = 0,$$

where c — is the elastic element stiffness coefficient;

m — is the mass of the vibrating body, considered to be concentrated at the center of inertia.

The equation expresses equilibrium of the inertial and elastic forces.

For systems of the type shown in Figure 1.1,c the differential equation of free torsional vibrations has the form

$$J\ddot{\varphi} + c\varphi = 0,$$

where c — is the torsional stiffness of the bar;

J — is the disk moment of inertia.

For small pendulum vibrations the equation will be

$$ml^2\ddot{\varphi} + mgl\varphi = 0.$$

All the equations are of the same type and reduce to the harmonic oscillator general differential equation

$$\ddot{q} + k^2 q = 0, \tag{1.1}$$

where k^2 is the ratio, respectively,

$$k^2 = \frac{c}{m}; \quad k^2 = \frac{c}{J}; \quad k^2 = \frac{g}{l}; \tag{1.2}$$

It will be shown later that k is an important parameter of the system — the circular frequency of the system natural vibrations.

There are several different forms of the solution of the harmonic oscillator equations.

We seek the solution in the form

$$q = e^{\lambda t};$$

A^c $\cdot$ substituting this solution into (1.1) we obtain the characteris $\cdot$ c equation, from which we find

$$\lambda = \pm ik; \quad i = \sqrt{-1};$$

then the general solution of (1.1) will be

$$q = C_1 e^{ikt} + C_2 e^{-ikt}; \tag{1.3}$$

We find the constants C_1 and C_2 after specifying the initial conditions.

For $t = 0$, $q = q_0$, $\dot{q}_0 = 0$ we obtain

$$C_1 = C_2 = \frac{1}{2} q_0.$$

The product Ce^{ikt} is a vector whose modulus is C and direction with respect to the reference axis is defined by the angle kt. Thus the solution (1.3) (Figure 1.2,a) is the sum of two identical vectors, positioned symmetrically with respect to the angle reference line and rotating in opposite directions with the angular velocity k. The latter is called the natural oscillation circular frequency and depends, in accordance with (1.2), on the mass, elastic, and geometric characteristics of the system.

Knowing k, it is easy to find the frequency of the natural oscillations per second

$$f = \frac{k}{2\pi}.$$

In the more general but less frequently used initial condition case

$$t=0,\ q=q_0,\ \dot{q}=\dot{q}_0$$

the coefficients C_1 and C_2 take the form

$$C_1 = \frac{1}{2}\left(q_0 - i\cdot\frac{\dot{q}_0}{k}\right);$$

$$C_2 = \frac{1}{2}\left(q_0 + i\cdot\frac{\dot{q}_0}{k}\right);$$
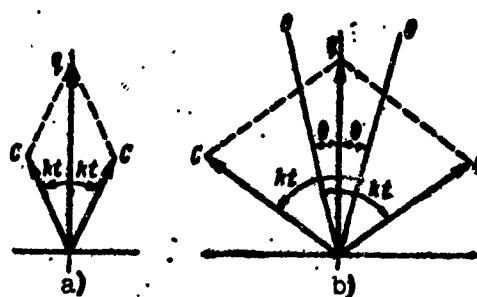
Figure 1.2. Vector representation of harmonic vibrations

They are complex conjugate numbers and are represented in the form of vectors

$$C_1 = Ce^{-i\theta}; \quad C_2 = Ce^{i\theta},$$

where the vector modulus is

$$C = \frac{1}{2}\sqrt{q_0^2 + \left(\frac{\dot{q}_0}{k}\right)^2}; \tag{1.4}$$

the angle of the initial vector position, associated with the initial conditions, is

$$\operatorname{tg}\theta = \frac{\dot{q}_0}{kq_0}; \tag{1.5}$$

In this case the general solution (1.3) takes the form

$$q = Ce^{i(kt-\theta)} + Ce^{-i(kt-\theta)}; \tag{1.6}$$

It is represented with the aid of vectors (see Figure 1.2,b). The vector form is more pictorial and in many complex problems yields simpler solution techniques.

The vector form of the solution can be replaced by the trigonometric form. In accordance with the known relation

$$\frac{1}{2}\left[e^{i(kt-\theta)} + e^{-i(kt-\theta)}\right] = \cos(kt-\theta),$$

(1.6) takes the form

$$q = A\cos(kt-\theta), \qquad (1.7)$$

where A = 2C.

The Solution (1.7) satisfies the original differential equation (1.1). If we take the general initial conditions, we find easily

$$A = \sqrt{q_0 + \left(\frac{\dot{q}_0}{k}\right)^2}, \qquad (1.8)$$

and the angle θ is defined by (1.5).

Another version of the trigonometric form of the solution is

$$q = A_1\cos kt + A_2\sin kt, \qquad (1.9)$$

in which A_1 and A_2 are easily found from the initial conditions.

1.2. Free Vibrations of Systems with Friction

Under real conditions vibrations always take place in the presence of friction forces. As a result of energy absorption by the friction forces and its transformation into heat, the free vibrations gradually decay and finally terminate.

Friction forces can be divided into two forms: the friction forces which arise in the material of the elastic parts of the system during their deformation, and the friction forces which arise from interaction of the vibrating parts of the system with the ambient medium. The latter include the forces of surface friction, hydrodynamic resistance, and so on.

The mechanism of friction force action is very complex, and many techniques for expressing the laws of friction force action lead to nonlinear problems. We shall examine two forms of friction forces within the limits of the linear problems.

1.2.1 Resistance Proportional to Velocity

The Vogt formula is widely used in linear vibration theory; in accordance with this formula the friction force is taken to be proportional to the vibration velocity

$$R = -\xi \dot{q}, \tag{1.10}$$

where ξ — is the friction force coefficient and is a small positive quantity.

This relation is valid to some degree for external friction, but is not suitable for expressing the internal friction forces, which are the fundamental resistance during vibrations. Numerous experiments have shown that internal friction is independent of the deformation velocity and depends on the hysteresis losses in the material. The latter are associated with the magnitude of the deformation, i.e., with the amplitudes of the vibrations. The use of the Vogt formula makes it possible to study the action of friction forces in the linear problem formulation, which is of theoretical interest. The results thus obtained in cases of small friction forces do not contradict experiment.

The linear equation of vibrations of a system with friction has the form

$$m\ddot{q} + \xi \dot{q} + cq = 0; \tag{1.11}$$

Referring to unit mass, we obtain

$$\ddot{q} + 2n\dot{q} + k^2 q = 0; \tag{1.12}$$

taking the solution of the equation in the form

$$q = e^{\lambda t},$$

we obtain the characteristic equation

$$\lambda^2 + 2n\lambda + k^2 = 0, \qquad (1.13)$$

from which we find, assuming n < k

$$\lambda = -n \pm i \sqrt{k^2 - n^2}.$$

The general solution of (1.12) takes the form

$$q = e^{-nt}(C_1 e^{ik_1 t} + C_2 e^{-ik_1 t}), \qquad (1.14)$$

where

$$k_1^2 = k^2 - n^2; \qquad (1.15)$$

k_1 is the natural vibration circular frequency of the system with friction. As a result of the smallness of n, the friction alters the natural frequency of the system very little; in practice this change is less than 1%.

We find the constants C_1 and C_2 for the initial conditions

$$t = 0; \quad q = q_0; \quad \dot{q}_0 = 0;$$

we obtain accordingly

$$C_1 = \frac{1}{2} q_0 \left(1 - i \frac{n}{k_1}\right); \quad C_2 = \frac{1}{2} q_0 \left(1 + i \frac{n}{k_1}\right).$$

The constants C_1 and C_2 are complex conjugate numbers, whose modulus is

$$C = \frac{1}{2} q_0 \sqrt{1 + \left(\frac{n}{k_1}\right)^2}; \qquad (1.16)$$

the initial position of the vectors is defined by the angle β (Figure 1.3)

$$\mathrm{tg}\,\beta = \frac{n}{k_1}. \qquad (1.17)$$

After finding C_1, C_2 and the angle β, the vector form of the solution (1.14) can be written in trigonometric form

$$q = 2Ce^{-nt}\cos(k_1 t - \vartheta). \qquad (1.18)$$

The law of motion of a system with damping is shown in Figure 1.3.

The free vibrations of a system with friction decay with time. The system deviations from the equilibrium position approach zero asymptotically. The decay of the deviations follows the geometric progression law.

The ratio of any two successive deviations is constant and is called the damping coefficient

$$\eta = \left| \frac{q_i}{q_{i+1}} \right| = e^{n\frac{T}{2}}, \qquad (1.19)$$

where T — is the period of the damped vibrations and equals

$$T = \frac{2\pi}{k_1}. \qquad (1.20)$$

The natural logarithm of the damping coefficient is termed the logarithmic decrement of the vibrations

$$\delta = \ln \eta = n \frac{T}{2} = n \frac{\pi}{k_1}. \qquad (1.21)$$

The larger its magnitude, the faster the vibrations decay. (In some handbooks the amplitude reduction is taken over an entire period rather than half the period. Then the logarithmic decrement of the vibrations will be twice as large: $\delta = 2n\pi/k_1$.)

Figure 1.3. Law of motion of system with damping
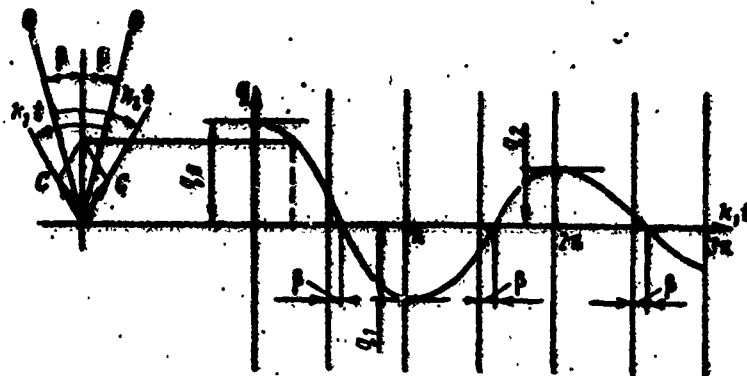
The damping coefficient and the logarithmic decrement remain constant in the course of the entire time of vibration. They can be found from an oscillogram of the damped vibrations, taking the ratio of the amplitudes of neighboring cycles.

In practice, because of the complexity of the action of the friction mechanism and the energy dissipation process, the vibration amplitude decay does not follow the geometric progression law. In this case the average value of the vibration decrement is determined.

Damped vibrations differ significantly from harmonic vibrations. Each half of the period (see Figure 1.3) divides into two parts which are not identical. The time for system motion from the position of maximal deflection to the equilibrium position is greater than the time for its motion from the equilibrium position to the next maximal deflection. The moment of passage through the equilibrium position is shifted with relation to the midpoint of the half-period by the angle β. Using the formulas presented above we can calculate, for example, that for a damping coefficient $\eta = 1.1$, the angle β of shift of the initial position reaches $1°40'$, and the ratio $n/k_1 = 0.029$.

1.2.2. Resistance of the Coulomb Friction Type

According to the Coulomb law the dry friction force is proportional to the specific pressure on the rubbing surfaces and is independent of the sliding velocity.

The magnitude of the friction force is determined by the friction coefficient, which has two values: the coefficient of kinetic friction and the coefficient of static friction. The first is always smaller than the second. The magnitude of the coefficients depends on the contacting materials, the quality and condition of the rubbing surfaces.

The action of dry friction during vibrations is detected by the nature of the damping. To illustrate the principle we shall examine the system shown in Figure 1.4. The kinetic friction force, which is a constant quantity, acts in the direction opposite the

velocity. At the instant the mass comes to rest this force changes sign; therefore the equation of motion is valid only in the c' ' 3e of half the period.

We write the equation for the motion segment from one extreme deflection position to the opposite extreme deflection position. In this segment the friction force has a positive sign

Figure 1.4. Diagram of system with Coulomb friction.

$$-m\ddot{q}-Cq+R=0, \qquad (1.22)$$

where R — is the constant friction force.

The particular solution of this equation will be

$$q_R=\frac{R}{C}. \qquad (1.23)$$

The general solution has the form

$$q=A_1\cos kt+A_2\sin kt+q_R; \qquad (1.24)$$

For the given initial conditions

$$t=0; \quad q=q_0; \quad \dot{q}_0=0$$

we obtain

$$q=(q_0-q_R)\cos kt+q_R; \qquad (1.25)$$

the system motion law in the course of the half-period is a cosinusoid whose axis is shifted in the direction of the initial deflection by the magnitude q_R, and the amplitude of the cosinusoid is $q_0 - q_R$. Plotting this part of the curve (Figure 1.5), we see that the system deflection in the opposite direction is less than the initial deflection by the amount $2q_R$:

Motion in the reverse direction
leads to change of the friction
force sign; therefore the motion
law remains valid and the curve
of the next half-period can be
plotted using the same rule.
The axis of the cosinusoid is now
shifted in the negative deflec-
tion direction by the amount q_R.

After plotting the cosinusoid
with the amplitude

Figure 1.5. Law of motion of
system with Coulomb friction

$$q_0 - 3q_R,$$

we see that the new deflection is less by $2q_R$ and so on.

Hence we see that the maximal deflection decay follows the
arithmetic progression law, i.e., each subsequent deflection is less
than the preceding by the amount $2q_R$. The line connecting the points
of maximal deflection on the vibration diagram is a straight line.

The vibration amplitude decay process will continue until the
next deflection becomes less than q_{R_0}.

$$(q_i < q_{R_0}) = \frac{R_0}{C},$$

where R_0 is the static friction force.

In this case the static friction force is greater than the
spring reaction force and the latter cannot move the mass from the
state of rest — the vibrations terminate. The system does not reach
the equilibrium position. For this reason vibrations with partici-
pation of the dry friction force are called stopping vibrations.

We see from the general solution (1.25) that the free vibra-
tion frequency of the system with dry friction is equal to the

frequency of the system without friction. In other words, dry friction forces have no effect on the free vibration period.

1.3. Forced Vibrations of System Without Friction .

Forced vibrations arise when external forces which vary in accordance with a definite law in the course of time act on a system.

We shall examine the properties of a system with forced vibrations and its laws of motion as a function of the form and nature of the excitation.

1.3.1. Vibrations Under Action of Harmonic Force. General Solution of the Differential Equation. Free, Accompanying Forced Vibrations

The differential equation of motion for this case has the form

$$\ddot{q} + k^2 q = h \cos \omega t, \tag{1.26}$$

where h — is the amplitude of the acting force, referred to unit mass;

ω — is the excitation circular frequency.

The particular solution of the equation will be

$$q = B \cos \omega t, \tag{1.27}$$

where B — is the amplitude of the forced vibrations, equal to

$$B = \frac{h}{k^2 - \omega^2}; \tag{1.28}$$

this formula is valid for $\omega \neq k$.

The general solution of the equation has the form

$$q = C_1 \cos kt + C_2 \sin kt + B \cos \omega t; \tag{1.29}$$

and constants C_1 and C_2 are determined from the initial conditions

$$t=0; \quad q=q_0; \quad \dot{q}=\dot{q}_0.$$

C_1 and C_2 are easily determined by substituting these initial values into (1.29), after which the solution takes the form

$$q=q_0\cos kt + \frac{\dot{q}_0}{k}\sin kt - B\cos kt + B\cos \omega t; \qquad (1.30)$$

the first two terms represent independent free vibrations. They are defined only by the initial conditions q_0 and $\dot{q}_0$. If the system was in the state of rest at the initial moment, these vibrations are not present.

The third term also represents free vibrations, but their occurrence is associated with the sudden application of an external force. Their amplitude equals the amplitude of the forced vibrations, and their frequency equals that of the free vibrations. These are called accompanying vibrations. The forced vibrations combine with the accompanying vibrations to yield nonharmonic vibrations of variable amplitude of the beat type.

If at the initial moment the system is given an initial displacement equal to the amplitude of the forced vibrations, i.e., the condition

$$t=0; \quad q_0=B; \quad \dot{q}_0=0,$$

is satisfied, the forced vibrations will take place without the accompanying vibrations.

The forced vibration frequency equals the frequency of the disturbing force. In accordance with (1.28) the forced vibration amplitude depends on the amplitude of the disturbing force and on the difference of the squares of the frequencies of the natural and forced vibrations (Figure 1.6). If $\omega < k$ the force and the displacement caused by it are in-phase, i.e., they have the same sign. For $\omega > k$ the disturbing force and the resulting displacement are opposite in sign, i.e., they are in opposite phases. The state $\omega = k$, when the disturbing force frequency equals the natural vibration frequency of the system, is termed resonance.

At the resonance condition the Formulas (1.27) and (1.28) become unsuitable for determining the system vibrations. In this case (1.26) takes the form

$$\ddot{q} + k^2 q = h\cos kt; \tag{1.31}$$

its particular solution is the function

$$q = \frac{ht}{2k}\sin kt, \quad \text{or} \quad q = \frac{ht}{2k}\cos\left(kt - \frac{\pi}{2}\right). \tag{1.32}$$

This solution contains the time; this means that the vibrations become anharmonic at resonance. The maximal deviations from the equilibrium position increase in proportion to the time (Figure 1.7). The vibration function has a phase shift by the angle π/2 relative to the disturbing force function.
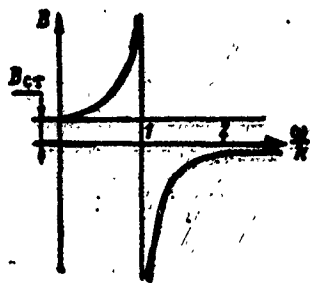
Figure 1.6. Forced vibration amplitude versus frequency
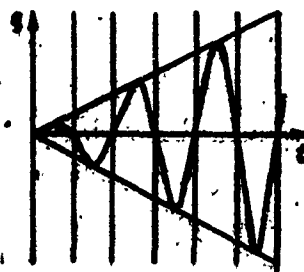
Figure 1.7. Vibration amplitude growth at resonance

The solution (1.32), containing the factor t, is termed the secular term in the general solution.

When the frequency ω is close to the natural vibration frequency k, forced vibrations take place in the form of beats. To clarify this phenomenon we use the general solution (1.30), assuming that $q_0 = 0$; $\dot{q}_0 = 0$; then

$$q = B(\cos\omega t - \cos kt).$$

Here the first term represents the forced vibrations, and the second term represents the accompanying vibrations. The value of B is defined by (1.28).

We represent the forced and accompanying vibrations as the projections of two vectors of equal magnitude B, rotating with the angular velocities ω and k (Figure 1.8).

At the initial time the vectors B occupy opposing positions and the deflection q = 0.

As a result of the small difference in the angular velocities ω and k, the angle between the vectors changes slowly. In the course of some definite time one vector performs a complete revolution relative to the other. This time is called the beat period and equals
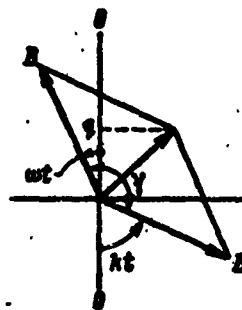
Figure 1.8. Beat vector diagram

$$T = \frac{2\pi}{k - \omega}.$$

(1.33)

The resultant of the vectors is the vibration amplitude during the beats. The vibration amplitude changes slowly as a result of change of the angle γ. Its maximal value is 2B and the minimal value is zero.

The vibration frequency during the beats is equal to the average velocity of the vectors

$$\Omega = \frac{k + \omega}{2}.$$

(1.34)

Figure 1.9 shows the nature of the beats for different relationships between the forced and natural frequencies.

The closer the values of the frequencies ω and k to one another, the longer the beat period and the larger the values reached by the maximal vibration amplitudes. The amplitude growth
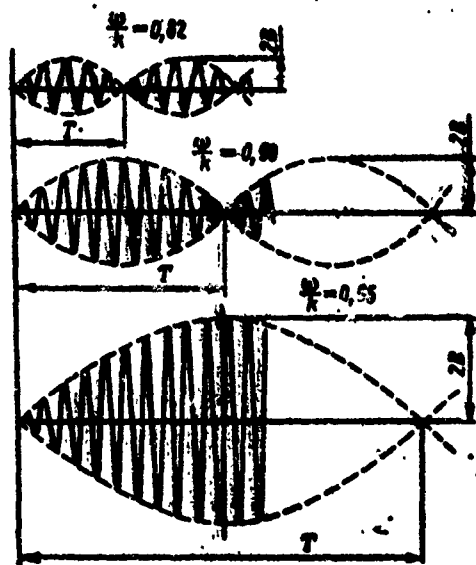
Figure 1.9. Beating as a function of ratio of forced and natural frequencies

process in the beginning of each beat period becomes more and more similar to the nature of the amplitude growth at resonance.

The beat phenomena are observed on oscillograms for forced vibration frequencies close to resonance.

1.3.2. Vibrations Under Action of Periodic Anharmonic Force

Decomposition of disturbing force into Fourier series. If a system is acted on by a periodic force Q (t) whose variation law differs from the harmonic law, such a force can be decomposed in a well-known fashion into a trigonometric Fourier series

$$Q(t) = \frac{1}{2} H_0 + \sum_{s=1}^{\infty} H_s \cos(s\omega t + \delta_s), \quad s = 1, 2, \ldots \quad (1.35)$$

The individual terms of this series are called harmonics of the disturbing force. Each harmonic differs in the amplitude H_s and the shift angle δ_s, which are determined in the decomposition process.

The system vibration differential equation takes the form

$$\ddot{q} + k^2 q = \sum_{s=1}^{\infty} h_s \cos(s\omega t + \delta_s), \quad (1.36)$$

where

$$k_s = \frac{H_s}{m}.$$

The constant first term of (1.35) is not taken into account. It is a constant force which yields the constant deflection defining the static equilibrium position. The displacement q given by (1.36) yields the position of the system relative to this equilibrium position.

The general solution of (1.36) will be

$$q = C_1 \cos kt + C_2 \sin kt + \sum_{s=1}^{\infty} B_s \cos(s\omega t + \delta_s), \qquad (1.37)$$

where

$$B_s = \frac{k_s}{k^2 - s^2\omega^2}; \qquad (1.38)$$

if at the initial time $q_0 = 0$ and $\dot{q}_0 = 0$, then

$$C_1 = -\sum_{s=1}^{\infty} B_s \cos \delta_s; \qquad (1.39)$$

$$C_2 = \sum_{s=1}^{\infty} B_s \frac{s\omega}{k} \sin \delta_s. \qquad (1.40)$$

In the general case of a periodic force the forced vibrations of the system are the result of superposing the vibrations from each harmonic of the disturbing force, taken separately. As we have noted above, the accompanying vibrations take place with the frequency of the natural vibrations of the system. Their amplitude and phase angle are the result of combining the initial deflections from all harmonics of the disturbing force and are defined by the formulas

$$\left. \begin{array}{l} C = \sqrt{C_1^2 + C_2^2}; \\ \mathrm{tg}\,\delta = \dfrac{C_2}{C_1}; \end{array} \right\} \qquad (1.41)$$

then the general solution of (1.37) will be

$$q = C \cos(kt - \delta) + \sum_{s=1}^{\infty} B_s \cos(s\omega t + \delta_s). \qquad (1.42)$$

If for any of the harmonics $k \approx n\omega$, this harmonic, having the large amplitude B_n, will stand out from the general sum. Therefore, we can assume that

$$q \approx q_n = -B_n \cos(kt + \delta_n) + B_n \cos(n\omega t + \delta_n); \qquad (1.43)$$

we obtain the beats caused by the nth harmonic.

If one of the harmonics of the disturbing force has a frequency equal to the system natural vibration frequency, i.e., $j\omega = k$, then in the general solution (1.42) there appears the forced vibration secular term

$$q_j = \frac{n_j}{2k} \sin(kt + \delta_j). \qquad (1.44)$$

It shows that in the course of time the vibration amplitudes grow without limit, characterizing resonant vibrations.

1.3.3. Forced Vibrations with Kinematic Excitation

In many cases forced vibrations of the system arise as a result of harmonic or periodic vibrations of the system support points rather than under the action of any external periodic force.

Let us examine a bar on two supports with a mass at the midpoint.

The bar supports perform harmonic vibrations, whose amplitude and frequency are given

$$q_a = q_b = B_i \cos \omega t. \qquad (1.45)$$

The kinetic and potential energies of the system are defined by the functions

$$T = \frac{1}{2} m \dot{q}^2 \text{ and } \Pi = \frac{1}{2} c (q - q_a)^2;$$

substitution of these functions into the Lagrange equation yields the vibration differential equation

$$m\ddot{q} + c(q - q_a) = 0;$$

substitution herein of (1.45) leads to the equation

$$\ddot{q} + k^2 q = k^2 B_0 \cos \omega t. \tag{1.46}$$

This equation is identical in form to (1.26). Here the role of the force amplitude value h is played by the product $k^2 B_0$ — the given kinematic excitation amplitude times the natural vibration frequency squared.

Consequently, all the solutions of (1.46) and (1.26) will be identical. The quantitative relations are obtained by replacing the quantity h by the product $k^2 B_0$ in the formulas.

If the kinematic excitation frequency equals the system natural vibration frequency, resonant vibrations will occur. If there is a small difference of the frequencies, vibrations will take place in the form of beats.

What we have said is equally valid for kinematic periodic excitation. In this case the support motion law must be represented in the form of a Fourier series, and we must examine the action of each harmonic separately. All the formulas previously obtained for periodic force excitation may be used for this purpose.

1.4. Forced Vibrations of System with Friction
Proportional to Velocity

1.4.1. General Solution of the Equation of the System

We examine a system with friction proportional to the velocity, subjected to the action of a harmonic force. The differential equation of such a system will be

$$\ddot{q} + 2n\dot{q} + k^2 q = h \cos \omega t; \tag{1.47}$$

the general solution of the equation will be

$$q = C e^{-nt} \cos(k_1 t - \theta) + q_\Lambda; \tag{1.48}$$

the first term represents free damped vibrations; the second term
represents forced vibrations. The amplitude C and the phase angle
θ of the free vibrations are determined from the given initial
conditions. In view of the fact that the free vibrations decay, we
shall not take the first term into account in the general solution.

The forced vibrations are defined by the solution

$$q_\Lambda = B \cos(\omega t - \beta). \qquad (1.49)$$

Substituting this solution into the differential equation
(1.47), we obtain

$$B(k^2 - \omega^2)\cos(\omega t - \beta) - 2n\omega B \sin(\omega t - \beta) = k \cos \omega t;$$

Expanding the cosine and sine of the difference using well-known
trigonometric formulas and then combining terms with the common
factor cos ωt and sin ωt, we obtain two equations

$$B(k^2 - \omega^2)\cos\beta + B 2n\omega \sin\beta = k;$$
$$B(k^2 - \omega^2)\sin\beta - B 2n\omega \cos\beta = 0,$$

The amplitude and phase angle of the forced vibrations are deter-
mined from these equations

$$B = \frac{k}{\sqrt{(k^2 - \omega^2)^2 + (2n\omega)^2}}; \qquad (1.50)$$

$$\mathrm{tg}\,\beta = \frac{2n\omega}{k^2 - \omega^2}. \qquad (1.51)$$

The solution obtained shows that forced vibrations of a system
with friction take place in accordance with a harmonic law.

Figure 1.10 shows the amplitude versus the ratio of the forced
and natural vibration frequencies.

For ω = 0 the system deflection equals the static deflection
for all n

$$B_{ct} = \frac{k}{k^2}.$$

The friction has a particularly large influence in the resonant
region. The greater the friction the smaller the vibration ampli-
tudes B. However, it should be emphasized that the amplitudes of

the forced vibrations remain larger than the static amplitudes in the region up to resonance and in a considerable portion of the region beyond resonance.

The peaks of the curves lie to the left of unity. The frequency ratios corresponding to the peaks can be found from the formula

$$\frac{\omega}{k} = \sqrt{1 - 2\left(\frac{n}{k}\right)^2} \approx 1 - \left(\frac{n}{k}\right)^2; \quad (1.52)$$

as a result of the smallness of n the shift of the peaks is slight.

Figure 1.10. Amplitude versus ratio of forced and natural vibration frequencies

Far from resonance, friction has very little effect on the vibration amplitudes. Therefore friction may be ignored when making a vibration analysis of systems far from resonance.

As a result of friction, the forced vibration function (1.49) is shifted relative to the disturbing force function by the angle β. We represent them as projections of the vectors h and B on the vertical axis (Figure 1.11). The shift angle β is connected with the friction, but depends strongly on the relationship of the frequencies ω and k. In the region ω < k (see Figure 1.11, a) the angle β is less than π/2; for ω = k (see Figure 1.11, b) it equals π/2, and beyond resonance (see Figure 1.11, c) it is greater than π/2. The existence of the shift angle indicates that forced vibrations of the system are performed with expenditure of energy to overcome friction forces.

The work of the disturbing force during a period equals

$$L_\lambda = \int_0^{\frac{2\pi}{\omega}} h\dot{q}_\lambda \cos\omega t\, dt; \quad (1.53)$$

Figure 1.11. Vector representation of forced
vibrations of system with friction

Substituting herein (1.49) and performing the integration, we obtain

$$L_h = \pi h B \sin \beta. \tag{1.54}$$

If $\beta = 0$ or $\beta = \pi$, the disturbing force work equals zero. If
$\omega = k$

$$\sin \beta = 1; \quad L_h = \pi h B.$$

The most work is expended at the frequency corresponding to the
amplitude peak, which is defined by (1.52).

The work of the friction forces equals

$$L_R = \int_0^{2\pi/\omega} R \dot{q} \, dt = - \int_0^{2\pi/\omega} 2n \dot{q}^2 \, dt; \tag{1.55}$$

substitution herein of (1.49) and integration yields

$$L_R = - 2n \pi \omega B^2; \tag{1.56}$$

For steady-state forced vibrations the work balance during a period
is defined by the equation

$$L_A + L_R = 0; \qquad (1.57)$$

hence, in accordance with (1.54) and (1.56), we obtain

$$h \sin \beta = 2nB\omega = R_A. \qquad (1.58)$$

This equation represents equality of the friction force amplitude and the disturbing force component performing the work (see Figure 1.11).

1.4.2. Vibration Source Isolation

The disturbing force which causes forced vibrations of the system is transmitted through the elastic elements to the supports.

The force transmitted to the supports is defined by the elasticity of the elements and the friction which develops in the elements

$$P = cq + \xi \dot{q}; \qquad (1.59)$$

substituting herein (1.49), we obtain

$$P = cB \cos (\omega t - \beta) - B\xi\omega \sin (\omega t - \beta);$$

By the replacement

$$cB = P_A \cos \delta; \quad B\xi\omega = P_A \sin \delta$$

the formula is reduced to the form

$$P = P_A \cos (\omega t - \beta + \delta). \qquad (1.60)$$

where P_A — is the amplitude of the force transmitted to the supports;

δ — is the phase angle;

$$P_A = cB \sqrt{1 + \left(\frac{2n\omega}{k^2}\right)^2}; \qquad (1.61)$$

$$\operatorname{tg} \delta = \frac{2n\omega}{k^2}; \qquad (1.62)$$

Substituting (1.50) into (1.61), we obtain the final form of the formula for the amplitude of the force acting on the supports

$$P_A = H \frac{\sqrt{h^2 + (2n\omega)^2}}{\sqrt{(h^2 + \omega^2)^2 + (2n\omega)^2}} = H\eta, \qquad (1.63)$$

i.e., the force transmitted through the elastic suspension to the supports is equal to the product of the excitation force H by the dynamic force coefficient η.

Figure 1.12 shows η as a function of frequency and the friction coefficient. For $\omega = 0$ and $(\omega/k) = \sqrt{2}$ the quantity $\eta = 1$; in the range from zero to $(\omega/k) = \sqrt{2}$ the coefficient η is larger than one, but its value diminishes with increase of the friction; for $(\omega/k) > \sqrt{2}$ the coefficient η becomes less than one, but its magnitude increases with increase of the friction.
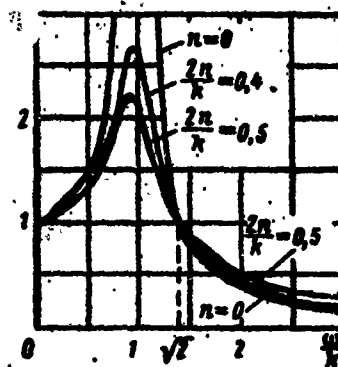
Figure 1.12. Coefficient of dynamic force transmitted to supports in the elastic support case

These curves show that in order to isolate the vibration source and reduce the dynamic forces on the supports the elastic suspension must be designed so that its natural frequency is no more than 70% of the exciting force frequency. The introduction of damping devices into the system in this case is not advisable, since this leads to increase of the forces transmitted to the supports.

If it is not possible to provide a soft suspension, then the mounting of the unit should be as rigid as possible in order that the coefficient η not exceed one significantly. In this case the introduction of damping devices is not mandatory, since their effectiveness is not high.

If the exciting force frequency changes over a wide range during operation and the occurrence of resonant vibrations is

possible, then damping devices must be introduced into the elastic suspension in order to reduce the amplitudes of the resonant vibrations, which leads to reduction of the forces transmitted to the supports.

1.5. Forced Vibrations of System with Internal
Inelastic Resistance

The primary form of energy losses during vibrations is energy expenditure on overcoming internal resistance in the material. Plastic deformations, in addition to the elastic deformations, occur in the elastic elements of the system when they are loaded. The energy expended on creating microplastic deformations is not returned when the load is removed. If the external load applied to the system has a cyclic nature, there are definite irreversible energy expenditures during each load variation cycle.

The losses due to inelastic resistance during a complete deformation cycle are defined by the so-called hysteresis loop (Figure 1.13); these losses are proportional to the area of this loop.

For an individual element or specimen the area of the hysteresis loop diagram depends on the material properties, the magnitude of the deformations, and depends very little on the deformation rate over quite a broad rate variation range.

Figure 1.13. Hysteresis loss diagram

The material properties with regard to energy absorption in inelastic resistance during vibrations are evaluated by the absorption coefficient

$$\psi = \frac{A_R}{\Pi},$$ (1.64)

where L_R — is the energy absorbed by the material during a deformation cycle and is proportional to the hysteresis loop area;

Π — is the system potential energy for the same amplitude.

This connection between the losses and the potential energy is very convenient, since it permits estimation of the losses as a fraction of the magnitude of the potential energy. This relation is applicable to the ent'~~ system, and to its individual segments and elements.

Experimental specimen loading and unloading diagrams make it possible to determine the coefficient ψ. At the same time they show that the inelastic resistance losses increase faster than the deformation amplitude squared. Therefore the absorption coefficient ψ, strictly speaking, is not constant, but increases with increase of the amplitude

$$\psi = \gamma A^{m-1}, \quad m > 1$$

where γ and m are the coefficients which depend on the material properties. The greater the plasticity of the materials, the larger these coefficients. However, for deformations lying within the elastic limits the variation of ψ for a given specimen is very small and is not taken into account in linear problems.

The values of the absorption coefficients ψ for some materials are shown in Table 1.1 (see [37] and [12]).

For materials having low inelastic resistance an approximate estimate of the coefficient ψ can be made on the basis of the damped vibrations.

We write the energy balance equation for two neighboring states, differing in time by one period

$$\Pi_s = \Pi_{s+1} + L_R;\qquad\qquad(1.65)$$

the potential energies at the beginning and end of the cycle are, respectively

$$\Pi_s = \frac{1}{2} c A_s^2; \quad \Pi_{s+1} = \frac{1}{2} c A_{s+1}^2; \quad L_R = \psi \overline{\Pi}_{s+1};$$

substituting these values into (1.65), we obtain

$$\left(\frac{A_s}{A_{s+1}}\right)^2 = 1 + \psi. \tag{1.66}$$

After recording the oscillogram of the damped vibrations and determining from this record the amplitude ratio of two neighboring vibrations, we can use this formula to find the absorption coefficient ψ.

TABLE 1.1.

Item no.	Material	ψ
1	Steel 3	0.01 − 0.03
2	Aluminum	0.03 − 0.044
3	Soft cold-drawn steel	0.01
4	Cold-drawn aluminum	0.0067
5	Cold-drawn copper	0.01
6	Cast tungsten	0.033

We note that in the beginning of the oscillogram the damped vibration amplitudes decrease more rapidly than at the end of the recording.

In spite of its small magnitude, inelastic resistance has a significant influence on the forced vibration amplitudes in the resonant region.

The Sorokin formula (see [36]) is used in vibration analysis of systems with account for inelastic resistance

$$S^* = \left(1 + i\frac{\psi}{2\pi}\right) cq. \tag{1.67}$$

which represents the overall internal resistance force. This force is expressed in complex form: the real part is the elastic resistance force, and the imaginary part is the inelastic resistance. The inelastic resistance is to be considered as a vector proportional to the elastic force, rotated through the angle $\pi/2$ relative to the latter.

Using the Sorokin formula, we write the differential equation of forced vibrations of the system in the form

$$m\ddot{q}+\left(1+i\frac{\psi}{2\pi}\right)cq=He^{i\omega t};\tag{1.68}$$

The right side — the disturbing force — is taken here in complex form, which corresponds to the form of the left side of the equation.

The particular solution of this equation should also be taken in complex form

$$q=Be^{i\omega t}.\tag{1.69}$$

Substituting this solution into the differential equation, we obtain

$$\left(k^2-\omega^2+i\frac{\psi}{2\pi}k^2\right)B=h;$$

hence

$$B=h.\frac{(k^2-\omega^2)-i\frac{\psi}{2\pi}k^2}{(k^2-\omega^2)^2+\left(\frac{\psi}{2\pi}k^2\right)^2}.\tag{1.70}$$

The quantity B is a complex number and is expressed by a vector shifted by the angle β relative to the disturbing force vector H (Figure 1.14).

Calculating on the basis of (1.70) the modulus of the vector B and the phase angle β, we obtain the final form of the Solution (1.69)

$$q=\frac{h}{\sqrt{(k^2-\omega^2)^2+\left(\frac{\psi}{2\pi}k^2\right)^2}}e^{i(\omega t-\beta)};\tag{1.71}$$

$$\operatorname{tg}\beta=\frac{\psi}{2\pi}\frac{k^2}{k^2-\omega^2}.\tag{1.72}$$

The formulas show that the forced vibration amplitude of a sys=
tem with inelastic resistance depends on the disturbing force fre-
quency and the coefficient ψ. The largest amplitude is obtained at
resonance $\omega = k$. In this case the phase angle β becomes equal to
$\pi/2$.

Figure 1.14 shows the relative
position of the vectors of the
forces acting on a mass during
vibrations.

The inelastic resistance
force

$$R_A = -i\frac{\psi}{2\pi} cB \qquad (1.73)$$

is rotated through the angle $\pi/2$
relative to the displacement
vector.

It is not difficult to verify
that the work expended during a
period on overcoming this resist-
ance is proportional to the maximal
deflection potential energy.
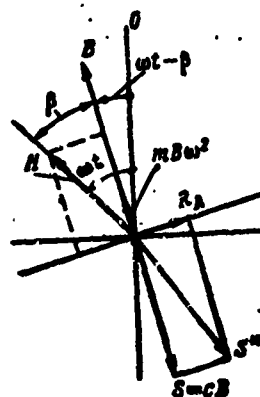
Figure 1.14. Vector dia-
gram of forced vibrations
of system with nonelastic
resistance

1.6. Solution of Forced Vibration Equation in Definite Integral Form

1.6.1. General Method for Constructing Solution in Defir e Integral
Form

It is not always convenient or even possible to solve the
forced vibration differential equation

$$\ddot{q} + k^2 q = Q(t) \qquad (1.74)$$

by representing its right side in the form of an infinite Fourier
series. For example, if Q (t) is a function having discontinuities
or is given in the form of systematic impulses, the decomposition
of such functions into a trigonometric Fourier series can be per-

formed only very arbitrarily because of the slow convergence of the series.

In such cases the solution can be obtained in the form of a definite integral, which yields the system deflection at a given time τ as the result of the action of the disturbing force during the entire time segment from the beginning up to τ.

If the disturbing force $Q(t)$ is an arbitrary function, the solution can be obtained by the arbitrary constant variation method. To do this, in the general integral of Equation (1.74) without the right side

$$q = C_1 \cos kt + C_2 \sin kt \qquad (1.75)$$

we consider C_1 and C_2 to be time functions, which we choose so as to satisfy the complete equation (1.74).

Differentiating (1.75), we obtain

$$\dot{q} = \dot{C}_1 \cos kt + \dot{C}_2 \sin kt + k(-C_1 \sin kt + C_2 \cos kt).$$

Since there are two unknown functions, in the process of seeking the solution we can take an additional condition which the functions C_1 and C_2 must satisfy.

We take the additional condition

$$\dot{C}_1 \cos kt + \dot{C}_2 \sin kt = 0; \qquad (1.76)$$

then we obtain

$$\ddot{q} = k(-\dot{C}_1 \sin kt + \dot{C}_2 \cos kt) - k^2(C_1 \cos kt + C_2 \sin kt);$$

substituting $\ddot{q}$ and q into (1.74), after transformations we obtain

$$k(-\dot{C}_1 \sin kt + \dot{C}_2 \cos kt) = Q(t).$$

Solving this equation together with (1.76), we find

$$\dot{C}_1 = -\frac{1}{k} Q(t) \sin kt; \quad \dot{C}_2 = \frac{1}{k} Q(t) \cos kt;$$

integrating, we obtain the unknown functions

$$C_1 = C_1^* - \frac{1}{k} \int_0^\tau Q(t) \sin kt \, dt; \quad C_2 = C_2^* + \frac{1}{k} \int_0^\tau Q(t) \cos kt \, dt, \qquad (1.77)$$

where C_1^* and C_2^* — are the initial values of the functions C_1 and

C_2 for $t = 0$;

τ — is the instantaneous upper integration limit.

The resulting Formulas (1.77) are functions of the time τ which include the given initial conditions.

Substituting (1.77) into the general solution (1.75) and replacing in the latter t by the value of τ corresponding to the upper integration limit we obtain

$$q = \left[C_1^* - \frac{1}{k} \int_0^\tau Q(t) \sin kt \, dt \right] \cos k\tau + $$
$$+ \left[C_2^* + \frac{1}{k} \int_0^\tau Q(t) \cos kt \, dt \right] \sin k\tau;$$

The quantities $\sin k_\tau$ and $\cos k_\tau$ can be put under the integral sign, since when integrating with respect to t they are constant factors. Then the solution reduces to the form

$$q = C_1^* \cos k\tau + C_2^* \sin k\tau + \frac{1}{k} \int_0^\tau Q(t) \sin k(\tau - t) \, dt. \qquad (1.78)$$

This solution is the general law of motion of the system under the influence of an arbitrary disturbing force in the form of the superposition of the free vibrations given by the initial conditions on the general displacement caused by the dynamic application of an external disturbance. We obtain the displacement velocity by differentiating (1.78) with respect to τ

$$\dot{q} = k(-C_1^* \sin k\tau + C_2 \cos k\tau) + \frac{1}{k} \frac{d}{d\tau} \int_0^\tau Q(t) \sin k(\tau - t) \, dt;$$

the derivative of the integral equals

$$\frac{d}{d\tau} \int_0^\tau Q(t) \sin k(\tau - t)\, dt = \int_0^\tau \frac{\partial}{\partial \tau} [Q(t) \sin k(\tau - t)]\, dt +$$

$$+ [Q(t) \sin k(\tau - t)]_{t=\tau};$$

upon substitution of the limit $t = \tau$, the expression in the square bracket vanishes.

The velocity formula finally takes the form

$$\dot{q} = k(-C_1^* \sin k\tau + C_2^* \cos k\tau) + \int_0^\tau Q(t) \cos k(\tau - t)\, dt. \qquad (1.79)$$

If at the initial moment of time ($\tau = 0$) $q = q_0$; $\dot{q} = \dot{q}_0$, then $C_1^* = q_0$; $C_2^* = \dfrac{\dot{q}_0}{k}$ and (1.78) takes the form

$$q = q_0 \cos k\tau + \frac{\dot{q}_0}{k} \sin k\tau + \frac{1}{k} \int_0^\tau Q(t) \sin k(\tau - t)\, dt. \qquad (1.80)$$

We shall examine some applications of the formulas obtained.

1.6.2. Case of Periodic Loading

General form of solution. If the disturbing force is a continuous periodic function, the forced vibrations will also be periodic. The vibration periodicity conditions will be

$$q(\tau) = q(\tau + T); \quad \dot{q}(\tau) = \dot{q}(\tau + T), \qquad (1.81)$$

where T — is the disturbing force period.

We find the periodic solution of the differential equation

$$\ddot{q} + k^2 q = Q(t)$$

with the aid of the general solution (1.78) and its derivative (1.79).

We select the constants C_1^* and C_2^* on the basis of the fact that the solution must be periodic. The solution will be carried out for the first period, assuming that for $\tau = 0$ and $\tau = T$ the quantities $q = q_0$ and $\dot{q} = \dot{q}_0$.

We write the periodicity equations

$$q_0 = C_1^* = C_1^* \cos kT + C_2^* \sin kT + \frac{1}{k} \int_0^T Q(t) \sin k(T-t) dt;$$

$$\left. \begin{array}{l} \dot{q}_0 = k C_2^* = k(-C_1^* \sin kT + C_2 \cos kT) + \\ \\ + \int_0^T Q(t) \cos k(T-t) dt; \end{array} \right\} \qquad (1.82)$$

Shifting the unknowns C_1^* and C_2^* to the left, we obtain the system of nonhomogeneous algebraic equations

$$C_1^*(1 - \cos kT) - C_2^* \sin kT = \frac{1}{k} \int_0^T Q(t) \sin k(T-t) dt;$$

$$C_1^* \sin kT + C_2^*(1 - \cos kT) = \frac{1}{k} \int_0^T Q(t) \cos k(T-t) dt;$$

We write the integrals on the right in the form of the following sums

$$\sin kT \int_0^T Q(t) \cos kt \, dt - \cos kT \int_0^T Q(t) \sin kt \, dt;$$

$$\cos kT \int_0^T Q(t) \cos kt \, dt + \sin kT \int_0^T Q(t) \sin kt \, dt.$$

Denoting

$$\int_0^T Q(t) \sin kt \, dt = S; \qquad \int_0^T Q(t) \cos kt \, dt = C, \qquad (1.83)$$

we can write the system of equations in the form

$$\left. \begin{array}{l} C_1^*(1 - \cos kT) - C_2^* \sin kT = \frac{1}{k}(C \sin kT - S \cos kT); \\ \\ C_1^* \sin kT + C_2^*(1 - \cos kT) = \frac{1}{k}(C \cos kT + S \sin kT). \end{array} \right\} \qquad (1.84)$$

Substituting

$$\frac{\sin kT}{1 - \cos kT} = \operatorname{ctg} \frac{kT}{2},$$

we find C_1' and C_2^*:

$$C_1^* = \frac{1}{2k}\left(S + C\,\mathrm{ctg}\,\frac{kT}{2}\right); \quad C_2^* = -\frac{1}{2k}\left(C - S\,\mathrm{ctg}\,\frac{kT}{2}\right). \qquad (1.85)$$

Substituting these coefficients into the general solution (1.78), we obtain the solution for the periodic functions in the form

$$q = \frac{1}{2k}\left[\left(S + C\,\mathrm{ctg}\,\frac{kT}{2}\right)\cos k\tau - \left(C - S\,\mathrm{ctg}\,\frac{kT}{2}\right)\sin k\tau\right] +$$
$$+ \frac{1}{k}\int_0^\tau Q(t)\sin k(\tau - t)\,dt. \qquad (1.86)$$

This is the final form of the periodic solution of the forced vibration equation in definite integral form. It is sufficient to construct the motion law for a single period, i.e., in the time interval τ from zero to T. The subsequent periods will be a repetition of the constructed period. The necessary condition for this is periodicity of the function Q (t). Any point of the given function Q (t) can be selected as the initial time for constructing the solution.

1.7. Determination of Forced Vibration Amplitudes upon Passage through Resonance

As we have shown previously, at resonance the vibration amplitudes gradually increase, reaching large values in the course of time.

Operation of machines and assemblies in the resonant regime is not permitted. Therefore, it is necessary to pass through the resonant frequency by smoothly varying the operating speed to the nominal value which is safe with regard to vibration. Nevertheless, passage through resonance is accompanied by increase of the vibration amplitudes. This increase depends on the rate at which resonance is passed and the power of the exciter. If the forced vibration frequency increases slowly, the vibration amplitudes will reach

large values. High accelerations and considerable power of the driving source are necessary for rapid passage through resonance.

Let us determine the connection between the resonance passage rate and the vibration amplitudes which develop for an ideal system with a single degree of freedom

$$\ddot{q} + k^2 q = Q(t),$$

where Q (t) — is a function of variable periodicity.

To make the problem definite we take the excitation function in the form

$$Q(t) = h \cos\left(\frac{1}{2} \varepsilon t^2 + \omega_0 t\right),$$ 　　　　(1.87)

i.e., the amplitude value of the function remains constant in the course of time, while the frequency increases monotonically with the angular acceleration ε, beginning with the initial value ω_0.

We seek the system displacement at any time τ with the aid of the definite integral (1.78).

Prior to initiation of the frequency increase, the system performs forced vibrations with the frequency ω_0:

$$q = \frac{h}{k^2 - \omega_0^2} \cos \omega_0 t.$$

At the initial time (t = 0) the system position is defined by the displacement and velocity

$$q_0 = \frac{h}{k^2 - \omega_0^2}; \quad \dot{q}_0 = 0.$$

Correspondingly,

$$C_1^* = q_0; \quad C_2^* = 0.$$

Then (1.78) is written as

$$q = q_0 \cos k\tau + \frac{1}{k} \int_0^\tau Q(t) \sin k(\tau - t)\, dt;$$

substituting (1.87) herein, we obtain

$$q = q_0 \cos k\tau + \frac{h}{k} \int_0^\tau \cos\left(\frac{1}{2} \varepsilon t^2 + \omega_0 t\right) \sin k(\tau - t)\, dt. \qquad (1.88)$$

This is the basic formula for determining the system displacement at any time τ.

After making trigonometric transformations and introducing new variables, (1.88) takes the form

$$q = q_0 \cos k\tau + \frac{h}{k \sqrt{2\varepsilon}} \left\{ \cos\beta \int_{\chi_0}^{\chi_\tau} \sin\chi^2 d\chi + \sin\beta \int_{\chi_0}^{\chi_\tau} \cos\chi^2 d\chi - \right.$$
$$\left. - \cos\beta' \int_{z_0}^{z_\tau} \sin z^2\, dz + \sin\beta' \int_{z_0}^{z_\tau} \cos z^2\, dz \right\}, \qquad (1.89)$$

where

$$\chi = \sqrt{\frac{\varepsilon}{2}}\, t - \frac{k - \omega_0}{\sqrt{2\varepsilon}}; \qquad \beta = k\tau - \frac{(k - \omega_0)^2}{2\varepsilon}; \qquad (1.90)$$

$$z = \sqrt{\frac{\varepsilon}{2}}\, t + \frac{k + \omega_0}{\sqrt{2\varepsilon}}; \qquad \beta' = k\tau + \frac{(k + \omega_0)^2}{2\varepsilon}. \qquad (1.91)$$

The integration limits χ_τ, χ_0 and z_τ, z_0 are determined from (1.90) and (1.91) after substituting therein $t = \tau$ and $t = 0$.

For $t = 0$ the quantity χ_0 has a large negative value. For $t = (k - \omega_0)/\varepsilon$ we obtain $\chi = 0$; at this moment the forced vibration frequency ω reaches the natural vibration frequency—the system passes through resonance:

$$\omega = \omega_0 + \varepsilon t = k. \qquad (1.92)$$

For $t > (k - \omega_0)/\varepsilon$ the quantity χ is positive, i.e., when passing through resonance the coordinate χ changes sign from negative to positive. The moment of passage through resonance is the origin of the χ coordinate.

- - Let us examine the integrals

$$\int_{\chi_0}^{\chi^*} \sin \chi^2 d\chi \text{ and} \int_{\chi_0}^{\chi^*} \cos \chi^2 d\chi. \qquad (1.93)$$

The functions $\sin \chi^2$ and $\cos \chi^2$ are symmetric about the coordinate $\chi = 0$. This circumstance is used in calculating the integrals in question

$$\int_{\chi_0}^{0} = \int_{0}^{-\chi_0}; \qquad (1.94)$$

correspondingly

$$\int_{\chi_0}^{\chi^*} = \int_{0}^{-\chi_0} + \int_{0}^{\chi^*}. \qquad (1.94)$$

Since the coordinate χ_0 is negative by definition, the upper limit $(-\chi_0)$ is positive and the integral has a positive value.

Integrals of the form

$$\int_{0}^{\chi} \sin \chi^2 d\chi; \quad \int_{0}^{\chi} \cos \chi^2 d\chi$$

cannot be expressed with the aid of elementary functions

Within narrow limits the calculation of the integrals can be carried out by numerical methods. Over wide limits their calculation is made with the aid of the Fresnel infinite integral

$$\int_{0}^{\infty} \sin \chi^2 d\chi = \int_{0}^{\infty} \cos \chi^2 d\chi = \frac{1}{2} \sqrt{\frac{\pi}{2}}. \qquad (1.95)$$

The upper limit $(-\chi_0)$ of the first integral of the right side of (1.94) is always a large number. Therefore the value of the integral differs very little from the limiting value. Then the calculation of the integrals (1.94) can be made in the form of the sums

$$\int_{\chi_0}^{\chi_\tau} \sin \chi^2 d\chi = \frac{1}{2} \sqrt{\frac{\pi}{2}} + \int_0^{\chi_\tau} \sin \chi^2 d\chi; \qquad (1.96)$$

$$\int_{\chi_0}^{\chi_\tau} \cos \chi^2 d\chi = \frac{1}{2} \sqrt{\frac{\pi}{2}} + \int_0^{\chi_\tau} \cos \chi^2 d\chi. \qquad (1.97)$$

During passage through resonance the vibration amplitudes reach maximal values near resonance. Therefore the upper limit χ_τ of the integrals is small. It suffices to examine values of this limit up to $3 - 4$. The values of the integrals in these limits are shown in Figure 1.15.
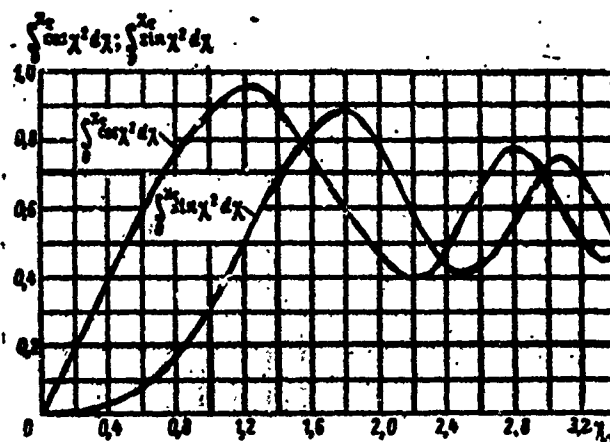
Figure 1.15. Determination of integrals.

The other two integrals of (1.89)

$$\int_{\chi_0}^{\chi_\tau} \sin z^2 dz; \qquad \int_{\chi_0}^{\chi_\tau} \cos z^2 dz$$

always have large integration limits. Therefore, the values of the integrals are close to zero and they can be neglected. Then (1.89) takes the simpler form

$$q = q_0 \cos k\tau + \frac{A}{k\sqrt{2\pi}} \left[\cos \beta \int_{\chi_0}^{\chi_\tau} \sin(\chi^2) d\chi + \sin \beta \int_{\chi_0}^{\chi_\tau} \cos(\chi^2) d\chi \right]. \qquad (1.98)$$

We denote

$$
\left.\begin{array}{l}
\int_{\chi_0}^{\chi_\tau} \sin(\chi^2)\,d\chi = C(\tau)\sin\theta; \\[2mm]
\int_{\chi_0}^{\chi_\tau} \cos(\chi^2)\,d\chi = C(\tau)\cos\theta;
\end{array}\right\}
\qquad (1.99)
$$

then

$$
q = q_0\cos k\tau + \frac{h}{k\sqrt{2\epsilon}}\,C(\tau)\sin(\beta+\theta). \qquad (1.100)
$$

The primary term in this formula, defining the vibrations during passage through resonance, is the second term. The first term yields the free vibrations, associated with the initial conditions, which are superposed on the resonance passage vibrations. Since the free vibrations are small in amplitude, this term is ignored hereafter.

The function $C(\tau)$ changes slowly in comparison with β, which in accordance with (1.90) is proportional to the natural vibration frequency k. Therefore the function $C(\tau)$ is the vibration amplitude coefficient for passage through resonance.

Figure 1.16 shows this function and also the phase angle θ, which are calculated from the formulas

$$
C^2(\tau) = I_s^2 + I_c^2; \qquad (1.101)
$$

$$
\operatorname{tg}\theta = \frac{I_s}{I_c}, \qquad (1.102)
$$

where I_S, I_C — are the integrals calculated using (1.96) and (1.97).

The largest value of $C(\tau)$, equal to 2.01, is obtained for $\chi_\tau = 1.5$. In accordance with (1.90) this value of χ_τ corresponds to the time

$$
\tau = \sqrt{\frac{2}{\epsilon}}\,\chi_\tau + \frac{k-\omega_0}{\epsilon}; \qquad (1.103)
$$

the first term indicates the time interval after passage through resonance. During this time the frequency increases with the given

acceleration ϵ and will be

$$\omega = k + \chi_\tau \sqrt{2\epsilon};$$

hence

$$\frac{\omega}{k} = 1 + \chi_\tau \frac{\sqrt{2\epsilon}}{k}; \qquad (1.104)$$

the larger the acceleration, the further the amplitude peak is
shifted in frequency relative to the resonant frequency.

According to (1.100), during passage through resonance the
vibration amplitude is proportional to C (τ) and is expressed by
the formula

$$A = \frac{h}{k\sqrt{2\epsilon}} C(\tau). \qquad (1.105)$$

The vibration amplitudes A are inversely proportional to $\sqrt{\epsilon}$.
The higher the acceleration, the smaller the amplitudes during
passage through resonance. Figure 1.17 shows the vibration ampli-
tude as a function of acceleration. The curves are shown in
relative units

$$\bar{A} = \frac{A}{A_{st}},$$

where A_{st} — is the deformation
with static applica-

tion of the force H:

$$A_{ct} = \frac{H}{e} = \frac{h}{M};$$

therefore

$$\bar{A} = \frac{h}{\sqrt{2\epsilon}} C(\tau). \qquad (1.106)$$

The curves are plotted on the
basis of the function C (τ),
shown in Figure 1.16.
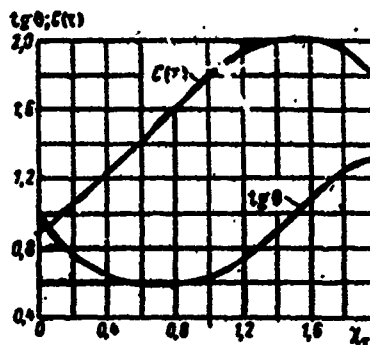
Figure 1.16. Value of
amplitude function for
passage through resonance

In the case of monotonic frequency decrease, the passage through resonance is also accompanied by increase of the amplitudes; they reach maximal values for vibration frequencies below the natural frequency.

In systems without friction the large vibration amplitudes are maintained in the course of all further time after passing through resonance. In this case the vibrations take place with the natural vibration frequency.

In systems with friction the resonant vibration amplitudes decrease in the course of time, and only the forced vibrations are maintained.

The dependence of the vibration amplitude increase on the acceleration indicates that passage through resonance should be accomplished with high acceleration in order to avoid large increase of the amplitudes.

For the experimenter, the fact that this maximal amplitude is shifted in frequency complicates the problem of finding natural vibration frequencies by the resonance method. If the experiment is conducted with

Figure 1.17. Vibration amplitudes as a function of acceleration on passing through resonance

continuous increase of the frequency or by the deceleration technique, then all the resonance peaks will be shifted in frequency by some magnitude relative to the natural vibration frequency. If the acceleration is known, this shift can be estimated using (1.104).

CHAPTER 2

SYSTEMS WITH MANY DEGREES OF FREEDOM

Idealized configurations composed of inertial elements connected
by weightless elastic links are termed systems with many degrees of
freedom. The number k of system degrees of freedom is determined by
the number of independent generalized coordinates q which define
uniquely the position of all the inertial elements of the system at
any moment of time.

The computational scheme is formulated on the basis of analysis
of the real system which is to be vibration analyzed. To this end
some of the system structural elements, for example, disks, drums,
cylinders, shaft or beam segments, and so on, are taken to be ideally
rigid bodies having definite mass and moments of inertia. Frequently,
these parts are replaced by point masses of equal magnitude, concen-
trated at the center of inertia of the corresponding body. In these
cases, the rotatory inertia of the inertial parts of the structure
will not be taken into account in the computational equations and
formulas.

The idealized elastic links between the inertial elements are
selected equal in stiffness to the real links. This means that equal
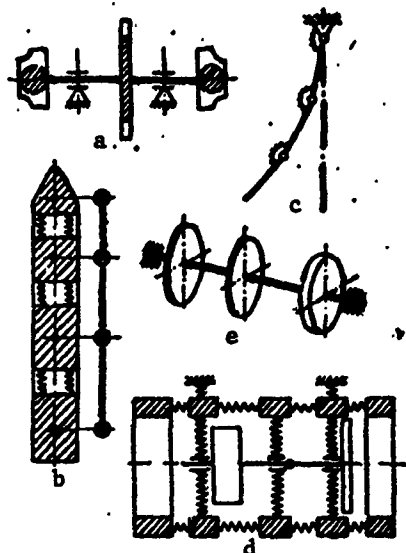
Figure 2.1. Schematics of multi-
mass systems for vibration
calculations.

forces cause equal deformations
in the actual and idealized links.
The mass centers of inertia are
used as points of application of
the forces and for the measure-
ment of the deformations.

As examples, Figure 2.1
shows the individual computational
schemes for several constructions.

For example, the turbopump
assembly rotor (see Figure 2.1a)
can be represented for plane
transverse vibration analysis in
the form of a system consisting
of three point masses located at
the centers of inertia of the
disks, which are connected by
weightless shafts. Such a system
will have three degrees of free-
dom. However, if all the wheels are represented as ideally rigid
disks with masses and moments of inertia equal to the corresponding
quantities for the wheels, then the computational system will have
six degrees of freedom.

The structure of a flight vehicle of the rocket type, with its
considerable length, is idealized for transverse vibration analysis
in the form of a free system consisting of point masses coupled to-
gether by elastic rods (see Figure 3.1b). The location of the point
masses, their magnitude, the bending stiffnesses of the coupling rods
are determined from the design of the vehicle in question. In the
case of longitudinal vibration analysis, the same structure may be
examined in the form of a chain-like system.

Certain designs of multi-panel thermal radiators, radio and
solar energy devices and so on, can be reduced to the multi-hinge
pendulum scheme (see Figure 2.1c).

In the torsional vibration analysis of shafts of piston machines, gas turbine engine rotors, and power generating station rotors, the configuration is examined in the form of a system consisting of several disks connected by shafts of different length and different diameters, working in torsion (see Figure 2.1d).

The gas turbine engine system can be represented by a scheme in which the rotor is replaced by the system shown in Figure 2.1e, in which the housing is represented in the form cf rigid annular masses connected by elastic segments. If in the analysis account is taken for rotation of the annular masses in the vibration plane, then the position of each of the masses must be defined by two generalized coordinates. All the elastic links, including the links between the rotor and the housing and also between the housing and the engine suspension points, are represented in the form of weightless elastic elements whose stiffnesses are equal to those of the corresponding real elements.

In formulating the analytic system, we can take as generalized coordinates either the absolute or the relative displacements of the inertial elements. These displacements appear in the form of rod deflections, section rotation angles, shaft twist angles, tensile or compressive deformations of the elastic elements, pendulum deviation angles, and so on. We emphasize that all the generalized coordinates are time functions.

2.1. Differential Equations of Free Vibrations of Systems With Several Degrees of Freedom and Their Integration

2.1.1. Formulation of the Differential Equations

The general method for formulating the differential equations is based on use of the Lagrange equations. To this end we formulate the expressions for the kinetic and potential energies.

In order to obtain linear differential equations, we consider only small vibrations about the equilibrium position, as a result of

which, as discussed .in courses in theoretical mechanics, the kinetic and potential energies are expressed in quadratic form.

The system kinetic energy is defined by the formula

$$T = \frac{1}{2}(a_{11}\dot{q}_1^2 + a_{22}\dot{q}_2^2 + \ldots + a_{kk}\dot{q}_k^2 + 2a_{12}\dot{q}_1\dot{q}_2 + $$
$$+ 2a_{13}\dot{q}_1\dot{q}_3 + \ldots + 2a_{1s}\dot{q}_1\dot{q}_s),$$

i.e.,

$$T = \frac{1}{2}\sum_{l=s=1}^{k} a_{ls}\dot{q}_l\dot{q}_s,$$ (2.1)

where a_{ls} – are inertial coefficients, containing the mass and moment of inertia J_i.
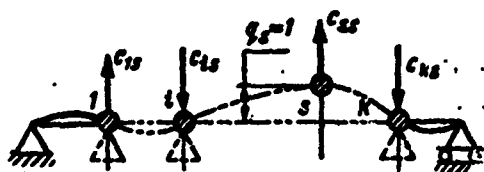
Figure 2.2. Determining static stiffness coefficients.

The system potential energy is expressed in the form

$$\Pi = \frac{1}{2}\sum_{l=s=1}^{k} c_{ls}q_l q_s,$$ (2.2)

where c_{ls} – are quasi-elastic coefficients.

To calculate these coefficients we impose on the system additional rigid constraints in the direction of all the generalized coordinates except that one with subscript s (Figure 2.2).

Then in the direction s we apply the force P_s, whose action leads to the displacement q_s and the reactions R_i of all the additional constraints. The ratio

$$c_{ss} = \frac{P_s}{q_s}$$ (2.3)

is termed the intrinsic quasi-elastic coefficient. The ratio of the support reactions to the displacement

$$c_{is} = \frac{R_i}{q_s} \qquad (2.4)$$

is called the extrinsic quasi-elastic coefficient.

In the calculations the subscript s takes values from one to k. Therefore, the system has k intrinsic coefficients and k(k - 1) extrinsic coefficients. The latter possess the reciprocity property

$$c_{is} = c_{si}.$$

After differentiating (2.1) and (2.2) in accordance with the requirements of the Lagrange equation, we obtain the system of differential equations of small vibrations of the linear system

$$\left. \begin{array}{l} a_{11}\ddot{q}_1 + a_{12}\ddot{q}_2 + \ldots + a_{1k}\ddot{q}_k + c_{11}q_1 + c_{12}q_2 + \ldots + c_{1k}q_k = 0; \\ a_{21}\ddot{q}_1 + a_{22}\ddot{q}_2 + \ldots + a_{2k}\ddot{q}_k + c_{21}q_1 + c_{22}q_2 + \ldots + c_{2k}q_k = 0; \\ \cdot\cdot\cdot\cdot\cdot\cdot\cdot\cdot\cdot\cdot\cdot\cdot\cdot\cdot\cdot\cdot\cdot\cdot\cdot\cdot\cdot\cdot\cdot\cdot\cdot\cdot\cdot\cdot; \\ \cdot\cdot\cdot\cdot\cdot\cdot\cdot\cdot\cdot\cdot\cdot\cdot\cdot\cdot\cdot\cdot\cdot\cdot\cdot\cdot\cdot\cdot\cdot\cdot\cdot\cdot\cdot\cdot \end{array} \right\} \qquad (2.5)$$

In general form, the system of equations is written as

$$\sum_{s=1}^{k} (a_{is}\ddot{q}_s + c_{is}q_s) = 0 \quad (i = 1, \ldots, k). \qquad (2.6)$$

Equations in direct form. The equations can be obtained in simpler form if we take as the generalized coordinates those which yield the expression for the kinetic energy in the form of the sum of squares

$$T = \frac{1}{2} \sum_{i=1}^{k} m_i \dot{q}_i^2. \qquad (2.7)$$

Then the differential equations are obtained in the form

$$m_i \ddot{q}_i + \sum_{s=1}^{k} c_{is}q_s = 0 \quad (i = 1, \ldots, k). \qquad (2.8)$$

The expanded system of equations has the form

$$
\left.
\begin{aligned}
-m_1\ddot{q}_1 &= c_{11}q_1 + c_{12}q_2 + \ldots + c_{1k}q_k; \\
-m_2\ddot{q}_2 &= c_{21}q_1 + c_{22}q_2 + \ldots + c_{2k}q_k; \\
&\cdots \cdots \cdots \cdots \cdots \cdots \cdots \\
&\cdots \cdots \cdots \cdots \cdots \cdots \cdots \\
-m_k\ddot{q}_k &= c_{k1}q_1 + c_{k2}q_2 + \ldots + c_{kk}q_k;
\end{aligned}
\right\}
\qquad (2.9)
$$

this form of the equations and the related further solutions are
usually termed the "direct form of the vibration equations".

If the inertial elements of the system perform angular vibrations
and among the generalized coordinates there are angular coordinates,
then the formula for the kinetic energy takes the form

$$
T = \frac{1}{2}\sum_{i=1}^{n} m_i \dot{q}_i^2 + \frac{1}{2}\sum_{i=n+1}^{k} J_i \dot{q}_i^2;
\qquad (2.10)
$$

Correspondingly, the left sides of (2.9) will contain the moments of
inertia. In view of the uniformity of the formulas, in the following
we shall not identify the terms containing the moments of inertia,
considering the latter as generalized masses.

Equations (2.9) are the equations of equilibrium of the inertia
forces and the elastic forces applied to the masses m_i. Therefore,
in many practical problems the vibration differential equations can
be obtained without use of the Lagrange equations, formulating them
as the equations of equilibrium based on the d'Alembert principle.

For chain-type systems (see Figure 2.1c,d) formulation of the
differential equations in the form (2.9) offers obvious conveniences,
since most of the coefficients c_{is} then vanish.

Equations in inverse form. For beam-type systems the form (2.9)
requires finding all the coefficients c_{is}. This involves tedious
calculations, since it is necessary to solve systems with a large
number of static indeterminacies.

In these cases, the equations in the so-called "inverse form" are more convenient. These equations can be obtained in two ways: either by transforming the system of Equations (2.9), solving it for the variables q_1, or with the aid of the generalized equation of the force method

$$\left.\begin{array}{l} q_1 = a_{11}P_1 + a_{12}P_2 + \ldots + a_{1k}P_k; \\ q_2 = a_{21}P_1 + a_{22}P_2 + \ldots + a_{2k}P_k; \\ \cdots\cdots\cdots\cdots\cdots\cdots\cdots; \\ \cdots\cdots\cdots\cdots\cdots\cdots\cdots; \\ q_k = a_{k1}P_1 + a_{k2}P_2 + \ldots + a_{kk}P_k. \end{array}\right\} \qquad (2.11)$$

where a_{is} — are the static influence or compliance coefficients. They denote the displacement in the direction of the q_1 coordinate under the action of a unit force in the q_s direction.

It is customary to call:

a_{11} — the intrinsic influence coefficient;

a_{is} — the extrinsic influence coefficient.

The influence coefficients have the reciprocity property

$$a_{is} = a_{si}.$$

From the d'Alembert principle we have

$$P_i = -m_i \ddot{q}_i \qquad (2.12)$$

and (2.11) become the vibration differential equations in inverse form

$$\left.\begin{array}{l} q_1 = -a_{11}m_1\ddot{q}_1 - a_{12}m_2\ddot{q}_2 - \ldots - a_{1k}m_k\ddot{q}_k; \\ q_2 = -a_{21}m_1\ddot{q}_1 - a_{22}m_2\ddot{q}_2 - \ldots - a_{2k}m_k\ddot{q}_k; \\ \cdots\cdots\cdots\cdots\cdots\cdots\cdots\cdots; \\ \cdots\cdots\cdots\cdots\cdots\cdots\cdots\cdots; \\ q_k = -a_{k1}m_1\ddot{q}_1 - a_{k2}m_2\ddot{q}_2 - \ldots - a_{kk}m_k\ddot{q}_k. \end{array}\right\} \qquad (2.13)$$

2.1.2. Integration of the Differential Equations of Free Vibrations

All the differential equations forming the Systems (2.5), (2.9), or (2.13) are second-order equations. The solutions of the equations are the harmonic functions

$$q_i = A_i \cos(pt + \varepsilon);$$

(2.14)

in accordance with these solutions all the masses perform harmonic vibrations with the same frequency p but different amplitudes A_1.

The phase angle ε is the same for all coordinates. This means that all the masses reach the extreme position or pass through the zero position simultaneously.

The choice of the phase angle corresponds to the choice of the initial conditions. If we set for t = 0

$$q_i(0) = A_i; \quad \dot{q}_i(0) = 0,$$

we obtain

$$\varepsilon = 0.$$

2.1.2.1. Solution of the Equations in Direct Form

We substitute (2.14) into (2.9) and obtain

$$m_i p^2 A_i = \sum_{s=1}^{k} c_{is} A_s \quad (i = 1, 2, \ldots, k).$$

(2.15)

We write this system in expanded form

$$\left.\begin{array}{l} (c_{11} - m_1 p^2) A_1 + c_{12} A_2 + \ldots + c_{1k} A_k = 0; \\ c_{21} A_1 + (c_{22} - m_2 p^2) A_2 + \ldots + c_{2k} A_k = 0; \\ \cdots\cdots\cdots\cdots\cdots\cdots\cdots\cdots \\ \cdots\cdots\cdots\cdots\cdots\cdots\cdots\cdots \\ c_{k1} A_1 + c_{k2} A_2 + \ldots + (c_{kk} - m_k p^2) A_k = 0. \end{array}\right\}$$

(2.16)

These equations are homogeneous. They contain the k unknown amplitudes A_i. Their nonzero values can be obtained from the equations, provided the system determinant equals zero

$$\Delta = \begin{vmatrix} c_{11}-m_1 p^2 & c_{12} & \dots & c_{1k} \\ c_{21} & c_{22}-m_2 p^2 & \dots & c_{2k} \\ \cdot & \cdot \cdot \cdot \cdot \cdot \cdot & \cdot & \cdot \\ \cdot & \cdot \cdot \cdot \cdot \cdot \cdot & \cdot & \cdot \\ c_{k1} & c_{k2} & \dots & c_{kk}-m_k p^2 \end{vmatrix} = 0. \qquad (2.17)$$

The determinant is a function of p^2. The roots of the determinant — the frequencies for which it vanishes — are termed the system natural vibration frequencies. Therefore, the determinant, equated to zero, is called the frequency equation.

The determinant is symmetric about the principal diagonal and has an order equal to the number of system degrees of freedom. Since p^2 appears in all the diagonal terms, the number p_j^2 of roots of the determinant is also equal to the number of degrees of freedom.

The theorem "On the positiveness and separation of the roots of the secular equation" is proved in general courses on vibration theory. This theorem has the following significance: If the system potential energy is a positive definite function of the generalized coordinates, all the roots of the frequency equation (frequency squared p^2) are positive and are separated by the roots of the minor corresponding to the first element of the determinant.

According to this theorem, all the k natural frequencies are real. They are usually numbered in increasing order by subscripts from 1 to k.

For each root of the frequency equation, the basic Equations (2.16) make it possible to find all the values of the natural oscillation amplitudes A_i. In this case, as a result of homogeneity of the equations one of them can be dropped, and the amplitude of the first mass, for example, can be taken as unity. Then the amplitudes found will be relative.

For each natural frequency the amplitudes form a quite definite ensemble of quantities, termed the vibration mode. Each frequency has its own vibration mode.

Thus, a system with k degrees of freedom has k natural frequencies and corresponding vibration modes. In vibration theory the natural frequencies and vibration modes are termed principal frequencies and modes.

By virtue of the linearity of the differential Equations (2 ..., we obtain their general solution as the sum of the particular solutions (2.14)

$$q_i = \sum_{j=1}^{k} A_{ij} \cos(p_j t + \epsilon_j),$$

(2.18)

where j — is the sequential natural vibration frequency number.

It follows from the general solution that each of the masses executes a complex vibratory motion which is the superposition of principal vibrations of different frequencies. Since the frequencies are not in general multiples, the combined vibrations will not be periodic.

The "natural vibration mode" and "natural vibration frequency" concepts are applicable only to the principal vibrations and have no meaning in application to their combinations. Therefore, the free vibrations in general form have neither a definite mode nor a definite frequency.

This important conclusion on independence and superpositioning of the principal vibrations has great theoretical and practical importance. As a result of this conclusion, the entire theory of linear vibrations is constructed as a theory of principal vibrations and the calculations are made as calculations of the natural modes and frequencies. This avoids the necessity for simultaneous examination of the entire ensemble of vibrations and makes it possible to

study the principal vibrations individually, with subsequent use of
the superposition principle.

In accordance with this principle, any vibrations of a system with
k degrees of freedom can be decomposed into k principal vibrations,
representing them in the form of the sum of the natural modes. To do
this, it is necessary to first know all the natural frequencies and
vibration modes of the system, whose determination is one of the
basic problems of vibration theory and analysis.

2.1.2.2. Solution of Equations in Inverse Form

If the Solutions (2.14) are substituted into the differential
Equations (2.13), we obtain another form of the algebraic equations

$$A_i = \sum_{s=1}^{k} a_{is} m_s p^2 A_s, \quad \text{where} \quad i = 1, 2, \ldots, k. \tag{2.19}$$

This system is written in expanded form as

$$
\begin{aligned}
&(a_{11}m_1 p^2 - 1) A_1 + a_{12} m_2 p^2 A_2 + \ldots + a_{1k} m_k p^2 A_k = 0; \\
&a_{21}m_1 p^2 A_1 + (a_{22} m_2 p^2 - 1) A_2 + \ldots + a_{2k} m_k p^2 A_k = 0; \\
&\quad \ldots \ldots \ldots \ldots \ldots \ldots \ldots \ldots \ldots ; \\
&\quad \ldots \ldots \ldots \ldots \ldots \ldots \ldots \ldots \ldots ; \\
&a_{k1}m_1 p^2 A_1 + a_{k2} m_2 p^2 A_2 + \ldots + (a_{kk} m_k p^2 - 1) A_k = 0.
\end{aligned}
\tag{2.20}
$$

The determinant of this system yields the frequency equation in
inverse form:

$$
\begin{vmatrix}
a_{11}m_1 p^2 - 1 & a_{12}m_2 p^2 & \ldots & a_{1k}m_k p^2 \\
a_{21}m_1 p^2 & a_{22}m_2 p^2 - 1 & \ldots & a_{2k}m_k p^2 \\
\ldots & \ldots & \ldots & \ldots \\
\ldots & \ldots & \ldots & \ldots \\
a_{k1}m_1 p^2 & a_{k2}m_2 p^2 & \ldots & a_{kk}m_k p^2 - 1
\end{vmatrix} = 0;
\tag{2.21}
$$

the determinant is asymmetric about the diagonal terms.

To symmetrize (2.21), which is advisable in many cases, we divide
each column with subscript i by $\sqrt{m_i}$ and multiply the corresponding

row by the same factor; after this, we introduce the notations

$$h_{i\sigma} = a_{i\sigma} \sqrt{m_i m_\sigma} \qquad (2.22)$$

and obtain the symmetrized equation

$$\begin{vmatrix} h_{11} - \dfrac{1}{p^2} & h_{12} & \cdots & h_{1k} \\ h_{21} & h_{22} - \dfrac{1}{p^2} & \cdots & h_{2k} \\ \cdot & \cdot \cdot \cdot \cdot \cdot \cdot \cdot & & \cdot \\ \cdot & \cdot \cdot \cdot \cdot \cdot \cdot \cdot & & \cdot \\ h_{k1} & \cdot \quad h_{k2} & \cdots & h_{kk} - \dfrac{1}{p^2} \end{vmatrix} = 0. \qquad (2.23)$$

The roots of the frequency Equations (2.17), (2.21) and (2.23) of a particular system are obviously identical.

It is advisable to use a digital computer to find the roots of the frequency equations for systems with four or more degrees of freedom. The use of computers eliminates practically all the difficulties in calculating the high-order determinants, associated with the large volume of the computational operations. The entire frequency spectrum can be found for any multimass system encountered in practice.

The calculation is made using the trial and error method. To this end, we can use the frequency equation in the form of the determinant (2.17), (2.21), or (2.23), using one of the standard programs for calculating determinants.

In the computational process the function $\Delta(p^2)$ is plotted. The function is discontinuous; the points of intersection of the curve with the abscissa axis correspond to the roots of the determinant.

We note that the slope of the curve at the points of intersection with the abscissa axis for the higher roots becomes nearly normal, which makes it difficult to identify the abscissa of the zero point.

To facilitate the calculation we can recommend plotting the function $\Delta(p^2)/(p^2)^j$, where j is the sequential number of the root in the region of which the indicated function is constructed.

When using the other technique, the determinant is expanded into a row. As a result, we obtain an algebraic equation of degree k. The coefficients of the equation are calculated in the determinant expansion process and must form an alternating series. Otherwise, among the roots of the equation there will be negative roots, which contradicts the general property of the frequency equation — the positive nature of its roots.

Expansion of the determinant into a row is a tedious process and is performed on a digital computer; however, the subsequent selection of the roots is simplified markedly.

When the roots of the frequency equation have been determined, its polynomial can be written in the form of the product

$$\Delta = M\Pi^k_{j=1}\left(p^2 - p^2_j\right),$$ (2.24)

where M — is the coefficient of the highest term of the polynomial. For the determinant (2.17) it equals the product

$$M = (-1)^k\Pi^k_{i=1}m_i.$$ (2.25)

2.1.3. Change of System Natural Vibration Frequencies With the Imposition of Additional Constraints

Let us examine the case in which a constraint is imposed on one of the sections, where the mass m_1 is located. We use the Equation (2.17) to evaluate the constraint effect.

When the constraint is imposed on the section i, the compliance coefficients α_{1s} for this section become zero. Therefore, the coefficients h_{1s} of the column and row i of the determinant (2.23) vanish, and the corresponding diagonal element becomes $-1/p^2$. The first solution of the frequency equation will be

$$\frac{1}{p^2} = 0;$$

which means that the highest frequency increases without limit.
From the system frequency spectrum there is removed the frequency
lying in the region

$$p_j^2 = \frac{1}{h_{ii}};$$ (2.26)

The remaining frequencies are altered only slightly in one direction
or the other.

Upon imposition of the additional constraint, the minor of the
i^{th} diagonal element becomes the system frequency equation. The
number of roots of the new frequency equation is one less than the
number of roots of the original equation, which corresponds to a
reduction of the number of system degrees of freedom because of
imposition of the constraint.

In accordance with the theorem presented above on the separation
of the roots of the frequency equation, the roots of the minor are
located between the roots of the original determinant. Consequently,
the natural vibration frequencies of the system with the imposed
constraint are located in any case between the frequencies of the
original system.

The numerical value of the roots in the case of restraint of one
or another of the coordinates will be different, but will lie within
the limits of the indicated bounds. In summary, all the frequencies
are shifted in the upward direction, and the highest frequency
approaches infinity.

If still another coordinate is constrained, the new frequency
equation is obtained by still another deletion of the corresponding
row and column of the original determinant. The frequencies of the
new system will be located between the roots of the preceding minor

and their number will be still one smaller. All the frequencies again increase.

If the constraint is imposed at a section which does not coincide with the location of one of the masses, but is located between the masses, then the number of degrees of freedom remains the same. All the frequencies in the spectrum increase. In this case, the frequencies which previously were in the region

$$p_j^2 = \frac{1}{h_{i,i}}; \quad p_i^2 = \frac{1}{h_{i+1,i+1}}, \tag{2.27}$$

where i, i + 1 are the numbers of the masses between which the rigid constraint is introduced, now move up into the high-frequency region.

2.1.4. Change of Natural Vibration Frequencies With Change of System Masses and Stiffnesses

The frequency equations in determinant form show that the system natural vibration frequencies depend only on the magnitudes of the masses and stiffnesses (compliances). Therefore, in order to change the frequencies we must change the construction of the system elements to increase or decrease their masses or stiffnesses.

The choice of the correct direction in which to alter the construction may be made without carrying out special calculations, on the basis of the general dependence of the frequencies on the stiffnesses and masses.

Reduction of one of the system masses m_i reduces the coefficients h_{is} of the corresponding row and column of the Determinant (2.23). This leads to increase of the natural vibration frequencies. If we examine the limiting case and set the mass m_i equal to zero, this will be equivalent to the introduction of an additional support. The roots of the minor of the ith diagonal element of the original determinant become the natural vibration frequencies. Since the roots of the minor lie in the intervals between the roots of the original determinant, in general all the frequencies are shifted in the

increasing direction. In the spectrum there will be no frequencies in the region

$$p^2 = \frac{1}{k_{11}}.$$

If m_i is small but not equal to zero, this frequency shifts beyond the limit of the previous spectrum into the higher frequency region.

Increase of the mass m_i has an effect opposite to that just described. This can be seen from the frequency equation in the direct form (2.17). If we divide all the elements of the ith row by m_i and imagine that m_i increases without limit, the coefficients c_{is}/m_i of the row vanish. With unlimited increase of one of the masses, the lowest frequency approaches zero. The roots of the minor to the ith element of the basic determinant become the natural frequencies. Since these roots lie between the basic roots, we can conclude that with increase of one of the masses all the natural vibration frequencies decrease.

The limit for the first frequency is zero, while the limits for the other frequencies are the roots of the minor of the diagonal element.

Simultaneous change of several masses provides a cumulative effect.

The system element stiffnesses also have a consistent influence on the natural vibration frequencies: increase of the stiffnesses always increases the frequencies, while reduction of the stiffnesses always reduces the frequencies.

Change of the stiffness of an individual element causes simultaneous change of several coefficients in the frequency equation. Therefore, all the frequencies undergo a change. The degree of change of the individual natural frequencies depends on the degree of mutual

influence of the elements in the system. For example, if the determinant consists of only diagonal elements

$$\begin{vmatrix} c_{11}-m_1p^2 & 0 & 0 \\ 0 & c_{22}-m_2p^2 & 0 \\ 0 & 0 & c_{33}-m_3p^2 \end{vmatrix}=0, \qquad (2.28)$$

the system natural frequencies depend only on the intrinsic stiffness coefficients. In such a system the frequencies can be altered separately and independently by increasing or decreasing the corresponding coefficient c_{ii}.

If the determinant contains only certain extrinsic coefficients, for example,

$$\begin{vmatrix} c_{11}-m_1p^2 & c_{12} & 0 \\ c_{21} & c_{22}-m_2p^2 & 0 \\ 0 & 0 & c_{33}-m_3p^2 \end{vmatrix}=0, \qquad (2.29)$$

the frequency equation can be represented in the form of the product

$$(c_{33}-m_3p^2)\cdot\begin{vmatrix} c_{11}-m_1p^2 & c_{12} \\ c_{21} & c_{22}-m_2p^2 \end{vmatrix}=0. \qquad (2.30)$$

This shows that only a single frequency is associated with the coefficient c_{33} and it is independent. The other two frequencies are interconnected by the coefficient c_{12}. They are separated by the frequencies of the diagonal elements

$$p_1^2 < \frac{c_{11}}{m_1} < \frac{c_{22}}{m_2} < p_2^2. \qquad (2.31)$$

In the general case, when the determinant of the frequency equation contains all the extrinsic coefficients, all the natural frequencies are interconnected. The degree of influence of the stiffness of an individual element of the system on each of the frequencies depends on the magnitude of the extrinsic coefficients c_{is}.

In spite of the mutual influence, the diagonal elements are the determining factors for the natural frequencies. If, as a result of

change of the system stiffnesses, only one of the diagonal coefficients c_{11} changes significantly, then the largest change will take place only in the single natural frequency which is closest to the frequency defined by the ratio c_{11}/m_1. This makes possible selective influence on the individual natural frequencies by finding in the system those elements whose stiffness has the strongest influence on certain coefficients and considerably less influence on the others.

2.2. Natural Vibration Modes and Their Properties

2.2.1 Vibration Mode Determination

The vibration amplitudes are found from the algebraic Equations (2.15) or (2.20). We have noted previously that the equations yield nonzero amplitude values when the frequency p in the equation takes a value equal to the natural vibration frequency.

Let us examine the system of Equations (2.15) in application to a three-mass system. We drop the first equation and take the amplitude of the first mass as one. The remaining equations yield the following system

$$(c_{22}-m_2 p^2)A_2 + c_{23}A_3 = -c_{21}; \quad \Big\}$$
$$c_{32}A_2 + (c_{33}-m_3 p^2)A_3 = -c_{31}. \quad \Big\} \qquad (2.32)$$

Hence we find the vibration amplitudes as the ratios

$$A_2 = \frac{\Delta_{12}}{\Delta_{11}}; \quad A_3 = \frac{\Delta_{13}}{\Delta_{11}}, \qquad (2.33)$$

where $\Delta_{11}, \Delta_{12}, \Delta_{13}$ are the respective determinants

$$\begin{vmatrix} c_{22}-m_2 p^2 & c_{23} \\ c_{32} & c_{33}-m_3 p^2 \end{vmatrix}; \quad \begin{vmatrix} -c_{21} & c_{23} \\ -c_{31} & c_{33}-m_3 p^2 \end{vmatrix}; \quad \Bigg\}$$
$$\begin{vmatrix} c_{22}-m_2 p^2 & -c_{21} \\ c_{32} & -c_{31} \end{vmatrix}; \qquad (2.34)$$

it is not difficult to verify that these determinants are the minors of the basic determinant of the system of equations (2.15) to the elements of the first row.

We form the amplitude ratios

$$A_1 : A_2 : A_3 = 1 : \frac{\Delta_{12}}{\Delta_{11}} : \frac{\Delta_{13}}{\Delta_{11}}.$$

Hence we also have

$$A_1 : A_2 : A_3 = \Delta_{11} : \Delta_{12} : \Delta_{13}, \qquad (2.35)$$

i.e., the amplitudes of the system mass free vibrations are proportional to the minors to the elements of the first row of the determinant of the frequency equation.

The result is not changed if in determining the amplitudes we drop some other equation rather than the first. The amplitudes of the free vibrations are proportional to the minors to the elements of any row of the determinant of the frequency equation.

The amplitude ratios are strictly defined for each natural frequency. Plotting to scale the vibration amplitudes of the masses (Figure 2.3), we obtain a definite pattern of the deflections of all the masses from the equilibrium position. The vibration amplitude relationship or the shape of the mass deflections is termed the natural vibration mode.

The number of natural vibration modes is equal to the number of system degrees of freedom.

2.2.2. Vibration Mode Norming
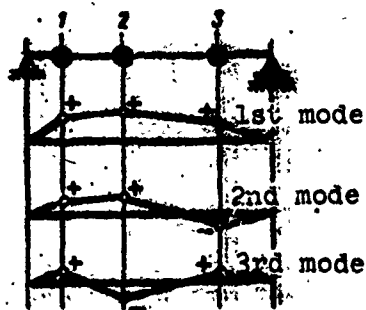
Figure 2.3 Vibration modes of single-span bar. 1,2,3 - mass numbers;

The normed natural vibration mode is that mode for which the sum of the products of the amplitudes squared by the masses equals one

$$\sum_{i=1}^{n} m_i u_{ij}^2 = 1;\qquad (2.36)$$

the first subscript of the normed amplitude is the mass number, the second subscript is the mode number.

The ratios of the normed amplitudes of a given vibration mode remain the same as for the un-normed mode. Therefore, conversion from un-normed to normed amplitudes reduces to multiplication of all the amplitudes by the same number N_j, which is called the norming factor. If the vibration mode is specified by the ratio of the minors, then the normed amplitudes will be

$$u_{1j} = \Delta_{1j} N_j;\ u_{2j} = \Delta_{2j} N_j;\ \ldots;\ u_{nj} = \Delta_{nj} N_j. \qquad (2.37)$$

Substituting these values of the normed amplitudes into (2.36), we obtain the formula for determining the norming factor of the vibration mode j

$$N_j^2 \sum_{i=1}^{n} m_i \Delta_{ij}^2 = 1. \qquad (2.38)$$

Writing the expression for the system kinetic energy for the given vibration mode

$$T = \frac{1}{2} \sum_{i=1}^{n} m_i \dot{q}_{ij}^2 = \frac{1}{2} \sum_{i=1}^{n} m_i u_{ij}^2 p_j^2 \sin^2(p_j t + \varepsilon),$$

it is easy to see that the expression takes a very simple form for the normed vibration modes

$$T_j = \frac{1}{2} p_j^2 \sin^2(p_j t + \varepsilon_j), \qquad (2.39)$$

i.e., the maximal system kinetic energy is numerically equal to half the natural vibration frequency squared.

2.2.3. Vibration Normal Mode Orthogonality Condition

The mass inertia force during vibrations is connected with the elastic forces by the equality (2.8)

$$-m_i\ddot{q}_i = \sum_{s=1}^{b} c_{is}q_s$$

the displacement of the mass m_1 for vibrations in each of the normal modes is defined by the harmonic function

$$q_{ij} = u_{ij}\cos(p_j t + \varepsilon_j). \tag{2.40}$$

We form the product of the inertia force of the mass m_1 in the vibration mode j by the displacement in the vibration mode ν

$$-m_i\ddot{q}_{ij}q_{i\nu} = q_{i\nu}\sum_{s=1}^{b}c_{is}q_{sj}.$$

Substituting herein the harmonic function (2.4) with the corresponding subscript, we obtain

$$m_i u_{ij}p_j^2 u_{i\nu}\cos(p_j t + \varepsilon_j)\cos(p_\nu t + \varepsilon_\nu) =$$
$$= u_{i\nu}\cos(p_\nu t + \varepsilon_\nu)\sum_{s=1}^{b}c_{is}u_{sj}\cos(p_j t + \varepsilon_j);$$

cancelling the common factor, we obtain the equality

$$m_i p_j^2 u_{ij}u_{i\nu} = u_{i\nu}\sum_{s=1}^{b}c_{is}u_{sj};$$

Forming these equalities for all the masses and combining them, we obtain

$$p_j^2\sum_{i=1}^{b}m_i u_{ij}u_{i\nu} = \sum_{i=1}^{b}u_{i\nu}\sum_{s=1}^{b}c_{is}u_{sj}. \tag{2.41}$$

If we form the sum of the products of the inertia forces in mode j by the displacement in mode ν, we obtain the analogous equality with inversion of the subscripts

$$p_v^2 \sum_{i=1}^{k} m_i u_{i\nu} u_{ij} = \sum_{i=1}^{k} u_{ij} \sum_{s=1}^{k} c_{is} u_{s\nu};$$ (2.42)

The stiffness coefficient c_{is} is not connected with the vibration mode; therefore, the right sides of (2.41) and (2.42) are equal. Consequently, the left sides must be equal

$$p_v^2 \sum_{i=1}^{k} m_i u_{i\nu} u_{ij} = p_j^2 \sum_{i=1}^{k} m_i u_{ij} u_{i\nu};$$

since $p_\nu \neq p_j$, this is possible provided

$$\sum_{i=1}^{k} m_i u_{ij} u_{i\nu} = 0.$$ (2.43)

This equality expresses the condition for orthogonality of the normal vibration modes. It is very important in both vibration theory and practical calculations. Several important theorems are proved with the aid of this condition. The orthogonality condition is necessary in calculating the second and following higher natural vibration modes and frequencies.

The orthogonality condition yields directly a very important conclusion: the work of the inertia forces of one vibration mode during displacements in another vibration mode equals zero. This means that the energy of one vibration mode cannot transfer into the energy of another vibration mode. A new vibration mode cannot develop as a result of existing energy and special external input is required for its development.

2.2.4. Theorem on Natural Vibration Mode Nodes

The theorem on normal mode nodes is the second corollary of the orthogonality condition.

A system with k degrees of freedom has k principal frequencies. To each frequency corresponds its own vibration mode. The definitive feature of each vibration mode is the number of mode nodes or the

number of amplitude sign changes. The nodes are the system points which remain stationary during vibration.

The normal mode node theorem, which is proved in specialized courses, defines the general rule: the number of amplitude sign changes (number of mode nodes) of normal mode j equals $j - 1$, i.e., one less than the mode number.

For simple systems, for example for single-span beams (see Figure 2.3), this means that during vibrations in the first mode the displacement of all the masses takes place on the same side of the equilibrium position — the vibration mode has no nodes.

By the orthogonality condition, the second vibration mode must have part of the amplitudes positive and part negative. Otherwise the sum of the products of the amplitudes of the first and second modes will not be equal to zero. This means that the second mode must have a single node, or a single amplitude sign change. The third vibration mode has two nodes, i.e., two amplitude sign changes, and so on.

In applying the nodal theorem to multi-support systems, particularly for multi-span beams, we must remember that a stationary point lying within the limits of a span is to be considered a vibration mode node. The stationary points at the supports are not considered vibration mode nodes.

The location of the vibration mode nodes is obvious if the elastic line of the beam is plotted. Usually this construction involves additional calculations and is not carried out. Then the analysis of the vibration modes is based on the signs of the vibration amplitudes.

We shall examine this question using the example of a three-support beam with cantilever (Figure 2.4).
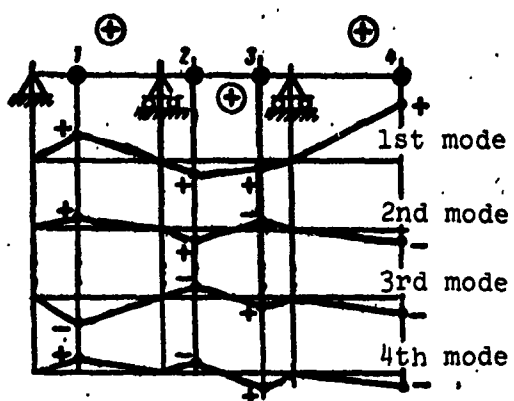
Figure 2.4. Vibration modes of multi-span bar. 1,2,3 - mass numbers.

The first vibration mode, constructed for the lowest frequency, has the following characteristics. The signs of the amplitudes within the limits of a span are the same and opposite to the signs of the amplitudes of the adjacent spans. If this rule is not satisfied, the elastic line for the first mode will have nodal points, which contradicts the nodal theorem.

We take the directions of the displacement of the masses in the first mode as the positive directions. Then for the second mode the left part of the beam will have positive amplitudes, while the right part will have negative amplitudes. The vibration mode has a single amplitude sign change and a single nodal point in the right-hand span.

The third and fourth modes have respectively two and three amplitude sign changes, although the locations of the nodal points for these modes are not identified.

In more complex cases, in order to determine the vibration mode number, it is necessary to resort to construction of the elastic line and determination of the number of vibration mode nodes.

The nodal theorem is used to check the calculation of the vibration natural frequencies and modes. In those cases in which, from the entire natural frequency spectrum only a single frequency is determined, it serves for determining the number of the vibration mode found.

2.2.5. Expansion of Arbitrary Modes in Normal Vibration Modes

Any ensemble of numerical quantities λ_i, consisting of k elements,

can be expanded in the normal vibration modes of some given system
having k degrees of freedom, representing them in the form of the
following linear relations

$$\begin{aligned}
\lambda_1 &= x_1 u_{11} + x_2 u_{12} + \dots + x_k u_{1k}; \\
\lambda_2 &= x_1 u_{21} + x_2 u_{22} + \dots + x_k u_{2k}; \\
&\dots \dots \dots \dots \dots \dots \dots; \\
\lambda_k &= x_1 u_{k1} + x_2 u_{k2} + \dots + x_k u_{kk},
\end{aligned}$$
(2.44)

or in general form

$$\lambda_i = \sum_{j=1}^{k} x_j u_{ij} \quad (i = 1, 2, \dots, k),$$

where λ_i is the given ensemble of k quantities;

  u_{ij} are the normed amplitudes of the system free vibrations; i
  is the mass number; j is the mode number;

  κ_j are the coefficients of the modal expansion from one to k.

The feasibility of this expansion follows directly from the
system of linear Equations (2.44), in which the expansion coefficients
κ_j are the unknowns. The basic system determinant is not equal to
zero; therefore the coefficients κ_j are always real and can be found
from the given equations.

The process of expansion in normal forms should be considered as
a purely formal procedure. It should not be associated with the
vibration superposition principle.

However, the technique of expansion of different modes in terms
of the normal vibration modes is convenient and finds application in
theoretical transformations and in developing practical methods for
the solution of problems — for example, in the study of questions of
forced vibrations of multi-mass systems, in developing successive
approximation methods, and in calculating the normal vibration modes
and frequencies.

The determination of the expansion coefficients by solving the
system of Equations (2.44) for the unknowns κ_i in the case of a large

number of terms of the expansion is unsuitable because of the complexity of this method. Application of the normal vibration mode orthogonality properties simplifies considerably the determination of the expansion coefficients.

In order to use the orthogonality condition (2.43), we multiply each equation by the mass m_i and by the amplitude of that vibration mode ν whose expansion coefficient is to be found

$$
\left.\begin{aligned}
m_1\lambda_1 u_{1\nu} &= x_1 m_1 u_{11} u_{1\nu} + \ldots + x_\nu m_1 u_{1\nu}^2 + \ldots + x_k m_1 u_{1k} u_{1\nu}; \\
m_2\lambda_2 u_{2\nu} &= x_1 m_2 u_{21} u_{2\nu} + \ldots + x_\nu m_2 u_{2\nu}^2 + \ldots + x_k m_2 u_{2k} u_{2\nu}; \\
&\ \ \ \ldots\ldots\ldots\ldots\ldots\ldots\ldots\ldots\ldots\ldots; \\
m_k\lambda_k u_{k\nu} &= x_1 m_k u_{k1} u_{k\nu} + \ldots + x_\nu m_k u_{k\nu}^2 + \ldots + x_k m_k u_{kk} u_{k\nu}.
\end{aligned}\right\}
\qquad (2.45)
$$

We combine all the equations

$$
\sum_{i=1}^{k} m_i\lambda_i u_{i\nu} = x_1 \sum_{i=1}^{k} m_i u_{i1} u_{i\nu} + \ldots + x_\nu \sum_{i=1}^{k} m_i u_{i\nu}^2 + \ldots + x_k \sum_{i=1}^{k} m_i u_{ik} u_{i\nu}. \qquad (2.46)
$$

By virtue of the orthogonality condition, all the terms in the right side of the equation, except the term containing κ_ν, vanish. The sum affiliated with κ_ν equals one by the normalization condition. Therefore, the expansion coefficient will be

$$
x_\nu = \sum_{i=1}^{k} m_i\lambda_i u_{i\nu}. \qquad (2.47)
$$

2.3 Methods for Calculating Natural Vibration Frequencies and Modes of Systems with Many Degrees of Freedom

2.3.1. Rayleigh Method

The natural vibration frequency can be determined on the basis of the energy conservation law. The sum of the kinetic and potential energies of each vibration mode is a constant. On this basis we write the equality

$$
T_{j\,max} = \Pi_{j\,max}, \qquad (2.48)
$$

where $T_{j\ max}$ is the maximal system kinetic energy at the moment of
passage through the equilibrium position;

$\Pi_{j\ max}$ is the maximal system potential energy at the moment
of greatest deflection.

Representing the vibrations with the aid of the normed amplitudes

$$q_{ij}=u_{ij}\cos(p_j t+z_j);\quad \dot{q}_{ij}=-p_j u_{ij}\sin(p_j t+z_j)$$

and substituting the values of the maximal deflections and velocities
into the potential energy (2.2) and kinetic energy (2.7) formulas,
we obtain

$$\Pi_{j\ max}=\frac{1}{2}\sum_{i,s=1}^{n}c_{is}u_{ij}u_{sj};\quad T_{j\ max}=\frac{1}{2}p_j^2\sum_{i=1}^{n}m_i u_{ij}^2. \tag{2.49}$$

Equating the energies and solving the equations for p_j^2, we obtain

$$p_j^2=\frac{\sum_{i,s=1}^{n}c_{is}u_{ij}u_{sj}}{\sum_{i=1}^{n}m_i u_{ij}^2}. \tag{2.50}$$

Formula (2.50) relates the natural vibration frequency and amplitudes.
It is valid for all vibration modes, but only with strict correspon-
dence of the vibration frequency and mode.

In practical calculations the vibration frequency and mode are
the unknowns; therefore (2.50) cannot be used for precise determination
of the natural frequencies.

Let us evaluate the calculation results if in (2.50), in place of
the exact values, we substitute the approximate values of the vibration
amplitudes Y_i, representing approximately some natural vibration
mode

$$R=\frac{\sum_{i,s=1}^{n}c_{is}Y_i Y_s}{\sum_{i=1}^{n}m_i Y_i^2}; \tag{2.51}$$

this formula is called the Rayleigh function.

We expand the approximate vibration mode, represented by the given amplitudes Y_i, in terms of the normal modes. In so doing each amplitude is represented in the form of the sum

$$Y_i = \sum_{j=1}^{k} \varkappa_j u_{ij}, \qquad (2.52)$$

where $\varkappa_j$ is the expansion coefficient of the given mode (determined as shown previously).

The denominator of (2.51) is transformed in accordance with (2.52) as follows

$$\sum_{i=1}^{k} m_i Y_i^2 = \sum_{i=1}^{k} m_i \left(\varkappa_1^2 u_{i1}^2 + \varkappa_2^2 u_{i2}^2 + \dots + \varkappa_k^2 u_{ik}^2 + 2\varkappa_1\varkappa_2 u_{i1} u_{i2} + \right.$$
$$\left. + 2\varkappa_1\varkappa_3 u_{i1} u_{i3} + \dots + 2\varkappa_j \varkappa_\nu u_{ij} u_{i\nu} + \dots \right).$$

We combine terms with common factors $\varkappa_j^2$ or $\varkappa_j \varkappa_\nu$. In so doing we take account of the norming and orthogonality conditions

$$\sum_{i=1}^{k} m_i u_{ij}^2 = 1; \quad \sum_{i=1}^{k} m_i u_{ij} u_{i\nu} = 0;$$

as a result we obtain

$$\sum_{i=1}^{k} m_i Y_i^2 = \varkappa_1^2 + \varkappa_2^2 + \dots + \varkappa_k^2 = \sum_{j=1}^{k} \varkappa_j^2. \qquad (2.53)$$

By means of the substitution (2.52) the numerator of (2.51) is reduced to the form

$$\sum_{i,s=1}^{k} c_{is} Y_i Y_s = \sum_{i=1}^{k} (\varkappa_1 u_{i1} + \varkappa_2 u_{i2} + \dots + \varkappa_k u_{ik}) \sum_{s=1}^{k} c_{is} (\varkappa_1 u_{s1} +$$
$$+ \varkappa_2 u_{s2} + \dots + \varkappa_k u_{sk}). \qquad (2.54)$$

Let us examine the individual sums on the right. In accordance with (2.15) we have

$$\sum_{s=1}^{k} c_{is} \varkappa_1 u_{s1} = \varkappa_1 m_i p_1^2 u_{i1};$$

similarly, for any of the sums

$$\sum_{s=1}^{k} c_{i_s} x_s u_{s_j} = x_j p_j^2 m_j u_{ij},$$

and (2.54) takes the form

$$\sum_{i,s=1}^{k} c_{is} Y_i Y_s = \sum_{i=1}^{k} (x_1 u_{i1} + x_2 u_{i2} + \dots + x_k u_{ik}) \times$$
$$\times (x_1 p_1^2 m_i u_{i1} + x_2 p_2^2 m_i u_{i2} + \dots + x_k p_k^2 m_i u_{ik}). \qquad (2.55)$$

The sum of the products on the right contains the following terms

$$\sum_{i=1}^{k} x_\nu u_{i\nu} \cdot x_j p_j^2 m_i u_{ij},$$

or

$$x_\nu x_j p_j^2 \sum_{i=1}^{k} m_i u_{i\nu} u_{ij};$$

those terms for which $\nu \neq j$ equal zero by the orthogonality condition.
The remaining terms of the right side of (2.55), for which $\nu = j$,
with account for the norming condition yield

$$\sum_{i=s=1}^{k} c_{is} Y_i Y_s = \sum_{j=1}^{k} x_j^2 p_j^2 \qquad (2.56)$$

substituting (2.56) into (2.51), we obtain the Rayleigh function
(2.51) in the form of the expansion

$$R = \frac{x_1^2 p_1^2 + x_2^2 p_2^2 + \dots + x_k^2 p_k^2}{x_1^2 + x_2^2 + \dots + x_k^2}. \qquad (2.57)$$

Formula (2.57) shows that, if the given initial mode Y_1 coincides
exactly with one of the principal modes, then all the expansion coef-
ficients except the one belonging to the given mode equal zero. Then
the Rayleigh function is exactly equal to the frequency of the
principal vibrations of the given mode. If the initial mode is not
exact, but is close to one of the principal modes, then the Rayleigh
function is close to the frequency of this mode squared.

Extremal Properties of the Rayleigh function. The minimal value of the Rayleigh functions equals the square of the first frequency

$$R_{min} = p_1^2 .$$ (2.58)

The Rayleigh function approaches this value when the initial mode approaches the first vibration mode. If the initial mode is not exact, then R is larger than p_1^2.

This property shows that in determining the first free vibration using (2.51) we should specify the amplitudes Y_1 as close as possible to the normal vibration mode. Of all the versions the most correct will be that which yields the smallest value of the vibration frequency. Naturally, all the selected vibration modes must correspond to the restraint conditions and, in particular, the displacements at the supports must be zero.

The extremality property does not hold if we use the Rayleigh formula to calculate the frequency of the second vibration mode. Small deviations from the exact form of the second mode can yield a Rayleigh function larger or smaller than the second frequency squared. This drawback can be eliminated if we take a mode orthogonal to the first mode as the approximate mode. Then $\kappa_1 = 0$ and the formula takes the form

$$R = \frac{\varkappa_2 p_2^2 + \varkappa_3 p_3^2 + \dots + \varkappa_k p_k^2}{\varkappa_2^2 + \varkappa_3^2 + \dots + \varkappa_k^2};$$

the Rayleigh function takes on the extremality property with respect to the second vibration mode.

The calculation of the first vibration frequency using (2.51) involves calculation of the quadratic form in the numerator. This is difficult, since it requires preliminary calculation of all the stiffness coefficients c_{is} and then all the combinations of products of three cofactors. Since the numerator is twice the potential

energy, it is more convenient to make its calculation in the form of the displacement work of some system of forces. Then (2.51) takes the form

$$R = \frac{\sum_{i=1}^{n} P_i Y_i}{\sum_{i=1}^{n} m_i Y_i^2}.$$ (2.59)

Rayleigh proposed taking as the initial mode the static displacements of the system masses under the action of the weight forces. Thus, following Rayleigh the weight forces are taken as the system of forces P_i. We determine the displacements Y_i resulting from the action of these forces and calculate the sums appearing in the numerator and denominator of (2.59). In this case the function R will be equal (with a slight excess) to the first vibration mode frequency squared. Usually the results of the calculation using the Rayleigh method differ from the exact values of the frequencies, obtained by exact methods, by 0.5 - 1%

In formulating the initial mode the static deflections can be determined by any of the techniques presented in courses on elasticity theory and resistance of materials, including the graphical methods. In so doing the weight forces must be directed toward positive displacements in the first vibration mode, i.e., the force system must not have a change of sign.

The accuracy of the Rayleigh calculation can be improved if we take the inertia forces as the initial force system

$$P_i = m_i p^2 Y_i;$$ (2.60)

the results of the preceding calculation are used to evaluate the inertia forces. New deflections are found from the inertia forces, and (2.59) is used to determine the vibration frequency. The new force system is more exact in comparison with the weight force system; therefore the results of the calculation of the vibration frequency and mode will be more exact.

If necessary, the refinements can be repeated several times until the newly obtained frequency repeats the previous value within the specified precision limits.

2.3.2. Method of Successive Approximations of the Vibration Modes (Iteration Method)

2.3.2.1. Iteration Method Formulas and Convergence

We take the system (2.19) of algebraic equations in expanded form

$$
\left.
\begin{aligned}
A_1 &= a_{11}m_1p^2A_1 + a_{12}m_2p^2A_2 + \ldots + a_{1k}m_kp^2A_k; \\
A_2 &= a_{21}m_1p^2A_1 + a_{22}m_2p^2A_2 + \ldots + a_{2k}m_kp^2A_k; \\
&\;\cdot; \\
&\;\cdot; \\
A_k &= a_{k1}m_1p^2A_1 + a_{k2}m_2p^2A_2 + \ldots + a_{kk}m_kp^2A_k.
\end{aligned}
\right\}
\qquad (2.61)
$$

As shown previously, this system of equations defines the k linearly independent orthogonal normal vibration modes and their frequencies. For each mode the relationship between the amplitudes A_i is strictly defined. In the normed case the amplitudes A_i are denoted by u_{ij}.

Let us take the Equations (2.61) to construct this computational sequence. We substitute into the right side in place of the unknown amplitudes A_i some sequence of initial numbers $Y_i^{(0)}$. Then in the left side we obtain the new system of numbers $Y_i^{(1)}$. In general form this is written as

$$
Y_i^{(1)} = p^2 \sum_{s=1}^{k} a_{is}m_sY_s^{(0)}, \quad i = 1, 2, \ldots, k; \qquad (2.62)
$$

after calculating the sums we obtain

$$
Y_i^{(1)} = p^2 \lambda_i^{(1)},
$$

where p^2 is some arbitrary frequency, written in general form, and

$$\lambda_j^{(1)} = \sum_{s=1}^{k} a_{is} m_s Y_s^{(0)}.$$

We repeat the calculation, substituting the resulting numbers $Y_i^{(1)}$ into the original system (2.62) in place of $Y_s^{(0)}$:

$$Y_j^{(2)} = p^2 \sum_{s=1}^{k} a_{is} m_s Y_s^{(1)} = (p^2)^2 \sum_{s=1}^{k} a_{is} m_s \lambda_s^{(1)},$$

or

$$Y_j^{(2)} = (p^2)^2 \lambda_j^{(2)},$$

where

$$\lambda_j^{(2)} = \sum_{s=1}^{k} a_{is} m_s \lambda_s^{(1)};$$

the superscript indicates the sequential number of the summation (iteration).

Repeating the computational process several times, we obtain

$$Y_j^{(n)} = (p^2)^n \sum_{s=1}^{k} a_{is} m_s \lambda_s^{(n-1)} = (p^2)^n \lambda_j^{(n)};$$

we take the ratio of two succeeding iterations

$$\frac{Y_j^{(n-1)}}{Y_j^{(n)}} = \frac{1}{p^2} \frac{\lambda_j^{(n-1)}}{\lambda_j^{(n)}}. \tag{2.63}$$

In order to establish the limit which the ratio of the iterations approaches for quite large n, we again carry out the iteration computation process, after first expanding the initial mode $Y_i^{(0)}$ in terms of the normal modes

$$Y_j^{(0)} = z_1 a_{i1} + z_2 a_{i2} + \ldots + z_j a_{ij} + \ldots + z_k a_{ik}. \tag{2.64}$$

We substitute this expansion into (2.62)

$$Y_j^{(1)} = p^2 \sum_{s=1}^{n} a_{js} m_s (x_1 u_{s1} + x_2 u_{s2} + \ldots + x_j u_{sj} + \ldots + x_k u_{sk});$$

we recall that the second subscript of the normed amplitude denotes the mode number. The overall sum breaks down into a series of sums with respect to the vibration modes

$$Y_j^{(1)} = p^2 \left(x_1 \sum_{s=1}^{n} a_{js} m_s u_{s1} + x_2 \sum_{s=1}^{n} a_{js} m_s u_{s2} + \ldots + \right.$$
$$\left. + x_j \sum_{s=1}^{n} a_{js} m_s u_{sj} + \ldots + x_k \sum_{s=1}^{n} a_{js} m_s u_{sk} \right). \qquad (2.65)$$

It is not difficult to see that in accordance with the general Equations (2.19) the following equality holds for each of the sums

$$\sum_{s=1}^{n} a_{js} m_s u_{sj} = \frac{1}{p_j^2} u_{ij};$$

Replacing in (2.65) the sums in accordance with this equality, we obtain

$$Y_j^{(1)} = p^2 \left(x_1 \frac{1}{p_1^2} u_{j1} + x_2 \frac{1}{p_2^2} u_{j2} + \ldots + x_j \frac{1}{p_j^2} u_{jj} + \ldots + x_k \frac{1}{p_k^2} u_{jk} \right) \qquad (2.66)$$

Comparing this formula with (2.64), we note that the expansion obtained for the first iteration in terms of the normal modes differs from the expansion of the initial mode by the common factor p^2 and by the denominator p_j^2 in each term of the expansion.

By virtue of the general nature of the transformations made, we can state that each subsequent iteration will differ from the preceding iteration by these additions. Therefore, the result of the nth iteration can immediately be written in the form

$$Y_j^{(n)} = \left(\frac{p^2}{p_1^2} \right)^n \left[x_1 u_{j1} + x_2 \left(\frac{p_1^2}{p_2^2} \right)^n u_{j2} + \ldots + x_j \left(\frac{p_1^2}{p_j^2} \right)^n u_{jk} + \right.$$
$$\left. + \ldots + x_k \left(\frac{p_1^2}{p_k^2} \right)^n u_{jk} \right]. \qquad (2.67)$$

We take the ratio of two successive approximations

$$\frac{y_i^{(n-1)}}{y_i^{(n)}} = \frac{p_1^2}{p_i^2} \cdot \frac{z_1 a_{i1} + z_2\left(\frac{p_1^2}{p_2^2}\right)^{n-1} a_{i2} + z_3\left(\frac{p_1^2}{p_3^2}\right)^{n-1} a_{i3} + \dots}{z_1 a_{i1} + z_2\left(\frac{p_1^2}{p_2^2}\right)^{n} a_{i2} + z_3\left(\frac{p_1^2}{p_3^2}\right)^{n} a_{i3} + \dots} \quad (2.68)$$

Equating (2.63) and (2.68), we obtain

$$\frac{\lambda^{(n-1)}}{\lambda^{(n)}} = p_1^2 \frac{z_1 a_{i1} + z_2\left(\frac{p_1^2}{p_2^2}\right)^{n-1} a_{i2} + z_3\left(\frac{p_1^2}{p_3^2}\right)^{n-1} a_{i3} + \dots}{z_1 a_{i1} + z_2\left(\frac{p_1^2}{p_2^2}\right)^{n} a_{i2} + z_3\left(\frac{p_1^2}{p_3^2}\right)^{n} a_{i3} + \dots}; \quad (2.69)$$

For sufficiently large n, the ratios of the squares of the principal frequencies to the powers n and (n - 1) become very small. The fraction in the right side of (2.69) approaches one. On the basis of (2.69) we obtain the formula

$$\lim_{n \to \infty} \frac{\lambda^{(n-1)}}{\lambda^{(n)}} = p_1^2 \quad (2.70)$$

where

$$\left.\begin{aligned}
\lambda^{(1)} &= \sum_{s=1}^{k} a_{is} m_s y_s^{(0)}; \\
\lambda^{(n)} &= \sum_{s=1}^{k} a_{is} m_s \lambda_s^{(n-1)};
\end{aligned}\right\} \quad (2.71)$$

These formulas form the basis of the successive approximation method. They show that the ratio of two successive approximations for a sufficiently large number of iterations yields the frequency squared of the first vibration normal mode with some excess, which depends on the number of iterations.

2.3.2.2. Calculation of the First Vibration Mode

The selection of the initial mode $Y_s^{(0)}$ can be made arbitrarily. The iteration convergence process is very stable. Formula (2.69) shows that the components of the higher modes disappear rapidly with

increase of n. If we have no idea of the unknown vibration mode, we can set all the initial amplitudes equal to unity

$$Y_s^{(0)} = 1.$$

The inaccuracy of the initial mode affects only the number of iterations required.

The number of iterations required depends on the required computational accuracy. The latter is evaluated by comparing neighboring frequencies squared

$$P_{1(n)}^2 = \frac{\lambda_j^{(n-1)}}{\lambda_j^{(n)}} \quad \text{and} \quad P_{1(n+1)}^2 = \frac{\lambda_j^{(n)}}{\lambda_j^{(n+1)}};$$

taking the ratio, we obtain

$$\frac{P_{1(n+1)}^2}{P_{1(n)}^2} = \frac{[\lambda_j^{(n)}]^2}{\lambda_j^{(n-1)}\lambda_j^{(n+1)}}; \tag{2.72}$$

with increase of the number of iterations this ratio approaches unity. After three or four iterations the ratio (2.72) is larger than 0.95 - 0.96. This means that the natural vibration frequency is determined to within 2 - 3%. The calculation must be continued to obtain higher precision.

Formula (2.70) shows that the limit of the iteration ratio for any mass is the same and is equal to the square of the lowest frequency. In practice this is not so. Because of the limited number of iterations, their ratios for different system masses differ somewhat from one another. The smallest ratio is the most correct, being closest to the limit, i.e., closest to the sought natural vibration frequency. In the computational process this smallest ratio is found without any difficulty, since all the iterations are calculated for all the masses. The definitive mass, for which this ratio is minimal, is that which has the largest vibration amplitude in the first mode.

What we have said is equally valid for Formula (2.72). The
mass having the smallest ratio (2.70) will have the ratio (2.72)
closest to unity.

The vibration mode is determined by each iteration as the ensemble
of quantities $x_i^{(n)}$. The larger the number of iterations, the closer
the calculated mode corresponds to the exact value of the normal
mode. Coincidence of the calculated modes in the process of carrying
out the iterations can also serve as a criterion of the computational
accuracy. Comparison of the vibration amplitudes again leads to the
Formula (2.70).

Application of the Rayleigh formula. The frequency calculation
can be simplified considerably and even reduced to a single iteration
if the Rayleigh Formula (2.59) is used.

In this case we take as the force system the products

$$P_i = m_i Y_i.$$

and we take as the amplitudes Y_i the first iteration $x_i^{(n)}$ from $Y_i^{(n)}$,
since it is the deflection from the given initial force system.

Substituting these notations into the Rayleigh formula (2.59),
we obtain

$$\lambda = \frac{\sum_i m_i Y_i^{(n)} Y_i^{(n)}}{\sum_i m_i x_i^{(n)} Y_i^{(n)}}.$$
(2.73)

In order to obtain sufficient computational accuracy we should try
to specify the initial amplitudes $Y_i^{(n)}$ as close as possible to the
assumed vibration mode.

If it is necessary to obtain an estimate of the accuracy of
the frequency found and improve this accuracy, we can use the
Rayleigh formula for the first and second iterations, writing it in
the form

$$p_1^2 \approx \frac{\sum_{i=1}^{k} m_i \lambda_i^{(1)} \lambda_i^{(2)}}{\sum_{i=1}^{k} m_i \left[\lambda_i^{(2)}\right]^2},$$ (2.74)

The result obtained using this formula yields a more exact upper limit of the sought frequency. Its comparison with the result obtained using the preceding formula shows the refinement which can be achieved as a result of making the second iteration.

2.3.2.3. Calculation of the Second Vibration Mode

Method of exclusion of the first mode. Formula (2.69) shows that, if the initial mode (2.64) does not contain components of the first vibration mode ($\kappa_1 = 0$), then the ratio of two successive iterations will be

$$\frac{\lambda^{(n-1)}}{\lambda^{(n)}} = p_2^2 \frac{\kappa_2 \varkappa_{i2} + \kappa_3 \left(\frac{p_2^2}{p_3^2}\right)^{n-1} \varkappa_{i3} + \cdots}{\kappa_2 \varkappa_{i2} + \kappa_3 \left(\frac{p_2^2}{p_3^2}\right)^{n} \varkappa_{i3} + \cdots}.$$ (2.75)

and (2.70) takes the form

$$\lim_{n \to \infty} \frac{\lambda^{(n-1)}}{\lambda^{(n)}} = p_2^2,$$ (2.76)

i.e., in the absence in the initial mode of components of the first mode, the iteration ratio yields the square of the second frequency.

The calculation of the second frequency can be made by this technique if the first vibration mode is known. Then for the calculation we specify the assumed mode very approximately, and exclude it from the first mode with the aid of the orthogonality condition.

Exclusion of the first mode is accomplished with the aid of the expansion coefficient using the formula

$$Y_{i2}^{(0)} = Y_i^{(0)} - \kappa_1 a_{i1}.$$ (2.77)

where $Y_i^{(0)}$ is the assumed mode;

   $Y_i^{(0)}$ is the orthogonalized assumed mode, with the first mode eliminated;

   u_{i1} are the amplitudes of the first vibration mode, determined by the previous calculation;

   $\varkappa_1$ is the first mode expansion coefficient.

We have noted previously that this expansion coefficient equals

$$\varkappa_1 = \sum_{i=1}^{k} m_i Y_i^{(0)} u_{i1}. \qquad (2.78)$$

The orthogonalized mode is then used to calculate the first approximation $\lambda_i^{(1)}$ using (2.71).

The resulting first approximation cannot be immediately used to calculate the second approximation. It contains as a result of iteration the magnified error present in the approximate solution of the first mode.

If we use the first approximation directly for the calculation of the succeeding approximations, then with increase of the number of iterations the error will increase, obscuring the second vibration mode and directing the calculation toward exhibiting the first mode, i.e., the posed problem is not solved.

For the further calculation we must re-orthogonalize the first approximation. To do this we again determine the expansion coefficient

$$\varkappa_1 = \sum_{i=1}^{k} m_i \lambda_i^{(1)} u_{i1}$$

and exclude the first mode from $\lambda_i^{(1)}$:

$$\lambda_{i2}^{(1)} = \lambda_i^{(1)} - \varkappa_1 u_{i3};$$

after which we use (2.71) in the usual way to find the second approximation.

Mode orthogonalization is necessary prior to each iteration and also for the final approximation, after which the vibration frequency in the second mode is found as the ratio

$$p_2^2 \approx \frac{\lambda_{j2}^{(z-1)}}{\lambda_{j2}^{(z)}}.$$ (2.79)

...e . ...lation of the higher vibration modes is made similarly, but t⁴ ... d modes must be orthogonalized with respect to all the prece ' ... .s.

Method of reduction. A rational technique for calculating the second normal vibration mode is the method of reduction of the order of the system of basic algebraic equations (see [41]). To use this method, just as before, we must have the previously calculated first vibration mode.

We take the system of algebraic equations in inverse form (2.19)

$$A_1 = a_{11}m_1p^2A_1 + a_{12}m_2p^2A_2 + \ldots + a_{1k}m_kp^2A_k;$$
$$A_2 = a_{21}m_1p^2A_1 + a_{22}m_2p^2A_2 + \ldots + a_{2k}m_kp^2A_k;$$
$$\ldots \ldots \ldots \ldots \ldots \ldots \ldots \ldots \ldots \ldots;$$
$$\ldots \ldots \ldots \ldots \ldots \ldots \ldots \ldots \ldots \ldots;$$
$$A_k = a_{k1}m_1p^2A_1 + a_{k2}m_2p^2A_2 + \ldots + a_{kk}m_kp^2A_k.$$

We drop the first equation, replacing it by the orthogonality equation

$$m_1A_1u_{11} + m_2A_2u_{21} + \ldots + m_kA_ku_{k1} = 0,$$

where u_{s1} are the normed amplitudes of the first vibration mode. With the aid of this equation we exclude from the remaining (k - 1) basic equations the amplitude A_1 of the first mass. As a result we obtain the new system of equations

$$A_i = p^2 \sum_{s=2}^{k} \left(a_{is} - a_{i1}\frac{u_{s1}}{u_{11}} \right) m_s A_s, \quad \text{where} \quad i = 2, 3, \ldots, k.$$ (2.80)

This system contains one less equation than the preceding system. In the new system all the vibration modes are orthogonal to the first

mode of the basic system. The lowest mode is the second mode for the basic system.

We denote for convenience

$$\alpha'_{is} = \alpha_{is} - \alpha_{i1} \frac{x_{s1}}{x_{11}}.$$ (2.81)

Then the new system of equations in general form is

$$A_i = p^2 \sum_{s=2}^{n} \alpha'_{is} m_s A_s.$$ (2.82)

The further calculations of the successive approximations are made in the usual sequence with the aid of the system of equations

$$\lambda_i^{(n)} = \sum_{s=2}^{n} \alpha'_{is} m_s \lambda_s^{(n-1)}.$$ (2.83)

The ratio of successive approximations yields

$$p_2^2 = \frac{\lambda_i^{(n-1)}}{\lambda_i^{(n)}}.$$ (2.84)

The amplitude of the excluded mass is found after completing the iterations from the orthogonality equation

$$A_1 = -\frac{1}{m_1 x_{11}} \sum_{s=2}^{n} m_s x_{s1} \lambda_s^{(n)}.$$ (2.85)

2.3.2.4. Determining the Highest Frequency by Direct Iteration

The direct iteration method can be used to calculate the highest vibration frequency and mode. To do this we must use the algebraic equations in the direct form (2.15)

$$\left.\begin{aligned}
m_1 p^2 A_1 &= c_{11} A_1 + c_{12} A_2 + \ldots + c_{1n} A_n; \\
m_2 p^2 A_2 &= c_{21} A_1 + c_{22} A_2 + \ldots + c_{2n} A_n; \\
&\cdot\cdot\cdot\cdot\cdot\cdot\cdot\cdot\cdot\cdot\cdot\cdot\cdot\cdot\cdot; \\
&\cdot\cdot\cdot\cdot\cdot\cdot\cdot\cdot\cdot\cdot\cdot\cdot\cdot\cdot\cdot; \\
m_n p^2 A_n &= c_{n1} A_1 + c_{n2} A_2 + \ldots + c_{nn} A_n.
\end{aligned}\right\}$$ (2.15, a)

Denoting temporarily

$$\frac{1}{p^2} = z$$

and dividing each equation by m_1, we obtain the system (2.15a) in the form

$$A_l = z \sum_{s=1}^{k} \frac{c_{ls}}{m_l} A_s, \quad l = 1, \ldots; k; \qquad (2.86)$$

we shall use this system for the method of successive approximations. We substitute into the right side some sequence of assumed numbers $Y_s^{(0)}$. Then we obtain on the left the corresponding approximations

$$Y_l^{(1)} = z \sum_{s=1}^{k} \frac{c_{ls}}{m_l} Y_s^{(0)}; \qquad (2.87)$$

and for the subsequent approximations

$$Y_l^{(n)} = z \sum_{s=1}^{k} \frac{c_{ls}}{m_l} Y_s^{(n-1)}. \qquad (2.88)$$

Hence, we obtain the system of computational equations

$$\lambda_l^{(n)} = \sum_{s=1}^{k} \frac{c_{ls}}{m_l} \lambda_l^{(n-1)}; \qquad (2.89)$$

this system has all the properties characteristic of the system (2.71). In the iteration process it leads to the smallest value of z and the corresponding mode

$$z_{min} = \frac{\lambda_l^{(n-1)}}{\lambda_l^{(n)}};$$

then

$$p_k^2 \approx \frac{\lambda_l^{(n)}}{\lambda_l^{(n-1)}}; \qquad (2.90)$$

Since in the iteration process we approached z_{min} from above, this means that the formula yields the lower limit of the highest frequency. Taking the iteration ratios for the different masses, the largest ratio is to be considered closest to the natural frequency squared.

The assumed mode for the calculation should be chosen in accordance with the theorem on the number of normal mode sign changes. The highest mode has (k - 1) sign changes. Consequently, we can take as the assumed mode the alternating series consisting of ones

$$Y_s^{(0)} = 1, -1, 1, -1 \text{ etc.}$$

In order to shorten the calculations, we can also use here the Rayleigh formula, which in the present case takes the following form (see [5])

$$z_{min} = \frac{1}{p_k^2} \approx \frac{\sum_{i=1}^{k} m_i \lambda_i^{(a-1)} \lambda_i^{(a)}}{\sum_{i=1}^{k} m_i \lambda_i^{(a)2}}. \tag{2.91}$$

2.4. Forced Vibrations of a System with
k Degrees of Freedom

2.4.1. Forced Vibrations under the Action of a Single Harmonic Force

We write the differential equations of forced vibrations of a system under the action of the harmonic force

$$Q_m = H_m \cos \omega t,$$

applied to the mass m_m, in direct form

$$-m_1 \ddot{q}_1 = \sum_{i=1}^{k} c_{1i} q_i;$$

$$-m_2 \ddot{q}_2 = \sum_{i=1}^{k} c_{2i} q_i;$$

$$\cdots \cdots \cdots \cdots;$$

$$\cdots \cdots \cdots \cdots; \tag{2.92}$$

$$Q_m - m_m \ddot{q}_m = \sum_{i=1}^{k} c_{mi} q_i;$$

$$\cdots \cdots \cdots \cdots;$$

$$\cdots \cdots \cdots \cdots;$$

(Equation continued on next page)

$$-m_k \ddot{q}_k = \sum_{s=1}^{k} c_{ks} q_s. \qquad (2.92)$$

We shall not consider the general solution of the system of equations, assuming that free vibrations are excluded by the choice of the initial conditions.

The particular solution defining the forced vibrations has the form

$$q_{im} = B_{im} \cos \omega t; \qquad (2.93)$$

the second subscript m denotes the number of the mass to which the harmonic force is applied.

After substituting the solution into (2.92), we obtain the system of algebraic equations

$$
\left.
\begin{aligned}
& m_1 \omega^2 B_{1m} = \sum_{s=1}^{k} c_{1s} B_{sm}; \\
& m_2 \omega^2 B_{2m} = \sum_{s=1}^{k} c_{2s} B_{sm}; \\
& \cdots \cdots \cdots \cdots \cdots \cdots; \\
& \cdots \cdots \cdots \cdots \cdots \cdots; \\
& H_m + m_m \omega^2 B_{mm} = \sum_{s=1}^{k} c_{ms} B_{sm}; \\
& \cdots \cdots \cdots \cdots \cdots \cdots; \\
& m_k \omega^2 B_{km} = \sum_{s=1}^{k} c_{ks} B_{sm}.
\end{aligned}
\right\}
\qquad (2.94)
$$

From this system of equations we find the amplitudes of the forced vibrations of all the masses

$$B_{im} = \frac{\Delta_{im}}{\Delta} H_m, \qquad (2.95)$$

where Δ is the basic determinant of the system

$$\Delta = \begin{vmatrix} c_{11}-m_1\omega^2 & c_{12}\ldots & c_{1m}\ldots & c_{1k} \\ c_{21} & c_{22}-m_2\omega^2\ldots & c_{2m}\ldots & c_{2k} \\ \cdots & \cdots & \cdots & \cdots \\ \cdots & \cdots & \cdots & \cdots \\ c_{m1} & c_{m2}\ldots & c_{mm}-m_m\omega^2\ldots & c_{mk} \\ \cdots & \cdots & \cdots & \cdots \\ \cdots & \cdots & \cdots & \cdots \\ c_{k1} & c_{k2}\ldots & c_{km}\ldots & c_{kk}-m_k\omega^2 \end{vmatrix}. \qquad (2.96)$$

Δ_{im} are the minors of the basic determinant to the elements of row m.

The ensemble of amplitudes (2.95) yields the forced vibration mode.

2.4.2. Dynamic Compliance Coefficients

The ratio Δ_{im}/Δ of the determinants is the vibration amplitude of the mass with subscript i under the action of unit harmonic force applied to the mass with subscript m. By analogy with the static compliance coefficient, this ratio is called the dynamic compliance coefficient and is denoted by e_{im}:

$$e_{im} = \frac{\Delta_{im}}{\Delta}; \qquad (2.97)$$

then

$$B_{im} = e_{im}H_m; \qquad (2.98)$$

since the harmonic force can be applied to any mass, the subscript m can take values from one to k.

Putting the dynamic compliance coefficient in place of that element of the determinant (2.96) with respect to which the minor is taken, we can formulate the dynamic compliance coefficient matrix of the system

$$\begin{vmatrix} e_{11} & e_{21} \dots e_{m1} \dots e_{k1} \\ e_{12} & e_{22} \dots e_{m2} \dots e_{k2} \\ \cdot & \cdot \cdot \cdot \cdot \cdot \cdot \cdot \cdot \cdot \cdot \cdot \cdot \cdot \\ e_{1m} & e_{2m} \dots e_{mm} \dots e_{km} \\ \cdot & \cdot \cdot \cdot \cdot \cdot \cdot \cdot \cdot \cdot \cdot \cdot \cdot \cdot \\ e_{1k} & e_{2k} \dots e_{mk} \dots e_{kk} \end{vmatrix}; \qquad (2.99)$$

Here the first subscript is the mass number; the second is the number of the unit force.

The diagonal coefficients e_{11} are termed the proper dynamic compliance coefficients. They show the amplitude of the forced vibrations of that mass to which the unit disturbing force is applied. The coefficients e_{im} with mixed subscripts are termed the mixed or improper dynamic compliance coefficients. They have the reciprocity property

$$e_{is} = e_{si}.$$

The dynamic coefficients e_{is} are variable quantities which depend on the disturbing force frequency ω. They can be expressed as functions of ω^2 with the aid of the roots of the basic determinant (2.96) and the roots of the minors. For the minors to the diagonal elements

$$e_{ii} = \frac{-\Pi_{p=1}^{k-1}\left(\omega^2 - p_p^2\right)}{m_i \Pi_{j=1}^{k}\left(\omega^2 - p_j^2\right)}, \qquad (2.100)$$

where p_j — are the roots of the basic determinant — the natural vibration frequencies of the system;

p_{j*} are the roots of the minor to the ith diagonal element. These are the natural vibration frequencies of the system with an additional constraint imposed on the mass m_i.

For the nondiagonal minors

$$e_{im} = \frac{\Delta_{im}}{\Pi_{j=1}^{k} m_i \cdot \Pi_{j=1}^{k}\left(\omega^2 - p_j^2\right)}. \qquad (2.101)$$

The numerator — the minor to the element im — contains one or more imaginary roots; therefore, it does not break down completely into a product of the characteristic roots, but is a polynomial in powers of ω^2.

A typical dependence of the dynamic compliance coefficients on the forced vibration frequency is shown in Figure 2.5. If the exciting force frequency equals one of the normal vibration frequencies ($\omega = p_j$), all the coefficient functions undergo a discontinuity. This corresponds to the resonance phenomenon, when the amplitudes of the forced vibrations increase without limit. The resonance phenomenon is independent of the point of application of the disturbing force.

The zero points on the segments between resonances show a change of the signs of the amplitudes of certain masses and denote transition of the vibration mode from a preceding (lower) mode to the next (higher) mode.

The dynamic coefficients e_{im} can be calculated with the aid of the equations in inverse form

$$B_{im} = \sum_{i=1}^{s} a_{is} m_s p^2 B_{is} + e_{im} H_m, \quad \text{rие } i = 1, \ldots k;\qquad(2.102)$$

here m is the index of the ma-s to which the disturbing force is applied.
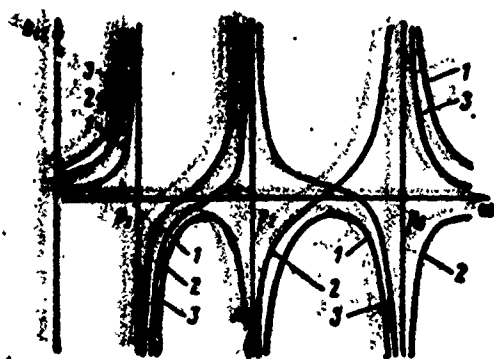
Figure 2.5 Dynamic compliance coefficients as a function of disturbing force frequency. 1,2,3 - mass numbers.

Expanding the general form into a system of equations and taking $H_m = 1$, we can find the coefficients e_{1m} as the ratio of the determinants

$$e_{im} = \frac{\Delta_{im}}{\Delta},$$

where Δ is the basic determinant of the system

$$\Delta = \begin{vmatrix} a_{11}m_1\omega^2 - 1 & a_{12}m_2\omega^2 \ldots \ldots a_{1k}m_k\omega^2 \\ a_{21}m_1\omega^2 & a_{22}m_2\omega^2 - 1 \ldots a_{2k}m_k\omega^2 \\ \ldots \ldots \ldots \ldots \ldots \ldots \ldots \ldots \ldots \ldots \\ \ldots \ldots \ldots \ldots \ldots \ldots \ldots \ldots \ldots \ldots \\ a_{k1}m_1\omega^2 & a_{k2}m_2\omega^2 \ldots \ldots a_{kk}m_k\omega^2 - 1 \end{vmatrix};$$

Δ_{im} is the basic determinant in which the column with order number i is replaced by the column consisting of the coefficients α_{sm}, where s = 1, 2, ..., k; m is the index of the mass to which the unit harmonic force is applied.

2.5. Determining Any Natural Vibration Frequency by the Dynamic Compliance Coefficient Method

Determining the natural vibration frequencies for systems having a large number of degrees of freedom involves a very considerable volume of computational work. However, in many practical cases we do not need to calculate the entire spectrum of natural frequencies of the system; we need only know the frequencies lying in the limits of some narrow range. In this case we obviously know that these are not the first frequencies. Examples of such problems are the analyses of aircraft structures — aircraft engines, turbopump assemblies, auxiliary powerplants, and so on — which are complex systems having a large number of natural frequencies and operating at high rotational speeds, so that the disturbing forces cause resonance in the intermediate vibration modes of the system.

The method using dynamic compliance coefficients makes it possible to determine the natural frequencies in any prespecified

89

range without requiring preliminary calculation of all the lower-lying frequencies. In using this method the calculation is made by means of successive approximations.

We begin the derivation of the computational formulas with the general equations in direct form (2.15a)

$$m_i p^2 A_i = \sum_{s=1}^{k} c_{is} A_s, \quad i = 1, 2, \ldots, k;$$

we make a formal substitution, representing the unknown root as the sum

$$p^2 = \omega^2 + \delta\omega^2, \tag{2.103}$$

where ω^2 is the square of the given frequency, near which we seek the root of the frequency equation;
$\delta\omega^2$ is the sought increment

$$m_i (\omega^2 + \delta\omega^2) A_i = \sum_{s=1}^{k} c_{is} A_s.$$

We write this system of equations in expanded form, denoting $m_1 \delta\omega^2 A_1 = P_1$

$$
\left.
\begin{aligned}
P_1 &= (c_{11} - m_1\omega^2) A_1 + c_{12} A_2 + \ldots + c_{1k} A_k; \\
P_2 &= c_{21} A_1 + (c_{22} - m_2\omega^2) A_2 + \ldots + c_{2k} A_k; \\
&\; \cdots \cdots \cdots \cdots \cdots \cdots \cdots \cdots \cdots ; \\
P_k &= c_{k1} A_1 + c_{k2} A_2 + \ldots + (c_{kk} - m_k\omega^2) A_k.
\end{aligned}
\right\} \tag{2.104}
$$

We solve the system of equations for A_i

$$A_i = \frac{\Delta_i}{\Delta}, \tag{2.105}$$

where Δ is the basic determinant of the system

$$
\Delta =
\begin{vmatrix}
c_{11} - m_1\omega^2 & c_{12} & \cdots & c_{1k} \\
c_{21} & c_{22} - m_2\omega^2 & \cdots & c_{2k} \\
\cdots & \cdots & \cdots & \cdots \\
\cdots & \cdots & \cdots & \cdots \\
c_{k1} & c_{k2} & & c_{kk} - m_k\omega^2
\end{vmatrix}
$$

Δ_1 is the determinant obtained from the basic determinant by replacing the column i by the column P_1.

After making this substitution, it is not difficult to see that the determinant equals the following sum

$$\Delta_i = \sum_{s=1}^{k} P_s \Delta_{is},$$

where Δ_{is} is the minor of the basic determinant to the element of column i and row s. Therefore, (2.105) takes the form

$$A_i = \sum_{s=1}^{k} P_s \frac{\Delta_{is}}{\Delta};$$

but according to (2.97) the ratio of the determinants is the dynamic compliance coefficient e_{is}. Therefore, after the replacement $P_s = m_s \delta \omega^2 A_s$ we obtain the following system of computational equations

$$A_i = \delta \omega^2 \sum_{s=1}^{k} e_{is} m_s A_s, \quad i = 1, 2, \dots, k. \qquad (2.106)$$

This system is identical to (2.61). It defines the k linearly independent orthogonal natural vibration modes and their frequencies. But the latter are defined here as the increments $\delta \omega^2$ to the frequency ω^2, which was used in calculating e_{is}.

The system of Equations (2.106) is used to calculate the smallest value of $\delta \omega^2$ by successive approximations. To do this, as before, we denote

$$\lambda_i^{(n)} = \sum_{s=1}^{k} e_{is} m_s \lambda_s^{(n-1)}; \qquad (2.107)$$

using these equations, after assuming the initial mode $\lambda_s^{(0)}$, we make a successive calculation of several approximations. After this we find the sought increment

$$(\delta \omega^2)_{min} \approx \frac{\lambda_i^{(n-1)}}{\lambda_i^{(n)}}. \qquad (2.108)$$

The result may be either positive or negative. In the latter case this means that the nearest natural vibration frequency is less than that value of ω which was taken for the calculation of the coefficients e_{is}. The frequency is found from (2.103). The number of the resulting natural vibration mode is determined from the number of sign changes of the final approximation $\lambda_i^{(n)}$. The mode number is one more than the number of sign changes.

The vibration mode is determined by the ratio of the quantities $\lambda_i^{(n)}$, from which the normed amplitudes are easily found.

The convergence of the computational results to the smallest value $(\delta\omega^2)$min is proved by the same technique used to find the basic frequency.

By expanding the assumed, approximately specified mode $\lambda^{(0)}$ terms of the normal modes

$$\lambda_i^{(0)} = z_1 x_{i1} + z_2 x_{i2} + \ldots + z_k x_{ik}$$

and making the first iteration, we obtain an equality similar to (2.65)

$$\lambda_i^{(1)} = z_1 \sum_{s=1}^{k} e_{is} m_s x_{s1} + z_2 \sum_{s=1}^{k} e_{is} m_s x_{s2} + \ldots + z_k \sum_{s=1}^{k} e_{is} m_s x_{sk}$$

replacing the sums in accordance with (2.106), we obtain

$$\lambda_i^{(1)} = z_1 \frac{1}{(\delta\omega^2)_1} x_{i1} + z_2 \frac{1}{(\delta\omega^2)_2} x_{i2} + \ldots + z_k \frac{1}{(\delta\omega^2)_k} x_{ik}$$

After making n sequential calculations, we find

$$\lambda_i^{(n)} = z_1 x_{i1} \frac{1}{(\delta\omega^2)_1^n} + z_2 x_{i2} \frac{1}{(\delta\omega^2)_2^n} + \ldots + z_k x_{ik} \frac{1}{(\delta\omega^2)_k^n}. \qquad (2.109)$$

We take the smallest value $(\delta\omega^2)_1^n$ outside the braces; then (2.109) takes the form

$$\lambda_j^{(n)} = \frac{1}{(\delta\omega^2)_{j\,min}} \left\{ x_1 u_{j1} \left[\frac{(\delta\omega^2)_{j\,min}}{(\delta\omega^2)_1} \right]^n + x_2 u_{j2} \left[\frac{(\delta\omega^2)_{j\,min}}{(\delta\omega^2)_2} \right]^n + \right.$$

$$\left. + \ldots + x_j u_{jj} + \ldots + x_n u_{jn} \left[\frac{(\delta\omega^2)_{j\,min}}{(\delta\omega^2)_n} \right]^n \right\};$$

With increase of the number of approximations the process converges

$$\lim_{n \to \infty} \lambda_j^{(n)} = \frac{x_j u_{jj}}{(\delta\omega^2)_{j\,min}^2}.$$

Taking the ratio of the limiting values, we obtain

$$\lim_{n \to \infty} \frac{\lambda_j^{(n-1)}}{\lambda_j^{(n)}} = (\delta\omega^2)_{j\,min}. \qquad (2.110)$$

Formula (2.110) shows that the iteration process using the dynamic compliance coefficients converges and yields the value of the smallest difference between the square of the natural frequency and the assumed value ω^2, from which the coefficients e_{is} were taken.

CHAPTER 3

VIBRATIONS OF BARS WITH CONTINUOUSLY DISTRIBUTED MASS

In the present chapter we examine small vibrations of bars with .
straight centerline and section which is constant or variable along
the length.

The mass of the bar is assumed to be distributed continuously
along the bar length in accordance with a definite law.

The bar centerline is the line of centers of gravity of its
sections. We assume that the bar centerline is straight in the
equilibrium position. This assumption excludes from consideration
static forces such as, for example, weight forces and the static
deformations caused by them. We know from general courses in
mechanics that static forces do not affect the vibrations in linear
systems. Their effect shows up only in a shift of the position of
the equilibrium state by the magnitude of the static deformation.
It is assumed that the bar has at least one longitudinal plane of
symmetry and the vibrations are examined in this plane.

In all the problems we consider vibrations with small ampli-
tudes, for which proportionality is maintained between the elastic
forces and the bar deflections from the equilibrium position or
(what is the same thing) between the elastic forces and the bar
deformations.

94

In vibration problems it is customary to call bars systems with an infinite number of degrees of freedom, since for the exact determination of the position of their centerline it is necessary to know an infinite number of coordinates of the displacement of the points of the centerline. In other words, it is necessary to know the bar deflection function along its length.

3.1. Derivation of General Differential Equation for

Transverse Bar Vibrations

We shall examine small transverse vibrations of a bar with mass $m(x)$ distributed arbitrarily along its length and stiffness $EJ(x)$, resting on two or more supports. An external load in the form of distributed forces of intensity q and distributed bending moment μ is applied to the bar.

We take the straight axis of the bar in the undeformed state as the x axis. In view of the smallness of the vibrations, the displacement of any point of the axis is defined by the coordinate y, and the section rotation is defined by the angle $\theta = dy/dx$. We neglect the small movements of the sections along the axis and the associated inertia forces.

We obtain the transverse vibration differential equation by formulating the equations of equilibrium of the forces and moments of an elementary segment of the bar, bounded by the sections with the coordinates x and x + dx (Figure 3.1).

The external distributed load q is represented by its projections $q_y(x, t)$ and $q_x x, t)$ and the effect of the discarded adjacent segments is represented by the moment and forces applied in the sections.

We write the force and moment equations in projections on the coordinate axes
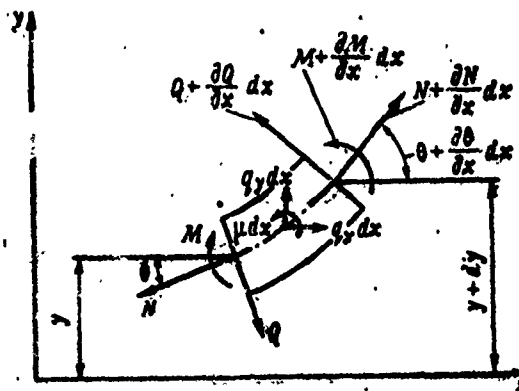
95

Figure 3.1. Forces and moments applied to bar element

$$\frac{\partial M}{\partial x}\, dx + Q\, dx + \mu\, dx + N\, \frac{\partial \theta}{\partial x}\, dx^2 = 0;$$

$$\frac{\partial Q}{\partial x}\, dx - N\theta + \left(N + \frac{\partial N}{\partial x}\, dx\right)\left(\theta + \frac{\partial \theta}{\partial x}\, dx\right) + q_y\, dx = 0;$$

$$\frac{\partial N}{\partial x}\, dx + Q\theta - \left(Q + \frac{\partial Q}{\partial x}\, dx\right)\left(\theta + \frac{\partial \theta}{\partial x}\, dx\right) + q_x\, dx = 0;$$

(3.1)

Cancelling dx and dropping infinitesimal terms, we obtain the equilibrium equation in the form

$$\frac{\partial M}{\partial x} + Q + \mu = 0;$$

$$\frac{\partial Q}{\partial x} + \frac{\partial}{\partial x}(N\theta) + q_y = 0;$$

$$\frac{\partial N}{\partial x} + q_x = 0.$$

(3.2)

The last equation defines the distribution of the longitudinal forces along the bar. For small deviations from the equilibrium position the forces N are independent of the vibrations and are completely defined by the initial conditions of the problem.

96

Solving jointly the first and second equations (3.2) and excluding Q, we obtain

$$\frac{\partial^2 M}{\partial x^2} + \frac{\partial \mu}{\partial x} - \frac{\partial}{\partial x}(N\theta) - q_y = 0. \qquad (3.3)$$

If shear deformations are ignored

$$\theta = \frac{\partial y}{\partial x}.$$

Substituting into (3.3) the known equality

$$M = EJ\frac{\partial^2 y}{\partial x^2},$$

we obtain in general form the differential equation of the bar deformations

$$\frac{\partial^2}{\partial x^2}\left(EJ\frac{\partial^2 y}{\partial x^2}\right) + \frac{\partial \mu}{\partial x} - \frac{\partial}{\partial x}\left(N\frac{\partial y}{\partial x}\right) - q_y = 0. \qquad (3.4)$$

The distributed loads q_y and μ are the inertial forces and moments of the mass of the bar itself

$$\left.\begin{aligned} q_y &= -m(x)\frac{\partial^2 y}{\partial t^2}; \\ \mu &= -J(x)\frac{\partial^2 \theta}{\partial t^2}, \end{aligned}\right\} \qquad (3.5)$$

where $m(x)$ and $J(x)$ are the mass and moment of inertia of the bar per unit length.

After substituting (3.5) into (3.4), the latter takes the form

$$\frac{\partial^2}{\partial x^2}\left(EJ\frac{\partial^2 y}{\partial x^2}\right) - \frac{\partial}{\partial x}\left[J(x)\frac{\partial^2 \theta}{\partial t^2} + N\frac{\partial y}{\partial x}\right] + m(x)\frac{\partial^2 y}{\partial t^2} = 0. \qquad (3.6)$$

This is the general differential equation of free vibrations of straight bars.

Provided the longitudinal force N is independent of time, the differential equation (3.6) is solved by the Fourier method. We represent the unknown function as a product of two independent functions

$$\left.\begin{aligned} y(x,t) &= Y(x)T(t); \\ \theta(x,t) &= \frac{\partial y}{\partial x} = \frac{dY(x)}{dx}T(t). \end{aligned}\right\} \qquad (3.7)$$

97

Substitution of (3.7) into (3.6) leads to separation of the latter
into two independent equations

$$\ddot{T}(t) + p^2 T(t) = 0 \qquad (3.8)$$

and

$$\frac{d^2}{dx^2}\left(EJ\frac{d^2Y}{dx^2}\right) - \frac{d}{dx}\left[N\frac{dY}{dx} - p^2 J(x)\frac{dY}{dx}\right] - m(x)p^2 Y = 0. \qquad (3.9)$$

Equation (3.8) for free harmonic vibrations has the general
solution

$$T(t) = A_1 \cos pt + A_2 \sin pt;$$

for the initial condition T(0) = 1; T (0) = 0 it takes the simple
form

$$\dot{T}(t) = \cos pt.$$

Then the Solution (3.7) will have the form

$$y(x,t) = Y(x)\cos pt; \quad \theta(x,t) = \frac{dY(x)}{dx}\cos pt. \qquad (3.10)$$

Let us examine (3.9).

The function Y(x) is the vibration amplitude. It shows the bar
free vibration mode shape.

The differential equation (3.9) is very general and allows the
solution of a large range of varied problems. Direct integration
of the equation is difficult and is feasible only for individual
particular cases. However, it is used in various approximate
methods. Specifically, we can note the Bubnov-Galerkin method, the
integral method, and the method of successive approximations.

Direct integration of the general equation is most fruitful for
uniform beams and bars. In this case (3.9) becomes a linear equa-
tion with constant coefficients and its solutions are simple
functions.

3.2. General Solution of the Differential Equation for
Bars of Constant Section in Krylov Functions

We obtain the differential equation for uniform bars from (3.9), assuming therein that the mass m and bending stiffness EJ(x) per unit length are constant within the limits of a span.

We take the longitudinal force to be zero and ignore rotary inertia of the bar elements

$$N = 0; \ J_{\bullet} = 0.$$

Under these conditions the differential equation (3.9) has the form

$$EJ \ \frac{d^4Y}{dx^4} - mp^2Y = 0; \tag{3.11}$$

we introduce the dimensionless coordinate

$$\xi = \frac{x}{l}, \tag{3.12}$$

where l — is the bar length.

Equation (3.11) is written as

$$\frac{d^4Y}{d\xi^4} - k^4Y = 0, \tag{3.13}$$

where

$$k^4 = l^4 \frac{mp^2}{EJ}. \tag{3.14}$$

Solved for p, this expression yields the general formula for calculating the natural vibration frequency of bars

$$p = \frac{k^2}{l^2} \sqrt{\frac{EJ}{m}}; \tag{3.15}$$

the coefficient k^2 depends on the bar restraint conditions and is defined later.

Equation (3.13) is the simplest and most frequently used equation, on the basis of which a large number of varied problems are solved.

The general integral (3.13) is made up of four particular solutions

$$\sin k\xi; \ \cos k\xi; \ \text{sh } k\xi; \ \text{ch } k\xi \qquad (3.16)$$

or their combinations. The solutions comprised of the Krylov functions is often used

$$
\left.
\begin{aligned}
S(\xi) &= \frac{1}{2}(\text{ch } k\xi + \cos k\xi); \\
T(\xi) &= \frac{1}{2}(\text{sh } k\xi + \sin k\xi); \\
U(\xi) &= \frac{1}{2}(\text{ch } k\xi - \cos k\xi); \\
V(\xi) &= \frac{1}{2}(\text{sh } k\xi - \sin k\xi).
\end{aligned}
\right\} \qquad (3.17)
$$

The Krylov functions are convenient in practical calculations, since they simplify the connection between the general solution and the boundary conditions. Upon differentiation, they have the circular permutation property, as shown in Table 3.1.

TABLE 3.1.

$Y_i(k\xi)$	$S(k\xi)$	$T(k\xi)$	$U(k\xi)$	$V(k\xi)$
$Y_i'(k\xi)$	$k V(k\xi)$	$k S(k\xi)$	$k T(k\xi)$	$k U(k\xi)$
$Y_i''(k\xi)$	$k^2 U(k\xi)$	$k^2 V(k\xi)$	$k^2 S(k\xi)$	$k^2 T(k\xi)$
$Y_i'''(k\xi)$	$k^3 T(k\xi)$	$k^3 U(k\xi)$	$k^3 V(k\xi)$	$k^3 S(k\xi)$
$Y_i''''(k\xi)$	$k^4 S(k\xi)$	$k^4 T(k\xi)$	$k^4 U(k\xi)$	$k^4 V(k\xi)$

The solution of (3.13) in Krylov functions has the following form

$$Y(k\xi) = C_1 S(k\xi) + C_2 T(k\xi) + C_3 U(k\xi) + C_4 V(k\xi). \qquad (3.18)$$

This general solution remains valid for all uniform bars, re-gardless of the end restraint conditions and form of support. The latter affect the values of the integration constants C_1, C_2, C_3, C_4.

To determine the coefficients C_1, C_2, C_3, C_4 and the free vibra-tion frequency it is necessary to specify the boundary conditions, i.e., to define the bar end restraint conditions.

The general problem solving technique is the same for all cases and consists of several steps, which we shall analyze using indivi-dual examples.

3.3. Bars on Rigid Supports

Rigid supports may be either hinged or built-in. The different combination of simple supports and free ends of the bar yields a large number of varied bar restraint conditions, which encompass most practical cases.

3.3.1. Bar on Rigid Hinged Supports (Figure 3.2a)

The displacement of the bar ends is zero; the bending moments in the hinge are also zero. Therefore the bar end restraint condi-tions are defined by the equalities

$$Y(0)=0; \ Y''(0)=0; \ Y''(1)=0; \ Y(1)=0.$$

Applying these equalities to the general solution (3.18), we obtain $C_1 = C_3 = 0$; the second pair of equalities yields two equations

$$C_2 T(k) + C_4 V(k) = 0;$$
$$C_2 V(k) + C_4 T(k) = 0.$$

These equations are homogeneous; therefore, to obtain nonzero solu-tions we must equate the system determinant to zero, i.e., we must satisfy the condition

$$T^2(k) - V^2(k) = 0. \tag{3.19}$$

$$\sin k = 0$$
$$k = n\pi, \ n = 1, 2, 3, \ldots$$

a)

$$1 + \text{ch} \, k \, \cos k = 0;$$
$$k_1 = 1{,}875; \ k_2 = 4{,}694;$$
$$k_n = (n - 0{,}5)\pi, n = 3, 4,$$

b)

$$1 - \text{ch} \, k \, \cos k = 0;$$
$$k_1 = 4{,}73; \quad k_n = (n + 0{,}5)\pi, \quad n = 2, 3, 4, \ldots$$

c)

d)

$$\text{tg} \, k - \text{th} \, k = 0;$$
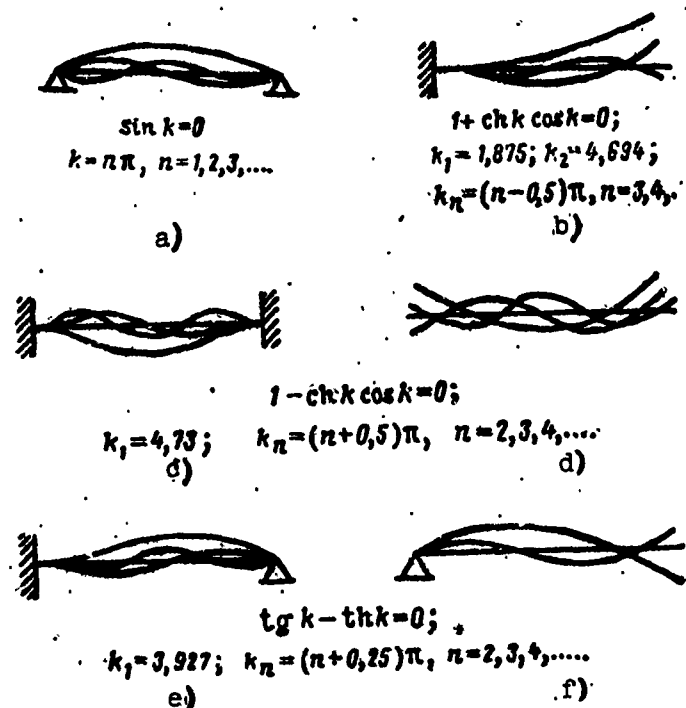$$k_1 = 3{,}927; \ k_n = (n + 0{,}25)\pi, \ n = 2, 3, 4, \ldots$$

e)

f)

Figure 3.2. Vibration modes of bars with different end fixity

Replacing the Krylov functions by their values from the Solutions (3.17), we obtain the equality

$$\sin k = 0; \tag{3.20}$$

the roots of the equality are the solutions

$$k = n\pi, \ \text{where} \ n = 1, 2, 3, \ldots, \tag{3.21}$$

where n — is the sequential number of the vibration mode.

The Solution (3.20) shows that the vibration mode of a uniform bar is a sinusoid. An integral number of sinusoid halfwaves occurs in the limits of the span.

The parameter k defined here makes it possible to calculate with with aid of (3.15) the normal vibration frequencies.

The Equality (3.20) has an infinite number of roots. This indicates that the bar with distributed mass has an infinite number of normal vibration modes and frequencies. The frequencies are related as the squares of the integers

$$p_1 : p_2 : p_3 : p_4 = 1 : 4 : 9 : 16 \text{ etc.}$$

Only the first few roots are of practical importance, which yield the frequencies characteristic for mechanical systems. In addition we note that the roots of the higher frequencies are determined with an error resulting from the fact that shear deformations are not taken into account. The errors increase with increase of the mode number.

3.3.2. Clamped Cantilever Bar (Figure 3.2b)

The displacement and section rotation angle are zero at the clamped end, which corresponds to the equalities

$$Y(0) = 0; \quad Y'(0) = 0.$$

For the free end

$$Y''(1) = 0; \quad Y'''(1) = 0.$$

The first two equalities yield for the Solution (3.18)

$$C_1 = 0; \quad C_2 = 0.$$

The second two equalities lead to the equations

$$\left. \begin{array}{l} C_3 S(k) + C_4 T(k) = 0; \\ C_3 V(k) + C_4 S(k) = 0. \end{array} \right\} \tag{3.22}$$

Hence we obtain the frequency equation

$$1 + \operatorname{ch} k \cos k = 0. \tag{3.23}$$

The roots of this equation are

$$k_1 = 1,875; \quad k_2 = 4,694; \quad k_n = (n - 0,5)\pi, \text{ where } n = 3, 4, \ldots$$

The normal vibration frequencies are found from (3.15).

In order to construct the vibration mode using (3.18) we must determine the coefficients C_3 and C_4. Setting one of them equal to

one (for example, $C_3 = 1$), we find the other coefficient from either of the Equations (3.22). After this we obtain the formula for calculating the vibration mode

$$Y(k\xi) = U(k\xi) - \frac{S(k)}{T(k)} V(k\xi).$$ (3.24)

Figure 3.2a, b, c, d, e, f, shows the most typical bar restraint schemes, the frequency equations and their roots (see [1]). The normal vibration frequencies are calculated with the aid of these roots using (3.15).

3.4. Vibrations of Bars on Elastic Supports

Bar supports, whether hinged supports or with built-in restraint, are not perfectly rigid. The supports deform under the action of the forces from the bars; as a result of this there are displacements and rotation of the bar sections at the supports.

The elastic deformations of the supports affect the bar vibration natural frequencies and modes. In many cases the supports are intentionally made elastic in order to alter the natural frequencies.

Support elasticity is taken into account in the calculations in formulating the boundary conditions. We shall examine the technique for solving the problem on the example of a cantilever beam with elastic end fixity (Figure 3.3).

The restraint elasticity is characterized by two coefficients: c_1 or the transverse stiffness coefficient, and c_2 or the moment stiffness coefficient. Therefore both varieties of elastic support deformations and the corresponding stiffness coefficients appear in the example in question.

Let us write the boundary condition equations. The boundary conditions for the root section ($\xi = 0$) will be: equality of the bending moment and the shearing force to the corresponding restraint elastic moment and force

$$\frac{1}{l^2} EJY''(0) = c^2 \frac{1}{l} Y'(0); \qquad (3.25)$$

$$\frac{1}{l^3} EJY'''(0) = c_1 Y(0). \qquad (3.26)$$

For the free end ($\xi = 1$) the boundary condition will be: vanishing of the bending moment and shearing force. This is equivalent to:

$$Y''(k) = 0; \ Y'''(k) = 0. \qquad (3.27)$$

Substituting into these equalities the general solution (3.18), we obtain the system of homogeneous equations

$$\frac{k^2}{l^2} EJC_3 = c_2 \frac{k}{l} C_2;$$

$$-\frac{k^3}{l^3} EJC_4 = c_1 C_1;$$

$$C_1 U(k) + C_2 V(k) + C_3 S(k) + C_4 T(k) = 0;$$

$$C_1 T(k) + C_2 U(k) + C_3 V(k) + C_4 S(k) = 0;$$

on the basis of these equations we formulate the frequency equation in determinant form

$$\begin{vmatrix} \bar{c}_1 & 0 & 0 & k^3 \\ 0 & \bar{c}_2 & -k & 0 \\ U(k) & V(k) & S(k) & T(k) \\ T(k) & U(k) & V(k) & S(k) \end{vmatrix} = 0, \qquad (3.28)$$

where

$$\bar{c}_1 = \frac{c_1 l^3}{EJ}; \quad \bar{c}_2 = \frac{c_2 l}{EJ}. \qquad (3.29)$$

Expanding the determinant into a row and substituting the Krylov functions (3.17), we obtain the equation in the form

$$\bar{c}_1 \bar{c}_2 (1 + \text{ch } k \cos k) + \bar{c}_1 k (\text{sh } k \cos k - \text{ch } k \sin k) -$$
$$- \bar{c}_2 k^3 (\text{sh } k \cos k + \text{ch } k \sin k) + k^4 (1 - \text{ch } k \cos k) = 0. \qquad (3.30)$$

The roots of (3.30) are the frequency coefficients, which can be found for any relationship and values of the restraint stiffness coefficients $\bar{c}_1$ and $\bar{c}_2$.

If we set $\bar{c}_1 = \bar{c}_2 = \infty$, ..., we consider the restraint absolutely stiff, we obtain the case shown in Figure 3.2b. For this case the frequency coefficients are respectively 1.875, 4.694, 7.85, and so on. In Figure 3.3 they are shown as the horizontal asymptotes for the solid lines — the frequency characteristics.
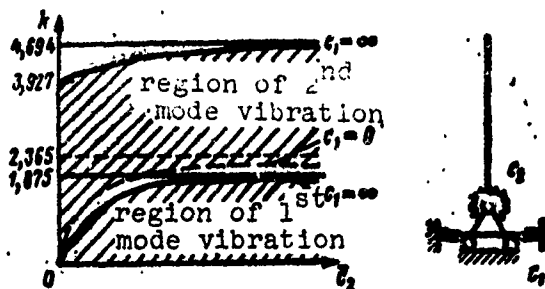

Figure 3.3. Frequency coefficients as a function of cantilever bar restraint stiffness

As the hinge moment stiffness is reduced, the frequency coefficients become smaller. For the first mode the coefficient reaches zero, and for the second it reaches a value corresponding to the case shown in Figure 3.2f. The bar vibration frequency decreases in this case in proportion to the square of the reduction of the coefficient, i.e., by 30%.

The lower limit of the coefficient k for the second mode is the dashed curve ($c_1 = 0$). Its asymptote is the straight line with the coordinate k = 2.365. Thus, transverse elasticity can reduce the frequency by 3 — 4 times. The curves show in general that cantilever bar restraint elasticity leads to change of the normal vibration frequency in the first and second modes over very wide limits.

Similar results are also obtained in other cases of elastic bar restraint.

3.5. Free Vibrations of Uniform Bars with Account for the Rotary Inertia of Their Elements

The calculation of free bar vibration frequencies is usually made without account for rotary inertia of the bar elements. This assumption, often used without any restriction, is valid for the

lower vibration modes, but becomes incorrect when calculating the frequencies of the higher vibration modes. It is also not valid if additional masses, which alter the bar stiffness little or not at all but alter significantly the mass moment of inertia per unit length, are added to the bar.

The differential equation of the problem is the Equation (3.9), in which we must set $N = 0$.

By elementary transformations the equation is reduced to a form with dimensionless parameters

$$\frac{d^4Y}{d\xi^4} + \varkappa^2 \frac{d^2Y}{d\xi^2} - k^4 Y = 0,$$
(3.31)

where

$$\xi = \frac{x}{l};$$

$$k^4 = \frac{ml^4}{EI} p^2;$$
(3.32)

$$\varkappa^2 = l^2 \frac{J_s p^2}{EI}.$$
(3.33)

The general integral of the equation is the sum

$$Y = C_1 \, \mathrm{ch} \, \lambda_1 \xi + C_2 \, \mathrm{sh} \, \lambda_1 \xi + C_3 \cos \lambda_2 \xi + C_4 \sin \lambda_2 \xi.$$
(3.34)

where

$$\lambda_1^2 = -\frac{1}{2} \varkappa^2 + \sqrt{\frac{1}{4} \varkappa^4 + k^4};$$
(3.35)

$$\lambda_2^2 = \frac{1}{2} \varkappa^2 + \sqrt{\frac{1}{4} \varkappa^4 + k^4};$$
(3.36)

The final form of the Solution (3.34) is obtained after determining the integration constants C_1, C_2, C_3, C_4. This requires four additional conditions, which are the bar end restraint conditions.

The boundary conditions for hinged supports are

$$Y(0) = 0; \; Y''(0) = 0; \; Y(1) = 0; \; Y''(1) = 0.$$

In accordance with the boundary conditions, we write the system of equations

$$C_1 + C_3 = 0;$$
$$C_1 \lambda_1^2 - C_3 \lambda_2^2 = 0,$$

hence

$$C_1 = C_3 = 0.$$

The second pair of conditions, with account for the preceding discussion, yields

$$C_2 \operatorname{sh} \lambda_1 + C_4 \sin \lambda_2 = 0;$$
$$C_2 \lambda_1^2 \operatorname{sh} \lambda_1 - C_4 \lambda_2^2 \sin \lambda_2 = 0.$$

From these two equations we obtain $C_2 = 0$; $\sin \lambda_2 = 0$. The latter equality yields the frequency coefficient

$$\lambda_2 = n\pi. \tag{3.37}$$

The general solution of (3.34) takes the simple form

$$Y(x) = C_4 \sin n\pi\xi. \tag{3.38}$$

To determine the free vibration frequency we substitute (3.32) and (3.33) into (3.36) and solve the resulting equation for the frequency p

$$p = \frac{\lambda_2^2}{l^2} \sqrt{\frac{EJ}{m + J_s \frac{\lambda_2^2}{l^2}}}. \tag{3.39}$$

We shall make an estimate of the rotary inertia effect on the vibration frequency.

For a bar of rectangular section

$$J_s = m \frac{h^2}{12},$$

where h — is the section height.

Formula (3.39) after substitution of J_s takes the form

$$\tag{3.40}$$
$$p = \frac{\lambda_2^2}{l^2} \sqrt{\frac{1}{1+s}} \sqrt{\frac{EJ}{m}},$$

where

$$s=\frac{\pi^2}{12}\frac{n^2h^2}{l^2}.$$ (3.41)

For thin-wall hollow round bars

$$J_s=\frac{1}{8}\,md^2$$

and correspondingly

$$s=\frac{\pi^2}{16}\frac{n^2d^2}{l^2}.$$ (3.42)

For the first harmonic the frequency correction is very small if the bar length is large in comparison with its height. For the higher vibration modes, the effect of rotary inertia becomes more significant.

Figure 3.4 shows the frequency reduction owing to the influence of rotary inertia for hollow bars of the drum type. The ratio of the length of a halfwave of the elastic line to the bar diameter can serve as the criterion. If

$$\frac{l}{nd}<6,$$ (3.43)

the rotary inertia of the bar sections must be considered.

Figure 3.4. Effect of section rotary inertia on vibration frequency for hollow circular bars

If distributed masses which increase the inertial moment but do not increase the stiffness (for example, thin plates or fins) are attached to the bar, the rotary inertia must be accounted for in all cases.
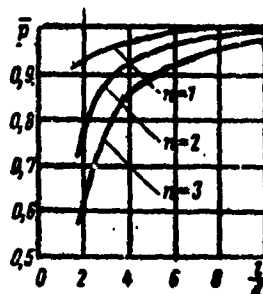
3.6. Free Vibrations of Bars in Compression and Tension

The differential equation (3.9) for compressed bars under the condition $J_c = 0$ reduces to the form

$$\frac{d^4Y}{d\xi^4} + x^2\frac{d^2Y}{d\xi^2} - k^4Y = 0; \qquad (3.44)$$

here the parameter accounting for the effect of the compressive force N is defined by the formula

$$x^2 = \frac{Nl^2}{EJ}. \qquad (3.45)$$

We obtain the frequency formula from (3.36) by means of minor transformations. After substituting (3.45) and (3.32) into this formula, we obtain the equation

$$\lambda_2^4 - \lambda_2^2\frac{Nl^2}{EJ} = \frac{m p^2 l^4}{EJ};$$

solving this equation for p, we obtain

$$p = \frac{\lambda_2^2}{l^2}\sqrt{\frac{EJ}{m}\left(1 - \frac{Nl^2}{\lambda_2^2 EJ}\right)} = \frac{\lambda_2^2}{l^2}\sqrt{\frac{EJ}{m}\left(1 - \frac{x^2}{\lambda_2^2}\right)}. \qquad (3.46)$$

3.6.1. Bar on Two Hinged Supports

For hinged supports the general integral of (3.44) reduces to the function (3.38)

$$Y(x) = \sin\lambda_2\xi,$$

where $\lambda_2 = n\pi$, which is found from the restraint conditions.

Substituting λ_2 into (3.46), we obtain

$$p = n^2\frac{\pi^2}{l^2}\sqrt{\frac{EJ}{m}\left(1 - \frac{N}{n^2 N_{cr}}\right)}, \qquad (3.47)$$

where N_{cr} — is the critical longitudinal force for the two-support bar, which is found from the formula

$$N_{cr} = \frac{\pi^2 EJ}{l^2}. \qquad (3.48)$$

The frequency for the first vibration mode (n = 1) decreases with increase of the longitudinal force N. When this force reaches the critical value, the frequency becomes equal to zero.

The longitudinal force has a similar but lesser effect on the normal vibration frequencies in the second and other higher modes; the larger n, the smaller this effect (Figure 3.5).

Formula (3.47) can be used to calculate the normal vibration frequency of filled fluid lines subjected to pressure (Figure 3.6). In this case the longitudinal force is the fluid static pressure force

$$N = \sigma f,$$

where σ — is the pressure in the line;

f — is the tubing cross section area.

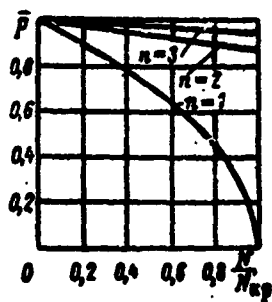

Figu 3.5. Effect of longitudinal compressive force on natural vibration frequency of two-support bar
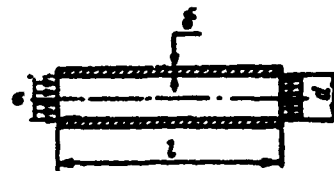

Figure 3.6. Diagram illustrating calculation of tubing vibrations

The critical force is defined by the stiffness of the tubing, and the mass per unit length is comprised of the tubing mass and the fluid mass

$$m = \rho_1 \pi d \delta + \rho f, \qquad (3.49)$$

where ρ_1 and ρ_2 — are the densities of the tubing material and the fluid, respectively;

δ — is the wall thickness.

In application to thinwall tubing, (3.47) takes the form

$$p = n^2 \frac{n^2}{l^2} \sqrt{\frac{E\delta d}{8\rho_1 \frac{\delta}{d} + 2\rho_2} \left(1 - \frac{2\sigma l^2}{n^2 \pi^2 E\delta d}\right)}. \tag{3.50}$$

This formula shows that internal pressure has a very significant effect on the line vibration frequency. This frequency is variable and depends on the operating regime, increasing in certain regimes and decreasing in others.

When the pressure in the line reaches the magnitude at which the longitudinal force becomes equal to the critical value, the line becomes unstable.

3.6.2. Compressed Cantilever Bar

The boundary conditions for the cantilever bar are defined by the equalities

1) $Y(0) = 0$; 2) $Y'(0) = 0$; 3) $Y''(1) = 0$; 4) $Q(1) = N_x \theta(1)$.

We obtain the expression for the transverse force Q in general form from (3.2). For any section we have the equality

$$Q = -\frac{d}{dx} EJ \frac{d^2Y}{dx^2} - \mu = N_x \frac{dY}{dx}. \tag{3.51}$$

For the problem in question (EJ = const; $\mu = 0$), (3.51) reduces to the form

$$\frac{EJ}{l^3}[Y'''(t) + x^2 Y'(t)] = 0. \tag{3.52}$$

In accordance with (3.52) the fourth boundary condition equality takes the form

$$Y''(1) + x^2 Y'(1) = 0. \tag{3.53}$$

Substituting the general solution of the form (3.34) into the boundary conditions, we obtain four homogeneous equations, which after obvious transformations reduce to the following characteristic equation

$$2k^4(1+\mathrm{ch}\,\lambda_1 \cos\lambda_2)+\varkappa^2(\varkappa^2\,\mathrm{ch}\,\lambda_1 \cos\lambda_2-k^2\,\mathrm{sh}\,\lambda_1 \sin\lambda_2)=0. \qquad (3.54)$$

The value of λ_2 found from this equation, when substituted into (3.46), yields the vibration frequency of a compressed bar as a function of the longitudinal force N.

If N = 0, then $\varkappa=0, \lambda_1=\lambda_2=k,$ and we obtain the case shown in Figure 3.2b. The vibration frequency decreases with increase of the compressive force N.

Let us determine the magnitude of the force for which the vibration frequency becomes equal to zero.

Setting k = 0, from (3.35) and (3.36) we obtain

$$\lambda_1=0; \ \lambda_2=\varkappa.$$

Correspondingly, (3.54) becomes

$$N=\frac{\varkappa^2 EJ}{4l^2}. \qquad (3.55)$$

hence we find that $\varkappa=\frac{\pi}{2}.$

Substitution of this result into (3.45) yields the limiting va‾ ɘ of the longitudinal force

$$\cos\varkappa=0;$$

This is the Euler critical longitudinal compressive force. Thus, when the longitudinal force reaches the critical value, the first vibration mode frequency becomes equal to zero. The other vibration mode frequencies also decrease, but to a lesser degree.

Stretched bars are calculated using (3.46). The tension force N is to be taken with reversed sign. Then the sign in the parentheses of (3.46) will be positive. This shows that a tensile force increases the normal vibration frequencies. In this case the force

N_{cr} does not cause loss of stability and is simply the scale of the tensile force acting.

For two-support bars $\lambda_2 = n\pi$. For cantilever bars λ_2 must be found from (3.54), using (3.35) and (3.36) as well. (The tensile force N is taken with minus sign.)
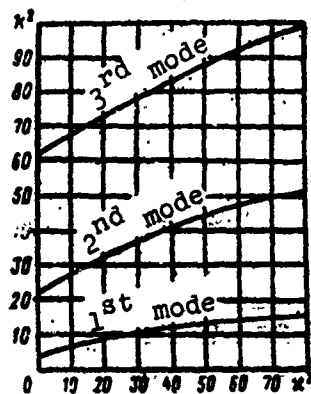

Figure 3.7. Effect of longitudinal tensile force on natural vibration frequency of two-support bar

Figure 3.7 show the increase of the free vibration frequency of a cantilever bar with increase of the tension force. We note that the tensile force has the largest effect on the first vibration mode.

3.7. Vibrations of Taut Wires and Tension Members

In engines there are a large number of stressed tensile elements — tiebolts, pins, tubes, braces, and so on. During engine operation the taut elements begin to vibrate, amplifying the general noise level and being subjected to additional stresses. In order to avoid resonant vibrations, these elements must be detuned from the operating frequencies. The limiting cases of taut elements are wires and tension braces.

The differential equation of taut wire vibrations is obtained from (3.9) if therein we set EJ = 0; J(x) = 0:

$$\frac{d}{dx}\left(N\frac{dY}{dx}\right) + mp^2Y = 0; \qquad (3.56)$$

Strictly speaking, the tensile force N depends on the taut wire deflection during vibration. The deflection of the taut wire from the rectilinear condition causes additional stretching and increase of the force N.

For small vibrations, long taut wire length, and large tension, the force increase is slight; the increase can be neglected and we can examine the vibration equation in the simpler form

$$\frac{d^2Y}{d\xi^2} + v^2Y = 0, \qquad (3.57)$$

where

$$v^2 = p^2 \frac{m}{N} l^2. \qquad (3.58)$$

The differential equation satisfies the following general solution

$$Y = C_1 \cos v\xi + C_2 \sin v\xi.$$

The boundary condition for the taut wire can be only geometric; these conditions are defined by the equalities

$$Y(0) = 0; \; Y(1) = 0,$$

accordingly

$$C_1 = 0; \; \sin v = 0;$$

he₁

$$v = \pi n. \qquad (3.59)$$

The general solution of the differential equation takes the final form

$$Y = C_2 \sin n\pi\xi, \qquad (3.60)$$

The taut wire or tension member has a multitude of free vibration modes, which differ in the number of halfwaves found within the limits of the wire length. Each mode has its own frequency, which in accordance with (3.58) and (3.59) is

$$p = n\frac{\pi}{l}\sqrt{\frac{N}{m}}. \qquad\qquad (3.61)$$

The basic vibration mode of the taut wire is the first mode, which has the lowest frequency. The vibration frequencies of all the higher modes are multiples of the frequency of the first mode.

The ratio of the tensile force to the mass per unit length of the taut wire, which appears under the radical sign, is replaced by the ratio of the wire tensile stress σ to the density ρ of the wire material. Then the fundamental frequency formula takes the form

$$p = \frac{\pi}{l}\sqrt{\frac{\sigma}{\rho}}. \qquad\qquad (3.62)$$

Since the tensile stress in the wire is limited by the material strength, each wire length has a corresponding maximal vibration frequency. The shorter the wire, the higher its fundamental frequency, and vice versa.

For tuning purposes, in . . tion to selecting the wire length and its tension, we can alter the effective density ρ. For example, for this purpose musical strings have an outer winding made from a second wire which does not operate in tension but constitutes an additional mass which is uniformly distributed along the entire length of the string. Thanks to the outer winding, excessively long strings are not required in order to obtain low-frequency vibrations.

3.8. Calculation of Bar Vibrations with Account
for Shear Deformations

Shear deformations have an influence on the natural vibration frequencies of bars when the latter are short in comparison with the cross-section dimensions.

We use well-known general relations in order to formulate the differential equation.

The bar element equilibrium conditions are defined by the equations

$$\frac{\partial M}{\partial x} = -Q; \quad \frac{\partial Q}{\partial x} = -q.$$

(3.63)

The bending deformation is characterized by rotation of the bar sections under the influence of the bending moment

$$\frac{\partial \theta_1}{\partial x} = \frac{M}{EJ}, \quad \text{where} \quad \theta_1 = \frac{\partial y_1}{\partial x};$$

(3.64)

The subscript one indicates bending deformations for which the bar cross sections remain at all times perpendicular to the bar axis.

The shear deformation from the action of the transverse force is characterized by the relative displacement of the element sections perpendicular to the bar axis without additional rotation of the sections. The connection between the shear deformations and the transverse force is given by the formula

$$\frac{\partial y_3}{\partial x} = \beta \frac{Q}{GF},$$

(3.65)

where β — is a coefficient which depends on the shape and dimensions of the bar cross section. This coefficient is calculated from the formula

$$\beta = \frac{F}{J^2} \int_{z_a}^{z_b} \frac{S^2(z)}{b(z)} \, dz.$$

(3.66)

Here F, J — are the area and moment of inertia of the bar cross section;

b(z) — is the bar width across the section;

S(z) — is the static moment of the part of the section above the coordinate z

$$S(z) = \int_{z_a}^{z_b} z b(z) \, dz;$$

(3.67)

z_a, z_b — are the distances to the extreme fibers of the section.

For the bar of rectangular cross section $\beta = 1.2$; for the round bar $\beta = 10/9$; for the round hollow thinwall bar $\beta \approx 1.5$.

The overall deflection of the bar at the section x is equal to the sum

$$y = y_1 + y_2. \tag{3.68}$$

Double differentiation and substitution of (3.64) into (3.65) leads to the equation

$$\frac{\partial^2 y}{\partial x^2} = \frac{M}{EJ} + \frac{\partial}{\partial x} \beta \frac{Q}{GF}. \tag{3.69}$$

For a bar with section which is constant along the length, further differentiation and substitution of (3.63) yields the differential equation

$$EJ \frac{\partial^4 y}{\partial x^4} + \beta \frac{EJ}{GF} \frac{\partial^4 y}{\partial x^2} - q = 0. \tag{3.70}$$

For harmonic vibrations the equation is solved by the substitution

$$y = Y(x) \cos pt;$$
$$q = -m \frac{\partial^2 y}{\partial t^2} = mp^2 Y(t) \cos pt;$$

Substitution yields

$$\frac{d^4 Y}{d\xi^4} + x^2 \frac{d^2 Y}{d\xi^2} - k^4 Y = 0, \tag{3.71}$$

where

$$k^4 = \frac{mp^2}{EJ} l^4; \quad x^2 = \beta \frac{mp^2}{GF} l^2 = k^4 \frac{EJ}{GFl^2}; \tag{3.72}$$

the equation is referred to the dimensionless coordinate $\xi = x/l$.

The general solution of the equation is

$$Y(x) = C_1 \operatorname{ch} \lambda_1 \xi + C_2 \operatorname{sh} \lambda_1 \xi + C_3 \cos \lambda_2 \xi + C_4 \sin \lambda_2 \xi. \tag{3.73}$$

Let us take the solution for the two-support beam and find the estimate of the effect of shear deformations on the frequency. The boundary conditions for this case will be

$$t = 0 \text{ and } t = 1; \quad Y(0) = Y(1) = 0; \quad Y''(0) = Y''(1) = 0;$$

the general solution corresponding to these conditions takes the form

$$\left. \begin{array}{l} Y(x) = \sin \lambda_n x; \\ \lambda_n = n\pi. \end{array} \right\} \tag{3.74}$$

Substituting this solution into the general differential equation (3.71), we obtain

$$\lambda_n^4 - \lambda_n^2 n^2 - k^4 = 0;$$

substituting herein (3.72), we obtain the frequency formula

$$p = \frac{n^2 \pi^2}{l^2} \sqrt{\frac{EJ}{m}} \sqrt{\frac{1}{1+s}}, \tag{3.75}$$

where

$$s = n^2 \pi^2 \frac{EJ}{GF l^2}; \tag{3.76}$$

the factor in the form of the second radical is the frequency correction for shear deformation. This correction is very large for short bars.

Let us find its numerical value for the hollow circular bar

$$\beta = 1, 5; \quad \frac{E}{G} = 2, 5; \quad \frac{J}{F} = \frac{1}{2} R^2.$$

Accordingly,

$$s = 1.875 \pi^2 \frac{n^2 R^2}{l^2}.$$

This formula shows that if

$$\frac{l}{2R} = 10, \text{ then } s \approx 0.05 n^2.$$

This means that as a result of shear deformation the first frequency is reduced by about 2.5%, the second by 9%, and the third by 20%.

We see from this example that shear deformations must be taken into account for a more exact calculation of the higher natural vibration frequencies.

For short bars, with length less than ten diameters, shear must also be taken into account in calculating the first frequency.

3.9. Longitudinal and Torsional Vibrations of Bars

3.9.1. Differential Equation of Longitudinal Vibrations

We obtain the longitudinal vibration differential equation by examining the equilibrium conditions and deformation of the bar element dx (Figure 3.8).

The element equilibrium equation will obviously be

$$\frac{\partial N}{\partial x}dx + qdx = 0. \qquad (3.77)$$

The element relative deformation at this moment equals

$$\varepsilon = \frac{N}{EF}.$$

The relative deformation is also determined by the difference of the displacements of the element sections

$$\delta y = \left(y + \frac{\partial y}{\partial x}dx\right) - y;$$

from this difference we determine ε as the ratio

$$\varepsilon = \frac{\delta y}{dx} = \frac{\partial y}{\partial x}.$$

Figure 3.8. Diagram illustrating derivation of equation of bar longitudinal vibrations

Equating the expressions for the relative deformations, we obtain

$$N = EF\frac{\partial y}{\partial x}. \qquad (3.78)$$

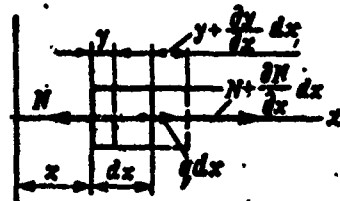Substituting (3.78) into (3.77), we obtain

$$\frac{\partial}{\partial x} EF \frac{\partial y}{\partial x} + q = 0. \qquad (3.79)$$

During vibration the inertia force is a distributed load

$$q = -m \frac{\partial^2 y}{\partial t^2}.$$

After substituting this expression into (3.79), we obtain the general differential equation for bar longitudinal vibrations

$$\frac{\partial}{\partial x} EF \frac{\partial y}{\partial x} - m \frac{\partial^2 y}{\partial t^2} = 0. \qquad (3.80)$$

The equation is solved by the substitution

$$y = Y(x) \cos pt, \qquad (3.81)$$

after which it becomes the vibration mode equation

$$\frac{d}{dx} EF \frac{dY}{dx} + m p^2 Y = 0. \qquad (3.82)$$

If EF does not change along the length of the bar, the equation transforms to the form

$$\frac{d^2 Y}{dx^2} + v^2 Y = 0, \qquad (3.83)$$

where

$$v^2 = \frac{m p^2}{EF} l^2. \qquad (3.84)$$

3.9.2. Longitudinal Vibrations of Uniform Bars

The general solution of (3.83) is expressed by the function

$$Y(x) = C_1 \cos v\xi + C_2 \sin v\xi. \qquad (3.85)$$

Boundary conditions are necessary in order to define the constants C_1 and C_2. The simplest and most widely used conditions are:

1) clamped bar end ($Y = 0$);

2) free bar end ($N = 0$), which in accordance with (3.78) becomes the equality $Y' = 0$.

Figure 3.9 shows various forms of bar restraint and the corresponding vibration modes.

The vibration modes, i.e., the amplitudes of the longitudinal vibrations of the bar sections, are represented by sinusoids or cosinusoids. In all cases an integral number of halfwaves fall within the limits of the span. The number of vibrations nodes is one less than the mode number; the only exception to this rule is the free bar. The free bar, having one extra degree of freedom, has one node more for all the vibration modes.
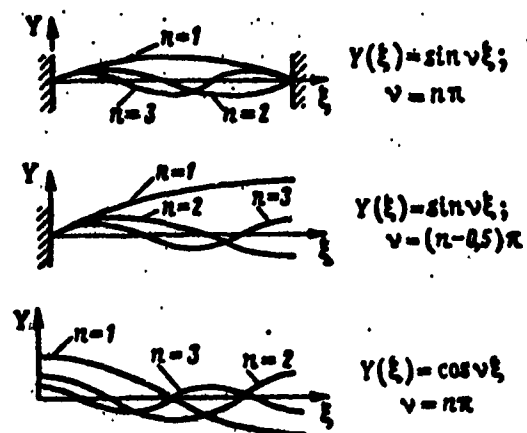

Figure 3.9. Longitudinal vibration modes for different bar end fixity conditions

The vibration frequencies are found from the general formula

$$p = \frac{v}{l}\sqrt{\frac{EF}{m}} = \frac{v}{l}\sqrt{\frac{E}{\varrho}}, \qquad (3.86)$$

where ρ is the material density.

This formula was obtained from (3.84); the values of the frequency coefficients v as a function of the type of constraint are shown in Figure 3.9.

The vibration frequencies of the clamped-clamped bar and the free bar are the same. For the different vibration modes the frequencies are related as the integers $1 : 2 : 3$, i.e., they form an arithmetic progression series with difference equal to the fundamental frequency.

The vibration frequencies of a bar clamped at one end lie in the interval for the frequencies of the bar clamped at both ends.

Formula (3.86) shows that the bar natural longitudinal vibration frequency depends only on its length and material properties and is independent of the magnitude of the cross section.

3.9.3. Longitudinal Vibrations of Compressible Fluid in Lines

We isolate in the line an elementary volume (Figure 3.10)

Equilibrium of the element is defined by the equation

$$-\frac{\partial p}{\partial x} = \varrho \frac{\partial^2 y}{\partial t^2}, \qquad (3.87)$$

which represents equality of the inertia force of the element and the axial force of the gas pressure on the element.

The pressure distribution along the line length and in time is related with the change of the element volume.

At the initial time the element volume equals $V = Fdx$, and the gas pressure is p_0. During the time δt the element moves the distance y and its volume changes by the amount $dV =$ $F \frac{dy}{dx} dx$; the pressure becomes equal to p.
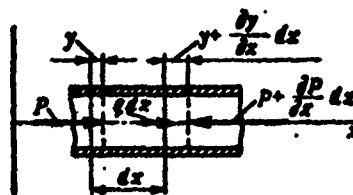
Figure 3.10. Diagram illustrating derivation of equation of longitudinal vibrations of gas in tubing

The change of the state of the gas inside the elementary volume in question can be considered to be adiabatic, since the volume changes with a high rate with a small pressure change. Therefore, the pressure change is determined by the adiabatic equation

$$p_0 V^n = p(V + dV)^n;$$

hence we obtain

$$p = p_0 \frac{1}{\left(1 + \frac{\partial y}{\partial x}\right)^n}; \qquad (3.88)$$

we differentiate (3.88)

$$\frac{\partial p}{\partial x} = -k p_0 \frac{\frac{\partial^2 y}{\partial x^2}}{\left(1 + \frac{\partial y}{\partial x}\right)^{k+1}}.$$

The denominator of this formula differs very little from one; therefore the derivative can be written in the simpler form

$$\frac{\partial p}{\partial x} = -k p_0 \frac{\partial^2 y}{\partial x^2}. \tag{3.89}$$

Substituting (3.89) into (3.87), we obtain the wave operation

$$a^2 \cdot \frac{\partial^2 y}{\partial x^2} = \frac{\partial^2 y}{\partial t^2}, \tag{3.90}$$

where a is the speed of sound in the gas filling the line

$$a^2 = kgRT^\circ.$$

Equation (3.90) is solved by the Fourier substitution

$$y = Y(x)T(t). \tag{3.91}$$

After substitution it separates into two equations

$$\left.\begin{array}{l} \ddot{T} + \lambda^2 T = 0; \\ Y'' + \nu^2 Y = 0, \end{array}\right\} \tag{3.92}$$

where λ is the vibration frequency; ν is a parameter, equal to

$$\nu = l \frac{\lambda}{a}. \tag{3.93}$$

The general solution of (3.90), corresponding to the solutions of (3.92), is obtained in the form

$$y = (C_1 \cos \nu\xi + C_2 \sin \nu\xi)(\cos \lambda t + A \sin \lambda t); \tag{3.94}$$

for the initial conditions

$$t = 0, \quad y = Y(x), \quad \dot{y} = 0$$

the solution simplifies

$$y = (C_1 \cos \nu\xi + C_2 \sin \nu\xi) \cos \lambda t. \tag{3.95}$$

For a line segment with both ends closed, the boundary conditions are the equalities

$$\xi=0; \; Y=0; \; \xi=1; \; Y=0;$$

substituting herein (3.95), we obtain

$$C_1=0, \; \sin v=0;$$

hence

$$v=n\pi.$$

In accordance with (3.93) the frequency of the longitudinal gas vibrations in a closed line is

$$\lambda=n\pi\frac{a}{l}, \qquad (3.96)$$

i.e., the vibration frequency decreases with increase of the line length and is proportional to the speed of sound in the gaseous medium, i.e., it depends on the gas properties and temperature.

The vibration period for the lowest frequency (n = 1) is

$$\tau=\frac{2\pi}{\lambda}=\frac{2l}{a}; \qquad (3.97)$$

the vibration period equals the time during which the pressure wave travels the distance along the tube to the end and back.

For the higher modes

$$\tau=\frac{2l}{na}; \qquad (3.98)$$

this is the time for the wave to travel between the nodal sections.

The longitudinal vibration function for the closed tube will be

$$y=C_2 \sin v\xi \cos \lambda t, \qquad (3.99)$$

where C_2 is the wave crest amplitude.

For a tube open at one end the boundary conditions will be

$$\xi=0, \; Y=0; \; \xi=1, \; \frac{dY}{dx}=0. \qquad (3.100)$$

This equality shows that, because of the invariability of the pressure at the open end of the tube, there is no change of the elementary volume at this end.

In accordance with the conditions (3.100), the general solution (3.95) yields

$$C_1 = 0; \quad \nu = \frac{\pi}{2}(2n - 1); \tag{3.101}$$

the vibration frequency is

$$\lambda = \frac{\pi}{2}(2n - 1)\frac{a}{l}, \tag{3.102}$$

The vibration frequency of gas in an open tube is lower than in a closed tube of the same length; for the first gas vibration mode in open and closed tubes of the same length the frequencies differ from one another by a factor of two.

The displacement of the gas particles during vibrations in an open tube is determined by the solution

$$y = C_2 \sin \nu \xi \cos \lambda t. \tag{3.103}$$

The longitudinal vibrations of uniform bars and gas in tubes are described by the same equations and are defined by the same solutions. Among these, the frequency formulas (3.86) and (3.96) are identical, since the speed of sound in metals equals

$$a = \sqrt{\frac{E}{\varrho}}. \tag{3.104}$$

In other words, small disturbances in the metals, just as in a gas, propagate with the speed of sound. Depending on the nature of the disturbance and the end conditions, in the bar there is formed either a traveling wave, which is reflected from the opposite end and returns to the initial point, or standing longitudinal vibration waves.

3.9.4. Torsional Vibrations

The differential equation for torsional vibrations is also the wave equation. It can be obtained directly from (3.80) by replacing the linear factors by angular factors

$$\frac{\partial}{\partial x} G J_0 \frac{\partial \varphi}{\partial x} - \rho J_0 \frac{\partial^2 \varphi}{\partial t^2} = 0, \qquad (3.105)$$

where J_0 — is the section torsional moment of inertia;

ρ — is the material density;

ϕ — are angular displacements.

For uniform bars (3.105) becomes the previously examined wave equation

$$\frac{\partial^2 \varphi}{\partial t^2} + v^2 \varphi = 0, \qquad (3.106)$$

where

$$v^2 = \frac{\rho \ell^2}{G} p^2. \qquad (3.107)$$

The solutions discussed previously for longitudinal vibrations are applicable in form and meaning for torsional vibrations as well. Therefore we shall not repeat these formulas.

We simply note that the shear deformation propagation velocity is defined by the relation

$$a = \sqrt{\frac{\sigma}{\rho}}; \qquad (3.108)$$

In accordance with the elastic modulus G, this velocity is less than that for longitudinal deformations.

3.10. General Properties of Small Natural Vibration Modes of Bars and Beams

3.10.1. Orthogonality condition of natural vibration forms

The orthogonality condition is a consequence of the work reciprocity theorem. According to this theorem, the work of the free vibration inertia forces of the mode j on displacements of another vibration mode ν is equal to the work of the inertia forces of mode ν on displacements of mode j.

The natural vibrations of modes j and ν are defined by the functions

$$y_j(x, t) = Y_j(x)\cos(p_j t + \beta_j);$$
$$y_\nu(x, t) = Y_\nu(x)\cos(p_\nu t + \beta_\nu).$$

The work reciprocity equation for the elementary time segment dt will be

$$p_j^2 \int m(x)Y_j(x)\cos(p_j t + \beta_j)\, y_\nu(x, t)\, dt\, dx =$$

$$= p_\nu^2 \int m(x)Y_\nu(x)\cos(p_\nu t + \beta_\nu)\, y_j(x, t)\, dt\, dx.$$

Substituting herein the vibration mode functions and taking outside the integral sign the factors which are not functions of x, we obtain

$$p_j^2 p_\nu \cos(p_j t + \beta_j)\sin(p_\nu t + \beta_\nu)\, dt \int m(x)Y_j(x)Y_\nu(x)\, dx =$$

$$= p_\nu^2 p_j \cos(p_\nu t + \beta_\nu)\sin(p_j t + \beta_j)\, dt \int m(x)Y_\nu(x)Y_j(x)\, dx;$$

Since the products preceding the integrals are not equal to one another, the equation is satisfied as a result of vanishing of the integral

$$\int m(x)Y_j(x)Y_\nu(x)\, dx = 0. \qquad (3.109)$$

This is the orthogonality condition for the bar natural vibration modes.

3.10.2. Norming the Vibration Mode Functions

The normed deflection is the function which satisfies the equation

$$\int m(x)u_j^2(x)dx = 1. \tag{3.110}$$

In order to normalize a known deflection function, obtained to an arbitrary scale, it is multiplied by the constant number N_j, which is called the norming factor

$$u_j(x) = N_j Y_j(x);$$

substitution of this relation into (3.110) yields the formula for finding the norming factor

$$N_j^2 \int m(x)Y_j^2(x)dx = 1. \tag{3.111}$$

3.10.3. Theorem on Number of Natural Vibration Nodes

The proofs of the theorem follow from the orthogonality condition. They are presented in special courses on vibration theory. We shall present only the theorem content which is of practical importance.

For single-span bars or beams, the number of nodes of the nth order normal mode is one less than the order number. The first vibration mode is always nodeless.

The theorem on the number of nodes remains valid for bars with any number of static indeterminacies, including multi-support beams. Hinged supports are not considered nodes. The coincidence of a node of one of the vibration modes with a hinged support is a particular case. Such a situation can occur in special problems and is ensured by selection of a definite location for the hinged support.

Systems which have a single static degree of freedom (for example, those shown in Figure 3.11a) do not have the first, nodeless, vibration mode. For these systems the equations of equilibrium of the forces and moments are not satisfied for vibrations in the first mode. The lowest vibration mode for these systems is the single-node mode, i.e., the second mode.

If a system has two static degrees of freedom (see, for example, Figure 3.11b), it will not have either the first or second vibration modes. The lowest mode will be the third — the two-node mode.
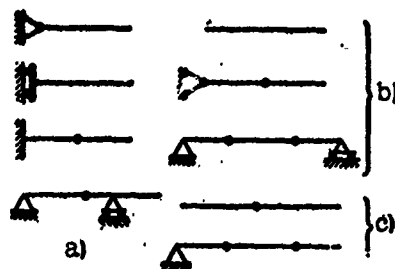

Figure 3.11. Diagram illustrating determination of the number of vibration mode nodes of systems with static degrees of freedom:

a, b, c) systems with one, two, and three degrees of freedom, respectively

In general, the number of missing lower vibration modes of a system equals the number of static degrees of freedom.

3.11. Approximate Methods for Determining Bar and Beam Natural Vibration Frequencies and Modes

Exact solutions of the differential equations of vibrations of bar elements with mass distributed continuously along their length are known only for a limited number of the simplest cases. The majority of practical vibration problems are solved by approximate methods. The Ritz, Rayleigh, and Bubnov-Galerkin variational methods are widely used. The integral method is quite effective. The initial parameter method and the discrete model method, which is based on the principles of the initial parameter methods, and also the successive approximation method in discrete form have been developed and applied quite successfully recently.

The development of the approximate computational methods is associated particularly with the use of digital computers. The latter make possible considerable increase of the precision and reliability of the calculations, but the most important aspect of digital computer use is that they have made it possible to carry out engineering calculations of systems which were previously not amenable to calculation. However, the use of the digital computer requires further development and improvement of the computational methods.

3.11.1. Ritz Method

The Ritz method is a very widely used technique for vibration analysis of complex beams and bars. This method makes it possible to obtain quite high computational accuracy with comparatively little expenditure of time. The computational formulas for the Ritz method follow from the expression for the Ostrogradskiy-Hamilton action functional

$$S = \int_{t_A}^{t_B} (T - \Pi)\,dt.$$

(3.112)

In solving a problem by the Ritz method, there is no need to formulate the differential equation of motion, but it is necessary to examine carefully the internal energy balance during the vibrations, formulating the expressions for the kinetic T and potential Π energies.

According to the Ostrogradskiy-Hamilton principle, of all the possible infinitely close paths for the system to transfer from position A to position B, that path is realized for which the action functional (3.112) has the minimal value.

For transverse bar vibrations, the kinetic and potential energies of the bar are defined by the formulas

$$T = \frac{1}{2} \int_0^l m(x) \left(\frac{\partial y}{\partial t}\right)^2 dx;$$

$$\Pi = \frac{1}{2} \int_0^l EJ(x) \left(\frac{\partial^2 y}{\partial x^2}\right)^2 dx.$$

Substituting these formulas into (3.112), we obtain the action functional in the form

$$S = \frac{1}{2} \int_{t_A}^{t_R} \int_0^l \left[m(x)\left(\frac{\partial y}{\partial t}\right)^2 - EJ(x)\left(\frac{\partial^2 y}{\partial x^2}\right)^2 \right] dx\, dt. \tag{3.113}$$

We substitute into (3.113) the harmonic vibration function

$$y(x, t) = Y(x)\cos pt.$$

After integrating with respect to time for the interval $(t_R - t_A)$, equal to the vibration period $T = 2/p$, the functional takes the form

$$S = \frac{\pi}{2p} \int_0^l \left[m(x) p^2 Y^2(x) - EJ(x) Y''^2(x) \right] dx, \tag{3.114}$$

where the double prime denotes second derivative with respect to x.

If $Y(x)$ is an exact function of the natural vibration mode, then $S = 0$, since the expression in the brackets is the difference of the maximal kinetic and potential energies for an elementary segment of the beam. As we know, this difference equals zero for the entire beam.

If we substitute into (3.114) the function $\phi(x)$, representing approximately the vibration mode, the functional will not equal zero. Of the entire family of functions $\phi(x)$, which are associated with the parameters embedded in $\phi(x)$, the closest to the exact expression will be that for which the functional has the minimal value.

We represent $\phi(x)$ as the sum

$$\phi(x) = \sum_{i=1}^{n} a_i \psi_i(x), \tag{3.115}$$

where α_i — are the parameters of the function;

ψ_i — are linearly independent functions, each of which is a possible beam deflection mode during vibration. Each of the functions must satisfy the geometric boundary conditions;

FTD-HC-23-780-70   132

n — is the number of separate functions, which must be minimal; this is associated with the accuracy of the computation.

Substituting (3.115) into (3.114) and equating the derivatives with respect to each of the parameters to zero, we obtain a system of linear and homogeneous equations in α_i

$$\int [m(x)p^2\varphi(x)\varphi_s(x)-EJ(x)\varphi''(x)\varphi_s''(x)]dx=0, \quad s=1,\ 2,\ldots,n. \tag{3.116}$$

In differentiating with respect to α_s, we use the usual sequence

$$\frac{\partial}{\partial\alpha_s}(\varphi^2)=\frac{\partial}{\partial\varphi}(\varphi^2)\frac{\partial\varphi}{\partial\alpha_s}=2\varphi(x)\varphi_s(x);$$

similarly

$$\frac{\partial}{\partial\alpha_s}(\varphi'')^2=\frac{\partial}{\partial\varphi''}(\varphi'')^2\frac{\partial\varphi''}{\partial\alpha_s}=2\varphi''(x)\varphi_s''(x).$$

Since $\phi(x)$ and $\phi''(x)$ are sums of the functions $\psi_i(x)$ and $\psi_i''(x)$, if we take α_i outside the integral sign we can write (3.116) in the form of the sum

$$\sum_{i=1}^{n}\alpha_i\left[p^2\int m(x)\varphi_i(x)\varphi_s(x)dx-\int EJ(x)\varphi_i''(x)\varphi_s''(x)\,dx\right]=0. \tag{3.117}$$

The system contains n equations, one for each subscript s; each equation consists of n terms, one for each subscript i.

We denote

$$T_{is}=\int m(x)\varphi_i(x)\varphi_s(x)dx; \tag{3.118}$$

$$\Pi_{is}=\int EJ(x)\varphi_i''(x)\varphi_s''(x)dx. \tag{3.119}$$

The coefficients have the reciprocity property

$$T_{is}=T_{si}; \quad \Pi_{is}=\Pi_{si}.$$

Equations (3.117) are written in the form

$$\sum_{i=1}^{n} a_i [p^2 T_{is} - \Pi_{is}] = 0, \quad s = 1, 2, \ldots, n.$$ (3.120)

Forming the determinant of (3.120) and equating it to zero, we obtain the frequency equation in Ritz form

$$\begin{vmatrix} p^2 T_{11} - \Pi_{11} & p^2 T_{12} - \Pi_{12} & \cdots \\ p^2 T_{21} - \Pi_{21} & p^2 T_{22} - \Pi_{21} & \cdots \\ \cdots & \cdots & \cdots \end{vmatrix} = 0.$$ (3.121)

The roots of (3.121) are the natural vibration frequencies with some excess. The frequency of the first vibration mode is determined with a high degree of precision, while the subsequent frequencies are defined with decreasing precision.

The larger the number of terms of the minimizing function $\phi(x)$, the more accurately the natural vibration frequencies are determined and the larger the number of roots which are evaluated as a result of the calculation.

Formula (3.118) for the kinetic energy coefficient takes into account only the kinetic energy of the mass of the bar itself. If there are any additional distributed or concentrated masses on the bar, then (3.118) must be supplemented.

For example

$$T_{is} = \int_0^l m(x) \phi_i(x) \phi_s(x) \, dx + \int_{x_1}^{x_2} \mu(x) \phi_i(x) \phi_s(x) \, dx + m_a \phi_i(a) \phi_s(a),$$

where $\mu(x)$ — is the distributed mass attached to the bar and located in the limits from x_1 to x_2;

m_a — is the mass concentrated at the point with coordinate $x = a$.

Similar arguments are also valid with regard to the potential energy coefficient. Formula (3.119) accounts for the potential energy of deformation of the bar only. If the bar supports are elastic or there are additional elastic elements within the limits of the span — for example, elastic hinges — then (3.119) must be

supplemented with the corresponding terms accounting for the potential energy of the deformation of these elements. For example, in the case of elastic supports we must take

$$\Pi_{ts} = \int_0^l EJ(x)\ddot{\psi}_i(x)\ddot{\psi}_s(x)\,dx + c_A\psi_i(x_A)\psi_s(x_A) + c_B\psi_i(x_B)\psi_s(x_B),$$

where c_A and c_B — are the stiffnesses of the supports located at the points with coordinates x_A and x_B.

The action of the additional elements may affect the selection of the minimizing function $\phi(x)$ as well as the formulas for the coefficients. In the case of concentrated masses this function must include terms defining the deflection of the bar from the action of the concentrated forces. In the case of elastic supports, the displacement and angle of rotation of the bar axis must be introduced.

If the minimizing function $\phi(x)$ is represented by a single term, then only the upper diagonal element remains in the Ritz frequency equation (3.121). Equating this element to zero and solving for p_2, we obtain the Rayleigh formula

$$p^2 = \frac{\int_0^l EJ(x)[\psi''(x)]^2\,dx}{\int_0^l m(x)\psi^2(x)\,dx}.$$

The function $\psi(x)$ must satisfy the geometric boundary conditions and must reflect as accurately as possible the assumed vibration mode.

In order to use the variational principle, we must introduce into the function the free parameter α. As a result of the presence of the parameter, the minimizing function $\psi(x, \alpha)$ will be a family of homogeneous curves. By varying the parameter α, we select its value so as to obtain a minimal value of the frequency from the Rayleigh formula. This value will be closest to the true value.

For example, for a clamped
cantilever beam the following
functions can be selected

$$\psi(x) = x^a \quad \text{or} \quad \psi(x) = x^2 - a x^3.$$

In practice the determination
of the minimum value of the fre-
quency is accomplished by select-
ing α and constructing a graph
of $p(\alpha)$ using the Rayleigh formula
(Figure 3.12). This graph yields
p_{min} and the value of the para-
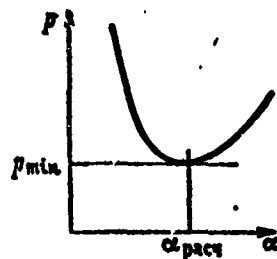meter α which defines the deflection function (x, α).

Figure 3.12. Minimizing
parameter of the Rayleigh
method

3.11.2. Vibrations of Blade of Variable Section with Account for the Action of Centrifugal Forces

Let us consider a blade of wedge shape which has a linear varia-
tion of the section along the length (Figure 3.13). The variation
of the mass per unit length and
section moment of inertia along
the blade length are defined by
the relations

$$m(x) = m_0 \left(1 - \frac{x}{L}\right);$$

$$J(x) = J_0 \left(1 - \frac{x}{L}\right)^3 . \qquad (3.122)$$

where m_0 and J_0 — are the mass
and section
moment of iner-
tia at the base
of the blade.
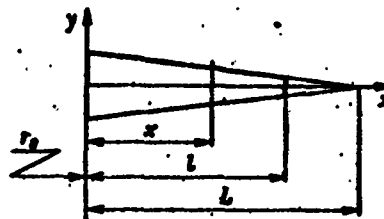
Figure 3.13. Diagram illus-
trating analysis of tapered
blade

Let us first examine the effect of taper on the natural vibra-
tion frequency without account for the action of the centrifugal
forces.

We take a two-term minimizing function

$$\varphi(x) = a_1 \xi^2 + a_2 \xi^2 (1-\xi), \quad \xi = \frac{x}{L}. \qquad (3.123)$$

The functions satisfy the geometric boundary conditions at the clamped end.

We calculate the coefficients (3.118) and (3.119) for the Ritz frequency equation

$$
\left.
\begin{aligned}
T_{11} &= m_0 L \int_0^{\xi_l} (1-\xi)\,\xi^4 d\xi = m_0 L \xi_l^5 \left(\frac{1}{5} - \frac{1}{6}\xi_l \right); \\
T_{12} &= m_0 L \int_0^{\xi_l} (1-\xi)^2 \xi^4 d\xi = m_0 L \xi_l^5 \left(\frac{1}{5} - \frac{1}{3}\xi_l + \frac{1}{7}\xi_l^2 \right); \\
T_{22} &= m_0 L \int_0^{\xi_l} (1-\xi)^3 \xi^4 d\xi = m_0 L \xi_l^5 \left(\frac{1}{5} - \frac{1}{2}\xi_l + \right. \\
&\qquad \left. + \frac{3}{7}\xi_l^2 - \frac{1}{8}\xi_l^3 \right);
\end{aligned}
\right\} \qquad (3.124)
$$

$$
\left.
\begin{aligned}
\Pi_{11} &= \frac{1}{L^3} EJ_0 4 \int_0^{\xi_l} (1-\xi)^3 d\xi = \frac{1}{L^3} EJ_0 [1 - (1-\xi_l)^4]; \\
\Pi_{12} &= \frac{1}{L^3} EJ_0 4 \int_0^{\xi_l} (1-\xi)^3 (1-3\xi)\, d\xi = \Pi_{11} + \\
&\qquad + \frac{1}{L^3} EJ_0 \frac{3}{5}[(1-\xi_l)^4 (1+4\xi_l)-1]; \\
\Pi_{22} &= \frac{1}{L^3} EJ_0 4 \int_0^{\xi_l} (1-\xi)^3 (1-3\xi)^2 d\xi = 2\Pi_{12} - \Pi_{11} + \\
&\qquad + \frac{36}{L^3} EJ_0 \xi_l^3 \left(\frac{1}{3} - \frac{3}{4}\xi_l + \frac{3}{5}\xi_l^2 - \frac{1}{6}\xi_l^3 \right).
\end{aligned}
\right\} \qquad (3.125)
$$

These formulas show that the Ritz coefficients depend on the relative blade length; the vibration frequency also depends on the blade length.

For a full wedge $\xi_l = 1$ the coefficients take the values

$$T_{11} = \frac{1}{30} m_0 L; \quad T_{12} = \frac{1}{105} m_0 L; \quad T_{22} = \frac{1}{280} m_0 L; \quad \Pi_{11} = \frac{EJ_0}{L^3};$$

$$\Pi_{12} = \Pi_{22} = 0.4 \frac{EJ_0}{L^3}.$$

Substitution of these coefficients into the determinant (3.121) after calculation yields the frequency formula

$$p = \frac{5.3187}{L^2} \sqrt{\frac{EJ_0}{m_0}}.$$

The exact value of the frequency coefficient, obtained by Kirchhoff, is 5.315. The error of the approximate solution amounts to 0.07%.

Assuming values of the relative length ξ_l less than one, calculating the coefficients (3.124), (3.125), and solving the Ritz determinant, we obtain the natural vibration frequency for a blade made in the form of a truncated wedge.

The frequency formula for these cases can be written in the general form

$$p = \frac{k^2}{l^2} \sqrt{\frac{EJ_0}{m_0}}.$$

The notation k^2 for the frequency coefficient is retained — the same as for beams of constant section.

The values of k^2 are shown in Figure 3.14 as a function of the taper ratio, which is expressed by the ratio of the blade cross-section areas at the tip and at the root. The taper provides an increase of the natural vibration frequency of up to 54%.

The centrifugal forces, acting parallel to the centerline (Figure 3.15), restrict deflection of the blade from this position. This action leads to increase of the blade natural vibration frequencies, and this increase becomes significant at high wheel rotational speeds ω.
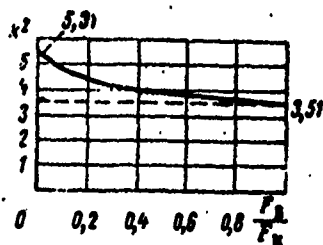
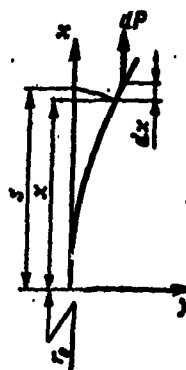Figure 3.14. Frequency co-efficients of tapered blade

Figure 3.15. Diagram illustrating calculation of blade deformation energy in centrifugal force field

The deformation energy of a blade on a rotating wheel is greater than on a stationary wheel. To the potential energy of elastic deformation there is added the displacement energy of the blade elements in the radial direction. Although this displacement, caused by blade bending, is small, the work of the inertial forces of this displacement must be taken into account.

To calculate the work of the centrifugal forces we find the blade element displacement in the radial direction. For the section x this displacement equals the difference of the length of the curved blade centerline and its projection on the x axis

$$s - x = \int_0^x dx \sqrt{1 + \left(\frac{dy}{dx}\right)^2} - x.$$

In view of the smallness of the quantity dy/dx, we replace the radical by its expansion

$$s - x = \int_0^x \left[1 + \frac{1}{2} (Y')^2 \right] dx - x =$$

$$= \frac{1}{2} \int_0^x (Y')^2 dx.$$

The additional energy is calculated as the centrifugal force work integral of the elementary blade segments

$$\Pi_\omega = \int_0^l (s-x)\,dP = \frac{1}{2}\int_0^l m(x)\,r\omega^2\,dx \int_0^x (Y')^2(x)\,dx,$$

where

$$r = r_0 + x.$$

In accordance with this formula, the addition to the potential energy coefficient (3.119) is determined by the formula

$$\Pi_{is}^\omega = \int_0^l m(x)\,r\omega^2\,dx \int_0^x \psi_i'(x)\,\psi_s'(x)\,dx. \qquad (3.126)$$

For the assumed section distribution law (3.1?2) and the minimizing function (3.123), the coefficients Π_{1s}^ω will be

$$\left.\begin{array}{l}
\Pi_{11}^\omega = m_0 r_0 \omega^2 \dfrac{4}{3}\left(\dfrac{1}{4}\,\xi_1^4 + \dfrac{b}{5}\,\xi_1^5 - \dfrac{c}{6}\,\xi_1^6\right); \\[2mm]
\Pi_{12}^\omega = \Pi_{11}^\omega - m_0 r_0 \omega^2 \dfrac{3}{2}\left(\dfrac{1}{5}\,\xi_1^5 + \dfrac{b}{6}\,\xi_1^6 - \dfrac{c}{7}\,\xi_1^7\right); \\[2mm]
\Pi_{22}^\omega = 2\Pi_{12}^\omega - \Pi_{11}^\omega + 0{,}9\left(\dfrac{1}{6}\,\xi_1^6 + \dfrac{b}{7}\,\xi_1^7 - \dfrac{c}{8}\,\xi_1^8\right),
\end{array}\right\} \qquad (3.127)$$

where

$$r = r_0\left(1 + \frac{x}{r_0}\right) = r_0(1 + c\xi);$$

$$b = c - 1; \quad c = \frac{L}{r_0}.$$

The frequency equation (3.121) with account for (3.127) takes the form

$$\begin{vmatrix}
p^2 T_{11} - (\Pi_{11} + \Pi_{11}^\omega) & p^2 T_{12} - (\Pi_{12} + \Pi_{12}^\omega) & \cdots \\
p^2 T_{12} - (\Pi_{12} + \Pi_{12}^\omega) & p^2 T_{22} - (\Pi_{22} + \Pi_{22}^\omega) & \cdots \\
\cdots & \cdots & \cdots
\end{vmatrix} = 0. \qquad (3.128)$$

Calculation of the frequency using (3.128) after substituting therein the coefficients (3.127) again leads to the formula

$$p_\omega = \frac{\varkappa}{l^2}\sqrt{\frac{EJ_0}{m_0}},$$

but here the coefficient k^2 depends on the rotational speed. Figure 3.16 shows the variation of this coefficient as a function of the dimensionless centrifugal force parameter κ^2

$$x^2 = \frac{m_0 r_0 l^2}{EI_0} \omega^2.$$ (3.129)

This parameter is proportional to ω^2; its value is also proportional to the stress in the blade. The quantity $\kappa^2 = 20$ corresponds, for the usual blade dimensional relations, to a centrifugal force stress equal to 1600 - 2000 kgf/cm^2 (for steel blades). We see in Figure 3.16 that the frequency increase with change of κ^2 from zero to 20 for blades of both types is very significant. For the tapered blade the frequency increases by nearly a factor of two, and for the blade of constant section it increases by more than two times. The blade of the latter type is more sensitive to the action of the centrifugal forces and shows a larger frequency increase — both relative and absolute.

The blade incidence angle relative to the wheel plane of rotation (Figure 3.17) has a large influence on the blade vibration frequencies. Since $\beta \neq 0$, as the blade bends in the vibration plane there appear transverse forces
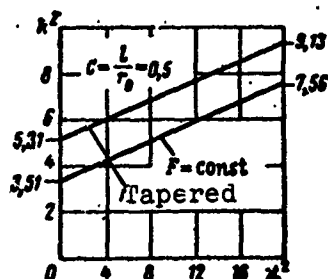

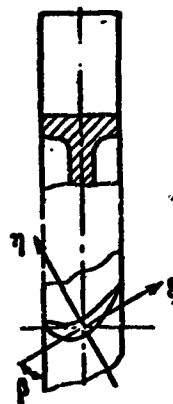Figure 3.16. Blade frequency coefficients as a function of rotor rpm

Figure 3.17. Diagram illustrating the influence of blade incidence angle on its vibration frequency

distributed along the blade length like the projection of the centrifugal forces

$$dP_y = m(x) Y(x) \omega^2 \sin \beta \, dx;$$

During bending these forces perform work, which must be added to the kinetic energy. The work of the transverse inertial force equals

$$T_\omega = \frac{1}{2} \int_0^l Y(x) \sin \beta \, dP_y = \frac{1}{2} \int_0^l m(x) Y^2(x) \omega^2 \sin^2 \beta \, dx;$$

in accordance with this formula the addition to the kinetic energy coefficients (3.118) is defined by the expression

$$T_{i s}^* = \omega^2 \sin^2 \beta \int_0^l m(x) \psi_i(x) \psi_s(x) \, dx.$$

Comparing this expression with Formula (3.118), we see that it differs from (3.118) by the constant factor $\omega^2 \sin^2 \beta$

$$T_{i s}^* = \omega^2 T_{i s} \sin^2 \beta. \qquad (3.130)$$

Therefore the Ritz frequency equation (3.128) can be written as

$$\begin{vmatrix} p_{\omega_0}^2 T_{11} - (\Pi_{11} + \Pi_{11}^*) & p_{\omega_0}^2 T_{12} - (\Pi_{12} + \Pi_{12}^*) & \dots \\ p_{\omega_0}^2 T_{12} - (\Pi_{12} + \Pi_{12}^*) & p_{\omega_0}^2 T_{22} - (\Pi_{22} + \Pi_{22}^*) & \dots \\ \dots & \dots & \dots \end{vmatrix} = 0. \qquad (3.131)$$

Here

$$p_{\omega_0}^2 = p_{\omega_\beta}^2 + \omega^2 \sin^2 \beta; \qquad (3.132)$$

p_{ω_0} — is the natural vibration frequency for zero incidence angle ($\beta = 0$);

p_{ω_β} — is the natural vibration frequency of a blade set at the angle β.

The resulting form (3.131) of the frequency equation shows that no additional calculations need be made in order to calculate the frequencies of a blade set at the angle β. The frequencies found from (3.131) are to be considered as the natural vibration frequencies in the axial plane of the rotating wheel, $\beta = 0$. If a blade

is set at the angle β its natural vibration frequencies are reduced because of the action of the additional transverse forces. The correction is found using (3.132).

When p_{ω_0} and ω are comparable quantities, the incidence angle β can have a significant effect on the change of the natural vibration frequency. For β ≠ 0 the frequency increase owing to wheel rotation will be less than shown in Figure 3.16 for zero incidence angle.

Blade heating during operation reduces its natural vibration frequency.

If the heating takes place uniformly along the entire blade length, all its frequencies are reduced in proportion to the square root of the reduction of the elastic modulus of the material

$$\frac{p_t}{p} = \sqrt{\frac{E_t}{E}}. \qquad (3.133)$$

In connection with the change of the operating temperatures, the reduction of the elastic modulus of the refractory materials lies in the range up to 20 − 25%. This means that the blade natural vibration frequencies may decrease 12 − 15% as a result of the temperature effect during engine operation.

If the blade is heated nonuniformly, (3.133) becomes invalid. The blade natural vibration frequencies depend on the nature of the temperature distribution along the blade length. A complete calculation must be carried out to determine the frequencies of a non-uniformly heated blade.

In this case the temperature distribution along t.e blade length and the associated variation of the elastic modulus E must be represented in the form of functions of the x coordinate. Then the product EJ(x) in (3.119) will be a general function of the stiffness along the blade length, and the coefficient Π_{1s} calculated in this case will account for the temperature variability. Further calculation using (3.121) yields the natural vibration frequencies of the nonuniformly heated blade.

3.11.3. Bubnov-Galerkin Method

The basis of this method are the Ostrogradskiy-Hamilton principles. The Bubnov-Galerkin variational equation for problems on bar vibrations is obtained on the basis of the general differential equation (3.9). The latter, as we know, is the equation of equilibrium of the transverse forces applied to an elementary segment of the bar.

We shall analyze this method using the general equation for the bar

$$\frac{d^2}{dx^2} EJ \frac{d^2Y}{dx^2} - mp^2 Y = 0.$$

The exact solution $Y(x)$ causes the left side of the equation to vanish. This solution is the form of bar free vibrations, taking place without participation of external forces.

If in place of the exact solution we substitute into the equation the approximate value of the function $\phi(x)$, the left side will not equal zero. It becomes the function $f(x)$

$$\frac{d^2}{dx^2} EJ \frac{d^2\phi}{dx^2} - mp^2\phi = f(x). \qquad (3.134)$$

The function $f(x)$ is the difference between the elastic force and the inertia force applied to an element of the bar.

If we form the integral

$$\int f(x)\phi(x)\,dx,$$

it will be the additional work which must be expended on deformation of the bar during vibrations in the $\phi(x)$ mode.

It follows from the Galerkin method that we can select the deflection function $\phi(x)$ so that it will be orthogonal to the force function $f(x)$. Then the additional work of deformation will be zero

$$\int f(x)\phi(x)\,dx = 0. \qquad (3.135)$$

Under these conditions the function $\phi(x)$ satisfies the energetic conditions for free vibrations without participation of an external input, but the energy balance is satisfied on the average for the entire bar. For the individual elements, the deformation potential energy of the element will not be equal to its kinetic energy.

We replace f(x) in (3.135) in accordance with (3.134)

$$\int_0^l \left[\frac{d^2}{dx^2} EJ \frac{d^2\varphi(x)}{dx^2} - mp^2\varphi(x) \right] \varphi(x)dx = 0. \qquad (3.136)$$

We represent the deflection function $\phi(x)$ in series form

$$\varphi(x) = a_1\psi_1(x) + a_2\psi_2(x) + \ldots + a_n\psi_n(x). \qquad (3.137)$$

Each term of the series is a suitable function, satisfying all the boundary conditions of the problem.

The coefficients α_1 are the parameters of the function $\phi(x)$ and are selected so as to satisfy the Condition (3.135) and the equivalent Equation (3.136).

We require that each of the functions $\psi_1(x)$ be orthogonal to the function f(x). Then the Condition (3.135) is satisfied termwise and on the whole. In this case (3.136) becomes the system of equations

$$\int_0^l \left[\frac{d^2}{dx^2} EJ \frac{d^2\varphi(x)}{dx^2} - mp^2\varphi(x) \right] \psi_i(x)dx = 0, \quad i = 1, 2, \ldots, n. \qquad (3.138)$$

These equations are called the Bubnov-Galerkin equations. They are linear in the unknown coefficients α_1 and are homogeneous.

We substitute (3.137) into (3.138)

$$\sum_{s=1}^n a_s \int_0^l \left[\frac{d^2}{dx^2} EJ \frac{d^2\psi_s(x)}{dx^2} - mp^2\psi_s(x) \right] \psi_i(x)dx = 0, \quad i = 1, 2, \ldots, n. \qquad (3.139)$$

We denote

$$W'_{si} = \int_0^l \frac{d^2}{dx^2} EJ \frac{d^2 \psi_s(x)}{dx^2} \psi_i(x)dx;$$ (3.140)

$$T_{si} = \int_0^l m\psi_s(x)\psi_i(x)dx;$$ (3.141)

then (3.139) takes the form

$$\sum_{s=1}^{n} a_s(W'_{si} - p^2 T_{si}) = 0.$$ (3.142)

Since the system of equations is homogeneous, its determinant must equal zero

$$\begin{vmatrix} W_{11} - p^2 T_{11} & W_{12} - p^2 T_{12} & \cdots \\ W_{21} - p^2 T_{21} & W_{22} - p^2 T_{22} & \cdots \\ \cdots & \cdots & \cdots \end{vmatrix} = 0.$$ (3.143)

We have obtained the frequency equation in the Bubnov-Galerkin form. If the number of terms of the Series (3.137) is sufficiently large and the functions themselves are selected properly with regard to the free vibration modes, the Galerkin frequency equation makes it possible to find the first few natural vibration frequencies, but this involves the necessity to solve a high-order determinant.

In practice the use of two or three terms in the Galerkin method permits calculation with high accuracy of the first vibration frequency and mode, and calculation with less accuracy of the second vibration mode.

To construct the vibration mode with the aid of the Series (3.137) we must determine the coefficients a_1. The latter are found as the minors to the elements of any row of the determinant (3.143).

In the Bubnov-Galerkin method the functions (3.140) and (3.141) and the frequency Equation (3.143) can be formulated not only on the basis of the Equation (3.133), but also on the basis of more general equations, which contain the friction forces and the disturbing forces. This broadens considerably the possibilities of the Bubnov-Galerkin method in comparison with the Ritz and Rayleigh

methods and makes it possible to solve problems on forced vibrations of systems with friction.

Example 3.1. Find the natural vibration frequency of a blade of variable section. The cross section areas and moments of inertia are specified by functions in polynomial form

$$F = (1 - a_1\xi + a_2\xi^2)\, F_0;$$
$$J = (1 - a_1\xi + a_2\xi^2)^3\, J_0.$$

The coefficients a_1 and a_2 are determined by the blade geometry. In the present example: $a_1 = 1.2$; $a_2 = 0.6$.

We find the first vibration mode frequency by the Galerkin method. We choose the blade bending function in polynomial form

$$\varphi = \xi^2 \left(1 - \frac{2}{3}\xi + \frac{1}{6}\xi^2\right).$$

The polynomial coefficients are selected so that the bending function satisfies all the boundary conditions. In this case the natural vibration frequency is defined by the relation

$$p^2 = \frac{W_{11}}{T_{11}},$$

where W_{11} and T_{11} are calculated using (3.140), (3.141):

$$W_{is} = \int_0^l (EJ\varphi_i'')^{''} \varphi_s\, dx = \int_0^l EJ\varphi_i''\varphi_s''\, dx;$$
$$T_{is} = \int_0^l m(x)\, \varphi_i\varphi_s\, dx.$$

Since we take the solution in the form of a single function, then $i = s = 1$. We calculate the coefficients, assuming that $x = \xi l$:

$$W_{11} = \frac{EJ_0}{l^3} \int_0^1 (1 - a_1\xi + a_2\xi^2)^3 (2 - 4\xi + 2\xi^2)^2\, d\xi = 0,486\, \frac{EJ_0}{l^3};$$

$$T_{11} = \rho l F_0 \int_0^1 (1 - a_1\xi + a_2\xi_2)\left(1 - \frac{2}{3}\xi + \frac{1}{6}\xi^2\right)^2 \xi^4\, d\xi = 0,028\rho l F_0;$$

$$p = \frac{4,16}{l^2}\sqrt{\frac{EJ_0}{\rho F_0}}.$$

To appraise the accuracy of this solution we form a minimizing function of two terms

$$\varphi = a_1 \psi_1(\xi) + a_2 \psi_2(\xi);$$

$$\psi_1(\xi) = \xi^2 \left(1 - \frac{2}{3}\xi + \frac{1}{6}\xi^2\right);$$

$$\psi_2(\xi) = \xi^3(1 - \xi + 0.3\xi^2);$$

both basis functions satisfy all the boundary conditions.

We use the formulas presented above to calculate the missing coefficients of the Galerkin determinant

$$W_{12} = \frac{EJ_0}{l^3} \int_0^1 (1 - a_1\xi + a_2\xi^2)^3 (2 - 4\xi + 2\xi^2)(6\xi - 12\xi^2 + 6\xi^3)\, d\xi =$$

$$= 0.164 \frac{EJ_0}{l^3};$$

$$W_{22} = \frac{EJ_0}{l^3} \int_0^1 (1 - a_1\xi + a_2\xi^2)^3 (6\xi - 12\xi^2 + 6\xi^3)^2\, d\xi = 0.1056 \frac{EJ_0}{l^3};$$

$$T_{12} = \varrho l F_0 \int_0^1 (1 - a_1\xi + a_2\xi^2)\left(1 - \frac{2}{3}\xi + \frac{1}{6}\xi^2\right)(1 - \xi + 0.3\xi^2)\xi^5\, d\xi =$$

$$= 0.0149 \varrho l F_0;$$

$$T_{22} = \varrho l F_0 \int_0^1 (1 - a_1\xi + a_2\xi^2)(1 - \xi + 0.3\xi^2)^2 \xi^6\, d\xi = 0.006 \varrho l F_0.$$

From these coefficients we form the frequency equation in Bubnov-Galerkin form in accordance with (3.143)

$$\begin{vmatrix} 0.466 - 0.028\,x & 0.164 - 0.0149x \\ 0.164 - 0.0149x & 0.1056 - 0.006x \end{vmatrix} = 0,$$

where

$$x = \frac{\varrho F_0}{F J_0} l^4 p^2;$$

Expanding the determinant, we obtain the quadratic equation

$$x^2 - 427.597x + 5237.286 = 0.$$

We note that the calculation of the coefficients of the Bubnov-Galerkin equation should be carried out with high precision, since in solving the quadratic equation for the first frequency we must determine the small difference of large numbers

$$x = 213,7985 \pm 201,1778;$$
$$x_1 = 12,62; \quad x_2 = 415. \quad \cdot \cdot$$

In accordance with the resulting solutions, the first and second natural frequencies are defined by the formulas

$$p_1 = \frac{3,55}{2}\sqrt{\frac{EJ_0}{\varrho F_0}}; \quad p_2 = \frac{20,35}{l^2}\sqrt{\frac{EJ_0}{\varrho F_0}}.$$

Comparing the coefficient 3.55 of the frequency formula with the coefficient 4.16 obtained previously, we conclude that the calculation of the first vibration mode frequency on the basis of only the single function $\psi_1(\xi)$ gives a larger error in comparison with the second, more exact solution.

The ratio of the coefficients α_1 and α_2 of the minimizing function ϕ is determined as the ratio of the minors (elements in the present case) of the Bubnov-Galerkin determinant

$$\frac{\alpha_1}{\alpha_2} = \frac{0,1056 - 0,0008x}{-(0,164 - 0,0149x)}.$$

For the first vibration mode ($x_1 = 12.62$) this ratio will be

$$\frac{\alpha_1}{\alpha_2} = 0,197.$$

Setting $\alpha_2 = 1$, in accordance with the previously selected basis function, we obtain the equation for the first vibration mode

$$\varphi(\xi) = 0,197\left(1 - \frac{2}{3}\xi + \frac{1}{6}\cdot\xi^2\right)\xi^2 + (1 - \xi + 0,3\xi^2)\xi^3;$$
$$\varphi(\xi) = (0,197 + 0,868\xi - 0,967\xi^2 + 0,3\xi^3)\xi^2.$$

For the second vibration mode ($x_2 = 415$)

$$\frac{\alpha_1}{\alpha_2} = -0,535.$$

The second vibration mode function will be:

$$\varphi(\xi) = (-0,535 + 1,356\xi - 1,089\xi^2 + 0,3\xi^3)\xi^2.$$

149

3.11.4. Initial Parameter Method

Usually, in practical calculations the bar, beam, or blade being analyzed, with a section which is variable along the length, is specified by the dime ·'ons of the individual sections, located by the coordinates relative to the initial section. In these cases it is not possible to formulate the Bubnov-Galerkin or Ritz functional because of the absence of any given functional dependence of the section dimensions on their coordinates.

It is more rational to make the vibration analysis of such bars by the initial parameter method. To this end we divide the bar into individual segments, which are taken to be segments of constant section (Figure 3.18). The relationship between the parameters of the beginning and end of the segment is formulated for each segment. In so doing the parameters of the beginning section — displacement, section rotation angle, bending moment and shearing force in the section — are considered to be known, while the parameters at the end of the segment are the unknowns.
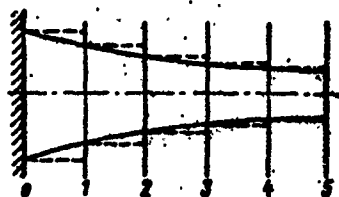
Figure 3.18. Schematization of bar for calculation by initial parameter method

The connection between the parameters of the beginning and end of the segment is constructed with the aid of the general solution of the vibration equation for a beam of constant section

$$Y_{(\kappa)} = C_1 S_{(\kappa l)} + C_2 T_{(\kappa l)} + C_3 U_{(\kappa l)} + C_4 V_{(\kappa l)};$$

the parameter k for a given segment is determined by the formula

$$k^4 = \frac{m l^3}{EJ} \Omega,$$

where l — is the segment length;

m — is the average mass per unit length of the segment;

J — is the moment of inertia of the initial section of the

segment, assumed constant within the limits of the
entire segment;

p — is the unknown vibration frequency.

The constants C_1, C_2, C_3, C_4 are found from the given initial
parameters. Taking $\xi = 0$, using well-known formulas we obtain

$$C_1 = Y_0; \quad C_2 = \frac{1}{\alpha}\theta_0; \quad C_3 = \frac{M_0}{\alpha^2 EJ}; \quad C_4 = -\frac{Q_0}{\alpha^3 EJ},$$

$$\alpha = k/L$$

With the aid of the general solution and the values of the
coefficients written out above, we write the expressions for the
parameters at the end of the segment ($\xi = 1$):

$$Y_{(k)} = Y_0 S_{(k)} + \frac{1}{\alpha}\theta_0 T_{(k)} + \frac{M_0}{\alpha^2 EJ} U_{(k)} - \frac{Q_0}{\alpha^3 EJ} V_{(k)};$$

$$\theta_{(k)} = \alpha Y_0 V_{(k)} + \theta_0 S_{(k)} + \frac{M_0}{\alpha EJ} T_{(k)} - \frac{Q_0}{\alpha^2 EJ} U_{(k)};$$

$$M_{(k)} = EJ\left[\alpha^2 Y_0 U_{(k)} + \alpha\theta_0 V_{(k)} + \frac{M_0}{EJ} S_{(k)} - \frac{Q_0}{\alpha EJ} T_{(k)}\right];$$

$$Q_{(k)} = -EJ\left[\alpha^3 Y_0 T_{(k)} + \alpha^2\theta_0 U_{(k)} + \alpha\frac{M_0}{EJ} V_{(k)} - \frac{Q_0}{EJ} S_{(k)}\right].$$

It is not difficult to see that the parameters of the end of
the segment are expressed with the aid of the parameters of the
beginning of the segment.

The resulting system of equalities is written in matrix form

$$P_{ki} = L_i P_{0i}, \tag{3.144}$$

where:
the segment matrix is

$$L_i = \begin{vmatrix} S_{(k)} & \frac{1}{\alpha} T_{(k)} & \frac{1}{\alpha^2 EJ} U_{(k)} & -\frac{1}{\alpha^3 EJ} V_{(k)} \\ \alpha V_{(k)} & S_{(k)} & \frac{1}{\alpha EJ} T_{(k)} & -\frac{1}{\alpha^2 EJ} U_{(k)} \\ \alpha^2 EJU_{(k)} & \alpha EJV_{(k)} & S_{(k)} & -\frac{1}{\alpha} T_{(k)} \\ -\alpha^3 EJT_{(k)} & -\alpha^2 EJU_{(k)} & -\alpha V_{(k)} & S_{(k)} \end{vmatrix}; \tag{3.145}$$

The column matrices of the parameters of the end and beginning of the segment are

$$P_{kl} = \begin{vmatrix} Y_{(k)} \\ \vartheta_{(k)} \\ M_{(k)} \\ Q_{(k)} \end{vmatrix}; \qquad P_{0l} = \begin{vmatrix} Y_0 \\ \vartheta_0 \\ M_0 \\ Q_0 \end{vmatrix}. \qquad (3.146)$$

To obtain the product of the matrices, we must multiply the elements of the first column of the matrix L_1 by the first element of the matrix P_{10}. Similarly, the second column is multiplied by the second element, the third column by the third element, and so on. Then all the products must be combined row-by-row; we obtain the column P_{k1}.

The parameters of the end of the preceding segment are at the same time the parameters of the beginning of the next segment. Therefore the parameters of the end of the last segment are associated with the parameters of the beginning of the first segment by the matrix product

$$P_{kn} = L_n L_{n-1} \ldots L_2 L_1 P_{01}. \qquad (3.147)$$

The parameters of the beginning of the first segment are determined by the bar end restraint conditions. They are expressed by the following columns for the hinged support, built-in support, and the free end

$$\begin{vmatrix} 0 \\ \vartheta_0 \\ 0 \\ Q_0 \end{vmatrix}; \qquad \begin{vmatrix} 0 \\ 0 \\ M_0 \\ Q_0 \end{vmatrix}; \qquad \begin{vmatrix} Y_0 \\ \vartheta_0 \\ 0 \\ 0 \end{vmatrix}.$$

More complex cases will be shown in section 4.6.

We see from the contents of the matrix P_{01} that two of the four parameters equal zero, and the other two are unknowns and will appear in all the products. Therefore the bar end matrix P_{kn} will be a column of binomials with multipliers of the remaining initial parameters θ_0, Q_0, or M_0, Q_0, or Y_0, θ_0.

The frequency p is determined by trial and error. We specify the frequency p and use the formulas presented above to calculate the parameters k_i, α_i of the segments and formulate all the matrices L_i. After this we perform sequential matrix multiplication and determine the parameters P_{kn}.

In accordance with the bar end restraint conditions, two of the resulting parameters must be equal to zero. This yields two homogeneous equations of the form (for the free end)

$$M_{kn} = a_1\theta_0 + a_2 Q_0 = 0; \\ Q_{kn} = b_1\theta_0 + b_2 Q_0 = 0, \quad \Big\}$$

(3.148)

where a_1, a_2, b_1, b_2 — are numerical coefficients

We formulate and calculate the determinant of the equations

$$\Delta = a_1 b_2 - a_2 b_1.$$

For the natural frequency the determinant must be equal to zero. If this does not occur in the calculation, we must specify a different frequency p and repeat the entire calculation until the determinant does equal zero.

The initial parameter method permits calculating the higher vibration modes as well as the first mode. If the entire bar is divided into a sufficiently large number of segments, this method makes it possible to obtain high computational accuracy. An attempt must be made to ensure that the moments of inertia of the sections of adjacent segments differ by no more than 10 — 15%.

The drawback of this computational method is the necessity for reformulation of the matrices of all the segments for each specification of the frequency p, since the parameters k_i and α_i change. This leads to a large volume of computational operations and presents difficulties in applying the method for hand computation and when using a large number of small segments. The method is very effective when using electronic computers.

3.11.5. Discrete Model Method

This method is based on replacing the actual bar of variable section by a multimass dynamically equivalent system with a finite number of degrees of freedom (Figure 3.19).

To construct the discrete model we divide the bar into several segments. The mass of each segment is concentrated at its center of gravity and is considered to be a point mass.

The bar segment connecting the sections at which the point masses are located is considered to be a weightless segment of constant section. If the section change along the segment length is significant, the segment must be subdivided into several subsegments of constant section.

The number of segments into which the entire bar must be divided depends on the number of vibration modes to be calculated. In order to obtain high computational accuracy the general criterion limiting the segment length should be the inequality (see [16])

$$\frac{EI_i}{m_i l_i^4} > \omega^2, \qquad (3.149)$$

where ω — is the largest value
      of the frequencies
      being calculated.

Comparing the general criterion with the formula for the frequency of the beam of constant section, we obtain a simpler inequality for the maximal acceptable relative segment length

$$\frac{l_i}{L} < \frac{1}{k_j},$$

where k_j — is the frequency coefficient of the highest vibration mode being calculated.
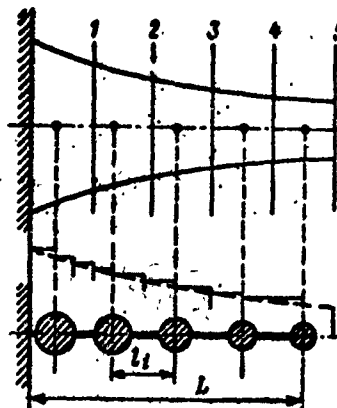

Figure 3.19. Schematization of bar in discrete model form

Using the frequency coefficients for the beam of constant section, we find that for the calculation of the first beam vibration mode it is sufficient to divide the beam into three segments. For the calculation of the first two modes, the number of segments should be 5 — 6; for the calculation of the third mode, 8 — 10 should be used.

The calculation of the natural vibration frequency of the discrete model is made using the initial parameter method. To this end we formulate the relationships between the parameters of the beginning and end of the elastic segments and the parameter change upon passing through a mass.

The connection between the parameters of the beginning and end of the weightless segment of a bar of constant section is determined on the basis of the polynomial

$$Y_{(\kappa)} = C_1 + C_2\xi + C_3\xi^2 + C_4\xi^3, \qquad (3.150)$$

which is the general solution of the differential equation of bending for a beam of constant section.

The coefficients C_1, C_2, C_3, C_4 are determined from the given segment initial parameters Y_0, θ_0, M_0, Q_0, acting in the section $\xi = 0$

$$C_1 = Y_0; \quad C_2 = l_i\theta_0; \quad C_3 = \frac{l_i^2}{2EJ}M_0; \quad C_4 = -\frac{l_i^3}{6EJ}Q_0.$$

The corresponding parameters of the end of the segment will be

$$Y_{(\kappa)} = Y_0 + l_i\theta_0 + \frac{l_i^2}{2EJ}M_0 - \frac{l_i^3}{6EJ}Q_0;$$

$$\theta_{(\kappa)} = \theta_0 + \frac{l_i}{EJ}M_0 - \frac{l_i^2}{2EJ}Q_0;$$

$$M_{(\kappa)} = M_0 - l_iQ_0;$$

$$Q_{(\kappa)} = Q_0.$$

In matrix form this system of equalities is written in the product form

$$P_{\kappa i} = L_i P_{6 i}. \qquad (3.151)$$

where the matrix of the weightless elastic segment is written as

$$L_i = \begin{vmatrix} 1 & l_i & \dfrac{l_i^2}{2EJ_i} & -\dfrac{l_i^3}{6EJ_i} \\ 0 & 1 & \dfrac{l_i}{EJ_i} & -\dfrac{l_i^2}{2EJ_i} \\ 0 & 0 & 1 & -l_i \\ 0 & 0 & 0 & 1 \end{vmatrix}. \qquad (3.152)$$

If the segment between the point masses is divided into subsegments, then the connection between the parameters of the beginning and end of the stepped weightless segment is found as the product

$$P_{ki} = L_i' L_i'' L_i''' P_{0i}, \qquad (3.153)$$

where L'_1, L''_1, L'''_1 — are the subsegment matrices, analogous to that presented above.

The parameters of the beginning of a segment located after a point mass are connected with the parameters of the end of the segment ahead of the mass by the matrix form

$$P_{0(i+1)} = M_i P_{ki}, \qquad (3.154)$$

where the point mass matrix is

$$M_i = \begin{vmatrix} 1 & 0 & 0 & 0 \\ 0 & 1 & 0 & 0 \\ 0 & 0 & 1 & 0 \\ -m_i p^2 & 0 & 0 & 1 \end{vmatrix}; \qquad (3.155)$$

here m_i — is the magnitude of the point mass.

The matrix is formulated under the conditions that the displacement Y, section rotation angle θ, and bending moment M do not change upon passing through the mass, and the shearing force after the mass is determined from the condition of equilibrium of the forces acting on the mass from the left and right and the inertia force.

As a result of the calculation the parameters P_{kk} of the end of the last segment are connected with the parameters of the beginning of the first segment as the matrix product

$$P_{hh} = M_n L_n M_{n-1} L_{n-1} \ldots M_1 L_1 P_{01}. \qquad (3.156)$$

The calculation of the discrete system is made by the trial and error method, as discussed in Section 3.11.4.

Example 3.2. Analyze a blade whose geometry is defined by sections, and the section areas and moments of inertia are given in Table 3.2.

TABLE 3.2.

Section No.	Section relative coordinates	F/F_0	J/J_0
0	0	1.00	1.00
1	0.2	0.784	0.480
2	0.4	0.616	0.235
3	0.6	0.496	0.122
4	0.8	0.424	0.076
5	1.0	0.400	0.064

Here F_0, J_0 — are, respectively, the area and moment of the blade root section.

The given sections define the division of the blade into five parts of equal length (Figure 3.20), which is sufficient for calculating the first two vibration modes.

We determine the mass of the segments using the formula

$$m_i = \frac{1}{2} \varrho \left(\frac{F_i}{F_0} + \frac{F_{i+1}}{F_0} \right) F_0 0.2 l.$$

where ρ, l — are the material density and blade length, respectively.

We obtain

i	1	2	3	4	5
$\dfrac{m_i}{\varrho F_0 l}$	0,1784	0,14	0,112	0,092	0,0824

The centers of gravity of
the segments do not coincide with
their midpoints, but this dis-
crepancy amounts to only 1 — 2%
of the segment length. There-
fore, to simplify the calculation
we concentrate the masses at
points located at the midpoint
of the segments. After this we
obtain a new division of the
blade length into segments
located between the masses. The
first segment has the length 0.11;
the remaining segments have the length 0.21 cach. We assume that
the segments have constant stiffness and section moment of inertia
equal to the moment of inertia of the average section of the seg-
ment. These will be the given sections 1, 2, 3, 4 (see Figure 3.20).

Figure 3.20. Schematization
of bar designed.

The segment lengths are linearly related with the overall
blade length l; the section moments of inertia and masses m_1 are
proportional to J_0 and F_0 of the root section. Therefore the blade
vibration frequency is defined by the formula

$$p = \frac{k^2}{l^2}\sqrt{\frac{EJ_0}{\varrho F_0}}.$$

where k^2 — is the frequency coefficient, characteristic for the
given blade geometry and having a different value for
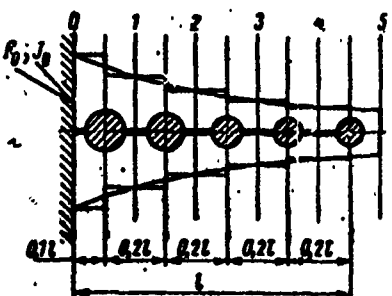each vibration mode.

We take in the calculation $E = 1$, $J_0 = 1$; $l = 1$; $\rho = 1$; $F_0 = 1$.

Then $p = k^2$ and the result of the calculation will be the frequency coefficient, suitable for calculating the entire family of similar blades.

For the assumed unit values of the blade parameters, we use (3.152) to formulate the segment matrices, which are entered in the corresponding locations of the computational table (see Table 3.3). Taking $p^2 = 12$, we use (3.155) to formulate the matrices of the point masses, which are also entered in the computational table. The root section has the initial parameters

$$Y_0 = 0; \quad \theta_0 = 0; \quad M_0 \neq 0; \quad Q_0 \neq 0.$$

The calculation of the blade end parameters is made by the two-calculation method. In the first calculation, the column matrix is taken with a one in the third place, i.e., in the place of the first unknown

$$P_{01} = [0, 0, 1, 0].$$

The entire table is calculated using this matrix. To do this, we multiply the columns of the matrix L_1 by the like elements of the column matrix P_{01}, and after combining the products row-by-row we obtain the parameters P_{k1} of the end of the segment. We multiply these parameters, in turn, by the mass matrix columns, and after combining we obtain the parameters P_{02} of the beginning of the next segment. At the end of the calculations, we obtain the coefficients

$$P_{kk}^{(M)} = [1{,}63677; \quad \ldots \ 565; \ 1{,}37082; \ -2{,}86809].$$

In the second calculation the one is taken in the fourth place, i.e., in the place of the second unknown. After making the second calculation of the table, we obtain the coefficients

$$P_{kk}^{(Q)} = [-0{,}644724; \ -3{,}443938; \ -0{,}981721; \ +1{,}940322].$$

TABLE 3.3. TABLE OF COEFFICIENTS M_0 FOR $p^2 = 12$

P_{01}	Matrix of segment L_1				P_{91}	Matrix of mass M_1				P_{91}
0	1	0.1	$0.5 \cdot 10^{-2}$	$-0.1667 \cdot 10^{-3}$	$0.5 \cdot 10^{-2}$	1	0	0	0	$0.5 \cdot 10^{-2}$
0	0	1	0.1	$0.5 \cdot 10^{-2}$	0.1	0	1	0	0	0.1
-1	0	0	1	0.1	1	0	0	1	0	1
	0	0	0	1	0	-2.1408	0	0	1	$-1.07 \cdot 10^{-3}$

P_{02}	Matrix of segment L_2				P_{92}	Matrix of mass M_2				P_{02}
$0.5 \cdot 10^{-2}$	1	0.2	$4.1669 \cdot 10^{-2}$	$-2.7778 \cdot 10^{-3}$	$6.6695 \cdot 10^{-2}$	1	0	0	0	$6.6695 \cdot 10^{-2}$
0.1	0	1	0.4167	$4.1669 \cdot 10^{-2}$	0.5171	0	1	0	0	0.5171
1	0	0	1	0.2	1.0022	0	0	1	0	1.0022
$-1.07 \cdot 10^{-2}$	0	0	0	1	$-1.07 \cdot 10^{-2}$	-1.64	0	0	1	-0.1228

P_{03}	Matrix of segment L_3				P_{93}	Matrix of mass M_3				P_{04}
$6.6695 \cdot 10^{-2}$	1	0.2	$8.5106 \cdot 10^{-2}$	$-0.5673 \cdot 10^{-2}$	$25.6101 \cdot 10^{-3}$	1	0	0	0	$25.6101 \cdot 10^{-2}$
0.5171	0	1	0.6511	$8.5106 \cdot 10^{-2}$	1.3904	0	1	0	0	1.3904
1.0021	0	0	1	0.2	1.0267	0	0	1	0	1.0267
-0.12278	0	0	0	1	-0.1228	-1.3584	0	0	1	-0.4706

P_{04}	Matrix of segment L_4				P_{94}	Matrix of mass M_4				P_{05}
$25.6101 \cdot 10^{-3}$	1	0.2	0.1639	$-1.0926 \cdot 10^{-2}$	0.70564	1	0	0	0	0.7054
1.3904	0	1	1.6393	0.1639	3.07127	0	1	0	0	3.07127
1.0267	0	0	1	0.2	1.12062	0	0	1	0	1.12062
-0.4706	0	0	0	1	-0.47063	-1.104	0	0	1	-1.24966

P_{05}	Matrix of segment L_5				P_{95}	Matrix of mass M_5				$P_{10}^{(4)}$
0.70564	1	0.2	0.26346	$-1.7543 \cdot 10^{-2}$	1.63677	1	0	0	0	1.63677
3.07127	0	1	2.63157	0.26316	6.34965	0	1	0	0	6.34965
1.12062	0	0	1	0.2	1.37082	0	0	1	0	1.37082
-1.24966	0	0	0	1	-1.24966	-0.9988	0	0	1	-2.95909

The parameters at the end of the blade are represented in the form of sums of the results of the two calculations

$$Y_k = 1.63677 M_0 - 0.844724 Q_0;$$
$$\theta_k = 6.34965 M_0 - 3.443938 Q_0;$$
$$M_k = 1.37082 M_0 - 0.981721 Q_0;$$
$$Q_k = -2.86809 M_0 + 1.940323 Q_0.$$

The boundary conditions for the end of the blade are $M_k = 0$; $Q_k = 0$. Equating the last two equalities to zero, we check their determinant

$$\Delta = 1.37082 \cdot 1.940323 - 2.86809 \cdot 0.981721 = -0.155584.$$

The determinant is not equal to zero; therefore we assume a different value $p^2 = 13$ and repeat the computation.

As a result we obtain

$$\Delta = 1.404285 \cdot 2.380299 - 3.150771 \cdot 1.042695 = 0.084355.$$

The zero value of the determinant occurs for a value of p^2 between 12 and 13. Interpolating, we obtain

$$p^2 = 12.65; \quad k^2 = p = 3.557.$$

To construct the vibration mode, after determining the value of p^2 and calculating for this value all the coefficients of the computational tables, we determine the ratio Q_0/M_0. This can be done using the third or fourth equality of the end parameters, which for $p^2 = 12.65$ are represented by the equalities

$$M_k = 1.39257 M_0 - 1.021354 Q_0 = 0;$$
$$Q_k = -3.035473 A_0 + 2.226831 Q_0 = 0.$$

From either equation we obtain

$$\frac{Q_0}{M_0} = 1.36.$$

The deflections of the ends of the segments, from which the vibration mode is constructed, are calculated from the data in the first line of the computational tables as the sums

$$Y_{\kappa i} = Y_{\kappa i}^{(M)} + \frac{Q_0}{M_0} Y_{\kappa i}^{(Q)}.$$

The calculation of the second vibration mode is made similarly.

3.11.6.   Integral Method.

The integral method of successive approximations for bars and beams with distributed mass is constructed on the basis of the general differential equation. We examine the equation

$$\frac{d^2}{dx^2}\left[EJ(x)\frac{d^2Y(x)}{dx^2}\right] = m(x)p^2Y(x).$$

Performing the integration within the limits of a segment, where the functions m(x), Y(x), EJ(x) are continuous, we obtain sequentially

$$-Q(x) = \frac{d}{dx}EJ(x)\frac{d^2Y(x)}{dx^2} = p^2\int_0^x m(x)Y(x)dx + C_1; \qquad (3.157)$$

$$M(x) = EJ(x)\frac{d^2Y(x)}{dx^2} = p^2\iint_0^{xx} m(x)Y(x)dx^2 + C_1x + C_2; \qquad (3.158)$$

$$\frac{dY(x)}{dx} = p^2\int_0^x \frac{1}{EJ(x)}\left[\iint_0^{xx} m(x)Y(x)dx^2 + \frac{1}{p^2}(C_1x + C_2)\right]dx + C_3; \qquad (3.159)$$

$$Y(x) = p^2\iint_0^{xx} \frac{1}{EJ(x)}\left[\iint_0^{xx} m(x)Y(x)dx^2 + \right.$$
$$\left. + \frac{1}{p^2}(C_1x + C_2)\right]dx^2 + C_3x + C_4. \qquad (3.160)$$

The constants of integration are found from the given boundary conditions at the ends of the segment.

The Equation (3.160) is the integral equation of the vibration modes. It is satisfied by the function Y(x), which is the exact expression for the natural vibration mode with account for all the boundary conditions. Here the right side of the equation, written in integral form on the basis of the function Y(x), is proportional to the function itself. The coefficient of proportionality is the square of the natural vibration frequency for the given node.

The integral equation (3.160) is written in abbreviated form as

$$Y(x) = p^2 K(Y),$$

where $K(Y)$ — is an integral operator which includes the set of constants of integration.

We formulate the system of successive approximations

$$\left.\begin{array}{l} \varphi^{(1)}(x) = K\,[\varphi^{(0)}]; \\ \varphi^{(2)}(x) = K\,[\varphi^{(1)}]; \\ \cdot\;\cdot\;\cdot\;\cdot\;\cdot\;\cdot\;\cdot\;\cdot \\ \varphi^{(n)}(x) = K\,[\varphi^{(n-1)}], \end{array}\right\} \qquad (3.162)$$

where $\phi^{(0)}(x)$ — is some initial function approximating the vibration mode. To shorten the calculations it is desirable that this function satisfy the geometric boundary conditions;

$\phi^{(1)}(x)$ — is the first approximation of the vibration mode and is a function satisfying all the boundary conditions.

The successive approximations are constructed using the cyclic rule.

We form the ratio of the last two approximations

$$\frac{\varphi^{(n-1)}(x)}{\varphi^{(n)}(x)} = \frac{K[\varphi^{(n-2)}(x)]}{K[\varphi^{(n-1)}(x)]}. \qquad (3.163)$$

Let us find the value of this ratio. To do this we write the initial function in the form of an eigenmode expansion

$$\varphi^{(0)}(x) = \varkappa_1 u_1(x) + \varkappa_2 u_2(x) + \varkappa_3 u_3(x) + \ldots, \qquad (3.164)$$

where $u_j(x)$ — are the normed natural vibration mode functions of the bar;

$\varkappa_j$ — are the expansion coefficients.

We write the first approximation on the basis of (3.164)

$$\varphi^{(1)}(x) = K\left[\sum_{j=1}^{\infty} \varkappa_j u_j(x)\right]. \qquad (3.165)$$

Since each of the functions is the exact solution of the integral
equation (3.161), we can make the replacement

$$K\{u_j(x)\} = \frac{1}{p_j^2} u_j(x);$$

then the first approximation (3.165) is written in the form

$$\varphi^{(1)}(x) = \sum_{j=1}^{\infty} x_j \frac{u_j(x)}{p_j^2}. \tag{3.166}$$

It differs from the initial function (3.164) in that each term is
divided by the square of the natural frequency. Using this rule,
we can write the expression for any n^{th} approximation

$$\varphi^{(n)}(x) = \sum_{j=1}^{\infty} x_j \frac{u_j(x)}{(p_j^2)^n}. \tag{3.167}$$

We take the first frequency outside the summation symbol

$$\varphi^n(x) = \frac{1}{(p_1^2)^n} \left[x_1 u_1(x) + \sum_{j=2}^{\infty} x_j u_j(x) \left(\frac{p_1^2}{p_j^2} \right)^n \right]. \tag{3.168}$$

The ratio of the frequencies squared, under the summation symbol,
is less than one. Therefore the limit of the nth approximation with
increase of n is

$$\lim_{n \to \infty} \varphi^{(n)}(x) = \frac{1}{(p_1^2)^n} x_1 u_1(x),$$

and the limit of the ratio of two successive approximations
approaches the first frequency squared

$$\lim_{n \to \infty} \frac{\varphi^{(n-1)}(x)}{\varphi^{(n)}(x)} = p_1^2. \tag{3.169}$$

Consequently, for a sufficiently large number of approximations
(3.163) yields the square of the first frequency. The approximation
process has good convergence, and in practice it is sufficient to
take two or three approximations in order to determine with high
precision the frequency and deflection function of the first vibra-
tion mode. The latter is the approximation function itself
$\phi^{(n)}(x)$.

For a limited number of approximations, the value of p_1^2 found from (3.169) is a function of x. Of all the possible values of p_1^2, the closest to the exact value is the one calculated for the section with maximal deflection in the first vibration mode. In accordance with the orthogonality conditions, the influence of the nearest second mode is minimal at this section.

The choice of the initial function $\phi^{(0)}(x)$ does not alter the process of convergence to the first vibration mode.

In using the integral method to calculate the second vibration mode, special measures must be taken in selecting the initial function and in the computation process.

The initial function $\phi(0)$ must not contain a term which is in proportion to the first vibration mode. For such a function $\kappa_1 = 0$, and in accordance with (3.168) the second vibration mode becomes dominant

$$\varphi_2^{(n)}(x)\frac{1}{(p_2^2)^n}\left[\varkappa_2 u_2(x)+\sum_{j=3}^{\infty}\varkappa_j u_j(x)\left(\frac{p_2^2}{p_j^2}\right)^n\right].\qquad(3.170)$$

In practice it is difficult to specify the initial function (except for obvious cases) such that it does not contain the first mode. Then it must be orthogonalized, i.e., the first mode must be removed. To do this we find the first mode expansion coefficient

$$\varkappa_1=\int_0^l m(x)\varphi^{(0)}(x)\varphi_1(x)dx,$$

where $\phi_1(x)$ -- is the previously determined first vibration mode function.

Then the first mode is subtracted from the given function, and the initial function for the calculation of the second vibration mode takes the form

$$\varphi_2^{(0)}(x)=\varphi^{(0)}(x)-\varkappa_1\varphi_1(x).$$

We have mentioned previously that the orthogonalization process must be carried out for each approximation in the course of the entire calculation.

Calculation of the successive approximations by multiple integration of the initial function is not possible, except for elementary cases which are of little interest for the present method. Therefore the integration is replaced by summation. The computational formulas in terms of finite differences, obtained on the basis of (3.157) — (3.160), will have the form

$$-Q(x)_i = \sum_{i=0}^{a} m(x)_i \varphi(x)_i \Delta x_i + C_1,$$ (3.171)

where i — is the number of the elementary segment;

$$M(x)_i = -\sum_{i=0}^{a} Q_i(x) \Delta x_i + C_2;$$ (3.172)

$$\varphi_i'(x) = \sum_{i=1}^{a} \frac{M_i(x)}{EJ_i(x)} \Delta x_i + C_3;$$ (3.173)

$$\varphi_i(x) = \sum_{i=0}^{a} \varphi_i'(x) \Delta x_i + C_4.$$ (3.174)

The constants C_1, C_2, C_3, C_4 are determined in the computational process on the basis of the problem boundary conditions.

Example 3.3. Calculate by the integral method the first and second vibration modes of the blade whose geometry is given by sections in accordance with Table 3.3 (see Example 3.2.).

Taking in the calculation $F_0 = 1$; $J_0 = 1$; $l = 1$; $\rho = 1$; $E = 1$, the dimensions shown in Table 3.3 can be considered to be absolute. Then the result of the calculation gives the frequency coefficient k^2, and the frequency for blades of similar geometric form is found from the formula

$$p = \frac{k^2}{l^2} \sqrt{\frac{EJ_0}{\gamma F_0}}.$$

The calculation of the successive approximations is made using (3.171) - (3.174). The computational technique reduces to sequential filling in of the columns of the computational table (see Table 3.4).

Lines 1 - 4 of Table 3.4 are filled in on the basis of the initial data. Line 5 is the initial function of the zero approximation. In the present example it is taken in the form of a quadratic parabola, satisfying the boundary conditions at the clamped end (zero section).

Line 9 is formed as the sum of the numbers appearing in the preceding columns of line 8. In accordance with the boundary conditions and Formula (3.171), the last number in line 9 is the coefficient C_1 with reversed sign ($C_1 = -15.1966$).

Line 10 gives the shearing forces (with minus sign) in the blade sections.

Lines 11 - 21 are sequential calculations using (3.172), (3.173), (3.174). Line 21 is the first approximation of the vibration mode. Using the data of this line in place of line 5 and making a repeat calculation, we obtain the second approximation, shown in line 22.

The ratio of the numbers of line 21 to the corresponding values of line 22 yields the square of the first vibration mode frequency. In our example this is the square of the frequency coefficient

$$p_1^2 = (k_1^{(1)})^2 = 12.2.$$

Further calculations yield very slight refinement.

The normalization of the first vibration mode is performed in lines 23 - 28. Line 28 is the normed vibration mode, which is necessary for the further calculation of the second vibration mode and frequency.

Line 29 gives, very approximately, the second vibration mode. The expansion coefficient of the first mode, which is used to

TABLE 3.4. INTEGRAL METHOD OF BLADE CALCULATION

Item No.	Function	Remark	Section No.					
			0	1	2	3	4	5
1	x_i	Section coordinates	0	0.2	0.4	0.6	0.8	1.0
2	$F_i = m_i$	Mass of segment	1.000	0.784	0.616	0.496	0.424	0.400
3	EI_i	Stiffness of segment	1.000	0.460	0.235	0.122	0.076	0.064
4	$\Delta x_i = x_i - x_{i-1}$	Length of segment	—	0.2	0.2	0.2	0.2	0.2
5	$\varphi_i^0 = 100\,x_i^2$	Zero approximation	0	4	16	36	64	100
6	$m_i \varphi_i^0$	(2)·(5)	0	3.136	9.856	17.856	27.136	40.0
7	$0.5(m_i\varphi_i^0 + m_{i-1}\varphi_{i-1}^0)$	Average of segment	—	1.568	6.496	11.856	22.496	33.568
8	$(7)\cdot\Delta x_i$	(7)·(4)	—	0.3136	1.2992	2.3712	4.499	6.7136
9	$\Sigma(10)$	Integral (8)	0	0.3136	1.6128	3.984	8.483	11.1966
10	$-Q_i = (9) + C_1$	$C_1 = -15.1966$	−15.1966	−14.883	−13.5838	−11.2126	−6.7136	−3.3568
11	$-Q_i$ av	Average of segment	—	−15.0398	−14.2334	−12.3982	−8.9631	−0.6714
12	$(11)\cdot\Delta x_i$	(11)·(4)	—	−3.0080	−2.8467	−2.4796	−1.7926	−10.7983
13	$\Sigma(12)$		0	−3.0080	−5.8546	−8.3343	−10.1260	−10.7983
14	$M_i = (13) + C_2$	$C_2 = 10.7983$	−10.7983	−7.7903	4.9436	2.4640	0.6714	0
15	M_i/EI_i	(14)/(3)	10.7983	16.2200	21.0365	20.1957	8.8342	0
16	(15) av	Average of segment	—	13.5142	18.6333	20.6166	14.5155	4.4171
17	$(16)\cdot\Delta x_i$	(16)·(4)	—	2.7028	3.7267	4.1238	2.9031	0.8834
18	$\varphi_i = \Sigma(17)$	$C_3 = 0$	0	2.7028	6.4295	10.5538	13.4559	14.3398
19	(φ_i) av	Average of segment	—	1.3514	4.5662	8.4912	12.0048	13.8976

TABLE 3.4. (Continued)

Item No.	Function	Remark	\(0\)	\(1\)	\(2\)	\(3\)	\(4\)	\(5\)
					Section No.			
20	$(19)\cdot\Delta x_i$	(19) · (4)	—	0,2703	0,9132	1,6982	2,4000	2,7706
21	$\psi_i^{(1)}=\Sigma(20)$	$C_4 = 0$. First approximation	0	0,2703	1,1835	2,8817	5,2826	8,0621
22	$\psi_i^{(2)}$	Second approximation	0	0,0222	0,6972	0,2365	0,4331	0,660⁵
23	$(\psi_i^{(2)})^2$	$\overline{(2)\cdot(23)}$	0	0,0004	0,0094	0,0449	0,1876	0,4353
24	$m_i\cdot(23)$	Average of segment	0	0,0003	0,0058	0,0277	0,0735	0,1745
25	$(24)_{av}$	(25) · (4)	—	0,0002	0,0031	0,0168	0,0536	0,1270
26	$(25)\cdot\Delta x_i$		—	0,0000	0,0006	0,0034	0,0107	0,0254
27	$\Sigma(26)-N-2$		—					0,0401
28	$\psi_i^{(3)}\cdot N-a_i^2$	N = 5. Normed amplitude of first mode	0	0,111	0,486	1,1825	2,1655	3,3025
29	$[\psi_i^0]_{11}$	Zero approximation of second mode	0	3	8	9	0	—20
30	$\psi_i^0\,a_i^2$	(29) · (28)	0	6,3330	3,8880	10,6425	0	—66,05
31	$\psi_i^0\,a_i m_i$	(30) · (2)	0	0,2611	2,325	5,2787	0	—26,42
32	$(31)_{av}$	Average of segment	—	0,1306	1,328	3,637	2,6394	—13,21
33	$(32)\cdot\Delta x_i$	(32) · (4)	—	0,0261	0,2656	0,7674	0,5279	—2,642
34	$\Sigma(33)-x_1$	Expansion coefficient $x_1 = -1.055$	—					—1,055
35	$(28)\cdot x_1$		0	—0,1171	—0,5127	—1,2475	—2,2046	—3,484
36	$(29)-(35)=[\psi_i^0]'$	Orthogonal approximation	0	3,1171	8,5127	10,2475	2,2046	—16,5159
37	$m_i\cdot(36)$	(2) · (36)	0	2,4438	5,2438	5,0828	0,9687	—6,8004
38	$(37)_{av}$	Average of segment	0	1,2219	3,8438	5,1633	3,0258	—2,8189
39	$(38)\cdot\Delta x_i$	(38) · (4)	—	0,2444	0,7688	1,0327	0,6052	—0,5658
40	$\Sigma(39)$	Integral (39)	0	0,2444	1,0132	2,0459	2,6511	2,0873
41	$-Q_i=(40)+C_i$	$C_1 = 2.0873$	—2,0873	—1,8429	—1,0741	—0,0414	0,5638	0
42	$(42)_{av}$	Average of segment	—	—1,9650	—1,4585	—0,5580	0,2512	—0,2819

TABLE 3.4. (Concluded)

Item No.	Function	Remark	Section No.					
			0	1	2	3	4	5
43	$(42)\cdot\Delta x_i$	$(42)\cdot(4)$	—	0,3630	-0,2917	-0,116	0,0522	0,0564
44	$\Sigma(43)$	Integral (43)	0	-0,3630	-0,6547	-0,7963	-0,7441	-0,6877
45	$M_j=-(44)+C_2$	$C_2=0.6877$	0,6877	0,2947	0,0030	-0,1096	-0,0564	0
46	M_i/EI_i	$(45)/(3)$	0,6877	0,6140	0,0128	-0,8902	-0,7421	0
47	(46)av	Average of segment	—	0,6509	0,3134	-0,4387	-0,8162	-0,3711
48	$(17)\cdot\Delta x_i$	$(47)\cdot(4)$	—	0,1302	0,0629	-0,0877	-0,1632	-0,0742
49	$\varphi_j=-\Sigma(48)$	$C_3=0$	0	0,1302	0,1931	0,1054	-0,0578	-0,1320
50	(49)av	Average of segment	—	0,0651	0,1617	0,1493	0,0238	-0,0949
51	$(50)\cdot\Delta x_i$	$(50)\cdot(4)$	—	0,0130	0,0323	0,0299	0,0048	-0,0190
52	$\varphi_j^{(1)}\cdot\Sigma(51)$	First approximation	0	0,0130	0,0453	0,0752	0,0900	0,0610
53	$\varphi_j^{(1)}\,u_j$	$(52)\cdot(28)$	0	0,0014	0,0220	0,0689	0,1732	0,2014
54	$(53)\cdot m_i$	$(53)\cdot(2)$	0	0,0011	0,0136	0,0441	0,0735	0,0905
55	(54)av	Average of segment	—	0,0006	0,0074	0,0289	0,0588	0,0771
55	$(55)\cdot\Delta x_i$	$(55)\cdot(4)$	—	0,0001	0,0015	0,0038	0,0118	8,0154
56	$x_j=-\Sigma(56)$	Expansion coefficient	0	—	—	—	—	0,0346
57	$x_j\cdot(28)$	$(57)\cdot(28)$	0	0,0038	0,0168	0,0400	0,0749	0,1143
58	$(52)—(58)=[\varphi_j^{(1)}]^a$	Refined first approximation	0	0,0092	0,0285	0,0343	0,0051	-0,0533
59	$[\varphi_j^{(2)}]^a\cdot10^i$	Refined second approximation	0	0,00037	0,00448	-0,11372	0,01743	-0,17461
60	$[(59)/(60)]=\omega_j^2$	Frequency coefficient	—	302,9	301,7	301,6	302,7	305,6

exclude the first vibration mode from the zero approximation, is
determined in lines 30 − 35. The result of clearing of the mode
is obtained in line 36.

A computational cycle using (3.171) − (3.174) is made in lines
37 − 52, the result being the first approximation of the vibration
mode. Excluding from the resulting mode the first vibration mode
(line 53 − 59), we obtain the first approximation of the second
vibration mode.

The values in line 59 are used to calculate the second approxi-
mation. To do this line 59 is used to replace line 36, and the
entire subsequent computational cycle is repeated. The results of
the calculation of the second approximation for the second vibration
mode after excluding the first mode are presented in line 60.

The ratio of the numbers of lines 59 and 60 (line 61) for
sections 3 or 5, where the amplitudes are largest, yields the
second vibration mode frequency squared

$$\mu_2^2 = \left(k_2^2\right)^2 = 302 + 305.$$

Calculation of the third approximation confirms the adequate
accuracy f the calculation of the second mode and frequency in the
first two approximations.

CHAPTER 4

VIBRATIONS AND CRITICAL SPEEDS OF ROTATING FLEXIBLE
SHAFTS AND ROTORS OF GAS TURBINE ENGINES
AND TURBOMACHINES

The shafts and rotors of turbomachines have extremely varied
construction, beginning with the very simple single-mass systems and
ending with the very complex systems consisting of several disks
connected by flexible segments with distributed mass, or composed
of several sections which are hinged together.

Rotor vibrations take place simultaneously in two mutually
perpendicular planes. The two forms of vibrations are coupled.
The coupling arises as a result of rotation, because of the action
of centrifugal forces and gyroscopic moments, and also in those cases
in which the shaft supports or the shaft itself do not have axial
symmetry.

These characteristics make it necessary to examine special
problems on the vibrations of rotating elastic systems.

4.1. Free Vibrations of Flexible Shaft with Single Disk

The rotor scheme with a single disk located arbitrarily on a flexible shaft is very widely used.

Most frequently we must analyze axisymmetric systems, when the rotor rotational axis coincides with one of the principal axes, the moments of inertia are the same with respect to the other axes, and the support and shaft stiffnesses are axisymmetric.

4.1.1. Kinetic Energy of a Rotating Body

As a result of shaft and support deformation, during rotation the rotor body performs regular or irregular precession. The rotor center of inertia travels along a circular or elliptical trajectory and the principal axis — tangent to the elastic line of the shaft — describes a complex surface. The body's kinetic energy is made up of two parts: the kinetic energy T_0 of the translational motion with the velocity of the center of inertia, and the kinetic energy T_1 of the rotational motion

$$T = T_0 + T_1;$$ (4.1)

In the fixed coordinate axis system (Figure 4.1) the former is defined by the simple formula

$$T_0 = \frac{1}{2} m (\dot{x}_0^2 + \dot{y}_0^2);$$ (4.2)

The second component is defined in the xyz rotating axis system, fixed with the body,

$$T_1 = \frac{1}{2} (J_1 \omega_x^2 + J_2 \omega_y^2 + J_3 \omega_z^2),$$ (4.3)

where ω_x, ω_y, ω_z — are the projections of the body angular velocity vector on the xyz principal axes;

J_1, J_2, J_3 — are the principal moments of inertia of the body.

In order to determine the position of the rotor body in space and its angular velocities, we introduce the $\xi \eta \zeta$ additional system
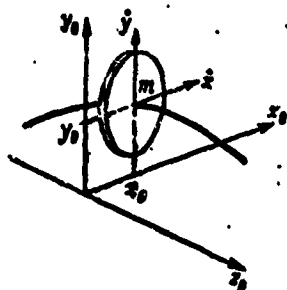
Figure 4.1. Single-mass rotor
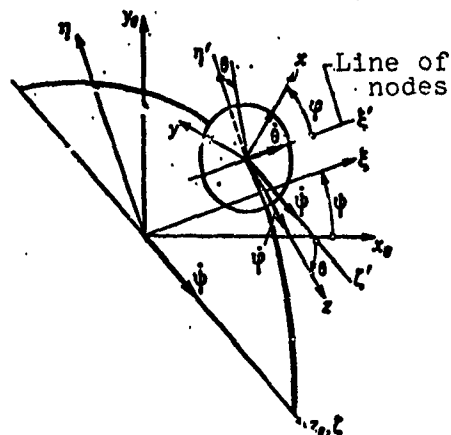
Figure 4.2. Eulerian axis system of rotating and precessing disk

of rotating coordinate axes (Figure 4.2); we align the ζ axis with the z_0 axis. Then the ξ, η axes will lie in the $x_0 y_0$ plane and will form the angle ψ with the $x_0 y_0$ axes. The position of the rotor (disk) body relative to the $\xi \eta \zeta$ axes is defined by the Euler angles θ and ϕ. The nutation angle θ between the z and ζ axes is formed by rotation of the body around the ξ axis, which is called the line of nodes. The proper rotation angle defines the relative rotation of the body about its z axis and is measured between the line of nodes ξ and the x axis. ψ is called the precession angle. The Euler angles ψ, θ, ϕ completely define the position of the rotating body in the $x_0 y_0 z_0$ fixed coordinate system.

The projections of the instantaneous absolute angular velocity of the body on its principal axes are defined with the aid of the Euler angles by the following formulas

$$\omega_x = \dot{\theta} \cos \varphi + \dot{\psi} \sin \theta \sin \varphi;$$
$$\omega_y = -\dot{\theta} \sin \varphi + \dot{\psi} \sin \theta \cos \varphi;$$
$$\omega_z = \dot{\psi} \cos \theta + \dot{\varphi}.$$

The overdots denote angular velocities with respect to the corresponding angles.

Formula (4.3) in terms of Euler angles takes the form

$$T_1 = \frac{1}{2} [J_1(\dot{\psi}\sin\theta\sin\varphi + \dot{\theta}\cos\varphi)^2 +$$
$$+ J_2(\dot{\psi}\sin\theta\cos\varphi - \dot{\theta}\sin\varphi)^2 + J_3(\dot{\psi}\cos\theta + \dot{\varphi})^2]. \tag{4.4}$$

This is the general expression for the kinetic energy of rotation.

For a circular body $J_1 = J_2$, and (4.4) takes the form

$$T_1 = \frac{1}{2} [J_1(\dot{\psi}^2\sin^2\theta + \dot{\theta}^2) + J_3(\dot{\psi}\cos\theta + \dot{\varphi})^2]. \tag{4.5}$$

4.1.2. Differential Equations of Axisymmetric Rotor Vibrations

The rotor bending potential energy is defined by the projections of the deformation of its elastic axis on the coordinate planes (Figure 4.3)

$$\Pi = \frac{1}{2} [c_{11}(x_0^2 + y_0^2) + 2c_{12}(y_0\alpha + x_0\beta) + c_{22}(\alpha^2 + \beta^2)]; \tag{4.6}$$

where x_0, y_0 — are the center of gravity displacement coordinates;

    α, β — are the slopes of the tangents to the projections of the elastic axis;

c_{11}, c_{12}, c_{22} — are the static stiffness coefficients.

The angles α and β are connected with the Euler angles by the relations

$$-\alpha = \theta\cos\psi;$$
$$\beta = \theta\sin\psi, \tag{4.7}$$

so that (4.6) may be written in the form

$$\Pi = \frac{1}{2} [c_{11}(x_0^2 + y_0^2) - 2c_{12}\theta$$
$$(y_0\cos\varphi - x_0\sin\varphi) + c_{22}\theta^2]. \tag{4.8}$$

The Formulas (4.2), (4.5) for the kinetic energies and (4.8) for the potential energy contain five
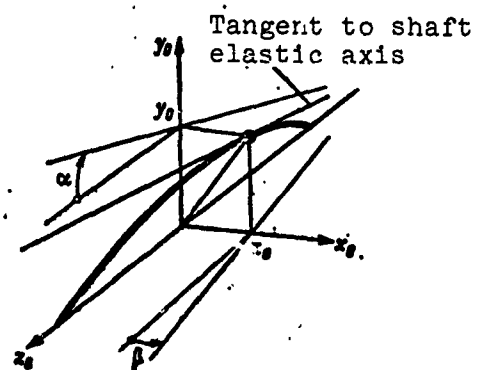
Figure 4.3. Coordinates of shaft elastic axis

independent coordinates x_0, y_0, θ, ψ, ϕ, which correspond to the five degrees of freedom of the system.

The coordinates x_0 and y_0 are connected with the ξ, η coordinates by the formulas

$$\xi = x_0 \cos \psi + y_0 \sin \psi; \qquad (4.9)$$

$$\eta = -x_0 \sin \psi + y_0 \cos \phi. \qquad (4.10)$$

We shall formulate the differential equations of the vibrations of the rotating rotor with the aid of the Lagrange equation

$$\frac{d}{dt}\left(\frac{\partial T}{\partial q}\right) - \frac{\partial T}{\partial q} + \frac{\partial \Pi}{\partial q} = 0.$$

Differentiating (4.2) and (4.8) respectively with respect to x_0 and y_0, we obtain

$$m\ddot{x}_0 + c_{11}x_0 + c_{12}\theta \sin \psi = 0; \qquad (4.11)$$

$$m\ddot{y}_0 + c_{11}y_0 - c_{12}\theta \cos \psi = 0; \qquad (4.12)$$

differentiation of (4.5) and (4.8) with respect to θ, ψ, ϕ yields

$$J_1\ddot{\theta} - [J_1\dot{\psi}\cos\theta - J_3(\dot{\psi}\cos\theta + \dot{\phi})]\dot{\psi}\sin\theta - c_{12}(y_0\cos\psi - \\ -x_0\sin\psi) + c_{22}\theta = 0. \qquad (4.13)$$

$$J_1\ddot{\psi}\sin^2\theta + 2J_1\dot{\psi}\dot{\theta}\sin\theta\cos\theta - J_3(\dot{\psi}\cos\theta + \dot{\phi})\dot{\theta}\sin\theta + \\ + J_3\cos\theta\frac{d}{dt}(\dot{\psi}\cos\theta + \dot{\phi}) + c_{12}\theta(x_0\cos\psi + y_0\sin\psi) = 0; \qquad (4.14)$$

$$\frac{d}{dt}(\dot{\psi}\cos\theta + \dot{\phi}) = 0. \qquad (4.15)$$

The last equality shows that the rotor absolute velocity of rotation about the z axis is constant. The precession of the circular rotor has no effect on the uniformity of its rotation

$$\omega = \dot{\psi}\cos\theta + \dot{\phi} = \text{const.} \qquad (4.16)$$

Formulas (4.13) and (4.14) take a simpler form after replacing therein certain terms in accordance with (4.9), (4.10), (4.15), (4.16), and making the replacement $\sin \theta = \theta$; $\cos \theta = 1$:

$$J_1\ddot{\theta} - (J_1\dot{\psi} - J_3\omega)\dot{\psi}\theta - c_{12}\eta + c_{22}\theta = 0; \qquad (4.17)$$

$$J_1\ddot{\psi}\theta + 2J_1\dot{\psi}\dot{\theta} - J_3\omega\dot{\theta} + c_{12}\xi = 0. \qquad (4.18)$$

These are the equations of equilibrium of the moments applied to the rotor in terms of projections on the ξ and ζ axes.

Equations (4.11), (4.12) and (4.17), (4.18) form a system of equations which defines completely the free vibrations of the rotating rotor.

4.1.3. Solutions of the Equations

4.1.3.1. Plane vibrations

During plane vibrations the line of nodes does not displace, and deflection of the rotor takes place in the η, ζ plane, i.e., plane vibrations correspond to the conditions

$$\ddot{\psi} = \dot{\psi} = 0; \quad \xi = 0; \quad \psi = \text{const.}$$

Equation (4.18) shows that we must have $\omega = 0$ in this case. Otherwise a gyroscopic moment develops relative to the η axis, which disturbs the plane vibrations.

If we take for simplicity $\psi = 0$, then $x_0 = 0$, $y_0 = \eta$ and (4.12) and (4.17) become the equations of plane vibrations

$$m\ddot{\eta} + c_{11}\eta - c_{12}\theta = 0; \left.\vphantom{\begin{matrix}1\\1\end{matrix}}\right\}$$
$$J_1\ddot{\theta} - c_{12}\eta + c_{22}\theta = 0. \quad\quad (4.19)$$

In accordance with the assumed initial conditions, the solutions of these equations may be taken in the form

$$\eta = A \cos pt; \quad \theta = \Theta \cos pt;$$

substitution of these solutions into (4.19) leads to the frequency equation in determinant form. Expanding this determinant into a row, we obtain

$$(c_{11} - mp^2)(c_{22} - J_1 p^2) - c_{12}^2 = 0. \quad\quad (4.20)$$

This equation has two roots, which are the free plane vibration frequencies.

This solution makes it possible to draw the important conclusion that plane vibrations can occur only with a nonrotating rotor. Plane vibrations are not possible for a rotating rotor.

4.1.3.2. Regular precession

Regular precession is characterized by constant precession rate $\dot{\psi}$ and constant shaft deflection

$$\dot{\psi} = \text{const}; \quad \dot{\eta} = \text{const}; \quad \theta = \text{const};$$

correspondingly

$$\ddot{\psi} = 0; \quad \dot{\theta} = \ddot{\theta} = 0; \quad \xi = 0;$$

Equation (4.18) is satisfied in this case term by term.

In accordance with (4.9) and (4.10), where we must set $\xi = 0$, we obtain

$$x_0 = -\eta \sin\psi; \quad y_0 = \eta \cos\psi, \text{where } \psi = \lambda t.$$

Substitution of these functions into (4.11) and (4.12) makes them identical and they become

$$m\lambda^2\eta = c_{11}\eta - c_{12}\theta, \tag{4.21}$$

and (4.17) for regular precession becomes

$$(J_1\lambda - J_2 w)\lambda\theta = -c_{12}\eta + c_{22}\theta. \tag{4.22}$$

The system of four differential equations has been reduced to two homogeneous algebraic equations with two unknowns — η and θ. Equations (4.21) and (4.22) are the equations of equilibrium. In (4.21) the centrifugal force of precession appears on the left side, and on the right side there is the elastic force associated with the magnitude of the deflection η and the angular deformation θ. The sum of the dynamic and gyroscopic moments appears on the left in (4.22), and the corresponding elastic force moment appears on the right.

These equations show that in the future there is no need to formulate all the differential equations every time for axisymmetric rotors; it is sufficient to formulate only the equations of equilibrium of the inertial and elastic forces and moments.

Nonzero solutions of (4.21) and (4.22) are possible only if the determinant of the system equals zero. The determinant for (4.21) and (4.22) yields the equation

$$(c_{11} - m\lambda^2)\left[c_{22} - \left(1 - \frac{J_2}{J_1}\frac{\omega}{\lambda}\right)J_1\lambda^2\right] - c_{12}^2 = 0. \qquad (4.23)$$

This equation is satisfied only for four definite values of λ — the regular precession rates. These roots of the equation are the natural circular vibration frequencies of the spinning rotor.

The free vibration frequencies λ depend on the proper rotation speed ω. Figure 4.4 shows the dependence of the roots of the frequency equation (4.23) on ω. The diagram consists of four branches, separated by three horizontal asymptotes (the middle one being the abscissa axis). The upper and lower branches have an inclined asymptote passing through the coordinate origin.
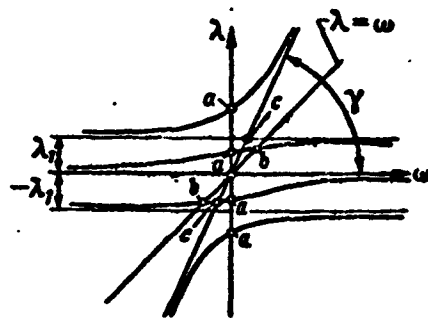
Figure 4.4. Roots of the frequency equation of a rotating shaft

We obtain the equation of the asymptotes from (4.23). For the horizontal asymptotes we must set $\omega \to \infty$. Then we obtain

$$c_{11} - m\lambda_1^2 = 0; \quad \lambda_1 = \pm\sqrt{\frac{c_{11}}{m}}. \qquad (4.24)$$

The more rigid the rotor, the more distant the asymptotes are from the abscissa axis.

For the inclined asymptote we must set $\lambda \to \infty$. After dividing all the terms by λ^4, we obtain the slope of the inclined asymptote

$$\text{tg}\,\gamma = \left(\frac{\lambda}{\omega}\right)_\infty = \frac{J_2}{J_1}. \qquad (4.25)$$

This formula shows that the slope of the asymptote depends on the ratio of the moments of inertia of the rotor body. For a thin disk

this ratio equals two. For a long rotor of drum construction or consisting of several rigidly connected disks this ratio may be less than one. Then the asymptote is positioned with correspondingly small slope to the abscissa axis.

The diagram is skew symmetric relative to the center. The first and third quadrants correspond to forward precession, when the direction of precession coincides with the direction of rotation.

The second and fourth quadrants correspond to backward precession, when the direction of precession is opposite the direction of rotation. For each rotational speed there are four vibration modes — two forward precession and two backward, which corresponds to the number of system degrees of freedom. In accordance with the general rule, the rotating shaft or rotor does not have any other free vibration modes. This makes it possible to draw the important conclusion that the free vibration modes of a rotating rotor can be only regular precession.

We shall note certain particular cases.

For $\omega = 0$ (4.23) becomes (4.20). Its roots are shown by the points a in Figure 4.4. Thus the nonrotating rotor, in addition to plane vibrations, can perform circular vibrations in the form of regular precession with the same circular frequency.

Vibrations of the nonrotating rotor are also possible in the form of irregular precession, which is obtained as the result of the combination of two oppositely directed regular precessions with different amplitudes.

Precession for which $\omega = \lambda$ is called forward synchronous precession. In this case the disk does not rotate relative to the shaft bending plane. The synchronous precession circular frequency is defined by the point b of intersection of the straight line with slope equal to one with the frequency characteristic curves.

The point c of intersection of the curve with the inclined asymptote corresponds to the ratio

$$\frac{\lambda}{\omega} = \frac{J_3}{J_1}.$$

In this case the parentheses in (4.23) vanish.   This means that
for this ratio of the velocities ω and λ the inertial moment vanishes,
and the circular frequency of the rotating shaft is equal to the
frequency of the vibrations of the same shaft with the point mass m.

In the case of free circular vibrations, the shaft bending
shape is determined by the relationship between the deflection η
and the rotation angle θ of the shaft section at the point where
the disk center of gravity is located.

There are two vibration modes for forward precession and two
modes for backward precession.

For each of the natural frequencies the ratio of the deforma-
tions can be found from either (4.21) or (4.22)

$$\frac{\theta}{\eta} = \frac{c_{11} - m\lambda^2}{c_{12}}.$$ (4.26)

In accordance with (4.23) the difference $(c_{11} - m\lambda^2)$ is posi-
tive for the first vibration mode; therefore, (4.26) is positive
(Figure 4.5a). For the second mode this ratio is negative (see
Figure 4.5b).
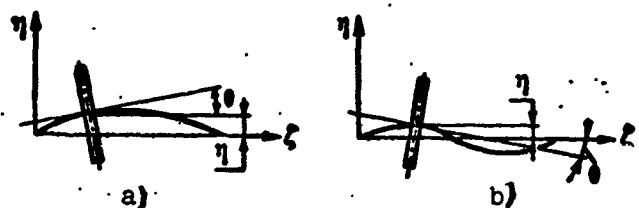
Figure 4.5.   Shaft vibration modes

4.1.4.   Reduction of Differential Equations to Stationary Coordinate
         Axis System

Problems on vibrations of rotating rotors are usually solved in
stationary coordinate axes. The Equations (4.7) and (4.10) are used
to refer the differential equations (4.11), (4.12), (4.17) to sta-
tionary axes.

In accordance with (4.7), the Equations (4.25) and (4.26) are immediately written in the form

$$m\ddot{x}_0 + c_{11}x_0 + c_{12}\beta = 0; \qquad (4.27)$$

$$m\ddot{y}_0 + c_{11}y_0 + c_{12}\alpha = 0. \qquad (4.28)$$

To transform (4.17) it is necessary to use (4.7) to find the expressions for $\ddot{\theta}$ and $\dot{\psi}\theta$, which are obtained in the form

$$\left. \begin{array}{l} \ddot{\theta} = -\ddot{\alpha}\cos\phi + \ddot{\beta}\sin\phi + \theta\dot{\psi}^2; \\ \theta\dot{\psi} = \dot{\beta}\cos\psi - \dot{\alpha}\sin\phi. \end{array} \right\} \qquad (4.29)$$

After substituting these expressions into (4.17), the latter breaks down into two equations

$$J_1\ddot{\alpha} - J_3\omega\dot{\beta} + c_{12}y_0 + c_{22}\alpha = 0; \qquad (4.30)$$

$$J_1\ddot{\beta} + J_3\omega\dot{\alpha} + c_{12}x_0 + c_{22}\beta = 0. \qquad (4.31)$$

These are the equations of equilibrium of the inertial and elastic force moments in terms of their projections on the stationary coordinate axes.

The system of four equations (4.27), (4.28), (4.30), (4.31) completely defines the free vibrations of the rotating rotor.

The following solutions of the equations correspond to regular precession

$$\left. \begin{array}{ll} x_0 = \eta\cos\lambda t; & \beta = \Theta\cos\lambda t \\ y_0 = \eta\sin\lambda t; & \alpha = \Theta\sin\lambda t. \end{array} \right\} \qquad (4.32)$$

Substitution of the solutions into (4.27), (4.28) and (4.30), (4.31) yields two pairs of identical equations

$$m\lambda^2\eta = c_{11}\eta + c_{12}\Theta; \qquad (4.33)$$

$$(J_1\lambda - J_3\omega)\lambda\Theta = c_{12}\eta + c_{22}\Theta; \qquad (4.34)$$

these equations are identical to (4.21) and (4.22), which were analyzed in detail above.

It is important to note that if we take as the solutions the functions for x_0, y_0 and α, β with different amplitudes, we obtain

a more complex system of four homogeneous equations. But further
calculations show that the frequency equation yields roots which are
identical with the roots of the equations (4.33), (4.34), and the
deflection and rotation angle amplitudes are pairwise identical,
i.e., the solution also reduces to regular precession.

4.2. Forced Vibrations of Shaft with Single Disk

4.2.1. Shaft Vibrations Due to Circular Excitation

We represent the external disturbing force Q acting on the
shaft as the rotating vector H (Figure 4.6.). Then

$$\bar{Q} = He^{i\Omega t}, \qquad (4.35)$$

where Ω — is the angular velocity of the disturbance vector, which
is not equal to the shaft rotation velocity ω.

The projections of the force Q on the coordinate axes will be

$$Q_x = H \cos \Omega t; \quad Q_y = H \sin \Omega t.$$

The differential equations of the forced vibrations are identi-
cal with (4.27), (4.28), and (4.30), (4.31), but they have a right
side

$$\left.\begin{aligned}
m\ddot{x}_0 + c_{11}x_0 + c_{12}\beta &= H \cos \Omega t; \\
m\ddot{y}_0 + c_{11}y_0 + c_{12}\alpha &= H \sin \Omega t; \\
J_1\ddot{\beta} + J_3\omega\dot{\alpha} + c_{12}x_0 + c_{22}\beta &= 0; \\
J_1\ddot{\alpha} - J_3\omega\dot{\beta} + c_{12}y_0 + c_{22}\alpha &= 0.
\end{aligned}\right\} \qquad (4.36)$$

We take the particular solutions of the equations for the
forced vibrations in the form

$$\left.\begin{aligned}
x_0 &= X \cos \Omega t; \quad y_0 = Y \sin \Omega t; \\
\beta &= B \cos \Omega t; \quad \alpha = A \sin \Omega t;
\end{aligned}\right\} \qquad (4.37)$$

the solutions represent forward precession of the shaft. Substi-
tution of these solutions into the differential equations leads to

the system of algebraic equations

$$-m\Omega^2 X + c_{11}X + c_{12}B = H;$$
$$-m\Omega^2 Y + c_{11}Y + c_{12}A = H;$$
$$-J_1\Omega^2 B + J_3\omega\Omega A + c_{12}X + c_{22}B = 0;$$
$$-J_1\Omega^2 A + J_3\omega\Omega B + c_{12}Y + c_{22}A = 0. \qquad (4.38)$$

The equations are pairwise identical and show that the deflection amplitudes and rotation angles are equal in magnitude

$$X = Y = \eta; \quad B = A = \theta. \qquad (4.39)$$

Figure 4.6. Vector form of representation of rotating shaft deformations and motion

This is easily verified by continuing the solution on the assumption of inequality of the amplitudes.

Thanks to the equality of the amplitudes, the solutions are completely defined by the two equations

$$H + m\Omega^2\eta = c_{11}\eta + \dot{c}_{12}\theta; \qquad (4.40)$$

$$(J_1\Omega - J_3\omega)\,\Omega\theta = c_{12}\eta + c_{22}\theta; \qquad (4.41)$$

from these equations we find the magnitudes of the shaft deflection η and the nutation angle θ for forced vibrations

$$\eta = \frac{c_{22} - J_1\Omega^2\left(1 - \frac{J_3}{J_1}\frac{\omega}{\Omega}\right)}{\Delta} H; \quad \theta = -\frac{c_{12}}{\Delta}H, \qquad (4.42)$$

where

$$\Delta = (c_{11} - m\Omega^2)\left[c_{22} - J_1\Omega^2\left(1 - \frac{J_3}{J_1}\frac{\omega}{\Omega}\right)\right] - c_{12}^2.$$

In Figure 4.6 vectors are used to show: the disturbing force H, the resulting deflection η and section rotation angle θ, and also their projections on the x_0 and y_0 axes. The shaft bending plane coincides with the plane of action of the force H.

In this connection the Solutions (4.37) can be represented in vector form

$$\bar{z} = \eta e^{i\Omega t}; \quad \bar{\vartheta} = i\theta e^{i\Omega t}. \tag{4.43}$$

The deflection η and the angle θ depend on the relationship between the natural frequencies λ_1 and λ_2 of the rotating shaft and the excitation frequency Ω. When Ω coincides with one of the frequencies, the determinant Δ in the denominator of (4.42) vanishes. In this case the shaft deformation amplitudes increase without bound — the resonance phenomenon occurs.

The resonant state is easily defined with the aid of the frequency diagram (Figure 4.7). If the excitation frequency Ω_1 is given, we can draw a horizontal line to find the point of intersection with the characteristic curve; this point shows the rotor speed at which resonance occurs. If the shaft speed ω_1 is given, we can draw the corresponding vertical line to obtain the four values of the resonant excitation frequencies.

Usually the excitation sources of the rotating shaft have frequencies which are proportional to the rotational speed

$$\Omega = s\omega, \tag{4.44}$$

where s — is the proportionality factor which, generally speaking, can be an integer or a fraction and can be either positive or negative.

Exciters with multiplicity factor s differing from zero can occur, for example, in two-shaft constructions; in cases of kinematic excitation in which the shaft vibrations are excited through its supports; in the form of gasdynamic forces — as a result of interaction of nozzle guide vanes and rotor blades.

Knowing the numbers s of the possible exciters and drawing on the frequency characteristic diagram straight lines with different slopes s (Figure 4.8), we find the resonant rotational speeds for the different exciters as the point of intersection of the straight lines with the frequency characteristic curves.
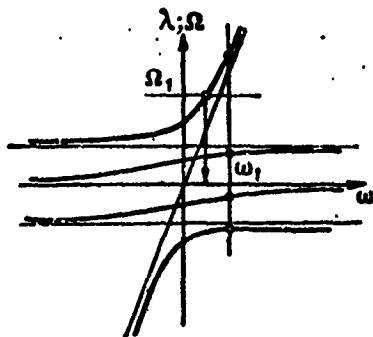
Figure 4.7. Illustrating
det rmination of shaft
resonant states
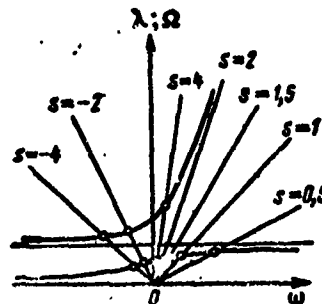
Figure 4.8. Resonance dia-
gram

We note that finding the external exciters for shaft and rotor
vibrations is a very complex problem. This problem is eased if we
know from experiments the resonant rotational speeds and the vibra-
tion frequencies at these speeds. Then, after determining the
multiplicity factor s, we can identify the possible vibration sources
for the given construction and the given operating conditions.

4.2.2. Critical Rotational Speeds

The primary exciter is rotor unbalance, for which s - 1, i.e.,
when the excitation vector rotates together with the shaft.

Drawing from the coordinate origin a straight line with the
slope $s = 1$ ($\Omega = \omega$) (Figure 49a), we obtain the point of intersection
with the curve, which yields the resonant rotational speed. This
resonant speed is termed the critical speed (ω_{cr}). At the critical
speed the shaft loses its stability under the influence of its own
unbalance.

For the thin disk, and in general for $J_3 > J_1$, the shaft has a
single critical speed. The long rotor, for which $J_3 < J_1$, has two
critical speeds (see Figure 4.9b).
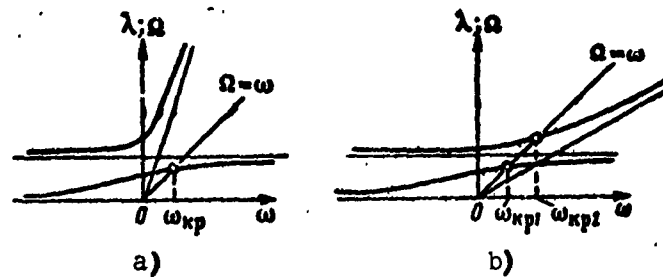
Figure 4.9. Determination of critical shaft speeds

The critical speed is calculated using the general equation (4.23). Setting $\lambda = \omega$ in this equation and solving for λ, we obtain

$$\omega_{\text{кр}}^2 = \frac{[c_{22}m - c_{11}(J_3 - J_1)] \pm \sqrt{[c_{22}m - c_{11}(J_3 - J_1)]^2 - 4m(J_3 - J_1)\delta}}{2m(J_3 - J_1)}, \quad (4.45)$$

where

$$\delta = c_{11}c_{22} - c_{12}^2.$$

The calculation of the shaft deflection and the nutation angle under the action of unbalance is made using (4.42). In these formulas we set

$$\dot{\Omega} = w; \quad H = ma\omega^2,$$

where a — is the unbalance, i.e., the shift of the center of gravity of the disk relative to the center of the shaft.

Then we obtain

$$\eta = \frac{c_{22} + (J_3 - J_1)\omega^2}{\Delta} ma\omega^2; \quad \theta = \frac{-c_{12}}{\Delta} ma\omega^2, \quad (4.46)$$

where

$$\Delta = (c_{11} - m\omega^2)[c_{22} + (J_3 - J_1)\omega^2] - c_{12}^2.$$

The shaft deflection η and the angle θ depend on the shaft rotational speed ω (Figure 4.10).
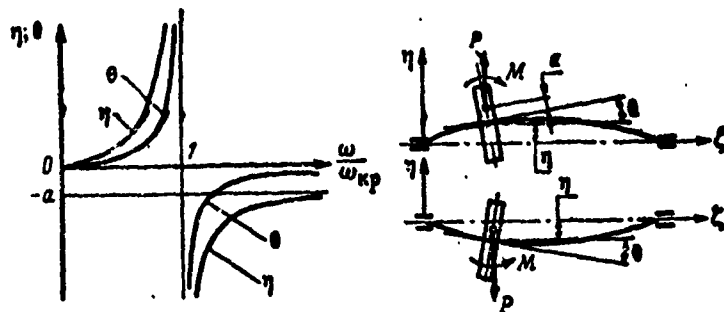
Figure 4.10. Dependence of deformations η and θ of
unbalanced shaft on rotation speed

In the subcritical region the deflections increase with increase
of the rotational speed. The direction of the shaft deflection is
the same as that of the unbalance a.

With approach to the critical speed, the deflection increases
without bound.

In the supercritical region the shaft deflections decrease with
increase of the rotational speed. In this case the shaft bends in
the direction opposite the direction of the unbalance a. The disk
mass center occupies a position between the axis of rotation and the
curved shaft centerline. The distance (η − a) between the axis of
rotation and the disk mass center determines the centrifugal force,
which balances the elastic force of the shaft.

In the limit, when the rotational speed increases without bound,
the shaft deflection η approaches a value equal to a, the disk cen-
ter of inertia tends to occupy a position on the axis of rotation,
and the angle θ approaches zero.

Shafts and rotors operating at speeds below the critical speed
are usually termed "rigid", while shafts and rotors operating in
the supercritical region are termed "flexible".

The forces which arise on the supports and are transmitted to the casing are connected with the shaft deformation

$$P = c_{11}\eta + c_{12}\theta; \atop M = c_{12}\eta + c_{22}\theta. \quad\Bigr\}$$

(4.47)

It is not difficult to calculate with the aid of (4.46) and (4.47) the dynamic forces and moments, which are then transferred to the supports. In the supercritical region, far from ω_{cr}, these forces become very small.

In addition to static unbalance, the rotor usually has so-called dynamic unbalance, in which its central axis does not coincide with the shaft axis, forming with the latter the angle θ_0. In this case Equations (4.40) and (4.41) for equilibrium of the rotating rotor will have the form

$$m\omega^2(\eta + a) = c_{11}\eta + c_{12}\theta; \atop (J_1 - J_3)(\theta + \theta_0)\omega^2 = c_{12}\eta + c_{22}\theta; \quad\Bigr\}$$

(4.48)

hence we obtain

$$\eta = \frac{c_{22} + (J_3 - J_1)\omega^2}{\Delta} m a \omega^2 + \frac{c_{12}}{\Delta}(J_3 - J_1)\theta_0\omega^2; \atop \theta = -\left[\frac{c_{12}}{\Delta} m a \omega^2 + \frac{c_{11} - m\omega^2}{\Delta}(J_3 - J_1)\theta_0\omega^2\right]. \quad\Biggr\}$$

(4.49)

Comparing these formulas with (4.46), we see that disk tilt on the shaft affects the shaft deflection during rotation.

With increase of the rotational speed far beyond the critical speed, the shaft deformations approach their limiting values

$$\eta \rightarrow -a; \quad \theta \rightarrow -\theta_0.$$

i.e., the disk center of gravity and its central axis tend to align themselves with the axis of rotation. In this case the elastic forces will be

$$P = c_{11}a + c_{12}\theta_0; \quad M = c_{12}a + c_{22}\theta_0.$$

(4.50)

4.2.3. Vibrations of Shaft Subject to Periodic Force of Constant
       Direction

Under the influence of the periodic force, the rotating rotor
will execute forced vibrations in the form of irregular precession.

In order to calculate these vibrations, we represent the periodic
force as the sum of two vectors rotating in opposite directions
(Figure 4.11)

$$\bar{Q} = 2H \cos \Omega t = H e^{i\Omega t} + H e^{-i\Omega t}. \tag{4.51}$$

After this we can use the preceding solutions, applying the
superposition principle.
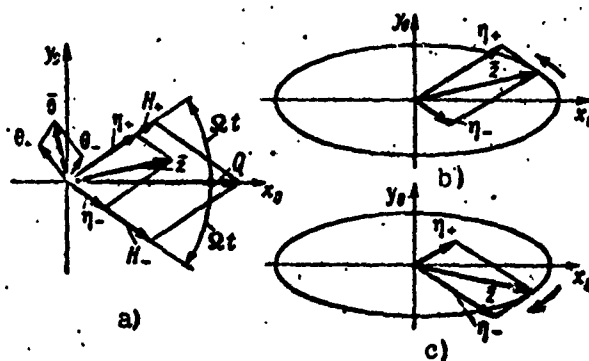
Figure 4.11. Vector diagram of rotating shaft
              forced vibrations

Each of the vectors, rotating in opposite directions, causes in
its plane the bending η_+, η_- and rotational θ_+, θ_- deformations.
The magnitudes of the deformations are calculated using (4.42); in
so doing we must consider the sign of Ω in relation to the shaft
rotational speed ω.

The combined displacement from the action of the two vectors
is equal to the sum of the displacements obtained for each vector
separately. We write this displacement in the form

$$\bar{z} = \eta_+ e^{i\Omega t} + \eta_- e^{-i\Omega t};$$
$$\bar{\delta} = i(\theta_+ e^{i\Omega t} + \theta_- e^{-i\Omega t}). \qquad (4.52)$$

The moduli of the vectors η_+, η_-, θ_+, θ_- are different in magnitude. Therefore the trajectory of the disk center-of-inertia motion has an elliptic form, elongated along the x_0 or y_0 axis.

If $\eta_+ > \eta_-$ and both values are of the same sign, the ellipse is elongated along the x_0 axis, and the describing point moves in the positive direction, i.e., the shaft vibrations take place in the form of irregular positive precession. If $\eta_+ < \eta_-$, the precession will be backward.

When the exciting force frequency approaches the natural frequency, the trajectory approaches a circle, since the second, non-resonant vector is small in comparison with the resonant vector. The direction of motion of the describing point is the same as that of the resonant vector.

Upon passing through resonance, one of the vectors changes sign; now the ellipse is elongated along the y_0 axis.

4.2.4. Kinematic Excitation

We have shown in Chapter I that kinematic excitation is identical to force excitation.

If the rotor supports are located in a casing which performs vibrations with a frequency which differs from the rotor rotational speed, these vibrations will cause forced vibrations of the rotor in the form of forward or backward precession.

Kinematic excitation can arise in the form of circular or plane excitation. In the first case the rotor supports displace along circles of definite radius with the angular frequency Ω. The second case can be considered as the combination of two circular motions of the supports in opposite directions with the same frequencies and amplitudes equal to half the amplitude of the plane vibrations.

Let us examine circular kinematic excitation. In accordance with the notations shown in Figure 4.12, the equations of equilibrium of the forces and moments acting in the rotor bending plane are written as

$$m\Omega^2\eta = c_{11}(\eta-\eta_0)+c_{12}(\theta-\theta_0);$$
$$(J_1\Omega^2-J_3\Omega\omega)\theta = c_{12}(\eta-\eta_0)+c_{22}(\theta-\theta_0),$$

(4.53)

where η_0, θ_0 — are the displacements in the plane of the rotor center of inertia caused by kinematic displacement of the supports. These displacements are easily determined from geometric considerations as a function of the given support displacements.

Considering the terms of the equations which are associated with kinematic excitation as external disturbing forces
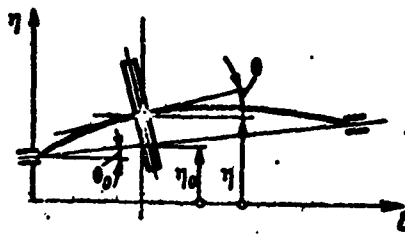
Figure 4.12. Kinematic excitation of shaft

$$H_\xi = c_{11}\eta_0+c_{12}\theta_0;$$
$$H_\eta = c_{12}\eta_0+c_{22}\theta_0,$$

(4.54)

we obtain the basic equations in the form

$$(c_{11}-m\Omega^2)\eta+c_{12}\theta = H_\xi;$$
$$c_{12}\eta+\left[c_{22}-J_1\Omega^2\left(1-\frac{J_3}{J_1}\frac{\omega}{\Omega}\right)\right]\theta = H_\eta;$$

(4.55)

hence we obtain

$$\eta = \frac{\Delta_1}{\Delta}; \quad \theta = \frac{\Delta_2}{\Delta},$$

(4.56)

where

$$\Delta = (c_{11}-m\Omega^2)\left[c_{22}-J_1\Omega^2\left(1-\frac{J_3}{J_1}\frac{\omega}{\Omega}\right)\right]-c_{12}^2;$$
$$\Delta_1 = H_\eta\left[c_{22}-J_1\Omega^2\left(1-\frac{J_3}{J_1}\frac{\omega}{\Omega}\right)\right]-H_\theta c_{12};$$
$$\Delta_2 = H_\theta(c_{11}-m\Omega^2)-H_\xi c_{12}.$$

The nature of the vibrations in the kinematic excitation case coincides completely with the vibrations examined above with circular force excitation.

The vibrations with plane kinematic excitation are completely defined by (4.52), for which the moduli of the vectors, with account for the direction of rotation, are found from (4.56).

4.3. Vibrations of Multimass Rotors

4.3.1. Vibration Equations in Direct and Inverse Form. Frequency Equation

The vibration equations of axisymmetric multimass rotors are formulated in the form of a system of equations of equilibrium. If in so doing we use the stiffness coefficients c_{is}, we obtain the direct form of the equations

$$m_i \lambda^2 \eta_i = \sum_{s=1}^{k} (c_{i,s} \eta_s + c_{i,k+s} \vartheta_{k+s}), \quad i = 1 \text{ to } k; \quad (4.57)$$

$$A_i J_{ai} \lambda^2 \vartheta_{k+i} = \sum_{s=1}^{k} (c_{k+i,s} \eta_s + c_{k+i,k+s} \vartheta_{k+s}), \quad i = 1 \text{ to } k, \quad (4.58)$$

where k — is the number of disks;

$c_{1,s}$; $c_{1,k+s}$; $c_{k+1, s}$; $c_{k+1,k+s}$ — is the system of stiffness coefficients, relating the unit deflections and rotation angles with the elastic forces and moments. The subscripting notation is as follows: the displacements from 1 to k are first numbered, then the rotation angles from k to 2k. The forces are numbered first and then the moments; the stiffness coefficients obey the reciprocity principle;

J_e, J_p, m — are the equatorial and polar moments of inertia of the disk and its mass, respectively;

A_1 — are coefficients accounting for the ratio of the disk moments of inertia and the precession mode. Its subscript corresponds to the disk number

$$A_i = 1 - \frac{I_\rho}{I_0} \frac{\omega}{\lambda}.$$ (4.59)

This coefficient takes into account the gyroscopic moment, which determines the form of the free vibrations as regular precession.

The inverse form of the equations is obtained if the influence coefficients α_{is} are used in writing the equations

$$\eta_i = \sum_{s=1}^{k} (\alpha_{is} m_s \lambda^2 \eta_s + \alpha_{i,k+s} A_s J_{os} \lambda^2 \theta_{k+s}), \quad i = 1 \text{ to } k;$$ (4.60)

$$\theta_{k+i} = \sum_{s=1}^{k} (\alpha_{k+i,s} m_s \lambda^2 \eta_s + \alpha_{k+i,k+s} A_s J_{os} \lambda^2 \theta_{k+s}), \quad i = 1 \text{ to } k.$$ (4.61)

The system is composed of 2k equations, since each disk has two degrees of freedom in the shaft bending plane.

All the equations of the Systems (4.57), (4.58) and (4.60), (4.61) are homogeneous. Therefore, to find their nonzero solutions we must formulate the system determinant and then equate it to zero to find the parameter λ^2, which will be the square of the shaft free circular vibration frequency. The system determinant, when equated to zero, is thus the frequency equation.

We shall formulate the determinant for the system of equations in inverse form, which is the form most often used in calculations. For simplicity we consider a shaft with only two disks, which does not alter the structure of the determinant

$$\begin{vmatrix} \alpha_{11} m_1 \lambda^2 - 1 & \alpha_{12} m_2 \lambda^2 & \alpha_{13} A_1 J_{o1} \lambda^2 & \alpha_{14} A_2 J_{o2} \lambda^2 \\ \alpha_{21} m_1 \lambda^2 & \alpha_{22} m_2 \lambda^2 - 1 & \alpha_{23} A_1 J_{o1} \lambda^2 & \alpha_{24} A_2 J_{o2} \lambda^2 \\ \alpha_{31} m_1 \lambda^2 & \alpha_{32} m_2 \lambda^2 & \alpha_{33} A_1 J_{o1} \lambda^2 - 1 & \alpha_{34} A_2 J_{o2} \lambda^2 \\ \alpha_{41} m_1 \lambda^2 & \alpha_{42} m_2 \lambda^2 & \alpha_{43} A_1 J_{o1} \lambda^2 & \alpha_{44} A_2 J_{o2} \lambda^2 - 1 \end{vmatrix} = 0.$$ (4.62)

The theorem on number of roots and degrees of freedom remains valid for a rotating rotor.

For any rotor rotational speed ω, the determinant has 2k positive roots corresponding to forward precession and the same number of negative roots corresponding to backward precession — in all there are 4k distinct real roots, which correspond to the total number of

degrees of freedom in the two planes. The values of the roots depend on ω. Various methods may be used to find the roots.

If the rotational speed ω, which appears in the coefficients A_1 and A_2, is given, the determinant expands into an equation of degree 4k. Its solution, even for a rotor with only two disks, becomes very lengthy and difficult to carry out in practice.

If the coefficients A_1 and A_2 are given, i.e., the precession mode — the ratio ω/λ, which appears in these coefficients — is given, then the determinant expands into an equation of degree 2k in terms of λ^2. The solution of this equation is possible in practice for no more than three disks. Here we must remember that in those cases in which the coefficients A_1, A_2, and so on, take a negative value there will be negative roots among the λ^2. The number of negative roots equals the number of negative coefficients A_1. These negative roots are discarded as being imaginary solutions for λ.

If the precession rate λ is given, then the determinant expands into an equation of degree k in ω or in ω/λ. This equation has the lowest degree and the resonant rotational speeds are most easily determined from it.

4.3.2. Frequency Equation Root Map

The dependence of the rotor natural circular vibration frequencies on the rotational speed for all the vibration modes is called the frequency map.

A map of the frequency equation roots for a rotor with two disks is shown in Figure 4.13. The system of curves in this diagram is skew symmetric. There are two pairs of horizontal asymptotes and two inclined asymptotes.

The location of the horizontal asymptotes λ_1 and λ_2 is determined from the frequency equation (4.62) if we set therein $\omega \to \infty$,

i.e., A_1 and $A_2 \to \infty$. The determinant takes the form

$$\begin{vmatrix} \alpha_{11}m_1\lambda^2 - 1 & \alpha_{12}m_2\lambda^2 & \alpha_{13} & \alpha_{14} \\ \alpha_{21}m_1\lambda^2 & \alpha_{22}m_2\lambda^2 - 1 & \alpha_{23} & \alpha_{24} \\ \alpha_{31}m_1\lambda^2 & \alpha_{32}m_2\lambda^2 & \alpha_{33} & \alpha_{34} \\ \alpha_{41}m_1\lambda^2 & \alpha_{42}m_2\lambda^2 & \alpha_{43} & \alpha_{44} \end{vmatrix} = 0. \qquad (4.63)$$

The locations of the inclined asymptotes are defined by the equations

$$A_1 = 0; \quad A_2 = 0.$$

If the rotor has thin disks with the same ratio J_p/J_e of the moments of inertia, the inclined asymptotes merge.

Knowledge of the location of the asymptotes facilitates the construction of the entire diagram and in many cases avoids the necessity for computing the curves point by point to obtain a rough estimate of the rotor frequency characteristic.

The general technique for constructing the maps is as follows. The number of horizontal asymptotes in each half of the diagram and the number of inclined asymptotes equals the number of disks. Their locations are known. For definiteness of the construction it is desirable to note on the vertical axis the nonrotating rotor frequencies λ_{0j}. To do

Figure 4.13. Roots of frequency equation of rotor with two disks

this we compute the determinant (4.62) for the condition $\omega = 0$. In this case all the coefficients $A_1 = 1$. The number of roots is equal to 2k. Then for the upper part of the diagram a family of k curves is drawn from the zero

asymptote (abscissa axis) from left to right. Each curve must pass through one of the points on the vertical axis and terminate approaching one of the asymptotes, beginning from below. From the left free end of each of the horizontal asymptotes, beginning from above, there runs upward and to the right a single curve, all of which pass through the remaining points and approach the inclined asymptotes. The number of these branches also equals the number of disks. Individual points can be computed using the general equation (4.62) to refine the position of the curves in questionable cases. The lower half of the diagram is skew symmetric to the upper half.

If among the rotor disks there are point masses, we must set $J_e = J_p = 0$ for these disks. In this case the corresponding column and row of the Determinant (4.62) are deleted. One inclined asymptote and one point on the vertical axis disappear on the root map. The number of horizontal asymptotes remains the same and their position is computed using (4.63).

The curves are constructed as described above, but now a number of curves equal to the number of inclined asymptotes begin from the abscissa axis. After the construction of the upper and lower parts of the diagram, there remain in the central part free asymptotes and points on the vertical axis through which the missing curves are drawn.

The frequency map is used to determine the resonant speeds. To do this we draw through the coordinate origin rays with definite slopes corresponding to the possible circular excitation or kinematic excitation frequencies. The points of intersection of the rays with the frequency curves yield the rotor resonant speeds.

The straight line with slope equal to one shows the critical rotor speeds. If necessary the latter can be refined by calculation using the general formula (4.62), where we take

$$A_i = 1 - \frac{J_p}{J_e}.$$

Then the equation for determining the rotor critical speeds can be written in the form

$$
\begin{vmatrix}
a_{11} - \dfrac{x}{m_1} & a_{12} & a_{13} & a_{14} \\
a_{21} & a_{22} - \dfrac{x}{m_2} & a_{23} & a_{24} \\
a_{31} & a_{32} & a_{33} + \dfrac{x}{(J_p - J_s)_1} & a_{34} \\
a_{41} & a_{42} & a_{43} & a_{44} + \dfrac{x}{(J_p - J_s)_2}
\end{vmatrix} = 0, \qquad (4.64)
$$

where we have used the notation $x = 1/\lambda^2$ for simplicity.

Usually $J_p > J_e$ and (4.64) has two positive roots. In general, in such cases the number of positive roots and the corresponding number of critical speeds equals the number of disks. If $J_p < J_e$ — for rotors of the drum type or with several rigidly coupled disks — the number of critical speeds increases.

4.3.3. Rotating Rotor Vibration Modes and Their Properties

The deflections η and rotation angles θ, which are used to construct the vibration mode, are determined for a known frequency from the general equation (4.62). We have shown in Chapter II that the deflections and rotation angles are proportional to the minors to the elements of any row of the Determinant (4.62). The first half of the numbers are proportional to the deflections; the second half are proportional to the rotation angles.

The vibration modes have all the properties characteristic of multimass systems. They have the orthogonality property, can be normalized, and the general theorem on the number of vibration mode nodes applies to them.

4.3.3.1. Orthogonality condition

We shall formulate the equation for reciprocity of the work performed by the vibration modes. To do this we multiply for all the disks the inertia forces and the inertia torques of one mode by the corresponding displacements in another mode and combine these

products. Then, formulating the same sum for the reciprocal mode and equating the sums, w. obtain the equation

$$\sum_{i=1}^{k} (m_i \lambda_j^2 \eta_{ij} \eta_{i,v} + J_{9i} A_{ij} \lambda_j^2 \theta_{(k+1),j} \theta_{(k+1),v}) =$$
$$= \sum_{i=1}^{k} (m_i \lambda_v^2 \eta_{i,v} \eta_{ij} + J_{9i} A_{ji} \lambda_v^2 \theta_{(k+1),v} \theta_{(k+1),j}). \qquad (4.65)$$

The subscripts j and ν indicate the vibration mode number.

The other subscript system remains the same as it was in (4.57) and (4.58).

The coefficients A_1 are also connected with the vibration mode number, since the frequency λ enters into their formula (4.59). Moreover, the rotational speed ω also enters into these coefficients.

If we examine modes taken for the same multiplicity factor s, i.e., if we take the frequencies (and the associated modes) determined by the points of intersection on the frequency map of a given ray with the frequency curves, then for all these frequencies the coefficient A_1 will remain constant. Then the orthogonalit condition is obtained in the following form from (4.65)

$$\sum_{i=1}^{k} (m_i \eta_{ij} \eta_{iv} + J_{9i} A_{i9} \theta_{(k+1)j} \theta_{(k+1)v} = 0; \qquad (4.66)$$

the subscript s on the coefficient A_1 indicates the slope of the ray from which the vibration natural frequencies and modes are taken.

The orthogonality condition (4.66) is valid, specifically, for the rotor critical speeds (s = 1).

The existence of orthogonality of the vibration modes indicates that the nodal theorem is applicable to the vibration modes. In accordance with this theorem and the orthogonality conditions, each branch of the frequency map (see Figure 4.13) is characterized by its own number of nodes.

We note that the vibration modes for forward and backward precession have these properties independently of one another, since in essence they belong to different rotational speeds.

Example 4.1. Calculate the critical speeds and bending modes of the rotor shown in Figure 4.14a. In view of their small diameter and considerable width, we take the overhanging wheels as point masses. The magnitudes of the masses are respectively: $m_1 = 3.5$ kg, $m_2 = 7$ kg, $m_3 = 3$ kg (the masses are numerically equal to the weights of the wheels). The moments of inertia of the turbine disk are: axial — $J_p = 0.05$ kg·m^2, equatorial — $J_e = 0.025$ kg·m^2.
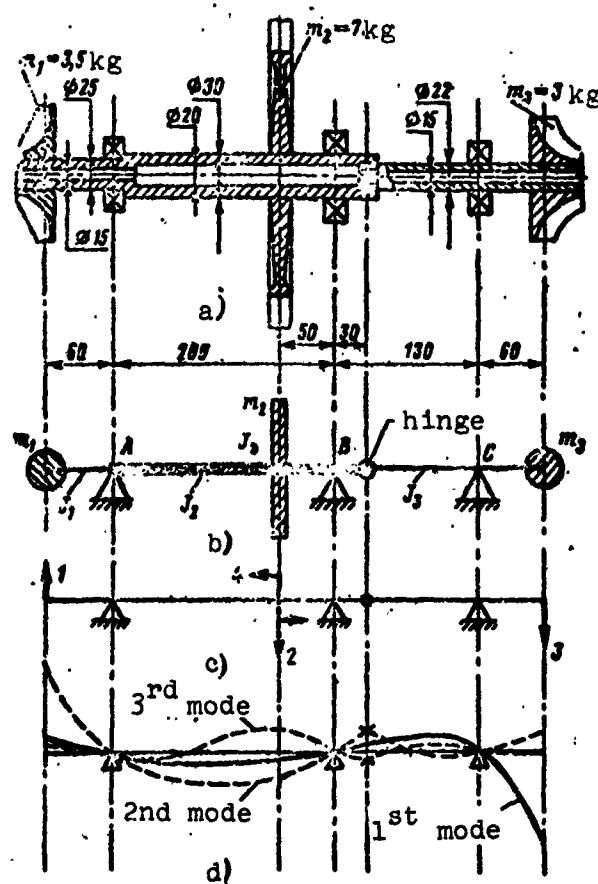

Figure 4.14. Rotor schematic for vibration calculation

The rotor shaft is stepped. The moments of inertia of the sections (see Figure 4.14b) are respectively: $J_1 = 1.7$ cm^4; $J_2 = 3.2$ cm^4; $J_3 = 0.9$ cm^4.

The compliance coefficients for the unit forces shown in Figure 4.14c are represented by the matrix

$$|\alpha_{is} \cdot 10^9| = \begin{vmatrix} 58.7 & 14.7 & 5.62 & 255 \\ 14.7 & 14.7 & 6.15 & 195 \\ 5.62 & 6.15 & 110.4 & 63.5 \\ 255 & 195 & 63.5 & 4550 \end{vmatrix} .$$

The coefficients α_{is} are computed in the SI system of units and have the respective dimensions: m/N, 1/N, 1/(N · m).

The coefficients are most easily found by the Vereshchagin technique; the linear dimensions are expressed in meters (m) and the forces in Newtons (N). In determining the compliance coefficients, the directions of the unit forces and moments are as shown in Figure 4.14c.

We formulate the frequency equation in determinant form (4.62). To do this we multiply each of the columns of the coefficient matrix by m_1, m_2, m_3, $- J_e$, respectively (the coefficient $A = - 1$)

$$\begin{vmatrix} 20.5 - x & 10.3 & 1.69 & -0.638 \\ 5.15 & 10.3 - x & 1.85 & -0.4488 \\ 1.97 & 4.3 & 33.1 - x & -0.159 \\ 89.3 & 137 & 19 & -11.4 - x \end{vmatrix} = 0,$$

where $x = 10^8/\lambda^2$.

Expanding the determinant into a row, we obtain

$$x^4 - 52.5x^3 + 565.2x^2 + 2953x - 22049 = 0.$$

The roots of the equation are

$$x_1 = 33.71; \quad x_2 = 20.57; \quad x_3 = 4.81; \quad x_4 = -6.59.$$

These roots correspond to the frequencies

$$\lambda_1 = 1722\frac{1}{\text{sec}}; \quad \lambda_2 = 2200\frac{1}{\text{sec}}; \quad \lambda_3 = 4530\frac{1}{\text{sec}}.$$

The fourth root yields an imaginary frequency.

The critical speeds are

$$n_{\kappa p 1} = 16\,500\,\text{rpm}; \quad n_{\kappa p 2} = 21\,000\,\text{rpm}; \quad n_{\kappa p 3} = 43\,300\,\text{rpm}.$$

The rotor bending modes at the critical speeds are determined by the deflections at the disks. The latter are proportional to the minors of the frequency equation determinant. Calculating these minors, we obtain the following amplitude ratios:

for the first root — 0.151 : 0.095 :: 1.0 : 1.005;

for the second root — 1.00 : 0.276 :: −0.20 : 3.8;

for the third root — −0.42 : 1.00 :: − 0.085 : 5.6

The vibration modes (see Figure 4.14d) show that at the first critical speed the largest deformations occur in the right-hand shaft overhang. At the second critical speed they occur in the left overhang, and at the third critical speed the maximal deflection occurs in the center span. The maximal inflection of the elastic line at the hinge is obtained at the second critical speed.

4.4. Critical Speeds of Rotors with Hinged Connection

The rotors of aircraft gas turbine engines and turbomachines often have three or four supports. Such rotors are usually made up of two parts connected by a hinge in order to avoid the danger of overloading and binding of the bearings because of the elastic and thermal deformations of the case, and to facilitate fabrication and assembly operations. The selection of the hinge location on the rotor is determined primarily by convenience in the arrangement of the entire assembly and various design considerations. In addition, the location of the hinge has a very significant effect on the natural vibration frequencies of the rotor and its critical speeds, and therefore this factor must also be considered during

design. Moreover, even a slight change of the location of the hinge in the rotor can serve as an effective technique for altering the frequency characteristic of the rotor in attempting to reduce vibrations.

It is obvious that the introduction of a hinge into the rotor design does not reduce the number of rotor natural vibration modes and frequencies or the number of critical speeds. The introduction of the hinge reduces the natural frequencies. Depending on the hinge location, its effect on certain frequencies may be considerable, while the influence on others may be small or completely negligible.
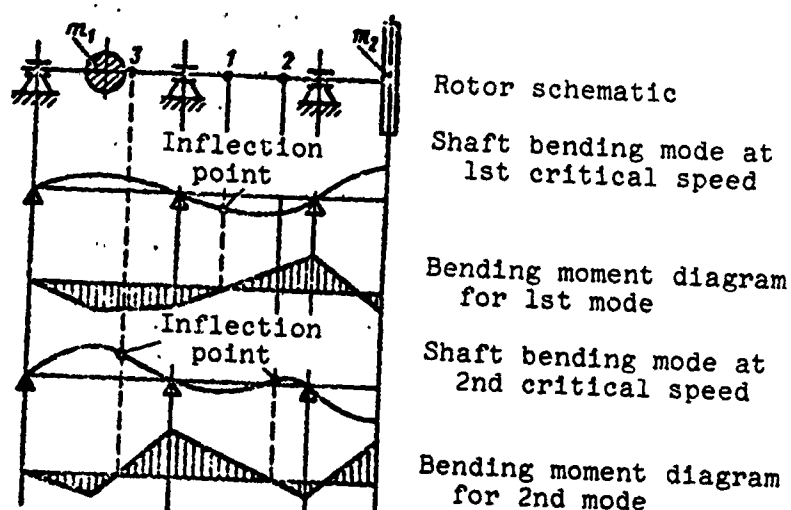
Figure 4.15. Shaft bending modes at critical speeds

Figure 4.15 shows a schematic of the rotor. According to the frequency map such a rotor has two critical speeds. Each speed corresponds to its own bending mode.

Knowing the critical speed, the shaft deflections at the points where the mass and disk are located, and also the rotation angle of

the disk, we can easily find the inertial forces and moments acting on the shaft

$$P_1 = m_1 \eta_1 \omega_{\text{кр}}^2; \quad P_2 = m_2 \eta_2 \omega_{\text{кр}}^2; \quad M = -J_\theta \theta \omega_{\text{кр}}^2. \tag{4.67}$$

We shall construct the elastic line and the bending moment diagram owing to the action of these loads. The construction is carried out for both critical speeds.

A hinge located at the point of inflection of the shaft's elastic line, where the bending moment is zero, does not alter the vibration mode or frequency. The hinge has the greatest effect if it is located at the section with the maximal bending moment. Then there is a significant change of the frequency of that mode which is disturbed by the hinge.

For example, if we locate the hinge at the point 1 (see Figure 4.15) the first critical speed is not changed while the second is reduced. The spread between the critical speeds is reduced.

If we locate the hinge at the point 2 or 3, the second critical speed is not changed while the first is reduced. The spread between the critical speeds is increased.

Location of the hinge away from the inflection points reduces both critical speeds but not to the same degree, the reduction is rather a function of the relationship between ratio of the bending moments at the sections.

The resolution of the hinge location problem depends on the objective, i.e., what critical speed spread needs to be increased and what frequencies need to be changed in order to shift the natural frequency region away from the operating conditions.

The use of a hinge or a splined coupling in the construction of a rotor (or a composite shaft) at rotational speeds above the critical speed can lead to the onset of self-excited vibrations of the rotor. This question is examined in Section 11.2.

The calculation of the vibration frequencies and modes of the hinged rotor is made using the general equation (4.62). The computational technique remains the same. The presence of the hinge

in the construction affects the magnitudes of the compliance co-efficients, which are the basis of the frequency equation.

4.5. Vibrations of Rotors on Elastic Supports

4.5.1. Estimating Overall Support Compliance

Elastic deformations in the supports lead, in general, to reduction of the vibration natural frequencies and rotor critical speeds. All rotor supports have some definite elasticity. Therefore the analysis of all rotors should be made with account for support elasticity in order to obtain more exact results.

The technique for analysis of the rotor with elastic supports remains general and is based on calculating the roots of the determinant (4.62) and its minors as the vibration modes.

The compliance coefficients which appear in this determinant are written as the sum

$$a_{is} = a'_{is} + a''_{is},$$ (4.68)

where a'_{is}, a''_{is} — are respectively the compliance coefficients associated with rotor deformation for absolutely rigid supports and for an absolutely rigid rotor. The latter are determined on the basis of the geometric relationships between the rotor dimensions and support stiffness.

As an example we shall present the formulas for calculating the support compliance coefficients of a two-support rotor (Figure 4.16).

The displacement at the point s from unit force factor at the point i will be

$$a''_{si} = (e_2 - e_1)\frac{l_s}{L} + e_1;$$ (4.69)

the angle of rotation at the point s from unit force factor at point i is
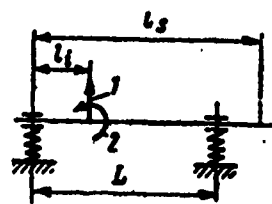
Figure 4.16. Determining support compliance coefficients

$$\alpha'_{si} = \frac{e_2 - e_1}{L},\qquad(4.70)$$

where the subscripts si are to be associated with the corresponding subscripts of the compliance coefficients from the deformation of the rotor itself; e_1, e_2 are the support deformations under the action of unit force or moment applied at the point i.

The deformations from the unit force are

$$c_1 = \frac{L - l_i}{Lc_I};\qquad e_2 = \frac{l_i}{Lc_{II}}.\qquad(4.71)$$

The deformations from the unit moment are

$$e_1 = -\frac{1}{Lc_I};\qquad e_2 = \frac{1}{Lc_{II}},\qquad(4.72)$$

where c_I and c_{II} — are the stiffness coefficient of the left and right supports.

Substituting (4.71) or (4.72) into (4.69) and (4.70), we obtain the compliance coefficients in the form of displacement or rotation angle at the point s from unit force or moment applied at point i. If $l_1 = l_s$, we obtain the eigenvalues of the compliance coefficients. It is not difficult to obtain similar formulas for any rotor configuration.

The support compliance, from which their stiffness is defined, is made up from the deformations of the bearings, webs or diaphragms in which the bearings are mounted, the deformation of the structural elements of the case, and so on.

The support compliance coefficients can be taken approximately in the ranges

$$(50 - 150)\cdot 10^{-9} \text{ m/N, or } (50 - 150)\cdot 10^{-6} \text{ cm/kgf.}$$

The compliance coefficients of antifriction bearings generally fall in the range:

for ball bearings:

$$(5 - 8) \cdot 10^{-9} \text{ m/N, or } \sim(5 - 8) \cdot 10^{-6} \text{ cm/kgf;}$$

for roller bearings:

$$(2.5 - 5.5) \cdot 10^{-9} \text{ m/N, or } \sim(2.5 - 5.5) \cdot 10^{-6} \text{ cm/kgf.}$$

These figures for the bearings constitute about 5 − 6% of the overall magnitude of the compliance.

The support stiffness coefficients are the reciprocals of the compliance coefficients. The magnitudes corresponding to the values shown above are:

$$(6 - 20) \cdot 10^{6} \text{ N/m, or } \sim (6 - 20) \cdot 10^{3} \text{ kgf/cm.}$$

In practical calculations of specific gas turbine engine and turbomachinery designs, the support compliance coefficients or stiffness coefficients are evaluated from the design drawing or are determined experimentally.

We note that the support compliance coefficients are comparable with the rotor compliance coefficients and in certain cases may even be larger than the latter. Therefore, calculation of the rotor critical speeds without account for at least the static compliances of the supports may lead to significant disagreement with experiment.

More profound studies and exact calculations are made with account for dynamic interaction of the rotor and case. The fundamentals of such calculations are presented in Chapter VI.

4.5.2. Selection of Special Elastic Supports

The primary objective of the use of special elastic rotor supports is to modify the rotor frequency characteristic and reduce the case vibrations created by the rotor.

It was shown in Section 4.2.1. that for a high rotational speed, far exceeding the critical speed, a tendency for rotor self-centering develops and the disk centers of gravity and principal

axes tend to align with the axis of rotation. In this case the forces which develop in the supports are minimal.

For multi-support rotors of complex construction, consisting of several disks, it is difficult to keep all the rotor critical speeds significantly below the rotor operating speed. It may happen that one of the critical speeds lies in the operating speed range, and as a result excessive engine vibrations develop.

By selection of the support stiffnesses, it is possible to broaden the spread between adjacent critical speeds and select the latter so that they differ markedly from the operating speeds.

At the same time it should be pointed out that the use of elastic supports is accompanied by several negative aspects. As a result of the large support compliances there appear large static radial displacements of the rotor under the action of the weight forces and accelerations during flight, and shock loads are possible when displacement limiters come into play. The large deformations create the danger of blade contact with the case, scoring of the labyrinth seals, and so on. Therefore the use of elastic supports requires the resolution of several design problems other than those associated with vibration.

When resorting to the use of special elastic supports, we must remember that change of the compliance of the individual supports has a different effect on the change of the critical speeds of the different modes. Their influence depends on the rotor configuration, its mass and stiffness, and also on the location of the supports.

An estimate of the effect of each of the supports can be made with the aid of the relation

$$\frac{\Delta \omega_{cr\,j}}{\Delta e_n}, \text{ where } \Delta e_n = e'_n - e_n; \qquad (4.73)$$

where $\Delta\omega_{cr\,j} = \omega_{cr\,j} - \omega_{cr\,j}$ — is the reduction of the critical speed of mode j with increase of the compliance of support n;

e'_n, e_n — are, respectively, the increased and original compliances of support n.

By varying in turn the compliances of all the supports within small limits and finding the new values of the critical speeds ω'_{cr}, we can determine the influence of each support with the aid of (4.73).

The resulting ratios make possible a more rational introduction of the elastic support in order to affect markedly one vibration mode in the desired direction while having relatively little effect on another mode.

The overall critical speed reduction as a result of changing the compliance of all the supports if found from the formula

$$\delta\omega_{\kappa p\,j} = \sum_{n=1}^{k} \frac{\Delta\omega_{\kappa p\,j}}{\Delta e_n}\, \delta e_n \tag{4.74}$$

where k — is the number of supports;

δe_n — is the compliance change of each support.

Figure 4.17 shows the variation of the rotor critical speeds of a gas turbine engine with change of the compliance of the first and second supports over a wide range. Because of the large compliance of the third support and the central location of the hinge, change of the compliance of the front supports has no effect on the first critical speed.

Example 4.2. Determine the critical speed reduction for the rotor of Example 4.1, which can be obtained by the use cf elastic supports.

The introduction of elastic supports leads to increase of the compliance coefficients. This increase is determined as the additional displacement from unit force in the corresponding directions (Figure 4.18) which appears as a result of deformation of the supports for an absolutely rigid shaft.

As a result of system linearity, we can determine the additional compliances from the elasticity of each support separately. These additional compliances are represented by the following tables
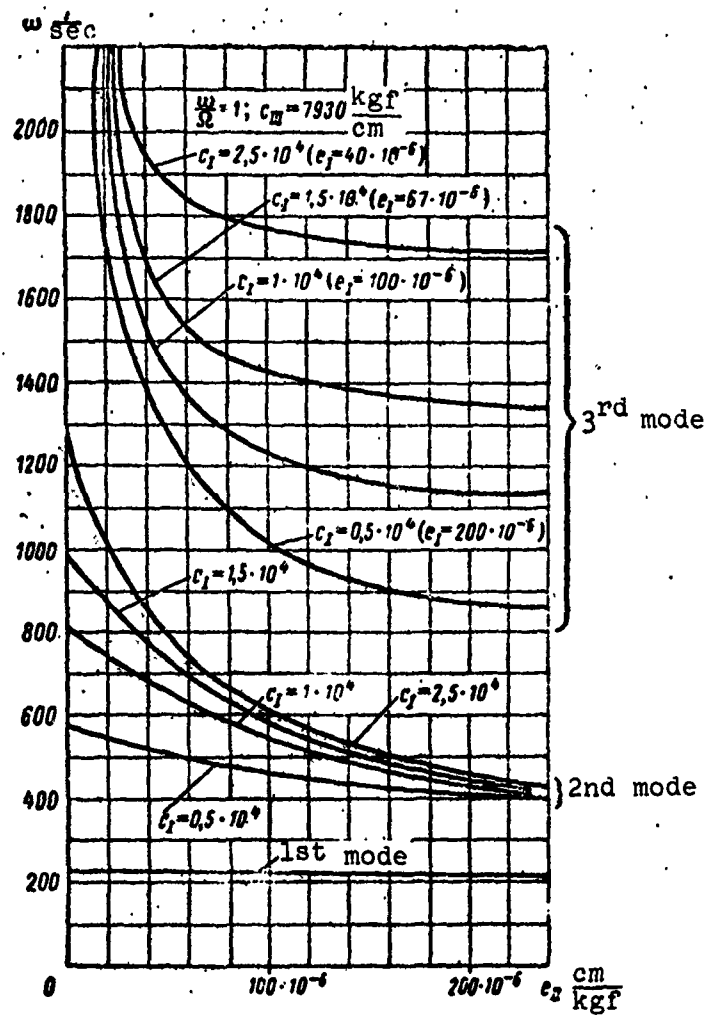
Figure 4.17. Effect of support compliance on gas turbine engine rotor critical speeds
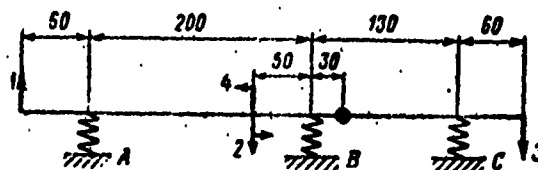
Figure 4.18. Schematic of rotor elastic supports

$$
\Delta a_{ls} = \begin{vmatrix}
1,690 & -0,325 & -0,117 & -6,500 \\
-0,325 & 0,063 & 0,023 & 1,250 \\
-0,117 & 0,023 & 0,008 & 0,450 \\
-6,500 & 1,250 & 0,450 & 25,00
\end{vmatrix} a_A;
$$

$$
\Delta a_{ls} = \begin{vmatrix}
0,090 & 0,225 & -0,207 & -1,500 \\
0,225 & 0,563 & -0,518 & -3,750 \\
-0,207 & -0,518 & 0,273 & 2,600 \\
-1,500 & -3,750 & 2,600 & 25,00
\end{vmatrix} a_B;
$$

$$
\Delta a_{33} = 2,56 a_C; \quad \Delta a_{ls}^C = 0,
$$

where α_A, α_B, α_C — are the compliance coefficients of the elastic supports.

We see from the rotor support arrangement that the introduction of compliance of support C yields a change only in the coefficient α_{33} and has no effect on the other coefficients.

We specify the compliance coefficient of the elastic supports by the quantity

$$a_A = a_B = a_C = 20 \cdot 10^{-9} \ \mathrm{m/N}.$$

Combining the additional compliances with the basic coefficient matrix (see Example 4.1), we obtain

$$
a_{ls}^A = \begin{vmatrix}
92,20 & 8,20 & 3,28 & 125 \\
8,20 & 15,95 & 6,60 & 220 \\
3,28 & 6,60 & 110,56 & 72,5 \\
125,00 & 220,00 & 72,5 & 50,0
\end{vmatrix} \cdot 10^{-9};
$$

$$a_{is}^B = \begin{vmatrix} 60,50 & 19,20 & 1,48 & 225 \\ 19,20 & 25,95 & -4,21 & 120 \\ 1,48 & -4,21 & 115,86 & 115,5 \\ 225,00 & 120,00 & 115,50 & 5050 \end{vmatrix} \cdot 10^{-9};$$

$$a_{is}^C = \begin{vmatrix} 5870 & 14,70 & 5,62 & 255 \\ 14,70 & 14,70 & 6,15 & 195 \\ 5,62 & 6,15 & 161,60 & 63,5 \\ 225,00 & 195,00 & 63,50 & 4550 \end{vmatrix} \cdot 10^{-9}.$$

Multiplying the columns respectively by $m_1 = 3.5$ kg, $m_2 = 7$ kg, $m_3 = 3$ kg, $-\varepsilon_e = 0.025$ kg $\cdot$ m, we construct the frequency equations for the rotor having one of the supports elastic with the compliance indicated above.

For elastic support A

$$\begin{vmatrix} 32,40-x & 5,75 & 0,984 & -0,312 \\ 2,87 & 11,20-x & 1,98 & -0,550 \\ 1,15 & 4,62 & 33,20-x & -0,181 \\ 43,70 & 154 & 21,80 & -12,6-x \end{vmatrix} = 0;$$

for elastic support B

$$\begin{vmatrix} 21,20-x & 13,43 & 0,444 & -0,563 \\ 6,72 & 18,20-x & -1,26 & -0,300 \\ 0,52 & -2,95 & 34,7-x & -0,269 \\ 78,80 & 84,00 & 34,6 & -12,6-x \end{vmatrix} = 0;$$

for elastic support C

$$\begin{vmatrix} 20,50-x & 10,3 & 1,69 & -0,638 \\ 5,15 & 10,3-x & 1,85 & -0,488 \\ 1,97 & 4,3 & 48,50-x & -0,159 \\ 89,30 & 137,0 & 19,0 & -11,4-x \end{vmatrix} = 0.$$

Expanding the determinant into a row, we obtain equations which have the following positive roots:

$$x^4-64,2x^3+918x^2+4320x-58000=0;$$
$$x_1=38,6; \quad x_2=26,2; \quad x_3=7,23;$$
$$\lambda_1=1615 \, 1/sec; \quad \lambda_2=1960 \, 1/sec; \quad \lambda_3=3720 \, 1/sec;$$
$$x^4-61,5x^3+805x^2+6190x-100500=0;$$
$$x_1=37,5; \quad x_2=23,0; \quad x_3=11,2;$$

$$\lambda_1 = 1640 \ 1/\text{sec}; \quad \lambda_2 = 2090 \ 1/\text{sec}; \quad \lambda_3 = 2980 \ 1/\text{sec};$$

$$x^4 - 67.9x^3 + 863x^2 + 4140x - 34\,900 = 0;$$

$$x_1 = 49.0; \quad x_2 = 20.9; \quad x_3 = 5.07;$$

$$\lambda_1 = 1430 \ 1/\text{sec}; \quad \lambda_2 = 2190 \ 1/\text{sec}; \quad \lambda_3 = 4460 \ 1/\text{sec}.$$

Comparison of the roots of these equations with the roots of the original equation (see Example 4.1) shows that the elastic supports provide different reduction of all the natural frequencies.

The elastic support A reduces the first frequency by 6.2%, the second by 11%, the third by 18%, i.e., it affects the higher frequencies more and the first frequency least.

The elastic support B provides only slight reduction of the first frequency — by 4.7%, and 5% reduction of the second; however, it has a marked effect on the third frequency, reducing it by 34%.

Conversely, the elastic support C provides marked reduction of the first frequency — 17%, but has practically no effect on the second and third frequencies, reducing them by 0.5% and 1.6% respectively.

By selecting the magnitudes of the support compliance, we can achieve the desired change of the rotor natural vibration frequencies (critical speeds).

4.6. Approximate Methods for Calculating Rotor
Natural Frequencies and Critical Speeds

Calculation of the natural frequencies using (4.62) becomes very time-consuming for even three disks. The determinant is of high order, a large number of influence coefficients must be calculated in order to formulate the determinant, and then the frequencies are found by trial and error.

Moreover, we note that this determinant does not take into account the distributed mass of the parts of the rotor and its

shafts. The introduction of these masses into the composition of the determinant increases its order and complicates the calculations still more.

Therefore approximate computational methods, which provide an accuracy which is quite adequate for practical purposes, are used to find the natural frequencies and the critical speeds.

Among the approximate methods, those most frequently used are the Rayleigh method, Ritz and Galerkin variational methods, the method of successive approximations, and the integral method. These methods were examined in Chapters II and III, and may be applied for calculating shafts and rotors without any essential changes.

For today's rotor designs, which have low natural frequencies because of the thin-wall construction, the most rational computational methods are those which make it possible to find the natural vibration frequencies and critical speeds in any frequency range without prior computation of the lower vibration modes. The following method is of this type.

4.6.1. Initial Parameter Method

We regard to the equations used and satisfaction of the boundary conditions, the initial parameter method belongs to the exact computational methods. It is constructed on the cyclic principle and consists of several repeating series of multiplication and addition operations. As a result of this, the method is convenient for computer programming and computing.

To carry out the calculation the rotor or shaft (Figure 4.19) is broken down into a series of individual segments. The boundaries of the segments are: locations of concentrated masses or disks, locations of supports, locations of stepwise change of the shaft cross section. The rigid supports divide the entire shaft or rotor into several segments.

Figure 4.19. Dividing the rotor into segments
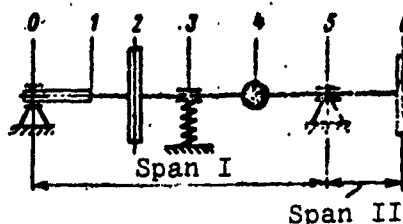
4.6.1.1. Segment matrices

In order to perform the calculation for each segment, we formulate the equations for converting from the parameters at the beginning of the segment to the parameters at the end of the segment.

If the calculation is made with account for the distributed masses of the segments, the basis for the formulation of the equations is the equation for the elastic line of a bar, which can be taken in the most general form (3.34) with account for rotary inertia of the section and the action of the longitudinal force. For the description of the method we shall restrict ourselves to the simpler but frequently used form (3.18) for simple uniform bars:

$$Y(k\xi) = C_1 S(k\xi) + C_2 T(k\xi) + C_3 U(k\xi) + C_4 V(k\xi).$$

The section rotation angle, bending moment, and shearing force will be defined respectively by the equations:

$$\theta(k\xi) = \frac{k}{l}[C_1 V(k\xi) + C_2 S(k\xi) + C_3 T(k\xi) + C_4 U(k\xi)];$$

$$M(k\xi) = EJ\frac{k^2}{l^2}[C_1 U(k\xi) + C_2 V(k\xi) + C_3 S(k\xi) + C_4 T(k\xi)];$$

$$Q(k\xi) = -EJ\frac{k^3}{l^3}[C_1 T(k\xi) + C_2 U(k\xi) + C_3 V(k\xi) + C_4 S(k\xi)].$$

Let us assume that the displacement and forces at the initial point of the segment ($\xi = 0$) are known. Then the constants are easily found from the equations

$$C_1 = Y(0); \quad C_2 = \frac{l}{k}\theta(0); \quad C_3 = \frac{l^2}{k^2 EJ}M(0); \quad C_4 = \frac{-l^3}{k^3 EJ}Q(0).$$

After substituting these values of the coefficients into the basic equations, we obtain a system of equations in which the displacements and forces are expressed in terms of the parameters of the initial section of the segment

$$
\left.
\begin{aligned}
Y(k\xi) &= Y(0)S(k\xi) + \theta(0)\frac{1}{a}T(k\xi) + \\
&+ M(0)\frac{1}{a^2 EJ}U(k\xi) - Q(0)\frac{1}{a^3 EJ}V(k\xi); \\
\theta(k\xi) &= Y(0)aV(k\xi) + \theta(0)S(k\xi) + \\
&+ M(0)\frac{1}{aEJ}T(k\xi) - Q(0)\frac{1}{a^2 EJ}U(k\xi); \\
M(k\xi) &= Y(0)a^2 EJU(k\xi) + \theta(0) \times \\
&\times aEJV(k\xi) + M(0)S(k\xi) - \\
&- Q(0)\frac{1}{a}T(k\xi); \\
Q(k\xi) &= -Y(0)a^3 EJT(k\xi) - \\
&- \theta(0)a^2 EJU(k\xi) - M(0)aV(k\xi) + \\
&+ Q(0)S(k\xi).
\end{aligned}
\right\}
\qquad (4.75)
$$

These formulas yield a linear relationship between the parameters of the beginning and end of the segment.

We write the system of equations for the displacements and forces at the right end of the segment ($\xi = 1$) in matrix form

$$
\left\|
\begin{array}{c}
Y(k) \\
\theta(k) \\
M(k) \\
Q(k)
\end{array}
\right\|_{M} =
$$

$$
= \left\|
\begin{array}{cccc}
S(k) & \frac{1}{a}T(k) & \frac{1}{a^2 EJ}U(k) & -\frac{1}{a^3 EJ}V(k) \\
aV(k) & S(k) & \frac{1}{aEJ}T(k) & -\frac{1}{a^2 EJ}U(k) \\
a^2 EJU(k) & aEJV(k) & S(k) & -\frac{1}{a}T(k) \\
-a^3 EJT(k) & -a^2 EJU(k) & -aV(k) & S(k)
\end{array}
\right\| \times
\qquad (4.76)
$$

$$
\times \left\|
\begin{array}{c}
Y(0) \\
\theta(0) \\
M(0) \\
Q(0)
\end{array}
\right\|_{M},
$$

where $a=\frac{k}{l}$; $k^4=\frac{m\lambda^2l^4}{EJ}$;

The indices ki and 0i denote the end and beginning of the segment i.

In accordance with the matrix multiplication rules, to obtain the displacement or forces at the right end of the segment we must take the sum of the products of the elements of the corresponding row by the column elements in their sequential order. The square matrix is called fundamental. Such matrices are constructed ahead of time for all the segments.

If the calculation is made without account for the distributed masses of the segments, then we take the following equations, formulated in accordance with the scheme shown in Figure 4.20, as the equations connecting the beginning and end of the segment

Figure 4.20. Determining connection between parameters of end and beginning of segment

$$\left.\begin{aligned}
Y_{ki} &= Y_{0i} + \theta_{0i}l + a_{12}M_{ki} + a_{11}Q_{ki}; \\
\theta_{ki} &= \theta_{0i} + a_{22}M_{ki} + a_{12}Q_{ki}; \\
M_{ki} &= M_{0i} - Q_{0i}l; \\
Q_{ki} &= Q_{0i}.
\end{aligned}\right\} \qquad (4.77)$$

Transforming the equations so that only the initial parameters remain on the right side, we obtain a system of equations which can be written in matrix form as follows:

$$\left\|\begin{matrix} Y \\ \theta \\ M \\ Q \end{matrix}\right\|_{ki} = \left\|\begin{matrix} 1 & l & a_{12} & a_{11}-a_{12}l \\ 0 & 1 & a_{22} & a_{12}-a_{22}l \\ 0 & 0 & 1 & -l \\ 0 & 0 & 0 & 1 \end{matrix}\right\| \times \left\|\begin{matrix} Y \\ \theta \\ M \\ Q \end{matrix}\right\|_{0i} \qquad (4.78)$$

where a_{11}, a_{12}, a_{22} — are the influence coefficients of the cantilever beam.

4.6.1.2. Matrices for transition between segments

It is also convenient to represent the transition through the separating element from the end of the preceding segment to the beginning of the next segment in matrix form.

Transition from a segment with one cross section to a segment with a different cross section is not accompanied by change of the parameters. Therefore, the transition matrix will have the form

$$\begin{vmatrix} 1 & 0 & 0 & 0 \\ 0 & 1 & 0 & 0 \\ 0 & 0 & 1 & 0 \\ 0 & 0 & 0 & 1 \end{vmatrix}. \qquad (4.79)$$

Multiplication of this matrix by the column of the parameters of the end of the preceding segment yields a repetition of the latter parameters in the form of the column of the initial parameters for the next segment.

Figure 4.21 shows the individual elements through which transition must be made in the computational process. Characteristic for all the cases other than that shown in Figure 4.21c is invariability of the kinematic parameters Y, θ, and change of the moments and shearing forces. After formulating the equations of equilibrium corresponding to the notations shown in Figure 4.21, we obtain the transition matrices in the form:

a) transition through a point mass

$$\begin{vmatrix} 1 & 0 & 0 & 0 \\ 0 & 1 & 0 & 0 \\ 0 & 0 & 1 & 0 \\ -m_i\lambda^2 & 0 & 0 & 1 \end{vmatrix}; \qquad (4.80)$$

b) transition through a rotating disk

$$\begin{vmatrix} 1 & 0 & 0 & 0 \\ 0 & 1 & 0 & 0 \\ 0 & -\left(1-\frac{\omega}{\lambda}\cdot\frac{J_p}{J_a}\right)J_a\lambda^2 & 1 & 0 \\ -m\lambda^2 & & 0 & 1 \end{vmatrix}; \qquad (4.81)$$
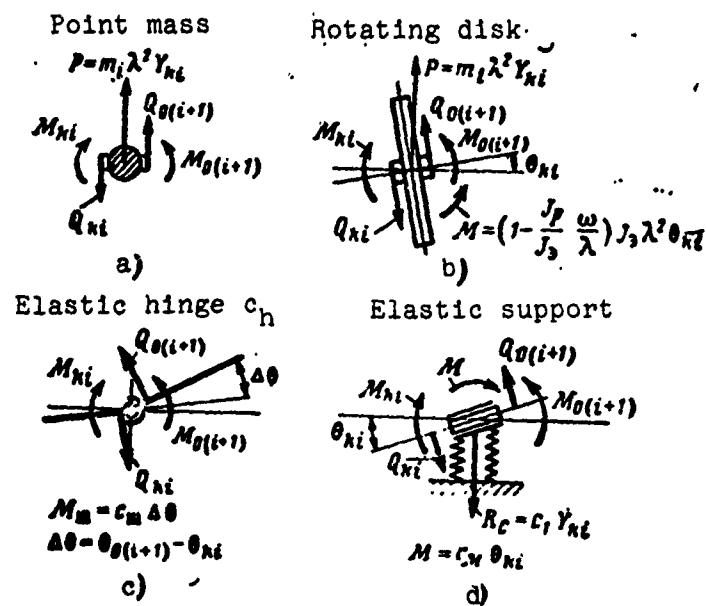
Figure 4.21. Schemes for passing through individual
elements of computational system

c) transition through an elastic hinge

$$\begin{vmatrix} 1 & 0 & 0 & 0 \\ 0 & 1 & \dfrac{1}{c_m} & 0 \\ 0 & 0 & 1 & 0 \\ 0 & 0 & 0 & 1 \end{vmatrix};$$

(4.82)

where c_h — is the hinge moment stiffness coefficient;

d) transition through an elastic support with elastic
restraint

$$\begin{vmatrix} 1 & 0 & 0 & 0 \\ 0 & 1 & 0 & 0 \\ 0 & c_m & 1 & 0 \\ c_Q & 0 & 0 & 1 \end{vmatrix};$$

(4.83)

if there is no elastic restraint, then $c_h = 0$.

Transition through rigid support.

The rigid support is th. ᵒnd of a span. The transverse displacement at the support is zerᵥ; therefore, the first of the four equations becomes a homogeneous linear equation relating the initial parameters

$$Y_{ki} = a_1 Y_0 + a_2 \theta_0 - a_3 M_0 + a_4 Q_0 = 0, \qquad (4.84)$$

where a_1, a_2, a_3, a_4 — are numerical coefficients formulated in the process of calculating the preceding segments.

This equation makes it possible to exclude any of the unknown initial parameters from the remaining three equations.

The initial parameters of the next $(i + 1)^{st}$ span are connected with the final parameters of the calculated i^{th} span by the following equations (Figure 4.22):

$$\left. \begin{array}{l} Y_{0(i+1)} = 0; \\ \theta_{0(i+1)} = \theta_{ki}; \\ M_{0(i+1)} = M_{ki}; \\ Q_{0(i+1)} = Q_{ki} - R_i, \end{array} \right\} \qquad (4.85)$$

where R_i — is the unknown reaction of the rigid support. This reaction enters into the further calculations of the entire span in place of the excluded parameter of the first span. The number of unknown parameters remains the same.
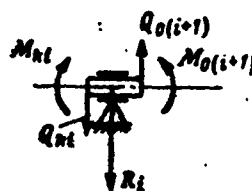
Figure 4.22. Scheme for passing through rigid support

4.6.1.3. Selection of assumed initial conditions.

The initial conditons at the zero section of the first span are selected on the basis of the restraint conditions and loading of the shaft being analyzed. For the most typical cases (Figure 4.23) they are represented in the form of one of the columns
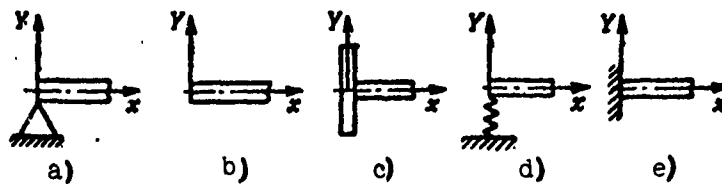
igure 4.23. Choice of initial conditions:
a — rigid support; b — free cantilever; c — cantilever
disk; d — elastic support; e — clamped

$$
a)\begin{vmatrix} 0 \\ \theta_0 \\ 0 \\ Q_0 \end{vmatrix}
\quad b)\begin{vmatrix} Y_0 \\ \theta_0 \\ 0 \\ 0 \end{vmatrix}
\quad c)\begin{vmatrix} Y_0 \\ \theta_0 \\ -\left(1-\dfrac{\omega}{\lambda}\dfrac{J_p}{J_s}\right)J_s\lambda^2\theta_0 \\ -m\lambda^2 Y_0 \end{vmatrix}
\quad d)\begin{vmatrix} Y_0 \\ \theta_0 \\ 0 \\ c_Q Y_0 \end{vmatrix}
\quad e)\begin{vmatrix} 0 \\ 0 \\ M_0 \\ Q_0 \end{vmatrix}.
\qquad (4.86)
$$

In all cases two of the four initial parameters are zero and
the other two appear as unknowns. Even in the most complex matrix
— column (c) — all four elements are functions of two parameters
— Y_0 and θ_0. This means that in the computational process all the
parameters of the beginning and end of all the segments will be
linear functions of the two unknown assumed parameters.

These initial parameter columns can serve as the parameters
for the end of the last span. In this case the signs of the moments
and the shearing forces must be reversed and the subscript 0 re-
placed by the subscript k.

An essential feature is the fact that all the parameters of
the end section are expressed in terms of two parameters, so that
the four equations for the end parameters can be reduced to two
homogeneous equations with two unknowns.

4.6.1.4. Two-calculation method

The determination of the natural vibration frequency, and for the rotating shaft the circular precession rate λ, is accomplished `︳ ⌢⌣⌢⌣⌢⌣` selection.

Taking some numerical value of λ, we formulate for all the segments of the shaft being analyzed the segment matrices and the transition matrices. Then we select one of the initial condition columns (4.86) in accordance with the conditions at the zero section [for the sake of definiteness we present the analysis for column (a)].

Using the linear connection between the parameters, we make two calculations of the first span. In the first calculation we $\theta_0 = 1$, $Q_0 = 0$; in the second calculation we take $\theta_0 = 0$; $Q_0 = 1$.

As a result we obtain two groups of coefficients a, b, c, d, from which we formulate the Equations (4.85) of the parameters of the last section of the first span and the first section of the second span

$$\left.\begin{aligned}
Y_{0II} &= Y_{kI} = a_2\theta_0 + a_4 Q_0 = 0; \\
\theta_{0II} &= \theta_{kI} = b_2\theta_0 + b_4 Q_0; \\
M_{0II} &= M_{kI} = c_2\theta_0 + c_4 Q_0; \\
Q_{0II} &= Q_{kI} + R_1 = d_2\theta_0 + d_4 Q_0 + R_1.
\end{aligned}\right\} \qquad (4.87)$$

The first equation of this system provides the relationship between θ_0 and Q_0. With the aid of this equation, we eliminate from the remaining equations one of the parameters (Q_0, for example), as a result of which we obtain the column for calculating the next span

$$\begin{vmatrix} Y_{0II} \\ \theta_{0II} \\ M_{0II} \\ Q_{0II} \end{vmatrix} = \begin{vmatrix} 0 \\ b\theta_0 \\ c\theta_0 \\ d\theta_0 + R_1 \end{vmatrix}. \qquad (4.88)$$

The basic column now contains two unknown parameters: θ_0 and R_I.

Two calculations are made of the second span. In the first calculation we take $\theta_0 = 1$; $R_I = 0$, and in the second $\theta_0 = 0$; $R_I = 1$. As a result we obtain a system of equations for the end of the second span which is similar to (4.87).

If there is a third span, we perform operations similar to those described and the next span is calculated. In this case the parameter R_I is excluded, and in its place there appears the parameter R_{II}.

If the third span is the last, we obtain the equations for its its end

$$
\left.
\begin{aligned}
Y_{kIII} &= a'_2\theta_0 + a'_4 R_{11}; \\
\theta_{kIII} &= b'_2\theta_0 + b'_4 R_{11}; \\
M_{kIII} &= c'_2\theta_0 + c'_4 R_{11}; \\
Q_{kIII} &= d'_2\theta_0 + d'_4 R_{11}.
\end{aligned}
\right\}
\tag{4.89}
$$

In accordance with the end conditions, two of these equations are set equal to zero, or on the basis of (4.89) and the end conditions, two homogeneous equations with the two unknowns θ_0 and R_{II} are formulated.

The frequency λ is considered to have been selected correctly if the second-order determinant Δ composed from the coefficients of the homogeneous equations equals zero. If this condition is not met the calculation must be repeated for a different value of λ.

The results of the calculation are represented in graphical form (Figure 4.24). The point of intersection of the curve with the abscissa axis is the sought frequency.

For a rotating shaft the number of roots is in general equal to twice the number of degrees of freedom of the shaft in one plane. In this case half of the roots are negative, which indicates backward precession.

In finding the critical speeds, after assuming the frequency λ, the condition $\omega = \lambda$ must be satisfied to formulate the matrices

for transition through the disks.
In this case the number of roots
will be equal to the number of
shaft masses, considering the
disk with $J_e > J_p$ as two masses.

4.6.1.5. Constructing shaft vibration mode shapes

Figure 4.24. Curve plotted from calculation results

Sometimes it is necessary to construct the vibration mode shape. We can judge the order number of the found frequency from the vibration mode shape; the vibration mode shape shows the most highly stressed segments of the shaft, the segments with the highest vibration amplitude, and so on

The vibration mode shape is constructed from the previously calculated parameters Y and θ of the beginning and end of the segments (we consider the parameters for the design frequency λ_d). To this end one of the basic parameters (θ_0, for example) is taken as unity and all the other parameters are calculated from the available relations. Then the displacement Y_1 and the angles θ_1 at the ends of the segmen , are plotted to a convenient scale, after which it is easy to construct the elastic line. If a more exact construction of the bending shape of any segment is required, this is accomplished using the general equation

$$Y(k\xi) = C_1 S(k\xi) + C_2 T(k\xi) + C_3 U(k\xi) + C_4 V(k\xi),$$

for which the constants C_1, C_2, C_3, C_4 are determined from the known parameters Y and θ at the beginning and end of the segment.

Example 4.3. Calculate by the initial parameter method the rotor examined in Example 4.1. The rotor shaft mass is to be neglected in the calculation.

The rotor consists of six segments of constant section separated by supports, a disk, and a hinge (see Figure 4.14b).

Let us formulate the segment matrices. The general expression for the weightless segment matrix is defined by (4.78).

The influence coefficients appearing in the matrices are

$$\alpha_{11} = \frac{l^3}{3EJ}; \quad \alpha_{12} = \frac{l^2}{2EJ}; \quad \alpha_{22} = \frac{l}{EJ}.$$

The numerical values of the segment matrices will be

segment 1
$l = 0,06\,\text{м}$
$J = 1,7 \cdot 10^{-6}\,\text{м}^4$.
$$\begin{vmatrix} 1 & 0,06 & 0,53 \cdot 10^{-6} & -1,06 \cdot 10^{-8} \\ 0 & 1,0 & 0,177 \cdot 10^{-4} & -0,53 \cdot 10^{-6} \\ 0 & 0 & 1,0 & -0,06 \\ 0 & 0 & 0 & 1,0 \end{vmatrix};$$

segment 2
$l = 0,15\,\text{м}$
$J = 3,2 \cdot 10^{-6}\,\text{м}^4$
$$\begin{vmatrix} 1 & 0,15 & 1,768 \cdot 10^{-6} & -8,79 \cdot 10^{-8} \\ 0 & 1,0 & 0,2343 \cdot 10^{-4} & -1,758 \cdot 10^{-6} \\ 0 & 0 & 1,0 & -0,15 \\ 0 & 0 & 0 & 1,0 \end{vmatrix};$$

segment 3
$l = 0,05\,\text{м}$
$J = 3,2 \cdot 10^{-6}\,\text{м}^4$
$$\begin{vmatrix} 1 & 0,05 & 0,195 \cdot 10^{-6} & -0,326 \cdot 10^{-6} \\ 0 & 1,0 & 0,0781 \cdot 10^{-4} & -0,195 \cdot 10^{-6} \\ 0 & 0 & 1,0 & -0,05 \\ 0 & 0 & 0 & 1,0 \end{vmatrix};$$

segment 4
$l = 0,03\,\text{м}$
$J = 3,2 \cdot 10^{-6}\,\text{м}^4$
$$\begin{vmatrix} 1 & 0,03 & 0,0702 \cdot 10^{-6} & -0,0705 \cdot 10^{-8} \\ 0 & 1,0 & 0,0469 \cdot 10^{-4} & -0,0702 \cdot 10^{-6} \\ 0 & 0 & 1,0 & -0,03 \\ 0 & 0 & 0 & 1,0 \end{vmatrix};$$

segment 5
$l = 0,1\,\text{м}$
$J = 0,9 \cdot 10^{-6}\,\text{м}^4$
$$\begin{vmatrix} 1 & 0,1 & 2,778 \cdot 10^{-6} & -9,261 \cdot 10^{-8} \\ 0 & 1,0 & 0,557 \cdot 10^{-4} & -2,778 \cdot 10^{-6} \\ 0 & 0 & 1,0 & -0,1 \\ 0 & 0 & 0 & 1,0 \end{vmatrix};$$

segment 6
$l = 0,06\,\text{м}$
$J = 0,9 \cdot 10^{-6}\,\text{м}^4$
$$\begin{vmatrix} 1 & 0,06 & 10^{-6} & -2 \cdot 10^{-8} \\ 0 & 1,0 & 0,333 \cdot 10^{-4} & -10^{-6} \\ 0 & 0 & 1,0 & -0,06 \\ 0 & 0 & 0 & 1,0 \end{vmatrix}.$$

The initial parameter column is

$$\begin{vmatrix} Y_{01} \\ \theta_{01} \\ M_{01} \\ Q_{01} \end{vmatrix} = \begin{vmatrix} Y_{01} \\ \theta_{01} \\ 0 \\ -m_1 \lambda^2 Y_{01} \end{vmatrix};$$

where m_1 = 3.5 kg. The minus sign is used for the last element of the column because the inertia force of the mass m_1 acts on the left end of the segment.

We take Y_{01} = 1 and after assuming a value of λ (λ = 1700 sec^{-1}, for example) we multiply the column by the matrix of segment 1; we obtain the segment end parameters

$$Y_{\lambda 1} = 1,1072 + 0,060\theta_{01} = 0;$$
$$\theta_{\lambda 1} = 5,36095 + \theta_{01};$$
$$M_{\lambda 1} = 60,69 \cdot 10^4;$$
$$Q_{\lambda 1} = -10,115 \cdot 10^6.$$

Since segment 1 terminates at the rigid support, where the deflection equals zero, the first equality is set equal to zero an θ_{01} is then excluded from the second equality

$$\theta_{01} \approx -18,4533;$$
$$\theta_{\lambda 1} = -13,0923;$$
$$M_{\lambda 1} = 60,69 \cdot 10^4;$$
$$Q_{\lambda 1} = -10,115 \cdot 10^6.$$

The column of the initial parameters of the next segment (2) after the support will be

$$\begin{vmatrix} Y_{02} \\ \theta_{02} \\ M_{02} \\ Q_{02} \end{vmatrix} = \begin{vmatrix} 0 \\ -13,0923 \\ 60,69 \cdot 10^4 \\ -10,115 \cdot 10^6 + R_A \end{vmatrix}$$

where R_A — the reaction of the rigid support — is an unknown quantity.

After multiplying the column and the matrix of segment 2, we obtain the parameters of the end of the segment

$$Y_{\lambda 2} = -0,007807 - 8,79 \cdot 10^{-8} R_\lambda;$$
$$\theta_{\lambda 2} = 18,9096 - 1,758 \cdot 10^{-6} R_A;$$
$$M_{\lambda 2} = 2,1242 \cdot 10^6 - 0,15 R_A;$$
$$Q_{\lambda 2} = -10,115 \cdot 10^6 + R_A.$$

In accordance with (4.81), the matrix for transition through the rotating disk will be

$$\begin{vmatrix} 1 & 0 & 0 & 0 \\ 0 & 1 & 0 & 0 \\ 0 & 0{,}025 \cdot 1700^2 & 1 & 0 \\ -7 \cdot 1700^2 & 0 & 0 & 1 \end{vmatrix}.$$

Multiplying the column of the end parameters of segment 2 by the transition matrix, we obtain the parameters of the beginning of the next segment 3

$$Y_{03} = -0{,}007807 - 8{,}79 \cdot 10^{-8} R_A;$$
$$\theta_{03} = -18{,}9006 - 1{,}758 \cdot 10^{-6} R_A;$$
$$M_{03} = 3{,}4904 \cdot 10^6 - 0{,}277 R_A;$$
$$Q_{03} = -9{,}9571 \cdot 10^6 + 2{,}7782 R_A.$$

Multiplication of the parameters of the beginning of the segment by the matrix 3 yields the parameters of the end of segment 3

$$Y_{k3} = 1{,}65076 - 23{,}8672 \cdot 10^{-8} R_A = 0;$$
$$\theta_{k3} = 48{,}1112 - 4{,}4631 \cdot 10^{-6} R_A;$$
$$M_{k3} = 3{,}9883 \cdot 10^6 - 0{,}41591 \cdot R_A;$$
$$Q_{k3} = -9{,}9571 \cdot 10^6 + 2{,}7782 R_A.$$

With the aid of the first equality, we exclude R_A from all the expressions, after which the parameters of the end of the segment will be

$$R_A = 6{,}910646 \cdot 10^6;$$
$$\theta_{k3} = 17{,}2683;$$
$$M_{k3} = 1{,}1141 \cdot 10^6;$$
$$Q_{k3} = 9{,}2421 \cdot 10^6.$$

The initial parameters of the next segment 4, after the support B, are

$$\begin{vmatrix} Y_{04} \\ \theta_{04} \\ M_{04} \\ Q_{04} \end{vmatrix} = \begin{vmatrix} 0 \\ 17{,}2683 \\ -1{,}1141 \cdot 10^6 \\ 9{,}2421 \cdot 10^6 + R_B \end{vmatrix}.$$

Multiplying the initial parameters by the matrix 4, we obtain the parameters of the end of the segment

$$Y_M = 0.58974 - 0.0705 \cdot 10^{-6} R_B;$$
$$\theta_M = 21.8446 - 0.0702 \cdot 10^{-6} R_B;$$
$$M_M = 06368 \cdot 10^6 - 0.03 R_B = 0;$$
$$Q_M = 9.2421 \cdot 10^6 + R_B.$$

The moment in the hinge is zero; therefore the third equation is set equal to zero and then used to exclude R_B from all the other equations

$$R_B = 27.8933 \cdot 10^6;$$
$$Y_M = 0.57008;$$
$$\theta_M = 19.8865;$$
$$Q_M = 37.1354 \cdot 10^6.$$

The initial parameters of segment 5 will be

$$\begin{vmatrix} Y_{05} \\ \theta_{05} \\ M_{05} \\ Q_{05} \end{vmatrix} = \begin{vmatrix} 0.57008 \\ 19.8865 + \theta_m \\ 0 \\ 37.1354 \cdot 10^6 \end{vmatrix}.$$

where θ_h — the rotation angle in the hinge — is an unknown quantity.

Multiplication of the initial parameters and the matrix 5 yields the parameters of the end of the segment

$$Y_{A5} = -0.88038 + 0.1 \theta_h = 6;$$
$$\theta_{A5} = -53.2758 + \theta_m;$$
$$M_{A5} = -3.71354 \cdot 10^6;$$
$$Q_{A5} = 37.1354 \cdot 10^6.$$

The initial parameters of the last segment, after excluding θ_h from the preceding equalities and passing through the support C, take the form

$$\begin{vmatrix} Y_{06} \\ \theta_{06} \\ M_{06} \\ Q_{06} \end{vmatrix} = \begin{vmatrix} 0 \\ -74.4718 \\ -3.71354 \cdot 10^6 \\ 37.1354 \cdot 10^6 + R_C \end{vmatrix}.$$

Multiplying by the matrix of the last segment 6, we obtain the parameters of the end of the segment

$$Y_{M6} = -8,9245 - 2 \cdot 10^{-8} R_C;$$
$$\theta_{M6} = -235,2681 - 10^{-6} R_C;$$
$$M_{M6} = -5,94164 \cdot 10^6 - 0,06 R_C;$$
$$Q_{M6} = 37,1354 \cdot 10^6 + R_C.$$

In accordance with (4.80) the matrix of the mass m_3 will be

$$\begin{vmatrix} 1 & 0 & 0 & 0 \\ 0 & 1 & 0 & 0 \\ 0 & 0 & 1 & 0 \\ -3 \cdot 1700^2 & 0 & 0 & 1 \end{vmatrix}.$$

Multiplying the matrix by the parameters of the end of the segment, we obtain the parameters after the mass — at the free right end of the shaft

$$Y_{M} = -8,9245 - 2 \cdot 10^{-8} R_C;$$
$$\theta_{M} = -235,2681 - 10^{-6} R_C;$$
$$M_{M} = -5,94164 \cdot 10^6 - 0,06 R_C = 0;$$
$$Q_{M} = 114,5108 \cdot 10^6 + 1,1734 R_C = 0.$$

The last segment is a cantilever and there is no external force or moment on the right; therefore the last two equations must be equal to zero. This is satisfied if the corresponding coefficients of the equations are proportional, or if the determinant composed from the coefficients of the equations is equal to zero. We verify the latter condition

$$-(5,94164 \cdot 1,1734 - 0,06 \cdot 114,5108) \cdot 10^6 = -0,10127 \cdot 10^6 \neq 0.$$

The determinant is not equal to zero; therefore the frequency $\lambda = 1700$ sec^{-1} used in the calculation is not correct. The calculation must be repeated after choosing a different frequency.

The calculation for the frequency $\lambda = 1725$ sec^{-1} yields the following parameters at the free end of the cantilever

$$Y_{M} = -8,4764 - 2 \cdot 10^{-8} R_C;$$
$$\theta_{M} = -223,4057 - 10^{-6} R_C;$$
$$M_{M} = -5,6387 \cdot 10^6 - 0,06 R_C = 0;$$
$$Q_{M} = 110,9089 \cdot 10^6 + 1,178536 R_C = 0.$$

The determinant of the last two equations equals

$$-(5.6367 \cdot 1.178536 - 110.9069 \cdot 0.06) \cdot 10^9 = 0.00971.$$

By interpolation from the values of the determinants obtained from the two calculations, we find that the critical frequency (first critical speed) is

$$\omega_1 = \lambda_1 = 1722.8 \ //\text{sec}.$$

If it is necessary to determine the support reactions and the parameters at the ends of all the segments for this frequency, we must carry out still another cycle of calculations with the frequency equal to $1722.8 \ \text{sec}^{-1}$. The quantities obtained as a result of this calculation pertain to deflection equal to one ($Y_{01} = 1$).

For the calculation of the second critical speed, we must assume higher values of the frequency λ. The value of the frequency for which the end-section determinant passes through zero, changing sign from positive to negative, will be the value of the sought critical speed.

It is convenient to systematize the calculation in the form of a table, whose arrangement can be arbitrary.

4.6.2. Variational Methods

The Rayleigh, Ritz, and Bubnov-Galerkin variational methods were examined in Chapters II and III. The application of these methods for the calculation of rotating shafts and rotors has certain peculiarities.

4.6.2.1. Rayleigh method

The free vibrations of a rotating shaft are executed in the form of regular precession. As a result of this, the inertial forces and moments of all the shaft masses and disks act in the shaft bending plane. Therefore we can examine the deformation of the shaft as being static, and we can formulate the sum of the work of all the inertial forces and moments

$$K = \frac{1}{2} \sum_{i=1}^{k} [m_i \lambda^2 \eta_i^2 + (J_{ei} \lambda^2 - J_{pi} \omega \lambda) \theta_i^2]. \qquad (4.90)$$

where   k — is the number of disks seated on the shaft;

λ — is the free vibration circular frequency — the regular precession rate;

m_i, J_{ei}, J_{pi} — are the mass, equatorial and polar moments of inertia of the disk, respectively;

ω — is the shaft rotational speed.

The work of the external forces equals the potential energy of the shaft deformation

$$K = \Pi. \qquad (4.91)$$

Substituting herein (4.90), we obtain the Rayleigh formula in the form

$$\lambda^2 = \frac{\Pi}{K_0},$$

where

$$K_0 = \frac{1}{2} \sum_{i=1}^{k} \left[m_i \eta_i^2 + \left(J_{ei} - J_{pi} \frac{\omega}{\lambda} \right) \theta_i^2 \right]. \qquad (4.92)$$

In accordance with the Rayleigh method, the potential energy is calculated as the work of some system of external forces and moments, which are numerically equal respectively to the masses and moments of inertia of the disks

$$\left. \begin{array}{l} P_i = m_i; \\ M_i = \left(J_{ei} - J_{pi} \frac{\omega}{\lambda} \right). \end{array} \right\} \qquad (4.93)$$

The calculation is made for precession of a definite form. Therefore the ratio ω/λ must be considered constant. In the calculation of the critical speeds, it is equal to one.

Applying the forces and moments to the shaft at the points where the disks are located, we calculate the deflections η_1 and the section rotation angles θ_1.

After this, we calculate the deformation potential energy

$$\Pi = \frac{1}{2} \sum_{i=1}^{k} (P_i \eta_i + M_i \theta_i).$$

The final form of the Rayleigh formula will be

$$p^2 = \frac{\sum\limits_{i=1}^{k} (P_i \eta_i + M_i \theta_i)}{\sum\limits_{i=1}^{k} \left[m_i \eta_i^2 + \left(I_{xi} - I_{pi} \frac{\omega}{\lambda} \right) \theta_i^2 \right]}. \tag{4.94}$$

It should be noted that in calculating the deflections η_1 and angles θ_1 the positive directions of the forces P_1 and the moments M_1 must coincide in sign with the directions of the deformations in the first vibration mode. Usually the first vibration mode shape is obvious, and the choice of the directions of the applied forces and moments does not cause any difficulty. The signs of the calculated η_1 and θ_1 can serve as a check of the correctness of the basic assumptions with regard to the directions of action of the forces and moments.

If in the calculations we neglect the effect of the inertial moments of the disks, then (4.94) simplifies

$$\lambda^2 = \frac{\sum\limits_{i=1}^{k} P_i \eta_i}{\sum\limits_{i=1}^{k} m_i \eta_i^2}.$$

4.6.2.2. Frequency equation in Ritz form

If the shaft deflection function $\eta(x)$ is known, the deformation potential energy is calculated with the aid of the integral

$$\Pi = \frac{1}{2} \int_0^l EJ \left(\frac{d^2\eta}{dx^2}\right)^2 dx;$$

in this connection (4.91) takes the form

$$\int_0^l EJ \left(\frac{d^2\eta}{dx^2}\right)^2 dx - \lambda^2 \sum_{l=1}^n \left[m_l \eta_l^2 + \left(J_{sl} - J_{pl} \frac{\omega}{\lambda}\right) \theta_l^2 \right] = 0, \qquad (4.95)$$

where η_1, θ_1 — are the discrete values of the functions $\eta(x)$ and $d\eta/dx$ for the disk location coordinates.

In view of the fact that the function $\eta(x)$ is not known, it is replaced by the approximate function $\phi(x)$, but then (4.95) is not satisfied and becomes the functional

$$S = \int_0^l EJ \left(\frac{d^2\varphi}{dx^2}\right)^2 dx - \lambda^2 \sum_{l=1}^n \left[m_l \varphi_l^2 + \left(J_{sl} - J_{pl} \frac{\omega}{\lambda}\right) \left(\frac{d\varphi_l}{dx}\right)^2 \right]. \qquad (4.96)$$

Of all the possible functions $\phi(x)$, the closest to the exact solution $\eta(x)$ will be that for which the functional S has the minimal value.

We represent $\phi(x)$ as the minimizing function

$$\varphi(x) = \sum_{n=1}^z \alpha_n \phi_m \qquad (4.97)$$

where ψ_n — are the basic functions, which must satisfy the geometric boundary conditions. In practical calculations it is desirable that the number z of basic functions not be made large, restricting ourselves to two or three functions;

α_n — are the variational coefficients.

We substitute (4.97) into (4.96), after which we take the derivative of S with respect to α_n and equate it to zero

$$\frac{dS}{d\alpha_s} = \int_0^l EJ \cdot \frac{d^2\varphi}{dx^2} \cdot \frac{d^2\psi_s}{dx^2} dx - \lambda^2 \sum_{l=1}^n \left[m_l \varphi_l \psi_{ls} + \right.$$
$$\left. + \left(J_{sl} - J_{pl} \frac{\omega}{\lambda}\right) \left(\frac{d\varphi}{dx}\right)_l \left(\frac{d\psi_s}{dx}\right)_l \right] = 0, \qquad (4.98)$$

where s — is the index of the variational coefficient with respect to which the differentiation is performed.

The number of equations in (4.98) equals the number of basic functions z. All the equations are homogeneous and contain the unknown coefficients α_n.

For convenience in formulating the subsequent equations, we denote the combinations of the basic functions

$$\int_0^l EJ \frac{d^2\psi_n}{dx^2} \frac{d^2\psi_s}{dx^2} dx = U_{ns};$$ (4.99)

$$\left[\sum_{i=1}^s m_i \psi_{ni} \psi_{si} + \sum_{i=1}^s \left(1 - \frac{J_p}{J_s} \frac{\omega}{\lambda}\right) J_{si} \left(\frac{d\psi_n}{dx}\right)_i \left(\frac{d\psi_s}{dx}\right)_i\right] = T_{ns}.$$ (4.100)

The coefficients U_{sn} and T_{sn} possess the reciprocity property. With the aid of the introduced notations, we write the system of equations (4.98). Assuming that the number of basic functions equals three, we obtain

$$\alpha_1(U_{11} - \lambda^2 T_{11}) + \alpha_2(U_{21} - \lambda^2 T_{21}) + \alpha_3(U_{31} - \lambda^2 T_{31}) = 0;$$
$$\alpha_1(U_{12} - \lambda^2 T_{12}) + \alpha_2(U_{22} - \lambda^2 T_{22}) + \alpha_3(U_{32} - \lambda^2 T_{32}) = 0;$$
$$\alpha_1(U_{13} - \lambda^2 T_{13}) + \alpha_2(U_{23} - \lambda^2 T_{23}) + \alpha_3(U_{33} - \lambda^2 T_{33}) = 0.$$

The determinant of this system of equations is the frequency equation in Ritz form

$$\begin{vmatrix} U_{11} - \lambda^2 T_{11} & U_{21} - \lambda^2 T_{21} & U_{31} - \lambda^2 T_{31} \\ U_{12} - \lambda^2 T_{12} & U_{22} - \lambda^2 T_{22} & U_{32} - \lambda^2 T_{32} \\ U_{13} - \lambda^2 T_{13} & U_{23} - \lambda^2 T_{23} & U_{33} - \lambda^2 T_{33} \end{vmatrix} = 0.$$ (4.101)

The smallest root λ^2 of (4.101) is the square of the sought circular vibration frequency of the rotating rotor or shaft. If $\lambda = \omega$, this frequency will be the critical rotational speed.

The minors of the Determinant (4.101) to the elements of any row, calculated for the found value of λ^2, yield a series of numbers proportional to the coefficients α_n

$$\Delta'_1 : \Delta'_2 : \Delta'_3 = \alpha_1 : \alpha_2 : \alpha_3. \tag{4.102}$$

Their determination makes it possible to construct the shaft bending mode shape in the form of the Function (4.97).

4.6.2.3. Construction of the Minimizing Function

The construction of the assumed minimizing function must correspond to the number and location of the supports. For example, for the two-support shaft with small overhang, the Function (4.97) can be taken in the form

$$\varphi(x) = \alpha_1 \sin \pi \xi + \alpha_2 \sin 2\pi \xi + \alpha_3 \sin 3\pi \xi; \tag{4.103}$$

$\xi = (x/l_1)$, x is taken in the range from zero to 1,

where l — is the overall shaft length;

l_1 — is the distance between supports.

For the three-support shaft with spans of different length, the minimizing function must consists of two parts

$$\varphi_1(x) = \alpha_1 \sin \pi \xi_1 + \alpha_2 \sin 2\pi \xi_1 + \alpha_3 \sin 3\pi \xi_1), \ 0 < \xi_1 < 1;$$
$$\varphi_2(x) = \beta(-\alpha_1 \sin \pi \xi_2 + \alpha_2 \sin 2\pi \xi_2 - \alpha_3 \sin 3\pi \xi_2, \ 0 < \xi_2 < 1,$$

where

for the first span $\xi_1 = \dfrac{x}{l_1}, \ 0 < x < l_1;$

for the second span $\xi_2 = \dfrac{x}{l_2}, \ 0 < x < l_2.$

Then the Integral (4.99) breaks down into two integrals, and the computation of the Coefficients (4.100) must be made with account for the fact that on each part of the shaft there is located a mass with the index i.

The coefficient β is found from the condition that the deflection curves match at the center support. This coefficient equals

$$\beta = \frac{l^2}{l_1}.$$

4.7. Special Problems of Vibrations of
Rotating Shafts and Rotors

4.7.1. Free Vibrations of Rotors on Anisotropically Elastic Supports

In practice, shaft supports may have different stiffness in mutually perpendicular — principal — directions. This is associated with the nature of the specific construction of the turbomachine or engine as .

If the difference in the stiffnesses is not large, it is not taken into consideration and the supports are assumed to be axisymmetric. For those cases in which the difference in support stiffnesses is significant, it is necessary to take into consideration the specific characteristics in the rotor vibrations which appear because of disruption of axial symmetry. Such supports are usually termed anisotropically elastic supports.

We consider a shaft with a single disk (Figure 4.25). We denote the stiffness of the supports and the shaft in the principal planes, referred to the center of gravity of the disk, as follows:

c_{11}^{x}, c_{12}^{x}; c_{22}^{x} — are the stiffnesses acting in the xOz plane;

c_{11}^{y}, c_{12}^{y}, c_{22}^{y} — are the stiffnesses acting in the yOz plane.

We write the differential equations of motion as the equations of equilibrium of the forces and moments in terms of projections on the coordinate axes

$$
\left.
\begin{array}{l}
m\ddot{x}_0 + c_{11}^{x} x_0 + c_{12}^{x}\beta = 0; \\
m\ddot{y}_0 + c_{11}^{y} y_0 + c_{12}^{y}\alpha = 0;
\end{array}
\right\} \quad (4.104)
$$

$$
\left.
\begin{array}{l}
J_s\ddot{\alpha} - J_p\omega\dot{\beta} + c_{12}^{y} y_0 + c_{22}^{y}\alpha = 0; \\
J_s\ddot{\beta} + J_p\omega\dot{\alpha} + c_{12}^{x} x_0 + c_{22}^{x}\beta = 0.
\end{array}
\right\} \quad (4.105)
$$
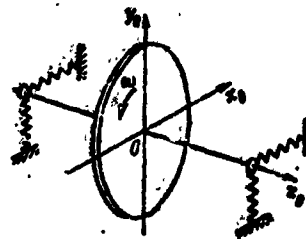
Figure 4.25. Rotor on anisotropically elastic supports

Equations (4.104) and (4.105) form a unified system, since the solutions in the z_0z_0 plane are connected with the solutions in the other y_0z_0 plane.

The solutions of the equations are the functions

$$\left.\begin{array}{l} x_0 = X \cos \lambda t; \\ y = B \cos \lambda t; \\ y_0 = Y \sin \lambda t; \\ \alpha = A \sin \lambda t. \end{array}\right\} \qquad (4.106)$$

Substitution of the Functions (4.106) into (4.104) and (4.105) yields a system of homogeneous algebraic equations

$$\left.\begin{array}{l} (c_{11}^x - m\lambda^2) X + c_{12}B = 0; \\ c_{12}^x X + (c_{22}^x - J_s\lambda^2) B + J_\rho \omega\lambda A = 0; \\ (c_{11}^y - m\lambda^2) Y + c_{12}^y A = 0; \\ J_\rho \omega\lambda B + c_{12}^y Y + (c_{22}^y - J_s\lambda^2) A = 0. \end{array}\right\} \qquad (4.107)$$

The arrangement of the equations and the terms within them is such that we obtain the same sequence of amplitude values X, B, Y, A, horizontally and diagonally.

The determinant of the System (4.107) has the form

$$\begin{vmatrix} c_{11}^x - m\lambda^2 & c_{12}^x & 0 & 0 \\ c_{12}^x & c_{22}^x - J_s\lambda^2 & 0 & J_\rho \omega\lambda \\ 0 & 0 & c_{11}^y - m\lambda^2 & c_{12}^y \\ 0 & J_\rho \omega\lambda & c_{12}^y & c_{22}^y - J_s\lambda^2 \end{vmatrix} = 0. \qquad (4.108)$$

The roots of this equation are the free vibration frequencies of a rotating rotor on anisotropically elastic supports.

For computational convenience, the determinant can be transformed to the form

$$(J_\rho \omega)^2 = \frac{\delta_0^x \delta_0^y}{(c_{11}^x - m\lambda^2)(c_{11}^y - m\lambda^2)}, \qquad (4.109)$$

where

$$\Delta_0^r = \begin{vmatrix} c_{11}^r - m\lambda^3 & c_{14}^r \\ c_{12} & c_{22}^r - J_s\lambda^3 \end{vmatrix}; \quad \Delta_1^r = \begin{vmatrix} c_{11}^r - m\lambda^3 & c_{12}^r \\ c_{12}^r & c_{22}^r - J_s\lambda^3 \end{vmatrix}. \tag{4.110}$$

The roots of the Determinants (4.110) are the free vibration frequencies of the nonrotating rotor in the horizontal and vertical planes. They are shown in the frequency diagram (Figure 4.26) by points lying on the ordinate axis.

The position of the horizontal asymptotes is determined by the condition $\omega \to \infty$. Therefore, the equations of the asymptotes are

$$c_{11}^r - m\lambda^3 = 0; \quad c_{11}^r - m\lambda^3 = 0. \tag{4.111}$$

The slope of the inclined asymptote is equal to the ratio J_p/J_e.

The frequency diagram is easily constructed approximately from the zero points and the asymptotes by following the rule: from each zero point there emerges only a single curve, which approaches

Figure 4.26. Natural frequencies of rotor on anisotropically elastic supports

one of the nearest asymptotes, including the abscissa axis. Only a single curve can approach each horizontal asymptote. The frequency diagram is symmetric about the abscissa axis and the ordinate axis, i.e., the numerical value of the natural frequencies is independent of the direction of rotation.

The rotor with a single disk has for any rotational speed four different natural vibration frequencies, which is the same as the total number of its degrees of freedom. Each frequency corresponds to its own vibration mode in the form of forward or backward irregular precession. The precession form can be established from the amplitude values of the Functions (4.106).

The relationship between the amplitude values X : B : Y : A is determined as the ratio of the minors to the elements of any row of the Determinant (4.108).

In the general case the center of gravity executes motion along an elliptical trajectory. If the signs of the amplitude values X and Y are the same, then the describing point travels along the ellipse in the positive direction — the precession is irregular and forward. If the signs of the amplitudes are opposite, the precession is backward. The ellipse is elongated along that axis for which the absolute value of the amplitude is larger.

During free vibrations, the principal central axis of the disk describes the surface of an elliptical cone. In accordance with (4.106) and the conventional rule for reckoning the angles of rotation α and β in the $x_0 y_0 z_0$ axes, the precession of the axis will be forward for positive signs of the amplitudes A and B. The precession will be backward if the signs of these amplitudes are opposite.

The overall vibration mode shape is formed as the superposition of the precession of the principal axis on the center-of-gravity motion trajectory.

If the stiffnesses in the principal planes are the same, (4.109) breaks down into two identical equations

$$(c_{11} - m\lambda^2)\left[c_{22} - J_*\lambda^2\left(1 - \frac{J_\rho}{J_*}\frac{\omega}{\lambda}\right)\right] - c_{12}^2 = 0,$$

which yield the free circular vibration frequencies.

4.7.2. Critical Speeds of Rotor on Anisotropically Elastic Supports

We shall examine the simplest case, in which the disk is located midway between the supports and the stiffness coefficients $c_{12}^x = c_{12}^y = 0$. Then, as the shaft bends, there is no rotation of the disk plane and inertial bending moments do not arise. We denote by c_x and c_y the stiffness coefficients along the x and y axes respectively. If the disk center of gravity is shifted by the

distance a, relative to the shaft axis, then the equations of the forced vibrations along the two axes will be

$$m\ddot{x} + c_x x = ma\omega^2 \cos\omega t; \\ m\ddot{y} + c_y y = ma\omega^2 \sin\omega t. \qquad \Big\} \qquad (4.112)$$

The solutions of the equations are defined by the functions

$$x = X\cos\omega t; \quad y = Y\sin\omega t, \qquad (4.113)$$

where

$$X = a\frac{\omega^2}{\lambda_x^2 - \omega^2}; \quad Y = a\frac{\omega^2}{\lambda_y^2 - \omega^2};$$

$$\lambda_x^2 = \frac{c_x}{m}; \quad \lambda_y^2 = \frac{c_y}{m}. \qquad (4.114)$$

The amplitudes of the forced horizontal and vertical vibrations are shown in Figure 4.27 as a function of the rotational speed. The rotor on anisotropically elastic supports has two critical speeds

$$\omega_{\text{кр}1} = \lambda_x; \quad \omega_{\text{кр}2} = \lambda_y.$$

For a rotational speed $\omega < \lambda_x$ (below the lowest natural frequency) both amplitudes have a positive sign. This means that the
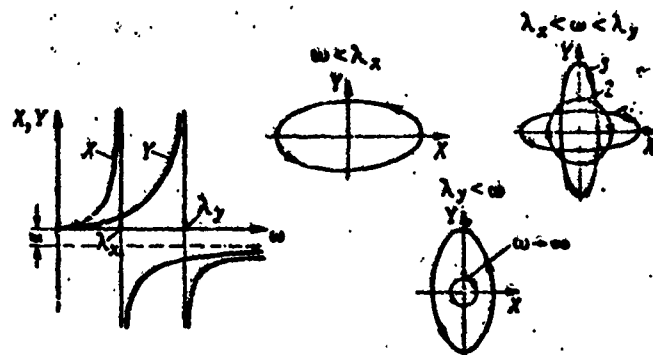
Figure 4.27.   Shaft precession at different rotatioral speeds

describing point travels along the elliptical trajectory in the positive direction — the shaft executes forward irregular precession. With approach to the first critical speed, the amplitude X of the vibrations along the x axis increases. This axis of the ellipse becomes longer.

For a rotational speed $\lambda_x < \omega < \lambda_y$, the amplitudes X and Y have different signs. In this connection, under the influence of unbalance the shaft executes backward precession. The axis of the ellipse is gradually elongated along the y axis. At the moment when the rotational speed equal to λ_y is reached, the vibrations become nearly planar in the vertical plane.

In the supercritical region both amplitudes are negative, and the precession becomes forward. As the rotational speed increases the ellipse approaches a circle of radius a, and the center of gravity of the disk tends to take a position on the axis of rotation.

In the more general case, with account for the gyroscopic moments of the disk, the critical speeds are found from the frequency diagram (see Figure 4.26) as the points of intersection of the characteristics with the straight line $\omega = \lambda$. The precession form at the critical speed is determined with the aid of the signs and magnitudes of the quantities X, Y, B, A, which are found as usual from the Determinant (4.108).

Thus, the effect of support anisotropicity shows up in an increase of the number of shaft vibration critical speeds and natural modes. The forced vibrations under the influence of unbalance may have the form of either forward or backward irregular precessio..

4.7.3. Vibrations of Rotor Having Different Stiffnesses in the Principal Bending Planes

The rotor which has different bending stiffness in the two principal directions has several singular properties during vibration. For such a rotor there is an increase of the number of natural vibration frequencies and modes, and also an increase of

the number of critical speeds. Rotor vibrations may be caused during rotation by static transverse loads.

Differences in the stiffnesses in the principal directions are connected primarily with the shape of the shaft. If the shaft has a noncircular cross section, slots, depressions, or protuberances, then its stiffnesses will be different. Differences of the stiffnesses may be associated with the specific characteristics of the mounting of the disks or other components on the shaft and with one another. For example, nonuniform fit of components shrunk onto the shaft, variable wall thickness of the shaft and sleeves, nonuniformity of the circumferential positioning of attach fittings, and so on.

4.7.3.1. General differential equations

In order to clarify the primary vibration characteristics of the rotor with unequal bending stiffnesses, we shall examine a shaft with a single disk located at the midpoint. We shall carry out the solution in the xOy moving coordinate axes (Figure 4.28), para_lel to the principal stiffness axes of the shaft, rotating together with the shaft with the angular velocity ω. The center of gravity of the disk does not coincide with the shaft axis, its displacement is defined by the projections a_1 and a_2 on the moving axes.
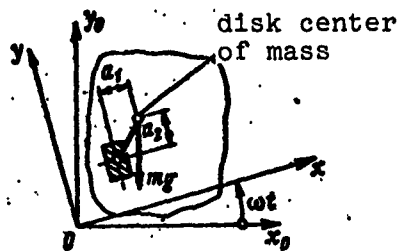
Figure 4.28. Coordinate axis system for shaft with different stiffness in different planes

We take as the generalized coordinates the coordinates x, y of the center of gravity in the moving coordinate axis system.

The potential energy of the system consists of the shaft bending energy and the work of the gravity forces. In the x, y axes, this potential energy will be

$$\Pi = \frac{1}{2}[c_x(x-a_1)^2 + c_y(y-a_2)^2] + mg(x\sin\omega t + y\cos\omega t). \qquad (4.115)$$

The projections of the absolute velocity of the center of gravity on the moving axes are equal to the sums of the relative and reference-frame velocities

$$\dot{x}-\omega y;\ \dot{y}+\omega x;$$

therefore the disk kinetic energy is

$$T=\frac{m}{2}\left[(\dot{x}-\omega y)^2+(\dot{y}+\omega x)^2\right]. \qquad (4.116)$$

We apply the Lagrange equation

$$\frac{d}{dt}\left(\frac{\partial T}{\partial \dot{q}}\right)-\frac{\partial T}{\partial q}+\frac{\partial \Pi}{\partial q}=0.$$

After differentiating (4.115) and (4.116) and substituting into the Lagrange equation, we obtain the differential equations of motion in the moving axes, which after minor transformations are written in the form

$$\left.\begin{array}{l}\ddot{x}-2\dot{y}\omega+(p_x^2-\omega^2)\,x=c_xa_1-g\sin\omega t;\\[4pt]\ddot{y}+2\dot{x}\omega+(p_y^2-\omega^2)\,y=c_ya_2-g\cos\omega t,\end{array}\right\} \qquad (4.117)$$

where

$$p_x^2=\frac{c_1}{m};\quad p_y^2=\frac{c_2}{m}. \qquad (4.118)$$

Equations (4.117) are linear and are conjugated by the Coriolis acceleration terms.

4.7.3.2. Free vibrations. Vibration instability conditions

The solutions of (4.117) without the right sides define the free vibration properties. The equations are solved by the substitution

$$x=Ae^{\lambda t};\ y=Be^{\lambda t}, \qquad (4.119)$$

after which we obtain a system of two homogeneous algebraic equations

$$A\lambda^2-2\lambda\omega B+(p_x^2-\omega^2)\,A=0;$$
$$B\lambda^2+2\lambda\omega A+(p_y^2-\omega^2)\,B=0.$$

The determinant of the system, equated to zero, yields the equation

$$\lambda^4 + (p_x^2 + p_y^2 + 2\omega^2)\lambda^2 + (p_x^2 - \omega^2)(p_y^2 - \omega^2) = 0. \qquad (4.120)$$

This equation is biquadratic and the coefficient of λ^2 is always positive. Therefore the roots of (4.120) depend on the sign of the free term. If

$$(p_x^2 - \omega^2)(p_y^2 - \omega^2) > 0, \qquad (4.121)$$

both roots of (4.120) are negative

$$\lambda^2 = -\frac{1}{2}(p_x^2 + p_y^2 + 2\omega^2) \pm$$
$$\pm \frac{1}{2}\sqrt{(p_x^2 + p_y^2 + 2\omega^2)^2 - 4(p_x^2 - \omega^2)(p_y^2 - \omega^2)}. \qquad (4.122)$$

i.e., briefly,

$$\lambda_1 = \pm i\mu_1; \quad \lambda_2 = \pm i\mu_2,$$

and the Solutions (4.119) take the form

$$x = A_1 e^{i\mu_1 t} + A_2 e^{-i\mu_1 t}; \quad y = B_1 e^{i\mu_1 t} + B_2 e^{-i\mu_1 t}. \qquad (4.123)$$

Analogous functions can be written for the second solution. The coefficients A_1, A_2, B_1, B_2 are found from the initial conditions.

Let us assume that for $t = 0$

$$\left. \begin{array}{l} x = A_0; \ \dot{x} = 0; \\ y = 0; \ \dot{y} = B_0\mu_1; \end{array} \right\} \qquad (4.124)$$

then (4.123) take the form

$$x = \frac{1}{2}A_0(e^{i\mu_1 t} + e^{-i\mu_1 t}) = A_0\cos\mu_1 t;$$
$$y = \frac{1}{2i}B_0(e^{i\mu_1 t} - e^{-i\mu_1 t}) = B_0\sin\mu_1 t.$$

In the moving axes the center of gravity executes harmonic vibrations. Its motion trajectory is an ellipse with axes A_0 and B_0. The vibrations are stable.

The Condition (4.121) is satisfied when both parentheses are simultaneously positive or negative, i.e., when the rotational speed is either lower than or higher than both natural frequencies (4.118).

If

$$(p_x^2 - \omega^2)(p_y^2 - \omega^2) < 0,$$ (4.125)

we see easily from (4.122) that one of the roots is positive. Therefore

$$\lambda = \pm \mu.$$

Then the Solutions (4.119) take the form

$$x = A_1 e^{\mu t} + A_2 e^{-\mu t}; \quad y = B_1 e^{\mu t} + B_2 e^{-\mu t}.$$ (4.126)

For the initial conditions (4.124), they reduce to the hyperbolic functions

$$x = A_0 \operatorname{ch} \mu t; \quad y = B_0 \operatorname{sh} \mu t.$$

This means that the rotor motion is unstable when the condition (4.125) is met. Hence we conclude that for a rotor speed ω in the range

$$p_x < \omega < p_y.$$ (4.127)

the rotor deflections increase without bound. A whole region of unstable rotational speeds appears as a result of the fact that the shaft section is not circular.

We shall examine separately the effect of unbalance and the effect of the weight force on rotor vibrations.

4.7.3.3. Forced vibrations due to unbalance

Under the condition g = 0, the differential equations (4.117) have particular solutions in the form of the constants

$$x^* = a_1 \frac{e_x}{p_x^2 - \omega^2}; \quad y^* = a_2 \frac{e_y}{p_y^2 - \omega^2}.$$ (4.128)

The solutions show that the rotor loses stability for $\omega = p_x$ and $\omega = p_y$, bending in one case along the x axis and in the other case along the y axis. In the absence of these resonant relations, the Solution (4.128) shows the direction of rotor bending. This direction does not coincide with the direction of the eccentricity and depends on ω.

The general solution of (4.117) is formulated as the sum of solutions of homogeneous equations in the form (4.123) or (4.126) and the particular solutions (4.128).

If $\omega < p_x < p_y$ or $p_x < p_y < \omega$, the general solutions will be

$$x = A_1 e^{i\mu_1 t} + A_2 e^{-i\mu_1 t} + x^*;$$
$$y = B_1 e^{i\mu_1 t} + B_2 e^{-i\mu_1 t} + y^*.$$

After determining the coefficients A_1, B_1 for the initial conditions (4.124), we obtain the solutions in the form

$$\left. \begin{array}{l} x = A_0 \cos \mu_1 t + x^* (1 - \cos \mu_1 t); \\ y = B_0 \sin \mu_1 t + y^* (1 - \cos \mu_1 t). \end{array} \right\} \qquad (4.129)$$

The solutions show that stable harmonic vibrations take place about the static equilibrium position. The amplitudes of the vibrations along the x and y axes are connected with the initial perturbation. The vibration frequency depends on the rotational speed ω and is found from (4.122).

If the rotational speed lies in the frequency range

$$p_x < \omega < p_y,$$

the general solution formulated on the basis of (4.126) and (4.128) for the Conditions (4.124) takes the form

$$\left. \begin{array}{l} x = A_0 \operatorname{ch} \mu t + x^* (1 - \operatorname{ch} \mu t); \\ y = B_0 \operatorname{sh} \mu t + y^* (1 - \operatorname{ch} \mu t). \end{array} \right\} \qquad (4.130)$$

The solution shows that the rotor is unstable for rotational speeds lying between the frequencies p_x and p_y. The rotor

deflections will increase in the course of time under the influence
of the unbalance.

Usually, passage through the critical speeds is accomplished
in short time intervals in order to avoid marked increase of the
vibration amplitudes. For the rotor with unequal stiffnesses rapid
passage through the entire unstable state region is necessary.

4.7.3.4. Vibrations due to weight force

The differential equations (4.117) correspond to the posed
conditions if we set therein $a_1 = a_2 = 0$.

The particular solutions of the equations will be the functions

$$x^* = A^* \sin \omega t; \quad y^* = B^* \cos \omega t, \qquad (4.131)$$

where A^*, B^* — are constants of integration, whose values are found
by substituting the functions (4.131) into (4.117).

After substituting, we obtain the algebraic equations

$$\left. \begin{array}{l} (p_x^2 - 2\omega^2)\, A^* + 2\omega^2 B^* = -g; \\ 2\omega^2 A^* + (p_y^2 - 2\omega^2)\, B^* = -g. \end{array} \right\} \qquad (4.132)$$

Hence

$$A^* = -\frac{g}{\Delta}\, (p_y^2 - 4\omega^2); \quad B^* = -\frac{g}{\Delta}\, (p_x^2 - 4\omega^2), \qquad (4.133)$$

where Δ is the determinant of the System (4.132)

$$\Delta = (p_x^2 - 2\omega^2)(p_y^2 - 2\omega^2) - 4\omega^4. \qquad (4.134)$$

The particular solution (4.131) represents harmonic vibrations.
The disk center of gravity, which in this case coincides with the
shaft axis, describes in the rotating coordinate axes an elliptical
trajectory with semiaxes A^* and B^*.

We obtain the equation of the center-of-gravity motion trajec-
tory in the $x_0 y_0$ fixed coordinate axis system by projecting the
Displacements (4.131) on these axes

$$x_0^* = x^* \cos \omega t - y^* \sin \omega t;$$
$$y_0^* = x^* \sin \omega t + y^* \cos \omega t;$$

Substituting herein (4.131), by means of simple transformations we reduce these equations to the form

$$x_0^* = \frac{A^* - B^*}{2} \sin 2\omega t;$$

$$y_0^* = \frac{A^* + B^*}{2} - \frac{A^* - B^*}{2} \cos 2\omega t.$$

Substitutic herein of (4.133) yields the final form of the equation of motion of the center of gravity in projections on the fixed axes

$$\left. \begin{array}{l} x_0^* = -\frac{g}{2\Delta}(p_y^2 - p_x^2) \sin 2\omega t; \\[2mm] y_0^* = -\frac{g}{2\Delta}(p_x^2 + p_y^2 - 8\omega^2) + \frac{g}{2\Delta}(p_y^2 - p_x^2) \cos 2\omega t; \end{array} \right\} \qquad (4.135)$$

this is the equation of a circle (Figure 4.29) of radius r

$$r = \frac{g}{2\Delta}(p_y^2 - p_x^2); \qquad (4.136)$$

The center of the circle is shifted downward along the y_0 axis by the distance y_c

$$y_c = -\frac{g}{2\Delta}(p_x^2 + p_y^2 - 8\omega^2). \qquad (4.137)$$

These formulas show that the rotor or shaft of unequal stiffness under the influence of the weight force executes forced vibrations about a center which is shifted downward by the distance y_c. The frequency of the circular vibrations is 2ω.
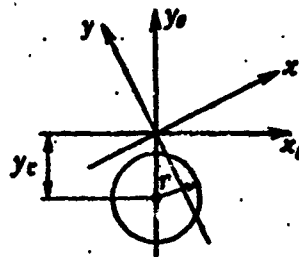
Figure 4.29. Trajectory of center of mass of shaft with different stiffness in different planes

Formulas (4.136) and (4.137) show that the circular vibration amplitude r and the shift y_c depend on the rotational speed.

The resonance phenomenon occurs at that rotational speed at which the determinant Δ becomes equal to zero. The shaft deflection and vibration amplitude increase without bound under the influence of the weight force.

We determine the resonant speed by equating (4.134) to zero

$$(p_x^2 - 2\omega^2)(p_y^2 - 2\omega^2) - 4\omega^4 = 0.$$

Hence we find

$$\omega = \sqrt{\frac{c_x c_y}{2m(c_x + c_y)}}.$$ (4.138)

This speed is called the "critical speed of the second kind".

4.7.4. Forced Vibrations with Account for External and Internal Friction Forces

The friction forces in rotating shafts and rotors must be divided into external and internal.

External friction arises as a result of interaction of the shaft with the external medium — friction with the air or liquid, friction in seals, friction on lateral supporting surfaces, and so on.

The internal friction is associated with deformation of the shaft. It appears when the shaft fibers experience alternating stresses. For example, if a shaft performs circular vibrations, i.e., it precesses with the angular velocity Ω but does not revolve in the process, such vibrations will be accompanied by energy losses in internal resistance and will damp out. If in the case of the same circular vibrations the shaft revolves in ideal bearings with the precessional velocity, then its fibers will not have alternating stresses and there will not be any losses in inelastic resistance.

In the general case the friction force depends on the relative velocity of the shaft deformation in the coordinate system fixed with the shaft.

Let us examine the simplest case — the shaft with a disk at the midpoint (Figure 4.30). The shaft precesses under the influence of the external rotating force

$$Q = He^{i\Omega t} \qquad (4.139)$$
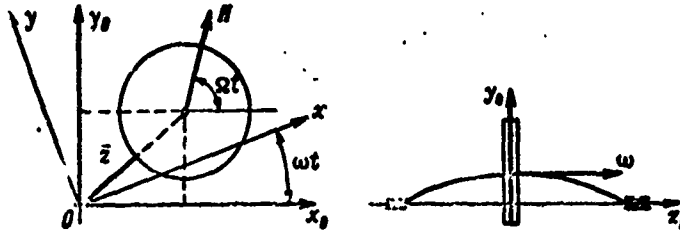
Figure 4.30. Illustrating effect of internal friction on shaft vibrations

The position of the disk center of gravity in the x_0, y_0 fixed coordinate system is defined by the vector

$$\bar{z}_0 = x_0 + iy_0. \qquad (4.140)$$

At the same time the shaft revolves about the curved axis with the velocity ω. The x, y coordinate axes, whose origin is located on the line of supports, rotates with the same velocity ω. The position of the center of the disk in the rotating axis system is defined by the vector

$$\bar{z} = \bar{z}_0 e^{-i\omega t}. \qquad (4.141)$$

In order to clarify the principle of the action of friction forces on the rotating shaft, we take the viscous friction law for these forces. Then the external and internal friction force vectors are expressed by the relations

$$R_e = -b\dot{\bar{z}}_0; \qquad (4.142)$$

$$R_n = -\mu\dot{\bar{z}}. \qquad (4.143)$$

where ξ and μ — are the external and internal friction coefficients.

Thus the external friction force is proportional to the absolute velocity, and the internal friction force is proportional to the relative velocity.

For external friction the viscous friction law corresponds quite well to the nature of the losses. This law is less suitable for internal friction, distorting somewhat the quantitative aspect, but it is convenient in that it avoids the necessity for resolving the question of the direction and sign of the internal friction force.

Differentiating (4.141) and substituting into (4.143), we obtain

$$R_{\mu} = -\mu \left(\dot{\bar{z}}_0 - i\omega\bar{z}_0 \right) e^{-i\omega t}. \tag{4.144}$$

This formula defines the internal friction force in the x, y rotating axes. To convert to fixed axes, it must be multiplied by $e^{i\omega t}$. Then we obtain

$$\dot{R}_{\mu,0} = R_{\mu} e^{i\omega t} = -\mu \left(\dot{\bar{z}}_0 - i\omega\bar{z}_0 \right). \tag{4.145}$$

The differential equation of forced vibrations with account for friction in vector form in fixed axes has the form

$$m\ddot{\bar{z}}_0 + \xi\dot{\bar{z}}_0 + \mu \left(\dot{\bar{z}}_0 - i\omega\bar{z}_0 \right) + c\bar{z}_0 = He^{i\omega t}. \tag{4.146}$$

We seek the solution of the equation without the right side, which defines ρ free vibrations, in the form

$$\bar{z}_0 = e^{(a+ib)t};$$

substituting this solution into (4.146) we obtain

$$(a+ib)^2 + (2n+\bar{\mu})(a+ib) - i\bar{\mu}\omega + k^2 = 0,$$

where

$$k^2 = \frac{c}{m}; \quad 2n = \frac{\xi}{m}; \quad \bar{\mu} = \frac{\mu}{m};$$

Separating the real and imaginary parts, we obtain the two equations

$$b^2 = k^2 + (2n + \bar{\mu}) a + a^2; \\ a = -n + \frac{1}{2} \bar{\mu} \left(\frac{\omega}{b} - 1 \right);$$ (4.147)

thest equations make it possible to draw an important conclusion concerning the effect of internal friction forces.

If there is no internal friction ($\bar{\mu} = 0$), we obtain from the equations

$$a = -n; \quad b = \pm \sqrt{k^2 - n^2}; \\ \bar{z}_0 = e^{(-n + ib)t}.$$ (4.148)

These are the previously considered damped free vibrations; b is the damped vibration frequency, close to the harmonic vibration frequency k. The negative value of the exponent characterizes the vibration decay.

The case when a = 0 is possible. Then b = k and the solution takes the form

$$\bar{z}_0 = e^{ikt}.$$

These are undamped harmonic vibrations. We find the conditions for which such vibrations are possible from (4.147):

$$\frac{\omega}{k} = 1 + \frac{\xi}{\mu}.$$ (4.149)

Undamped vibrations in the case with external and internal friction forces acting are possible if the shaft rotational speed ω is greater than the natural vibration frequency k, i.e., greater than the critical speed. The required speed differential is determined by the ratio of the external and internal friction coefficients.

If the internal friction is large or the speed a exceeds the critical speed considerably, the exponent a will have a positive value. This means that vibrations will take place with increase of the amplitudes. The speed of the developing precession will be somewhat greater than the critical speed k. In this case the internal friction forces will be the vibration exciter.

The particular solution of the complete equation for forced vibrations is taken in the form of the right side

$$\bar{z}_0 = A e^{i\Omega t} \qquad (4.150)$$

After substituting this expression into (4.146) and minor transformations, we obtain the formula for the circular vibration amplitude

$$A = \frac{H}{m} \frac{k^2 - \Omega^2 - i\left[2n\Omega + \bar{\mu}(\Omega - \omega)\right]}{(k^2 - \Omega^2)^2 + \left[2n\Omega + \bar{\mu}(\Omega - \omega)\right]^2} . \qquad (4.151)$$

The vibration amplitude is expressed by a complex number, which indicates the existence of an angular shift of the displacement vector relative to the disturbing force vector. The phase angle and the vibration amplitude modulus are easily found on the basis of (4.151).

The final formula for the shaft deflection with account for friction in the forced vibration case will be

$$\bar{z}_0 = h\left[(k^2 - \Omega^2)^2 + \{2n\Omega + \bar{\mu}(\Omega - \omega)\}^2\right]^{-\frac{1}{2}} e^{i(\Omega t - \epsilon)}, \qquad (4.152)$$

where

$$\operatorname{tg}\epsilon = \frac{2n\Omega + \bar{\mu}(\Omega - \omega)}{k^2 - \Omega^2} . \qquad (4.153)$$

In the particular case in which the disturbing force is an unbalanced force

$$\Omega = \omega; \quad H = ma\omega^2,$$

(4.152) simplifies, taking the usual form for a system with viscous friction

$$\bar{z}_0 = h\left[(k^2 - \Omega^2) + (2n\Omega)^2\right]^{-\frac{1}{2}} e^{i(\Omega t - \epsilon)}; \qquad (4.154)$$

the internal friction component cancels out. This is logical, since under the influence of the unbalanced force the shaft executes forward synchronous precession, having a deformed static state. In this case the magnitude of the deflection depends only on the external friction.

4.7.5. Rotor Passage Through Critical Speed

The majority of aviation gas turbine engines and turbomachines have rotor operating speeds exceeding their critical speeds. This situation is associated with the necessity for having high rotor tip speeds and the desire at the same time to minimize structural weight.

Engine starting speeds are low. Therefore, as the rotor accelerates and approaches the operating speeds, it is necessary to pass through one or more critical speeds.

We have shown above that under the influence of unbalance the forced vibration amplitudes tend toward infinitely large values. But this increase takes place gradually, in the course of time.

Therefore the rate at which the critical speeds are passed through is of importance, i.e., the acceleration or deceleration of the rotation. If the critical speed is passed rapidly; the vibration amplitudes cannot increase markedly.

Passage through the critical speed is associated with the expenditure of power. The faster the a   `eration, the greater the required power. If the rotor driving power is inadequate, the acceleration will be slow, with a large increase of the vibration amplitudes. In certain cases (if there are losses in the system), passage through the critical speed with the aid of a small energy source may be impossible.

During passage through the critical speed, the rotor vibrations are unsteady. The processes taking place in passage through the critical speed for a given rotor acceleration law have been examined in [14], [15], [11], and others.

Let us consider a two-support shaft with unbalanced disk located at the midpoint. As the generalized coordinates we take the coordinates x, y of the position of the disk mass center and the rotation angle ϕ (Figure 4.31). As a result of the location of the disk at the midpoint, its axis always remains parallel to the rotor rotational axis.

The rotor kinetic energy is defined by the formula

$$T = \frac{1}{2}\left[m(\dot{x}^2 + \dot{y}^2) + J_p\dot{\varphi}^2\right]. \qquad (4.155)$$

Let us assume that the shaft is absolutely rigid in torsion. Then the bending potential energy will be

$$\Pi = \frac{1}{2}c\left[(x - a\cos\varphi)^2 + (y - a\sin\varphi)^2\right]. \qquad (4.156)$$

Figure 4.31. Coordinates of shaft and center-of-mass location for nonuniform rotation

Substituting the formulas for T and Π into the Lagrange equations, we obtain three differential equations

$$\left.\begin{aligned}
&\ddot{x} + k^2 x = k^2 a \cos\varphi; \\
&\ddot{y} + k^2 y = k^2 a \sin\varphi; \\
&J_p\ddot{\varphi} + a\dot{\varphi}(x\sin\varphi - y\cos\varphi) = M(t),
\end{aligned}\right\} \qquad (4.157)$$

where M(t) — is the moment required to accelerate the rotor, which depends on the acceleration law and the variation of the x and y coordinates.

Let us examine the first two Equations (4.157), which define the mass center motion law. We assume that the rotor is accelerated with the constant acceleration ε. Then its angular velocity varies linearly

$$\omega = \omega_0 + \varepsilon t,$$

and the rotation angle equals

$$\varphi = \omega_0 t + \frac{1}{2}\varepsilon t^2, \qquad (4.158)$$

where ω_0 — is the initial rotational speed.

To study the dynamics of rotor passage through the critical speed, we use the solutions obtained in Sections 1.6 and 1.7.

We write the general solution of (4.157) in definite integral form. In accordance with (1.78) the solutions will have the form

$$x = C_1^x \cos k\tau + C_2^x \sin k\tau + ka \int_0^\tau \cos \varphi \sin k(\tau - t)\, dt; \qquad (4.159)$$

$$y = C_1^y \cos k\tau + C_2^y \sin k\tau - ka \int_0^\tau \sin \varphi \sin k(\tau - t)\, dt. \qquad (4.160)$$

At the initial moment the rotor rotates at the speed ω_0, which is less than k. In this case the disk mass center travels along a circle of radius

$$r_0 = \frac{a k^2}{k^2 - \omega_0^2};$$

In view of the fact that the acceleration begins from low speeds and ω_0 is significantly lower than k, the radius $r_0 \approx a$, i.e., it is a very small quantity. These initial conditions are ignored hereafter and we take

$$C_1^x = C_2^x = C_1^y = C_2^y = 0.$$

Formulas (4.159) and (4.160), with account for substitution of (4.158), take the form

$$x = ka \int_0^\tau \cos \left(\omega_0 t + \frac{1}{2} \varepsilon t^2 \right) s^! \quad {}^{\cdot}(\tau - t)\, dt; \qquad (4.161)$$

$$y = ka \int_0^\tau \sin \left(\omega_0 t + \frac{1}{2} \varepsilon t^2 \right) \sin k(\tau - t)\, dt. \qquad (4.162)$$

We replace the products of the trigonometric functions under the integral signs by differences and after making some transformations we write (4.161) and (4.162) in the form

$$x = \frac{ka}{\sqrt{2\varepsilon}} \left\{ \cos\beta \int_{\chi_0}^{\chi_\tau} \sin \chi^2 d\chi + \sin\beta \int_{\chi_0}^{\chi_\tau} \cos \chi^2 d\chi - \right.$$
$$\left. - \cos\beta' \int_{f_0}^{f_\tau} \sin f^2 df + \sin\beta' \int_{f_0}^{f_\tau} \cos f^2 df \right\}; \qquad (4.163)$$

$$y = \frac{ka}{\sqrt{2\varepsilon}} \left\{ \sin\beta \int_{\chi_0}^{\chi_\tau} \sin \chi^2 d\chi - \cos\beta \int_{\chi_0}^{\chi_\tau} \cos \chi^2 d\chi + \right.$$

$$+\sin\beta'\int_{f_\bullet}^{f_\tau}\sin f^2 df+\cos\beta'\int_{f_\bullet}^{f_\tau}\cos f^2 df\Big\}. \qquad (4.164)$$

where

$$\chi=\sqrt{\frac{\epsilon}{2}}\,t-\frac{k-\omega_0}{\sqrt{2\epsilon}}; \qquad \beta=k\tau-\frac{(k-\omega_0)^2}{2\epsilon};$$
$$f=\sqrt{\frac{\epsilon}{2}}\,t+\frac{k+\omega_0}{\sqrt{2\epsilon}}; \qquad \beta'=k\tau+\frac{(k+\omega_0)^2}{2\epsilon}. \qquad (4.165)$$

The limits of integration are obtained from these expressions by substituting therein t = τ and t = 0 respectively.

To find the vibration amplitudes when passing through the critical speed, we write the shaft deflection in the complex form

$$\bar{z}=x+iy.$$

Multiplying (4.164) by i and combining with (4.163), we obtain

$$\bar{z}=\frac{ka}{\sqrt{2\epsilon}}\Big\{e^{i\beta}\int_{\chi_\bullet}^{\chi_\tau}\sin\chi^2 d\chi-ie^{i\beta}\int_{\chi_\bullet}^{\chi_\tau}\cos\chi^2 d\chi-$$
$$-e^{-i\beta'}\int_{f_\bullet}^{f_\tau}\sin f^2 df+ie^{-i\beta'}\int_{f_\bullet}^{f_\tau}\cos f^2 df\Big\}. \qquad (4.166)$$

The following replacements were used in the process of transforming the complex expressions:

$$\cos\beta+i\sin\beta=e^{i\beta};$$
$$\sin\beta-i\cos\beta=-i(\cos\beta+i\sin\beta)=-ie^{i\beta};$$
$$-\cos\beta'+i\sin\beta'=-(\cos\beta'-i\sin\beta')=-e^{-i\beta'};$$
$$\sin\beta'+i\cos\beta'=i(\cos\beta'-i\sin\beta')=ie^{-i\beta'}.$$

The integrals appearing in (4.166) were examined in Chapter I. The first and second integrals are defined by (1.96) and (1.97).

The third and fourth integrals are small because of the large values of the limits f_0 and f_τ. Their magnitudes constitute fractions of a percent in relation to the magnitude of the first two integrals. Therefore, they can be neglected and we can write (4.166) in simplified form

$$\bar{z} = -\frac{ka}{\gamma \sqrt{2}\varkappa} \left\{ \int_{\chi_o}^{\chi_\tau} \sin\chi^2 d\chi - i \int_{\chi_o}^{\chi_\tau} \cos\chi^2 d\chi \right\} e^{i\theta}. \tag{4.167}$$

This formula in vector form defines the position of the disk mass center at the time τ.

The modulus of the vector — the quantity preceding the factor $e^{i\beta}$ — is a variable quantity and is defined by the values of the integrals for the given time τ. The direction of the vector is defined by the angle β. In accordance with (4.165) the vector rotates with the natural vibration frequency k.

In accordance with this discussion, we write (4.167) in the form

$$\bar{z} = Re^{i(k\tau - a - \gamma)}, \tag{4.168}$$

where

$$R = \frac{ka}{\gamma \sqrt{2}\varkappa} \sqrt{J_1^2 + J_2^2}; \quad \operatorname{tg}\gamma = \frac{J_2}{J_1}; \quad a = \frac{(k - \omega_0)^2}{2\varkappa};$$

$$J_1 = \int_{\chi_o}^{\chi_\tau} \sin\chi^2 d\chi; \quad J_2 = \int_{\gamma_o}^{\chi_\tau} \cos\chi^2 d\chi.$$

It was shown in Chapter I (see Figure 1.15) that the integrals J_1 and J_2 have maxima in the limits of the first period χ_τ. Therefore (see Figure 1.16) the maximum of their geometric sum is obtained for

$$\chi_\tau = 1.5;$$

in magnitude it equals

$$C(\tau) = \sqrt{J_1^2 + J_2^2} = 2.01.$$

Let us determine the time when the amplitude reaches the maximal value when passing through the critical speed. To do this we express the time from the first formula (4.165)

$$t = \sqrt{\frac{2}{\varepsilon}} \left(\chi_\tau + \frac{k - \omega_0}{\sqrt{2\varepsilon}} \right).$$

At this time the shaft speed will be

$$\omega = \omega_0 + \varepsilon t = k + \chi_\tau \sqrt{2\varepsilon};$$

in relation to the critical speed this will be

$$\frac{\omega}{k} = 1 + \chi_\tau \frac{\sqrt{2\varepsilon}}{k} \qquad (4.169)$$

Formula (4.169) shows that at the moment when the maximal vibration amplitude is reached (χ_τ = 1.5) the shaft rotational speed exceeds the critical speed k. The magnitude of the difference is determined by the second term of the formula.

The value of the maximal amplitude is found from the formula

$$R = 2{,}01 \frac{ke}{\sqrt{2\varepsilon}}. \qquad (4.170)$$

This formula shows that increase of the acceleration ε prevents the development of large vibration amplitudes during passage through the critical speed region.

Thus, rotor passage through the critical speed region during acceleration is accompanied by marked increase of the rotor deflections (vibration amplitudes). The latter reach their maximal values for a rotational speed exceeding the critical speed by a few percent. The greater the acceleration, the larger the shift of the deflection peak relative to the critical speed but the smaller the magnitude of the maximal deflection.

Figure 1.17 can serve as an illustration of the variation of rotor vibration amplitudes when passing through the critical speed.

Passage through the critical speed region during deceleration leads to shift of the peak toward a lower speed.

CHAPTER 5

BENDING VIBRATIONS OF CIRCULAR PLATES AND DISKS

5.1. Circular Plate Vibration Modes

Circular plates of constant thickness and disks of variable profile find very wide application in the structures of flight vehicle engines.

The problems concerning vibrations of circular plates and disks, differential equations used, methods for their solution, and so on have certain specific characteristics; the methods for solving these problems have been developed extensively and therefore must be examined separately from the plates of noncircular form.

The natural vibration modes of circular plates are quite varied but they can be divided into three forms — based on the number of nodal diameters (Figure 5.1).

Umbrella-type vibrations (see Figure 5.1a), in which no nodal diameters are formed. Such vibrations arise with axial excitation and cause axial forces along the disk attach contour. If the disk

is mounted on a shaft, a longitudinal force appears on the shaft; if the disk is mounted along the outer edge, forces develop along the contour which yield a resultant parallel to the disk axis. In both cases the disk interacts with the supporting system by means of the resultant of the axial forces.

Figure 5.1. Disk vibration modes.
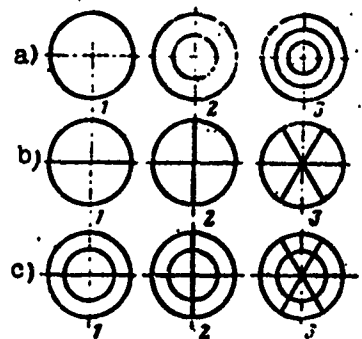
The umbrella-type vibrations have a large number of modes — one for each of the nodal circles. In accordance with the general theory, the number of nodal circles is one less than the mode number.

Skew-symmetric vibratio (see Figure 5.1, b1, c1), in which only a single nodal diameter is formed on the disk and several nodal circles are possible. Such vibrations arise when the mounting contour rotates around a diametral axis. For example, during bending vibrations of a shaft, bending vibrations of a disk mounted on the shaft will develop with a single nodal diameter as a result of the angular oscillations of the section where the disk is mounted.

During skew-symmetric vibrations there is inevitable interaction of the disk with the supporting system in the form of a moment, which arises as the resultant of the contour forces.

The skew-symmetric vibration modes differ in the number of nodal circles.

Fan-wise vibrations (see Figure 5.1, b2, b3, c2, c3), in which several nodal diameters together with nodal circles are formed on the disk. This vibration mode is the most varied, since an entire spectrum of modes with nodal circles is possible for each number of nodal diameters.

In spite of the great variety, all the fan-wise modes have one common property — their vibrations are dynamically self-equilibrated, i.e., the resultant of all the inertia forces and their moment are equal to zero. Therefore, the fan-wise modes do not cause axial forces or bending moments on the supports.

The fan-wise vibration modes are easily excited and arise under the action of the always-present axial asymmetry of the forces acting, disk restraint conditions, circumferential distribution of the structural elements, and also because of nonhomogeneity of the disk material.

Naturally, each vibration mode has its own frequency. The modes without nodal circles have the lowest frequencies. The larger the number of circles, the higher the frequencies.

The structures of modern flight vehicle engines consist primar-. ily of thinwall elements, including disks and plates; therefore these engines must be analyzed not only for the basic simple modes, but also for the more complex vibration modes.

5.2. Differential Equation of Bending Vibrations of Circular Plates of Variable Thickness

Let us examine the general case of deformation of a circular plate in polar coordinates.

We isolate a plate element (Figure 5.2). We apply to the edges of the element the forces and moments which replace the action of the internal forces. The forces and moments are referred to unit length of the corresponding circle or radius. The force and moment directions shown in Figure 5.2 are taken as positive.

At the center of mass of the element, we apply the mass and surface forces, whose intensity is denoted in the projections q_z
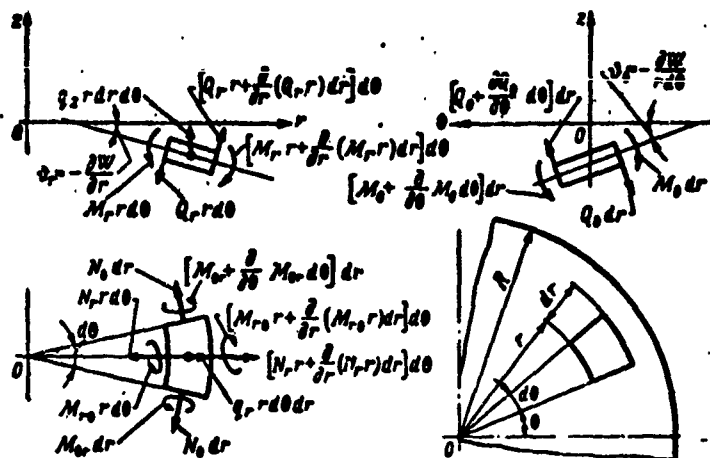
Figure 5.2. Forces and moments acting on
circular plate element.

and q_r. The latter are referred to unit surface area of the plate.

The plate stress state is determined by the forces N_r and N_θ. There forces arise from the action of centrifugal forces, thermal stresses, and so on. We shall restrict ourselves to examination of the axisymmetric stress states of plates; therefore, we shall assume that the forces N_r and N_θ are given as functions of r only.

We write the projections of the forces on the z axis, corresponding to the element position shown in Figure 5.2

$$N_r \vartheta_r r d\theta - \left[N_r \vartheta_r r d\theta + \frac{\partial}{\partial r} (N_r \vartheta_r r d\theta) dr \right].$$

This expression equals

$$- \frac{\partial}{\partial r} (N_r \vartheta_r r) d\theta dr.$$

We find the projections of the other pairs of components similarly

$$\frac{\partial}{\partial r}(Q_r r)\,d\theta dr; \quad \frac{\partial Q_\theta}{\partial r}\,dr\,d\theta;$$

$$-\frac{\partial}{\partial \theta}(N_\theta \vartheta_\theta)\,d\theta dr; \quad q_s r\,d\theta\,dr.$$

Combining all the projections, we obtain the equation of equilibrium of all the components. Dividing this equation by rdrdθ, we obtain

$$\frac{1}{r}\left[\frac{\partial}{\partial r}(Q_r r)+\frac{\partial Q_\theta}{\partial \theta}-\frac{\partial}{\partial r}(N_r r\vartheta_r)-\frac{\partial}{\partial \theta}(N_\theta \vartheta_\theta)\right]+q_s=0. \tag{5.1}$$

The sum of the projections of the moments on the radius yields

$$\frac{1}{r}\left[\frac{\partial}{\partial r}(rM_{r\theta})+\frac{\partial M_\theta}{\partial \theta}-M_{r,r}\right]-Q_\theta=0. \tag{5.2}$$

The sum of the projections of the moment on the circumferential direction yields

$$\frac{1}{r}\left[\frac{\partial}{\partial r}(rM_r)+\frac{\partial M_{\theta r}}{\partial \theta}-M_\theta\right]-Q_r=0. \tag{5.3}$$

With the aid of these equations we exclude from (5.1) the derivatives of the transverse forces rQ_r and Q_θ. In so doing we consider that $M_{\theta r} = M_{r\theta}$. We obtain the equation

$$\frac{1}{r}\left[\frac{\partial^2}{\partial r^2}(rM_r)-\frac{\partial M_\theta}{\partial r}+\frac{1}{r}\frac{\partial^2 M_\theta}{\partial \theta^2}+\frac{2}{r^2}\frac{\partial^2}{\partial r\partial \theta}(rM_{r\theta})-\right.$$
$$\left.-\frac{\partial}{\partial r}(N_r r\vartheta_r)-\frac{\partial}{\partial \theta}(N_\theta \vartheta_\theta)\right]+q_s=0. \tag{5.4}$$

To relate this equation with the bending deformations, we replace the bending and torsional moments by their expressions

$$M_r=-D\left[\frac{\partial^2 W}{\partial r^2}+v\left(\frac{1}{r}\frac{\partial W}{\partial r}+\frac{1}{r^2}\frac{\partial^2 W}{\partial \theta^2}\right)\right]; \tag{5.5}$$

$$M_\theta=-D\left(v\frac{\partial^2 W}{\partial r^2}+\frac{1}{r}\frac{\partial W}{\partial r}+\frac{1}{r^2}\frac{\partial^2 W}{\partial \theta^2}\right); \tag{5.6}$$

$$M_{r\theta}=-D(1-v)\frac{\partial}{\partial r}\left(\frac{1}{r}\frac{\partial W}{\partial \theta}\right). \tag{5.7}$$

where W is the plate deflection;

    ν is the Poisson coefficient;

    D is the cylindrical stiffness, equal to:

$$D = \frac{Eh^3}{12(1-\nu^2)}. \tag{5.8}$$

Substitution of the moment formula into (5.4) leads to the basic equation for the bending deformations

$$D\nabla^2\nabla^2 W + \frac{dD}{dr}\left(2\frac{\partial^3 W}{\partial r^3} + \frac{2+\nu}{r}\frac{\partial^2 W}{\partial r^2} - \frac{1}{r^2}\frac{\partial W}{\partial r} + \frac{2}{r^2}\frac{\partial^3 W}{\partial r\partial\theta^2} - \frac{3}{r^3}\frac{\partial^2 W}{\partial\theta^2}\right) +$$
$$+ \frac{d^2 D}{dr^2}\left[\frac{\partial^2 W}{\partial r^2} + \nu\left(\frac{1}{r}\frac{\partial W}{\partial r} + \frac{1}{r^2}\frac{\partial^2 W}{\partial\theta^2}\right)\right] + \frac{1}{r}\frac{\partial}{\partial r}(N_r r\vartheta_r) + \tag{5.9}$$
$$+ \frac{1}{r}\frac{\partial}{\partial\theta}(N_\theta\vartheta_\theta) - q_z = 0;$$

where the Laplace operator in polar coordinates defines the action

$$\nabla^2 W = \frac{\partial^2 W}{\partial r^2} + \frac{1}{r}\frac{\partial W}{\partial r} + \frac{1}{r^2}\frac{\partial^2 W}{\partial\theta^2}; \tag{5.10}$$

$$\vartheta_r = -\frac{\partial W}{\partial r}; \qquad \vartheta_\theta = -\frac{\partial W}{r\partial\theta}. \tag{5.11}$$

For disks and plates of constant thickness, the equation takes the quite simple form

$$D\nabla^2\nabla^2 W + \frac{1}{r}\frac{\partial}{\partial r}(N_r r\vartheta_r) + \frac{1}{r}\frac{\partial}{\partial\theta}(N_\theta\vartheta_\theta) - q_z = 0. \tag{5.12}$$

In (5.9) and (5.12) the terms containing the tangential forces $Q_{r\theta}$ and Q_r are dropped. For the axisymmetric stress state these forces equal zero.

The normal forces N_r and N_θ, acting in the plane of the disk, are axisymmetric functions. They depend on the stress distribution in the disk and are connected with the restraint conditions, thermal stresses, and the action of the centrifugal or other radial forces. For small vibrations they can be considered independent of the deflection and can be found on the basis of strength calculations —

from the distribution of the radial and circumferential stresses in the disk

$$N_r = \sigma_r h; \quad N_\theta = \sigma_\theta h. \tag{5.13}$$

The transverse load intensity during vibrations is defined by the formula

$$q_\epsilon = -\rho h \ddot{W}, \tag{5.14}$$

where ρ is the plate material density.

After substituting (5.14) into (5.12) we obtain the general linear differential equation for the vibrations of a circular plate, in which the deflections are expressed in the polar coordinates r and θ and are, in addition, functions of time

$$D\nabla^2\nabla^2 W + \frac{1}{r}\frac{\partial}{\partial r}(N_r r \theta_r) + \frac{1}{r}\frac{\partial}{\partial \theta}(N_\theta \theta_\theta) + \rho h \ddot{W} = 0. \tag{5.15}$$

We write the general solution (5.15) in the form of the product of three independent functions

$$W = U(r)V(\theta)T(t). \tag{5.16}$$

The functions T(t) and V(θ) are trigonometric and, with account for the initial condition chosen, can be taken in the form

$$\left.\begin{array}{l} T(t) = \cos pt; \\ V(\theta) = \cos n\theta. \end{array}\right\} \tag{5.17}$$

The first is a harmonic vibration function with the circular frequency p, while the second shows the distribution of the deflections along the circumference of the disk. The number n equals the number of nodal diameters which form on the disk during vibrations.

In connection with (5.17) the general solution (5.16) can be written in the form

$$W = U(r)\cos n\theta \cdot \cos pt. \tag{5.18}$$

Substituting this into (5.15), we obtain the differential equation of the disk bending shape in the meridional plane

$$D\nabla_1^2\nabla_1^2 U - \frac{1}{r} \cdot \frac{d}{dr}\left(N_r r \frac{dU}{dr}\right) + \frac{n^2}{r^2} N_\theta U - \varrho h p^2 U = 0, \tag{5.19}$$

where

$$\nabla_1^2 U = \frac{d^2U}{dr^2} + \frac{1}{r} \frac{dU}{dr} - n^2 \frac{1}{r^2} U. \tag{5.20}$$

The further solution of the equations requires specification of the distribution of the normal forces N_r and N_θ.

5.3. Different Cases of Solution of the Differential Equation for the Conditions $N_r = N_\theta = 0$

5.3.1. General Solution

If there are no normal forces in the disk midplane ($N_r = N_\theta = 0$), the equation takes the form

$$\nabla_1^2\nabla_1^2 U - \lambda^4 U = 0, \tag{5.21}$$

where

$$\lambda^4 = \frac{\varrho h p^2}{D}. \tag{5.22}$$

The equation is satisfied by the substitution

$$\nabla_1^2 U = \mp \lambda^2 U. \tag{5.23}$$

This means that it breaks down into two Bessel equations

$$\frac{d^2U}{dr^2} + \frac{1}{r}\frac{dU}{dr} + \left(\lambda^2 - \frac{n^2}{r^2}\right)U = 0; \qquad (5.24)$$

$$\frac{d^2U}{dr^2} + \frac{1}{r}\frac{dU}{dr} - \left(\lambda^2 + \frac{n^2}{r^2}\right)U = 0. \qquad (5.25)$$

The solutions of these equations are known and are expressed with the aid of the Bessel functions, respectively

$$U_1 = C_1 J_n(\lambda r) + C_2 Y_n(\lambda r); \qquad (5.26)$$

$$U_2 = C_3 I_n(\lambda r) + C_4 K_n(\lambda r), \qquad (5.27)$$

where $J_n(\lambda r)$, $Y_n(\lambda r)$ are Bessel functions of the first and second
kind of nth order of real argument;

$I_n(\lambda r)$, $K_n(\lambda r)$ are Bessel functions of first and second kind
of nth order and purely imaginary argument.

The values of the Bessel functions are found from the corresponding tables.

The general solution of (5.21) equals the sum of the solutions of both Bessel equations

$$U = C_1 J_n(\lambda r) + C_2 Y_n(\lambda r) + C_3 I_n(\lambda r) + C_4 K_n(\lambda r), \qquad (5.28)$$

where C_1, C_2, C_3, C_4 are constants which are found from the given
conditions at the outer and inner contours of
the plate.

5.3.2. Plate Without Center Hole, Clamped Along the Outer Contour

In all cases with continuous disks the coefficients C_2 and C_4
are to be taken as zero, since the Bessel functions of the second
kind for r = 0 become infinite and must be excluded from the general
solution. Then the solution is

$$U = C_1 J_n(\lambda r) + C_2 I_n(\lambda r). \tag{5.29}$$

If the plate is clamped along the contour, the boundary conditions will be

$$U_R = 0; \quad \left(\frac{dU}{dr}\right)_R = 0.$$

Substitution herein of the general solution (5.29) leads to the algebraic equations

$$\left.\begin{aligned}
C_1 J_n(\lambda R) + C_2 I_n(\lambda R) &= 0; \\
C_1 J_n'(\lambda R) + C_2 I_n'(\lambda R) &= 0.
\end{aligned}\right\} \tag{5.30}$$

Hence, we obtain the frequency equation

$$I_n(\lambda R) J_n'(\lambda R) - J_n'(\lambda R) I_n(\lambda R) = 0. \tag{5.31}$$

The products J'_n and I'_n are expressed with the aid of the Bessel functions themselves by known relations

$$\left.\begin{aligned}
J_n' &= \frac{1}{2}\lambda[J_{n-1}(\lambda R) - J_{n+1}(\lambda R)]; \\
I_n' &= \frac{1}{2}\lambda[I_{n-1}(\lambda R) + I_{n+1}(\lambda R)].
\end{aligned}\right\} \tag{5.32}$$

For each number n of nodal diameters (5.31) has its roots, arr͇ ͘d in ascending order. For the first vibrations modes of the circular plate clamped along the contour, the value of the roots squared $\alpha^2 = (\lambda R)^2$ is presented in Table 5.1 (see [40]).

TABLE 5.1

Number of nodal circles S	Number of nodal diameters n			
	$n=0$	$n=1$	$n=2$	$n=3$
	Values of α^2			
0	10,24	21,25	33,60	51
1	39,80	60,80	84,60	111
2	89,00	120,00	153,80	190
3	158,3	199	243	—

Using this table, we can easily determine the frequency for any of these natural vibration modes from the formula

$$p = \frac{\alpha^2}{R^2} \sqrt{\frac{D}{\varrho h}},$$ (5.33)

which is obtained in accordance with the previously adopted notation (5.22).

Knowing the coefficients α, it is easy to construct the free vibration modes (Figure 5.3). To do this we use one of the Equations (5.30) to find C_3, taking $C_I = 1$. The mode shape is constructed using the general solution (5.29).

For each number n of nodal diameters the vibration mode shapes differ in the number of nodal circles. The lowest frequency corresponds to the mode shape without nodal circles, the next frequency corresponds to the mode shape with a single nodal circle, and so on.

The disposition of the circles can be found by setting (5.29) equal to zero. Then we obtain the equation

$$J_n \left(\alpha \frac{r}{R} \right) + C_3 I_n \left(\alpha \frac{r}{R} \right) = 0,$$

from which we find the radii of the nodal circles.

5.3.3. General Boundary Condition Cases

The general geometric boundary condition case is the specification on the contour of definite displacements and rotation angles

$$U(R); \quad \left(\frac{dU}{dr} \right)_{r=R}.$$

Frequently these displacements are related with the elastic deformations of the plate mounting or with other conditions of interaction with the supporting system.
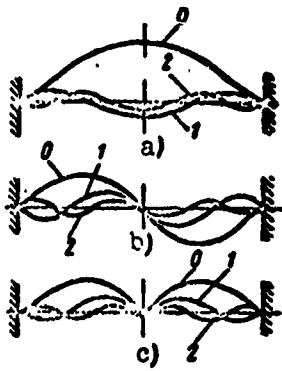
Figure 5.3. Plate vibration modes: a - umbrella; b,c - modes with odd and even numbers of nodal diameters, respectively; 0,1,2 - number of nodal circles.

In addition to the geometric conditions, there may be dynamic boundary conditions, which are defined by specifying on the disk contour either zero or certain definite values of the bending moment M_r and the torsional moment $M_{r\theta}$, expressed by (5.5) and (5.7), and also the shearing force Q_r

$$Q_r = -D \frac{\partial}{\partial r} \nabla^2 W -$$
$$- \frac{dD}{dr} \left[\frac{\partial^2 W}{\partial r^2} + \nu \left(\frac{1}{r} \frac{\partial W}{\partial r} + \frac{1}{r^2} \frac{\partial^2 W}{\partial \theta^2} \right) \right]. \quad (5.34)$$

In accordance with general plate and shell theory, the shearing force Q_r and the torsional moment $M_r\theta$ reduce on the contour to the generalized shearing force

$$Q_r^* = Q_r + \frac{1}{r} \frac{\partial M_{r\theta}}{\partial \theta}. \quad (5.35)$$

Accordingly,

$$Q_r^* = -D \left[\frac{\partial}{\partial r} \nabla^2 W + (1-\nu) \frac{1}{r} \frac{\partial}{\partial r} \left(\frac{1}{r} \frac{\partial^2 W}{\partial \theta^2} \right) \right]. \quad (5.36)$$

Let us transform (5.5) and (5.36) with application to the Bessel functions.

Complementing Formula (5.5) for the bending moment up to the complete value of the Laplace operator (5.10), we can write it in the form

$$M_r = -D \left[\nabla^2 W - (1-\nu) \left(\frac{1}{r} \frac{\partial W}{\partial r} + \frac{1}{r^2} \frac{\partial^2 W}{\partial \theta^2} \right) \right].$$

In accordance with the general solution (5.18)

$$\nabla^2 W = \nabla_1^2 U \cos n\theta \cos pt.$$

and the moment formula can be transformed to the form

$$M_r = -D\left[\mp \lambda^2 U - (1-\nu)\left(\frac{1}{r}\frac{dU}{dr} - \frac{n^2}{r^2}U\right)\right]\cos n\theta \cos pt. \tag{5.37}$$

The upper — negative — sign of the first term is to be used when the Bessel functions of real argument J_n or Y_n are substituted into the formula. The lower — positive — sign is to be used when Bessel functions of imaginary argument I_n or K_n are substituted.

Denoting

$$F_M(U) = \left[\mp \lambda^2 U - (1-\nu)\left(\frac{1}{r}\frac{dU}{dr} - \frac{n^2}{r^2}U\right)\right], \tag{5.38}$$

we obtain the shorter form of the moment formula

$$M_r = -DF_M(U)\cos n\theta \cos pt. \tag{5.39}$$

Similar transformations of (5.36) yield

$$Q_r^i = -D\left[\mp \lambda^2\frac{dU}{dr} - (1-\nu)\frac{n^2}{r^2}\left(\frac{dU}{dr} - \frac{U}{r}\right)\right]\cos n\theta \cdot \cos pt. \tag{5.40}$$

The remarks concerning the signs made with reference to (5.37) remain valid here also.

We denote

$$F_Q(U) = \left[\mp \lambda^2\frac{dU}{dr} - (1-\nu)\frac{n^2}{r^2}\left(\frac{dU}{dr} - \frac{U}{r}\right)\right]; \tag{5.41}$$

then

$$Q_r^* = -DF_Q(U)\cos n\theta \cdot \cos pt. \tag{5.42}$$

5.3.4. Plate Hinged Along Outer Contour (Figure 5.4a)

The boundary conditions for this case will be the equalities

$$U_R = 0; \quad M_R = 0.$$
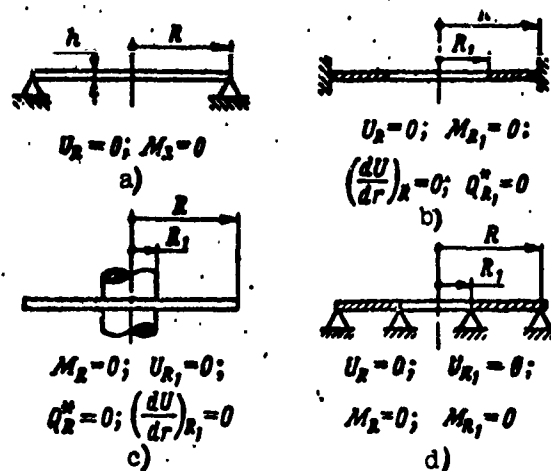
Figure 5.4. Plate restraint conditions.

In accordance with the general solution (5.29) and Formula (5.39), we obtain the following boundary condition equations

$$C_1 J_n(\lambda R) + C_3 I_n(\lambda R) = 0;$$
$$C_1 F_M(J_n)_R + C_3 F_M(I_n)_R = 0.$$

Forming the system determinant and equating it to zero, we obtain the equation

$$J_n(\lambda R) \cdot F_M(I_n)_R - I_n(\lambda R) \cdot F_M(J_n)_R = 0, \qquad (5.43)$$

whose roots are the condition for the existence solutions for non-zero C_1 and C_3.

Expanding the functions $F_M(I_n)$ and $F_M(J_n)$ in accordance with (5.38) and using the formulas for the derivatives (5.32), we obtain the frequency equation

$$4\alpha^2 J_n(\alpha) \cdot I_n(\alpha) - (1-\nu)\alpha \{J_n(\alpha)[I_{n-1}(\alpha) + I_{n+1}(\alpha)] - I_n(\alpha)[J_{n-1}(\alpha) - J_{n+1}(\alpha)]\} = 0, \qquad (5.44)$$

where

$$\alpha = \lambda R.$$

The roots of this equation, when squared, are the coefficients of (5.33). Their values are presented in Table 5.2.

TABLE 5.2

Number of nodal circles S	Number of nodal diameters n		
	$n=0$	$n=1$	$n=2$
	Values of α^2		
0	4,928	13,913	25,705
1	29,812	48,442	70,057
2	74;304	—	—

In the more general case in which the disk is also restrained along an inner contour of large radius R_1 (see Figure 5.4d) or there is a free central hole (see Figure 5.4b), the complete solution (5.28) must be used. In this connection, to find the coefficients C_1, C_2, C_3, C_4 we must specify four boundary conditions and formulate a more complex frequency equation, for which we use (5.39) and (5.42) and their Functions (5.38) and (5.41).

5.3.5 Plate Restrained at the Center

We write the following equations on the basis of the boundary conditions shown in Figure 5.4c.

$$C_1 J_n(\lambda R_1) + C_2 Y_n(\lambda R_1) + C_3 I_n(\lambda R_1) + C_4 K_n(\lambda R_1) = 0;$$
$$C_1 J'_n(\lambda R_1) + C_2 Y'_n(\lambda R_1) + C_3 I'_n(\lambda R_1) + C_4 K'_n(\lambda R_1) = 0;$$
$$C_1 F_M(J_n)_R + C_2 F_M(Y_n)_R + C_3 F_M(I_n)_R + C_4 F_M(K_n)_R = 0;$$
$$C_1 F_Q(J_n)_R + C_2 F_Q(Y_n)_R + C_3 F_Q(I_n)_R + C_4 F_Q(K_n)_R = 0.$$

The determinant of this system of equations is the frequency equation. Its elements are calculated using (5.32), (5.38), (5.41) as complex functions of $\alpha = \lambda R$.

For a large value of R_1 the roots α of the frequency equation depend essentially on the magnitude of R_1 and must be calculated

each time as a function of the given conditions.

If the restraint radius R_1 is comparatively small

$$R_1 < 0{,}2R_\bullet$$

its effect on the results of the α calculation is slight. For such cases we can use the frequency coefficients shown in Table 5.3 (see [40]).

TABLE 5.3

Number of nodal circles S	Number of nodal diameters n		
	$n=0$	$n=2$	$n=3$
	Values of α^2		
0	3,75	5,39	12,49
1	20,91	34,80	53,30
2	60,68	—	—

Examining vibrations of a disk with a single nodal diameter, we identify two cases (Figure 5.5). In case a, the support is stationary, but during the vibrations it is acted upon by the moments which arise as a result of the skew-symmetric disk vibration mode. In case b the support can rotate freely about the hinge (about the nodal diameter). The disk vibrations are free and the resultant of the inertia forces from the vibrations and their moment are equal to zero.

The natural vibration frequencies in cases a and b are different; their coefficients are shown in Table 5.4 (see [44]).

We note that the first mode shape a without a nodal circle is not clearly observed experimentally, since the circumferential deflection distribution proportional to sin θ is not maintained. In this
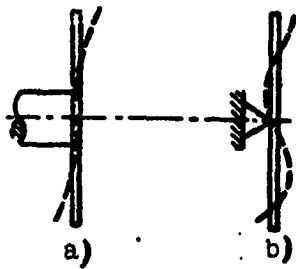
Figure 5.5. Restraint
conditions for vibra-
tions with single nodal
diameter.

connection, the experimentally measured
frequency of this lowest vibration mode
shape is somewhat lower than the calcu-
lated value based on the coefficient
shown in Table 5.4.

5.3.6. Vibrations of Composite Plates
and Closures

There are many structures in which
the plate consists of three layers
(Figure 5.6). The outer, load-carrying
layers are metal, while the middle layer is a filler which does not
take any load (see Figure 5.6a).

TABLE 5.4

Number of nodal circles S	Case a	Case b
	Values of α^2	
0	3.42	—
1	27.56	20.25
2	—	60.84
$R_1/R=0.1$		

Structures in which the space between the plates is free or
filled with fluid, but the plates are attached with one another by
uniformly distributed bonds (see Figure 5.6b), are of this same type.
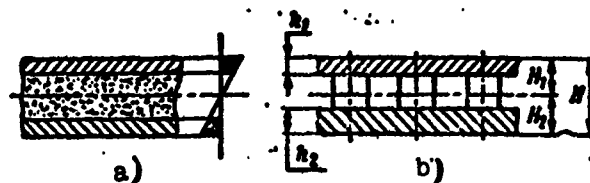
Figure 5.6. Diagram for determining stiffness of
sandwich plate.

Vibrations of such plates can be realized in all the modes examined above. The calculation of the free vibration frequencies can be made on the basis of (5.33), using the coefficients α^2 presented for continuous plates.

The cylindrical stiffness and material density used in the formula should be the equivalent values.

Assuming that the deformation is distributed linearly through the thickness of the plate, we can define the reduced cylindrical stiffness by the formula

$$D_{np} = \frac{E_1 h_1}{3(1-v_1^2)} (3 H_1^2 - 3 H_1 h_1 + h_1^2) +$$
$$+ \frac{E_2 h_2}{3(1-v_2^2)} (3 H_2^2 - 3 H_2 h_2 + h_2^2),$$

(5.45)

where E_1, v_1, E_2, v_2 are respectively the elastic moduli and Poisson coefficients of the outer layer materials.

The position of the middle surface for given layer thicknesses and overall thickness H is defined by

$$H_1 = \frac{h_1^2 + \frac{E_2}{E_1} \frac{1-v_1^2}{1-v_2^2} (2 H h_2 - h_2^2)}{2 \left(h_1 + h_2 \frac{E_2}{E_1} \cdot \frac{1-v_1^2}{1-v_2^2} \right)}.$$

(5.46)

The reduced material density of the composite plate can be defined approximately by the formula

$$\varrho_{np} = \frac{1}{H} (\varrho_1 h_1 + c_2 h_2 + c_0 h_0),$$

(5.47)

where

$$h_0 = H - h_1 - h_2;$$

ρ_0 is the filler density.

For a hollow plate with spot bonds, filled with a fluid, ρ_0 is defined by the formula

$$\varrho_0 = \varrho_\mathrm{A}(1 - \overline{v}) + \varrho_\mathrm{c}\overline{v}, \qquad (5.48)$$

where ρ_{liq} is the liquid density;

ρ_b is the average density of the bond material;

$\overline{v}$ is the relative volume of the bonds, referred to unit volume of the filled space.

5.4. Circular Plate Natural Vibration Mode Orthogonality Property

All the plate natural vibration modes are orthogonal. We obtain the orthogonality condition on the basis of the displacement reciprocity principle.

For a given load distribution $q_j(r\theta)$ the displacement of any point of the plate can be written in the form of the integral

$$W'_j = \int_F k_{xs} q_{js}(r\theta)\, dF, \qquad (5.49)$$

where k_{xs} — the influence function — is the displacement at point x caused by a unit force acting at point s.

This form is valid for linear systems with distributed parameters.

The same expression can be written for another loading $q_v(r\theta)$

$$W_v = \int_F k_{xs} q_{vs}(r\theta)\, dF. \qquad (5.50)$$

We write the integral for the work of the first load times displacement from the second load

$$\int_F W \cdot q_{jx}(r\theta)dF = \int_F q_{jx}(r\theta)dF \int_F k_{xs}q_{vs}(r\theta)dF. \qquad (5.51)$$

We obtain a similar expression for the second load

$$\int_F W_j q_{vx}(r\theta)dF = \int_F q_{vx}(r\theta)dF \int_F k_{xs}q_{js}(r\theta)dF. \qquad (5.52)$$

The influence functions have the reciprocity property

$$k_{xs} = k_{sx};$$

Therefore, the order of integration of the right sides of (5.51) and (5.52) with respect to the x and s coordinates is not important.

On this basis we equate the left sides of (5.51) and (5.52)

$$\int_F W \cdot q_{jx}(r\theta)dF = \int_F W_j q_{vx}(r\theta)dF, \qquad (5.53)$$

where

$$dF = rd\theta\, dr.$$

This equation is the expression of the generalized Rayleigh reciprocity principle.

Let us apply this principle for free vibrations of a plate. As is known, the displacements are expressed by the formulas

$$W'_j = U_j(r)\cos n_j\theta \cos p_j t;$$
$$W_v = U_v(r)\cos n_v\theta \cos p_v t.$$

Correspondingly, the distributed loads are the free vibration inertia forces

$$q_{jx} = m(r)p_j^2 W_j;$$
$$q_{vx} = m(r)p_v^2 W_v.$$

where m(r) is the mass of the plate per unit surface area.

Substituting the displacements and loads into (5.53), we obtain the equation

$$p_j^2 \int_{R_1}^{R} m(r) \dot{U}_v(r) U_j(r) r dr \int_0^{2\pi} \cos n_j \theta \cdot \cos n_v \theta d\theta =$$

$$= p_v^2 \int_{R_1}^{R} m(r) U_j(r) U_v(r) r dr \int_0^{2\pi} \cos n_j \theta \cdot \cos n_v \theta d\theta.$$

Since the different vibration modes have different frequencies $n_j = n_v = n$, the condition must be satisfied

$$\int_{R_1}^{R} m(r) U_j(r) U_v(r) r dr \int_0^{2\pi} \cos n_j \theta \cdot \cos n_v \theta d\theta = 0. \qquad (5.54)$$

For modes which differ in the number of nodal diameter ($n_j \neq n_v$), the condition (5.54) is always satisfied as a consequence of the second integral

$$\int_0^{2\pi} \cos n_j \theta \cdot \cos n_v \theta d\theta = 0. \qquad (5.55)$$

This yields the first orthogonality condition — the circular plate vibration modes which have a different number of nodal diameters are orthogonal.

If $n_j = n_v = n$, then integral (5.55) is not equal to zero. Then the orthogonality condition for the vibration modes becomes the equation

$$\int_{R_1}^{R} m(r) U_j(r) U_v(r) r dr = 0. \qquad (5.56)$$

This is the second orthogonality condition, which shows the sequence of vibration modes with the same number of nodal circles. The number of nodal circles of a given mode equals the mode number minus one.

The mode normalization condition is the equality

$$\int_{R_1}^{R} m(r) U_j^2(r) r dr = 1. \qquad (5.57)$$

5.5. Natural Vibrations of Rotating Disks of Constant Thickness

The turbine disks of the modern flight vehicle engines have small thickness, comparatively large dimensions, and blades of considerable weight mounted on the disk. The vibrations of such disks are performed as vibrations of the entire system with nodal diameters and circles which may be located both on the disk and on the blades.

The natural vibration frequencies of the disk with blades lie below the natural vibration frequencies of the isolated blades, and the number of natural frequencies is considerably greater than for the isolated blade. Therefore, the calculation of the combined vibrations of the disk and blades for modern turbomachines is extremely important.

The analysis of rotating turbine disks is among the most difficult problems. The analysis difficulties are associated with the complexity of the geometric shape of the disk and blades, and also with the presence of centrifugal forces and thermal stresses.

Calculation of rotating disks on the basis of the solution of the general differential equation is possible only for the simplest cases, and this calculation requires considerable idealization. However, this calculation makes it possible to identify and study the general, most significant properties of the vibrations.

5.5.1. Disks with Rigid Blades

As the contour load, we shall examine rigid blades which are spaced uniformly along the outer rim of the disk. We shall assume that the principal longitudinal axis of the blade is positioned radially, and we neglect the moment of inertia about the longitudinal axis in view of its smallness.

We denote the mass of the blade together with the locking part of the disk by the symbol m_b and the moment of inertia about the Oy_0 axis by the symbol J_b. The number of blades is z. We assume that the disk fixity along the circle R_1 is ideally rigid.

In the middle plane of the rotating disk, there act the normal forces

$$N_r = \sigma_r h; \quad N_\theta = \sigma_\theta h.$$ (5.58)

These forces are determined by the centrifugal forces of both the disk itself and the blades. They are axisymmetric and are functions of the radius.

The differential equation of the vibration mode of such a disk is the Equation (5.19)

$$D \nabla_1^2 \nabla_1^2 U - \frac{1}{r} \frac{d}{dr}\left(N_r r \cdot \frac{dU}{dr}\right) + \frac{n^2}{r^2} N_\theta U - \varrho h p^2 U = 0.$$

The general solution of this equation for variable N_r and N_θ is difficult and requires tedious calculations. Therefore, we resort to simplifying assumptions.

As is known, the variability of the radial and circumferential stresses in the disk is created by the centrifugal forces of the mass of the disk itself. The stresses σ_{rb} from the action of the blade centrifugal forces are constant at all points (Figure 5.7).

If the disk is thin and the blades have large dimensions and weight, the variability of the stresses can be neglected, taking the stress for the entire disk equal to the stress from the blades. Then

$$N = N_r = N_\theta = \sigma_r h.$$ (5.59)

and the differential Equation (5.19) takes the form

Figure 5.7. Stress distribution in rotating wheel: shaded part are stresses from centrifugal forces of the disk mass.

$$\Gamma_1^2\Gamma_1^2 U - \varkappa^2 \Gamma_1^2 U - \lambda^4 U = 0; \qquad (5.60)$$

where

$$\varkappa^2 = \frac{N}{D}; \qquad \lambda^4 = \frac{\varrho h}{D} p^2. \qquad (5.61)$$

The equation is solved by the substitution

$$\Gamma_1^2 U = \mp \lambda_i^2 U, \qquad (5.62)$$

after which we obtain the characteristic equation
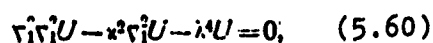
$$\lambda_i^4 \pm \varkappa^2 \lambda_i^2 - \lambda^4 = 0, \qquad (5.63)$$

whose roots are

$$\lambda_1^2 = -\frac{1}{2}\varkappa^2 + \sqrt{\frac{1}{4}\varkappa^4 + \lambda^4}; \qquad (5.64)$$

$$\lambda_2^2 = \frac{1}{2}\varkappa^2 + \sqrt{\frac{1}{4}\varkappa^4 + \lambda^4}. \qquad (5.65)$$

The general solution is formed from Bessel functions as the sum of the solutions of the two Bessel Equations (5.62)

$$U = C_1 J_n(\lambda_1 r) + C_2 Y_n(\lambda_1 r) + C_3 I_n(\lambda_2 r) + C_4 K_n(\lambda_2 r). \qquad (5.66)$$

The transverse force and moment on the outer contour of the disk with account for the action of the blade centrifugal forces are defined by the formulas (Figure 5.8)

$$Q_R = Q_a - N_a \left(\frac{dU}{dr}\right)_R \cos n\theta \cdot \cos pt; \qquad (5.67)$$

$$M_R = M_a - Q_a x_e + N_a x_e \left(\frac{dU}{dr}\right)_R \cos n\theta \cdot \cos pt; \qquad (5.68)$$

The blade vibration inertia force, referred to unit length of the circle of radius R, is

$$Q_a = \frac{1}{t_R} m_a p^2 \left[U_R + x_c \left(\frac{dU}{dr} \right)_R \right] \cos n\theta \cdot \cos pt; \qquad (5.69)$$

the blade centrifugal force is

$$N_a = \frac{1}{t_R} m_a R_c \omega_a^2; \qquad (5.70)$$
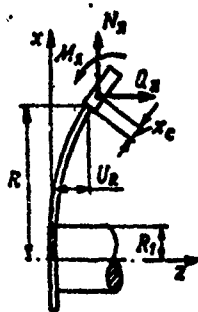
Figure 5.8. Diagram
of forces created
by blades on outer
contour of disk.

the blade inertial moment is

$$M_a = \frac{1}{t_R} J_a (\omega_a^2 - p^2) \left(\frac{dU}{dr} \right)_R \cos n\theta \cdot \cos pt, \qquad (5.71)$$

where J_b is the blade moment of inertia about an axis passing through the blade mass center, perpendicular to the plane of vibration;

t_R is the blade pitch along the outer disk circle of radius R;

ω_a is the disk angular velocity.

Equating (5.67) and (5.68) to (5.42) and (5.39), respectively, and replacing Q_b, N_b, and M_b by their reduced expressions, we obtain the equations for the dynamic boundary conditions

$$D \cdot F_Q(U)_R + \frac{m_a}{t_R} \left\{ p^2 \left[U_R + x_c \left(\frac{dU}{dr} \right)_R \right] - \omega_a^2 R_c \left(\frac{dU}{dr} \right)_R \right\} = 0; \qquad (5.72)$$

$$D \cdot F_M(U)_R - \frac{m_a}{t_R} x_c \left\{ p^2 \left[U_R + x_c \left(\frac{dU}{dr} \right)_R \right] - \right.$$
$$\left. - \omega_a^2 R_c \left(\frac{dU}{dr} \right)_R \right\} + \frac{J_a}{t_R} (\omega_a^2 - p^2) \left(\frac{dU}{dr} \right)_R = 0. \qquad (5.73)$$

The geometric boundary conditions for the inner contour of the disk will be

$$\left. \begin{array}{l} U(R_1) = 0; \\ \left(\frac{dU}{dr} \right)_{R_1} = 0. \end{array} \right\} \qquad (5.74)$$

Substituting into these four equations the general solution (5.66), we obtain a system of homogeneous equations from which we find the frequency coefficient $\alpha^2 = \lambda^2 R^2$. This coefficient not only depends on the geometric dimensions of the disk and blades, but is also a function of the angular velocity ω_a, i.e., κ.

Figure 5.9 shows the curves constructed on the basis of these equations. The curves are shown plotted in dimensionless coordinates and make possible direct determination of the natural vibration frequency of a disk with blades as a function of the angular velocity. The first mode has not nodal circles, the second mode has a single nodal circle.
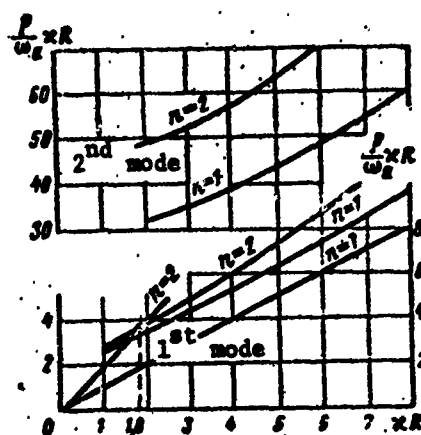
Figure 5.9. Natural vibration frequencies of rotating disk. Curves plotted for following geometric dimensions: $x_c = 0.2R$, $R_1 = 0.4R$

Figure 5.10 shows the nomogram for n = 2, which provides a greater degree of generality than the preceding curves. On the nomogram a particular disk will correspond to its own sloping straight line emanating from the coordinate origin. This line relates the coefficients κ and α, the angular velocity ω_a and the frequency.

Example 5.1. Use the nomogram (see Figure 5.10) to find the first and second natural vibration frequencies of a rotating turbine disk with respect to the mode with two nodal diameters.

Given: mass of all the blades M_b = 2 kg; radius of circle of centers of gravity of the blades R_c = 120 mm; outer design disk radius R = 100 mm; average disk thickness h = 10 mm; disk mass M_d = 2.5 kg; turbine speed n = 12,500 rpm.
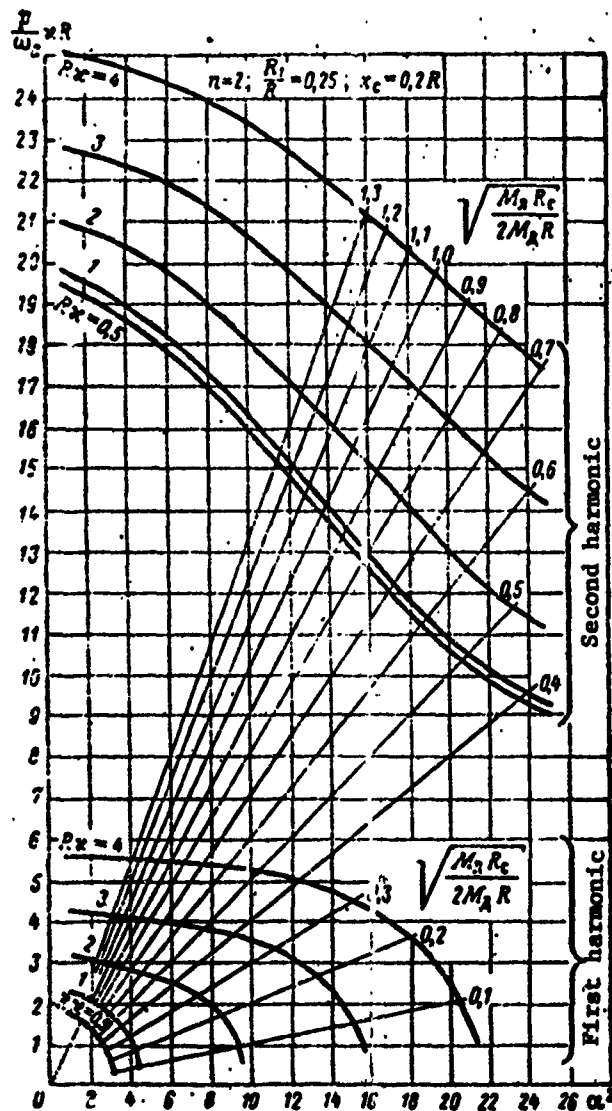
Figure 5.10. Nomogram for calculating natural
vibration frequencies of rotating disks:
M_b and M_d are blade and disk masses; R_c is the
radius of the circle of blade mass centers; R is
the outer design radius of the disk; x_c is the
distance from the root section to the blade center
of mass; R_1 is the radius of the disk restraint
circle.

We calculate the diagram ray coefficient

$$\sqrt{\frac{M_\delta R_c}{2M_\delta R}} = \sqrt{\frac{2 \cdot 12}{2 \cdot 2,5 \cdot 10}} \approx 0,69.$$

The blade force is calculated using (5.70)

$$N_\delta = \frac{1}{t_R} m_\delta R_c \omega_\delta^2 = \frac{M_\delta}{2\pi} \cdot \frac{R_c}{R} \omega_\delta^2 = \frac{2 \cdot 1,2}{2\pi \cdot 981} \omega_\delta^2 \, \text{kgf/cm};$$

$$\omega_\delta = 1310 \, 1/\text{sec}; \quad N_\delta = 670 \, \text{kgf/cm}.$$

The disk cylindrical stiffness

$$D = \frac{Eh^3}{12(1-\nu^2)} = \frac{2 \cdot 10^5}{12(1-0,3^2)} = 0,183 \cdot 10^5 \, \text{kgf/cm};$$

$$\varkappa^2 = \frac{N_\delta}{D} = \frac{670}{183 \cdot 10^3} = 0,365 \cdot 10^{-2} \, 1/\text{cm}^2;$$

$$\varkappa R = \sqrt{0,365} \approx 0,605.$$

The points of intersection of the ray for the coefficient 0.69 with the curves for the parameter κR = 0.6 yield the frequency coefficients:

for the first vibration mode . . . . α^2 = 2.1;

for the second vibration mode . . . . α^2 = 17.

The vibration frequencies of the rotating disk are calculated from the formula

$$p = \frac{\alpha^2}{R^2} \sqrt{\frac{D}{\varrho h}}.$$

For the material density ρ = 8·10⁻⁶ (kgf·sec²)/cm⁴ the frequencies will have the values p_1 = 3150 sec⁻¹, p_2 = 25,500 sec⁻¹.

The curves shown in Figures 5.9 and 5.10 for calculating the rotating disk frequencies yield results which are somewhat high in comparison with experiment because of the inevitable deviations from the ideal conditions in the retention of the disk and blades, and also because of the assumptions in the distribution of the normal stresses over the disk and because of blade flexibility.

We also note that these figures do not permit determining the
natural vibration frequency when the angular velocity is low and the
coefficient κ has a small value. In these cases it is better to
consider the nonrotating disk.

The natural vibration frequencies of the nonrotating disk with
rigid blades can be found from the formula

$$p = \frac{\alpha^2}{R^2} \sqrt{\frac{D}{\varrho h}},$$

where $\alpha = \lambda R$ is a coefficient obtained as a result of the solution
         of the system of Equations (5.72), (5.73), (5.74)
         under the condition that $\omega_a = 0$.

Figure 5.11 shows the values of this coefficient for the first
two vibration modes of a disk (without nodal circle and with a single
nodal circle) with two nodal diameters. The coefficients are given
as a function of the ratio

$$\frac{1}{2} \frac{M_b}{M_d} \frac{R_c}{R},$$

where M_b is the mass of all the blades; M_d is the disk mass.

If the blades are not long and their center of gravity lies
near the base, we can consider them as point masses uniformly dis-
tributed around the outer periphery of the disk.

In this case the calculation of the disk vibrations can be made
using the formulas presented above for rigid blades. Setting $x_c = 0$,
we obtain considerable simplification of the equations.

Figure 5.12 presents curves of the dimensionless coefficients
which make it possible to determine the natural vibration frequencies
of rotating disks with point masses for the modes with one, two, and
three nodal diameters.
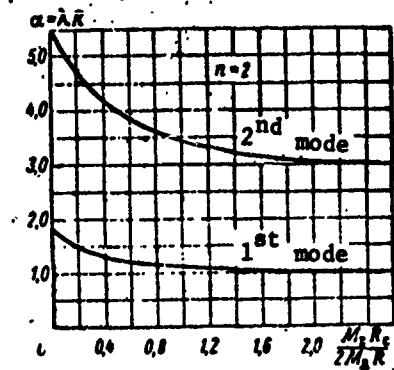
Figure 5.11. Frequency coefficients of nonrotating disk with blades: $x_c = 0.2$ R; $\bar{\rho}_1 = R_1/R = 0.25$.
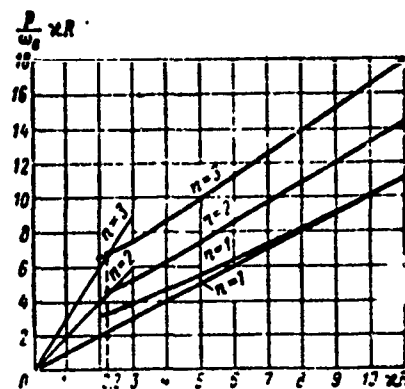
Figure 5.12. Natural vibration frequency coefficients of rotating disk with point masses on the outer contour: radius of circle of disk restraint on the shaft is $\bar{\rho}_1 = 0.2$.

5.5.2. Resolution of Disk Natural Vibrations Into Two Waves Traveling in Opposite Directions

The general solution (5.18) for free vibrations of a disk

$$W = U(r)\cos n\theta \cdot \cos pt$$

can be represented in the form of a sum, expanding the product of the cosines using the formula

$$\cos n\theta \cdot \cos pt = \frac{1}{2}[\cos(n\theta - pt) + \cos(n\theta + pt)]; \qquad (5.75)$$

then

$$W = \frac{1}{2}U(r)[\cos(n\theta - pt) + \cos(n\theta + pt)]. \qquad (5.76)$$

Each of the terms individually satisfies the general differential equation of disk vibrations. Therefore, they can be considered as independent solutions. Each of the solutions yields the vibrations of disk points which are shifted in phase by an angle proportional

to the θ coordinate. As a result of this the vibrations have the
form of phase waves traveling around the disk with a definite
velocity.

The first solution is a wave with n nodal diameters, traveling
around the disk in the positive θ direction; the second solution is
a wave traveling in the opposite direction.

It is convenient to define the position of the wave relative to
coordinate axes fixed with the disk by the position of some nodal
diameter (Figure 5.13). The equation for the position of the nodal
diameter is the equality

$$\cos(n\theta_0 \mp pt) = 0;$$

hence

$$\theta_0 = \pm \frac{p}{n}t + \frac{\pi}{2n}. \tag{5.77}$$

The plus sign relates to the wave traveling forward; the minus sign
relates to the wave traveling backward.
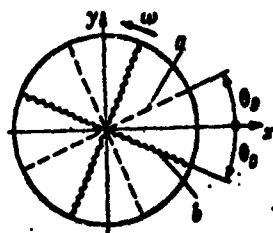
Figure 5.13. Arrangement
of traveling waves on
disk: a - mode traveling
in direction of disk
rotation; b - mode
traveling opposite disk
rotation.

We obtain the rate of displace-
ment of the nodal diameters around the
disk, and, consequently, the velocity
of the phase waves, by differentiating
(5.77):

$$\dot{\theta}_0 = \pm \frac{p}{n}. \tag{5.78}$$

The waves travel in opposite directions
with the same velocity, proportional
to the natural vibration frequency.
The number of possible phase wave
shapes and their velocities corresponds

to the number of disk natural vibration modes. The phase waves are
a different form of disk free vibrations.

The rule for the motion of the phase waves also holds for the
rotating disk, with account for the change of the natural vibration
frequency owing to the rotation. Moreover, the velocities of the
phase waves relative to stationary coordinate axes are of great
importance. If we denote the disk rotational velocity by ω_a, the
absolute angular velocities of the phase waves will be

$$\Omega = \omega_a \pm \frac{p}{n},$$ (5.79)

where p . ' · sk natural vibration frequency with account for
rotation.

Hence, we see that the absolute angular velocities of the phase
waves traveling forward and of the phase waves traveling backward
are different.

Representation of free vibrations in the form of phase wave
oscillations is very convenient and permits the solution of several
special problems.

5.5.3. Critical Disk Rotation Speeds

The absolute velocity Ω of the backward traveling wave decreases
with increase of the disk angular velocity ω_a. There is an angular
velocity at which the absolute velocity of the wave becomes equal
to zero. In this case the mode shape is itself stationary relative
to the fixed axes, and all the points of the rotating disk, follow-
ing this mode shape, perform transverse oscillations. This state
is very dangerous and the rpm corresponding to this condition has
been termed the disk critical speed.

At the critical speed the disk loses stability and cannot counter-
act static forces acting on its side surface or on the blades, as

a result of which large bending deformations arise and lead to disk failure or blade rupture.

In accordance with (5.79), the critical speed can be defined from the formula

$$\omega_{a\,кр} = \frac{p}{n},\qquad\qquad(5.80)$$

where p is the disk natural vibration frequency at a rotational speed equal to the critical speed.

To find the critical speed we must know the disk vibration frequency as a function of the angular velocity.

Plotting the curve $p(\omega_a)$ (Figure 5.14) and drawing the straight line $p = n\omega_a$ from the coordinate origin, we find the critical speed as the point of intersection of the frequency function with the line.
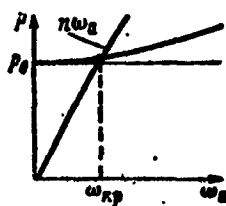
Figure 5.14. Diagram for determining disk critical speed.

Disks of constant thickness with rigid blades can be calculated with the aid of the curves shown in Figure 5.9, which are analogous to Figure 5.14 but are plotted in dimensionless quantities. The straight line drawn from the coordinate origin with the slope n gives the point of intersection with the corresponding frequency curve. The point of intersection shows the value of the parameter R corresponding to the disk critical speed.

The vibration mode shape without nodal circles, n = 2, corresponds to the parameter

$$\alpha_{кр} = R x_{кр} = 1,8.$$

In accordance with the previously introduced notations (5.61), the

general formula for calculating the critical speed takes the form

$$\omega_{a\,\text{кр}} = \frac{a_{\text{кр}}}{R} \sqrt{\frac{Dt_R}{m_s R_c}}.$$ (5.81)

The critical speeds for the vibration modes with nodal circles cannot be reached in practice because of limitations in the strength of the disk. Therefore, determination of their coefficients a_{cr} is not required.

In accordance with Figure 5.12, the critical speed coefficients a_{cr} for disks with ponnt masses distributed along the outer circumference are

$$a_{\text{кр}} = R \varkappa_{\text{кр}} = 2,\ 2.$$

We note that the critical speed coefficients a_{cr} for vibrations with a different number of nodal diameters lie in a narrow range. This indicates that the disk has an entire region of critical speeds, although quite narrow, within the limits of which it can have large amplitudes of forced vibrations in the different modes, interacting with the static pressure field on its side surface.

The curves presented in Figures 5.9 and 5.12 show that there are no critical rotational speeds for the vibration modes with a single nodal diameter. This is explained by a peculiarity of the vibration mode with a single nodal diameter.

For n = 1 all points of the disk travel along planar curves — circles. The resultants of the inertia forces from rotation and the transverse vibrations pass through the center of the disk and balance one another. As a result of this, the deformed state of the disk cannot occur without the participation of external forces.

Thus, the critical speeds of disks are connected with vibrations in the modes with two or more nodal diameters.

In most cases the vibrations of turbomachine disks arise as a result of nonuniformity of the gas stream approaching the working blades. The impulse of the flow acting per unit surface area swept by the blades depends on the velocity and density of the gas, and also on the static pressure in the stream. This impulse can be determined on the basis of a special gasdynamic calculation of the flow passage or by experimental measurements of the velocity and pressure field ahead of and behind the rotor.

Figure 5.15 shows examples of the impulse distribution, referred to the average radius of the flow passage. Developing the surface of the impulse diagram onto a plane, we can decompose the impulse diagram into a Fourier series, representing them as the sum

$$I = I_0 + \sum_{i=1}^{p} I_i \cos(n_i \theta - \gamma_i),$$

(5.82)

where n_i is the number of sinusoid waves within the limits of the circumference.

Among the Fourier series harmonics, there will be those with large amplitude of the impulse I_i. Usually these harmonics are determined by the peculiarities of the flow passage construction: the number of entrance channels, the number of combustion chambers, number of different struts or ribs; number of guide vanes, and so on.

Each of the harmonics of the overall impulse causes its own vibration mode respectively n_i, which occurs when the disk angular velocity reaches the critical speed for the given vibration mode. We note that there is always nonuniformity present in the velocity and pressure field in turbomachines. Therefore, (to avoid dangerous resonant phenomena) it is recommended that the existence of critical disk angular velocities, particularly those with number of nodal diameters $n = 2, 3, 4$, not be permitted in the operating speed region.

If a turbine is constructed with partial gas admission or with individual nozzle channels, then disk passage through the critical
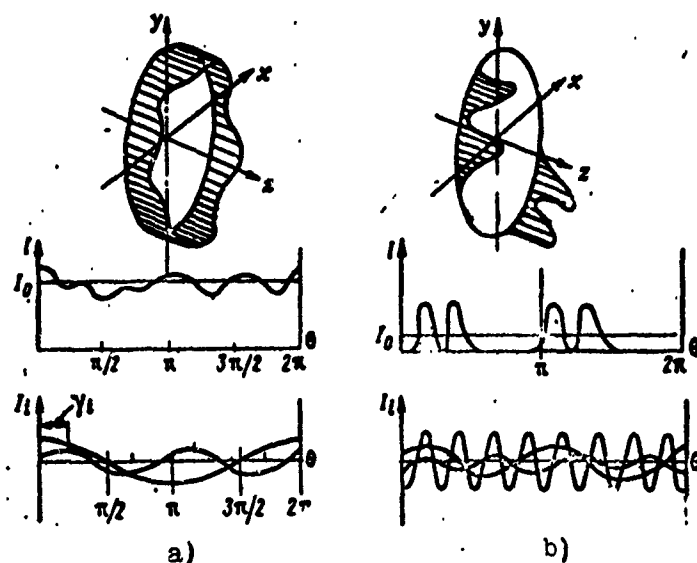
Figure 5.15. Decomposition of exciting pulses
into harmonic series: a - distributed pulses
along circumference of flow passage; b - local
pulses along circumference of flow passage.

speed should be avoided, since the excitation is very strong in
these cases.

5.6. Discrete Model Method for Calculating
Natural Vibration Frequencies of Turbomachine Disks

The computational method is based on replacing the real disk
and blades by an equivalent model, consisting of weightless ring
and bar segments and inertial masses concentrated at the boundaries
of the segments. The discrete model method makes it possible to
analyze disks of any shape subjected to various loading conditions.

The use of a digital computer for the calculation makes it
possible to select a computational model which is very close to the
actual system and obtain computational results which are in very
good agreement with experiment.

To construct the discrete model, the disk being analyzed is broken down into several annular segments (Figure 5.16). The number of disk segments should be at least three or four in calculating the first two vibration modes for disks with long blades.

The mass of the annular segment is concentrated on the section center-of-gravity circle. The mass per unit length of the circle is

$$m_p = \varrho F_p;$$

the mass and section indices p correspond to the segment indices.

The blade masses are also replaced by several discrete masses, as was shown in Section 3.11.5.
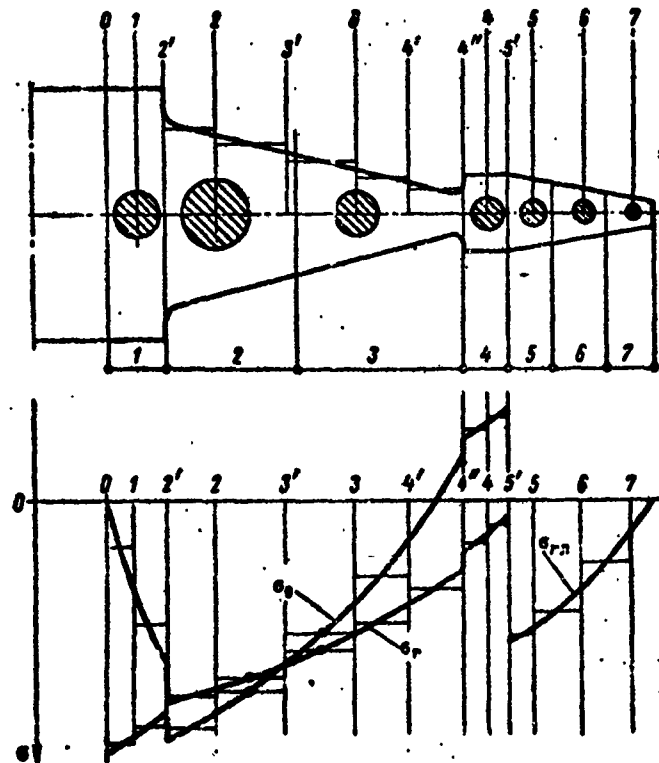
Figure 5.16. Discrete model of disk.

It is convenient to use a continuous sequential notation for the annular masses and the numbering of the segments for the disk and blades.

The segment located between the annular masses is considered weightless and is replaced by a segment of constant thickness equal to its average value. If the disk thickness or the radial and circumferential stresses in the disk from the action of the centrifugal forces and the temperature gradients vary significantly, the segment is broken down into several smaller weightless subsegments. The boundaries of the subsegments are designated by primes.

Let us find the connection between the deflection, section rotation angle, bending moment, and shearing force at the $(p + 1)^{st}$ section and the corresponding parameters at the section p.

From the general Equation (5.19) for the deformations of a circular plate, setting $\rho = 0$, we obtain the differential equation of deformation of a weightless ring of constant thickness

$$D\hat{\nabla}_1^2\hat{\nabla}_1^2 U - \frac{1}{r}\frac{d}{dr}\left(N_r r \frac{dU}{dr}\right) + n^2\frac{1}{r^2} N_t U = 0. \qquad (5.83)$$

The general solution of this equation consists of the sum of four particular solutions

$$U = C_1 U_1 + C_2 U_2 + C_3 U_3 + C_4 U_4.$$

the form of the particular solutions depends on the nature of the stresses σ_r and σ_θ acting in the midplane of the disk.

Taking the quantities σ_r and σ_θ constant within the limits of a segment, we seek the solutions in the form of the function

$$U = r^s. \qquad (5.84)$$

Substituting this function into the differential equation, we obtain

$$D(s^2 - n^2)[(s-2)^2 - n^2] - N_r r_{cp}^2 s^2 + N_t r_{cp}^2 n^2 = 0, \qquad (5.85)$$

where r_{av} is the average radius of the segment.

The four roots of this equation yield the four particular solutions which comprise the overall deflection function for the segment

$$U = C_1 r^{s_1} + C_2 r^{s_2} + C_3 r^{s_3} + C_4 r^{s_4}. \qquad (5.86)$$

If $\sigma_r = \sigma_\theta = 0$, i.e., there are no stresses in the disk mid-plane, then (5.85) becomes

$$(s^2 - n^2)[(s-2)^2 - n^2] = 0, \qquad (5.87)$$

which has the roots

$$s = \pm n; \quad s = 2 \pm n.$$

The general solution of (5.83) for $\sigma_r = \sigma_\theta = 0$ will be

$$U = C_1 r^{2+n} + C_2 r^n + C_3 r^{2-n} + C_4 r^{-n}. \qquad (5.88)$$

If $N_r = N_\theta = N$, (5.83) takes the form

$$\nabla_1^2 \nabla_1^2 U - \varkappa^2 \nabla^2 U = 0; \qquad (5.89)$$
$$\varkappa^2 = \frac{N}{D}.$$

Its general solution is known

$$U = C_1 r^n + C_2 r^{-n} + C_3 I_n(\varkappa r) + C_4 K_n(\varkappa r), \qquad (5.90)$$

where $I_n(\varkappa r)$ and $K_n(\varkappa r)$ are Bessel functions of the first and second kind of imaginary argument.

If it is desirable to avoid use of the Bessel functions, we can replace the exact solution by an approximate solution in the form of the Function (5.84). The exponents s are found from the characteristic Equation (5.85), which for the case $N_r = N_\theta = N$ takes the form

$$(s^2 - n^2)\left[(s-2)^2 - n^2 - \frac{Nr_{cp}^2}{D}\right] = 0. \tag{5.91}$$

Two roots of this equation coincide with the preceding roots and yield the exact solution. The other two roots differ somewhat from those found perviously because of the additional term in the brackets. These roots can be found by equating the bracketed quantity to zero.

The equation for the deformations of the outer segment of the disk, where the blade retainers are located, depends on the retained design. This equation can be obtained by special calculations on or the basis of experiments.

For an approximate evaluation, the retainer portion of the disk can be considered continuous.

To formulate the equations for transition through a segment of the disk, we write the formulas for the bending moment and generalized shearing forces acting in an annular section of a circular plate.

In accordance with (5.5), the moment formula is written as

$$M_r = -D\left[\frac{d^2U}{dr^2} + \nu\left(\frac{1}{r}\frac{dU}{dr} - \frac{n^2}{r^2}U\right)\right]\cos n\theta \cdot \cos pt.$$

In accordance with (5.36) the generalized shearing force will be

$$Q_r^* = -D\left[\frac{d}{dr}\nabla_1^2 U - (1-\nu)n^2\frac{1}{r}\frac{d}{dr}\left(\frac{1}{r}U\right)\right]\cos n\theta \cdot \cos pt.$$

Examining the amplitude values of M_r and Q_r^*, we drop the factor $\cos n\theta \cdot \cos pt$.

The formulas for the deflection functions (5.84) take the form

$$M_r = -D\sum_{i=1}^{4} C_i[s_i(s_i-1) + \nu(s_i - n^2)]r^{s_i r^{-2}};$$

$$Q_r^* = -D\sum_{i=1}^{4} C_i[(s_i^2 - n^2)(s_i - 2) - (1-\nu)n^2(s_i-1)]r^{s_i r^{-3}};$$

Denoting the bracketed quantities by μ_1 and q_1 respectively, we write these formulas in the shorter form

$$M_r = -D \sum_{i=1}^{4} C_i \mu_i r^{s_i-2};$$ (5.92)

$$Q_r^* = -D \sum_{i=1}^{4} C_i q_i r^{s_i-3};$$ (5.93)

The constants C_1 are found from the parameters of the beginning of the segment from the system of equations, in which we set $r = r_p$:

$$\left. \begin{aligned} U &= \sum_{i=1}^{4} C_i r^{s_i}; \\ \theta_r &= \sum_{i=1}^{4} C_i s_i r^{s_i-1}; \\ -\frac{1}{D} M_r &= \sum_{i=1}^{4} C_i \mu_i r^{s_i-2}; \\ -\frac{1}{D} Q_r^* &= \sum_{i=1}^{4} C_i q_i r^{s_i-3}; \end{aligned} \right\}$$ (5.94)

hence, we find

$$C_i = \frac{\Delta_i}{\Delta_p},$$ (5.95)

where Δ_p is the determinant composed of the coefficients of the right side of (5.94)

$$\Delta_p = \left| r_p^{s_i}, \ s_i r_p^{s_i-1}, \ \mu_i r_p^{s_i-2}, \ q_i r_p^{s_i-3} \right|_{i-1};$$ (5.96)

Δ_1 is the determinant formed from Δ_p by replacing the ith column by the column of parameters of the left side of (5.94)

$$U_p, \ \theta_p, \ -\frac{1}{D} M_{rp}, \ -\frac{1}{D} Q_{rp}^*.$$

After determining C_1, we then find the parameters of the end of the segment from (5.94), where we set $r = r_{p+1}$.

If a segment is broken down into subsegments, the parameters found for the end of the preceding subsegment are taken as the parameters for the beginning of the following subsegment and the calculation is continued. This process is continued until all the parameters of the end of the segment at the section ahead of the annular mass are determined.

Transition through the annular mass is accomplished using the known matrix formula

$$P_{p,0} = M_p P_{(p-1)K},$$
(5.97)

where $P_{(p-1)K}$ and $P_{p,0}$ are the parameters of the section p ahead of and behind the mass, respectively;

M_p is the mass matrix

$$M_p = \begin{vmatrix} 1 & 0 & 0 & 0 \\ 0 & 1 & 0 & 0 \\ 0 & 0 & 1 & 0 \\ -m_p p^2 & 0 & 0 & 1 \end{vmatrix}.$$
(5.98)

For the blade we obtain the segment deformation equation from the general Equation (3.9).

For a weightless segment of constant section, this equation takes the form

$$EJ \frac{d^4 Y}{dx^4} - N \frac{d^2 Y}{dx^2} = 0,$$
(5.99)

where EJ is the average stiffness of the blade segment relative to the axis of minimal stiffness;

N is the average value of the centrifugal force within the limits of the segment.

The differential Equation (5.99) has the solution
$$Y(x) = C_1 ch(\varkappa x) + C_2 sh(\varkappa x) + C_3 x + C_4;$$
$$\varkappa^2 = \frac{N}{EJ}.$$
(5.100)

If the calculation is made for the nonrotating wheel, $N = 0$, and the general solution will be

$$Y(x) = C_1 x^3 - C_2 x^2 + C_3 x + C_4. \qquad (5.101)$$

The calculation of the blade segments is made by the matrix method, as outlined in Section 3.11.5. The formula for transition through the segments will be

$$P_{p+1} = L_p P_p.$$

For the deflection function (5.100) the matrix L_p has the form

$$L_p = \begin{vmatrix} 1 & l & \dfrac{\mathrm{ch}\,(\varkappa l) - 1}{\varkappa^2 EJ} & -\dfrac{\mathrm{sh}\,(\varkappa l) - \varkappa l}{\varkappa^3 EJ} \\[2mm] 0 & 1 & \dfrac{\mathrm{sh}\,(\varkappa l)}{\varkappa EJ} & -\dfrac{\mathrm{ch}\,(\varkappa l) - 1}{\varkappa^2 EJ} \\[2mm] 0 & 0 & \mathrm{ch}\,(\varkappa l) & -\dfrac{1}{\varkappa}\,\mathrm{sh}\,(\varkappa l) \\[2mm] 0 & 0 & -\varkappa\,\mathrm{sh}\,(\varkappa l) & \mathrm{ch}\,(\varkappa l) \end{vmatrix}. \qquad (5.102)$$

The length l, average stiffness EJ, and parameter $\varkappa$ in this matrix have different values for each blade segment.

Transition through the mass is accomplished using (3.155).

The compatibility conditions for the disk and blades at Section 5' (see Figure 5.16) reduce to equality of the bending moments and shearing forces of the disk and blades

$$M_{d5'} = t_{5'} \cdot M_{r5'};$$
$$Q_{d5'} = t_{5'} \cdot Q_{5'}^o; \qquad (5.103)$$

$$t_{5'} = \frac{2\pi r_{5'}}{z}, \qquad (5.104)$$

where t_5 is the blade pitch along the circle $r_{5'}$;

z is the number of blades.

In addition to the bending vibrations, the blade performs torsional vibrations. The result of this is the development in the blade root of a twisting moment which acts on the outer contour of the disk. The magnitude of the twisting moment is small, and may be neglected in calculating the natural frequencies of the disk and blades. Account for the twisting moment does not present any difficulty and can be carried out within the limits of the discrete model method.

The transition through the joining section is written in matrix form

$$P_{v',0} = S_{5'} \cdot P_{4,x'}$$
(5.105)

where S_5, is the joining matrix

$$S_{5'} = \begin{vmatrix} 1 & 0 & 0 & 0 \\ 0 & 1 & 0 & 0 \\ 0 & 0 & t_{g'} & 0 \\ 0 & 0 & G & t_{g'} \end{vmatrix} \cdot$$
(5.106)

The calculation begins with the zero section, where usually $U_0 = 0$, $\vartheta = 0$. Selecting a frequency p, we calculate all the segments — from zero to the blade tip (the section after the last discrete mass). The bending moment and the shearing force equal zero at the blade tip. This condition is used to formulate the boundary condition equations and check the validity of the choice of the frequency p in the beginning of the calculation.

The determination of the frequency is made by trial and error, as was shown in the calculation of the blade alone.

When calculating the disk critical speed, the frequency p is associated with the wheel angular velocity and should be specified as the product

$$p = n\omega.$$

Moreover, the stresses in the disk and blades owing to the action of the centrifugal forces vary in proportion to ω^2. Therefore, each angular velocity must have its own diagram of the stress distribution in the disk and blades.

The natural vibration frequency found as a result of the calculation yields at the same time the value of the disk critical speed.

Calculation by the discrete model method is convenient for computer programming, and if a sufficiently large number of segments are used makes it possible to obtain good computational accuracy. The stress distribution in the disk and blades, from the action of centrifugal forces and temperature gradients can be calculated by any technique and should be specified among the initial data. In the case of computation on a digital computer, these stresses are determined in the process of the general computation with the aid of a special subprogram.

5.7. Calculation of Circular Plates and Disks by the Rayleigh Method

The Rayleigh method is used quite successfully to calculate the simple vibration modes of circular plates — the modes without nodal circles. The calculation is made with the aid of the known formula

$$p^2 = \frac{\Pi}{T^*} ,$$

(5.107)

which requires formulation of expressions for the maximal deformation potential energy Π and the maximal kinetic energy T^*, calculated for a frequency equal to unity.

5.7.1. Formulas for Disk Bending Deformation Potential Energy

To calculate the potential energy, we use the formulas which are familiar from general courses on theory of elasticity.

The potential energy of a plate for bending deformation is

$$\Pi = \frac{1}{2} \iint D \left[\left(\frac{\partial^2 W}{\partial x^2} \right)^2 + \left(\frac{\partial^2 W}{\partial y^2} \right)^2 + 2\nu \frac{\partial^2 W}{\partial x^2} \frac{\partial^2 W}{\partial y^2} + \right.$$
$$\left. + 2(1-\nu) \left(\frac{\partial^2 W}{\partial x \partial y} \right)^2 \right] dx\,dy, \tag{5.108}$$

where

$$D = \frac{Eh^3}{12(1-\nu^2)}; \tag{5.109}$$

this quantity is variable for plates of variable thickness.

Several transformations permit writing (5.108) in polar coordinates

$$\Pi = \frac{1}{2} \int_0^{2\pi} \int_{R_1}^{R} D \left\{ \left(\frac{\partial^2 W}{\partial r^2} + \frac{1}{r} \frac{\partial W}{\partial r} + \frac{1}{r^2} \frac{\partial^2 W}{\partial \theta^2} \right)^2 - \right.$$
$$\left. - 2(1-\nu) \left[\frac{\partial^2 W}{\partial r^2} \left(\frac{1}{r} \frac{\partial W}{\partial r} + \frac{1}{r^2} \frac{\partial^2 W}{\partial \theta^2} \right) - \left\{ \frac{\partial}{\partial r} \left(\frac{1}{r} \frac{\partial W}{\partial \theta} \right) \right\}^2 \right] \right\} r\,dr\,d\theta. \tag{5.110}$$

We note that for plates clamped along the contour the integral

$$\iint \left[\frac{d^2 W}{dr^2} \left(\frac{1}{r} \frac{dW}{dr} + \frac{1}{r^2} \frac{\partial^2 W}{\partial \theta^2} \right) - \left\{ \frac{\partial}{\partial r} \left(\frac{1}{r} \frac{\partial W}{\partial \theta} \right) \right\}^2 \right] r\,dr\,d\theta$$

vanishes.

The potential energy for bending vibrations in the fan-wise mode with several nodal diameters is obtained after substituting into (5.110) the deflection function

$$W_{max} = U(r) \cos n\theta, \tag{5.111}$$

$$\Pi_{max} = \frac{\pi}{2} \int_{R_1}^{R} D \left\{ \left(\frac{d^2 U}{dr^2} + \frac{1}{r} \frac{dU}{dr} - \frac{n^2}{r^2} U \right)^2 - \right.$$
$$\left. - 2(1-\nu) \left[\frac{d^2 U}{dr^2} \left(\frac{1}{r} \frac{dU}{dr} - \frac{n^2}{r^2} U \right) - \left\{ \frac{d}{dr} \left(\frac{n}{r} U \right) \right\}^2 \right] \right\} r\,dr. \tag{5.112}$$

For axisymmetric (umbrella) vibrations, for which the deflection is a function only of r, the potential energy formula takes the form

$$\Pi_{m,x} = \pi \int_{R_1}^{R} D \left\{ \left(\frac{d^2 U}{dr^2} + \frac{1}{r} \frac{dU}{dr} \right)^2 - (1-\nu) \frac{d^2 U}{dr^2} \frac{1}{r} \frac{dU}{dr} \right\} r \, dr. \qquad (5.113)$$

5.7.2. Middle Surface Deformation Potential Energy

This expression is not complete for rotating and nonuniformly heated disks, which have normal stresses in the midplane. In these disks the bending deformations are accompanied by elongation of the middle surface, which is easily visualized, since the area of the deformed wave surface is greater than the surface of the flat plate.

For small deflections the normal stresses which arise in the disk midplane because of its elongation are negligibly small, and the elongation potential energy can be ignored. However, if large stresses from centrifugal forces or thermal stresses act in the midplane, then the elongation potential energy becomes very significant and neglect of this energy is not admissible.

We find the elongation potential energy by examining the plate as an absolutely flexible membrane.

The work of elongation of an elemental volume of the membrane is equal to the sum of the work in the principal directions

$$d\Pi_N = \left[dx \sqrt{1 + \left(\frac{\partial W}{\partial x} \right)^2} - dx \right] \sigma_x h \, dy +$$
$$+ \left[dy \sqrt{1 + \left(\frac{\partial W}{\partial y} \right)^2} - dy \right] \sigma_y h \, dx;$$

where we assume that the bending deformations do not alter the normal stresses σ_x and σ_y in the midplane. In view of the smallness of the deflections, this expression can be simplified

$$d\Pi_N = \frac{1}{2} h \left[\sigma_x \left(\frac{\partial W}{\partial x} \right)^2 + \sigma_y \left(\frac{\partial W}{\partial y} \right)^2 \right] dx \, dy. \qquad (5.114)$$

In polar coordinates this expression has the form

$$dΠ_N = \frac{1}{2} h \left[σ_r \left(\frac{∂W}{∂r} \right)^2 + σ_θ \frac{1}{r^2} \left(\frac{∂W}{∂θ} \right)^2 \right] r dr dθ. \tag{5.115}$$

Substituting herein for the fan-wise mode the deflection function (5.111) and integrating, we obtain the formula

$$Π_N = \frac{π}{2} \int_{R_1}^{R} h \left[σ_r \left(\frac{dU}{dr} \right)^2 + σ_θ \frac{n^2}{r^2} U^2 \right] r dr. \tag{5.116}$$

The stresses $σ_r$ and $σ_θ$ are axisymmetric and are determined in the strength calculations for the given radial plate loads and the temperature distribution.

For the umbrella vibration mode, the formula will have the form

$$Π_N = π \int_{R_1}^{R} h σ_r \left(\frac{dU}{dr} \right)^2 r dr. \tag{5.117}$$

5.7.3. Disk Vibration Kinetic Energy

The disk vibration kinetic energy is found from the obvious formula

$$dT = \frac{1}{2} \, dm \dot{W}^2, \tag{5.118}$$

where

$$dm = ρh r dθ dr;$$
$$\dot{W} = \frac{∂W}{∂t} = -pU(r) \cos nθ \sin pt. \tag{5.119}$$

After substitution, (5.118) takes the form

$$dT = \frac{1}{2} ρ p^2 h r U^2(r) \cos^2 nθ \sin^2 pt dr dθ.$$

To determine the maximal kinetic energy of the vibrations of the entire disk we set sin pt = 1 and integrate the expression over the entire surface, after which we obtain

$$T_{max} = \frac{π}{2} ρ p^2 \int_{R_1}^{R} h U^2(r) r dr; \tag{5.120}$$

for umbrella vibrations

$$T_{max} = \pi \varrho p^2 \int_{R_1}^{R} hU^2(r)rdr. \qquad (5.121)$$

Equating the potential energy, taken in the form of the sum $\Pi_{max} + \Pi_N$, to the kinetic energy [(5.120) or (5.121)], we can write the Rayleigh formula in the form

$$p^2 = \frac{\Pi_{max} + \Pi_N}{T_{max}^s}. \qquad (5.122)$$

5.7.4. Initial Function Choice

As is known, to calculate the frequency we must assume the vibration mode, expressing it with the aid of a definite function $U(r)$. The function $U(r)$ must correspond to the vibration mode and must of necessity satisfy the geometric boundary conditions.

For example, for the disk rigidly clamped along a circle of radius R the conditions must be satisfied

$$U(R) = 0; \quad \left(\frac{dU}{dr}\right)_{r=R} = 0.$$

If the plate is hinged, only the first condition is satisfied.

For disks without central restraint the correspondence of the deflection function $U(r)$ to the vibration mode lies in the fact that, for the umbrella and fan-wise vibration modes with an even number of nodal diameters, the derivative of the function $U(r)$ at the disk center ($r = 0$) is equal to zero.

For the fan-wise modes with an odd number n, the derivative of the function $U(r)$ may not vanish at the center.

The disk deflection function must be minimizing. Therefore, it must contain a parameter ε, which is selected in the course of the calculation so that the unknown frequency will be minimal. Here

the parameter ε identifies, from the entire given function family, the most likely vibration mode.

The following are examples of the assumed functions which may be used in the calculations.

$$U(r) = \left(1 - \frac{r^2}{R^2}\right)^2. \qquad (5.123)$$

For umbrella vibrations with clamping along the outer contour

$$U(r) = (1 + \varepsilon r^2)\left(1 - \frac{r^2}{R^2}\right)r^2, \qquad (5.124)$$

where ε is the minimizing parameter.

For disks restrained at the center of along an inner contour at the radius R_1, the deflection functions are taken in the form:

If the inner disk restraint radius R_1 is small (it does not exceed the value 0.15 - 0.2 R), the simplest expression which can be taken as the initial disk elastic line has the form (Stodola)

$$U(r) = r^4. \qquad (5.125)$$

Another simple function is (see [7])

$$U(r) = r^2(1 + \varepsilon r). \qquad (5.126)$$

Both functions do not satisfy the dynamic boundary conditions and yield approximately the same accuracy of the disk vibration frequency calculation. The value of the fan-wise vibration frequency found using these functions may exceed the exact value by 3 - 4%. The big advantage of these functions is the simplicity of their application. This is particularly notable with regard to the second function, which yields simple algebraic equations for the sought parameter ε.

As a more refined function, we can take

$$U(r) = r^2(1 + Ar + Br^2);$$ (5.127)

the constants A and B are selected so that the dynamic boundary
conditions at the outer edge of the disk are satisfied.

If the radius R_1 is sufficiently large, according to Stodola
the deflection function in the following form is recommended

$$U(r) = (r - R_1)^2.$$ (5.128)

This formula yields good results for values of R_1 no larger than
(0.25 - 0.30) R.

5.8. Vibrations of Heated Circular Plates and Disks

A large number of engine components operate at high temperatures.
The degree of temperature rise of the individual parts is different,
and therefore thermal stresses develop in the components. These
stresses have a significant effect on the vibrations of the parts,
altering the resonant frequencies, making the vibrations unstable,
and altering the vibration level. The combustion chamber dome,
flat diaphragms, casing walls, and turbine disks are examples of
circular nonuniformly heated plates in the engines which operate under
the action of thermal stresses. The thermal stresses in these parts
depend on the temperature field, and also on the degree of freedom
or restrictedness of the thermal deformations. The change of the
material elastic modulus with temperature rise also affects the
vibrations.

5.8.1. Uniformly Heated Plate Clamped Along the Outer Contour

If the outer contour of the plate is clamped so that radial
deformations are not allowed, compressive stresses develop in the
plate when it is heated. The stresses will be the same at all sec-
tions and will depend on the magnitude of the temperature rise

$$\sigma = \frac{E}{1-\nu}\, \alpha \Delta t^\circ, \tag{5.129}$$

where α is the linear expansion coefficient;
Δt° is the temperature rise.

The appearance of compressive stresses leads to reduction of the natural vibration frequency, which depends on Δt°, and particularly markedly for thin plates of large diameter.

The equation for the plate vibrations is (5.60), in which the second term is to be taken with the positive sign in view of the fact that the stresses have a minus sign

$$\nabla_1^2 \nabla_1^2 U + \varkappa_t^2 \nabla_1^2 U - \lambda^4 U = 0, \tag{5.130}$$

where

$$\varkappa_t^2 = \frac{\sigma h}{D}; \quad \lambda^4 = \frac{\varrho h}{D} p^2. \tag{5.131}$$

The general solution of (5.130) is expressed in Bessel functions

$$U = C_1 J_n(\lambda_1 r) + C_2 Y_n(\lambda_1 r) + C_3 I_n(\lambda_2 r) + C_4 K_n(\lambda_2 r), \tag{5.132}$$

where

$$\lambda_1^2 = \frac{1}{2}\varkappa_t^2 + \sqrt{\frac{1}{4}\varkappa_t^4 + \lambda^4}; \tag{5.133}$$

$$\lambda_2^2 = -\frac{1}{2}\varkappa_t^2 + \sqrt{\frac{1}{4}\varkappa_t^4 + \lambda^4}. \tag{5.134}$$

When treating a plate without central hole, we set $C_2 = C_4 = 0$. The clamped outer contour conditions yield the equations

$$C_1 J_n(\lambda_1 R) + C_3 I_n(\lambda_2 R) = 0;$$
$$C_1 J_n'(\lambda_1 R) + C_3 I_n'(\lambda_2 R) = 0;$$

hence, we obtain the frequency equation for the plate

$$J_n(\lambda_1 R)\, I'_n(\lambda_2 R) - J'_n(\lambda_1 R)\, I_n(\lambda_2 R) = 0. \tag{5.135}$$

The roots λ of the frequency equation are the frequency coefficients; the frequency being found from the formula

$$p = \lambda^2 \sqrt{\frac{D}{\varrho h}}. \tag{5.136}$$

As usual, the coéfficients λ are related with the vibration mode, i.e., they depend on the number n of nodal diameters and the number s of nodal circles. In addition, they depend on the temperature rise Δt, which defines the coefficient x_t^2.

The frequency Equation (5.135) makes it possible to calculate the entire frequency spectrum of the plate in question for any value of Δt.

The calculation of the frequencies of the fundamental vibration modes, without nodal circles, is easily made using the Rayleigh formula

$$p^2 = \frac{\Pi_{max} + \Pi_N}{T^\bullet_{max}},$$

where $\Pi_{max}, \Pi_N, T^\bullet_{max}$ are found from the Formulas (5.113), (5.117), (5.121).

For umbrella vibrations, the function must be symmetric about the center of the plate.

The simplest function satisfying the conditions listed above is

$$U(r) = \left(1 - \frac{r^2}{R^2}\right)^2; \tag{5.137}$$

Although this function does not contain a minimizing parameter, the frequency determined using it differs from the exact value by only 1 - 2%.

The potential and kinetic energies calculated using (5.113) and (5.121) are

$$\Pi_{max} = \pi D \frac{32}{3R^2};$$

$$T_{max} = \pi p^2 \varrho h \frac{R^2}{10}.$$

The potential energy associated with the thermal stresses is calculated using (5.117). Because of the compressive stresses, it has a minus sign

$$\Pi_N = -\frac{2}{3} \pi h \sigma.$$

Equating the sum of the potential energies to the kinetic energy, we obtain the frequency formula

$$p = \sqrt{\frac{320}{3R^4} \frac{D}{\varrho h} - \frac{20}{3} \frac{\sigma}{\varrho R^2}}.$$ (5.138)

The first term of the radicand is the unheated plate frequency squared; the second term yields the correction for the influence of the thermal stresses.

Removing the fundamental frequency from the radical, we obtain

$$p = p_0 \sqrt{1 - \frac{\sigma h R^2}{16 D}},$$ (5.139)

where

$$p_0 = \frac{10.33}{R^2} \sqrt{\frac{D}{\varrho h}};$$

the elastic modulus E in the cylindrical stiffness D must be taken with account for the temperature.

Formula (5.139) shows that thermal stresses reduce the plate natural vibration frequency significantly. This effect is the stronger, the thinner the plate.

The frequency calculation may yield better results if we take as the initial function

$$U(r) = \left(1 - \frac{r^2}{R^2}\right)^2 \left[1 + \varepsilon\left(1 - \frac{r^2}{R^2}\right)\right]. \tag{5.140}$$

The minimizing parameter ε is selected so as to obtain the minimal value of the frequency for the given thermal stress. At the same time the vibration mode shape is refined.

The vibrations of a plate clamped in an elastic ring (Figure 5.17) are calculated using the same Formula (5.139). The thermal stresses in the plate, which are necessary for the calculation, can be found from the formula

$$\sigma\left[\frac{1-\nu}{E_1} + \frac{1}{E_2}\frac{Rh}{B\delta}\left(1 + \frac{\delta}{2R}\right)\right] = \alpha\Delta t^\circ, \tag{5.141}$$

where E_1, E_2 are the elastic moduli of the heated plate and the cold supporting ring, respectively.

5.8.2. Nonuniformly Heated Plate with Freely Supported Contour

If the supporting wall has small thickness δ, its action in restraining radial deformations of the plate is small. Therefore, we can examine the plate with freely supported edge (Figure 5.18). The plate is nonuniformly heated, the temperature rise being higher in the center and less along the edges. As a result of this, thermal stresses develop in the plate — compression in the central part and tension along the edges. This alters the plate natural vibration frequencies.

If the radial temperature distribution law is given, the stresses are calculated using the strength equations (see [12])

$$\sigma(r) = -E\alpha\Delta t_0^\circ f(r). \tag{5.142}$$

where Δt_0^o is the difference of the temperatures of the center and
edges of the plate;

$f(r)$ is the function of the radial and circumferential thermal
stresses in the free circular plate, which depends on
the temperature distribution law.

For the cubic temperature distribution law

$$\Delta t = \Delta t_0^o \left[1 - \left(\frac{r}{R} \right)^3 \right] \qquad (5.143)$$

we have

$$f_r(r) = \frac{1}{5} \left[1 - \left(\frac{r}{R} \right)^3 \right]; \quad f_t(r) = \frac{1}{5} \left[1 - 4 \left(\frac{r}{R} \right)^3 \right]. \qquad (5.144)$$

For the quadratic temperature distribution law

$$f_r(r) = \frac{1}{4} \left[1 - \left(\frac{r}{R} \right)^2 \right];$$
$$f_t(r) = \frac{1}{4} \left[1 - 3 \left(\frac{r}{R} \right)^2 \right]. \qquad (5.145)$$

The initial plate deflection function can be taken in the
form of the polynomial

$$U(r) = (1 + er^2)(1 + ar^2), \qquad (5.146)$$

which does not require satisfaction of the dynamic condition $M_R = 0$
at the outer contour. In accordance with the condition ($U_R = 0$) on
the contour, the coefficient a equals
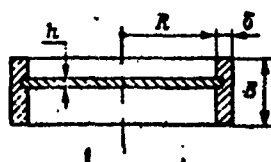
Figure 5.17. Diagram for
calculating vibrations of
a plate mounted in an
elastic ring.

$$a = -\frac{1}{R^2}.$$

The potential and kinetic energies
for the adopted initial function with
$n = 0$ are expressed by the formulas

$$\Pi_{max}=\pi D \frac{4}{R^2}\left[(1+v)(1+\imath R^2)^2+\frac{8}{3}\imath^2 R^4\right];\qquad (5.147)$$

$$T_{max}=\frac{\pi}{6}\varrho h R^2\left(1+\frac{1}{2}\imath R^2+\frac{1}{5}\imath^2 R^4\right). \qquad (5.148)$$

Equating these energies, we obtain the formula for calculating the unheated plate frequencies

$$p^2=\frac{24D}{R^4\varrho h}\,\frac{(1+v)(1+y)^2+\frac{8}{3}y^2}{1+\frac{1}{2}y+\frac{1}{5}y^2}, \qquad (5.149)$$

where $y = \varepsilon R^2$ is a parameter which is to be selected so that the minimal value of p^2 is obtained.

Taking the derivative of the fraction with respect to y and equating it to zero, we obtain an equation whose roots correspond to the minimal frequency values

$$y_1=-0{,}25;\ \ y_2=14{,}5;$$

The first root yields the coefficient for calculating the first vibration mode frequency, while the second root makes possible a rough estimate of the frequency of the second mode with a single nodal circle. Calculating the value of the fraction (5.149) for these roots, we obtain

$$p_1=\frac{4{,}92}{R^2}\sqrt{\frac{D}{\varrho h}};\quad p_2=\frac{20{,}4}{R^2}\sqrt{\frac{D}{\varrho h}}. \qquad (5.150)$$

To introduce the corrections for heating, we must calculate the middle surface deformation energy Π_N. This energy is calculated using (5.117) in accordance with the thermal stress distribution law. Its calculation for the cubic law leads to the formula

$$\Pi_N=-\pi\frac{4}{5}hE\alpha\Delta t_0^{\circ}\left[\frac{3}{28}(\imath R^2-1)^2-\frac{2}{9}(\imath R^2-1)\imath R^2+\frac{3}{22}\imath^2 R^4\right], \qquad (5.151)$$

where Δt_0° is the temperature difference between the center and contour of the plate.
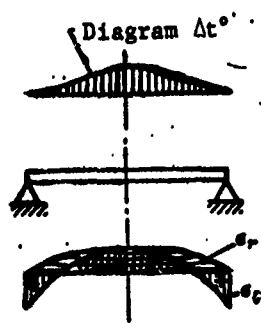
Figure 5.18. Diagram for calculating vibrations of nonuniformly heated plate.

Writing the equation

$$T_{max} = \Pi_{max} + \mathfrak{I}_N$$

and substituting therein (5.147), (5.148) and (5.151), we obtain the frequency formula

$$p^2 = \frac{24D}{R^4 \varrho h} f_1(y) - \frac{24}{5} \frac{E\alpha\Delta t_0^\circ}{R^2 \varrho} f_2(y), \qquad (5.152)$$

where

$$f_1(y) = \frac{(1+\nu)(1+y)^2 + \frac{8}{3} y^2}{1 + \frac{1}{2} y + \frac{1}{5} y^2};$$

$$f_2(y) = \frac{\frac{3}{28}(1-y)^2 + \frac{2}{9}(1-y)y + \frac{3}{22} y^2}{1 + \frac{1}{2} y + \frac{1}{5} y^2}.$$

Here we must again determine the parameter $\varepsilon R^2 = y$, which yields the minimal value of the frequency; this parameter will be a function of Δt_0°.

In view of the fact that in the extremum region the function changes only slightly with variation of ε, we shall use the parameters calculated previously for the estimate of the influence of heating nonuniformity on the frequency.

Calculating $f_1(y)$ and $f_2(y)$ for $y_1 = -0.25$, we obtain

$$p^2 = \frac{24,3D}{R^4 \varrho h} - 0,58 \frac{E\alpha\Delta t_0^\circ}{R^2 \varrho};$$

The first term is the unheated plate frequency squared, and the second term yields the correction for heating nonuniformity. The formula can finally be written in the form

$$p = p_0 \sqrt{1 - 2,4 \frac{EhR^2}{D} \alpha\Delta t_0^\circ 10^-} \qquad (5.153)$$

where

$$p_0 = \frac{4.92}{R^2} \sqrt{\frac{D}{\varrho h}}.$$

Figure 5.19 shows the plate vibration frequency as a function of the degree of temperature differential of its central part.
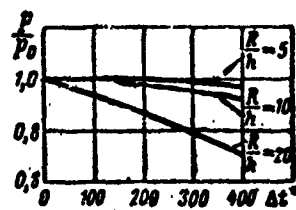
Figure 5.19. Effect of non-uniform heating on vibration frequency of freely supported plate.

Heating nonuniformity has a particularly large effect on the vibrations of relatively thin freely supported plates.

5.8.3. Fan-Wise Vibrations of Nonuniformly Heated Disk With Rigid Blades

It is well known that turbine disks operate with nonuniform heating. The peripheral part of the disk has a temperature which is several hundred degrees higher than the central part. This leads to significant reduction of the natural vibration frequency.

Particularly large temperature gradients arise during the startup period of the engine or turbomachine. A temporary transient frequency reduction appears, which reaches a large magnitude at certain moments. This phenomenon creates special conditons during starting, which are discussed below.

We shall assume that the disk temperature varies in accordance with a power law along the radius

$$\Delta t^\circ = \Delta t_0^\circ \left(\frac{r}{R} \right)^s, \tag{5.154}$$

where Δt_0° is the temperature difference between the periphery and center of the disk.

The stresses in the disk are found from the formula

$$\sigma = Ea\Delta f_0 f(r),\qquad (5.155)$$

where $f(r)$ are the distribution functions of σ_r and σ_θ, which are found using (5.144) and (5.145) as a function of the exponent s.

We take the initial function for fan-wise vibrations in the form

$$U(r) = \bar{\varrho}^2(1 + \varepsilon\bar{\varrho}^2),\qquad (5.156)$$

where

$$\bar{\varrho} = \frac{r}{R}.$$

We calculate the potential and kinetic energy functions for $n = 2$. In so doing we consider the relations

$$\frac{dU}{dr} = \frac{dU}{d\bar{\varrho}} \cdot \frac{d\bar{\varrho}}{dr} = \frac{1}{R} \cdot \frac{dU}{d\bar{\varrho}} \quad \text{etc.}$$

In accordance with (5.112), for the adopted deflection function we obtain

$$\Pi_{max} = \frac{\pi}{2} \frac{D}{R^2}\left[24\varepsilon^2 + 8(1-\nu)\left(1 + 3\varepsilon + \frac{3}{2}\varepsilon^2\right)\right].\qquad (5.157)$$

The potential energy of the midplane deformation resulting from differential heating is defined by (5.116)

$$\Pi_N = \frac{\pi}{2} h \int_0^1 \left[\sigma_\varrho\left(\frac{dU}{d\bar{\varrho}}\right)^2 + \sigma_\theta \frac{n^2}{\bar{\varrho}^2} U\right]\bar{\varrho}\,d\bar{\varrho};$$

We find the thermal stresses from the formulas

$$\sigma_\varrho = \frac{1}{5}Ea\Delta f_0(1 - \bar{\varrho}^2) \quad \text{and} \quad \sigma_\theta = \frac{1}{5}Ea\Delta f_0(1 - 4\bar{\varrho}^2).$$

319

Substitution of these formulas into the expression for Π_N, followed by integration and substitution of the limits, yields

$$\Pi_N = -\frac{\pi}{2} hEa\Delta f_0^2 \frac{4}{5}\left(\frac{6}{28} + \frac{1}{3}\epsilon + \frac{9}{11}\epsilon^2\right). \tag{5.158}$$

The disk kinetic energy is calculated from (5.120)

$$T_{max} = \frac{\pi}{2}\varrho hR^2 p^2 \int_0^1 [\bar\varrho^2(1 + \epsilon\bar\varrho^2)]^2 \bar\varrho\, d\bar\varrho;$$

after integration we obtain

$$T_{max} = \frac{\pi}{2}\varrho hR^2 p^2\left(\frac{1}{6} + \frac{\epsilon}{4} + \frac{\epsilon^2}{10}\right). \tag{5.159}$$

The kinetic energy of the rigid blades is defined by the deformation of the disk outer contour using the formula

$$T = \frac{\pi}{2}\frac{R}{\ell} p^2 \int_0^\ell m(x)\left[U_{\varrho=1} + \frac{x}{R}\left(\frac{dU}{d\bar\varrho}\right)_{\bar\varrho=1}\right]^2 dx; \tag{5.160}$$

We neglect rotation of the blade about the longitudinal axis. $m(x)$ is the mass per unit length of the blade, which for the linear area distribution law is expressed by the formula

$$m(x) = m_0\left(1 - c\frac{x}{\ell}\right). \tag{5.161}$$

where m_0 is the mass at the root section;

   c is the taper ratio.

Substituting into (5.160)

$$U_{\varrho=1} = 1 + \epsilon; \quad \frac{dU}{d\bar\varrho} = 2 + 4\epsilon,$$

we obtain the expression for the kinetic energy of all the blades (c = 0.5)

$$T = \frac{\pi}{2}\frac{R}{\ell} m_0\ell p^2\left[\frac{3}{4}(1 + \epsilon)^2 + \frac{2}{3}(1 + \epsilon)(1 + 2\epsilon)\frac{\ell}{R} + (1 + 2\epsilon)^2\frac{\ell^2}{R^2}\right]. \tag{5.162}$$

For convenience of the further calculations we express the blade mass in terms of the disk mass

$$M_{\pi} = kM_{\pi},\qquad(5.163)$$

where k is the weight ratio coefficient

$$m_0 l \,\frac{2\pi R}{t} = k\varrho\pi R^2 h;$$

In this connection the coefficient multiplying the bracketed quantity in (5.162) alters its form

$$T = \frac{\pi}{2}\,\frac{k}{2}\varrho R^2 h p^2 \left[\frac{3}{4}(1+\epsilon)^2 + \frac{2}{3}(1+\epsilon)(1+2\epsilon)\frac{l}{R} + (1+2\epsilon)^2\frac{l^2}{R^2} \right].\qquad(5.164)$$

We write the equation

$$\Pi_{max} + \Pi_N = T_{max} + T;$$

after substituting herein (5.157), (5.158), (5.159), (5.164), we obtain the formula

$$p^2 = \frac{D}{R^4\varrho h}\,\frac{S_R(\epsilon) - x_t^2 S_1(\epsilon)}{S_T(\epsilon) + kS_2(\epsilon)},\qquad(5.165)$$

in which

$$x_t^2 = \frac{Ea\Delta t_0^2 hR^2}{D} = 12(1-\nu^2)a\Delta t_0 \frac{R^2}{h^2};$$
$$S_R(\epsilon) = 5{,}6 + 16{,}8\epsilon + 32{,}4\epsilon^2;$$
$$S_1(\epsilon) = 0{,}172 + 0{,}267\epsilon + 0{,}653\epsilon^2;\qquad(5.166)$$
$$S_T(\epsilon) = 0{,}167 + 0{,}25\epsilon + 0{,}1\epsilon^2;$$
$$S_2(\epsilon) = \frac{3}{8}(1+\epsilon)^2 + \frac{1}{3}(1+\epsilon)(1+2\epsilon)\frac{l}{R} + (1+2\epsilon)^2\frac{l^2}{R^2}.$$

In (5.165) the parameter ϵ is to be selected so that p^2 will have the minimal value for the given conditions.

Disk without blades and without heating. In this case ($k = 0$;
$\kappa_t = 0$) the vibration frequency is defined by the formula

$$p^2 = \frac{D}{R^4\rho h} \; \frac{5.6 + 16.8\epsilon + 32.4\epsilon^2}{0.167 + 0.25\epsilon + 0.1\epsilon^2} \; . \qquad (5.167)$$

Finding the extremum of the fraction, we see that the minimal
frequency corresponds to

$$\epsilon = -0.164.$$

This root yields the frequency coeffic.ent for the first vibration
mode. Using this root to calculate the fraction (5.167), we obtain

$$p^2 = 28.8 \frac{D}{R^4\rho h} \quad \text{or} \quad p = \frac{5.36}{R^2} \sqrt{\frac{D}{\rho h}} \; . \qquad (5.168)$$

Disk with blades without heating. In this case the vibration
frequency depends on the blade mass and is defined by the formula

$$p^2 = \frac{D}{R^4\rho h} \; \frac{S_\pi(\epsilon)}{S_T(\epsilon) + k S_2(\epsilon)} \; . \qquad (5.169)$$

The fraction on the right is the frequency coefficient squared
$(\alpha^2)^2$. It depends on the number of blades and their dimensions.
Selecting the minimizing coefficient ϵ, we calculate α^2 for several
values of k and l/R (Figure 5.20). The resulting curves make it
possible to calculate the natural vibration frequencies of disks with
blades for different blade dimensional relationships using the
formula

$$p = \frac{\alpha^2}{R^2} \sqrt{\frac{D}{\rho h}} \; . \qquad (5.170)$$

It is obvious that the presence of blades on the disk reduces
the disk natural vibration frequencies significantly. Even compara-
tively small blades, whose weight amounts to 25% of the disk weight,
reduce the vibration frequency by 30 - 40%.

The nonuniformly heated disk with blades is calculated using the complete Formula (5.165). Selection of the parameter ϵ and calculation of the frequency coefficients leads to the formula

$$p_i^2 = \frac{D}{\rho h R^4}(\alpha^4 - \varkappa_i^2 \alpha_i^2),$$ (5.171)

where α^2 and α_t^2 are taken from the curves shown in Figures 5.20 and 5.21 as a function of the blade dimensions.

The ratio of the frequencies of the heated and unheated disks is

$$\frac{\bar{p}_i}{p} = \sqrt{\frac{\alpha^4 - \varkappa_i^2 \alpha_i^2}{\alpha^4}} = \sqrt{1 - \varkappa_i^2 \frac{\alpha_i^2}{\alpha^4}} \cdots$$ (5.172)

The ratio of the coefficients α_t^2/α^4 lies in a narrow range

$$\frac{\alpha_i^2}{\alpha^4} = 0{,}036 \div 0{,}039;$$

Therefore, the approximate estimate of the vibration frequency reduction owing to heating nonuniformity can be made using the formula

$$\frac{p_i}{p} = \sqrt{1 - 0{,}038 \varkappa_i^2},$$ (5.173)

where $\varkappa_t^2$ is calculated from (5.166) and depends on the temperature difference Δt_0° and on the disk dimensional relationship.

The thinner the disk, the larger its frequency reduction (for the same heating nonuniformity). The frequency reduction may reach 20 - 25%.

The temperature effect is increased if the disk has a rim with large temperature gradient at the point where the rim transitions into the disk.

If the disk temperature changes during operation, there will
be a corresponding change of its natural vibration frequency.

5.8.4. Change of Disk Critical Speed Resulting From Nonuniform
Heating

The critical speed change in the case of nonuniform disk heat-
ing is proportional to the frequency change

$$\omega_{\kappa p\,i}=\omega_{\kappa p}\sqrt{1-x_i^2\frac{a^2_i}{a^4}}.$$
(5.174)

This phenomenon creates dangerous conditions during startup
if the gas turbine engine or turbomachine is accelerated to maximal
speed immediately after starting, without warmup at low speed.
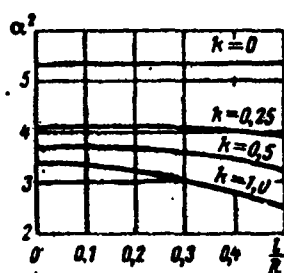
Figure 5.20. Effect of blade
dimensions on disk vibration
frequency.
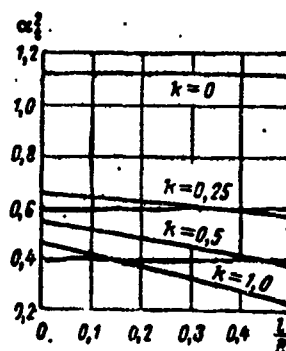
Figure 5.21. Coefficient of
influence of heating nonuni-
formity on vibration frequency
of disk with blades.

In this case the temperature rise of the blades and outer part
of the wheel is very rapid, while the central part heats up more
slowly (Figure 5.22). The temperature rise of the central part of
the disk is delayed because of intense heat removal into the shaft
and bearings.

As a result of the different heating rate of the peripheral
and central parts of the wheel, large temperature differences develop
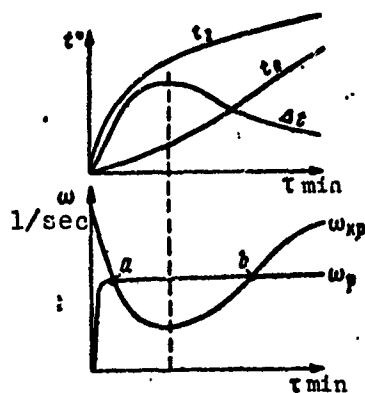
Figure 5.22. Effect of disk heating-up process on its resonant states: t_0 and t_2 are the temperatures of the center and blade part of the disk, respectively; Δt is the temperature difference; ω_r is the rotor speed; ω_{cr} is the critical speed of the nonuniformly heated disk.

in the disk which leads to marked reduction of its critical speeds. If the rotor has a small critical speed margin, then at certain times (a and b) the critical speed becomes equal to the rotational speed and the resonant state develops. In this case serious rotor and blade damage may arise as a result of the large amplitudes of the vibrations and stresses.

We note that fan-wise vibrations of the rotor are dynamically balanced. Therefore, even with large amplitudes of the vibrations they are not transmitted to the case and cannot be sensed from the case vibrations.

Nor can wheel vibrations at the critical rotational speed be detected with the aid of a sensor located on the case and measuring the clearance between the sensor and the wheel rim. As a result of the fact that the vibrations at the critical speed occur in the form of the so-called standing wave, the distance between the sensor and the wheel rim remains constant all the time, and in any case its change will not characterize the amplitude of the vibrations of the resonating critical speed mode. Strain gages must be mounted directly on the wheel itself in order to measure the rotor vibrations.

Critical speed margins of 1.5 - 2 must be provided in order to eliminate the possibility of the occurrence of these resonant states.

5.9. Damping of Plate and Disk Vibrations By Damping Coatings

The internal inelastic resistance of the usual constructional

materials — steels, aluminum, titan., and other alloys — is small.
Therefore, large vibration amplitudes develop at resonance, which
lead to the appearance of various defects. Increase of the internal
resistance of the material without significant deterioration of its
mechanical qualities is not possible. Therefore, wherever possible
it is advisable to use multilayer plates and disks, in which the
structural loads are taken by layers consisting of strong construc-
tional materials and damping is provided by layers made from materials
with a large absorption coefficient.

It is advantageous to make the damping layers the outer layers,
where the bending deformations are largest, and therefore the largest
energy absorption and the best damping effect will be observed.

Thus, from the viewpoint of improving damping and efficient
construction is the sandwich arrangement in which the center layer
is the structural layer, which accepts the radial and axial bending
loads, and the outer layers are the damping layers.

As was shown in Section 1.5, the energy absorbed by a material
during a vibration period is proportic i to the deformation potential
energy. Therefore, the total energy abs .oed by the sandwich plate
during a period is equal to the sum

$$L_R = \psi_0 \Pi_0 + \psi_s \Pi_s.$$

(5.175)

where ψ_0, ψ_s are the absorption coefficients for the materials of
the center (metal) layer and the coatings, respectively;

Π_0, Π_s are the deformation potential energies of the same parts
of the plate.

If we assume that the deformations are distributed linearly
through the plate thickness (Figure 5.23a), the potential energies of
the center and outer layers can be calculated using the same general
Formula (5.112). The energies will differ from one another because
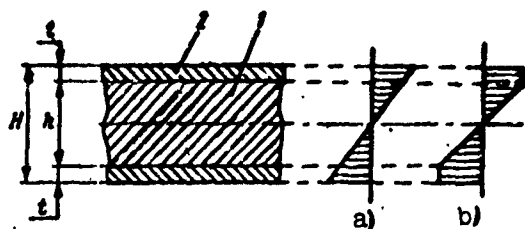
Figure 5.23. Stress distribution through thickness of coated plate: 1 - basic plate; 2 - coating.

of the difference in the cylindrical stiffnesses. The cylindrical stiffness for the center layer is found from (5.109), while that for the outer layers is calculated from the formula

$$D_s = \frac{E_s(H^3 - h^3)}{12(1 - v_s^2)}. \qquad (5.176)$$

The ratio of the energies dissipated in the outer damping layers and in the central layer is defined by the formula

$$\frac{L_s}{L_0} = \frac{\psi_s \Pi_s}{\psi_0 \Pi_0} = \frac{\psi_s D_s}{\psi_0 D_0} = \frac{\psi_s}{\psi_0} \frac{E_s}{E} \frac{H^3 - h^3}{h^3} \frac{1 - v^2}{1 - v_s^2}. \qquad (5.177)$$

This formula shows that to obtain large damping of the plate vibrations materials must be selected for the outer layers which have the largest product $\psi_s \Pi_s$ — the product of the absorption coefficient by the elastic modulus. Such materials are the fiberglasses, which in addition to the noted properties also have other important qualities — good ability to bond with the metals, ability to operate at temperatures up to 250° C, and long-term retention of the damping properties.
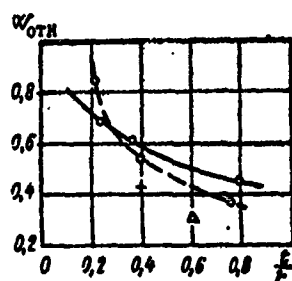
Figure 5.24. Effect of coating thickness on vibration damping: —— glass fiber T and epoxy resin; - - - glass fiber and polyester resin; + __KAST-V , Δ — nonwoven material — and phenol formaldehyde resin.

The properties of some materials are presented in Table 5.5 (see [32] and [14]). The data shown in this table indicate that the glass reinforced plastics have better damping qualities than the metals. However, they do not have high strength and stiffness and therefore cannot be used as independent structural elements of the structure. The combination of glass reinforced plastics with

TABLE 5.5

Material	ψ	$E \cdot 10^{-11}$ N/m^2	$\psi E \cdot 10^{-11}$	Remarks
Steel 3	0.01 - 0.03	2.1	0.021 - 0.063	ϵ up to 10^{-3}
Aluminum	0.03 - 0.044	0.58	0.017 - 0.026	ϵ up to 10^{-3}
High-temperature steel E1437B	0.01	-	-	σ up to $15 \cdot 10^7$ N/m^2
Cold drawn copper	0.01	1.0	0.01	-
Cast molybdenum	0.014	3.46	0.048	-
Cast tungsten	0.033	3.86	0.127	-
Epoxy fiberglass*	0.2	0.15	0.03	ϵ up to $5 \cdot 10^{-3}$.
Polyester fiberglass*	1.0	0.15	0.15	ϵ up to $5 \cdot 10^{-3}$
LKF1 plastic	0.46	-	-	σ more than $0.5 \cdot 10^7$ N/m^2
VFT-S fiberglass	0.2	-	-	σ more than $0.2 \cdot 10^7$ N/m^2

*V. M. Chernyshev, Transactions of NAMI (Central Scientific Research Institute of Automobiles and Automobile Engines), No. 49, 1962.

metals or the use of polymer coatings yield a stiff and strong structure which has good damping qualities.

Formula (5.177) yields a somewhat high estimate of the potential energy of the outer layers; and therefore a somewhat high estimate of the energy absorbed in these layers.

It would be more correct to take the deformation distribution across the thickness of the plate as shown in scheme b (see Figure 5.23).

Then the following expression should be used for the cylindrical stiffness in (5.177)

$$D_s = \frac{E_s (H - h)^3}{4(1 - v_s^2)}.$$ \hfill (5.178)

Figure 5.24 shows results of experiments with the use of glass reinforced plastics to damp circular steel plates. The excitation force: were the same in all the experiments, but the vibration amplitudes decreased sharply with increase of the thickness of the coatings. For an outer layer thickness $t/h = 0.8$, the vibration amplitude amounts to only 40% of the vibration amplitude for the undamped plate.

CHAPTER 6

CALCULATION OF VIBRATIONS OF COMPLEX COMPOSITE SYSTEMS

The structures of aircraft gas turbine engines, turbopump units, and their components consist of a large number of lightweight parts of various configurations. With regard to vibrations they form a complex elastic system having a large number of vibration natural frequencies and modes. Any components and systems can serve as examples: turbomachine casing-rotor, turbo-unit and its supply plumbing, the rotor system consisting of shaft, disks, and blades; the engine and propeller; heat exchangers, and so on.

The individual parts of the structures are usually vibration analyzed as isolated elements. To this end the element being analyzed is isolated from the overall system and its connections with the rest of the system are replaced by definite restraint conditions, formulated in the form of boundary conditions. Most often these connections are taken in the form of rigid restraints — clamped ends or hinges. Sometimes these restraints are considered elastic, having constant stiffnesses which are independent of the frequency.

This computational approach is justified for many typical problems. It permits considerable simplification of the problem and

makes it possible to identify the characteristic element parameters which affect its vibrations.

However, this approach makes it impossible to obtain any idea of the vibration characteristics of the individual elements in the system, which in many cases are very significant, and also excludes the possibility of studying the properties of the entire system.

First of all, we note that the individual elements in the system or parts of the system do not have their own natural vibration frequencies. The complete natural frequency spectrum and associated vibration modes, and also the stress distribution in the element an only be obtained by examining the system as a unified whole.

The interaction of the elements in the system depends on the vibration frequency. Therefore, analysis of the elements as isolated parts is justified only within the limits of the definite frequency range, to which the boundary conditions selected for the calculation correspond.

Certain natural vibration frequencies found by analysis for the isolated elements may be close in magnitude to certain natural frequencies of the entire system. This circumstance will confirm the correctness of the choice of the analytic scheme and the boundary conditions for the given isolated element, and will also show the frequencies for which analysis of the isolated element yields satisfactory results in comparison with the complete analysis of the entire system.

When we speak of forced vibrations and resonances, we must bear in mind that resonant vibrations of the individual elements show up as a result of resonance of the entire system. Isolated resonances of the individual parts of the system do not exist.

One of the most effective methods for vibration analysis of complex systems is the dynamic stiffness method. The dynamic compliance method is of the same type.

These methods are being developed at the present time in connection with the use of electronic computers, which broadens their capabilities considerably.

6.1. Concepts of Dynamic Stiffness Coefficients

The dynamic stiffness method is based on use of dynamic stiffness coefficients and formulation from these coefficients of the dynamic equilibrium and frequency equations. The dynamic stiffness concept is associated with forced vibrations.

As is known, if an elastic system is subjected at some point to a harmonically varying force

$$Q = X \cos pt,$$

the system performs forced harmonic vibrations following the same law

$$q = B \cos pt.$$

The ratio of the harmonic force to the displacement of a point of the system caused by this force in the direction of action of the force is called the dynamic stiffness coefficient

$$K = \frac{Q}{q} = \frac{X}{B}; \qquad (6.1)$$

Since the forced vibration function is identical to the disturbing force function, the dynamic stiffness coefficient is defined as the ratio of the disturbing force amplitude to the forced vibration amplitude.

The system dynamic stiffness coefficient depends on the system properties, point of application of the force, and disturbing force frequency.

We shall define this coefficient for some elementary cases. A free solid body performs harmonic vibrations under the action of a harmonic force. For a point mass m (Figure 6.1a) the differential equation of motion will be

$$m\ddot{q} = X \cos pt;$$ (6.2)

its solution is

$$q = -\frac{X}{mp^2} \cos pt,$$ (6.3)

Hence, the dynamic stiffness coefficient is

$$K = \frac{Q}{q} = -mp^2.$$ (6.4)

Analogous expressions for the dynamic stiffness coefficient are obtained for the free disk (see Figure 6.1,b) under the action of a harmonic moment, and for the ideally rigid bar (see Figure 6.1c) under the action of a moment about the hinge

$$K = \frac{M}{\varphi} = -Jp^2.$$ (6.5)

The dynamic stiffness coefficient of a weightless cantilever bar with point mass m attached to its end (see Figure 6.1,d) is equal to the sum of the static stiffness coefficients of the bar and the dynamic stiffness coefficient of the mass

$$K = c - mp^2.$$ (6.6)

The condition K = 0 corresponds to natural vibrations of the bar. Equation (6.6) yields the value of the natural vibration frequency

$$k^2 = \frac{c}{m}.$$

With the aid of the natural vibration frequency, the dynamic stiffness Formula (6.6) can be written in the form
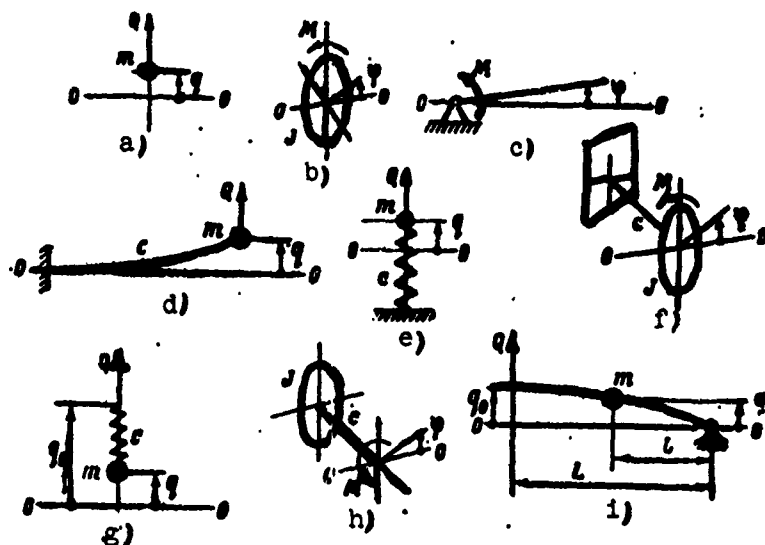
Figure 6.1. Elementary schemes for determining dynamic stiffness coefficients.

$$K = c(1 - \bar{p}^2),$$ (6.7)

where

$$\bar{p}^2 = \frac{p^2}{\lambda^2}.$$

Analogous expressions are obtained for the systems shown in Figure 6.1, e and f.

In certain problems, systems are encountered in which the harmonic force is applied to an elastic element (see, for example, Figure 6.1g, h, i).

Let us find the dynamic stiffness coefficient for the scheme shown in Figure 6.1,g. The differential equation of forced vibrations for the system will be

$$m\ddot{q} - c(q_0 - q) = 0; \tag{6.8}$$

while

$$c(q_0 - q) = X \cos pt. \tag{6.9}$$

Therefore

$$m\ddot{q} = X \cos pt;$$

hence

$$q = -\frac{X}{mp^2} \cos pt. \tag{6.10}$$

Substitution of (6.9) yields

$$q_0 = \left(\frac{X}{c} - \frac{X}{mp^2}\right) \cos pt;$$

taking the ratio Q/q_0, we obtain the dynamic stiffness coefficient

$$K = -\frac{cmp^2}{c - mp^2}. \tag{6.11}$$

We denote the natural vibration frequency of the system in question with the zero section fixed

$$k_0 = \frac{c}{m}.$$

Then the formula for the dynamic stiffness coefficient takes the form

$$K = -mp^2 \frac{1}{1 - \bar{p}_0^2}, \tag{6.12}$$

where

$$\bar{p}_0^2 = \frac{p^2}{k_0^2}.$$

For the arrangement shown in Figure 6.1,h, the moment of inertia J is substituted in place of m in the dynamic stiffness formula.

For the arrangement shown in Figure 6.1,i, a factor associated with the position of the mass on the bar appears in the formula

$$K = -mp^2 - \frac{1}{1-\bar{p}_*^2}\left(\frac{l}{L}\right)^2; \quad \cdot \tag{6.13}$$

to calculate the natural frequency p_* the left end of the bar must be restrained on a hinged support.

In practical problems, systems are encountered on which there act simultaneously several force factors of the same frequency — long'tudinal or transverse forces, bending and twisting moments, and so on.

Figure 6.2 shows as an example the rotor of a turbomachine. The harmonic forces of the interaction with the case are applied to the rotor support journals. The forces are connected with the displacements in the direction of action of the forces by the canonical equations. These equations are written in the following form for the force and displacement amplitudes

$$\left.\begin{array}{l} X_1 = K_{11}Y_1 + K_{12}Y_2 + K_{13}Y_3; \\ X_2 = K_{21}Y_1 + K_{22}Y_2 + K_{23}Y_3; \\ X_3 = K_{31}Y_1 + K_{32}Y_2 + K_{33}Y_3. \end{array}\right\} \tag{6.14}$$

The canonical equations are analogous to the canonical equations used in the displacement method in elasticity theory.

The number of equations in the system and the number of terms in the right side of each equation is equal to the number of forces acting on the system. The dynamic stiffness coefficients K_{is} are the basis for all the equations. The first subscript in the coefficient notation shows the force number, the second indicates the direction

of the unit displacement with which the given dynamic stiffness coefficient is connected. All the coefficients are functions of the frequency.

The method for determining the dynamic stiffness coefficients follows from (6.14). We impose on the system additional constraints, so that the displacements in the directions of action of all the forces other than the first will be equal to zero: $Y_2 = 0$; $Y_3 = 0$. Then the harmonic force with respect to the first direction with amplitude X_1 yields vibrations only with respect to the first direction with the amplitude Y_1. Harmonic reactions with the amplitudes X_2 and X_3 arise from the additional constraints.

The dynamic stiffness coefficients will be the ratios

$$K_{11} = \frac{X_1}{Y_1}; \ K_{21} = \frac{X_2}{Y_1}; \ K_{31} = \frac{X_3}{Y_1}. \tag{6.15}$$

If the direction 2 is left free, we obtain the coefficients K_{12}, K_{22}, K_{32}, and so on.

The dynamic stiffness coefficients for which both subscripts are the same are termed proper, since they represent the ratio of the force to the displacement in the proper direction.

The coefficients for which the two subscripts are different are termed improper and represent the reactions of the additional constraints. The improper coefficients possess the reciprocity property

$$K_{is} = K_{si}. \tag{6.16}$$

The determination of the dynamic stiffness coefficients is made on the basis of the problem of forced vibrations of the given system under the influence of all the forces applied to it.
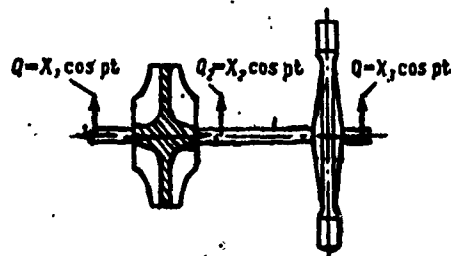
Figure 6.2. Determining rotor dynamic
stiffness.

6.2. Singly-Connected Systems

Singly-connected systems are those which can be cut into two
parts, replacing the action of the discarded part by only a single
force factor — shearing force, bending moment, torsional moment, or
longitudinal force.

In order to perform this division, it is sufficient that the
system have at least one section satisfying the single-connectedness
condition. The two component parts obtained after dividing the
system may no longer by singly connected.

If a system has several sections of singly-connected interaction,
its division into two systems can be accomplished along any of these
sections, depending on which path yields the simplest solution of
the problem.

In the majority of systems performing torsional or longitudinal
vibrations, any section satisfies the single-connectedness condition.
For such systems the choice of the place to divide the system is
determined by the technique used to solve the problem.

The singly-connected systems are among the simplest cases of vibration problems; nevertheless, their solution by conventional methods is not always simple. The dynamic stiffness method yields the most easily visualized solution and analysis of the singly-connected systems.

6.2.1. Cantilever Bar With Mass at End

In this problem we examine the vibrations of a bar with account for its own mass.

Let us first examine the cantilever bar of constant section (Figure 6.3). The bar mass per unit length is m; the concentrated mass is m_k.
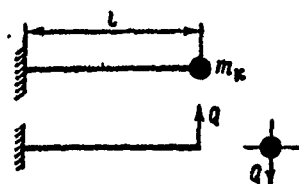
Figure 6.3. Partition of beam into two parts in order to use the dynamic stiffness method.

We cut the system into two parts, applying at the cuts the internal interaction forces Q. In the case of harmonic vibrations Q varies harmonically

$$Q = X \cos pt.$$

Let us examine the forced vibrations of each of the parts under the influence of the forces Q and find the dynamic stiffness coefficients for these parts.

For the cantilever bar this dependence is obtained on the basis of the general solution

$$y = [C_1 S(k\xi) + C_2 T(k\xi) + C_3 U(k\xi) + C_4 V(k\xi)] \cos pt. \qquad (6 \cdot 17)$$

The boundary conditions for the forced vibrations are

$$\xi = 0; \ y = y' = 0, \text{ hence } C_1 = C_2 = 0;$$
$$\xi = 1; \ y'' = 0; \ -EJ\left(\frac{d^3 y}{dx^3}\right)_{x=l} = Q.$$

The last two equalities yield the equations

$$C_3 S(k) + C_4 T(k) = 0;$$
$$-\frac{EI}{l^3} k^3 [C_3 V(k) + C_4 S(k)] = X,$$ (6.18)

Thus, we find C_3 and C_4, after which substitution into (6.17) yields the bar vibration amplitude function, connected with the exciting force amplitude X

$$Y(\xi) = X \frac{l^3}{EI k^3} \left[\frac{T(k)}{\Delta(k)} U(k\xi) - \frac{S(k)}{\Delta(k)} V(k\xi) \right],$$ (6.19)

where

$$\Delta(k) = S^2(k) - T(k) V(k);$$ (6.20)

The deflection of the bar end is

$$Y(1) = X \frac{l^3}{EI k^3} \frac{T(k) U(k) - S(k) V(k)}{\Delta(k)}.$$

Taking the ratio of the exciting force amplitude to the vibration amplitude of the bar end, where this force is applied, we obtain the dynamic stiffness coefficient

$$K = \frac{X}{Y};$$ (6.21)

In the case in question it equals

$$K = \frac{EI}{l^3} k^3 \frac{\Delta(k)}{T(k) U(k) - S(k) V(k)}.$$ (6.22)

The parameter k is connected with the vibration frequency p by the known formula

$$k^4 = \frac{m p^2}{EI} l^4.$$

The dependence of the dynamic stiffness coefficient K on the frequency is shown in Figure 6.4.
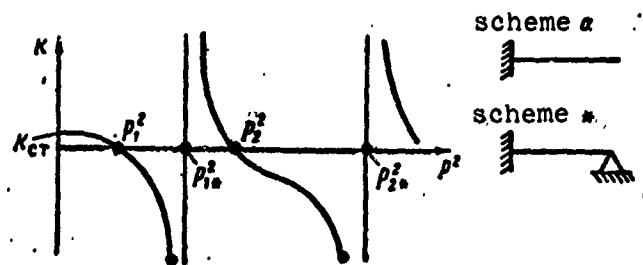
Figure 6.4. Cantilever dynamic stiffness
coefficient in direction of force Q.

The numerator $\Delta(k)$ of the fraction (6.22) vanishes for frequencies equal to the natural vibration frequencies of the cantilever bar (see scheme a in Figure 6.4). At these frequencies K equals zero.

The denominator of the fraction (6.22) vanishes at frequencies equal to the natural vibration requencies of the cantilever bar with additional constraint in the X direction (see scheme * in Figure 6.4). At these frequencies K increases without bound.

For $p = k = 0$ the dynamic stiffness coefficient becomes equal to the static stiffness coefficient

$$K(0) = K_{cr} = \frac{3EJ}{l^3}.$$

Transition to this expression from (6.22) can be accomplished by expanding the numerator and denominator into expressions consisting of trigonometric and hyperbolic functions and applying the l'Hopital rule

$$\lim_{k \to 0} \frac{k^3 \Delta(k)}{T(k)U(k) - S(k)V(k)} = 3,$$

Omitting the proof, we note that (6.22) can be reduced to the form:

$$K(p^2) = K_{cr} \frac{\left(1 - \frac{p^2}{p_1^2}\right)\left(1 - \frac{p^2}{p_2^2}\right)\left(1 - \frac{p^2}{p_3^2}\right) \cdots}{\left(1 - \frac{p^2}{p_{1*}^2}\right)\left(1 - \frac{p^2}{p_{2*}^2}\right)\left(1 - \frac{p^2}{p_{3*}^2}\right) \cdots},$$ (6.23)

where p_1, p_2 are the roots of the expression in the numerator of (6.23); in the present case they are the natural vibration frequencies of the free cantilever bar (scheme a in Figure 6.4);

p_{1*}, p_{2*} are the roots of the denominator — the natural vibration frequencies of the cantilever bar with additional constraint in the direction of action of the force (scheme * in Figure 6.4).

All the frequencies are found using the general formula

$$p^2 = \frac{k^4}{l^4} \cdot \frac{EI}{m},$$

where the natural vibration frequency coefficient k is taken in accordance with the particular scheme.

The structure of (6.23) is common for any linear elastic system. It is convenient in that it expresses the dependence of the dynamic stiffness coefficient on the vibration frequency with the aid of the natural vibration frequencies ⌐f the free system (type a) and with an imposed constraint (type *).

The number of factors which must be taken in the numerator and denominator of (6.23) depends on the range of frequencies within the limits of which it is necessary to construct the bar dynamic stiffness function and the computational accuracy required. If we restrict ourselves to three factors in the numerator and the same number in the denominator, the computational error will not exceed 2% for the first and second natural vibration frequencies.

We take the dynamic stiffness coefficient for the free mass in accordance with (6.4)

$$K_m(p^2) = -m_k p^2.$$

Since the forces X applied to the cutoff parts are internal, their sum equals zero. This is equivalent to a zero value of the sum of the dynamic stiffness coefficients

$$K + K_m = 0. \qquad (6.24)$$

This is the frequency equation of the dynamic stiffness method for singly-connected systems. The roots of the equation are the natural vibration frequencies of a bar with a mass at the end. The equation can be solved analytically or graphically. In the latter case (Figure 6.5), the roots of the equation will be the points of intersection of the dynamic stiffness curve of the left part of the system with the dynamic stiffness curve of the right part of the system — the point mass taken with reversed sign.

The graphical form of solution with the aid of the dynamic stiffness coefficients is very easily visualized. It is easy to determine the influence of a particular parameter from this presentation. For exmple, drawing straight lines for different magnitudes of the attached mass m_k, we see that the frequency of the first vibration mode decreases significantly with increase of the mass m_k. A similar change but in lesser degree takes place with the frequency of the second vibration mode. The frequencies of the higher natural vibration modes are close (slightly higher) to the frequencies of the bar with rigid support (scheme * in Figure 6.4). Change of the mass m_k has little effect on these frequencies.

Analysis of the bar with section variable along the length differs from the above analysis only in the dynamic stiffness diagram.
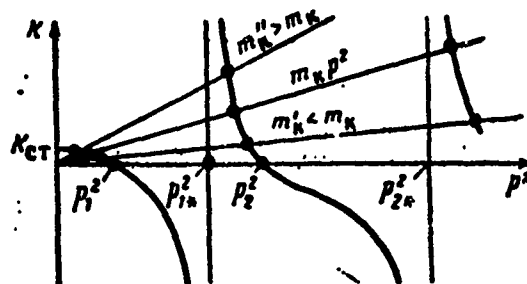
Figure 6.5. Determination of beam natural
vibration frequencies by the dynamic
stiffness method.

To construct the diagram by calculation or experimentally, we
determine the frequencies of the natural vibrations of the free can-
tilever bar (scheme a in Figure 6.4) and of the bar with an additional
support (scheme # in Figure 6.4). After this we use (6.23) to
construct the dynamic stiffness diagram.

As before, with the aid of the diagram, we determine the natural
vibration frequencies of the bar of variable section with the mass
attached to it.

6.2.2. Vibrations of Bar on Elastic Hinge (Figure 6.6)

The system has a single section, passing through the hinge, where
the single-connectedness condition is satisfied.

We cut the system into two parts through the hinge, applying in
the cuts the internal force moment

$$M = X \cos pt.$$
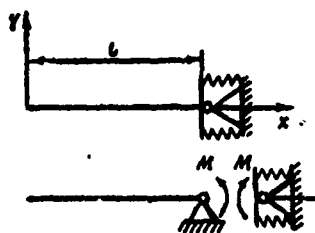
Figure 6.6. Beam with elastic
hinge and its partition into
two parts.

We shall determine the
dynamic stiffness coefficients
for the left and right parts.

On the basis of the general
solution (6.17), we find the
deflection equation for the left
part. The boundary conditions
will be

$$\xi=0; \quad Y''=Y'''=0;$$
$$\xi=1; \quad Y=0; \quad \frac{EJ}{l^2}\frac{d^2Y}{d\xi^2}=X.$$

Substituting into the boundary conditions the general solution

$$Y=C_1 S(k\xi)+C_2 T(k\xi)+C_3 U(k\xi)+C_4 V(k\xi),$$

we obtain for the first two conditions $C_3 = C_4 = 0$. The second two
equalities yield the equations

$$C_1 S(k)+C_2 T(k)=0;$$
$$\frac{k^2 EJ}{l^2}[C_1 U(k)+C_2 V(k)]=X.$$

After determining C_1 and C_2 from these equations, we obtain the
solution in the form

$$Y=-X\frac{l^2}{k^2 EJ}\left[\frac{T(k)}{\Delta(k)}S(k\xi)-\frac{S(k)}{\Delta(k)}T(k\xi)\right], \qquad (6.25)$$

where

$$\Delta(k)=S(k)V(k)-T(k)U(k).$$

Differentiating (6.25) with respect to $x=\xi l$, we obtain the
formula for the rotation angles, which for the bar end ($\xi=1$) yields
the dependence of the section rotation angle on the magnitude of the
moment X

$$\Phi(1) = -X \cdot \frac{l}{kEJ} \cdot \frac{T(k)V(k) - S^2(k)}{S(k)V(k) - T(k)U(k)}. \qquad (6.26)$$

Hence, the dynamic stiffness coefficient for the bar section passing through the hinge will be

$$K = \frac{X}{\Phi} = -\frac{kEJ}{l} \cdot \frac{S(k)V(k) - T(k)U(k)}{T(k)V(k) - S^2(k)}. \qquad (6.27)$$

To emphasize the definite physical significance of (6.27), we transform its coefficient

$$\frac{kEJ}{l} = \frac{k^4EJ}{lk^3} = \frac{1}{3} ml^3 p^2 \cdot \frac{3}{k^3} = J_0 p^2 \cdot \frac{3}{k^3},$$

where J_0 is the moment of inertia of the absolutely rigid bar about the hinge.

Then (6.27) takes the form

$$K = -J_0 p^2 \frac{3[S(k)V(k) - T(k)U(k)]}{k^3[T(k)V(k) - S^2(k)]}; \qquad (6.28)$$

for low frequencies, when $k \to 0$, as shown previously the fraction in (6.28) approaches one. Therefore

$$K(0) = -J_0 p^2,$$

i.e., for low frequencies the moment dynamic stiffness of the bar equals the moment dynamic stiffness of a mass with moment of inertia J_0 rotating freely about the hinge.

The roots of the expression in the numerator of (6.28) correspond to the natural vibration frequencies p_j of the bar on a free hinge, while the roots of the expression in the denominator correspond to the frequencies p_{j_*} of the clamped bar, i.e., the roots in the denominator correspond to the system with an additional constraint

in the direction of the force factor X. Therefore, the dynamic stiffness Formula (6.28) can be written in the form

$$K = -J_0 p^3 \frac{\left(1-\frac{p^2}{p_1^2}\right)\left(1-\frac{p^2}{p_2^2}\right)\left(1-\frac{p^2}{p_3^2}\right)\cdots}{\left(1-\frac{p^2}{p_{1*}^2}\right)\left(1-\frac{p^2}{p_{2*}^2}\right)\left(1-\frac{p^2}{p_{3*}^2}\right)\cdots};$$
(6.29)

The frequencies p_j and p_{j_*} are found from the known formula

$$p = \frac{k^2}{l^2}\sqrt{\frac{EI}{m}},$$

where k^2 is taken for the shaft with hinged and clamped support, respectively.

Figure 6.7 shows the dynamic stiffness coefficients as a function of frequency. The dashed line shows the dynamic stiffness of the absolutely rigid bar.

The hinge stiffness is constant and independent of the frequency. Therefore, the frequency equation for the system in question will be

$$K + K_\blacksquare = 0.$$
(6.30)

The horizontal lines, corresponding to the static stiffnesses of the hinge, plotted with reversed sign on the bar dynamic stiffness diagram, yield points of intersection with the dynamic stiffness curves. These points show the system natural vibration frequencies. The point of intersection with the dashed line yields the natural vibration frequency of the absolutely rigid bar with elastic hinge. Because of the bar elasticity, the natural vibration frequency is lower in comparison with the vibration frequency of the rigid bar, and higher vibration modes appear. If the hinge stiffness approaches zero, we arrive at the natural vibration frequencies of the bar on a free hinge. If the hinge stiffness increases, the frequencies approach those of the clamped cantilever bar.
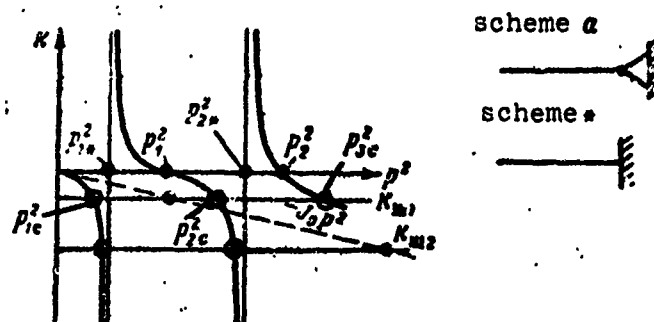
Figure 6.7. Diagram of dynamic stiffnesses
of beam with elastic hinge.

This analysis is completely applicable to the blade of variable
section, with the sole difference that the natural vibration frequen-
cies will be numerically different for the blade.

6.2.3. Analysis of Two-Support Shaft With Overhang (Figure 6.8)

We divide the system into two parts by a cut through the left
support A. The dynamic stiffness coefficie. of the left cantilever
part was obtained in the preceding example and is defined by (6.29).

The dynamic stiffness coefficient for the right side is defined
by (6.23). But here, K_{st} corresponds to the moment static stiffness
of the two-support bar.

This coefficient equals

$$K_{cr} = \frac{3EI}{l}.$$

The natural vibration frequencies p_1 and p_{1_*} must be taken for
the beam with hinged supports (scheme a) and with the left end
clamped (scheme * in Figure 6.8). The frequency coefficients for
these cases are, respectively, (see [1])
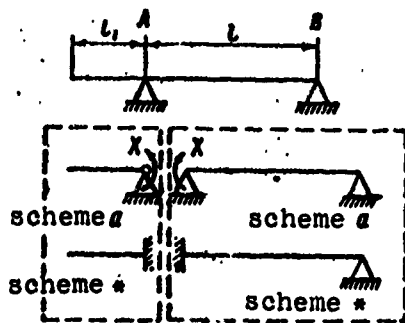
Figure 6.8. Beam with cantilever on two supports and its partition.
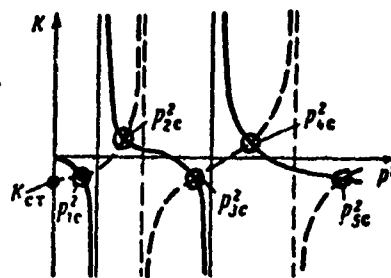
Figure 6.9. Dynamic stiffnesses of component parts: solid curves are for cantilever part of system; dashed curves are for two-support part of system; points of intersection of the curves are the natural vibration frequencies of the system in question.

$$k_i^2 = \pi^2;\ 4\pi^2;\ 9\pi^2 \quad \text{etc.;}$$
$$k_{j*}^2 = 15.418;\ 49.96;\ 104.25 \quad \text{etc.}$$

Superposing the dynamic stiffness coefficient diagram for the two-support part (with reversed sign) on the analogous diagram for the cantilever part, we obtain the natural vibration frequencies of the two-support beam with overhang (Figure 6.9) as the points of intersection of the dynamic stiffness curves. The problem solution is very easily visualized and makes it possible to evaluate the influence of the length and stiffness of the cantilever and primary parts of the beam, and also permits solving the problem in the case of stiffness which is variable along the length.

6.3. Multiply-Connected Systems

In vibration analysis, the multiply-connected systems are those which consist of several unlike simpler systems which are connected with one another by several characteristic constraints. For example, the turbopump assembly and its support (Figure 6.10) can be analyzed as a system consisting of three parts — rotor, case, and support. The rotor, in turn, can be analyzed as a system consisting of an integral or composite shaft, disks, and blades. The disk with its blades is also a multiply-connected system, since the connection between the blades and the disk is expressed with the aid of several components — transverse forces, bending and rotational moments (Figure 6.11).

6.3.1. Formulation of General Equations of the Dynamic Stiffness Method

In order to formulate the computational equations, the complex system is divided into several simpler parts (see Figure 6.10).

At each section along which the system is divided, the corresponding forces and moment replacing the action of the discarded constraints are applied. Since the system performs harmonic vibrations, the force factors at the sections are harmonic functions of the frequency p.

The forces and moments applied at the cuts are considered as external disturbing factors

$$Q_i = X_i \cos pt.$$

For each isolated part we solve the forced vibration problem, in which the method presented in Section 6.1 is used to find the dynamic stiffness coefficients K_{is}. After this, systems of canonical Equations (6.14) of the following form are written for all the parts
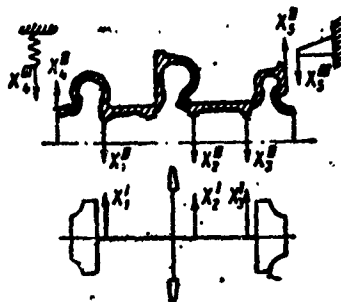
Figure 6.10. Diagram for vibration analysis of multiply-connected system.
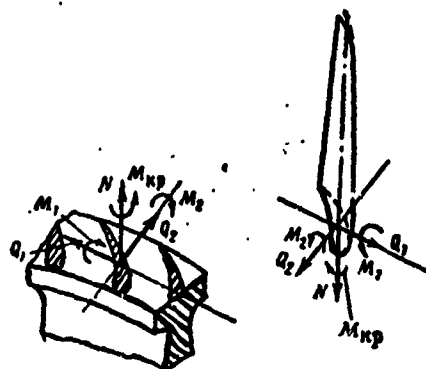
Figure 6.11. Schematic showing multiple-connectedness of disk and blades.

$$X_i^N = \sum_{s=1}^{n} K_{is}^N Y_s, \quad i = 1, 2, ..., n, \tag{6.31}$$

where N is the index of the system part;

   n is the number of constraints for the system N.

For each constraint there are two expressions X_1^N and X_1^{N+1}, with the condition being satisfied

$$X_i^N + X_i^{N+1} = 0. \tag{6.32}$$

Combining these expressions pairwise, we obtain the system of dynamic stiffness equations. With application to Figure 6.10, this system will be

$$\sum_{s=1}^{3} (K_{is}^I + K_{is}^{II}) Y_s + K_{i4}^{II} Y_4 + K_{i5}^{II} Y_5 = 0, \quad i = 1, 2, 3;$$

$$\sum_{s=1}^{3} K_{is}^{II} Y_s + (K_{i4}^{II} + K_{i4}^{III}) Y_4 + (K_{i5}^{II} + K_{i5}^{III}) Y_5 = 0, \quad i = 4, 5.$$

The equations are homogeneous; therefore, the condition for the existence of solutions is vanishing of the determinant

$$\Delta = \begin{vmatrix} K^{\text{I}}_{11}+K^{\text{II}}_{11} & K^{\text{I}}_{12}+K^{\text{II}}_{12} & K^{\text{I}}_{13}+K^{\text{II}}_{13} & K^{\text{II}}_{14} & K^{\text{II}}_{15} \\ K^{\text{I}}_{21}+K^{\text{II}}_{21} & K^{\text{I}}_{22}+K^{\text{II}}_{22} & K^{\text{I}}_{23}+K^{\text{II}}_{23} & K^{\text{II}}_{24} & K^{\text{II}}_{25} \\ K^{\text{I}}_{31}+K^{\text{II}}_{31} & K^{\text{I}}_{32}+K^{\text{II}}_{32} & K^{\text{I}}_{33}+K^{\text{II}}_{33} & K^{\text{II}}_{34} & K^{\text{II}}_{35} \\ K^{\text{II}}_{41} & K^{\text{II}}_{42} & K^{\text{II}}_{43} & K^{\text{II}}_{44}+K^{\text{III}}_{44} & K^{\text{II}}_{45}+K^{\text{III}}_{45} \\ K^{\text{II}}_{51} & K^{\text{II}}_{52} & K^{\text{II}}_{53} & K^{\text{II}}_{54}+K^{\text{III}}_{54} & K^{\text{II}}_{55}+K^{\text{III}}_{55} \end{vmatrix} = 0. $$

(6.33)

This is the basic frequency equation of the system. Its roots are the natural vibration frequencies.

The solution of the equation can be carried out in various ways. One way is the trial and error method. Assuming a frequency, the equations associated with the determination are used to calculate the values of the dynamic stiffness coefficients. Then the determinant itself is calculated. In the computational process, the curve $\Delta(p^2)$ is plotted, which shows the zero points of the determinant. Although the value of the determinant is a continuous function, its calculation is made difficult by the large number of points of discontinuity of the dynamic stiffness functions, and this calculation is very tedious for a determinant of high order.

Another method is to expand the determinant into a row. After replacing the dynamic stiffness coefficients in the row by their functions, a frequency equation which does not contain points of discontinuity can be obtained for systems which are not too complex. This method is in essence the method for composing the frequency equation of the system with the aid of the dynamic stiffness coefficients.

In principle, the dynamic stiffness method is one of the exact methods for analysis of linear systems. It permits determining the frequencies of all the natural vibration modes in any sequence. Moreover, this method makes it possible to introduce simplifications by replacing the exact expressions for the dynamic stiffness

coefficients of the individual elements by approximate expressions, and also makes it possible to include in the calculations the coefficients found experimentally.

6.3.2. Vibrations of Blades Connected by an External Shroud Ring

The shroud ring connecting the turbine rotor blade tips (Figure 6.12) usually is very thin. Therefore, we can assume that the shroud axial circle — the circle of centers of gravity of its sections — coincides with the blade tip circle. We assume that the connection of the blades with the shroud is ideally rigid; therefore, the angle between the blade longitudinal axis and the shroud axis is the same in the undeformed and deformed states.
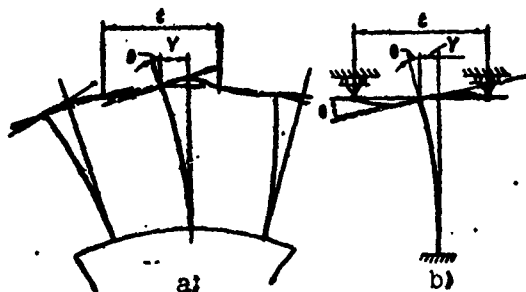
Figure 6.12. Schematic of shroud ring operation.

The primary vibration mode of the shrouded blades is that in which all the blades vibrate synchronously and uniformly (see Figure 6.12a). In this case, the shroud ring displaces with respect to the circle by the magnitude Y of the deflection of the blade tips, and the angle θ of rotation of the shroud sections at the points of connection with the blades equals the angle of rotation of the blade tip sections.

As a result of shroud bending, the restoring moment of the shroud elastic forces acts on the blade tips.

As a result of the identity of the deformations of all the blades and all the shroud segments, on the curved shroud axial line, there are inflection points at which the bending moment equals zero, and only a shearing force acts. We note also that the inflection points lie on the initial shroud circular axis.

We isolate one of the blades and the shroud segments adjacent to it by sections passing through the inflection points. We replace the action of the adjacent segments by hinged supports (see Figure 6.12b). The vibrations of the isolated blade of the resulting scheme will be identical to the vibrations of the same blade in the complete assembly.

We shall use the dynamic stiffness method to solve the problem. We divide the system into two parts (Figure 6.13) by sections passing through the blade tip and apply to both parts the force and moment replacing the internal interaction forces.

Figure 6.13. Determining the dynamic stiffnesses and natural vibration frequencies of shrouded blades.

For the lower part (I), the connection between the force and moment and the deformations — deflection Y and rotation angle θ — is defined by the equations

$$\left. \begin{array}{l} X_1^I = K_{11}^I Y + K_{12}^I \theta; \\ X_2^I = K_{21}^I Y + K_{22}^I \theta. \end{array} \right\} \qquad (6.34)$$

For the upper part (II), as a result of the fact that the force and moment are applied at the midpoint of the span, the mixed stiffness coefficients are missing

$$K_{12}^{II} = K_{21}^{II} = 0.$$

Therefore, we have for the upper part of the system

$$X_1^{11} = -m_6 p^2 Y; \quad X_2^{11} = c_6 \theta, \tag{6.35}$$

where m_s and c_s are, respectively, the mass and moment stiffness of the shroud segment.

Combining the corresponding equalities (6.34) and (6.35) and equating the sum to zero, we obtain homogeneous equations. The determinant composed of the equation coefficients must equal zero

$$\begin{vmatrix} K_{11}^1 - m_6 p^2 & K_{12}^1 \\ K_{12}^1 & K_{22}^1 + c_6 \end{vmatrix} = 0. \tag{6.36}$$

We expand the determinant and solve it for c_s

$$K_{22}^1 - \frac{(K_{12}^1)^2}{K_{11}^1 - m_6 p^2} = -c_6. \tag{6.37}$$

The left side of this equality is the moment dynamic stiffness coefficient of the blade with the shroud mass m_s attached to it (Figure 6.14). In order to verify this we must examine the problem of forced vibrations of a bar having a concentrated mass at the end under the action of the harmonic bending moment M.

This coefficient, which we denote by K^I, can be found using the formula

$$K^1 = \frac{EJ}{l} \frac{\left(1 - \frac{p^2}{p_1^2}\right)\left(1 - \frac{p^2}{p_2^2}\right)\left(1 - \frac{p^2}{p_3^2}\right) \cdots}{\left(1 - \frac{p^2}{p_{1*}^2}\right)\left(1 - \frac{p^2}{p_{2*}^2}\right)\left(1 - \frac{p^2}{p_{3*}^2}\right) \cdots}, \tag{6.38}$$

where the coefficient EJ/l is the static moment stiffness coefficient of the uniform bar (for the blade of variable section this coefficient has a different value); p_1, p_2, p_3, and so on are the natural vibration frequencies of the free blade with mass at the end (scheme a in

Figure 6.14); p_{1_*}, p_{2_*}, p_{3_*}, and so on are the natural vibration frequencies of the blade with additional constraint (scheme *).

The static moment stiffness of the shroud segment is found from the formula

$$c_t = 12\frac{EI}{t}. \qquad (6.39)$$

Plotting the dynamic stiffness characteristic using (6.38) and drawing the straight line c_s parallel to the abscissa axis (Figure 6.15), we obtain points of intersection which yield the natural vibration frequencies of blades connected by a common shroud ring.

The system frequencies p_{1c}, p_{2c}, and so on, differ from one another in the number of nodes on the blades.
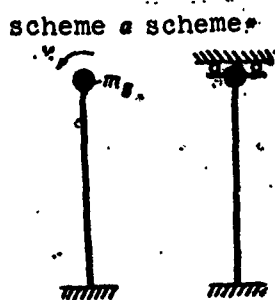
Figure 6.14. Determining the dynamic moment stiffness coefficient.
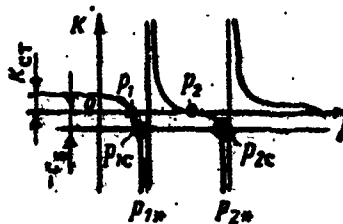
Figure 6.15. Determining the frequencies of shrouded blades.

6.3.3. Vibrations of Blades Connected by Lashing Wire

One version of lashed blade vibrations is that for which the blade vibration amplitudes are different and are distribute sinusoidally along the wheel periphery. Correspondingly, an even number of radial nodal lines is formed on the blade portion of the rotor. The

blade vibration amplitudes equal zero on the nodal lines. Between the nodal lines there are located the crests, where the amplitudes have the largest value.

Let us examine this case for blades connected by a lashing wire (Figure 6.16). As is known, the wire ring is passed through holes in the blades. The ring diameter and the wire diameter are determir by the lashing design.

As a result of the small blade thickness, we can consider that the wire lashing is hinged with the blade. The constraint arises by virtue of the friction force owing to the action of the centrifugal force of the lashing wire.

During vibration, the effect of the ring on the blades shows up in the form of transverse forces, and the lashing wire is subjected to longitudinal loads. In this process the ring points which coincide with the nodal lines remain stationary all the time (the case of possible slippage of the lashing wire in the hole is not considered).

We delete the constraints between the blades and the lashing wire, replacing their action by the corresponding forces

$$Q_i = X_i \cos pt.$$

The amplitude X_1 of the transverse force acting on the blade is connected with the amplitude Y_1 of the blade vibrations at this same section by the dynamic stiffness coefficient

$$X_i = K_s Y_i. \qquad (6.40)$$

The blade dynamic stiffness coefficient is found from (6.23). In this formula K_{st} is taken for the static force at the point of contact between the blade and lashing ring (see Figure 6.16). The frequencies p_1 in the numerator of (6.23) are the natural vibration frequencies of the free blade (scheme a in Figure 6.16). The

scheme *a*   scheme *#*
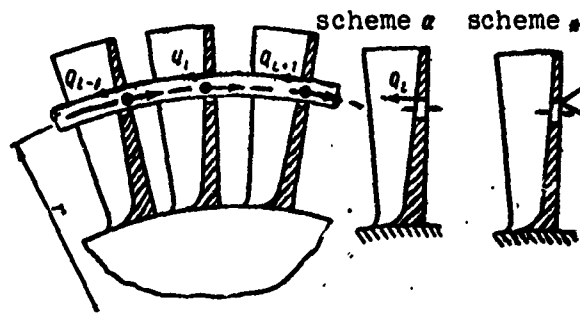
Figure 6.16.   Diagram for determining blade dynamic
stiffness coefficients at point of connection of
lashing wire.
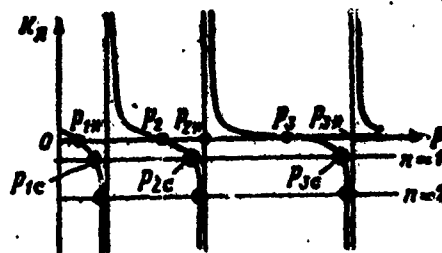
Figure 6.17.   Determining frequencies of shrouded
blades with band working in axial compression.

frequencies $p_{1_{#}}$ in the denominator are the natural vibration frequen-
cies of the blade with additional constraint as shown in scheme * in
Figure 6.16. These frequencies can be found by calculation or experi-
mentally. The dynamic stiffness coefficient is shown in Figure 6.17
as a function of frequency. In view of the fact that the construction
of all the blades is the same, the plotted function K_b and (6.40)
are valid for all the blades.

We consider the lashing ring weightless, since its mass is small
in comparison with the mass of all the blades. We represent the

longitudinal load on the ring from the action of all the blades as a distributed load. The load intensity is

$$q = \frac{X_l^6}{t} = -\frac{K_s}{t} Y,$$ (6.41)

where t is the blade pitch along the lashing ring.

The ratio K_b/t is constant for a given frequency; therefore, the wire longitudinal load is proportional to its longitudinal deformation.

We write the differential Equation (3.79) for the longitudinal deformations of the lashing wire

$$EF \frac{d^2Y}{dx^2} + q = 0,$$
$$x = r\varphi,$$ (6.42)

where EF is the lashing wire compressional stiffness;

    r is the lashing wire radius;

    ϕ is the coordinate.

After substitution from (6.41), (6.42) is written in more general form

$$\frac{d^2Y}{d\varphi^2} + v^2 Y = 0,$$ (6.43)

where

$$v^2 = -\frac{K_s r^2}{tEF}.$$ (6.44)

The general solution of (6.43) is

$$Y = C_1 \cos v\varphi + C_2 \sin v\varphi.$$ (6.45)

The lashing wire deformation distribution along its circumference must satisfy the periodicity condition

$$Y(\varphi)=Y(\varphi+2\pi). \qquad (6.46)$$

Substituting herein the general solution, we obtain the condition

$$n=1, 2, 3 \text{ . etc.} \qquad (6.47)$$

i.e., within the limits of the circumference there must be a whole number of lashing ring longitudinal deformation waves.

Replacing ν^2 in (6.44) by n^2, we obtain the frequency equation for the vibrations of blades connected by a lashing wire

$$K_s = -n^2 \frac{iEF}{r^2}. \qquad (6.48)$$

The equation is solved graphically (see Figure 6.17) by drawing on the blade dynamic stiffness characteristic curve, plotted using (6.23), horizontal lines corresponding to the right side of (6.48). The points of intersection yield the natural vibration frequencies p_{1c}, p_{2c}, p_{3c}, and so on, of the lashed blades.

Each value of n corresponds to its own natural vibration frequency spectrum of the lashed blades. The vibration modes within the limits of the spectrum differ in the number of nodes on the blade. The vibration modes of all the blades are similar.

The case n = 1 corresponds to a single lashing ring longitudinal deformation wave and, therefore, to a single direction of the blade deflections. For these vibration modes, the deformation of the lashing ring gives the most significant reduction of the natural frequencies in comparison with the ideally rigid band. The larger the number of blades and the smaller the section of the lashing wire, the greater the frequency reduction.

For n = 2 and more, the effect of band deformations is considerably less. The natural frequencies are close to those of the blade with ideally rigid band.

This is explained by the fact that the length of the band segment between the nodal points is reduced, and the number of blades loading the given segment is reduced. The band longitudinal deformations become negligible, and the band operates as a rigid connection between the blades.

With respect to the number of waves lying in the limits of the circumference, the number of natural vibration modes lashed blades depends on the number of blades on the rotor:

~~ · ;ven number of blades

$$n = \frac{z}{2};$$
(6.49)

for an odd number of blades

$$n = \frac{z-1}{2}.$$
(6.50)

6.3.4. Determination of Shaft Critical Speed With Account for Disk Deformation

Usually, in calculating the critical speed of a shaft, it is assumed that the disks seated on the shaft are absolutely rigid. This assumption may be the cause of considerable discrepancy between experimental and calculated values of the critical speed in light-weight designs with thin disks and heavy blades mounted on the disks. The error depends on where the disk is mounted on the shaft, with the error increasing when the disk is located at sections which rotate through a large angle during bending.

Analysis of the shaft with account for disk deformation is made by the dynamic stiffness method.

Let us consider a shaft with cantilever disk (Figure 6.18). We divide the system into two parts by a cut passing through the point where the disk is mounted on the shaft. Since during deformation of

scheme а

scheme *

Figure 6.18. Partitioning of shaft with flexible disk for determining dynamic stiffness coefficients.
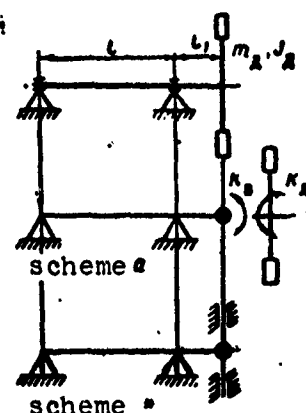
the shaft the disk rotates about the principal axis, its mixed dynamic stiffness coefficients equal zero. This makes it possible to examine a singly-connected system, leaving the disk mass in the form of a point at the end of the shaft and isolating only the moment dynamic stiffness of the disk.

The frequency equation of the system will be

$$K_{\text{в}}+K_{\text{д}}=0. \tag{6.51}$$

The shaft dynamic stiffness is found from the formula

$$K_{\text{в}}=\frac{3EJ}{3l_1+l} \cdot \frac{\left(1-\frac{p^2}{p_1^2}\right)\left(1-\frac{p^2}{p_2^2}\right)\cdots}{\left(1-\frac{p^2}{p_{1*}^2}\right)\left(1-\frac{p^2}{p_{2*}^2}\right)\cdots}, \tag{6.52}$$

where p_1 and p_{1*} are the natural vibration frequencies of schemes a and * respectively (Figure 6.18).

The vibration frequencies of these systems can be determined by any method, including the dynamic stiffness method.

If we neglect the shaft mass proper, assuming that the disk mass exceeds that of the shaft considerably, the dynamic stiffness coefficient of interest to us is found from the formula

$$K_{\text{в}}=\frac{a_{11}m_{\text{д}}\omega^2-1}{a_{22}-\left(a_{11}a_{22}-a_{12}^2\right)m_{\text{д}}\omega^2}, \tag{6.53}$$

where a_{11}, a_{12}, a_{22} are the influence coefficients;

ω is the shaft angular velocity.

The disk dynamic stiffness is proportional to its dynamic moment for forward precession

$$K_{\pi} = \frac{\mu_{\pi}}{\theta}. \qquad (6.54)$$

The calculation of this moment is made with account for disk bending under the action of the centrifugal forces of the blades and the disk itself.

Figure 6.19 shows curves of the specific dynamic stiffness of a disk with blades as a function of the dimensionless angular velocity.
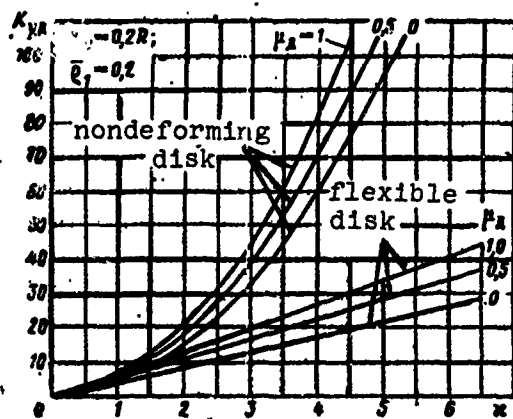
Figure 6.19. Specific dynamic stiffness of disk for forward synchronous precession

The moment dynamic stiffness is calculated with the aid of the graph, using the formula

$$K_{\pi} = K_{y\pi} D, \qquad (6.55)$$

where $D = \dfrac{Eh^3}{12(1-v^2)}$ is the cylindrical stiffness of the disk.

The parameter x equals

$$x = \sqrt{\frac{NR^3}{D}},\qquad(6.56)$$

where R is the disk radius; N is the blade centrifugal force, referred to unit length of the disk circumference:

$$N = \frac{1}{t} m_s r_c \omega^2.\qquad(6.57)$$

The parameter μ_d indicates the disk weight in relation to blade weight

$$\mu_s = \frac{m_s}{z m_s},\qquad(6.58)$$

where z and m_b are the number of blades and mass of a single blade, respectively.

The upper series of curves shows the dynamic stiffnesses for the nondeforming disk. We see that the difference between the dynamic stiffnesses of the rigid and flexible disks is very significant, particularly for high angular velocities and heavy blades.

We obtain the critical speed of the shaft with account for disk bending by solving (6.51). To do this, the dynamic stiffness curve of the disk with reversed sign is superposed on the shaft dynamic stiffness curve (Figure 6.20). The points of intersection of the curves correspond to the critical speeds of the shaft with flexible disk. In the same figure the dashed curve shows the dynamic stiffness curve of the nondeforming disk, which indicates the critical speed for rigid disks.

The value of the critical speed for the flexible disk lies in the range
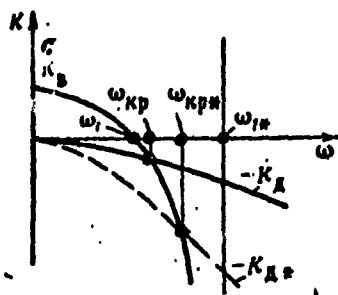
Figure 6.20. Use of dynamic stiffnesses to determine critical speed of shaft with flexible disk.

$$\omega_i < \omega_{\kappa p} < \omega_{\kappa p.m.}; \qquad (6.59)$$

i.e., between the shaft critical speed obtained without account for the restoring moment of the disk and the critical speed of the shaft with a rigid disk. Depending on the degree of disk flexibility, the critical speed may be close to one limit cr the other. For the first critical speed, the correction can reach 20 - 30%.

If the shaft is analyzed with account for its distributed mass, the second and higher critical speeds are less sensitive to disk flexibility.

6.3.5. Generalized Dynamic Stiffness and Initial Parameter Method

The generalized method is finding more and more application recently in connection with the advances in computer technology. Further development of this method is opening up vast promise for more complete and exact studies of the vibrations of complex elastic systems.

The initial parameter method was examined in Section 4.6.1. We shall dwell here on the characteristics of its combination with the dynamic stiffness method, using the example of the configuration shown in Figure 6.10.

As we have mentioned previously, the system is divided into three parts — I, II, III — by deleting the internal constraints and replacing them by equal and opposite forces.

The system I is calculated first. The purpose of the calculation is to find the dynamic stiffness coefficients at tne points of the

deleted constraints. To this end the system I is rigidly restrained with respect to all the constraints in question. Releasing in turn one of the constraints and applying in its place a disturbing harmonic force of given frequency, we calculate the displacement amplitude in the direction of action of the force and the reaction of the imposed constraints. The ratios of the amplitudes of the force acting and the constraint reactions to the resulting displacement amplitude are the dynamic stiffness coefficients. The calculation is made by the initial parameter method using the scheme discussed previously.

The transition through the section where the harmonic force acts is accomplished with the aid of the matrix

$$\begin{vmatrix} 1 & 0 & 0 & 0 \\ 0 & 1 & 0 & 0 \\ 0 & 0 & 1 & 0 \\ -K_{li}^{l} & 0 & 0 & 1 \end{vmatrix}. \tag{6.60}$$

This matrix is similar to that used for transition through an elastic support. The proper dynamic stiffness coefficient K_{li}^{l} is unknown; it will appear in general form in all the expressions for the initial and final parameters of the subsequent segments. The numerical value of the coefficient K_{li}^{l} is found after the formulas are obtained for the parameters of the ened of the next segment of system I. Applying the boundary conditions, we form from the formulas for the parameters a system of two homogeneous equations. The system determinant, equated to zero, forms the equation from which we find the numerical value of K_{li}^{l} for the frequency assumed in the beginning of the calculation.

Transition through sections with rigid additional constraints is accomplished like the transition through a conventional rigid support. The support reactions are the improper dynamic stiffness coefficients.

As a result of the calculation for a given frequency, we obtain the values of all the dynamic stiffness coefficients of system I.

Then system II is calculated. In this case, the dynamic stiffness coefficients for the constraints discarded on the system I side are considered known, and those on the system II side are unknown.

In the first case, the numerical values of the dynamic stiffness coefficients found in calculating system I are used, with reversed sign. With the aid of these coefficients, the forces oacting on system II from system I can be written in the form of the sums

$$X_i^{II} = \sum_{s=1}^{s} -K_{is}^{I} Y_s, \quad i = 1, 2, \ldots, n,$$ (6.61)

where n is the number of constraints between systems I and II.

In calculating the dynamic coefficients for the constraints facing system III, system II is rigidly restrained in the direction of all the constraints being calculated. The calculation is performed by the initial parameter method by freeing in turn one of the constraints and applying in its place the harmonic force

$$Q_i = X_i \cos pt.$$

As a result of the calculation, we find the vibration amplitude in the direction of the applied harmonic force and all the reactions of the additional constraints, which yields the dynamic stiffness coefficients.

After making the calculation for several values of the frequency p, we obtain the coefficients as a function of frequency.

In the calculation using the initial parameter method, transition through the sections where the constraints facing system III act is accomplished with the aid of the matrix (6.60), just as in the calculation of system I.

Transition through the section where the harmonic forces from system I act is accomplished in accordance with (6.61), using the following matrix formula

$$
\begin{vmatrix} Y_1 \\ \theta_1 \\ M_1 \\ Q_1^{ah} \end{vmatrix} = \begin{vmatrix} 1 & 0 & 0 & 0 & 0 & 0 \\ 0 & 0 & 0 & 1 & 0 & 0 \\ 0 & 0 & 0 & 0 & 1 & 0 \\ K_{11}^1 & K_{12}^1 & K_{13}^1 & 0 & 0 & 1 \end{vmatrix} \begin{vmatrix} Y_1 \\ Y_2 \\ Y_3 \\ \theta_1 \\ M_1 \\ Q_1^{be} \end{vmatrix}. \tag{6.62}
$$

where Q_1^{ah}, Q_1^{be} are the transverse forces ahead of and behind the section.

The dynamic stiffness coefficients appearing in the large matrix are known and have numerical values. In accordance with (6.62), the parameters Y_1, θ_1, M_1 do not change when passing through the section. The parameter Q_1^{be} acquires temporarily three unknown values — Y_1, Y_2, Y_3. The first value is excluded immediately, since it is expressed with the aid of the assumed parameters of the beginning of the segment. The remaining values are excluded in the course of passage through the corresponding sections.

The transition matrices for the second section will have the form

$$
\begin{vmatrix} Y_2 \\ \theta_2 \\ M_2 \\ Q_2^{ah} \end{vmatrix} = \begin{vmatrix} 0 & 1 & 0 & 0 & 0 & 0 \\ 0 & 0 & 0 & 1 & 0 & 0 \\ 0 & 0 & 0 & 0 & 1 & 0 \\ K_{21}^1 & K_{22}^1 & K_{23}^1 & 0 & 0 & 1 \end{vmatrix} \begin{vmatrix} Y_1 \\ Y_2 \\ Y_3 \\ \theta_2 \\ M_2 \\ Q_2^{be} \end{vmatrix}. \tag{6.63}
$$

For the last section of segment II, as before, we obtain two closing homogeneous equations, from which we find the dynamic stiffness coefficient K_{ii}^{11}, and then the reactions of the imposed rigid constraints — the improper dynamic stiffnesses K_{ie}^{11}.

For the calculation of the last part — system III — we use the dynamic stiffness coefficients found in calculating system II, with reversed sign.

The system III is the support and represents a series of several isolated elastic or rigid devices. We formulate the equations of equilibrium of the effective external forces and elastic forces for this support

$$c_4 Y_4 = -K_{44}^{11} Y_4 - K_{45}^{11} Y_5;$$
$$c_5 Y_5 = -K_{54}^{11} Y_4 - K_{55}^{11} Y_5.$$

$$(6.64)$$

where c_4, c_5 are the support static stiffness coefficients.

The equations are homogeneous and their determinant must equal zero

$$\begin{vmatrix} c_4 + K_{44}^{11} & K_{45}^{11} \\ K_{54}^{11} & c_5 + K_{55}^{11} \end{vmatrix} = 0.$$

$$(6.65)$$

The frequencies for which the determinant vanishes are the natural vibration frequencies of the entire system.

PART II

NONLINEAR VIBRATIONS

The real structures of mechanisms of various devices, particular-
ly flight vehicle engines, are nonlinear systems. Their nonlinearity
lies in the fact that one or more of the principal parameters, such
as stiffnesses, internal resistance and friction, and in certain
cases the masses, depend on the displacements. Because of these non-
linearities the system motion is described by nonlinear equations.

The nonlinearities are a consequence of violation of Hooke's
law, which is associated with the materials and working stresses
used, nonlinearity of the boundary conditions, and in certain cases
singularities of the mechanism kinematics.

A typical nonlinearity in machines is created by clearances,
loose fit of articulations or excessive tightening of joints, when
the material in the joint region is subjected to a stress close to
the proportional limit. The sliding supports of shafts and rotors
have characteristic nonlinear properties. The self-oscillating
systems are a special class of nonlinear systems.

Nonlinearity of the parameters imparts several special properties
to the systems, differing markedly from those which are described by

linear vibration theory. For example, the free vibration frequencies of the nonlinear systems depend on the amplitudes. In this connection, the concept of resonance in the form in which it is discussed in linear systems does not exist in nonlinear systems.

In the solution of the nonlinear differential equations, we do not use the principle of particular solution superpositioning. Therefore, in nonlinear system vibration theory the formulation of the question of principal vibrations and their forms does not appear, and the principle of vibration summation is not used. The self-oscillating systems have the property under certain conditions of performing steady-state harmonic vibrations in the absence of an external harmonic exciter, and so on.

One of the basic problems for nonlinear systems is vibration stability and determination of the conditions under which stable vibrations may become unstable. The majority of the studies concern equations with small parameters of the nonlinear terms. In these studies it is shown what phenomena can be expected because of the presence of small nonlinearities.

Nonlinear vibration theory and the problems examined in this theory yield more profound and complete understanding of the vibrations of mechanical systems than is given by linear theory, based on the linearized equations, from which the small but sometimes important nonlinear terms are excluded.

However, we note that nonlinear system vibration theory, in view of its complexity, has been developed primarily for simple systems and in application to individual specific problems. This remark is particularly valid in relation to systems with large nonlinearities.

CHAPTER 7

VIBRATIONS OF NONLINEAR CONSERVATIVE SYSTEMS

7.1. Phase Plane Method

In all conservative systems the sum of the kinetic and potential energies remains constant in the course of time

$$T + \Pi = E = \text{const},\qquad (7.1)$$

where E is the overall energy level of the system.

Substituting into (7.1) the expression for the kinetic energy, we obtain the equation of motion of the conservative system in general form

$$\frac{1}{2} m\dot{q}^2 + \Pi = E.\qquad (7.2)$$

The nature of the motion defined by this equation depends on the form of the potential energy function Π. A particular form of the motion is periodic motion, i.e., vibrations.

For nonlinear systems the potential energy is expressed by a polynomial of order higher than second or by some other complex function; therefore, integration of (7.2) is not possible in practice. Nevertheless, it does permit study of many systems and determination of the nature and properties of their vibrations.

One of the general analysis methods is the phase plane method. In accordance with this method the motion of an oscillating point is represented in the "velocity-displacement" coordinates or in quantities proportional to them. The coordinate plane is called the phase plane.

For a linear system

$$\Pi = \frac{1}{2} c q^2. \tag{7.3}$$

The vibration equation takes the form

$$m \dot{q}^2 + c q^2 = 2E; \tag{7.4}$$

denoting

$$y = \frac{\dot{q}}{k}; \quad A^2 = 2 \frac{E}{c}; \quad k^2 = \frac{c}{m}, \tag{7.5}$$

we obtain

$$y^2 + q^2 = A^2. \tag{7.6}$$

Harmonic vibrations are represented in the q, y phase plane in the form of a family of circles of radius A (Figure 7.1). The radius of the describing point circle is the larger, the larger the magnitude of the energy E imparted to the system at the initial moment.

If we take as the reference time the moment when the system passes through the equilibrium position, then

$$q_0 = 0; \quad E = \frac{1}{2} m \dot{q}_0^2.$$

If we take as the reference time the position of maximal deflection, then

$$\dot{q}_0 = 0; \quad E = \frac{1}{2} c q_0^2.$$

The position of the describing point on the phase trajectory defines at each moment of time the system displacement and velocity.
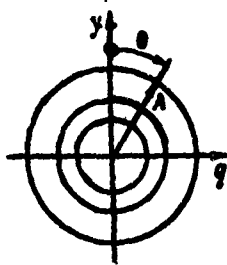
Figure 7.1. Representation of harmonic vibrations in phase plane.

The motion of the point along the phase trajectory always takes place in the clockwise direction. This is easily seen directly from the phase diagram: the upper part of the trajectory corresponds to positive velocities. This means that displacement can take place on the diagram only from left to right. Conversely, the lower part of the diagram corresponds to negative velocities. This means that the displacement here takes place from right to left. This all leads to motion of the describing point, as noted above, in the clockwise direction.

For harmonic vibrations the motion of the describing point along the phase trajectory takes place at constant velocity. To verify this, we calculate the angle θ between the radius vector of the describing point and the y axis

$$\sin \theta = \frac{q}{A}; \quad \cos \theta = \frac{y}{A} = \frac{\dot{q}}{kA};$$

differentiating $\sin \theta$, we obtain

$$\dot{\theta} = \frac{\dot{q}}{A \cos \theta} = k,$$

i.e., the angular velocity of the radius vector is constant and equal to the circular frequency of the harmonic vibrations.

In the general case the describing point velocity along the phase trajectory is variable.

7.1.1. General Method for Determining Motion of Nonlinear Conservative System

Equation (7.2)

$$\frac{1}{2}m\dot{q}^2 + \Pi = E$$

yields an extremely simple, and at the same time comprehensive, condition for the motion of a nonlinear conservative system. It is not limited by the magnitudes of the velocities and displacements, nor by the condition that the motion be periodic.

The total energy E in a conservative system remains constant in the course of the entire time. If the potential energy is known as a function of the displacement, then the distribution of the energy E between potential and kinetic for any position can be found from the graph (Figure 7.2). The points of intersection of the curve $\Pi(q)$ with the straight line characterizing the level E correspond to the instantaneous states of rest. The motion velocity is found easily from the difference between the total energy and the potential energy

$$\dot{q} = \pm\sqrt{\frac{2}{m}}\sqrt{E - \Pi(q)}. \tag{7.7}$$

Formula (7.7) connects the velocity and displacement and is the most general form of the equation of the system phase trajectory. The choice of the level from which the potential and total energy are reckoned is not important, since the velocity is determined by their difference.

Equation (7.7) shows that the phase trajectories are symmetric about the q axis. The derivative yields the phase trajectory slope

$$\frac{d\dot{q}}{dq} = \frac{1}{\sqrt{2m[E - \Pi(q)]}}\frac{d\Pi}{dq}. \tag{7.8}$$
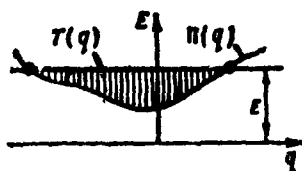
Figure 7.2. Energy
distribution in con-
servative system

At the point of intersection of the
phase trajectory with the q axis, the denomi-
nator of the fraction equals zero. This
means that the phase trajectory crosses the
axis at a right angle. These properties are
general and facilitate the construction and
analysis of the phase trajectories.

Let us examine the motion of some conservative system whose
potential energy function is given by the curve shown in Figure 7.3.
If the system is disturbed from the rest state, imparting to it the
energy E_1, the nature of its possible motions can be defined with the
aid of the phase trajectories shown in this same figure. System
motion is possible within the limits of the segments ab and cd and
also for $q < q_e$. On the segments ab or cd the phase trajectories
are closed; consequently, here the motion has the form of periodic
stable vibrations. As for the left side of the diagram, here within
the limits of the segment shown the motion is irreversible, of the
so-called "runaway type."

If the system energy level is reduced, the phase trajectories
on segments ab and cd will contract to a point. This indicates that
for a low energy level periodic motions become impossible on the
segments cd and ab. It is true that, in accordance with the potential
function being considered, motion on segment cd can be obtained for
a lower energy level than on segment ab. For a system energy level
below E_0, periodic motions in the system become impossible.

If the system energy level is increased, the ranges of possible
periodic motions will increase. When the energy imparted reaches the
value E_2, corresponding to the first maximum of the curve $\Pi(q)$, the
points b and c merge at the point f. The system is unstable in the
position q_f. From this position it can travel to the right — into
the region of periodic motion cd — but it can also travel to the
left — into the region ab.
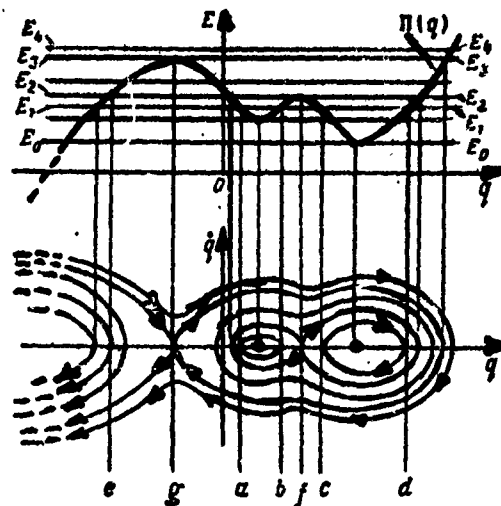
Figure 7.3. Phase trajectories of
periodic motions of a system with
different energy levels.

Further increase of the system energy leads to merging of zones
ab and cd. The phase trajectory becomes a curve surrounding both
zones. The motion on this segment retains the stable periodic motion
form, but the velocity varies in a complex fashion within the limits
of a period. The system oscillates, jumping from zone ab into zone
cd and back.

For the energy level E_3, corresponding to the second maximum
of the potential function, an unstable position q_g again appears in
the system. From the position q_g the system can perform periodic
motion, but it can also move out into the region of the runaway
trajectory.

If excessive energy (more than E_3) is imparted to the system,
it becomes unstable, since the system departs along a runaway
trajectory from any position.

This example indicates the well known relationship, which is
that an elastic system is stable in the minimum region of the

potential energy function, while in the maximum region it is unstable.

For those regions where the phase trajectory is closed, the vibration period can be found from (7.7). To this end, after separating variables we write this equation in the form

$$dt = \sqrt{\frac{m}{2}} \frac{dq}{\sqrt{E - \Pi(q)}};$$ (7.9)

Integrating in the limits from one extreme position to the other, for example, from a to b (see Figure 7.3), and doubling the result, we obtain the vibration period

$$\tau = 2\sqrt{\frac{m}{2}} \int_{q_a}^{q_b} \frac{dq}{\sqrt{E - \Pi(q)}};$$ (7.10)

the vibration period has its own value for each closed phase trajectory. In other words, the system vibration period depends on the initial conditions, which define the energy level E.

In many practical cases direct integration of (7.2) to obtain the system motion law of (7.10) to determine the vibration period is difficult, even if graphical integration methods are used. This is associated with the fact that the denominator of (7.10) vanishes at the integration limits. These problems are solved by approximate methods.

7.1.2. Free Vibrations of System with Backlash

In practice, systems with backlash are encountered quite frequently. The motion of the oscillating mass in a system with backlash consists of two parts. The first part is free motion in the limits permitted by the backlash; this motion takes place at constant velocity. The second part is the motion which arises as a result of deformations of the elastic elements of the system. In this case there is conversion of kinetic energy into deformation potential energy.

Restricting ourselves to a quadratic relationship, we write the potential energy equation in the form

$$\Pi = \frac{1}{2} c (q \mp q_0)^2, \tag{7.11}$$

where c is the system stiffness coefficient;

q_0 is the free displacement, corresponding to half the backlash. The minus sign is taken for $q > q_0$; the plus sign, for $q < q_0$.

Substituting (7.11) into (7.2), we obtain

$$m\dot{q}^2 + c(q \mp q_0)^2 = 2E; \tag{7.12}$$

denoting

$$\frac{\dot{q}}{p} = y; \quad \frac{2E}{c} = A^2, \tag{7.13}$$

where $p = \sqrt{\frac{c}{m}}$, we obtain for $q > q_0$

$$y^2 + (q - q_0)^2 = A^2. \tag{7.14}$$

This is the equation of a circle with center at the point O' at the distance q_0 from the coordinate origin (Figure 7.4). It is valid only for half the circle, when $q > q_0$. For $q < q_0$ the mass moves freely and the phase trajectory is parallel to ᵗ q axis. The left side of the diagram, for negative displacements, is symmetric to the right side.

The phase diagram shows that the phase trajectories of the system with backlash are a family of closed curves with common pole at the center. This means that free vibrations of the system are always stable and can continue infinitely long. The vibration range depends on the magnitude of the initial energy.

The motion law is not harmonic, but consists of segments of harmonic motion and segments of constant velocity (Figure 7.5). The
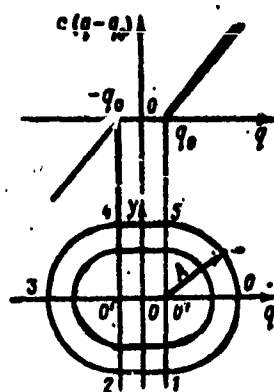
Figure 7.4. Characteristic of elastic force of system with backlash and phase trajectory of its oscillations
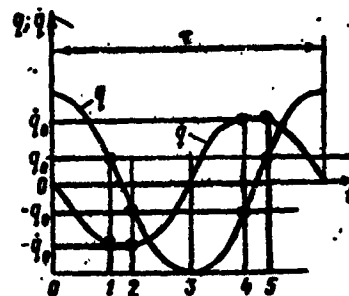
Figure 7.5. Law of motion of system with backlash.

complete period of the system vibrations is

$$\tau = \frac{2\pi}{p} + \frac{4q_0}{\dot{q}_0}. \qquad (7.15)$$

The first term of this formula is the period of the purely harmonic vibration of the system without backlash. The second term is the time required for taking up the backlash in one direction or the other at the maximal velocity $\dot{q}_0$. The latter is found from (7.12), where we set

$$q - q_0 = 0.$$

Then

$$\dot{q}_0 = \sqrt{\frac{2E}{m}} = p \sqrt{\frac{2E}{c}},$$

substituting this expression into (7.15), we obtain

$$\tau = \frac{2\pi}{p} + \frac{4q_0}{p\sqrt{\frac{2E}{c}}} = \frac{2\pi}{p} \left(1 + \frac{2q_0}{\pi\sqrt{\frac{2E}{c}}} \right). \qquad (7.16)$$

The vibration period of a system with backlash is longer than that of the system without backlash. This difference may be quite large.

For example, if the backlash is commensurate with the amplitude of
the harmonic part of the vibrations

$$2q_0 \approx \sqrt{\frac{2E}{c}} = A,$$

the vibration period increases by more than 30%. The vibration
frequency decreases correspondingly. Depending on the magnitude of
the backlash, a particular system may have different free vibration
frequencies.

7.1.3. Vibrations of System with Preload

The characteristic of the elastic force of a system with preload
is shown in Figure 7.6. The characteristic may be asymmetric
relative to zero. Such systems are
frequently encountered in machinery
in the form of special devices.
Examples are flexible couplings,
elastic supports, and under-torqued
connections.
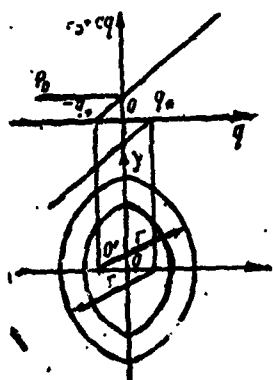
Figure 7.6. Characteristic
of elastic force of system
with preload and phase
trajectory of system
oscillations.

The system potential energy is
defined by the function

$$\Pi = P_0 q + \frac{1}{2} c q^2,$$

where P_0 is the preload force;

   c is the stiffness of the
   elastic elements.

The phase trajectory equation of a half-period will be

$$m\dot{q}^2 + 2P_0 q + cq^2 = 2E. \tag{7.17}$$

Denoting

$$\frac{\dot{q}}{p} = y; \quad (q + q_*) = x; \quad \frac{2E}{c} + q_*^2 = r^2,$$

where

$$q_* = \frac{P_0}{c}; \quad p^2 = \frac{c}{m},$$ (7.18)

we reduce (7.17) to the equation of a circle

$$y^2 + x^2 = r^2.$$

The center 0' of the circle has the coordinate $x_{0'} = -q_*$ (see Figure 7.6).

The curve for the second half-period is symmetric to that for the first half. The two circles intersect on the diagram axis.

All the phase trajectories are formed by concentric arcs drawn from the centers 0' and are closed curves. This indicates that the system vibrations are stable. The vibration period is defined by the formula

$$\tau = \frac{2}{p} \left(\pi - 2 \arcsin \frac{q_*}{r} \right).$$ (7.19)

The vibration period of the system in question is shorter than that of the linear system with the same stiffness. This means that the introduction of preload increases the natural vibration frequency. The increase may be quite large; it is determined by the ratio q_*/r. Using the notation (7.18), this ratio equals

$$\frac{q_*}{r} = \sqrt{\frac{q_*^2}{\frac{2E}{c} + q_*^2}} = \sqrt{\frac{1}{\frac{2E}{cq_*^2} + 1}} = \sqrt{\frac{1}{\frac{2E}{P_0 q_*} + 1}}.$$ (7.20)

The fraction in the denominator of (7.20) is the ratio of the energy imparted to the system at the initial moment and the elastic element pre-compression energy. For example, if this ratio equals one, in accordance with (7.19) the vibration period is reduced by a factor of two, i.e., the vibration frequency will be twice that of the linear system. The higher the system energy, i.e., the larger the

vibration range in comparison with the preload, the closer the frequency of the nonlinear system is to that of the linear system.

7.2. Small Parameter Method

The phase trajectories show that nonlinear conservative systems may perform periodic vibrations in the minimum region of the potential energy function.

According to Lyapunov's general theory, the solution of the nonlinear system vibration equation may be constructed in the form of the sum of functions arranged in a series in powers of an initial parameter

$$q(\varphi) = A\psi_1(\varphi) + A^2\psi_2(\varphi) + A^3\psi_3(\varphi) + \ldots ,$$
$$\varphi = \frac{2\pi}{T} t, \qquad (7.21)$$

where A is the initial parameter, associated with the system energy level. The amplitude q_0 (vibration range) or the maximal velocity $\dot{q}_0$ can be taken as this parameter. The parameter A must be sufficiently small in the region of the potential energy minimum. The nonlinear vibration period T is the unknown quantity. In constructing the solution, it is also represented in the form of an expansion

$$T = \frac{2\tau}{k}(1 + Ah_1 + A^2h_2 + \ldots). \qquad (7.22)$$

The coefficients h , h_2 and so on are found in the process of constructing the solution from the motion periodicity conditions. The functions ψ_1, ψ_2, ψ_3, appearing in the general construction, must satisfy the initial conditions. The latter may be taken in two forms:

a) for t = 0; ϕ = 0 we have q = q_0, $\dot{q}_0$ = 0;

then

$$q_0 = A\psi_1(0) + A^2\psi_2(0) + A^3\psi_3(0);$$
$$\dot{q}_0 = A\dot{\psi}_1(0) + A^2\dot{\psi}_2(0) + A^3\dot{\psi}_3(0) = 0;$$

hence

$$A = q_0; \quad \phi_1(0) = 1; \quad \phi_2(0) = 0; \quad \phi_3(0) = 0; \atop \dot{\phi}_1(0) = 0; \quad \dot{\phi}_2(0) = 0; \quad \dot{\phi}_3(0) = 0; \qquad (7.23)$$

b) for t = 0; ϕ = 0 we have q_0 = 0; $\dot{q}(0)$ = $\dot{q}_0$;

then

$$A\dot{\phi}_1(0) + A^2\dot{\phi}_2(0) + A^3\dot{\phi}_3(0) = 0;$$
$$\dot{q}_0 = A\dot{\phi}_1(0) + A^2\dot{\phi}_2(0) + A^3\dot{\phi}_3(0);$$

hence

$$A = \dot{q}_0; \quad \dot{\phi}_1(0) = 1; \quad \dot{\phi}_2(0) = 0; \quad \dot{\phi}_3(0) = 0; \atop \phi_1(0) = 0; \quad \phi_2(0) = 0; \quad \phi_3(0) = 0. \qquad (7.24)$$

7.2.1. Free Vibrations of Asymmetric Nonlinear Systems

In engineering problems we may encounter cases in which the characteristic of the elastic system is asymmetric relative to the center. This may occur in the case of asymmetry of the structure, in the case of differential preload of elastic elements which then operate differently in the direction of positive and negative displacements, in the case of action of weight force or acceleration force which shifts the zero point from the axis of symmetry.

For asymmetric systems the potential energy function is expressed in the form of a power-law polynomial

$$\Pi = \frac{1}{2} cq^2 + \frac{1}{3} aq^3 + \frac{1}{4} bq^4;$$

The system asymmetry is associated with the second term of the potential energy function. The larger the coefficient a, the more marked the asymmetry of the system. In the general case all the odd-power terms of the polynomial reflect the system asymmetry properties.

Substituting the function Π into the Lagrange equation, we obtain the nonlinear asymmetric system differential equation of motion

$$m\ddot{q}+cq+aq^2+bq^3=0. \qquad\qquad (7.25)$$

The phase plane method shows that the periodic solutions for
the nonlinear systems should be sought in the region of the potential
energy minimum. Therefore, before seeking the solution of the
differential equation we should analyze the function Π for minimum
and maximum.

The coordinates of the extremum of the function Π are found
from the derivative. A minimum of the function Π is located at
$q = 0$. The other two coordinates are found from the equation

$$c+aq+bq^2=0, \qquad\qquad (7.26)$$

hence

$$q=\frac{-a\pm\sqrt{a^2-4bc}}{2b}. \qquad\qquad (7.27)$$

Let us examine this solution when the coefficients a, b, c
are positive. If the asymmetry coefficient a is small, other extrema
do not exist. The form of the function $\Pi(q)$ and the elastic charac-
teristic of the system are shown in Figure 7.7a.

If a^2 > 4bc the curve $\Pi(q)$ has another minimum (see Figure
7.7b) at

$$q_{min}=-\frac{a+\sqrt{a^2-4bc}}{2b} \qquad\qquad (7.28)$$

and a single maximum at

$$q_{max}=-\frac{a-\sqrt{a^2-4bc}}{2b}. \qquad\qquad (7.29)$$

In this case the construction of the periodic solution of the
differential Equation (7.25) in the region of the first minimum may
be carried out, provided the maximal shift in the negative direction
does not exceed the coordinate defined by (7.29).
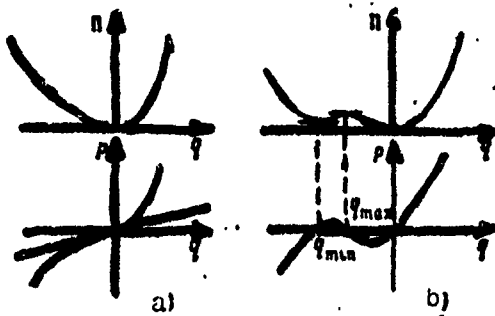
Figure 7.7. Characteristic of asymmetric systems.

We shall find the periodic solution of (7.25) in the form of an expansion in powers of the small deflection q_0. But we first divide all the terms of the equation by m

$$\ddot{q} + k^2 q + \gamma q^2 + \beta q^3 = 0, \qquad (7.30)$$

where

$$k^2 = \frac{c}{m}; \quad \gamma = \frac{a}{m}; \quad \beta = \frac{b}{m}.$$

and we refer the equation to the characteristic time. Reduction of the equation to characteristic time is accomplished by the substitution

$$\varphi = pt,$$

where p is the average circular frequency of free vibrations of the nonlinear system. This is the average angular velocity of the radius vector of the describing point on the phase trajectory

$$p = \frac{2\pi}{T},$$

where T is the vibration period.

As a result of nonharmonicity of the vibrations, the true angular velocity of the radius vector differs from the average value.

The time derivatives are replaced

$$\dot{q} = \frac{dq}{d\varphi} \frac{d\varphi}{dt} = p \frac{dq}{d\varphi};$$

similarly

$$\ddot{q} = p^2 \frac{d^2 q}{d\varphi^2}.$$

Equation (7.30) takes the form

$$\frac{d^2q}{d\varphi^2} + \frac{k^2}{p^2} q + \frac{\gamma}{p^2} q^2 + \frac{\zeta}{p^2} q^3 = 0. \tag{7.31}$$

In accordance with Lyapunov's theory and Krylov's method, limiting the solution of the equation to three terms, we construct the solution in the form of a sum in powers of the small parameter q_0

$$q(\varphi) = q_0 \psi_1(\varphi) + q_0^2 \psi_2(\varphi) + q_0^3 \psi_3(\varphi). \tag{7.32}$$

In the following we take the conditions (7.23) as the initial conditions for the sought solutions.

At the same time, as suggested by Drylov, we represent the circular frequency in the form of the expansion

$$p^2 = k^2 + q_0 h_1 + q_0^2 h_2; \tag{7.33}$$

hence

$$\frac{k^2}{p^2} = 1 - \frac{h_1}{p^2} q_0 - \frac{h_2}{p^2} q_0^2.$$

The coefficients h_1, h_2 are to be determined. We note that they are dimensional.

We substitute (7.32) and (7.33) into the differential Equation (7.31) and, collecting terms with the same powers of q_0, we obtain the equations

$$\left.\begin{array}{l} \psi_1^{\cdot\cdot} + \psi_1 = 0; \\[4pt] \psi_2^{\cdot\cdot} + \psi_2 = \frac{h_1}{p^2} \psi_1 - \frac{\gamma}{p^2} \psi_1^2; \\[4pt] \psi_3^{\cdot\cdot} + \psi_3 = \frac{h_1}{p^2} \psi_2 + \frac{h_2}{p^2} \psi_1 - \frac{\zeta}{p^2} \psi_1^3 - 2 \frac{\gamma}{p^2} \psi_1 \psi_2. \end{array}\right\} \tag{7.34}$$

In accordance with the initial conditions (7.23), we obtain from the first equation

$$\psi_1 = \cos\varphi \tag{7.35}$$

After substituting this value of ψ_1 into the second equation, it takes the form

$$\psi_2'' + \psi_2 = \frac{h_1}{\rho^2}\cos\varphi - \frac{Y}{\rho^2}\cos^2\varphi.$$

The solution of this equation is composed of the general solution of the homogeneous equation and the particular solutions

$$\psi_2 = C_1\cos\varphi + C_2\sin\varphi + B_1\varphi\sin\varphi + B_0 + B_2\cos 2\varphi,$$

where

$$B_1 = \frac{h_1}{2\rho^2}; \quad B_0 = -\frac{Y}{2\rho^2}; \quad B_2 = \frac{Y}{6\rho^2}. \tag{7.36}$$

To avoid the nonperiodic solution, which does not correspond to periodic motion of the system in question, we make use of the free coefficient h_1, setting it and therefore B_1 equal to zero. Then the solution of the equation will be

$$\psi_2 = C_1\cos\varphi + C_2\sin\varphi + B_0 + B_2\cos 2\varphi.$$

In accordance with the initial conditions $\dot\psi_2(0) = 0$; $\psi_2(0) = 0$, we obtain $C_2 = 0$ and also $C_1 = -(B_0 + B_2)$.

The final form of the second solution will be

$$\psi_2 = B_0 - (B_0 + B_2)\cos\varphi + B_2\cos 2\varphi. \tag{7.37}$$

Substituting ψ_1 and ψ_2 into the third equation (7.34), we obtain this equation in the form

$$\psi_3'' + \psi_3 = \frac{h_2}{\rho^2}\cos\varphi - \frac{3}{\rho^3}\cos^3\varphi - 2\frac{Y}{\rho^2}\psi_2\cos\varphi.$$

We replace

$$\cos^3\varphi=\frac{1}{4}(3\cos\varphi+\cos3\varphi);$$

$$\cos^2\varphi=\frac{1}{2}(1+\cos2\varphi);$$

$$\cos\varphi\cos2\varphi=\frac{1}{2}(\cos\varphi+\cos3\varphi);$$

after this we obtain

$$\ddot{\psi}_2+\psi_2=\left[\frac{h_2}{p^2}-\frac{3}{4}\frac{\beta}{p^2}-2\frac{\gamma}{p^2}\left(B_0+\frac{1}{2}B_2\right)\right]\cos\varphi+$$
$$+\frac{\gamma}{p^2}(B_0+B_2)(1+\cos2\varphi)-\left(\frac{\beta}{4p^2}+\frac{\gamma}{p^2}B_2\right)\cos3\varphi. \qquad (7.38)$$

The particular solution of this equation contains a term with the factor

$$\psi_2=D_0+D_1\varphi\sin\varphi+D_2\cos2\varphi+D_3\cos3\varphi. \qquad (7.39)$$

Substitution of the solution (7.39) into the differential Equation (7.38) permits finding the coefficients

$$\left.\begin{array}{l} D_0=\frac{\gamma}{p^2}(B_0+B_2);\quad D_2=-\frac{1}{3}D_0;\\[2mm] D_1=\frac{1}{2}\left(\frac{h_2}{p^2}-\frac{3}{4}\frac{\beta}{p^2}-2\frac{\gamma}{p^2}\left(B_0+\frac{1}{2}B_2\right)\right];\\[2mm] D_3=\frac{1}{8}\left(\frac{\beta}{4p^2}+\frac{\gamma}{p^2}B_2\right). \end{array}\right\} \qquad (7.40)$$

To exclude the secular term from the solution (7.39), we equate D_1 to zero, which yields

$$h_2=\frac{3}{4}\beta+2\gamma\left(B_0+\frac{1}{2}B_2\right); \qquad (7.41)$$

The complete solution of the equation will be

$$\psi_2=C_3\cos\varphi+C_4\sin\varphi+D_0\left(1-\frac{1}{3}\cos2\varphi\right)+D_3\cos3\varphi.$$

In accordance with the initial conditions

$$\psi_2(0)=0;\quad \dot{\psi}_2(0)=0;$$

therefore

$$C_3 = -\left(\frac{2}{3} D_0 + D_3\right); \quad C_4 = 0;$$

and finally

$$\psi_3 = D_0\left(1 - \frac{1}{3}\cos 2\varphi\right) - \left(\frac{2}{3}D_0 + D_3\right)\cos\varphi + D_3\cos 3\varphi. \tag{7.42}$$

Restricting ourselves to the terms found for the expansion, we write the general solution of (7.31)

$$q(\varphi) = q_0\cos\varphi + q_0^2[B_0 - (B_0 + B_2)\cos\varphi + B_2\cos 2\varphi] +$$
$$+ q_0^3\left[D_0\left(1 - \frac{1}{3}\cos 2\varphi\right) - \left(\frac{2}{3}D_0 + D_3\right)\cos\varphi + D_3\cos 3\varphi\right]; \tag{7.43}$$

To convert to the time t in the solution, we must make the substitution $\phi = pt$.

In accordance with (7.33), the average circular frequency is

$$p^2 = k^2 + q_0^2\left[\frac{3}{4}\beta + 2\gamma\left(B_0 + \frac{1}{2}B_2\right)\right]. \tag{7.44}$$

p^2 appears in the denominator of the formulas for the coefficients B_0 and B_2. Therefore, the calculation of p^2 using (7.44) is made by successive approximation. We substitute k^2 in place of p^2 in the right side of the formula and then make a refinement.

7.2.2. Free Vibrations of Symmetric System

If there is no system asymmetry, then a = 0 and the governing differential equation takes the form

$$m\ddot{q} + cq + bq^3 = 0;$$

in this equation the nonlinearity is represented by a single term with the small parameter b.

The solution of this equation is obtained from (7.43) if therein we set $\gamma = 0$. Then $B_0 = B_2 = 0$. Therefore, $D_0 = D_2 = 0; \; D_3 = \beta/32p^2$

and the solutions will be

$$q(\varphi) = q_0 \cos\varphi + q_0^3 \frac{\beta}{32p^2}(\cos 3\varphi - \cos\varphi); \qquad (7.45)$$

$$p^2 = k^2 + \frac{3}{4}\beta q_0^2. \qquad (7.46)$$

The vibrations differ from harmonic vibrations by a small quantity which is proportional to the cube of the small deflection q_0. This quantity is a third-order harmonic.

The average circular frequency p is greater than the harmonic oscillator natural frequency k by some magnitude. The larger the nonlinearity coefficient β, the more the periodic vibrations differ from harmonic vibrations.

7.2.3. Case of Negative Coefficient β

The system potential energy corresponding to a negative value of β is expressed by the function

$$\Pi(q) = \frac{1}{2}k^2q^2 - \frac{1}{4}\beta q^4. \qquad (7.47)$$

The potential energy and elastic force characteristics of the system are shown in Figure 7.8. The so-called soft springs used in various devices have such characteristics.

Taking the derivative of Π and equating it to zero, we find the displacements q for which the potential energy has minimal and maximal values.

The potential energy has a minimum for q = 0. In the region of this minimum the subject system may have periodic motion. For a displacement reaching the magnitude

$$q_{max} = \frac{k}{\sqrt{\beta}}.$$
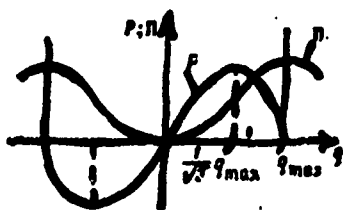
Figure 7.8. Nonlinear "soft" characteristic.

the potential energy has a maximum. This is the limit of the stable periodic motion.

If the vibration amplitude is significantly less than these limits, (7.45) and (7.46) can be used to find the displacement function and the frequency function, altering the signs of the terms containing β in these expressions. Then we obtain

$$q(pt) = q_0 \cos \cdots - q_0^3 \frac{1}{32} \frac{\beta}{p^2} (\cos 3pt - \cos pt); \qquad (7.48)$$

$$p^2 = k^2 - \frac{3}{4} q_0^2 \beta. \qquad (7.49)$$

Formula (7.49) shows that, for elastic systems having a soft characteristic, increase of the free vibration amplitudes is accomplished by reduction of the frequency, i.e., increase of the vibration period.

Figure 7.9 shows the vibration period as a function of vibration amplitude, expressed as a fraction of its maximal value. The increase of the vibration period because of the presence of the soft nonlinearity of the system for amplitudes significantly less than the stability limit lies in the range of 10%.

7.3. Forced Vibrations of Nonlinear System Subject to Harmonic Force

The equations of forced vibrations of nonlinear systems must be examined in their complete form, and we must seek directly the general solutions satisfying both the equations themselves and the boundary and initial conditions. Here the superpositioning method for finding the general solution is not applicable because of the system nonlinearity. Specifically, if the disturbing force, i.e., the right side of the equation, is represented in the form of a

Fourier series expansion, then in view of the nonlinearity we cannot write the general solution in the form of a sum consisting of individual particular solutions obtained independently for each separate harmonic of the exciting force. An integrated solution must be sought.

The exact solutions of nonlinear equations cannot be obtained; therefore, the solutions are constructed in the form of approximations. The solution methods are based on the general principles of mechanics. The variational methods based on the Ostrogradskiy-Hamilton general principle of possible displacements are quite effective. These include the Ritz and Bubnov-Galerkin methods.

7.3.1. Bubnov-Galerkin Method

We examine the equation of motion in the form

$$m\ddot{q} + cq + bq^3 = H \cos \omega t. \tag{7.50}$$

By the substitution

$$\varphi = \omega t$$

(7.50) is put into the form

$$\omega^2 \frac{d^2 q}{d\varphi^2} + k^2 q + \lambda q^3 = h \cos \varphi. \tag{7.51}$$

The Galerkin variational equation for the subject problem will have the form

$$\int_0^{2\pi} (\omega^2 q'' + k^2 q + \lambda q^3 - h \cos \varphi) \, \lambda q \, d\varphi = 0. \tag{7.52}$$

The minimizing function is written in the form of a linear sum of functions, termed basis functions

$$q(\varphi) = \sum_{i=1}^{s} a_i \vartheta_i (\varphi). \tag{7.53}$$
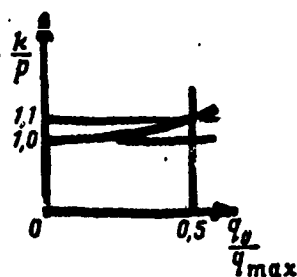
Figure 7.9. Increase of vibration period with increase of vibration amplitude for a "soft" characteristic.

Each of the functions must be periodic, a multiple of the forced vibration period, must satisfy the initial conditions, and must correspond as exactly as possible to the assumed solution form. Moreover, we must bear in mind that we should not try to use a large number of basis functions, since this leads to the necessity of solving a complex system of nonlinear algebraic equations.

The parameter α_1 is found by substituting the minimizing function into the Galerkin integral and then solving.

We compose a minimizing function of two terms

$$q = \alpha_1 \cos \varphi + \alpha_2 \cos 3\varphi; \qquad (7.54)$$

here we have selected functions of odd order. Functions of even order are excluded.

Substituting (7.54) into (7.52), we obtain the Bubnov-Galerkin variational equations in the form

$$\int_0^{2\pi} [-\omega^2(\alpha_1 \cos \varphi + 9\alpha_2 \cos 3\varphi) + k^2(\alpha_1 \cos \varphi +$$

$$+ \alpha_2 \cos 3\varphi) + \beta(\alpha_1 \cos \varphi + \alpha_2 \cos 3\varphi)^3 - k \cos \varphi](\delta \alpha_1 \cos \varphi +$$

$$+ \delta \alpha_2 \cos 3\varphi) d\varphi = 0.$$

By virtue of the independence of the variations of the parameters α_1 and α_2, this equation breaks down into two equations which are written in the form

$$\int_0^{2\pi} \{[(k^2 - \omega^2)\alpha_1 - k] \cos \varphi + (k^2 - 9\omega^2)\alpha_2 \cos 3\varphi +$$

$$+ \beta(\alpha_1 \cos \varphi + \alpha_2 \cos 3\varphi)^3\} \cos \varphi \, d\varphi = 0;$$

$$\int_0^{2\pi} \{[(k^2 - \omega^2)\alpha_1 - h]\cos\varphi + (k^2 - 9\omega^2)\alpha_2\cos 3\varphi +$$

$$+ \beta(\alpha_1\cos\varphi + \alpha_2\cos 3\varphi)^3\}\cos 3\varphi\, d\varphi = 0.$$

Integration of the equations and substitution of the limits leads to two algebraic equations

$$\left.\begin{aligned}
&\alpha_1(k^2 - \omega^2) + \beta\,\tfrac{3}{4}(\alpha_1^3 + \alpha_1^2\alpha_2 + 2\alpha_1\alpha_2^2) - h = 0; \\
&\alpha_2(k^2 - 9\omega^2) + \beta\,\tfrac{3}{4}(\alpha_1^3 + 3\alpha_1^2\alpha_2 + 3\alpha_2^3) = 0.
\end{aligned}\right\} \qquad (7.55)$$

The solution of these equations yields the parameters α_1 and α_2. The magnitude of the parameters and their relationship depend on the amplitude and frequency of the forced vibrations, on the magnitude of the coefficients k^2 and β.

If we take as the minimizing function only a single term

$$q = \alpha_1\cos\varphi, \qquad (7.56)$$

after substituting this term into the variational equation we obtain

$$\alpha_1(k^2 - \omega^2) + \tfrac{3}{4}\beta\alpha_1^3 = h. \qquad (7.57)$$

Equation (7.57) permits determining in the first approximation the amplitude α_1 of the nonlinear forced vibrations. The solution of (7.57) can be represented graphically. To do this we write the equation as

$$\alpha_1 k^2 + \tfrac{3}{4}\beta\alpha_1^3 = h + \omega^2\alpha_1, \qquad (7.58)$$

and plot the functions α_1 expressed by the left and right sides of (7.58) (Figure 7.10a). The left side of (7.58) yields a third-order curve, whose parameters are k^2 and β. This curve is not the elastic characteristic of the system, but is close to it (the elastic characteristic has the equation $k^2 q + \beta q^3$).

The right side of (7.58) is a straight line which intersects the ordinate axis at the point with coordinate h and has the slope
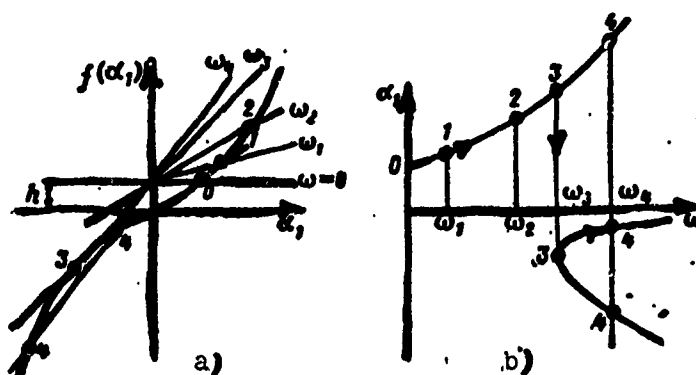
Figure 7.10. Forced vibration amplitude
versus nonlinear system vibration frequency.

ω^2. The larger ω^2, the steeper the straight line; in the limit it
approaches $\pi/2$.

The point of intersection of the curve and line described
above yields the amplitude of the forced vibrations. For a low
frequency ω of the forced vibrations, there is only a single point
of intersection, i.e., the ar-itude of the forced vibrations is
uniquely defined (the other t. oots of the equation are imaginary).
For some value of the frequency ω there appear three points of inter-
section — one for a positive value of the amplitude α_1 and two for
a negative value. For a given frequency ω, the system can vibrate only
with one of these three amplitude values. The stable vibrations are
those for which the system energy is minimal, i.e., vibrations with
the smallest amplitude.

Figure 7.10,b shows the forced vibration amplitude as a function
of the disturbing force frequency. The curves shown in the figure
can be constructed either directly from (7.57) or by graphical
construction. The arrows on the curves show the nature of the
amplitude variation with increase of the frequency.

An abrupt amplitude change takes place at a quite definite
value of the frequency, which we shall term the critical frequency.

At the critical frequency, both the magnitude and sign of the amplitude change abruptly. This means that the vibrations are in phase opposition with the disturbing force. Thus, for excitation of the system by frequencies below the critical value, the vibrations are in-phase with the exciting force and their amplitude increases with increase of the frequency. For excitation of the system by frequencies above the critical value, the vibrations take place in phase opposition with the force and as the frequency increases the vibration amplitudes decrease, approaching zero in the limit.

This dependence of the vibration amplitudes on the excitation frequency is confirmed well by experiments. The only experimental difference is the instability of the moment of system transition from the subcritical regime to the supercritical regime and vice versa. As a rule there is some lag — with increasing vibration frequency the transition takes place at the frequency $\omega' > \omega_{cr}$ (Figure 7.11), while with decreasing frequency the transition from supercritical to subcritical regimes takes place at the frequency $\omega'' < \omega'$.

We note that the amplitude-frequency characteristic plotted using (7.57) is not exact for frequencies close to zero. For $\omega = 0$ the static force h causes elastic defromation and is balanced only by the elastic force, which corresponds to the equilibrium equation

$$\alpha_1 k^2 + \beta \alpha_1^3 = h. \tag{7.59}$$

This equality differs from (7.57) in the coefficient multiplying β.

A significant change in the amplitude-frequency characteristic takes place with change of the amplitude of the disturbing force.

Figure 7.12 shows the characteristics for different magnitudes of the disturbing force amplitudes. The curves for the subcritical and supercritical regimes are plotted without account for the sign.
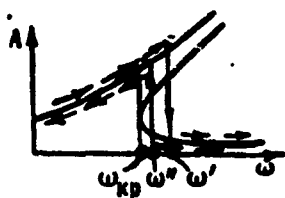
Figure 7.11. Experimental curve of passage through critical regime.
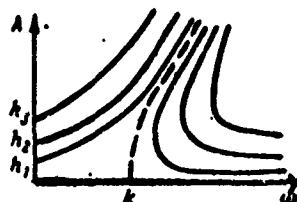
Figure 7.12. Vibration characteristics of nonlinear system as a function of perturbing force amplitude.

Setting h = 0, we can use (7.57) to construct the dependence of the amplitudes on the vibration frequency (dashed curve)

$$k^2 + \frac{3}{4}\beta a_1^2 = \omega^2.$$

This will be the characteristic of the nonlinear free vibrations. All the curves located to the left of the dashed curve correspond to subcritical regimes; the curves lying to the right of the dashed curve correspond to the supercritical vibration regimes, where the vibrations are in phase opposition with the force.

As the disturbing force amplitude increases, the curves shift away from the dashed curve; at the same time the critical frequency increases. This shows that in the nonlinear system there is no stable value of the critical frequency, upon reaching which the system transitions into the phase-opposition vibration regime. The critical frequency depends on the amplitude value of the disturbing force.

According to (7.46) the frequency of the nonlinear free vibrations is

$$k^2 + \frac{3}{4}\beta a_1^2 = p^2.$$

This equality makes it possible to write (7.58) in the form

$$a_1 p^2 = h + \omega^2 a_1. \qquad (7.60)$$

Hence, we obtain the very important conclusion: the forced vibration amplitude of a nonlinear system for small disturbing force amplitude ($h \to 0$) is equal to the free vibration amplitude for the frequency $p = \omega$.

For the calculation of forced vibrations, this conclusion makes it possible to use (7.46), derived to calculate free vibrations of nonlinear systems, and avoids the necessity for solving the equations with right sides in these cases.

CHAPTER 8

VIBRATIONS ON ELASTIC SUPPORTS
WITH BACKLASH

8.1. Differential Equations of Motion

The displacement of a mass on a horizontal shaft resting on elastic supports with backlash (Figure 8.1) is determined by the magnitude of this backlash and by the elastic deformations of the supports and the shaft itself.

Let us examine the general case of free vibrations when the weight force acts on the mass. This arrangement can be replaced by the system shown in Figure 8.2. We assume the stiffness of the pendulum's elastic support to be linear and axisymmetric. The pendulum length l is equal to half the total backlash. We represent the pendulum as a filament which does not absorb compressive forces. The pendulum can execute circular or oscillatory motions.

The characteristic of the elastic system is shown in Figure 8.2.

The system potential energy is defined by the formula
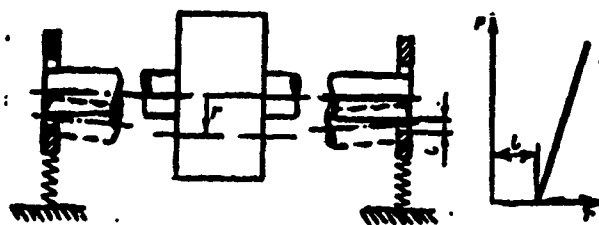
Figure 8.1. Horizontal shaft on elastic supports with backlash.

$$\Pi = \frac{1}{2} c (x_0^2 + y_0^2) + mq [l(1 - \cos \varphi) - x_0], \qquad (8.1)$$

where c is the support stiffness coefficient;

x_0, y_0 are the suspension point displacements owing to support elastic deformation.

We have the obvious connection between the coordinates x_0, y_0 of the suspension point and the coordinates x, y of the mass center

$$\left. \begin{array}{l} x = x_0 + l \cos \varphi; \\ y = y_0 + l \sin \varphi. \end{array} \right\} \qquad (8.2)$$

The potential energy is referred to the position $x_0 = y_0 = \phi = 0$.

The system kinetic energy is

$$T = \frac{1}{2} m (\dot{x}^2 + \dot{y}^2). \qquad (8.3)$$

Substituting the expressions for the potential and kinetic energies into the Lagrange equation, we obtain the differential equations of motion

$$\left. \begin{array}{l} \ddot{x}_0 - \ddot{\varphi} l \sin \varphi - \dot{\varphi}^2 l \cos \varphi + p^2 x_0 - g = 0; \\ \ddot{y}_0 + \ddot{\varphi} l \cos \varphi - \dot{\varphi}^2 l \sin \varphi + p^2 y_0 = 0; \\ \ddot{x}_0 \sin \varphi - \ddot{y}_0 \cos \varphi - l \ddot{\varphi} - g \sin \varphi = 0, \end{array} \right\} \qquad (8.4)$$

where $p^2 = \frac{c}{m}$.

Multiplying the first equation by sin ϕ, the second by cos ϕ, and subtracting the second from the first, we obtain

$$\ddot{x}_0 \sin\varphi - \ddot{y}_0 \cos\varphi - \ddot{\psi}l + p^2(x_0\sin\varphi - y_0\cos\varphi) - g\sin\varphi = 0;$$

Substracting from this expression the third Equation (7.4), we obtain the condition

$$x_0 \sin\varphi - y_0\cos\varphi = 0, \quad \text{or} \quad \frac{y_0}{x_0} = \text{tg}\,\varphi. \tag{8.5}$$

This condition shows that the displacement of the suspension point always coincides with the direction of the pendulum motion, i.e., $\phi = \theta$. This reduces the problem to the requirement for solution of the first two Equation (8.4), which we represent in a different form by excluding the angle ϕ.

We differentiate the equalities (8.2) twice and substitute the resulting expressions into (8.4), after which we obtain

$$\left.\begin{array}{l} \ddot{x} + p^2 x_0 - g = 0; \\ \ddot{y} + p^2 y_0 = 0; \end{array}\right\} \tag{8.6}$$

which is the simplest form of tne differential equations of motion of a pendulum on an elastic suspension, where the displacements of the suspension and of the mass m are connected with the position of the pendulum by the condition (8.5)

$$\frac{y_0}{x_0} = \frac{l}{x} = \text{tg}\,\varphi. \tag{8.7}$$

Equations (8.6) in projections on the moving axes ξ and η (Figure 8.3) have the form

$$\ddot{r}_0 - (r_0 + l)\dot{\varphi}^2 + p^2 r_0 - g\cos\varphi = 0; \tag{8.8}$$

$$(r_0 + l)\ddot{\varphi} + 2\dot{\varphi}\dot{r}_0 + g\sin\varphi = 0. \tag{8.9}$$
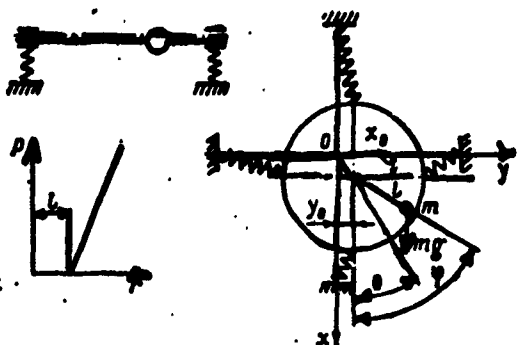
Figure 8.2. General scheme of vibrations of shaft on elastic supports with backlash.
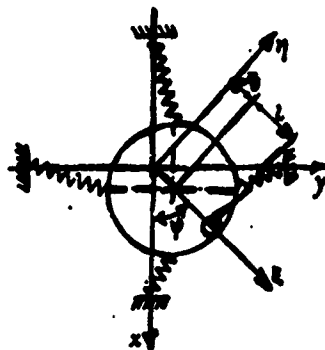
Figure 8.3. Illustrating derivation of vibration equations in moving axes.

The first equation is the condition for equilibrium of the radial forces, and the second is the condition for equilibrium of the forces perpendicular to the pendulum axis, applied to the mass m.

Before solving the resulting equations, we note that the shaft resting on elastic supports with backlash may execute pendulous oscillations or may execute continuous circular motion.

There is a discontinuous form of motion between the first and second forms of motion. This is the result of the existence of backlash in the supports and by the flexible filament of the pendulum. When the filament tension reaches zero and changes its sign, the connection is lost between the moving mass and the supporting system, the mass travels freely for some time with subsequent impact restoration of the connection. The conditions under which this motion develops are defined later.

8.2. Free Pendulous Vibrations of Shaft on Rigid Supports with Backlash

Setting $r_0 = 0$, we obtain two equations from (8.8) and (8.9)

$$l\dot{\varphi}^2 + g\cos\varphi = 0;$$
$$l\ddot{\varphi} + g\sin\varphi = 0, \qquad (8.10)$$

where l is the radial clearance for the shaft and the length for the pendulum.

The first Equation (8.10) yields the boundaries of stable motion in the presence of backlash. It defines the magnitude of the pendulum string tension or the force created by the shaft on the support. This equation can be written in the more general form

$$P = ml\dot{\varphi}^2 + mg\cos\varphi > 0,$$

where P is the force acting on the support. Hence, we obtain the condition

$$l\dot{\varphi}^2 + g\cos\varphi > 0. \qquad (8.11)$$

If the shaft performs oscillatory motion in the supports, in the extreme position $\dot{\varphi} = 0$. Then the condition for unseparated motion takes the form

$$\cos\varphi > 0; \qquad (8.12)$$

this means that unseparated motion is maintained for vibration amplitudes in the range $\pm \pi/2$.

If the vibration amplitudes are greater than $\pi/2$, contact between the shaft and the journal is lost and the shaft will move freely for some time.

If the shaft performs circular motion, the following condition must be satisfied for the upper point $\varphi = \pi$

$$\dot{\varphi}_{min} > \sqrt{\frac{g}{l}}, \qquad (8.13)$$

i.e., for unseparated motion the angular velocity of the precessional motion of the shaft at any moment of time must be greater than the circular frequency of the pendulous oscillations.

Equating the pendulum energy for the upper and lower points

$$\frac{1}{2} m l^2 \dot{\varphi}^2_{min} + 2mql = \frac{1}{2} m l^2 \dot{\varphi}^2_{max}, \tag{8.14}$$

we obtain with account for (8.13)

$$\dot{\varphi}^2_{max} > 5 \frac{g}{l}, \tag{8.15}$$

i.e., for the existence of circular motion of the pendulum its maximal angular velocity must exceed by more than a factor of two the circular frequency of the pendulous oscillations.

The second Equation (8.10) is the conventional pendulum equation. For small vibration amplitudes, when we can take sin $\phi = \phi$, the equation becomes linear

$$\ddot{\varphi} + \frac{g}{l} \varphi = 0, \tag{8.16}$$

having the solution

$$\varphi = A \cos kt, \text{ where } k = \sqrt{\frac{g}{l}}.$$

For large amplitudes the second Equation (8.10) for the system vibrations is nonlinear. To solve this equation, sin ϕ is replaced by its power series expansion

$$\sin \varphi = a_0 + a_1 \varphi + a_2 \varphi^2 + a_3 \varphi^3 + \ldots$$

The power series coefficients in the region $\phi = 0$ are found by sequential differentiation

$$(\sin \varphi)' = \cos \varphi = a_1 + 2a_2 \varphi + 3a_3 \varphi^2;$$
$$(\sin \varphi)'' = -\sin \varphi = 2a_2 + 6a_3 \varphi;$$
$$(\sin \varphi)''' = -\cos \varphi = 6a_3;$$

Substituting herein $\phi = 0$, we obtain

$$a_0 = 0; \quad a_1 = 1; \quad a_2 = 0; \quad a_3 = -\frac{1}{6}.$$

Then, to within the third term of the expansion, we obtain

$$\sin \varphi = \varphi - \frac{1}{6} \varphi^3; \tag{8.17}$$

the expansion yields adequate accuracy for vibration amplitudes up to $\pm \pi/3$.

The second Equation (8.10) takes the form

$$\ddot{\varphi} + \frac{g}{l}\left(\varphi - \frac{1}{6}\varphi^3\right) = 0. \tag{8.18}$$

The solution of this equation can be obtained by the Krylov method. To this end, without reducing the equation to characteristic time, we write the solution in expansion form

$$\varphi = A\varphi_1 + A^2\varphi_2 + A^3\varphi_3. \tag{8.19}$$

We also represent the nonlinear vibration frequency in the form of a sum

$$p^2 = \frac{g}{l} + Ah_1 + A^2h_2. \tag{8.20}$$

Substituting this expression into the differential Equation (8.18), we obtain

$$A\ddot{\varphi}_1 + A^2\ddot{\varphi}_2 + A^3\ddot{\varphi}_3 + (p^2 - Ah_1 - A^2h_2) \times$$
$$\times \left[A\varphi_1 + A^2\varphi_2 + A^3\varphi_3 - \frac{1}{6}(A\varphi_1 + A^2\varphi_2 + A^3\varphi_3)^3\right] = 0.$$

Collecting terms with the same power of A, we obtain a system of recurrence differential equations

$$\ddot{\phi}_1 + p^2\phi_1 = 0;$$
$$\ddot{\phi}_2 + p^2\phi_2 = h_1\phi_1;$$
$$\ddot{\phi}_3 + p^2\phi_3 = h_1\phi_2 + h_2\phi_1 + \frac{1}{6}p^2\phi_1^3. \qquad (8.21)$$

The solutions of all the equations must satisfy the initial conditions

$$\phi_1(0) = 1; \quad \dot{\phi}_1(0) = 0;$$
$$\phi_2(0) = 0; \quad \dot{\phi}_2(0) = 0;$$
$$\phi_3(0) = 0; \quad \dot{\phi}_3(0) = 0. \qquad (8.22)$$

Accordingly, the solution of the first Equation (8.21) will be

$$\phi_1 = \cos pt. \qquad (8.23)$$

To avoid obtaining a secular term, in the solution of the second Equation (8.21) we must set $h_1 = 0$ and the initial conditions lead to the solution

$$\phi_2 = 0. \qquad (8.24)$$

The third Equation (8.21), after substituting therein the preceding solutions, takes the form

$$\ddot{\phi}_3 + p^2\phi_3 = h_2 \cos pt + \frac{1}{6}p^2\cos^3 pt.$$

Using the substitution

$$\cos^3 pt = \frac{1}{4}(\cos 3pt + 3\cos pt),$$

we obtain

$$\ddot{\phi}_3 + p^2\phi_3 = \left(h_2 + \frac{1}{8}p^2\right)\cos pt + \frac{1}{24}p^2\cos 3pt; \qquad (8.25)$$

As before, here we must set

$$h_2 + \frac{1}{8}p^2 = 0; \quad \text{hence} \quad h_2 = -\frac{1}{8}p^2. \qquad (8.26)$$

Then

$$\psi_3 = C_1 \cos pt + C_2 \sin pt - \frac{1}{192} \cos 3pt.$$

In accordance with the initial conditions (8.22)

$$C_1 = \frac{1}{192}; \quad C_2 = 0;$$

then

$$\psi_3 = \frac{1}{192} (\cos pt - \cos 3pt). \tag{8.27}$$

The general solution of (8.18), to within the first two terms of the expansion, is written in the form of the sum

$$\varphi = A \cos pt + \frac{A^3}{192} (\cos pt - \cos pt). \tag{8.28}$$

The frequency of the nonlinear vibrations is found from the equality formulated in accordance with (8.20)

$$p^2 \left(1 + \frac{1}{8} A^2\right) = \frac{g}{l}. \tag{8.29}$$

Hence, we see that nonlinearity of the system leads to reduction of the vibration frequency. However, we note that this frequency change is very slight. For example, for A = π/4

$$p = 0.963 \sqrt{\frac{g}{l}}.$$

i.e., a frequency reduction of about 4% for very large amplitude of the pendulous oscillations.

8.3. Forced Pendulous Vibrations of Shaft on Elastic Supports with Backlash

As before, in examining free vibrations we replace the shaft resting on elastic supports with clearance by a pendulum with elastic filament.

Forced vibrations of a shaft in a support arise under the action of an unbalanced force. Therefore, we examine vibrations of the pendulum under the action of a circular force, represented by the vector H rotating with the constant angular velocity ω (Figure 8.4).
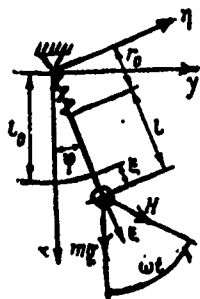
Figure 8.4. Forced oscillations of pendulum under the action of circular vector.

The basic equations are (8.8) and (8.9), which are complemented by a right side

$$(r_0+l)\ddot{\varphi}+2\dot{\varphi}\dot{r}_0+g\sin\varphi=h\sin(\omega t-\varphi); \quad (8.30)$$

$$\ddot{r}_0-(r_0+l)\dot{\varphi}^2+p^2r_0-g\cos\varphi=h\cos(\omega t-\varphi). \quad (8.31)$$

We represent the length of the elastic pendulum in motion in the form of the sum

$$r_0+l=l_0+\xi, \qquad (8.32)$$

where l_0 is the pendulum length in the static state

$$l_0=l+\xi_{cr};$$

ξ_{st} is the elongation under the action of the weight force

$$\xi_{cr}=\frac{mg}{e}; \qquad (8.33)$$

l is the filament length or support backlash;

ξ is a variable which is a function of φ.

We substitute (8.32) into (8.30) and (8.31); we then expand the right sides as the sine and cosine of the difference of the angles and replace sin φ and cos φ by their expansions in powers of φ

$$\sin\varphi = \varphi - \frac{1}{6}\varphi^3;$$
$$\cos\varphi = 1 - \frac{1}{2}\varphi^2.$$

After this, the equations take the form

$$(l_0+l)\ddot{\varphi} + 2\dot{\eta}\dot{\xi} + g\left(\varphi - \frac{1}{6}\varphi^3\right) =$$
$$= h\left[\left(1 - \frac{1}{2}\varphi^2\right)\sin\omega t - \varphi\left(1 - \frac{1}{6}\varphi^2\right)\cos\omega t\right]; \qquad (8.34)$$

$$\ddot{\xi} - (l_0+l)\dot{\varphi}^2 + p^2\xi + \frac{1}{2}g\varphi^2 =$$
$$= h\left[\left(1 - \frac{1}{2}\varphi^2\right)\cos\omega t + \left(\varphi - \frac{1}{6}\varphi^3\right)\sin\omega t\right]. \qquad (8.35)$$

Assuming that the ratios k/ω and p/ω are not integers, we seek the solution of (8.34) and (8.35) by the small parameter method, representing them in the form of sums

$$\varphi = A\psi_1 + A^2\psi_2;$$
$$\xi = A\xi_1 + A^2\xi_2.$$

We substitute into (8.34) and (8.35)

$$(l_0 + A\xi_1 + A^2\xi_2)(A\ddot{\psi}_1 + A^2\ddot{\psi}_2) + 2(A\dot{\xi}_1 + A^2\dot{\xi}_2)(A\dot{\psi}_1 + A^2\dot{\psi}_2) +$$
$$+ g\left[A\psi_1 + A^2\psi_2 - \frac{1}{6}(A^3\psi_1^3 + \ldots)\right] =$$
$$= h\left\{\left[1 - \frac{1}{2}(A\psi_1 + A^2\psi_2)^2\right]\sin\omega t -\right.$$
$$\left. - \left[A\psi_1 + A^2\psi_2 - \frac{1}{6}(A^3\psi_1^3 + \ldots)\right]\cos\omega t\right\};$$
$$A\ddot{\xi}_1 + A^2\ddot{\xi}_2 - (l_0 + A\xi_1 + A^2\xi_2)(A\dot{\psi}_1 + A^2\dot{\psi}_2)^2 + p^2(A\xi_1 + A^2\xi_2) +$$
$$+ \frac{1}{2}g(A\psi_1 + A^2\psi_2)^2 = h\left\{\left[1 - \frac{1}{2}(A\psi_1 + A^2\psi_2)^2\right]\cos\omega t +\right.$$
$$\left. + \left[A_1\psi_1 + A^2\psi_2 - \frac{1}{6}(A_1\psi_1 + A^2\psi_2)^3\right]\sin\omega t\right\}.$$

We collect terms with the same powers of A, taking as the small parameter $A = h$

$$l_0\ddot{\psi}_1 + g\psi_1 = \sin\omega t; \qquad (8.36)$$

$$l_0\ddot{\psi}_2 + g\psi_2 = -\ddot{\psi}_1\xi_1 - 2\dot{\psi}_1\dot{\xi}_1 - \psi_1\cos\omega t; \qquad (8.37)$$

$$\ddot{\xi}_1 + p^2\xi_1 = \cos \omega t;$$ (8.38)

$$\ddot{\xi}_2 + p^2\xi_2 = l_0\dot{\varphi}_1^2 - \frac{1}{2}g\varphi_1^2 + \varphi_1 \sin \omega t.$$ (8.38)

We formulate the solutions, satisfying the periodicity conditions

$$\begin{rcases} \varphi_i(0) = \varphi_i\left(\frac{2\pi}{\omega}\right); \\[2mm] \dot{\varphi}_i(0) = \dot{\varphi}_i\left(\frac{2\pi}{\omega}\right); \end{rcases}$$ (8.40)

$$\begin{rcases} \xi_i(0) = \xi_i\left(\frac{2\pi}{\omega}\right); \\[2mm] \dot{\xi}_i(0) = \dot{\xi}_i\left(\frac{2\pi}{\omega}\right). \end{rcases}$$ (8.41)

We finally obtain for (8.36)

$$\varphi_1 = a_1 \sin \omega t,$$ (8.42)

where

$$a_1 = \frac{1}{g - l_0\omega^2} = \frac{1}{l_0(k^2 - \omega^2)}.$$

We note that the pendulum natural vibration frequency k is calculated here from the formula

$$k^2 = \sqrt{\frac{g}{l_0}},$$

where we take as the pendulum length the filament length with account for its stretching by the weight force. For the elastic support with backlash, this will be the sum of the magnitudes of the backlash and elastic deformation of the support under the action of the weight force.

For (8.38)

$$\xi_1 = b_1 \cos \omega t,$$ (8.43)

where

$$b_1 = \frac{1}{p^2 - \omega^2}.$$

We substitute (8.42) and (8.43) into (8.37)

$$I_0 \ddot{\psi}_2 + g \psi_2 = a_1 (3b_1 \omega^2 - 1) \sin \omega t \cos \omega t;$$

hence, we obtain

$$\ddot{\psi}_2 + p^2 \psi_2 = \frac{1}{2I_0} a_1 (3b_1 \omega^2 - 1) \sin 2\omega t.$$

The solution of this equation will be

$$\psi_2 = a_2 \sin 2\omega t, \qquad (8.44)$$

where

$$a_2 = \frac{1}{2I_0} a_1 \frac{3b_1 \omega^2 - 1}{k^2 - 4\omega^2}.$$

After substituting (8.42) into (8.39), the latter takes the form

$$\ddot{\xi}_2 + p^2 \xi_2 = \frac{k^2}{4I_0 (k^2 - \omega^2)^2} \left[1 + \left(4 \frac{\omega^2}{k^2} - 1 \right) \cos 2\omega t \right];$$

its solution will be

$$\xi_2 = b_2 + b_3 \cos 2\omega t, \qquad (8.45)$$

where

$$b_2 = \frac{k^2}{4p^2 I_0 (k^2 - \omega^2)^2}; \quad b_3 = \frac{4\omega^2 - k^2}{4 I_0 (k^2 - \omega^2)^2 (p^2 - 4\omega^2)}.$$

To within two terms of the expansion, the general solution of (8.34) and (8.35) is written as the sum of (8.42), (8.44) and (8.43), (8.45):

$$\varphi = a_1 h \sin \omega t + a_2 h^2 \sin 2\omega t;$$ (8.46)

$$\xi = b_1 h \cos \omega t + h^2 (b_2 + b_3 \cos 2\omega t).$$ (8.47)

The forced vibrations of the elastic pendulum are performed in the form of motions along closed trajectories. If ω is smaller than k, the trajectories will be elongated in the direction of the oscillation arc (Figure 8.5a). The larger h and the closer ω to the frequency k of the pendulous oscillations, the larger the oscillation arc. We note that (8.46) and (8.47) for the pendulum motion are valid within the limits of accuracy of the replacement of sin ϕ and cos ϕ by their expansions, which were used in solving the differential equations. In practice these formulas can be used for pendulum deflection angles which do not exceed 0.8-0.9 radians.

a)

b)
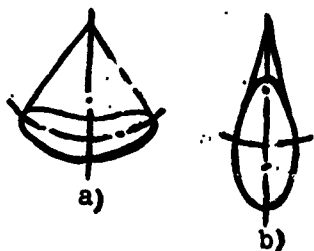
Figure 8.5. Trajectories of pendulous forced oscillations for different ratios ω/k and ω/p.

The natural frequency k of the pendulum longitudinal oscillations is larger than k. For ω close to p, the oscillation trajectory is elongated along the pendulum (see Figure 8.5b).

For forced oscillation frequencies significantly higher than p, the trajectory contracts into a circle of small radius, which approaches zero with unbounded increase of ω.

The motion trajectory remains continuous only if the condition of positive elongation of the filament is satisfied — when the amplitude of the pendulum longitudinal oscillations is less than the static elongation of the string by the weight force. This condition is defined by the following inequalities

$$b_1 h = \frac{h}{p^2 - \omega^2} < \xi_{cr} \text{ for } \omega < p;$$

$$b_1 h = \frac{h}{\omega^2 - p^2} < \xi_{cr} \text{ for } \omega > p,$$ (8.48)

where

$$t_{cr} = \frac{mg}{c} = \frac{g}{p^2};$$

from which we obtain

$$\left| \frac{h}{1 - \frac{\omega^2}{p^2}} \right| < g.$$
(8.49)

The inequality (8.49) makes it possible to find for a given
frequency ω the limiting value of the disturbance force for which
separated motion occurs, or from the magnitude of the force h to find
the frequency for which separation occurs.

If the disturbing force is the centrifugal force, then

$$h = e\omega^2,$$

where e is the mass eccentricity relative to the axis of rotation.

Inequality (8.49) takes the form

$$\left| \frac{e\omega^2}{1 - \frac{\omega^2}{p^2}} \right| < g;$$
(8.50)

from which we obtain the angular velocity limits for unseparated
pendulous vibrations under the influence of the centrifugal force.
Inequality (8.50) shows that for high-precision rotor balancing,
when e is close to zero, separation occurs only for angular velocities
close to p.

8.4. Circular Forced Vibrations

Circular vibrations of the pendulum-shaft can occur in two
cases:

(1) if the circular vector acting on the pendulum mass is
larger than the weight force. Then circular motion occurs immediately,

as soon as the force begins to act;

(2) if the circular vector is smaller than the weight force. Then circular motion is possible only if the pendulum is brought into the circular trajectory by some outside impulse, and the circular frequency of the force is no less than some value which depends on the magnitude of the force.

In accordance with (8.6), the circular vibration differential equations can be written in the form

$$\begin{aligned} \ddot{x} + p^2 x_0 - g &= h\cos\omega t; \\ \ddot{y} + p^2 y_0 &= h\sin\omega t. \end{aligned} \right\} \qquad (8.51)$$

In accordance with (8.6), the right sides of the equations are the projections on the x,y axes of the excitation H, rotating with the angular velocity ω. As a result of the effect of the weight force, the direction of the vector H does not coincide with the direction of the pendulum deflection. The connection between the angles is defined by the equality

$$\varphi = \omega t - \alpha. \qquad (8.52)$$

The coordinates x, x_0 and y, y_0 are connected with one another by the formulas

$$\begin{aligned} x_0 &= x - l\cos\varphi; \\ y_0 &= y - l\sin\varphi. \end{aligned} \right\} \qquad (8.53)$$

Substituting (8.52) and (8.53) into (8.51) and replacing the angle ϕ by the difference, we obtain the differential equations in the form

$$\ddot{x} + p^2 x - p^2 l(\cos\omega t\cos\alpha + \sin\omega t\sin\alpha) - g = h\cos\omega t;$$

$$\ddot{y} + p^2 y - p^2 l(\sin\omega t\cos\alpha - \cos\omega t\sin\alpha) = h\sin\omega t.$$

For circular motion the angle α is small; therefore, we replace $\cos\alpha = 1$, $\sin\alpha = \alpha$. The angle α is a periodic function. In the first approximation it can be represented by the relation

$$a = A \sin \omega t.$$

This relation corresponds to motion of the mass center $\dot{m}$ along a circle whose center is shifted relative to the coordinate origin by the distance a_0. In reality the trajectory of this point will not be a true circle. After the indicated simplifications and certain transformations, the equations take the form

$$
\left.
\begin{aligned}
&\ddot{x} + p^2 x = (h + p^2 l)\cos \omega t + g + \\
&+ \frac{1}{2} p^2 l A (1 - \cos 2\omega t); \\
&\ddot{y} + p^2 y = (h + p^2 l)\sin \omega t - \\
&- \frac{1}{2} p^2 l A \sin 2\omega t.
\end{aligned}
\right\}
\tag{8.54}
$$

We take the solutions of the equations in the form

$$
\left.
\begin{aligned}
x &= a_0 + a_1 \cos \omega t + a_2 \cos 2\omega t; \\
y &= b_1 \sin \omega t + b_2 \sin 2\omega t.
\end{aligned}
\right\}
\tag{8.55}
$$

We substitute these solutions into (8.54) and collect coefficients with the same trigonometric multipliers into individual algebraic equalities. Solving the resulting equalities, we find the formulas for the coefficients

$$
\left.
\begin{aligned}
a_1 &= b_1 = \frac{h + p^2 l}{p^2 - \omega^2}; \\
a_2 &= b_2 = - \frac{1}{2} \cdot \frac{p^2 l}{p^2 - 4\omega^2} A; \\
a_0 &= \frac{g}{p^2} + \frac{1}{2} l A.
\end{aligned}
\right\}
\tag{8.56}
$$

On the basis of approximate geometric relationships (see Figure 8.6), the amplitude of the angular nonuniformity can be taken as the ratio

$$A = \frac{a_2}{b_1}.$$

Then the formulas for the coefficients a_0 and a_2 take the form

$$a_0 = \frac{g}{p^2} \cdot \frac{2(h + p^2 l)}{2h + l(p^2 + \omega^2)}; \tag{8.57}$$

$$a_2 = b_2 = -l \cdot \frac{p^2 - \omega^2}{p^2 - 4\omega^2} \cdot \frac{\ell}{2h + l(p^2 + \omega^2)}. \qquad (8.58)$$

This solution is valid for well-known particular cases.

If there is no backlash, $l = 0$. Then $a_2 = b_2 = 0$;

$$a_0 = \frac{mg}{e} = x_{cr}; \quad a_1 = b_1 = \frac{h}{p^2 - \omega^2}.$$
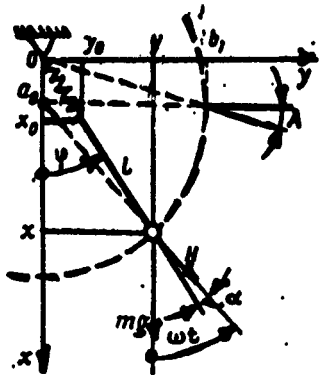
Figure 8.6. Circular motion of shaft in bearing with backlash at subcritical and supercritical rotation speeds.

We have obtained the exact solution for an elastic suspension without backlash. Under the action of the force h, the mass center moves along a circle of radius a_1, whose center is shifted under the action of the weight force downward by the magnitude of the static deformation $a_0 = x_{st}$. If $\omega < p$, a_1 will have the same sign as the direction of the force h; if $\omega > p$, a_1 and h will have different signs.

If there is no weight force, we must set $g = 0$ in (8.57) and (8.58). Then $a_0 = a_2 = 0$;

$$a_1 = \frac{h + p^2 l}{p^2 - \omega^2}.$$

This is the exact solution for the elastic system with backlash. As the disturbing force we usually consider the centrifugal force owing to unbalance. For this force $h = e\omega^2$, where e is the eccentricity of the mass center.

Then

$$a_1 = \frac{e\omega^2 + p^2 l}{p^2 - \omega^2}; \qquad (8.59)$$

in view of the presence of the backlash l, the radius a_1 of the mass center trajectory must be a positive quantity. Otherwise contact

between the shaft and the support is lost. Therefore, (8.59) is valid for $\omega < p$.

For velocities $\omega > p$ the eccentricity direction is established opposite the radius a_1. Then (8.59) takes the form

$$a_1 := \frac{-e\omega^2 + p^2 l}{p^2 - \omega^2};$$ (8.60)

Hence, we see that a_1 will be positive if the eccentricity e is greater than the clearance l. If $l > e$, the shaft will rotate about its mass center and the elastic support will not take part in the operation.

In the general case the following condition must be satisfied for unseparated circular motion:

for

$$\omega l = x, \quad x_0 < 0;$$ (8.61)

this means that the journal is forced against the supporting surface at the upper point. For the pendulum this means that it is loaded by a tensile force.

For this situation, according to (8.53) and (8.55)

$$x_0 = x + l = a_1 - a_1 + a_2 + l < 0.$$ (8.62)

Calculating using (8.56), (8.57), (8.58) the coefficients appearing in (8.62), we then find the value of the velocities for which circular motion is disrupted.

If the unbalance is small, circular motion is possible if ω/p is larger than 0.35-0.4.

Moreover, the unstable regime shows up for velocities lying in the range (0.5-0.8). The exact bounds are found from (8.62) as a function of the clearance, support stiffness, and magnitude of the unbalanced force.

In the region $\omega > p$ circular motion develops if the eccentricity e is larger than the magnitudeoof the clearance, i.e., for very large shaft unbalance.

CHAPTER 9

FORCED VIBRATIONS OF ROTOR ON NONLINEAR SUPPORTS
SUBJECT TO CIRCULAR DISTURBANCE AND WEIGHT FORCE

Let us examine a weightless shaft with a single mass m located arbitrarily with respect to the supports (Figure 9.1). The system stiffness at the point where the mass is located is defined by a nonlinear characteristic, which takes into account both the stiffness of the shaft itself and the stiffness of the nonlinear supports.

Let us assume that the elastic characteristic is axisymmetric. and is defined by the function

$$R = cr + br^3. \qquad (9.1)$$
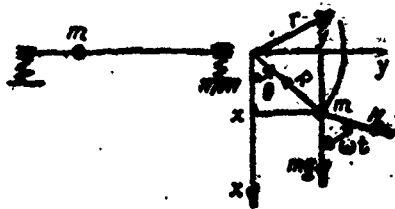
Figure 9.1. Illustrating derivation of vibration equations of shaft on nonlinear supports

The shaft will perform periodic vibrations under the influence of the circular disturbance H. Because of the effect of the weight force, the mass motion trajectory will not be strictly circular, but will depend on the relationship between the weight

force and the circular force, the elastic characteristic of the system, and the disturbance frequency.

We write the mass equation of motion in vector form

$$-m\ddot{z}-(c+br^2)z+He^{i\omega t}+nmg=0, \qquad (9.2)$$

where z is the vector defining the position of the mass center m

$$z=re^{i\theta}; \qquad (9.3)$$

r, θ are the polar coordinates of the point m, which in the general case are time functions;

n is the static overload coefficient.

The direction of the weight force is taken as the reference for measuring vector position angles.

The exact solution of (9.2) is not known. We shall seek its approximate solution.

9.1. Construction of General Solution in the First Approximation by the Bubnov-Galerkin Method

We represent (9.2) in projections on the coordinate axes

$$-m\ddot{x}-(c+br^2)x+H\cos\omega t+nmg=0; \qquad (9.4)$$

$$-m\ddot{y}-(c+br^2)y+H\sin\omega t=0. \qquad (9.5)$$

We use the Bubnov-Galerkin method and write the variational equations in the form

$$\int_0^T [\ddot{x}+(k^2+\beta r^2)x-h\cos\omega t-ng]\,\delta x\,dt=0; \qquad (9.6)$$

$$\int_0^T [\ddot{y} + (k^2 + \beta r^2)y - h \sin \omega t] \delta y \, dt = 0, \qquad (9.7)$$

where

$$k^2 = \frac{c}{m}; \quad \beta = \frac{b}{m}; \quad h = \frac{H}{m}; \quad T = \frac{2\pi}{\omega}. \qquad (9.8)$$

We restrict ourselves to the first approximation and take minimizing functions of the form

$$\begin{aligned} x &= A_0 + A_1 \cos \omega t; \\ y &= B_1 \sin \omega t. \end{aligned} \right\} \qquad (9.9)$$

In accordance with these functions, the motion trajectory of the point m is represented in the form of an ellipse (Figure 9.2), whose center is shifted relative to the x axis by the amount A_0. The ellipse semiaxes are A_1 and B_1.

The radius of displacement of the point m equals

$$r^2 = x^2 + y^2 = A_0^2 + A_1^2 \cos^2 \omega t + 2A_0 A_1 \cos \omega t + B_1^2 \sin^2 \omega t. \qquad (9.10)$$

Substituting (9.9) and the value of r^2 into the variational equations (9.6) and (9.7), we obtain these equations in the form

$$\int_0^T \{ -A_1 \omega^2 \cos \omega t + [k^2 + \beta (A_0^2 + A_1^2 \cos^2 \omega t + 2A_0 A_1 \cos \omega t +$$
$$+ B_1^2 \sin^2 \omega t)](A_0 + A_1 \cos \omega t) - h \cos \omega t - \eta g](\delta A_0 +$$
$$+ \delta A_1 \cos \omega t) dt = 0; \qquad (9.11)$$

$$\int_0^T \{ -B_1 \omega^2 \sin \omega t + [k^2 + \beta (A_0^2 + A_1^2 \cos^2 \omega t + 2A_0 A_1 \cos \omega t +$$
$$+ B_1^2 \sin^2 \omega t)] B_1 \sin \omega t - h \sin \omega t] \sin \omega t \, dt = 0. \qquad (9.12)$$

· Integrating the first equation initially with respect to the first variation and then with respect to the second, we obtain
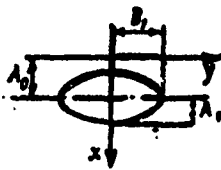
Figure 9.2. Trajectory of periodic vibrations in the first approximation.

$$A_0\left[k^2+\beta\left(A_0^2+\frac{3}{2}A_1^2+\frac{1}{2}B_1^2\right)\right]=ng; \quad (9.13)$$

$$A_1\left[k^2+\beta\left(3A_0^2+\frac{3}{4}A_1^2+\frac{1}{4}B_1^2\right)-\omega^2\right]=h. \quad (9.14)$$

Integrating the second equation, we obtain

$$B_1\left[k^2+\beta\left(A_0^2+\frac{1}{4}A_1^2+\frac{3}{4}B_1^2\right)-\omega^2\right]=h. \quad (9.15)$$

The resulting equations relate the static deflection A_0, vibration amplitudes A_1 and B_1, with the weight force and the circular disturbance force.

We shall apply the resulting equations to certain particular cases:

(a) no system nonlinearity, i.e., $\beta = 0$. Then (9.13), (9.14), (9.15) become independent and yield the conventional linear theory solutions

$$A_0=\frac{ng}{k^2}=n\frac{m}{c}g; \quad A_1=B_1=\frac{h}{k^2-\omega^2}; \quad (9.16)$$

in this case the motion trajectory is a circle with center shifted relative to the coordinate origin;

(b) no circular vector, i.e., h = 0. Then, in accordance with (9.14) and (9.15) $A_1 = 0$; $B_1 = 0$.

From (9.13) we find

$$A_0(k^2+\beta A_0^2)=ng. \quad (9.17)$$

The displacement A_0, defined by (9.17), is the st tic deflection of the shaft and supports under the action of the static force.

9.2. Rotor Vibrations in Absence of Weight Force

If no weight force acts, $ng = 0$. Then, according to (9.13) $A_0 = 0$, i.e., there is no static deformation. In accordance with (9.14) and (9.15)

$$A_1 = B_1;$$

their values are found from either (9.14) or (9.15)

$$A_1(k^2 + \beta A_1^2 - \omega^2) = h. \qquad (9.18)$$

The motion trajectory of the mass m under the action of the circular force h is a circle of radius A_1 with center at the coordinate origin.

We rewrite (9.18) in the form

$$A_1(k^2 + \beta A_1^2) = h + A_1 \omega^2. \qquad (9.19)$$

We shall consider the circular disturbance vector to be the centrifugal force owing to unbalance. In this case

$$h = e\omega^2,$$

where e is the displacement of the mass center m from the shaft axis owing to unbalance.

Substituting this expression for h into (9.19), we obtain

$$(k^2 + \beta A_1^2)A_1 = (e + A_1)\omega^2. \qquad (9.20)$$

This is the equation of static equilibrium of the rotating system.

The left side of (9.20) is the system elasticity force, and the right side is the centrifugal force per unit mass.

Equation (0.20) is easily solved graphically, for which we plot the function A_1, corresponding to the left side of the equation, and the straight lines corresponding to the right side (Figure 9.3). The points of intersection of these functions yield the solution of the equation in question. The slope of the straight lines is proportional to ω^2. For all values of ω^2 the straight lines pass through a common point with coordinate minus e. For small values of ω the equation has a single solution, yielding the radius A_1 of the circle. The larger ω, the larger A_1. For some value of ω the straight line becomes tangent to the curve, after which three solutions appear.
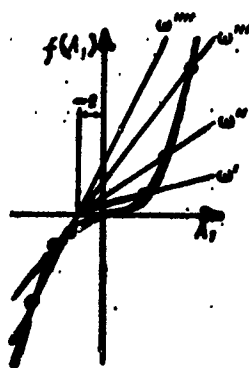
Figure 9.3. Graphical construction of deflection curve of shaft on nonlinear supports subject to unbalance.
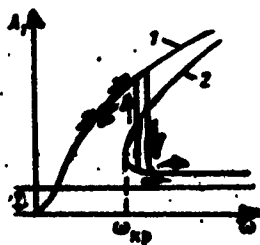
Figure 9.4. Shaft deflection as a function of rotation speed.

Figure 9.4 shows the solutions of the equation as a function of ω. The roots corresponding to the second branch of the curve have a negative sign, i.e., the shaft axis shift is in the direction opposite that of the static eccentricity e.

The shaft motion in the supercritical region is characterized by the fact that the radius A_1 decreases with increase of the angular velocity ω, approaching a value equal to e. In this case the mass tends to move to the axis of rotation. The upper part of curve 2 shows the unstable equilibrium state positions.

The transition from the subcritical regime 1 to the supercritical regime 2 takes place in the form of rapid restructuring of the system with marked reduction of the vibration amplitudes. The moment of transition depends on the magnitude of the initial
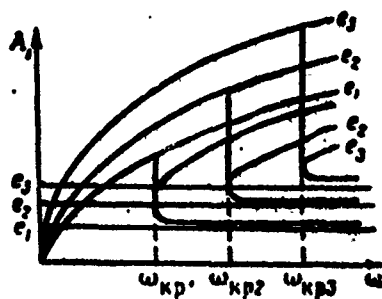
Figure 9.5. Critical speed of shaft on nonlinear supports as a function of initial unbalance.

unbalance, i.e., on the eccentricity e. The larger e, the higher the critical speed (Figure 9.5). The curves show that a large unbalance hinders transition of the shaft into the supercritical regime, extending its operation in the subcritical regime with large amplitudes.

9.3. General Case of Action of Unbalanced Force and Static Overload Force

In the case of combined action of a circular force $h = e\omega^2$ and the static force ng, the static displacement A_0 and the amplitudes A_1 and B_1 are interrelated. They are determined by solving the nonlinear system of Equations (9.13), (9.14) and (9.15).

We write (9.13), (9.14) and (9.15) in the form

$$A_0 = \frac{ng}{\mu^2 + \beta\left(A_0^2 + \frac{3}{2}A_1^2 + \frac{1}{2}B_1^2\right)};$$ (9.21)

$$A_1 = \frac{e\omega^2}{\mu^2 + \beta\left(3A_0^2 + \frac{3}{4}A_1^2 + \frac{1}{4}B_1^2\right) - \omega^2};$$ (9.22)

$$B_1 = \frac{e\omega^2}{\mu^2 + \beta\left(A_0^2 + \frac{3}{4}B_1^2 + \frac{1}{4}A_1^2\right) - \omega^2}.$$ (9.23)

The quantities A_0, A_1, B_1 can be calculated by trial and error or by successive approximations. For example, setting initially $\beta = 0$ we find from the formulas the approximate values of A_0, A_1, B_1. Then we repeat the calculation, now with account for the nonlinearity, and we refine the values found for the unknowns.

The equations show that the center-of-gravity motion trajectory is an ellipse (see Figure 9.2). The ellipse axes depend on the magnitude of the static force — the larger the force, the larger the shift A_0 of the center of the ellipse, but the smaller the dimensions of the ellipse. With increase of the static force, the horizontal and vertical amplitudes of the vibrations decrease.

The reverse phenomenon shows up in the fact that increase of the vibration amplitudes because of increase of the unbalance reduces the static deflection.

What we have said is valid for values of the velocity ω lying far from the critical speed, at which there is a restructuring of the system from the subcritical regime into the supercritical regime or vice versa.

The region of transition from the subcritical to the supercritical regime is a typical characteristic of the nonlinear system (Figure 9.6).
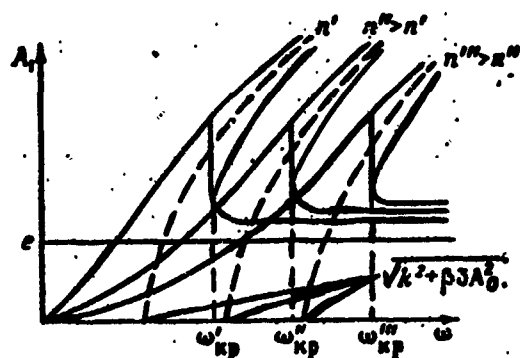
Comparison of the characteristics for different overload coefficients n indicates a very important property of the nonlinear system: the critical speed of this system depends on the magnitude of the static force. Increase of the static force leads to increase of the critical speed.

Figure 9.6. Vibration amplitude and critical speed as a function of static overload force magnitude.

A variable static force can be the cause for the appearance at different moments of time of large vibrations at the same rotational speed. For example, if an unbalanced shaft subject to a weight force has supercritical

speed, then if overload forces develop its rotational speed becomes subcritical. There is a corresponding sharp increase of the amplitude of the circular motion and along with this an increase of the centrifugal force. This process affects the condition of turbomachinery casings, where the vibrations increase markedly in this time segment.

CHAPTER 10

FREE VIBRATIONS OF DISSIPATIVE SYSTEMS

The vibrations of dissipative systems have a decaying nature because of energy absorption by the friction forces if energy is not supplied from outside. In this case the vibratory motion is not strictly harmonic, and the nature of the decay depends on the law of the resistance forces acting.

The differential equation of damped vibrations for a nonlinear resistance law is written in general form as

$$\ddot{q} + k^2 q + f(q, \dot{q}) = 0, \qquad (10.1)$$

where $f(q, \dot{q})$ — is the resistance function. Usually this function contains a small parameter in the form of the friction or loss coefficient.

The equation cannot be integrated in the general case of a nonlinear resistance function. An idea of the nature of the vibrations can be obtained with the aid of the phase plane.

The construction of the phase trajectory does not necessarily require solution of the differential equation, and can be carried out by transformations of the differential equation and graphical construction.

There are several methods for plotting the phase trajectories for a given differential equation. Usually the isocline method and the Lienard method are described in handbooks on nonlinear vibrations. We shall discuss here the so-called delta method.

10.1. Delta Method for Plotting Phase Trajectories

The delta method is the most general, and is quite simple and easily visualized (see [30] and [23]). It is applicable for the general forms of nonlinear equations in which the nonlinear part is represented by the function $f(q, \dot{q})$.

We reduce (10.1) to characteristic time by the substitution

$$\tau = \lambda t;$$
$$\frac{d^2 q}{d\tau^2} + q + \frac{1}{\lambda^2} f(q, \dot{q}) = 0.$$

Denoting

$$\frac{dq}{d\tau} = v; \tag{10.2}$$

$$\delta(q, v) = \frac{1}{\lambda^2} f(q, v), \tag{10.3}$$

we write the equation as

$$\frac{dv}{d\tau} = -[q + \delta(q, v)];$$

dividing by (10.2), we obtain

$$\frac{dv}{dq} = -\frac{q + \delta(q, v)}{v}. \tag{10.4}$$

For a small time interval we can consider the function δ constant. Then (10.4) can be integrated and yields

$$v^2 + [q + \delta(v, q)]^2 = \text{const} = r^2. \tag{10.5}$$

This is the equation of a circle of radius r, plotted in the coordinates v, q, with center lying on the q axis at the point M, shifted along the q axis by the distance $-\delta$ (Figure 10.1)

The initial point for the construction of the phase trajectory is given by the initial conditions

$$t = 0; \quad q(0) = q_0; \quad \dot{q}(0) = \dot{q}_0.$$

The last equality corresponds to

$$v(0) = k\dot{q}_0.$$

These same values are used with (10.3) to calculate the value of δ, which yields the initial position of the center of curvature — the point M_0.

... iting on the phase tra-
... the initial point, we
dr.. .rom this point a short arc
of radius r_0 with center at the
point M_0 in the clockwise direc-
tion. The end of this small arc
gives the new coordinates q_1 and
v_1. Using these coordinates and
(10.3), we find the new position
M_1 of the center, from which we
continue the construction of the
trajectory in the form of the

Figure 10.1. Delta method of constructing phase trajectory

next small arc of radius r_1. Such constructions make it possible to construct quite accurately the entire phase trajectory.

For a dissipative system the phase trajectory will be a convolute spiral with focus at the coordinate origin. The condition for convolutionality of the spiral is coincidence of the signs of δ and v.

We shall examine the construction of the phase trajectories by the delta method for some friction laws.

10.2. Linear Friction Law

The equation of motion for a linear friction law is

$$\ddot{q} + k^2 q + 2n\dot{q} = 0; \qquad (10.6)$$

here the friction force function is

$$f(\dot{q}) = 2n\dot{q} = 2nkv.$$

In accordance with (10.3)

$$\delta(v) = \frac{2n}{k} v,$$

i.e., the function δ is proportional to v.

To construct the phase trajectory we draw in the q, v coordinates the auxiliary function $\delta(v)$ in the form of a straight line with slope $-2n/k$ (Figure 10.2). Taking as the initial conditions $q(0) = q_0$, $v_0 = 0$, we obtain $\delta_0 = 0$, $r = q_0$, i.e., the initial segment is represented by an arc with center at the coordinate origin. To determine the position of the center of the arc of the next segment, we draw from the point q_1 a straight line parallel to the abscissa axis till it intersects the straight line representing the function $\delta(v)$. The perpendicular dropped from the point of intersection to the q axis yields the new center M_1. The follow-

Figure 10.2. Phase trajectory construction for the viscous friction case

ing centers M_2, M_3, and so on, are found in the same way in the course of the entire trajectory construction process. Use of the

auxiliary line δ(v) makes it possible to avoid the necessity for making any calculations in the plotting process and permits selecting any sufficiently small segments of the arcs being plotted.

10.3. Combined Action of Viscous and Coulomb
Friction Forces

The differential equation is written in the form

$$\ddot{x} + k^2 x + 2n\dot{x} \pm R = 0, \tag{10.7}$$

where R — is the friction force per unit mass. The sign of R is selected as a function of the motion direction. A plus sign is used for motion in the positive direction and a minus sign for motion in opposite direction.

The function δ is represented here by the expression

$$\delta(\dot{x}) = \frac{1}{k^2}(2n\dot{x} \pm R);$$

replacing $\dot{x} = kv$, we obtain

$$\delta(v) = \frac{1}{k^2}(2nkv \pm R). \tag{10.8}$$

Let us first plot the function δ(v) (Figure 10.3). This function has a piecewise linear form. The segment on the upper half of the plane is used for positive values of v; the segment on the lower half of the plane is used for negative values.

We take the initial point $x = x_0$, $v_0 = 0$. The center of the initial segment circle is the point M_0.

The construction is continued by the method outlined above, in accordance with which the auxiliary function is used to determine the position of the centers of the curve segments. Upon reaching the point x_0, the center is shifted to the point 0' and the plotting of the upper segment of the phase trajectory is continued.

The phase trajectory terminates on the x axis, when the describing point reaches the region lying within the zone R_{CT}/k^2, where the vibrations terminate.

10.4. Quadratic Friction Force Law

The equation of motion has the form

$$\ddot{x} + k^2 x \pm \mu \dot{x}^2 = 0; \tag{10.9}$$

in this equation the "minus" sign is used for a negative velocity x.

The delta function for (10.9) has the form

$$\delta(v) = \pm \frac{1}{\mu k} \mu \dot{x}^4 = \pm \mu v^4, \tag{10.10}$$

where μ, the loss coefficient, is a small quantity.
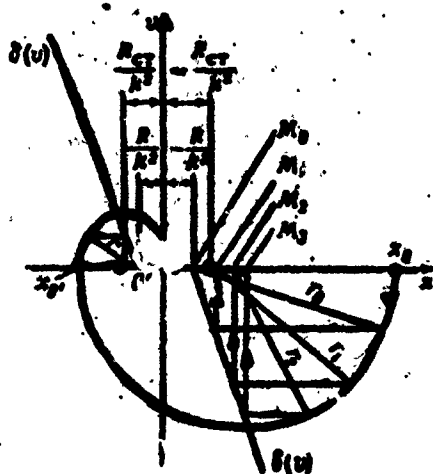
Figure 10.3. Phase trajectory construction with combined action of viscous and Coulomb friction forces
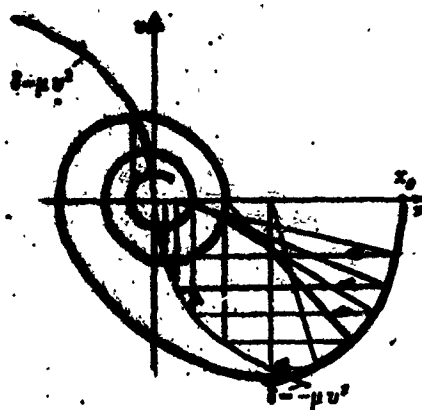
Figure 10.4. Phase trajectory for quadratic friction loss

The delta function is represented on the figure by segments of parabolas with account for the sign (Figure 10.4.). The initial

center is located at the coordinate origin. The curve is plotted in the usual way.

The phase trajectory is a converging spiral, asymptotically approaching the focus — the coordinate origin. The amplitude decrease is large for large amplitudes and nearly zero near the focus.

The phase trajectory defines the nature of the motion completely — it gives the value of the velocities for any position of the system, although it does not yield the time dependence of the motion parameters.

The delta method described above makes possible graphical construction of the phase trajectories for any friction force velocity dependence.

If the delta function has q and $\dot{q}$ as its arguments, it is not possible to construct it in the form of the auxiliary curve. Then the positions of the centers of curvature of the segments are found by calculation using (10.3).

CHAPTER 11

SELF-EXCITED VIBRATIONS

11.1. Methods for Studying Self-Excited
Vibrationo of Systems

A necessary condition for the existence of stable periodic vibrations of an elastic system is equality of the energy supplied to the system from the vibration exciter and the energy lost as a result of the action of various absorbers.

The principal energy absorbers are the various forms of friction, such as: internal friction in the system, in the material, and between individual parts of the system; external friction in couplings or special devices of the system (for example, friction in supports, guides, special braking devices, dampers).

Energy removal can also take place as a result of interaction of the vibrating system with the surrounding medium (for example, blade vibrations in a liquid or air medium; performance of compression or displacement work in the vibration process, and so on). In all cases of interaction with the surrounding medium, those factors are important which change in the course of the vibration period and depend on the velocity and amplitude of the vibrations. The

mathematical expression for the interaction must reflect as exactly as possible the principles involved, although the numerical quantities characterizing this interaction may be very small.

The energy input sources in the self-excited systems are external steady-state factors — for example, the weight force, uniform stream, constant velocity, constant flowrate of a liquid or gas, and so on. But in all these cases it is mandatory that there be interaction between the system and these "constant" factors. This interaction is expressed in the fact that the energy input to the system and the forces which arise in this interaction are controlled by the system vibrations.

In the self-excited systems the energy balance is not the same over different segments of the period, having a positive value at certain moments of time and a negative value at other moments. The energy balance is equal to zero on the whole during a period for steady-state self-excited vibrations.

Self-excited vibrations can occur only under definite conditions in nonlinear systems. In many cases the mechanism of self-excited vibration onset is very complex and is a peculiarity of the system itself.

The differential equation of motion of a system with a single degree of freedom, capable of performing self-excited vibrations, in the general case has the form

$$m\ddot{q} + c\dot{q} + \mu(q, \dot{q}) = 0. \qquad (11.1)$$

The excitation and resistance forces are concealed in the nonlinear term of this equation, which includes the small parameter μ. The exact solution of the equation is not possible in general. Therefore the study of the system properties and the determination of the conditions for onset of self-excited vibrations is made with the aid of the phase planes.

11.1.1. Graphic Method for Constructing Limit Cycles — the Delta Method

To construct the phase trajectory, we shall use the delta method. Making transformations of (11.1) similar to those of Section 10.1, we obtain the equation

$$v^2 + [q + \delta(q, v)]^2 = \text{const} = r^2, \qquad (11.2)$$

where

$$v = \frac{\dot{q}}{h}; \qquad (11.3)$$

$$\delta(q, v) = \frac{1}{mh^2} f(q, \dot{q}). \qquad (11.4)$$

We recall that the centers of curvature of the phase trajectory always lie on the q axis; their position is defined by the function δ.

.For harmonic vibrations μ = 0, δ = 0, and the phase trajectory is a circle. If δ is positive, the centers of curvature lie to the left of the coordinate origin, and the phase trajectory segments for these centers are represented by converging spirals in the upper half of the phase plane and diverging spirals in the lower half (Figure 11.1). If δ is negative, the centers of curvature lie to the right of the coordinate origin and the phase trajectories are represented by outward spirals in the upper half of the phase plane and by inward spirals in the lower half. We emphasize that in those regions in which the signs of δ and v are the same the phase trajectory converges, while — where their signs are different — the trajectory spirals outward.

Assuming δ equal to zero, we obtain the equation of the curve which divides the phase plane into regions which differ in the sign of δ. This facilitates the use of the rule presented above for determining the nature of the phase trajectory.

As an example we consider the Rayleigh equation

$$\ddot{q} + h^2 q + \mu(q^2 - 1)\dot{q} = 0. \qquad (11.5)$$

This equation defines the periodic vibrations of a system with a single degree of freedom subject to the action of a nonlinear force which is a function only of the velocity. Certain practical problems reduce to such an equation.

According to (11.4), the delta function of the Rayleigh equation has the form

$$\delta(v) = -\frac{1}{k}\,\mu(k^2 v^2 - 1)\,v; \qquad (11.6)$$

equating it to zero, we obtain

$$v = 0; \quad v = \pm\frac{1}{k}. \qquad (11.7)$$

The first solution yields the abscissa axis, lying at an equal distance on both sides of the axis. These lines divide the phase plane into four regions, in which δ alternately takes positive and negative signs (Figure 11.2).

According to (11.6), in the regions $v > \frac{1}{k}$ and $-\frac{1}{k} < v < 0$ the sign of δ is positive. In regions $0 < v < \frac{1}{k}$ and $v < -\frac{1}{k}$ the sign of δ is negative. In accordance with the general rule in region $-\frac{1}{k} < v < \frac{1}{k}$ the phase trajectories spiral outward. Consequently the coordinate origin, i.e., the position $q_0 = 0$; $\dot{q}_0 = 0$,

Figure 11.1. Connection between parameter δ and form of phase trajectory
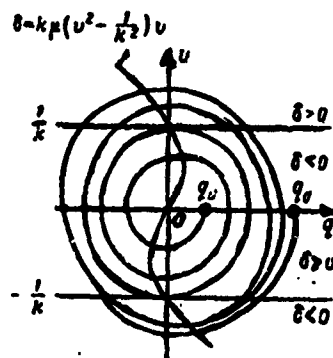
Figure 11.2. Limit cycle of Rayleigh equation and transition phase trajectories

is a point of unstable equilibrium. If an initial impulse disturbs the system from this position, it begins to perform vibrations with increase of the amplitudes. In the course of time the amplitudes
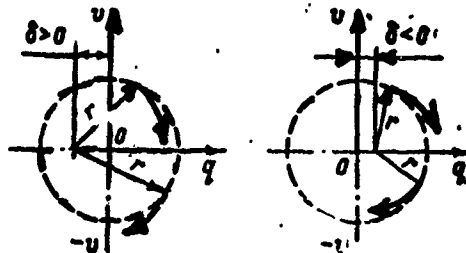
grow so much that the phase trajectory diverges beyond the limits of the bounds $\pm \frac{1}{k}$.

The regions $v > \frac{1}{k}$ and $v < -\frac{1}{k}$ yield converging phase trajectories. Therefore, the increase of the self-excited vibration amplitudes is slowed. The amplitudes will approach some definite value, and the phase trajectory will approach a closed curve. This limiting form of periodic motion is stable, and its phase trajectory is called a limit cycle.

If we examine the beginning of a motion with large amplitudes, the phase trajectory will pass through zones of stable and unstable motion. In this case the stability tendency will be dominant and the phase trajectory for the cycle will be a converging curve. As the amplitudes decrease, the action of the forces in the retardation segments is balanced by the action of the forces in the perturbation segments, and the phase trajectory approaches the limit cycle. The process of self-excited vibration approach to the limit cycle is termed the transition process.

The transition phase trajectories for the Rayleigh equation, starting from small and large values of q_0, approach the same limit cycle, which can be represented by a circle of radius $R_a = \frac{2}{k\sqrt{3}}$.

The Van der Pol equation is still another example of self-excited vibratory systems

$$\ddot{q} + k^2 q + \mu (q^2 - 1)\dot{q} = 0. \tag{11.8}$$

The delta function of (11.8) will be

$$\delta(v, q) = \mu \frac{1}{k} (q^2 - 1)v. \tag{11.9}$$

Equating it to zero, we obtain

$$v = 0; \quad q = \pm 1. \tag{11.10}$$

These roots divide the phase plane into several zones with respect to the values of the delta function (Figure 11.3). Comparing the signs of δ and v, we come to the conclusion that the center
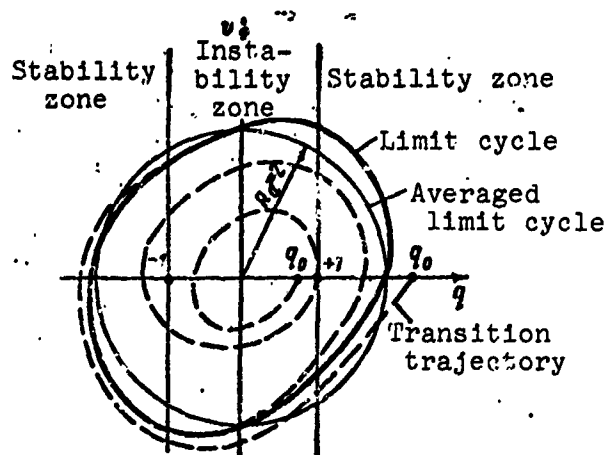
Figure 11.3. Limit cycle and transition trajectories
of Van der Pol equation

strip, lying in the limits q = ± 1, where δ and v have opposite
signs, is the instability zone of the periodic motion. Beyond the
limits q = ± 1 there lie regions with domination of the friction
forces, in which the phase trajectories have a decaying form. Con-
sequently, the system has a limit cycle, which the phase trajec-
tories approach from both small and large amplitudes.

Figure 11.3 shows the transition phase trajectories for the
Van der Pol equation. The limit cycle is a nearly circular closed
curve. The system represented by the Van der Pol equation is self-
oscillatory and does not have a stable rest position.

11.1.2. Van der Pol Averaging Method

The study of the properties of self-excited oscillatory systems
and finding the limit cycles by graphical construction of the phase
trajectories makes it difficult to obtain generalizing conclusions.
Therefore the analytic methods for studying phase trajectories, the

vibration transition processes, and finding the limit cycles are of great theoretical and practical interest.

One such method is that of Van der Pol. The essence of this method lies in the fact that the phase trajectory is represented in coordinate axes rotating with an angular velocity equal to the circular frequency of the self-excited vibrations. After this the nature of the phase trajectories is used to establish the limit cycle existence conditions and parameters.

We take an equation of general form with small nonlinear term

$$\ddot{q} + k^2 q + \mu f(q, \dot{q}) = 0. \tag{11.11}$$

For convenience we use the substitution $\phi = kt$ to reduce (11.11) to characteristic time

$$q'' + q + \mu \frac{1}{k^2} f_k(q, q') = 0. \tag{11.12}$$

where the prime denotes derivative with respect to ϕ.

Denoting

$$q' = v, \tag{11.13}$$

we obtain

$$v' + q + \mu \frac{1}{k^2} f(q, v) = 0. \tag{11.14}$$

Equalities (11.13) and (11.14) are the differential equations of the phase trajectory in the q, v coordinates.

We transform these equations into polar coordinates, taking (Figure 11.4)

$$v = R \cos \theta; \quad q = R \sin \theta; \tag{11.15}$$

R and θ are variables and are time functions; therefore

$$\left. \begin{array}{l} v' = R' \cos \theta - R\theta' \sin \theta; \\ q' = R' \sin \theta + R\theta' \cos \theta. \end{array} \right\} \tag{11.16}$$

Substituting (11.15) and (11.16) into (11.13) and (11.14), we obtain these equations in polar coordinates

$$R' \sin \theta + R\theta' \cos \theta = R \cos \theta;$$
$$R' \cos \theta - R\theta' \sin \theta = -R \sin \theta - \mu \frac{1}{k^2} f(R, \theta).$$

We solve these equations for the derivatives, which leads to the following equalities

$$R' = -\mu \frac{1}{k^2} f(R, \theta) \cos \theta; \left.\begin{array}{l}\\\\\end{array}\right\}$$
$$R\theta' = R + \mu \frac{1}{k^2} f(R, \theta) \sin \theta. \quad\quad\quad (11.17)$$

We introduce the ξ, ζ axes, rotating uniformly with the angular velocity k. The position of these axes at the time t is defined by the angle $\phi \approx kt$ (see Figure 11.4). Then

$$\theta = \varphi + \psi, \quad\quad (11.18)$$

where ψ is the polar coordinate of the describing point in the moving axes.

Figure 11.4. Polar coordinates of phase trajectory describing point in moving coordinate axes

To transform (11.17) into equations in the moving axes, we replace θ in accordance with (11.18)

$$\theta' = 1 + \psi'.$$

Substitution of θ and θ' into (11.17) yields

$$R' = -\mu \frac{1}{k^2} f(R, \varphi, \psi) \cos(\varphi + \psi); \quad\quad (11.19)$$

$$\psi' = \mu \frac{1}{Rk^2} f(R, \varphi, \psi) \sin(\varphi + \psi). \quad\quad (11.20)$$

This is the equation of the phase trajectories in the ξ and ζ moving axes.

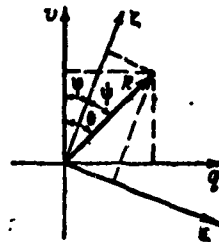For the harmonic oscillator $\mu = 0$. Therefore $R' = 0$; $\psi' = 0$; hence $R = $ const; $\psi = $ const.

This means that in the ξ, ζ axes the describing point is stationary. Its position is defined by the constant coordinates R and ψ, which are given by the initial position. In the stationary axes this describing point will yield a circle, which corresponds to harmonic vibrations.

Integration of (11.19) and (11.20) in the limits $\phi_1 - \phi_2$ yields the increment of the polar coordinates R and ψ during the time the axes rotate through the angle $\phi_2 - \phi_1$. Exact integration is possible only in rare particular cases; therefore, the exact integral is replaced by its approximate value.

We obtain the approximate value of the integrals under the assumption that the variation of R and ψ is small in the limits of integration and these quantities can be considered constants.

The validity of the assumptions made follows from the Equalities (11.19) and (11.20) themselves, in which the coefficient μ is always small and the derivatives R' and ψ' are not large. This can be seen by plotting the phase trajectory graphically. This is particularly valid with approach to the limit cycle, when the phase trajectory parameters change only slightly even after several cycles.

Integration of (11.19) and (11.20) in the limits of the ϕ variation period yields the following expressions for the coordinate increments

$$\Delta R = -\mu \frac{1}{k^2} \int_0^{2\pi} f(R, \psi, \phi)\cos(\phi + \psi)\, d\phi; \tag{11.21}$$

$$\Delta \psi = \mu \frac{1}{kR} \int_0^{2\pi} f(R, \psi, \phi)\sin(\phi + \psi)\, d\phi, \tag{11.22}$$

where R and ψ are considered constant parameters in the integration; $f(R, \psi, \phi)$ — is a function which is formulated on the basis of the governing differential equation by successive coordinate replacement

$$f(\psi, \dot{\psi}) = f(R\sin\theta, kR\cos\theta) =$$
$$= f[R\sin(\phi + \psi), kR\cos(\phi + \psi)]. \tag{11.23}$$

Equation (11.21) yields the vibration amplitude variation law during the period. Equation (11.22) yields the frequency correction. If $\Delta\psi$ is positive, this means that the describing point described the arc $2\pi + \Delta\psi$ during the period of integration $\phi = 2\pi$, i.e., the vibration circular frequency is higher than k

$$p = k\left(1 + \frac{\Delta\psi}{2\pi}\right); \tag{11.24}$$

if $\Delta\psi$ is negative, the circular vibration frequency is lower than k.

The limit cycle is found from the condition

$$\Delta R = 0. \tag{11.25}$$

In accordance with this condition, the integral (11.21) yields the equation

$$\int_0^{2\pi} f(R, \psi, \varphi)\cos(\varphi + \psi)\,d\varphi = 0. \tag{11.26}$$

Hence we find the radius of the limit cycle circle.

The form of the limit cycle phase trajectory, representable in the form of a circle of radius R, differs from the more exact phase trajectory form indicated previously. Thus, the circle is the limit cycle phase trajectory in the first approximation.

The limit cycle is stable if the phase trajectories approach it from within and without, and is unstable if the phase trajectories recede from it. Stable limit cycles correspond to self-excited vibrations.

The question of limit cycle stability is easily resolved with the aid of (11.21). If for $R = R_a - \epsilon$ (where R_a is the limit cycle radius and ϵ is a small quantity) we obtain $\Delta R > 0$, while for $R = R_a + \epsilon$ we obtain $\Delta R < 0$, then the limit cycle is stable, since the phase trajectories converge. If for $R = R_a - \epsilon$ we obtain $\Delta R < 0$ while for $R = R_a + \epsilon$ we obtain $\Delta R > 0$, then the limit cycle is unstable.

In connection with the fact that (11.21) and (11.22) show the phase trajectory changes near the limit cycles, they have been called the transition equations.

We shall present some examples of phase trajectory analysis.

Linear damped oscillator

Its differential equation will be

$$\ddot{q} + k^2 q + 2n\dot{q} = 0.$$

The defining function for this equation will be

$$f(\dot{q}) = \dot{q} = kv = kR \cos \theta = kR \cos (\varphi + \psi);$$

we substitute it into (11.21) and (11.22)

$$\Delta R = -\frac{2n}{k^2} \int_0^{2\pi} kR \cos^2 (\varphi + \psi) d\varphi;$$

$$\Delta \psi = \frac{2n}{Rk^2} \int_0^{2\pi} kR \sin(\varphi + \psi) \cos(\varphi + \psi) d\varphi.$$

Integrating, considering R and ψ constants, we obtain

$$\left.\begin{array}{l} \Delta R = -\frac{2n}{k}\ \pi R; \\ \Delta \psi = 0. \end{array}\right\} \tag{11.27}$$

This result indicates that in the rotating axes the describing point N moves toward the center. In the stationary phase plane it yields a converging logarithmic spiral. Self-excited oscillations cannot arise in such a system, since its stable state is the static equilibrium position. This is indicated by the fact that the coordinate origin is the focus of the phase trajectory.

Rayleigh equation

The Rayleigh equation is written as

$$\ddot{q} + k^2 q + \mu(\dot{q}^2 - 1)\dot{q} = 0.$$

The defining function of this equation will be

$$f(\dot{q}) = (\dot{q}^2 - 1)\dot{q} = (k^2v^2 - 1)kv =$$
$$= [k^2R^2\cos^2(\varphi + \psi) - 1]kR\cos(\varphi + \psi).$$

Substitution into (11.21) and (11.22) yields

$$\Delta R = -\mu \frac{1}{k^2} \int_0^{2\pi} [k^2R^2\cos^2(\varphi + \psi) - 1]kR\cos^2(\varphi + \psi)d\varphi;$$

$$\Delta\psi = \mu \frac{1}{Rk^2} \int_0^{2\pi} [k^2R^2\cos^2(\varphi + \psi) - 1]kR\sin(\varphi + \psi)\cos(\varphi + \psi)d\varphi.$$

Integration for constant R and ψ offers no difficulty and leads to the formulas

$$\left.\begin{array}{l} \Delta R = -\frac{\mu}{k}\pi\left(\frac{3}{4}k^2R^2 - 1\right)R; \\ \Delta\psi = 0. \end{array}\right\} \tag{11.28}$$

The phase trajectory in the moving coordinate system is a radial ray. The system has a limit cycle. To find its radius we set ΔR in (11.28) equal to zero

$$R\left(\frac{3}{4}k^2R_a^2 - 1\right) = 0;$$

hence

$$R_a = \frac{2}{k\sqrt{3}}; \ R = 0. \tag{11.29}$$

This limit cycle is stable, while the equilibrium position for R = 0 is unstable. This is easily seen on the basis of analysis of (11.28). Substituting therein R smaller than R_a, we obtain ΔR with a plus sign; substituting R larger than R_a, we obtain ΔR with a minus sign. This means that the phase trajectories are spirals which approach the limit cycle R_a. Therefore, the system whose vibrations are described by the Rayleigh equation is self-excited.

The Van der Pol equation (11.8) is also the equation of a self-excited system. The transition equation for this system will have the form

$$\Delta R = -\mu \frac{1}{k^2} \int\limits_0^{2\pi} [R^2 \sin^2(\varphi+\psi)-1] kR \cos^2(\varphi+\psi) d\varphi;$$

$$\Delta\psi = \mu \frac{1}{Rk^2} \int\limits_0^{2\pi} [R^2 \sin^2(\varphi+\psi)-1] kR \sin(\varphi+\psi) \cos(\varphi+\psi) d\varphi.$$

Integration of these equations yields

$$\left. \begin{aligned} \Delta R &= -\mu \frac{\pi}{k} \left(\frac{1}{4} R^2 - 1\right) R; \\ \Delta\psi &= 0. \end{aligned} \right\} \tag{11.30}$$

Setting ΔR equal to zero, we find

$$R = 0; \quad R_a = 2. \tag{11.31}$$

Equations (11.30) have a focus at the coordinate origin and a self-excited limit cycle. In the limits $0 < R < 2$ the increment ΔR is positive. This shows that the position $q = 0$; $\dot{q} = 0$ is unstable, the system enters self-excited oscillations and approaches the limit cycle $R_a = 2$. If $R > 2$, then ΔR is negative, i.e., the limit cycle is stable. Equality of $\Delta\psi$ to zero shows that self-excited oscillations take place with the free vibration frequency k.

11.2. Excitation of Rotor Self-Excited Vibrations

by Articulated Spline Coupling

Turbomachine rotors are often of composite construction. The sections are coupled with the aid of spherical hinges, cylindrical collars, or centering rings, and torque transmission from one part to another is accomplished with the aid of splined or sometimes pinned couplings. The articulated spline couplings make it possible to have some misalignment of the shaft axes, which inevitably occurs during operation for several reasons.

The hinged support under the action of an axial force, the cylindrical centering ring when tightly seated, the splined couplings

when transmitting torque, and also the pin-type couplings may be a source of rotor self-excitation, as a result of which deflections of the rotor appear and considerable vibration develops at a frequency equal to the critical rotor speed. The excitation is the result of the action of the friction forces on the supporting surfaces of the couplings.

To explain the mechanism of the disturbing force onset, we shall examine a splined flange coupling (Figure 11.5). The shafts which are connected by the coupling rotate with the angular velocity ω; their axes intersect at the small angle β. The clearance in the splines is quite large and wedging of the teeth doe. not occur for the small angle β. We shall assume that the force from the torque transmitted by the coupling is distributed uniformly over the entire circumference of the toothed ring. As a result of shaft misalignment, longitudinal slippage develops in th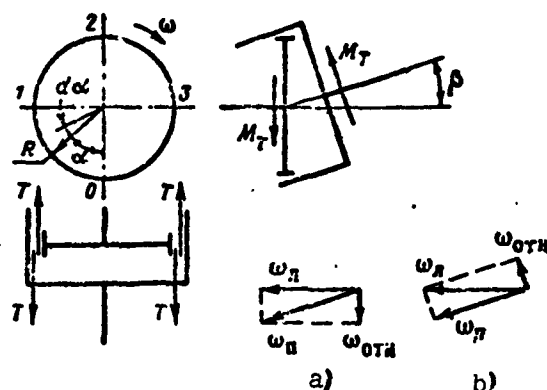e coupling teeth, which leads to the development of friction forces along the teeth. At the points 0 and 2 the teeth are in the expreme positions — least and most engaged; here the sliding velocities are zero. On the segment 0 − 1 − 2 the teeth gage further as the shafts rotate, while on the segment 2 − 3 − 0 they move apart. The friction forces act correspondingly: on the left half of the circumference they have one sign, on the right half they have the opposite sign.

Figure 11.5. Action of friction forces in splines with shaft axes misaligned

The friction forces create a torque which acts in the horizontal plane 1 − 3, i.e., in the plane perpendicular to the shaft misalignment plane. If the dependence of the friction forces on

the sliding velocity in the splines is known, the resultant bending moment is easily calculated from the sliding velocities, forces on the teeth, and friction coefficient.

Let us assume that the dry friction law is effective in the splines. Then the moment is found as the moment of all the friction forces relative to the vertical axis 0 − 2

$$M_f = 2 \int_0^\pi \mu P R^2 \sin\alpha\, d\alpha = 4\mu P R^2, \qquad (11.32)$$

where μ — is the friction coefficient, independent of the sliding velocity;

P — is the circumferential force per unit circumferential length:

$$P = \frac{M_{\kappa p}}{2\pi R^2}.$$

After substituting this expression for P, (11.32) takes the form

$$M_f = \frac{2}{\pi}\mu M_{\kappa p}. \qquad (11.33)$$

Similar moments arise on the hinged support under the influence of axial forces, in pin-type couplings, and in other similar couplings.

The direction of the friction torque vector acting on each half of the coupling coincides with the direction of the relative angular velocity vector.

For the left half of the coupling, the relative velocity vector equals (see Figure 11.5a)

$$\bar\omega_{OTH} = \bar\omega_{\text{II}} - \bar\omega_{\text{I}};$$

parallel to it is the friction moment vector acting on the left side of the coupling.

For the right half (see Figure 11.5b)

$$\bar\omega_{OTH} = \bar\omega_{\text{I}} - \bar\omega_{\text{II}};$$

to it corresponds the moment vector acting on the right side of the coupling.

Let us examine the question of the stability of the rectilinear axis of a high-speed composite rotor. In the absence of misalignment of the axes, no additional moment will arise in the articulated spline coupling and the rotor will not have any vibration. We deflect the rotor from the rectilinear position, forcing it to precess with the angular velocity $\Omega < \omega$. As a result of rotor bending, misalignment of the shafts in the splined coupling develops and a friction moment arises in the plane perpendicular to the rotor bending plane.

Figure 11.6 shows the inertia forces and friction moments in the splined coupling in terms of projections on the axes rotating with the precessional velocity Ω.

In the general case the projections of the inertia force are

$$
\left.
\begin{aligned}
P_\xi &= m(\xi\Omega^2 - \ddot{\xi} - \eta\dot{\Omega} + 2\Omega\dot{\eta}); \\
P_\eta &= m(\eta\Omega^2 - \ddot{\eta} - \xi\dot{\Omega} - 2\Omega\dot{\xi}).
\end{aligned}
\right\}
\tag{11.34}
$$

The terms of these formulas are respectively the centrifugal forces, radial acceleration forces, circumferential forces associated with angular acceleration, and the forces caused by Coriolis acceleration.

The coordinates of the mass m in the rotating axes are connected with the inertia forces and friction moment in the coupling by the equations

$$
\left.
\begin{aligned}
\xi &= a_{11}P_\xi - a_{12}M_\eta; \\
\eta &= a_{11}P_\eta + a_{12}M_\xi.
\end{aligned}
\right\}
\tag{11.35}
$$

Substituting herein the expressions for the force projections from (11.34) and then multiplying the second equation
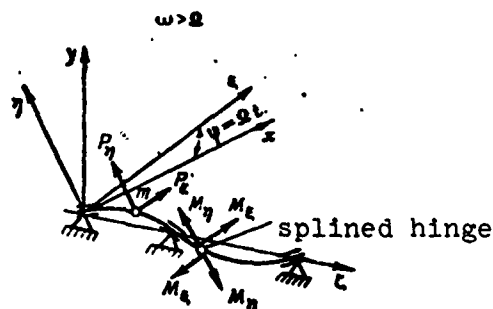

Figure 11.6. Interaction of inertia forces and moments arising in splined couplings

by 1 and again combining the resulting expressions, we obtain the equation in complex form

$$z = ma_{11}(\Omega^2 z - \ddot{z} - iz\dot{\Omega} -$$
$$- i2\Omega\dot{z}) + ia_{12}M_{f}, \qquad (11.36)$$

where

$$z = \xi + i\eta; \quad M_f = M_\xi + iM_\eta.$$

In view of the smallness of the friction moment, we can assume that the shaft has a planar bending mode. In this case the vector M_f lies in the shaft bending plane, and its effect shows up in the plane perpendicular to $\bar{z}$.

Separating the real and imaginary parts in (11.36), we obtain the equations

$$\ddot{z} + (k^2 - \Omega^2)z = 0; \\ z\dot{\Omega} + 2\dot{z}\Omega - k^2 a_{12}M_f = 0, \qquad (11.37)$$

where

$$k^2 = \frac{1}{a_{11}m}.$$

The first equation (11.37) is satisfied by the solutions

$$z = \text{const}; \quad \ddot{z} = 0; \quad \Omega = k; \quad \dot{\Omega} = 0. \qquad (11.38)$$

Then the second equation, for a constant value of the friction moment M_f, yields the solution

$$z = \frac{1}{2} \frac{k^2}{\Omega} a_{12}M_f t + z_0. \qquad (11.39)$$

These solutions show that the velocity Ω of the disturbed precession equals k — the shaft critical speed. The deflection z increases in the course of time. This means that for a rotor angular velocity higher than the critical value ($\omega > \Omega$) the rectilinear position of its axis is unstable. Under the influence of the friction forces in the articulated spline coupling there appear self-excited vibrations, which lead to increase of the deflections, inertia forces,

loads on the supports, and vibration. In this case the vibration frequency remains equal to the critical speed, regardless of the proper rotational speed ω. The larger the friction forces in the coupling, the greater the tendency to loss of stability.

If the proper rotational speed ω is less than the critical speed, the sign of the friction force moment M_f becomes negative. This means that in accordance with (11.39) the precession damps out under the influence of the friction forces. Friction in the couplings improves the rotor stability for subcritical rotational velocities.

The internal friction forces in the material create a similar effect in the excitation of self-excited shaft vibrations (see [15]).

11.3. Self-Excited Vibrations of Compressor Blades

Self-excited vibrations of blades are a frequently encountered and very hazardous problem of axial compressor rotor blades. Their appearance depends on the blade construction, the aerodynamic characteristics of its profile, and on the air or gas flow conditions over the blade. Variation of the blade profile and flow conditions along its length have a significant effect on the self-excited vibrations. For thin and light-weight disk structures, interaction between the blades on the wheel appears, involving transfer of energy from one blade to another. Part of the energy is absorbed by the friction forces in the disk.

As a result of the great variety of different factors on which the self-excited vibrations depend, they may have different forms and different nature of their onset. A large number of special studies have been made of self-excited blade vibrations. We shall examine here the simplest cases.

11.3.1. Plane-Parallel Self-Excited Vibrations

We shall examine plane-parallel vibrations of a profile of unit length under the influence of a uniform approaching stream (Figure 11.7). The lift force P_y develops on the profile, applied at the center of pressure

$$P_y = c_y b \frac{\varrho v^2}{2}.$$ \hfill (11.40)

The blade attachment is such that it does not permit rotation of the profile; therefore we ignore the influence of the aerodynamic moment.

The profile equilibrium condition is defined by the equation

$$m\ddot{q} + cq = P_y,$$ \hfill (11.41)

where m — is the profile mass per unit length;

   c — is the bending stiffness coefficient for the given profile segment.

The lift coefficient c_y depends on the angle of attack α, and for each profile this relation is represented in the form of the characteristic curve (Figure 11.8). The angle α is connected with the vibratory motion curve

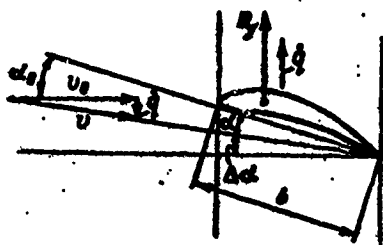$$\alpha = \alpha_0 + \Delta\alpha,$$ \hfill (11.42)

Figure 11.7. Illustrating development of plane-parallel, self induced blade vibrations
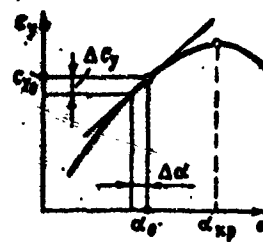

Figure 11.8. Variation of profile lift coefficient during vibrations

where α_0 — is the incidence angle corresponding to the nominal
value P_0 of the lift force;

$\Delta\alpha$ — is the angle change caused by vibration:

$$\Delta\alpha = -\frac{\dot{q}}{v}. \tag{11.43}$$

In view of the smallness of $\dot{q}$ in comparison with v, the angle $\Delta\alpha$ is small; therefore the lift force can be found from the formula

$$P_y = P_0 + \frac{dc_y}{d\alpha} \Delta\alpha \cdot b \frac{\rho v^2}{2} = P_0 - B \frac{dc_y}{d\alpha} \dot{q}, \tag{11.44}$$

where

$$B = \frac{1}{2} \rho b v.$$

Equation (11.41), reduced to characteristic time, has the form

$$\ddot{q} + q = \frac{1}{\varepsilon}\left(P_0 - B\frac{dc_y}{d\alpha}\dot{q}\right). \tag{11.45}$$

We make use of the Van der Pol transition equations and calculate the integral in (11.21)

$$\Delta R = \frac{1}{\varepsilon}\int_0^{2\pi}\left[P_0 - B\frac{dc_y}{d\alpha}kR\cos(\varphi+\psi)\right]\cos(\varphi+\psi)d\varphi; \tag{11.46}$$

after integration, we obtain

$$\Delta R = -\frac{B}{\varepsilon}\frac{dc_y}{d\alpha}kR\pi. \tag{11.47}$$

Formula (11.47) shows that plane-parallel self-excited vibrations cannot occur in the operating regimes corresponding to the left segment of the lift force curve for laminar flow over the blade. Random external disturbances are damped out by the aerodynamic forces, and the blade takes a stable equilibrium position specified by the incidence angle α_0.

If, because of significant reduction of air flowrate through the compressor, the angle of attack α_0 increases to values exceeding

α_{cr} (see Figure 11.8), then as a result of the change of the sign of $dc_y/d\alpha$ the sign of ΔR becomes positive. This means that self-excited vibrations appear, for which the amplitudes will increase without bound.

In practice this process is accompanied by the formation of vortices which separate from the blades, and the self-excitation mechanism changes its nature.

The friction forces in the blade material make it more resistant to self-excited vibrations. The formula for the amplitude increase for this case will have the form

$$\Delta R = -\frac{1}{e} B \frac{dc_y}{d\alpha} kR\pi - \frac{2\pi}{h}\pi R. \tag{11.48}$$

For the appearance of self-excited vibrations, the flow conditions over the blade must differ markedly from the design conditions, in order that the aerodynamic excitation can overcome the resistance forces.

More general is the case in which the blade bending oscillations are accompanied by blade twisting.

11.3.2. Bending-Torsion Self-Excited Vibrations

This self-excited vibration mode carries the general name of **flutter**. Flutter for compressor blades has its significant peculiarities which differentiate it from airplane wing flutter.

The compressor blade is a beam fixed at one end. Because of the complexity of its configuration, blade bending vibrations are always accompanied by torsional vibrations. This is explained by the fact that the blade does not have an elastic axis which is common for all sections, and the centers of gravity of the sections do not coincide with the elastic centers.

Let us examine a blade element of unit length (Figure 11.9). When located in a steady airstream, this element experiences the action of the aerodynamic forces. We shall identify three points

on the profile: the center of
gravity s, the elastic center d,
and the center of pressure a.
We note that the location of the
center of pressure is not con-
stant. It depends on the angle
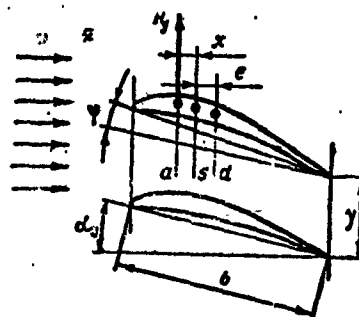of attack and the flow velo-
city v.

The displacements of the
subject element as a result of
elastic deformations are con-
nected with the forces acting
by the well-known equations

Figure 11.9. Illustrating
bending torsion self-induced
blade vibrations

$$(P_y+P_j)=c_{11}y+c_{12}\varphi;$$
$$(P_yx+M_j)=c_{12}y+c_{22}\varphi,$$ (11.49)

where y; ϕ — are, respectively, the displacement of the center of
gravity and the element rotation angle resulting from
elastic deformations;

P_j; M_j — are, respectively, the inertia forces and moment of the
element.

The coefficients c_{11}, c_{12}, c_{22} can be expressed with the aid
of the principal stiffness coefficients c_p and c_ϕ

$$c_{11}=c_p; \quad c_{12}=c_{21}=-ec_p; \quad c_{22}=c_\phi+e^2c_p.$$ (11.50)

The forces acting are defined by the equalities:

the aerodynamic force

$$P_y=c_yb\frac{\rho v^2}{2};$$

the lift coefficient

$$c_y=c_{y_0}+\frac{dc_y}{d\alpha}(\varphi+\Delta\alpha),$$ (11.51)

where c_{y_0} — is the lift coefficient for the incidence angle α_0;

$\Delta\alpha$ — is the angle of attack change resulting from the vibration velocity

$$\Delta\alpha = -\frac{\dot{y}}{v}.$$

As a result the formula for the lift force takes the form

$$P_y = P_0 + \frac{dc_y}{d\alpha}\left(\varphi - \frac{\dot{y}}{v}\right)b\frac{\varrho v^2}{2},\tag{11.52}$$

where

$$P_0 = c_{y_0}b\frac{\varrho v^2}{2}.$$

The inertia force and moment are

$$P_j = -m\ddot{y}; \qquad M_j = -J\ddot{\varphi},\tag{11.53}$$

where m is the element mass; J is the element moment of inertia about the center of gravity.

Substituting (11.52) and (11.53) into (11.49) and making minor transformations, we obtain

$$m\ddot{y} + c_{11}y + c_{12}\varphi = P_0 + \frac{dc_y}{d\alpha}\left(\varphi - \frac{\dot{y}}{v}\right)b\frac{\varrho v^2}{2};\tag{11.54}$$

$$J\ddot{\varphi} + c_{12}y + c_{22}\varphi = \left[P_0 + \frac{dc_y}{d\alpha}\left(\varphi - \frac{\dot{y}}{v}\right)b\frac{\varrho v^2}{2}\right]x.\tag{11.55}$$

Before examining with the aid of these equations the conditions for dynamic equilibrium of the profile, let us find its static equilibrium position under the influence of the air stream. To do this we set $\ddot{y} = \dot{y} = \ddot{\varphi} = 0$ in (11.54) and (11.55).

Then

$$\left.\begin{array}{l} c_{11}y_{ct} + c_{12}\varphi_{ct} = P_0 + c_\alpha\varphi_{ct} \\ c_{21}y_{ct} + c_{22}\varphi_{ct} = (P_0 + c_\alpha\varphi_{ct})x, \end{array}\right\}\tag{11.56}$$

where

$$c_\alpha = \frac{dc_y}{d\alpha}b\frac{\varrho v^2}{2};\tag{11.57}$$

hence

$$y_{cr} = P_0 \frac{c_{22} - c_{12}x}{\Delta}; \quad \varphi_{cr} = P_0 \frac{c_{11}x - c_{12}}{\Delta},$$ (11.58)

where

$$\Delta = \begin{vmatrix} c_{11} & c_{12} - c_a \\ c_{21} & c_{22} - c_a x \end{vmatrix}.$$ (11.59)

The profile loses static stability at the flow velocity v, when the Determinant (11.59) vanishes

$$c_{11}(c_{22} - c_a x) - c_{21}(c_{12} - c_a) = 0;$$

hence

$$c_{a\,cr} = \frac{c_{11}c_{22} - c_{12}^2}{c_{11}x - c_{12}}.$$

After substituting herein the notations of (11.50), we obtain

$$c_{a\,cr} = \frac{e_\varphi}{x + e}.$$ (11.60)

According to (11.57), the critical value of the coefficient c_a corresponds to the critical speed v_{cr}, upon reaching which the blade loses static stability. Obviously, the blade structure and its attachment must be such that its critical speed exceeds considerably the operating flow velocities.

The bending-torsion vibrations of the blade have dual coupling. As a result of the noncoincidence of the center of gravity and the elastic center they have elastic coupling, and as a result of noncoincidence of the center of pressure and center of gravity they also have aerodynamic coupling. The latter situation is defined by the right sides of (11.54) and (11.55). This is the basic condition for the possibility of onset of self-excited vibrations of the flutter type.

Having two degrees of freedom, the blade in question has two free vibration modes, which differ from one another in the relationship and sign of the vibration amplitudes and frequencies.

In examining vibrations relative to the static equilibrium position, which is established under the influence of the aerodynamic force P_0, we discard this force from (11.54) and (11.55) and write them in the form

$$m\ddot{y} + c_{11}y + (c_{12} - c_a)\varphi = -c_a \frac{\dot{y}}{v}; \qquad (11.61)$$

$$J\ddot{\varphi} + c_{12}y + (c_{22} - c_a x)\varphi = -c_a x \frac{\dot{y}}{v}. \qquad (11.62)$$

The free vibration mode shape and frequency of the blade in the air stream are defined by the left sides of (11.61) and (11.62). The right sides of these equations differ by the small quantity $\dot{y}/v$. They define the possibility of damping or excitation of the vibrations.

Setting the right sides of (11.61) and (11.62) equal to zero, we find the frequencies and mode shapes of the blade free vibrations.

The equations are solved by the substitution

$$\left. \begin{array}{l} y = Y\cos pt; \\ \varphi = \Phi \cos pt; \end{array} \right\} \qquad (11.63)$$

after which we obtain the frequency equation

$$\begin{vmatrix} c_{11} - mp^2 & c_{12} - c_a \\ c_{12} & c_{22} - c_a x - Jp^2 \end{vmatrix} = 0. \qquad (11.64)$$

Expanding the determinant and making the replacement $c_{12} = -ec_p$, we obtain

$$(c_{11} - mp^2)(c_{22} - c_a x - Jp^2) = ec_p(ec_p + c_a). \qquad (11.65)$$

The relative blade stiffness in torsion is greater than that in bending. Usually

$$\frac{c_{11}}{m} < \frac{c_{22}}{J},$$

Therefore the frequencies of the coupled bending-torsion vibrations with forward location of the center of pressure $(x > 0)$ are separated by the following boundaries

$$p_1^2 < \frac{c_{11}}{m} \; ; \; \frac{c_{22} - c_a x}{J} < p_2^2 \qquad (11.66)$$

(in both cases the product of the parentheses in the left side of (11.65) yields a positive number, equal to the right side of the equation).

With increase of the flow velocity, and consequently of the coefficient c_a, the boundary of the second frequency shifts to the left. In practice, the effect of the approaching flow velocity on the blade natural vibration frequencies is very slight. Nevertheless, designs may be encountered in which the influence of the flow may be more significant.

The ratio of the bending and torsional vibration amplitudes, in accordance with the Determinant (11.64), is calculated from the formulas

$$\frac{Y}{\Phi} = \frac{c_{22} - c_a x - J p^2}{-c_{12}}, \; \text{or} \; \frac{Y}{\Phi} = \frac{-(c_{12} - c_a)}{c_{11} - m p^2} . \qquad (11.67)$$

Using the notations (11.50), these formulas are conveniently written as

$$\frac{Y}{\Phi} = \frac{c_{22} - c_a x - J_{p^2}^2}{e c_p}, \; \text{or} \; \frac{Y}{\Phi} = \frac{e c_p + c_a}{c_{11} - m p^2} . \qquad (11.68)$$

Substituting herein the values of p_1^2 and p_2^2 found from the frequency equation, we obtain the amplitude ratios and their sign. In accordance with the general rules, the bending and torsional vibrations for one frequency will be in phase, while for the other frequency they will be in phase opposition (i.e., the amplitude ratio has a minus sign).

Now let us examine the complete equations (11.61) and (11.62). The right sides of these equations are respectively the external, small in magnitude, aerodynamic force and moment, proportional to the velocity of the bending vibrations. Under certain conditions these aerodynamic forces may damp the vibrations, while under other conditions they will excite the vibrations.

Let us determine the work of these forces during a period, assuming (in view of the smallness of the forces) that the perturbed vibrations take place with the frequency and in the mode shape of the natural vibrations

$$dL_1 = -c_a \frac{\dot{y}}{v} dy = -\frac{c_a}{v} \dot{y}^2 dt;$$

$$\Delta L_1 = -\frac{c_a}{v} \int_0^{\frac{2\pi}{p_i}} Y_i^2 p_i^2 \cos^2 p_i t \, dt = -\frac{c_a}{v} Y_i^2 p_i.$$ (11.69)

Formula (11.69) shows that in all cases the bending vibrations are accompanied by absorption of energy by the aerodynamic forces

$$dL_2 = -c_a x \frac{\dot{y}}{v} d\varphi = -x \frac{c_a}{v} \dot{y}\dot{\varphi} dt;$$

substituting herein (11.63) and integrating, we obtain

$$\Delta L_2 = -x \frac{c_a}{v} \int_0^{\frac{2\pi}{p_i}} p_i^2 Y_i \Phi_i \sin^2 p_i t \, dt = -x \frac{c_a}{v} \pi Y_i \Phi_i p_i.$$ (11.70)

The work of the aerodynamic moment may be positive. This means that under these conditions the aerodynamic moment is an exciter of self-excited vibrations.

Self-excited vibrations arise and will develop if the second work magnitude is greater than the first, i.e., if

$$\Delta L_1 + \Delta L_2 > 0;$$ (11.71)

Substituting herein (11.69) and (11.70), we obtain

$$-\pi \frac{c_a}{v} Y_i^2 p_i \left(\frac{\Phi_i}{Y_i} x + 1 \right) > 0.$$ (11.72)

The condition for occurrence of blade self-excited vibrations under operating flow conditions reduces to the inequality

$$\frac{\Phi_i}{Y_i} x + 1 < 0.$$ (11.73)

In the case of a forward center of pressure location ($x > 0$), the moment excites the out-of-phase bending-torsion vibration mode; in the case of an aft center of pressure location ($x < 0$), the moment excites the in-phase vibration mode. Here the value of the amplitude ratio is important

Self-excited vibrations occur when the vibration mode being excited has sufficiently large angular amplitudes. This depends on the flow velocity and the displacement e of the elastic center. An unfavorable case is that in which e is negative, i.e., the elastic center lies ahead of the center of gravity. Formula (11.68) shows that in this case the amplitude ratio

$$\frac{\phi}{\gamma} = \frac{c_{11} - m p^2}{c_a - e c_p}$$

becomes sufficiently large for excitation of blade self-excited vibrations as a result of the minus sign in the denominator.

The general conclusion from this analysis is that the blade for which the elastic center is located between the section center of gravity and the aft-positioned center of pressure will be most stable — both statistically and with respect to self-excited vibrations.

If a blade is designed so that the center of gravity of the section coincides with the center of pressure ($x = 0$), for example by special weighting of the leading edge, such a blade will not be disposed toward self-excited vibrations. In accordance with (11.70) the work of the aerodynamic moment is zero for such a blade, and bending vibrations are always accompanied by energy absorption. This is also indicated by the Condition (11.73).

If the center of gravity and the elastic center coincide ($e = 0$), then such a blade will also not tend to have self-excited vibrations. For $e = 0$ the torsional and bending vibrations become independent. The bending vibrations damp out rapidly under the influence of aerodynamic damping, and the torsional vibrations (in the absence of bending vibrations) are not excited.

This scheme describing the onset of blade self-excited vibrations is valid for the segment within the limits of which the aerodynamic and geometric parameters remain unchanged.

The conventional blade has a complex shape. The flow conditions and locations of the centers of gravity and elastic centers vary along the blade length. Therefore it may be that individual segments will operate with a positive energy balance, while others operate with a negative balance.

The overall energy balance for the entire blade serves as the criterion for the possibility of the onset of self-excited vibrations. If under any conditions the overall energy balance is positive, this means that the blade has a tendency toward self-excited vibrations.

Using (11.69) and (11.70), we wr$\cdot$ the overall balance in integral form

$$\Delta L = -\pi p_i \int_0^l \left(\frac{c_a}{v} Y_i^2 + x \frac{c_a}{v} Y_i \Phi_i \right) dl, \tag{11.74}$$

where Y_1, Φ_1 — are the natural vibration amplitudes, variable along the blade length;

v, c_a, and x — are respectively the flow velocity, aerodynamic force coefficient (11.57), and coordinate of its application — all these quantities also vary along the blade length.

The amplitude functions Y_1 and Φ_1 for calculating the integral are determined from the blade free vibration mode with account for the action of the aerodynamic forces and also with account for the action of the centrifugal forces.

In view of the complexity of the integrand, its calculation is replaced by summation over segments. A positive value of the Integral (11.74) indicates a tendency of the blade toward self-excited vibrations.

The blade self-excited vibration mechanisms are extremely complex and varied. Therefore the calculation scheme examined above and the corresponding criteria must be considered the simplest scheme, which reflects the actual phenomenon only in the first approximation. In the further refinement we must take into consideration friction forces in the material, interaction of the torsional vibrations with the blade aerodynamics, interaction of the vibration modes of the different blades within the limits of the rotor, and so on.

11.4. Self-Excited Vibrations of Rotor Turning

in Sliding Bearings

The bearing may serve as the exciter of self-excited vibrations of the rotor. If the bearings are of the plane sliding type, then in most cases as a result of high rotational speed and the abundant lubricant supply they operate in the hydrodynamic lift force regime.

General Equations

To clarify the excitation mechanism for self-excited vibrations, we shall examine the shaft motion in the bearing and the equations of equilibrium of the forces acting on the shaft (Figure 11.10). In so doing we assume that the rotor is perfectly balanced and its center of gravity coincides with the center of the shaft. Given: shaft angular velocity ω, bearing
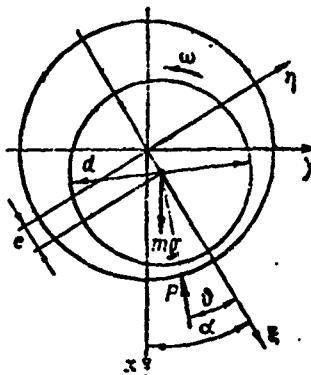

Figure 11.10. Forces and moments acting on journal in hydrodynamic bearing

radial clearance δ, bearing dimensions d and l; and the absolute
oil viscosity ν is also known.

The shaft position in the bearing is defined by the angle α
and the eccentricity e. Generally speaking, these quantities must
be considered variables, but for steady-state motion in the static
equilibrium position they are constants and define the condition
of equilibrium between the weight force G = mg and the hydrodynamic
force P.

Equilibrium for unsteady motion is defined by the equations

$$\left.\begin{array}{l} m\ddot{x}-G+P_x=0; \\ m\ddot{y}+P_y=0. \end{array}\right\} \tag{11.75}$$

In projections on the η, ξ moving axes, these equations have the
form

$$\left.\begin{array}{l} m(\ddot{e}-e\dot{\alpha}^2)-G\cos\alpha+P\ :\ \dot{w}=0; \\ m(2\dot{e}\dot{\alpha}+e\ddot{\alpha})+G\sin\alpha-P_\iota\qquad=0. \end{array}\right\} \tag{11.76}$$

The hydrodynamic force P depends on the shift e of the center
of the shaft relative to the center of the bearing and the shaft
angular velocity ω. Its magnitude is defined by the formula

$$P=\varphi(\chi)\cdot\nu l d\cdot\left(\frac{d}{2\delta}\right)^2, \tag{11.77}$$

where χ is the relative eccentricity

$$\chi=\frac{e}{\delta}; \tag{11.78}$$

here d and l are the bearing dimensions; $\phi(\chi)$ in (11.77) is the
bearing loading coefficient.

The loading coefficient is usually presented in graphical form
(Figure 11.11) as a function of χ and bearing relative length l/d.
For individual segments of these curves it can be expressed with
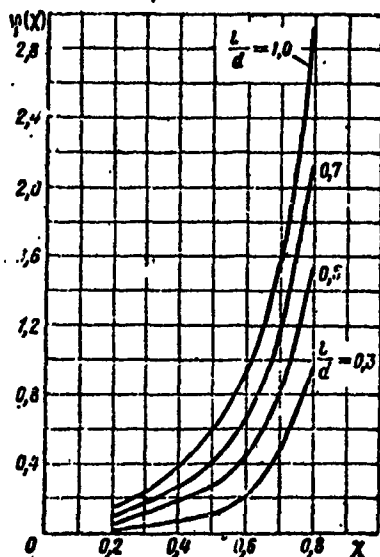the aid of the formula

Figure 11.11. Hydrodynamic bearing loading coefficient.

$$\varphi(\chi)=\frac{b_0+b_1\chi+b_2\chi^2}{(1-\chi)^n}, \qquad (11.79)$$

where the coefficients b_1, b_2, b_3, and n are determined by inspection from the corresponding curve (see Figure 11.11).

Sufficiently correct results can also be obtained using the simpler formula

$$\varphi(\chi)=\frac{b_1\chi}{1-\chi}. \qquad (11.80)$$

The direction of the vector P depends on the magnitude of the relative eccentricity χ and is defined by the angle ϑ:

$$\cos\vartheta=\chi. \qquad (11.81)$$

These formulas are analyzed in hydrodynamic lubrication theory and are used here without any special analysis or refinement.

The bearing lift force is determined by the volume of oil forced into the oil wedge by the viscous friction forces. For the steady-state stationary position of the eccentricity e, this volume is equal to (Figure 11.12a) $V_{av}\delta$, where

$$V_{cp}=\frac{1}{2}\,\omega r. \qquad (11.82)$$

If the angle α is variable and the eccentricity changes, the average input velocity must be calculated from the relative velocities (see Figure 11.12b)

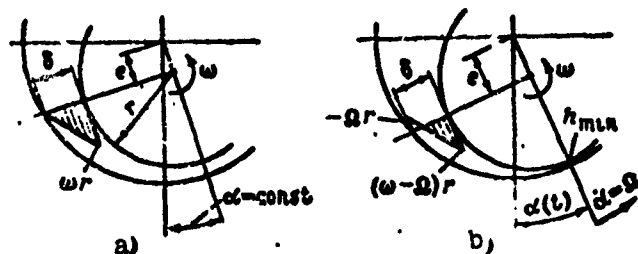$$V_{cp}=\frac{1}{2}\,(\omega-2\Omega)r.$$

Figure 11.12. Bearing operating zone
in the case of stationary (a) and
precessing (b) shaft.

Then the pumped oil volume will be

$$\frac{1}{2}(\omega - 2\Omega)\, r\delta. \qquad (11.83)$$

If $\Omega < \frac{1}{2}\omega$, the oil wedge and lift force are located behind the section h_{min}; if $\Omega > \frac{1}{2}\omega$, the oil wedge forms ahead of the section h_{min} and the lift force will hinder precession of the shaft.

To express the pumped oil volume in conventional form, we formulate the equality

$$\frac{1}{2}\omega_{np}\, r\delta = \frac{1}{2}(\omega - 2\Omega)\, r\delta, \qquad (11.84)$$

from which we obtain the reduced velocity

$$\omega_{np} = \omega - 2\Omega. \qquad (11.85)$$

This velocity is to be substituted into (11.77) in place of ω when the force P is determined for precessing shaft motion; in this case (11.77) takes the form

$$P = \varphi(\chi)(\omega - 2\Omega)\, \nu l d \cdot \left(\frac{d}{2\delta}\right)^2. \qquad (11.86)$$

We note that the lift force P is found from the absolute magnitude of the difference $(\omega - 2\Omega)$. If this difference is negative

the angle ϑ, which determines the direction of the force, must be taken with a negative sign.

The vertically positioned shaft or the shaft operating under weightless conditions does not experience the influence of gravity forces. Therefore, (11.76) take the form

$$m\,(\ddot{e}-e\dot{a}^2)+P\cos\vartheta=0;$$
$$m\,(2\dot{e}\dot{a}+e\ddot{a})-P\sin\vartheta=0. \qquad (11.87)$$

These equations are satisfied by the steady precession conditions

$$\dot{a}=\Omega=\text{const}; \quad \ddot{a}=0; \quad \dot{e}=\ddot{e}=0;$$

from (11.87) we obtain

$$P=me\Omega^2; \quad \sin\vartheta=0.$$

According to (11.81) and (11.78)

$$\chi=1; \quad e=\delta,$$

i.e., the shaft displaces in the bearing by the magnitude of the radial clearance. Thus, in accordance with Figure 11.11 and the Formula (11.79), $\lim_{x\to 1}\varphi(\chi)=\infty$ and then in accordance with (11.86) we have

$$\lim_{x\to 1}(\omega-2\Omega)=\frac{P}{\varphi(1)}=0.$$

Hence, we find the steady shaft precession rate

$$\Omega=\frac{1}{2}\,\omega. \qquad (11.88)$$

Shaft autorotation is a stable motion. If something leads to reduction of the precession rate Ω, the difference $(\omega - 2\Omega)$ becomes positive and a force appears, acting on the shaft in the direction of the precession (Figure 11.13), and restores the previous rate.
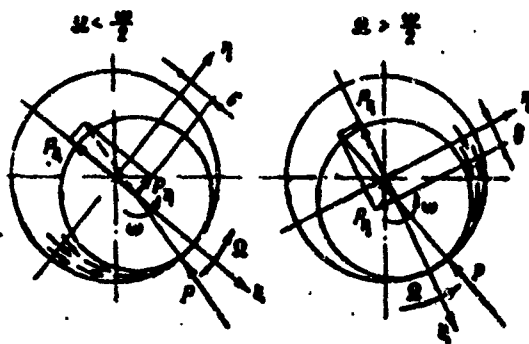
Figure 11.13. Diagram of hydro-
dynamic force action in the
autorotational speed region.

Conversely, if Ω increases under
the influence of some external
factor, the difference $(\omega - 2\Omega)$
becomes negative; this means that
a force develops from the opposite
side and cancels out the excess
rate.

The autorotation rate Ω
increases in proportion to ω.
When the velocity Ω reaches the
critical value, the resonance
phenomenon occurs, accompanied
by marked increase of shaft de-
flection and the loads on the supports.

For the simplest shaft arrangement (on two supports)

$$\omega_{\text{c}} = \sqrt{\frac{c}{m}};$$

therefore, the resonant angular velocity at which the self-excited
vibrations reach their maximal magnitudes will be

$$\omega_{\text{res}} = 2\omega_{\text{c}}.$$

When accounting for the gyroscopic moment of the disk, the
resonant speed is easily found from the frequency diagram (Figure
11.14).

Drawing from the coordinate origin a straight line with the
slope 0.5, we find the resonant angular velocity ω_{res} as the point
of intersection of this ray with the shaft frequency characteristic.

Self-excited vibrations of the rotor terminate when the angular
velocity exceeds ω_{res}. Experiments show that in this case the shaft
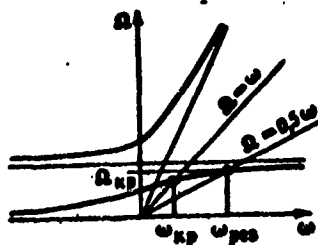
Figure 11.14. Determining critical autorotation speed.

centers, and every disturbance tending to disrupt the central position of the shaft, will be damped out by the hydrodynamic forces.

Self-excited vibrations of horizontal shaft. A similar autorotation phenomenon develops with the shaft axis horizontal.

In general hydrodynamic lubrication theory, the assumption is made that static equilibrium is established in the bearing between the external forces and the lift force of the oil layer. Accordingly, the shaft occupies a position which is characterized by the magnitude of the eccentricity e and its direction — the angle θ.

If the external force is the weight, the following equality is established

$$G = P = \varphi(\chi) \, \omega \nu l d \cdot \left(\frac{d}{2\delta}\right)^2.$$

(11.89)

The relative eccentricity χ and then the angle θ are easily found from this expression for given conditions. Since the weight force is constant, with increase of the angular velocity ω the eccentricity e will decrease, while the angle θ will increase.

The static equilibrium is not absolutely stable. At high rotational speeds self-excited vibrations of the autorotation type can develop, in which the shaft begins to precess with velocity equal to half the rotational velocity.

The precession velocity is not constant; therefore, in (11.76) we make the substitution

$$\alpha = \varphi + \beta, \text{ где } \dot{\varphi} = \frac{\omega}{2} t;$$

(11.90)

β is the deviation from the average value.

In this case the derivatives are transformed to the variable φ

$$\dot{e}=\frac{de}{d\varphi}\cdot\frac{\omega}{2}; \quad \ddot{e}=e''\frac{\omega^2}{4};$$

$$\dot{a}=\frac{\omega}{2}+\dot{\beta}; \quad \ddot{a}=\ddot{\beta};$$ (11.91)

$$\dot{\beta}=\beta'\frac{\omega}{2}; \quad \ddot{\beta}=\beta''\frac{\omega^2}{4};$$

here the primes denote derivatives with respect to φ.

After substitution and transformations, (11.76) take the form

$$e''-e(1+\beta')^2-\frac{4g}{\omega^2}\cos(\varphi+\beta)+\frac{4}{m\omega^2}P\cos\vartheta=0;$$

$$2e'(1+\beta')+e\beta''+\frac{4g}{\omega^2}\sin(\varphi+\beta)-\frac{4}{m\omega^2}P\sin\vartheta=0.$$ (11.92)

In these equations the hydrodynamic force P is calculated using (11.86), in which

$$\Omega=\dot{a}=\frac{\omega}{2}+\dot{\beta};$$

after substitution of this value into (11.86), the latter takes the form

$$P=-2\bar{\tau}(\chi)\dot{\beta}rld\cdot\left(\frac{d}{2\delta}\right)^2.$$

The direction of the force is oriented at the angle ϑ relative to the eccentricity e (see Figure 11.10). Since the angle α, which defines the direction of e changes, the direction of the force P also changes.

The angle β changes only slightly in the course of a period. The velocity β̇ is also small; therefore χ approaches one and the eccentricity of the journal in the bearing is close to the radial clearance $e\approx\delta$. As a result of this, the change of e during the period is small, and in (11.92) we can neglect the derivatives e' and e". Then (11.92) simplify and separate

$$me(1+\beta')^2\frac{\omega^2}{4}+G(\cos\varphi-\beta\sin\varphi)=P\cos\theta; \tag{11.93}$$

$$\beta''=-\frac{4g}{e\omega^2}(\sin\varphi+\beta\cos\varphi)+\frac{4}{em\omega^2}P\sin\theta. \tag{11.94}$$

Equation (11.93) for radial equilibrium yields the lower bcund for ω for stable autorotation. Since P cannot have a negat_ve value, its minimal value equals zero. Then the minimal velocity is found from the condition for $\varphi=\pi$: :

$$me\frac{\omega^2}{4}>G;$$

$$\omega_{min}>2\sqrt{\frac{g}{e}}, \text{ where } e=\delta. \tag{11.95}$$

For an angular velocity ω less than twice the pendulous frequency, separated precession may take place in the bearing, accompanied by bouncing and unstable phenomena. Stable autorotation is not possible.

Equation (11.94) for equilibrium of the external forces can be reduced to the transition equation. To do this we write its solution in phase trajectory polar coordinates

$$\left.\begin{array}{l}\beta=R\sin\gamma;\\ \beta'=R\cos\gamma.\end{array}\right\} \tag{11.96}$$

Differentiating the first equality and equating it to the second, and substituting the derivative of the second equality into (11.94), we obtain two equations

$$R'\sin\gamma+R\gamma'\cos\gamma=R\cos\gamma;$$

$$R'\cos\gamma-R\gamma'\sin\gamma=F(\beta,\beta'),$$

where $F(\beta,\beta')$ is the function which is the right side of (11.94).

Solving these equations for the derivatives, we obtain the formulas

$$R' = F(\beta, \beta') \cos \gamma + R \sin \gamma \cos \gamma;$$
$$\gamma' = -\frac{1}{R} F(\beta, \beta') \sin \gamma + \cos^2 \gamma.$$

Converting to the phase plane rotating coordinate axes by the substitution

$$\gamma = \varphi + \psi, \tag{11.97}$$

we obtain

$$R' = F(\beta, \beta') \cos(\varphi + \psi) + R \sin(\varphi + \psi) \cos(\varphi + \psi);$$
$$\psi' = -\frac{1}{R} F(\beta, \beta') \sin(\varphi + \psi) - \sin^2(\varphi + \psi). \tag{11.98}$$

Equations (11.98) show the variation of the phase trajectory polar coordinates R and ψ within the limits of a period. Since this change is small, in integrating (11.98) within the limits of a period we can consider these coordinates constant in the right side. Then we obtain the asymptotic equations:

$$\Delta R = \int_0^{2\pi} F(\beta, \beta') \cos(\varphi + \psi) d\varphi; \tag{11.99}$$

$$\Delta \psi = -\frac{1}{R} \int_0^{2\pi} F(\beta, \beta') \sin(\varphi + \psi) d\varphi - \pi. \tag{11.100}$$

We express the function $F(\beta, \beta')$, in accordance with (11.94) in polar coordinates by replacing β and β' using (11.96):

$$F(\beta, \beta') = -\frac{4g}{\omega^2} [\sin \varphi + R \sin(\varphi + \psi) \cos \varphi] -$$
$$- \frac{4B}{\omega m \omega^2} \varphi(\chi) \sqrt{1 - \chi^2} \omega R \cos(\varphi + \psi). \tag{11.101}$$

Here the oil layer lift force P is represented by the formula

$$P = -B \varphi(\chi) \omega R \cos(\varphi + \psi),$$

which was obtained from (11.86) by the replacement

$$(\omega - 2\dot{\alpha}) = \omega - 2\left(\frac{\omega}{2} + \dot{\beta}\right) = -2\dot{\beta} = -\omega\gamma' = -\omega R\cos(\varphi + \psi);$$

$$B = vld \cdot \left(\frac{d}{2\omega}\right)^2;$$

$$\sin\theta = \sqrt{1 - \chi^2};$$

the minus sign in the lift force formula indicates the direction of the circumferential component of the lift force.

Substituting the function $F(\beta, \beta')$ (11.101) into (11.99) and (11.100) and integrating, we obtain:

$$\Delta R = \frac{4\pi}{\omega^3}\left[g\sin\psi - BR\omega\varphi(\chi)\sqrt{1 - \chi^2}\right]; \qquad (11.102)$$

$$\Delta\psi = \pi\left(\frac{4g}{\omega^2 R}\cos\psi - 1\right). \qquad (11.103)$$

Formulas (11.102) and (11.103) show that for certain values of R and ψ the increments ΔR and $\Delta\psi$ become equal to zero. These values are the parameters of the self-excited vibration limit cycle. In accordance with (11.96) and (11.97), the quantity R is the amplitude angle β, and ψ is the phase angle.

The limit cycle is stable. This can be seen by taking disturbances of R larger than and smaller than the limiting value. In the first case ΔR and $\Delta\psi$ become negative, and in the second they become positive, which indicates return of the system to the limit state.

Formulas (11.102) and (11.103) are valid for sufficiently large values of ω. We recall that the lower limit of the angular velocity is defined by the inequality (11.95). For lower angular velocities separated autorotation appears, the deviations of the angle β within the limits of a period become significant, and integration of (11.98) under the assumption of slow change of the parameters β and β' is not permissible.

Just as for the vertical shaft, the upper limit of the angular velocity range within which self-excited vibrations can occur is the velocity equal to twice the critical speed.

Thus, the region of angular velocities for which shaft autorotation is possible in hydrodynamic bearings is defined by the inequality

$$2\sqrt{\frac{I}{b}} < \omega < \omega_{pos} \approx 2\omega_{\kappa p}. \tag{11.104}$$

In this case the autorotation speed under the influence of the hydrodynamic forces is equal to half the shaft rotation speed.

These conclusions are valid for the ideal case, in which the rotor center of gravity lies exactly on the axis of rotation. In real structures there is always some rotor unbalance, which results in the appearance of centrifugal forces owing to the unbalance. The unbalanced force vector rotates with the angular velocity of the shaft and forces the latter to precess with the same velocity, which hinders the onset of self-excited vibrations.

In this case the possibility of self-excited vibration onset depends on the relationship between the out-of-balance and hydrodynamic forces. The rotor which is precisely balanced has more tendency toward self-excited vibrations of this type.

The equations of motion of the journal in bearings for the unbalanced rotor case are analogous to (11.76), with the addition of the projections of the unbalanced forces:

$$\left.\begin{array}{l} m(\ddot{e} - e\dot{\alpha}^2) - G\cos\alpha + P\cos\psi - H\cos(\omega t - \alpha) = 0; \\ m(2\dot{e}\dot{\alpha} + e\ddot{\alpha}) + G\sin\alpha - P\sin\psi - H\sin(\omega t - \alpha) = 0, \end{array}\right\} \tag{11.105}$$

where H is the amplitude of the unbalanced force:

$$H = m a \omega^2;$$

a is the rotor unbalance.

The Bubnov-Galerkin method can be used to obtain the averaged solution of these equations.

11.4.2. Case of Semidry Bearing Friction

Pendulous self-excited vibrations. If bearing lubrication is insufficient or there is none at all, pendulous vibrations of the rotor under the action of the friction forces can arise. A schematic of the action of the forces on the rotor journal is shown in Figure 11.15. Here we assume that there are no unbalanced forces. The position of the rotor in the support is defined by the angle α, which is to be considered variable. The journal radial displacement equals the radial clearance δ. The angular velocity ω is constant. As a result of shaft rotation, the friction force F acting on the journal arises at the point of contact. The friction force F is replaced by the same force applied at the center and the moment F · r. The moment is overcome by the external driving moment and is excluded from further examination.

The rotor dynamic equilibrium conditions are defined by the equations in projections on the ξ, η axes:

$$m\delta\ddot{\alpha} + mg \sin \alpha + F = 0;$$
$$m\delta\dot{\alpha}^2 + mg \cos \alpha = N;$$
$$F = \mu N,$$

(11.106)

where μ is the semidry or dry friction coefficient.

The friction coefficient is a function of the sliding velocity v at the point of contact (Figure 11.16). The form of the function depends on the nature of the lubrication, the quality of the rubbing surfaces, the magnitude of the specific pressure, and so on. No matter what the characteristics of this function, the rest friction coefficient is always greater than the motion friction coefficient. Therefore, there is always a descending segment on the μ curve which,
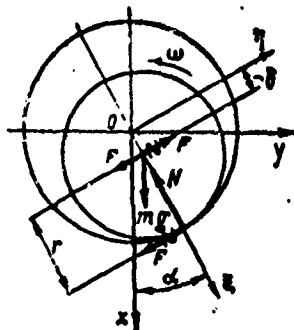
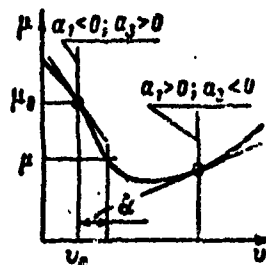Figure 11.15. Action of forces in semidry friction case.

Figure 11.16. Semidry friction coefficient as a function of sliding velocity.

as will be shown later, is the condition for the onset of self-excited vibrations.

In the absence of vibrations $\dot{a}=0; \ddot{a}=0$, and (11.106) define the position of the journal in the bearing:

$$tg\, a_0 = -\mu_0 \qquad (11.107)$$

where a_0 is the angle defining the equilibrium position of the the journal;

μ_0 is the friction coefficient in the equilibrium position, determined from the sliding velocity $v_0 = \omega r.$.

In accordance with (11.107), the equilibrium position is opposite that shown in Figure 11.15. Under the action of the friction force the shaft rolls up onto the bearing surface.

The equilibrium position may be stable or unstable. In the latter case there are pendulous vibrations of the journal about the equilibrium position. The instability conditions are clarified with the aid of the complete equations (11.106).

For variable α the sliding velocity is defined by the formula

$$v = \omega r + \delta \dot{\alpha},$$
(11.108)

which is the sum of the relative and reference-frame velocities of the point of contact.

In this connection, the friction coefficient μ is also variable. It depends on the zero sliding velocity and may be defined by both the ascending and descending segments of the μ characteristic curve. In the semidry and dry friction regimes the characteristic is descending.

In the equilibrium position region, the dependence of μ on α can be written in series form

$$\mu = \mu_0 + a_1 \dot{\alpha} + a_2 \dot{\alpha}^2 + a_3 \dot{\alpha}^3 + \ldots,$$
(11.109)

where

$$a_1 = \frac{d\mu}{d\dot{\alpha}}; \quad a_2 = \frac{1}{2} \frac{d^2\mu}{d\dot{\alpha}^2}; \quad a_3 = \frac{1}{6} \frac{d^3\mu}{d\dot{\alpha}^3}.$$

According to (11.108), the connection between the derivatives with respect to α and with respect to v is defined by the equality

$$\frac{dv}{d\dot{\alpha}} = \delta,$$

Therefore, the formulas for the series coefficients take the form:

$$a_1 = \delta \frac{d\mu}{dv}; \quad a_2 = \frac{1}{2} \delta^2 \frac{d^2\mu}{dv^2}; \quad a_3 = \frac{1}{6} \delta^3 \frac{d^3\mu}{dv^3}.$$
(11.110)

The derivatives of μ with respect to v and also the values of μ_0 in the equilibrium region are determined by the given friction coefficient characteristic curve.

Excluding the reaction N from (11.106), we obtain the differential equation:

$$\ddot{a} + k^2 \sin\alpha + \mu(\dot{a}^2 + k^2 \cos\alpha) = 0, \tag{11.111}$$

where

$$k^2 = \frac{g}{l}.$$

Substituting into (11.111) in place of μ its expansion (11.109) and reducing the equation to characteristic time by the substitution $\phi = kt$, we obtain

$$\alpha'' + \sin\alpha + (\mu_0 + a_1 k\alpha' + a_2 k^2 \alpha'^2 + a_3 k^3 \alpha'^3)(\alpha'^2 + \cos\alpha) = 0,$$

where the prime denotes derivative with respect to ϕ.

We replace

$$\alpha = \alpha_0 + \varepsilon \tag{11.112}$$

where ε is the disturbance with respect to the equilibrium position.

Then we obtain

$$\varepsilon'' + \sin(\alpha_0 + \varepsilon) + (\mu_0 + a_1 k\varepsilon' + a_2 k^2 \varepsilon'^2 +$$
$$+ a_3 k^3 \varepsilon'^3)[\varepsilon'^2 + \cos(\alpha_0 + \varepsilon)] = 0. \tag{11.113}$$

In the brackets the quantity ε'^2 is small in comparison with the quantity $\cos(\alpha_0 + \varepsilon)$, which differs very little from one; therefore, the bracketed expression is taken as one. After transformations, using (11.107) and considering the smallness of ε, we write (11.113) in the form:

$$\varepsilon'' + \varepsilon = -(a_1 k\varepsilon' + a_2 k^2 \varepsilon'^2 + a_3 k^3 \varepsilon'^3). \tag{11.114}$$

The Van de Pol method examined above can be used to reduce this equation to the transition Equations (11.21) and (11.22)

$$\Delta R = \int_0^{2\pi} F(\varepsilon') \cos(\varphi + \psi) d\varphi;$$

$$\Delta \psi = -\frac{1}{R} \int_0^{2\pi} F(\varepsilon') \sin(\varphi + \psi) d\varphi.$$

(11.115)

where $F(\varepsilon')$ is the function denoting the right side of (11.114).

In the integration of (11.115) we replace ε' in the function F by the phase trajectory parameters:

$$\varepsilon' = R \cos(\varphi + \psi); \quad \varepsilon = R \sin(\varphi + \psi).$$

(11.116)

Integration yields:

$$\Delta R = -\pi a_1 k R \left(1 + \frac{3}{4} R^2 k^2 \frac{a_3}{a_1} \right);$$

$$\Delta \psi = 0.$$

(11.117)

The first equality indicates the existence of the self-excited vibration limit cycle and defines the conditions for its existence.

Equating ΔR to zero, we find the two equilibrium states:

$$R = 0; \quad R_a^2 = -\frac{4}{3} \frac{a_1}{k^2 a_3}.$$

(11.118)

In accordance with (11.116) the first solution yields $\varepsilon = 0$, i.e., it indicates the static equilibrium position $a = a_0$. The second solution indicates the amplitude of the limit cycle.

The coefficients a_1 and a_3 of the expansion of the function in the equilibrium region usually have opposite signs, which corresponds to the nature of this function (see Figure 11.16). In this case R_a is real.

The stability of the equilibrium position of the center and of the limit cycle depends on the sign of the coefficient a_1. For dry

friction a_1 is negative, which corresponds to the descending part of the μ characteristic curve. In this case the center position is unstable and the limit cycle is stable. This is easily seen from (11.117). Taking values of R differing somewhat from the stable values, for $R \approx 0$ and $R < R_a$ we obtain positive ΔR, while for $R > R_a$ we obtain negative ΔR. This means that the system approaches the self-excited vibration state.

The condition Δψ = 0 indicates that the self-excited vibrations take place with the frequency of the pendulous vibrations:

$$k = \sqrt{\frac{f}{b}}.$$

The descending branch of the μ curve is usually located in the region of small sliding velocities. Therefore, the self-excited vibration mode in question can arise at low angular velocities.

The amplitude of the self-excited vibrations depends on the shaft angular velocity ω. This dependence is defined by the coefficients a_1 and a_3. There is a specific relationship of these coefficients for every point of the μ curve.

If $a_3 = 0$, or if both a_3 and a_1 are negative, the system does not have a stable position in this region. Under the influence of the friction forces there will be increasing oscillations of the rotor in the support, and the vibration amplitudes will become so large that the further behavior of the system must be examined with the aid of other equations.

<u>Circular self-excited rotor vibrations</u> under the influence of the semidry friction force can arise as a result of intense oscillation buildup or as a result of a random pulse which imparts to the journal a sufficiently large backward precession velocity.

For a vertical shaft or a rotor operating under weightless conditions, circular self-excited oscillations are defined by the equation
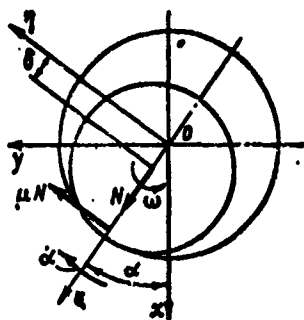
Figure 11.17. Forces causing circular self-induced vibrations in the semidry friction case.

$$m\delta\ddot{\alpha}=\mu\dot{\alpha}^2 m\delta, \qquad (11.119)$$

which represents equality of the circumferential forces — the inertia force and the shaft sliding friction force (Figure 11.17). As noted previously, the friction coefficient is a function of the sliding velocity v. Here the sliding velocity is defined by the difference:

$$v=r\omega-\dot{\alpha}\delta. \qquad (11.120)$$

As v decreases, the friction coefficient μ increases. The disturbance force is always positive and increases with increase of $\dot{\alpha}$. This, in turn, indicates continuous increase of the backward precession velocity. The kinematic limit of the velocity $\dot{\alpha}$ is the condition of rolling without sliding, i.e., v = 0. In accordance with (11.120) we obtain

$$\dot{\alpha}_{max}=\omega\frac{r}{\delta}. \qquad (11.121)$$

This velocity cannot be achieved in practice, since long before reaching it dynamic phenomena arise which are associated with rotor passage through the critical speeds. The dynamics of a flexible rotor on supports with backlash was examined in Chapter 8.

For the horizontal rotor the circular self-excited vibrations are defined by the equation

$$\ddot{\alpha}+k^2\sin\alpha=\kappa(\dot{\alpha}^2-\kappa^2\cos\alpha), \qquad (11.122)$$

which takes into account the effect of the gravity force.

The sum in the parentheses is proportional to the normal pressure of the journal on the bearings at the point of contact. This force is always positive for circular motion of the journal.

Multiplying both sides of (11.122) by $\dot{\alpha}$ and integrating the left side, we obtain

$$\frac{1}{2}\dot{\alpha}^2 - k^2\cos\alpha = \int_0^{\dot{\alpha}} \mu(\dot{\alpha}^2 + k^2\cos\alpha)d\alpha + C,$$ (11.123)

$$N = m l \dot{\alpha}^2 \qquad \text{where} \qquad C = \frac{1}{2}\Omega_0^2 - k^2.$$

The velocity change during a single period is calculated using the formula

$$\dot{\alpha}^2 - \Omega_0^2 = 2\int_0^{2\pi} \mu(\dot{\alpha}^2 + k^2\cos\alpha)d\alpha,$$ (11.124)

where Ω_0 is the initial value of the precession rate.

For circular motion the integral has a positive value. Therefore the backward precession which arises under the influence of the friction force increases with increase of the precession velocity. As the precession velocity increases, the role of the weight force becomes insignificant and the limiting velocity to which the shaft can be accelerated theoretically under the influence of the friction force is the kinematic limit (11.121).

Sometimes long and slender shafts are equipped with so-called false supports (Figure 11.18a) to permit passage through the critical speed. The false supports limit shaft deflection at speeds close to the critical value and thus prevent the onset of excessively large bending stresses in the shaft. The shaft does not contact the support at speeds far from the critical value.

Under certain conditions false supports can be the reason for the onset of circular self-excited backward-precession vibrations.
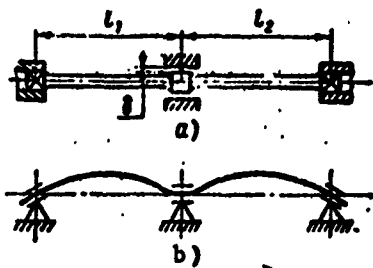
We shall analyze the mechanism for the onset of self-excited vibrations using the example in which the false support is located at the midpoint of the span

$$l_1 = l_2 = l.$$

The first critical speed of such a shaft is found from the well-known formula

Figure 11.18. Flexible shaft with additional support.

$$\omega_1 = \frac{\pi^2}{4l^2}\sqrt{\frac{EJ}{m}},$$
(11.125)

where EJ is the shaft stiffness;
m is the mass per unit length.

Upon approach to this speed the shaft begins to bend markedly, the clearance δ will be taken up, and when the angular velocity reaches the critical value the shaft will contact the surface of the center support. A friction force directed opposite the motion will arise at the point of contact. From this moment the shaft begins to operate as a three-support shaft. Further increase of the angular velocity will be accompanied by increase of the deflections (in accordance with the scheme shown in Figure 11.18b) and increase of the pressure on the center support.

If the support friction coefficient is sufficiently large and the shaft unbalance is small, under the influence of the friction force backward precession may develop with velocity equal to the critical velocity of the three-support shaft. For the scheme in question this angular velocity is defined by the formula

$$\omega = \frac{15.4}{l^2}\sqrt{\frac{EJ}{m}}.$$

After passage through this speed the danger of the appearance of self-excited vibrations disappears.

Such self-excited vibrations can arise in rotors of the vertical type: with large clearances in the supports or in the presence of slotted and labyrinth seals this can occur if the shaft comes into contact with the casing; in the presence of sleeve seals this can occur if the sleeves have high stiffness and radial displacement of the shaft leads to the appearance of a nonuniform friction force along the circumference of the shaft; under the influence of the friction force in a thrust bearing or axial support this can occur if the friction force does not pass through the center of rotation of the shaft.

CHAPTER 12

PARAMETRIC VIBRATIONS

12.1. General Principles

There are systems whose vibrations are defined by linear differential equations with variable coefficients. For the single-mass system this equation can be written in the general form

$$m(t)\ddot{q} + \xi(t)\dot{q} + c(t)q = 0. \tag{12.1}$$

The equation coefficients are time functions which are not associated with the position of the system, and their physical meaning depends on the concrete form of the system and the conditions of its motion.

If the coefficients vary periodically, vibrations which are termed parametric may develop under the influence of the variable parameter.

Equation (12.1) has the simplest solution

$$q(t) = 0.$$

This means that the system has an equilibrium position, although the stability of the system in this position is not defined by the solution.

The equilibrium state is unstable if the system when disturbed from this position begins to execute parametric vibrations.

Stable parametric vibrations are to be considered a particular case. Usually they have the form of decaying or increasing oscillations. In the first case the system approaches the equilibrium position in the course of time, in the second case the oscillations increase without bound, i.e., the parametric resonance phenomenon takes place.

In contrast with conventional resonance in linear systems, which occurs only when the exciting force frequency coincides with the natural vibration frequency, parametric resonance does not require coincidence of the parameter variation frequency with the natural vibration frequency, therefore its occurrence is possible over a wide range of disturbing parameter frequencies.

It is not possible to find the general solution of (12.1) and there is no need to do so, since the parametric vibration amplitudes vary in one direction or the other in the course of time. It is far more important to use the equation to find the system stability and parametric resonance zones, relating them with the system physical property coefficients.

In many engineering problems the general solution of (12.1) reduces to the Hill equation

$$\ddot{q} + \Psi(t)q = 0, \qquad (12.2)$$

where $\Psi(t)$ is a periodic function with period τ.

A particular case of the Hill equation, but more frequently encountered, is the Mathieu equation

$$\ddot{q} + [b + \mu\Phi(t)]q = 0, \tag{12.3}$$

where b is a constant;

  $\Phi(t)$ is the harmonic function sin t or cos t, having a period
    equal to 2π;

   μ is a small parameter characterizing the amplitude $\Phi(t)$ or,
    as we say, defining the pulsation intensity.

The argument t of the function $\Phi(t)$ is to be considered in the
equation as the characteristic time, with respect to which the deriva-
tives are taken, and which is the argument of the sought solution.
Reduction of differential equations to the characteristic time was
examined in the preceding chapters of the second part of the book.

The general solutions of the Hill and Mathieu equations for a
small parameter μ have the form

$$q = e^{\lambda t} f(t), \tag{12.4}$$

where f(t) is a periodic function with period 2π, equal to the
    parameter period;

   λ is the coefficient which defines the nature of the
    parametric vibrations. Positive values of λ characterize
    increase of the amplitudes, i.e., they indicate the
    parametric resonance case.

As a result of the periodicity of the function f(t), the ampli-
tude increase per period is defined by the ratio

$$s = \frac{q(t + 2\pi)}{q(t)} = e^{\lambda 2\pi}. \tag{12.5}$$

The amplitudes increase in geometric progression

$$q(t + 2\pi n) = s^n q(t), \tag{12.6}$$

where n is the number of periods elapsed.

The vibration velocities grow in the same proportion

$$\dot{q}(t+2\pi n) = s^n \dot{q}(t).$$ (12.7)

12.2. Meissner Equation

12.2.1. General Method for Estimating System Stability

Let us determine the stability of a system with stepwise stiffness parameter variation law (Figure 12.1.).

For this case, the Hill parametric vibration equation (12.2) has the form

$$\ddot{q} + (b \pm \Delta)q = 0.$$ (12.8)

Equation (12.8) is reduced to the stiffness parameter pulsation period by the substitution

$$t = \omega \tau,$$

where ω is the stiffness parameter pulsation frequency; $b = c/m_\omega^2$ and $\Delta = \Delta c/m_\omega^2$; the plus sign in (12.8) corresponds to the first half of ten stiffness parameter pulsation period, the minus sign corresponds to the second half of the period.

The reduced form of (12.8) has been studied in detail by Prof. Meissner and is therefore associated with his name.

The stiffness coefficient of (12.8) keeps a constant value within the limits of each half-period. Therefore, we can use the solutions for simple harmonic oscillations

$$\left.\begin{array}{l} q_1 = C_1 \sin p_1 t + C_2 \cos p_1 t; \\ q_2 = C_3 \sin p_2 t + C_4 \cos p_2 t, \end{array}\right\}$$ (12.9)

Figure 12.1. Stepped stiffness parameter variation law.
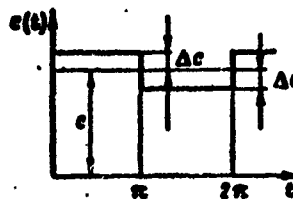
where

$$p_1^2 = b + \Delta; \quad p_2^2 = b - \Delta. \tag{12.10}$$

The integration constants C_i must satisfy the conditions for continuity of the velocity and displacement functions, and also their periodicity

$$\left.\begin{array}{l} q_1(\pi) = q_2(\pi); \quad \dot{q}_1(\pi) = \dot{q}_2(\pi); \\ q_2(2\pi) = s q_1(0); \quad \dot{q}_2(2\pi) = s \dot{q}(0). \end{array}\right\} \tag{12.11}$$

Substituting herein the solutions (12.9), we obtain the system of equations

$$\begin{array}{l} C_1 \sin \pi p_1 + C_2 \cos \pi p_1 - C_3 \sin \pi p_2 - C_4 \cos \pi p_2 = 0; \\ C_1 p_1 \cos \pi p_1 - C_2 p_1 \sin \pi p_1 - C_3 p_2 \cos \pi p_2 + \\ \quad + C_4 p_2 \sin \pi p_2 = 0, \\ C_2 s - C_3 \sin 2\pi p_2 - C_4 \cos 2\pi p_2 = 0; \\ C_1 p_1 s - C_3 p_2 \cos 2\pi p_2 + C_4 p_2 \sin 2\pi p_2 = 0. \end{array} \tag{12.12}$$

The system determinant must equal zero. Formulating this determinant and expanding it into a row, we obtain the characteristic equation

$$s^2 - 2sA + 1 = 0, \tag{12.13}$$

where

$$A = \cos \pi p_1 \cos \pi p_2 - \frac{p_1^2 + p_2^2}{2 p_1 p_2} \sin \pi p_1 \sin \pi p_2. \tag{12.14}$$

Solution of the quadratic Equation (12.13) yields

$$s = A \pm \sqrt{A^2 - 1}. \tag{12.15}$$

We see that the factor s depends on the magnitude of A. If A is positive and larger than one, then one of the roots s is larger than one. This is the parametric resonance condition, indicating increase of the vibration amplitudes after each pulsation period.

Several complete oscillation periods may fall in a single parameter pulsation period. Therefore, the parametric resonance vibration frequency for the cases A > (+1) may be equal to or a multiple of the pulsation frequency

$$p = n; \quad n = 1, 2, 3, \ldots \tag{12.16}$$

where n is the multiplicity number.

If A = 1, then s = 1, and the vibrations are stable, since they take place with constant amplitude. If A is negative and less than minus one, then one of the values of s is negative and numerically larger than one, and the vibrations are correspondingly unstable. This is the second parametric resonance condition. The negative sign indicates that the deflections are of alternating sign. Therefore, during one parameter pulsation period half of an oscillation period is performed. This also means that a whole odd number of oscillation half-periods fall in a single pulsation period.

Under these conditions, the parametric vibrations take place with the frequency

$$p = n - \frac{1}{2}; \quad n = 1, 2, 3, \ldots \tag{12.17}$$

If A = -1, then s = -1, and we have steady-state parametric vibrations with the indicated frequency.

When the value of A lies between +1 and -1, the value of s is complex

$$s = A \pm i \sqrt{1 - A^2}. \tag{12.18}$$

The modulus of the complex number equals one. This means that the vibrations amplitudes do not have a tendency to grow in this zone. The condition A = ±1 indicates the boundaries of the stable regions.

The coefficient A depends only on two quantities — b and Δ. Utilizing (12.14) and setting A equal to +1 or -1, we can plot the boundaries of the stable zones in the coordinates Δ and b (Figure 12.2). This diagram is called the system stability map. The full lines correspond to A = +1, the dashed are for A = -1. The shaded regions are the stability zones.

It can be shown that parametric resonance zones with a frequency which is a multiple of the parameter pulsation frequency are located between the full curves. Between the dashed curves there are zones of parametric resonance with a frequency which is a multiple of half the parameter frequency. The apexes of the parametric resonance zones lie on the abscissa axis. The coordinates of these apexes correspond to the square of the multiplicity number

$$b = n^2 \quad \text{or} \quad b = \left(n - \frac{1}{2}\right)^2. \tag{12.19}$$

These equalities are easily obtained using (12.14). In accordance with (12.10), for Δ = 0, $p_1 = p_2 = \sqrt{b}$. In this case, (12.14) becomes the equality

$$A = \cos 2\pi \sqrt{b};$$
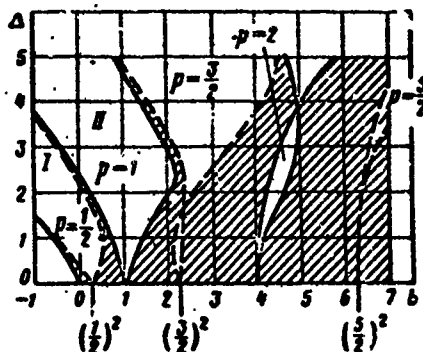
Setting A = +1 or A = -1, we obtain (12.19)

Figure 12.2. Stability map of system with stepped stiffness parameter variation.

p) number of oscillations per period of stiffness parameter variation.

In practice the first two instability regions — I and II — are the most important, since large vibrations may be expected corresponding to the parameters of these regions.

The magnitude of the coefficient Δ, which shows the parameter pulsation intensity, has a significant effect on the possibility of parametric resonance occurrence. Increase of Δ broadens the limits of the values of b within which resonance occurs.

The stability map plotted in terms of dimensionless parameters avoids the necessity to solve the Hill equation.

To resolve the question of the stability of a system with pulsating parameters, we need only reduce the differential equation of the system to the standard form (12.8) and use the coefficients of this equation together with the stability map to resolve the stability question.

12.2.2. Effect of Friction Forces on Parametric Resonance

The action of friction forces can lead to different results. In certain cases the friction forces may disrupt system stability; in other cases, the system may be stabilized by the friction forces.

Let us examine the influence of friction forces on a system with pulsating parameter. After introduction of viscous friction into (12.9), it takes the form:

$$\ddot{q} + 2\varkappa\dot{q} + (b \pm \Delta)q = 0. \tag{12.20}$$

The solutions of this equation for each pulsation half-period will be

$$q_1 = e^{-\varkappa t}(C_1 \sin p_1 t + C_2 \cos p_1 t); \\ q_2 = e^{-\varkappa t}(C_3 \sin p_2 t + C_4 \cos p_2 t), \tag{12.21}$$

where

$$p_1^2 = b - \xi^2 + \Delta; \quad p_2^2 = b - \xi^2 - \Delta. \tag{12.22}$$

The conditions for joining of the segments (12.11) lead to the same system of Equations (12.12) and Formula (12.14), with the sole difference that the values of p_1 and p_2 are to be taken in accordance with (12.22), accounting for the friction forces. Considering $(b - \xi^2)$ as the new parameter

$$b_t = b - \xi^2, \tag{12.23}$$

we can use the stability map (see Figure 12.2).

The friction forces shift the stability boundaries in the direction of the instability regions, narrowing the latter. In practice this shift is negligibly small.

The apexes of the instability regions do not reach the abscissa axis for the systems with friction. This means that small pulsations of the stiffness parameter are not capable of causing parametric vibrations in a system with friction.

Systems are possible in which the stiffness parameter pulsation is represented by more complex programs (Figure 12.3a and b). In this case, the period breaks down into unequal segments. Analysis of such systems and the construction of their stability map can be accomplished using the approach discussed above. But in this case, the system of equations for joining of the segments becomes more complicated, and the volume of calculations required to plot the stability map increases significantly.

12.3. Mathieu Equation

12.3.1. General Method for Constructing Stability Map
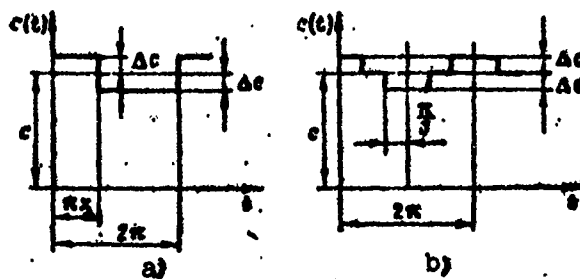
We examine the Mathieu equation in the form

Figure 12.3. Versions of stiffness
variation laws:

x - fraction of half-period.

$$\ddot{q}+(b+\mu \cos t)q=0. \qquad (12.24)$$

To plot the stability map we must plot the bounding curves for
the conditions A = +1 and A = -1.

For the condition A = +1 we write the solution of (12.24) in
Fourier series form

$$q=B_0+A_1\sin t+B_1\cos t+A_2\sin 2t+B_2\cos 2t+ \\ +A_3\sin 3t+ \ldots ; \qquad (12.25)$$

the arguments of the functions of the series terms are multiples of
the fundamental frequency.

Substituting the solution into (12.24) and equating the coeffi-
cients of like trigonometric functions to zero, we obtain the system
of linear homogeneous equations

$$(b-1)A_1+\frac{1}{2}\mu A_3=0;$$
$$\frac{1}{2}\mu A_1+(b-4)A_2+\frac{1}{2}\mu A_3=0;$$
$$\frac{1}{2}\mu A_2+(b-9)A_3+\frac{1}{2}\mu A_4=0; \qquad (12.26)$$

$$\dot{b}\bar{B}_0 + \frac{1}{2}\mu\bar{B}_1 = 0;$$

$$\mu B_0 + (b-1)B_1 + \frac{1}{2}\mu B_2 = 0;$$

$$\frac{1}{2}\mu B_1 + (b-4)B_2 + \frac{1}{2}\mu B_3 = 0;$$

$$\frac{1}{2}\mu B_2 + (b-9)B_3 + \frac{1}{2}\mu B_4 = 0. \tag{12.27}$$

Forming the determinants of each group of equations and equating them to zero, we obtain two equations for determining the multiple frequency boundary curves.

The determinant of the system (12.26) has three roots, i.e., it yields three branches; the determinant of (12.27) has four roots and yields four corresponding branches. These branches are shown on the stability map (Figure 12.4) by the full lines. The apexes of the parametric resonance zone, formed by the full boundary lines, lie at the values

$$b = 0; \quad b = 1; \quad b = 4, \ldots$$

Figure 12.4. Stability map for the Mathieu equation — Ince-Strutt diagram:

p - number of oscillations per period of stiffness parameter variation.

As the number of terms of the basic solution (12.25) is increase, the order of the determinant increases. At the same time there is an increase of the number of branches defined and the accuracy of their location on the stability map.

The resulting boundary lines can be represented with accuracy which is quite satisfactory for practical purposes by the following equations, which are obtained from (12.27) and (12.26)

$$b = -\frac{1}{2}\mu^2; \qquad b = 1 - \frac{1}{12}\mu^2;$$

$$b = 1 + \frac{5}{12}\mu^2; \qquad b = 4 + \frac{1}{12}\mu^2.$$

$$b = 4 + \frac{1}{30}\mu^2;$$

$$b = 9 + \frac{1}{20}\mu^2;$$

<div align="right">(12.28)</div>

The boundary curves for half-multiplicity (A = -1) are obtained by writing the solution of the equation in Fourier series form

$$q = A_1 \sin\frac{t}{2} + B_1 \cos\frac{t}{2} + A_3 \sin 3\frac{t}{2} +$$

$$+ B_3 \cos 3\frac{t}{2} + \ldots$$

<div align="right">(12.29)</div>

Substituting the solution (12.29) into the Mathieu Equation (12.24) and collecting terms with the same trigonometric functions, we obtain two more systems of equations

$$\left(b - \frac{1}{4} - \frac{1}{2}\mu\right)A_1 + \frac{1}{2}\mu A_3 = 0;$$
$$\frac{1}{2}\mu A_1 + \left(b - \frac{9}{4}\right)A_3 = 0;$$

<div align="right">(12.30)</div>

$$\left(b - \frac{1}{4} + \frac{1}{2}\mu\right)B_1 + \frac{1}{2}\mu B_3 = 0;$$
$$\frac{1}{2}\mu B_1 + \left(b - \frac{9}{4}\right)B_3 = 0.$$

<div align="right">(12.31)</div>

If we restrict ourselves to the first equations of each pair, dropping terms containing A_3 and B_3, we obtain the equations of the boundary lines, beginning at the point b = 1/4

$$b = \frac{1}{4} + \frac{1}{2}\mu; \qquad b = \frac{1}{4} - \frac{1}{2}\mu.$$

<div align="right">(12.32)</div>

A more exact position of the boundary curves is found from the formula based on both pairs of equations:

$$b = \frac{1}{4}(5+\mu) \pm \sqrt{1 - \frac{1}{2}\mu + \frac{5}{16}\mu^2};$$
$$b = \frac{1}{4}(5-\mu) \pm \sqrt{1 + \frac{1}{2}\mu + \frac{5}{16}\mu^2}. \qquad (12.33)$$

The formulas remain quite accurate for values of μ not exceeding 2. They yield the dashed boundaries shown in Figure 12.4.

The Mathieu equations containing the trigonometric function cos t or sin t are identical. One equation is easily transformed into the other by the substitution

$$t = z - \frac{\pi}{2}.$$

Therefore, the stability map is applicable for both forms of the equations.

12.3.2. Parametric Oscillations of Mathematical Pendulum

The motion of ε mathematical pendulum under the action of a circular vector is described by the equation

$$\ddot{\varphi} + k^2\varphi = h\sin(\omega t - \varphi), \qquad (12.34)$$

where ω is the circular frequency of the disturbance vector H

$$h = \frac{H}{ml^2}.$$

For small deviations ϕ the equation reduces to the form

$$\ddot{\varphi} + (k^2 + h\cos\omega t)\varphi = h\sin\omega t. \qquad (12.35)$$

The equation is further reduced to characteristic time by the substitution $\chi = \omega t$:

$$\varphi'' + \left(\frac{k^2}{\omega^2} + \frac{h}{\omega^2}\cos\chi\right)\varphi = \frac{h}{\omega^2}\sin\chi; \qquad (12.36)$$

Here the primes denote derivative with respect to χ.

Equation (12.36) without the right side is the Mathieu equation. The parametric resonance regions can be indicated with the aid of the general stability map (see Figure 12.4). Here the governing parameters are

$$b=\frac{\Omega}{\omega^2}; \quad \mu=\frac{h}{\omega^2}.$$

In accordance with the stability map, for a small value of h parametric oscillations of the pendulum occur in the region of the following frequency ratios

$$\frac{\Omega}{\omega^2}=\frac{1}{4}; \ 1; \ \frac{9}{4} \quad \text{etc.}$$

The complete Equation (12.36) must be examined if the parameters b and μ correspond to the stable region. Then the forced oscillations of the pendulum may be defined in series form

$$\varphi=A_1\sin\chi+A_2\sin 2\chi+A_3\sin 3\chi+\ldots \qquad (12.37)$$

Substituting this solution into (12.36), grouping terms with common trigonometric factor, and equating the resulting sums to zero, we obtain a system of equations analogous to (12.26), but with a right side

$$(b-1)A_1+\frac{1}{2}\mu A_2=\frac{h}{\omega^2};$$
$$\frac{1}{2}\mu A_1+(b-4)A_2+\frac{1}{2}\mu A_3=0;$$
$$\frac{1}{2}\mu A_2+(b-9)A_3+\frac{1}{2}\mu A_4=0. \qquad (12.38)$$

The system of Equations (12.38) makes it possible to find the entire sequence of coefficients of the series (12.37).

The equation of the oscillations of a pendulous mass m_1 under the influence of an unbalanced mass m_2 rotating uniformly around the mass m_1 (Figure 12.5) reduces to (12.34) and then to (12.36).

The position of each of the masses is defined by the coordinates

$$
\left.
\begin{aligned}
x_1 &= l\cos\varphi; \quad y_1 = l\sin\varphi; \\
x_2 &= l\cos\varphi + r\cos\omega t; \\
y_2 &= l\sin\varphi + r\sin\omega t.
\end{aligned}
\right\}
\tag{12.39}
$$

Differentiating each expression twice, we obtain the accelerations, which we on the ξ, η axes, fixed with the pendulum, and as a result we the acceleration projections

$$
\left.
\begin{aligned}
\ddot{\xi}_1 &= -l\dot{\varphi}^2; \quad \ddot{\xi}_2 = -l\dot{\varphi}^2 - r\omega^2\cos(\omega t - \varphi); \\
\ddot{\eta}_1 &= l\ddot{\varphi}; \quad \ddot{\eta}_2 = l\ddot{\varphi} - r\omega^2\sin(\omega t - \varphi).
\end{aligned}
\right\}
\tag{12.40}
$$

Forming the sum of the projections of the inertia forces and the weight forces on the η axis, we obtain the equation of motion of the pendulum:

$$
(m_1 + m_2)(l\ddot{\varphi} + g\sin\varphi) = m_2 r\omega^2\sin(\omega t - \varphi);
$$

Dividing all the terms by $(m_1 + m_2)l$, we obtain

$$
\ddot{\varphi} + k^2\sin\varphi = \frac{m_2}{m_1 + m_2}\,\frac{r}{l}\,\omega^2\sin(\omega t - \varphi).
\tag{12.41}
$$

This equation is analogous to (12.34) and reduces to the Mathieu equation:

$$
\varphi'' + (b + \mu\cos\alpha)\varphi = \mu\sin\alpha,
\tag{12.42}
$$

where

$$
\alpha = \omega t; \quad B = \frac{k^2}{\omega^2}; \quad \mu = \frac{m_2}{m_1 + m_2}\,\frac{r}{l}.
\tag{12.43}
$$

Equation (12.52) shows that a mass which is free to perform pendulous oscillations under the influence of an unbalanced force
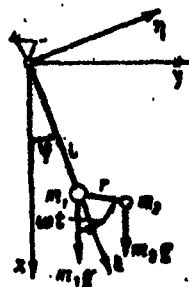
Figure 12.5. Parametric pendulous   Figure 12.6. Schematic of pendu-
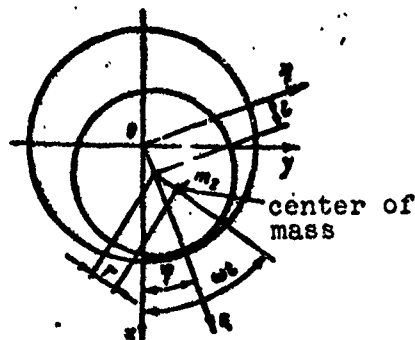oscillations under the action of   lous parametric oscillations of
unbalance.   shaft in journal with backlash.

has parametric resonances in the region of angular velocities ω which
are multiples of half the pendulous oscillation natural frequency.
Just as in conventional systems, the primary resonance is equality
of the angular velocity to the pendulous oscillation frequency —
$\omega = k$.

This system is realized in practice in rotors of gas turbine
engines and pump assemblies. In these cases, in which there are
radial clearances in the rotor bearings (Figure 12.6) the rotor can
execute pendulous oscillations with the frequency

$$k = \sqrt{\frac{L}{i}}.$$

The parametric force arises as a result of rotor unbalance,
defined by the static moment of its mass relative to the center of
the journal.

In using (12.43) to determine the parameters of the rotor
system, we must take

$$b = \frac{L}{i\omega}; \quad p = \frac{a}{\omega i}, \tag{12.44}$$

where l is the radial clearance in the supports;

   m is the rotor mass;

   a is the balancing precision — the static moment of the
   center of mass relative to the axis of rotation.

Parametric pendulous oscillations cannot develop with unbounded increase of the amplitudes. The nonlinear properties of the system begin to show up more and more strongly with increase of the amplitudes, and this limits the growth of the amplitudes.

However, we note that for an angular velocity exceeding the pendulous oscillation circular frequency parametric oscillations can transition into the circular motion which was examined in the preceding sections.

12.3.3. Inverted Pendulum

The inverted pendulum is usually unstable. However, if the support points are imparted periodic motion along the vertical, under certain conditions the upper position of the pendulum becomes stable.

Let us write the equation of motion of the pendulum. The position of its mass in the x,y coordinates (Figure 12.7) is defined by the equalities

$$x = x_0 + l \cos \varphi; \quad y = l \sin \varphi,$$

where x_0 is a variable coordinate defining the motion of the support point.

Differentiating, we obtain the accelerations:

$$\left. \begin{aligned} \ddot{x} &= \ddot{x}_0 - l\ddot{\varphi} \sin \varphi - l\dot{\varphi}^2 \cos \varphi; \\ \ddot{y} &= l\ddot{\varphi} \cos \varphi - l\dot{\varphi}^2 \sin \varphi. \end{aligned} \right\} \tag{12.45}$$
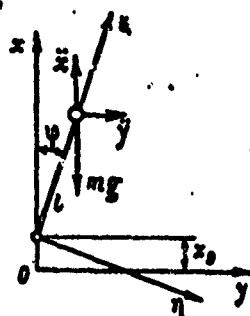
For harmonic support point motion law

Figure 12.7. Inverted
pendulum.

$$x_0 = X \cos \omega t; \\ \ddot{x}_0 = -X \omega^2 \cos \omega t, \qquad (12.46)$$

where X and ω are respectively the amplitude and frequency of the support point oscillations.

Projecting the accelerations on the η axis, we write the equation of equilibrium of the projections of the inertia forces and the weight force on this axis

$$\ddot{\eta} = l\ddot{\varphi} + X\omega^2 \cos \omega t \sin \varphi; \qquad (12.47)$$
$$-m\ddot{\eta} + mg \sin \varphi = 0. \qquad (12.48)$$

After substituting $\ddot{\eta}$ from (12.47) into (12.48) and minor transformations, (12.48) takes the form

$$\ddot{\varphi} + \left(-k' + \frac{X}{l} \omega^2 \cos \omega t\right) \sin \varphi = 0. \qquad (12.49)$$

After the substitution $\alpha = \omega t$ this equation reduces to the proper form of the Mathieu equation

$$\varphi'' + (b + \mu \cos \alpha)\varphi = 0, \qquad (12.50)$$

where

$$b = -\frac{k}{\omega^2}; \quad \mu = \frac{X}{l}. \qquad (12.51)$$

The stability map (Figure 12.8) of the inverted pendulum shows that a stable upper position of the pendulum can be obtained for a negative value of the parameter b. To this end it is necessary to select the amplitude X and frequency ω of the support oscillations so that the describing point lies in the shaded zone of the stability map. This requires satisfaction of the inequality

$$\sqrt{-2b} < \mu < \frac{1}{2} - 2b.$$

This inequality is easily obtained with the aid of the equations of the stability boundaries shown in the figure.

Substituting herein b and μ from (12.51), we obtain the stability condition:

$$\sqrt{\frac{2gl}{\omega^2}} < X < \left(\frac{l}{2} + \frac{2g}{\omega^2}\right). \tag{12.52}$$

The left side of the inequality shows that the amplitudes of the support point oscillations required for stability of the upper position of the pendulum decrease with increase of the support oscillation frequency.
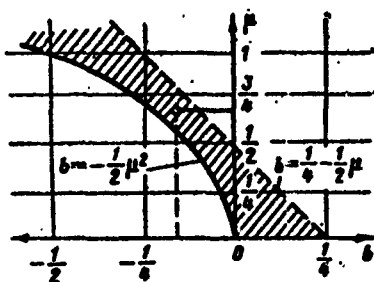

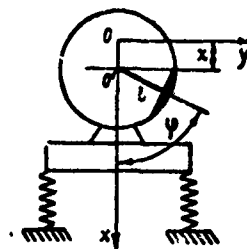Figure 12.8. Stability map of inverted pendulum.

Figure 12.9. Self-synchronization of unbalanced mass.

12.4. Synchronization of Rotational and Vibrational Motions

Let us examine an unbalanced mass (Figure 12.9) capable of performing free rotational motion, mounted on a base which executes harmonic oscillations

$$x = X \cos \omega t.$$

We shall find the conditions under which the mass under the influence of the harmonic oscillations of the base will perform stable rotational motion around the restraint point 0'.

The differential equation of motion is obtained in the same way as for the inverted pendulum and will have the form

$$\ddot{\varphi} + \left(k^2 + \frac{X}{l} \omega^2 \cos \omega t \right) \sin \varphi = 0. \tag{12.53}$$

Equation (12.53) differs from (12.49) in the sign of k^2 only because the position of the coordinate axes has been changed.

The rotational motion has an angular velocity which is not constant within the limits of the period. We represent this motion in the form of the sum

$$\varphi = \omega t + \psi(t), \tag{12.54}$$

where $\psi(t)$ is the deviation of the rotation angle from the average value.

By substitution of the expression adopted for ϕ into (12.53), we reduce the equation to the form

$$\ddot{\varphi} + \left(k^2 + \frac{X}{l} \omega^2 \cos \omega t \right) \sin(\omega t + \psi) = 0;$$

By the substitution $\alpha = \omega t$ we reduce this equation to characteristic time

$$\varphi'' + \left(\frac{k^2}{\omega^2} + \frac{X}{l} \cos \alpha \right) \sin(\alpha + \psi) = 0. \tag{12.55}$$

Assuming that ψ is not large, we transform (12.55) to the form:

$$\psi'' + \left(\frac{k^2}{\omega^2} + \frac{X}{l}\cos\alpha\right)\psi\cos\alpha = -\left(\frac{M}{\omega^2} + \frac{X}{l}\cos\alpha\right)\sin\alpha$$

and we finally obtain

$$\psi'' + (\mu + b\cos\alpha + \mu\cos 2\alpha)\psi = -(b\sin\alpha + \mu\sin 2\alpha), \qquad (12.56)$$

where

$$b = \frac{k^2}{\omega^2}; \quad \mu = \frac{1}{2}\frac{X}{l}. \qquad (12.57)$$

We have obtained the Hill equation with a right side.

The general solution of this linear equation consists of the solution of the homogeneous equation and the particular solution of the complete equation.

The solution of the homogeneous equation can be reduced to the construction of the stability map. The stability zones of this map show the conditions for stability of the adopted solution (12.54) as the solution for the rotational motion with small deviation from the average motion.

To construct the stability map we take the solution in Fourier series form

$$\psi = B_0 + A_1\sin\alpha + B_1\cos\alpha + B_2\sin 2\alpha + B_2\cos 2\alpha + \ldots \qquad (12.58)$$

As was done previously, we substitute this solution into (12.56) without the right side. We equate to zero the sums of terms having the same trigonometric factors. From the coefficients of the two resulting systems of equations we formulate determinants which we equate to zero; they yield the equations of the continuous boundary curves of the stability map (Figure 12.10).
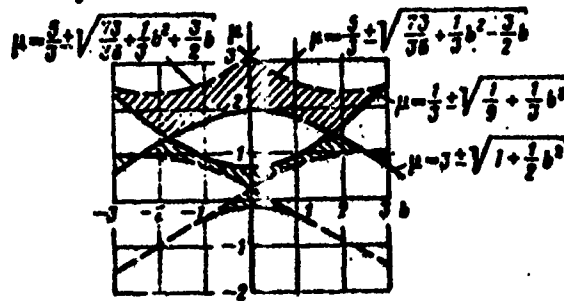
Figure 12.10. Stability map of synchronized
rotation.

The construction of the dashed boundary curves is carried out
similarly on the basis of the solution taken in the form of a Fourier
series with half-arguments

$$\phi = A_1 \sin \frac{\alpha}{2} + B_1 \cos \frac{\alpha}{2} + A_2 \sin 3 \frac{\alpha}{2} + B_2 \cos 3 \frac{\alpha}{2} + \cdots \qquad (12.59)$$

As is known, the zones of parametric resonance lie between like
curves, and the stability zones lie between unlike curves (shaded
regions).

The stability zones show the parameters (12.57) for which self-
synchronization of the free circular motion of the pendulum with the
harmonic oscillations of the table is possible.

If the parameters b and μ correspond to unstable zones, this
indicates that the amplitudes of the relative oscillations begin to
increase and grow beyond the small oscillation limit.

The stability map shown in Figure 12.10 is constructed for three
terms of the Fourier series. To refine the position of the boundary
curves in the region of large values of μ, it is necessary to increase
the number of terms of the Fourier series in the solutions (12.58)
and (12.59).

The solution of the complete Equation (12.56) yields the forced
vibrations and indicates the nonuniformity of the circular motion in
the stability zone. This solution is represented in Fourier series
form with arguments which are multiples of the arguments of the right
side of (12.56)

$$\varphi = A_1 \sin \alpha + A_2 \sin 2\alpha + A_3 \sin 3\alpha + \ldots \qquad (12.60)$$

Substituting (12.60) into (12.56) and collecting after transform-
ations coefficients with the same trigonometric factor, we obtain the
system of equations

$$\left.
\begin{aligned}
\left(\frac{1}{2}\mu - 1\right) A_1 + \frac{1}{2} b A_2 - \frac{1}{2}\mu A_3 &= -b; \\
\frac{1}{2} b A_1 + (\mu - 4) A_2 + \frac{1}{2} b A_3 &= -\mu; \\
\frac{1}{2}\mu A_1 + \frac{1}{2} b A_2 + (\mu - 9) A_3 &= 0,
\end{aligned}
\right\} \qquad (12.61)$$

which yields the possibility of finding the coefficients A_i of the
Fourier series and thereby defining completely the solution for
forced vibrations of the pendulum and the nonuniformity of its
rotation.

The solutions become meaningless for parameters lying on the
boundary of the stability zones, when the determinant of the system
(12.61) vanishes. This means that the zone boundaries themselves
should be considered part of the instability zones.

This self-synchronization phenomenon can show up in assemblies
having several rotors rotating with the same speed and mounted on a
common elastic base, or or coaxial shafts which are not mechanically
coupled with one another. As a result of the vibrations of the common
base, taking place under the influence of rotor unbalance, the rotor
disbalances gradually occupy a parallel position and will rotate in
synchronism. As a result, all the unbalances combine, and the dynamic
load on the supports increases.

The self-synchronization property can be utilized in those cases in which it is necessary to synchronize the rotation of two objects without the use of mechanical coupling — for example, in the installation of vibrators, one of which is driving and the others are synchronized with it.

The self-synchronization property depends on the magnitude of the friction forces acting in the system. The friction forces narrow the self-synchronization zones and also lead to the appearance of a phase shift in the motion of the individual elements. The driven element has a phase lag from the driving element. The phase shift leads to energy transfer from one element to another.

For example, in synchronized vibrators the driving vibrator must have a large shift angle and be sufficiently powerful to maintain the required amplitude of the vibrations of the common base.

REFERENCES

1. А н а н ь е в И. В., Т и м о ф е е в П. Г., Колебания упругих систем в авиационных конструкциях и их демпфирование, изд-во «Машиностроение», 1965.

2. А н д р о н о в А. А., В и т т А. А., Х а й к и н С. Э., Теория колебаний, Физматгиз, 1959.

3. Б а б а к о в И. М., Теория колебаний, изд-во «Наука», 1965.

4. Б и р г е р И. А., Вариационные методы в строительной механике турбомашин, Оборонгиз, 1959.

5. Б и ц е н о К. Б. и Г р а м м е л ь Р., Техническая динамика, т. II, Гостехиздат, 1952.

6. Б о г о л ю б о в Н. Н., М и т р о п о л ь с к и й Ю. А., Асимптотические методы з теории нелинейных колебаний, Физматгиз, 1958.

7. Б о г о м о л о в С. И., Совместные колебания рабочих лопаток и дисков турбомашин, «Энергомашиностроение», 1965, № 2.

8. Б у л г а к о в Б. В., Колебания, Гостехиздат, 1954.

9. Г а н т м а х е р Ф. Р., К р е й н М. Г., Осцилляционные матрицы и ядра и малые колебания механических систем, Гостехиздат, 1950.

10. Г р и г о р ь е в Н. В., Нелинейные колебания элементов машин и сооружений, Машгиз, 1961.

11. Г р о б о в В. А., Асимптотические методы исследования колебаний, изд-во АН СССР, 1960.

12. Г у р о в А. Ф., Расчеты на прочность и колебания в ракетных двигателях, изд-во «Машиностроение», 1966.

13. Д е н - Г а р т о г Дж. П., Механические колебания, Физматгиз, 1960.

14. Д и м е н т б е р г Ф. М., Изгибные колебания вращающихся валов, изд-во АН СССР, 1959.

15. Д и м е н т б е р г Ф. М., Ш а т а л о в К. Т., Г у с а р о в А. А., Колебания машин, изд-во «Машиностроение», 1964.

16. Д о н д о ш а н с к и й В. К., Расчет колебаний упругих систем на электронных вычислительных машинах, изд-во «Машиностроение», 1965.

17. Ж у р а в л е в а А. М., К р а в ц о в В. Я., Расчет собственных частот и форм колебаний ротора диско-барабанной конструкции, Сб. «Динамика и прочность машин», вып. 6, издание Харьковского университета, 1967.

18. З е й т м а н М. Ф., О выборе оптимальных конструкционных параметров многоопорных роторов при изгибных колебаниях, Сб. «Машиноведение», № 2, изд-во АН СССР, 1966.

19. К е м п н е р М. Л., Методы динамических податливостей и жесткостей для расчета изгибных колебаний упругих систем со многими степенями свободы, Сб. «Поперечные колебания и критические скорости», № 1, изд-во АН СССР, 1951.

20. К о в а л е н к о А. Д., Круглые пластины переменной толщины, Физматгиз, 1959.

21. К р ю к о в К. А., Связанные изгибные колебания ротора и корпуса авиационного газотурбинного двигателя, Труды МАИ, вып. 100, Оборонгиз, 1959.

22. К э н н и н х э м В., Введение в теорию нелинейных систем, Госэнергоиздат, 1952.

23. Л е в и н А. В., Лопатки и диски паровых турбин, Госэнергоиздат, 1953.

24. Лойцянский Л. Г., Лурье А. И., Курс теоретической механики, т. 2, Гостехиздат, 1955.

25. Митропольский Ю. А., Асимптотические методы в теории нелинейных колебаний, изд-во «Наука», 1964.

26. Обморшев А. Н., Введение в теорию колебаний, изд-во «Наука», 1965.

27. Огуречников А. Н., Динамические жесткости вращающихся валов, Труды МАИ, вып. 55, Оборонгиз, 1966.

28. Пановко Я. Г., Губанова И. И., Устойчивость и колебания упругих систем, изд-во «Наука», 1964.

29. Пановко Я. Г., Основы прикладной теории упругих колебаний, изд-во «Машиностроение», 1967.

30. Писаренко Г. С., Рассеяние энергии при механических колебаниях, изд-во АН УССР, 1962.

31. Пономарев С. Д., Бидерман В. Л., Лихарев К. К., Макушин В. М., Малинин Н. Н., Феодосьев В. И., Расчет на прочность в машиностроении, Машгиз, 1960.

32. Прочность. Устойчивость. Колебания, Справочник, под ред. д-ра техн. наук проф. И. А. Биргера и чл.-корр. АН Латвийской ССР Я. Г. Пановго, изд-во «Машиностроение», 1968.

33. Скубачевский Г. С., Авиационные газотурбинные двигатели. Конструкция и расчет деталей, издание 3-е, изд-во «Машиностроение», 1969.

34. Слива О. К., Дискретные модели колеблющихся лопаток турбомашин, Сб. «Динамика и прочность машин», вып. 4, издание Харьковского университета, 1966.

35. Сойфер А. Л., Бузицкий В. Н., Цельнометаллические упруго-демпфирующие элементы, их изготовление и применение, Сб. «Вибрационная прочность и надежность авиационных двигателей», Труды Куйбышевского авиационного института, вып. XIX, Куйбышев, 1965.

36. Сорокин Е. С., К вопросу неупругого сопротивления при колебаниях, Госстройиздат, 1954.

37. Сорокин Е. С., Динамический расчет несущих конструкций зданий, Госстройиздат, 1956.

38. Стокер Д. Ж., Нелинейные колебания в механических и электрических системах, ИЛ, 1952.

39. Теодорчик К. Ф., Автоколебательные системы, Физматгиз, 1957.

40. Тимошенко С. П., Колебания в инженерном деле, Физматгиз, 1959.

41. Фадеев В. Н., Вычислительные методы линейной алгебры, Гостехиздат, 1950.

42. Филекин В. П., Конструктивный гистерезис во фланцевых и шовных соединениях, Известия ВУЗов, серия «Авиационная техника», № 4, 1960.

43. Филиппова А. П., Колебания механических систем, изд-во АН УССР, 1965.

44. Харкевич А. А., Автоколебания, Гостехиздат, 1953.

45. Хронин Д. В., Совместные колебания дисков, валов и лопаток роторов турбокомпрессорных машин, Известия ВУЗов, серия «Авиационная техника», № 1, 1966.

46. Хронин Д. В., Расчет критических чисел оборотов валов турбомашин с учетом деформаций дисков и лопаток, Труды МАИ, вып. 136, Оборонгиз, 1961.

47. Шорр Б. Ф., Основы теории закрученных лопаток с непрямой осью, Сб. «Прочность и динамика авиационных двигателей», вып. 3, изд-во «Машиностроение», 1966.